HOMOGENEOUS CATALYSIS

Understanding the Art

Piet W.N.M. van Leeuwen

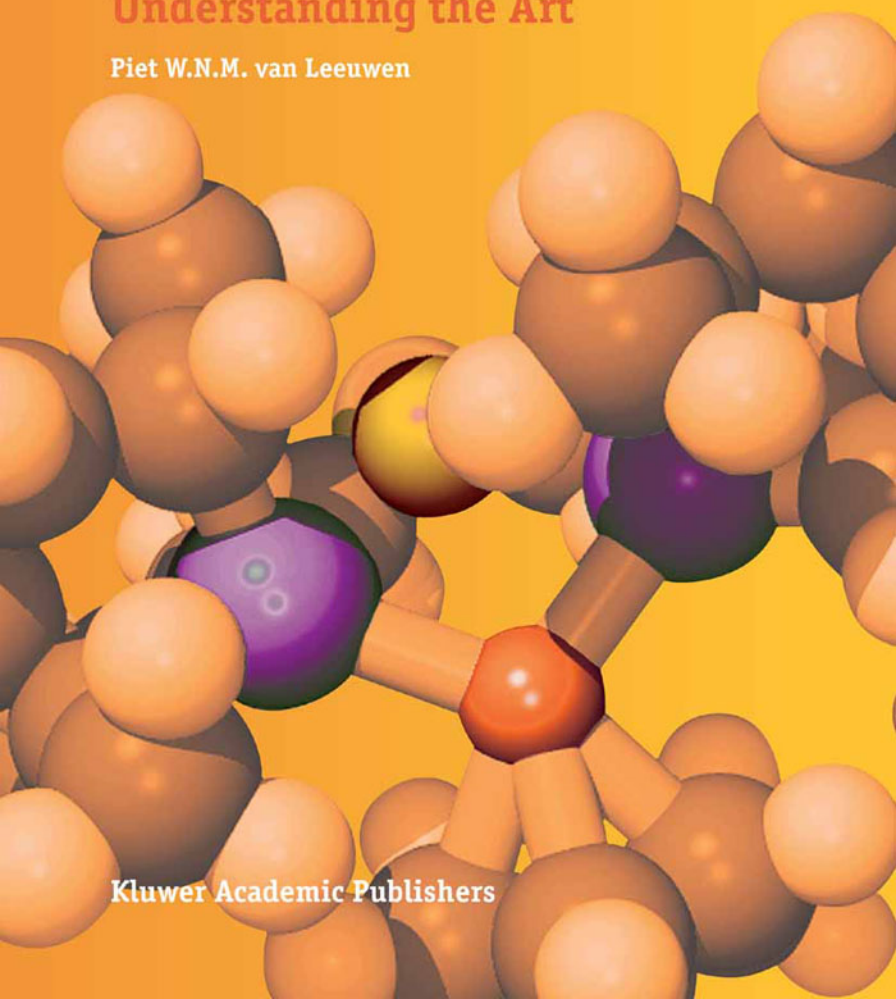

Kluwer Academic Publishers

Homogeneous Catalysis

Homogeneous Catalysis

Understanding the Art

by

Piet W.N.M. van Leeuwen
University of Amsterdam,
Amsterdam, The Netherlands

KLUWER ACADEMIC PUBLISHERS
DORDRECHT / BOSTON / LONDON

A C.I.P. Catalogue record for this book is available from the Library of Congress.

ISBN 1-4020-3176-9 (PB)
ISBN 1-4020-1999-8 (HB)
ISBN 1-4020-2000-7 (e-book)

Published by Kluwer Academic Publishers,
P.O. Box 17, 3300 AA Dordrecht, The Netherlands.

Sold and distributed in North, Central and South America
by Kluwer Academic Publishers,
101 Philip Drive, Norwell, MA 02061, U.S.A.

In all other countries, sold and distributed
by Kluwer Academic Publishers,
P.O. Box 322, 3300 AH Dordrecht, The Netherlands.

Printed on acid-free paper

Printed in the Netherlands.

Table of contents

Preface

Homogeneous catalysis using transition metal complexes is an area of research that has grown enormously in recent years. Many amazing catalytic discoveries have been reported by researchers both in industry and in academia. Reactions that were thought to be well understood and optimised have now been revolutionized with completely new catalysts and unprecedented product selectivities. Our knowledge in this area has increased accordingly, but much of this information is still only to be found in the original literature. While the field of homogeneous catalysis is becoming more and more important to organic chemists, industrial chemists, and academia, until now there has been no book available that gives real insight in the many new and old reactions of importance. This book aims to provide a balanced overview of the vibrant and growing field of homogeneous catalysis to chemists trained in different disciplines, and to graduate students who take catalysis as a main or secondary subject.

The book presents a review of sixteen important topics in modern homogeneous catalysis. While the focus is on concepts, many key industrial processes and applications that are important in the laboratory synthesis of organic chemicals are used as real world examples. After an introduction to the field, the elementary steps needed for an understanding of the mechanistic aspects of the various catalytic reactions have been described. Chapter 3 gives the basics of kinetics, thus stressing that kinetics, so often neglected, is actually a key part of the foundation of catalysis.

The approach in the catalysis chapters has been to introduce the key concepts and important examples, rather than to present a complete listing of catalysts, ligands, and processes, which would anyway be impossible within this single

volume. Readers requiring this level of depth and completeness on a given reaction are pointed (through references) toward many dedicated books that present the individual topics with all the details in a comprehensive way. The literature chosen is a very personal choice of what I thought crucial to the development of an understanding of a given reaction. A few chapters remain descriptive in the absence of better studies, but they have been included because of their importance, and in order to cover the full range of topics such as fine chemicals, bulk chemicals, polymers, high-tech polymers, pharmaceuticals, reaction types, etc. For a few reactions, I have included the process schemes, environmental concerns and safety aspects, in an attempt to encourage catalyst researchers to think about these topics at an early stage of their projects and communicate with chemical engineers, customers and the end-users.

Astonishment and awe signalled the early chapters of modern day science; a deeper understanding is not the end of this era of marvel and amazement, but simply the next exciting chapter.

Acknowledgments

I gratefully acknowledge my indebtness to many people for their input in this project. During many years my co-workers at Shell, the University of Amsterdam, and colleagues in many other places have contributed with their presentations, their observations, and discussions to my courses in "homogeneous catalysis", which eventually condensed in this book. A book like this requires more than just the writing, as being read is the primary goal. The students in the course of spring 2003 in Amsterdam worked a lot on the drafts and they made many suggestions, more than I could follow up. I am indebted to Alessia Amore, David Dominguez, Tanja Eichelsheim, René den Heeten, Mark Kuil, Renske Lemmens, Tomasso Marcelli, Maayke Mars, Angelica Marson, Teresa Monzón, Erica Nöllen, and Fabrizio Ribaudo for their valuable contributions.

I am grateful to many colleagues who read one of the chapters for their valuable discussions and corrections: Lily Ackerman, Peter Budzelaar, Sergio Castellón, Carmen Claver, Neil Grimmer, Marco Haumann, Henk Hiemstra, Paul Kamer, Hans Mol, Christian Müller, Joost Reek, Gino van Strijdonck, Dieter Vogt, and Matthew Wilkinson. I owe many thanks to Brian Goodall for reading many chapters and for making many useful contributions. After changing and editing the danger is that new mistakes are introduced and I am very grateful to Zoraida Freixa for reading the whole manuscript and for making the ultimate suggestions for improvements seaking a balance between time and result. I am indebted to Annemieke Pratt-Teurlings for the finishing touch in removing many errors and for polishing the last draft.

I am very pleased with the encouragement I received right from the start from my fellow-editor Brian James and the publishing editor Emma Roberts. Many thanks to all,

Amsterdam, December 2003, Piet van Leeuwen

Chapter 1

INTRODUCTION

What it is all about

1.1 Catalysis

Catalysis plays a key role in the industrial production of liquid fuels and bulk chemicals. More recently the producers of fine chemicals have started to utilise catalytic conversions in their processes. For oil processes heterogeneous catalysts are preferred with one exception, the alkylation reaction for which liquid acids are being used. For the conversion of petrochemicals both homogeneous and heterogeneous catalysts are used. The number of homogeneously catalysed processes has been steadily growing in the eighties and nineties. For fine chemicals a variety of sophisticated homogeneous catalysts is being used. In the laboratory a wide range of catalytic reactions has become indispensable.

The term catalysis was coined by Berzelius over 150 years ago when he had noticed changes in substances when they were brought in contact with small amounts of certain species called "ferments". Many years later in 1895 Ostwald came up with the definition that we use until today: *A catalyst is a substance that changes the rate of a chemical reaction without itself appearing into the products.* This means that according to Ostwald a catalyst can also slow down a reaction! The definition used today reads as follows: *A catalyst is a substance which increases the rate at which a chemical reaction approaches equilibrium without becoming itself permanently involved.*

The "catalyst" may be added to the reactants in a different form, the catalyst precursor, which has to be brought into an active form ("activated"). During the catalytic cycle the catalyst may be present in several intermediate forms when we look more closely at the molecular level. An active catalyst will pass a number of times through this cycle of states; in this sense the catalyst remains unaltered. The number of times that a catalyst goes through this cycle is the turnover number. The turnover number (TON) is the total number of substrate

molecules that a catalyst converts into product molecules. The turnover frequency (TOF) is the turnover number in a certain period of time. Substrates are present in larger amounts than the catalyst; when we report on catalytic reactions the ratio of substrate to catalyst is an important figure.

An inhibitor is a substance that retards a reaction. An inhibitor is also present in "catalytic" or sub-stoichiometric amounts. In a radical chain reaction an inhibitor may be a radical scavenger that interrupts the chain. In a metal catalysed reaction an inhibitor could be a substance that adsorbs onto the metal making it less active or blocking the site for substrate co-ordination. We also talk about a poison, a substance that stops the catalytic reaction. A poison may kill the catalyst. The catalyst dies, we say, after which it has to be regenerated wherever possible. We will often see the word co-catalyst, a substance that forms part of the catalyst itself or plays another role somewhere in the catalytic cycle. We inherited a florid language from our predecessors to whom catalysis was black magic. Naturally, these words are rather imprecise for a description of catalysis at the molecular level.

Organometallic catalysts consist of a central metal surrounded by organic (and inorganic) ligands. Both the metal and the large variety of ligands determine the properties of the catalyst. The success of organometallic catalysts lies in the relative ease of catalyst modification by changing the ligand environment. Crucial properties to be influenced are the rate of the reaction and the selectivity to certain products.

The following types of selectivity can be distinguished in a chemical reaction:

chemoselectivity, when two chemically different functionalities are present such as an alkene and an aldehyde in the example in Figure 1.1 which both can be hydrogenated, the chemoselectivity tells us whether the aldehyde or the alkene is being hydrogenated; or when more than one reaction can take place for the same substrate e.g. hydrogenation or hydroformylation;

regioselectivity, as in the example shown for the hydroformylation reaction, the formyl group can be attached to either the primary, terminal carbon atom or the secondary, internal carbon atom, which leads respectively to the linear and the branched product;

diastereoselectivity, the substrate contains a stereogenic centre and this together with the catalyst can direct the addition of dihydrogen in the example to give two diastereomers, the selectivity for either one is called the diastereoselectivity;

enantioselectivity, the substrate is achiral in this instance, but the enantiopure or enantio-enriched catalyst may give rise to the formation of one specific product enantiomer.

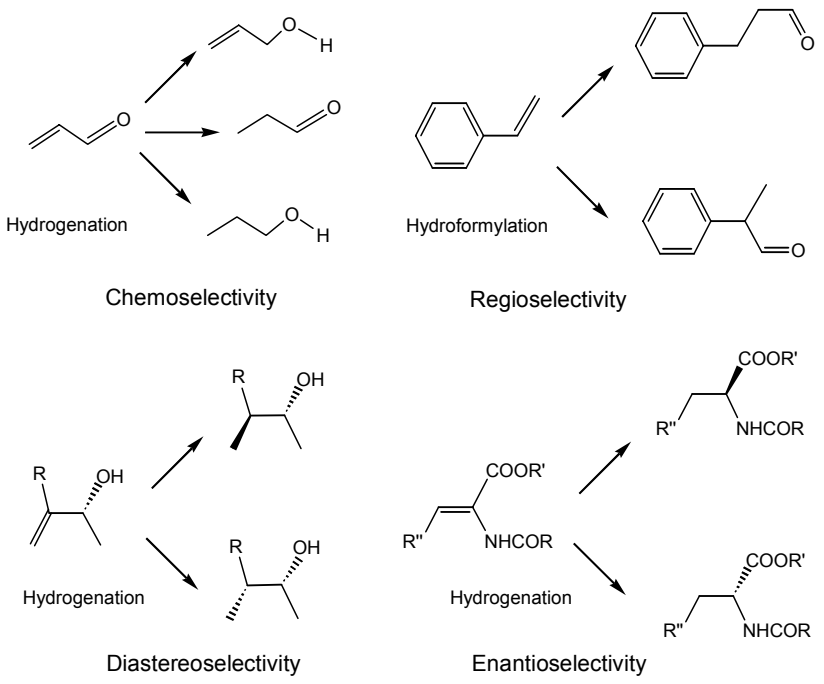

Figure 1.1. Selectivity of chemical conversions

High selectivity is a means

1) to reduce waste,
2) to reduce the work-up equipment of a plant, and
3) to ensure a more effective use of the feedstocks.

Rate enhancements of many orders of magnitude can be obtained in catalysis, often by very subtle changes. Rates represent a cost factor, higher rates allowing higher space-time yields (kg of product per time and reactor volume) and hence smaller reaction vessels. Higher rates and higher overall catalyst yields (i.e. mass of product per unit mass of catalyst) reduce the incremental contribution of catalyst costs per unit mass of product generated: In the case of metallocene catalysts for olefin polymerisation for example (Chapter 10) the higher catalyst cost contribution of these catalysts (around \$0.04 per kg of polyolefin) has significantly reduced their impact and ability to displace Ziegler-Natta catalysts (where the catalyst cost contribution is only \$0.006-0.011 per kg of polymer).

Kinetics are an important part of catalysis; after all, catalysis is concerned with accelerating reactions. In order to describe the effectiveness of a catalyst one would like to determine the acceleration that has been achieved in the

catalysed reaction as compared with the non-catalysed reaction. This is an impossibility. Suppose we have a bimolecular reaction of species A and B with a rate of product P formation:

$$d[P]/dt = k_1[A][B]$$

We don't know what the rate equation for the catalysed reaction might look like, but it is reasonable that at least the catalyst concentration will also occur in it, e.g.:

$$d[P]/dt = k_2[Cat][A][B] \quad (\text{or } d[P]/dt = k_3[Cat][A], \text{ etc.})$$

Hence the dimension ("the order") of the reaction is different, even in the simplest case, and hence a comparison of the two rate constants has little meaning. Comparisons of rates are meaningful only if the catalysts follow the same mechanism and if the product formation can be expressed by the same rate equation. In this instance we can talk about rate enhancements of catalysts relative to another. If an uncatalysed reaction and a catalysed one occur simultaneously in a system we may determine what part of the product is made via the catalytic route and what part isn't. In enzyme catalysis and enzyme mimics one often compares the k_1 of the uncatalysed reaction with k_2 of the catalysed reaction; if the mechanisms of the two reactions are the same this may be a useful comparison. A practical yardstick of catalyst performance in industry is the “space-time-yield” mentioned above, that is to say the yield of kg of product per reactor volume per unit of time (e.g. kg product/m^3.h), assuming that other factors such as catalyst costs, including recycling, and work-up costs remain the same.

In practice the rate equation may take a much more complicated form than the ones shown above. The rate equation may tell us something about the mechanism of the reaction.

Before we turn to "mechanisms" let us repeat how a catalyst works. We can reflux carboxylic acids and alcohols and nothing happens until we add traces of mineral acid that catalyse esterification. We can store ethene in cylinders for ages (until the cylinders have rusted away) without the formation of polyethylene, although the formation of the latter is exothermic by more than 80 kjoule/mol. We can heat methanol and carbon monoxide at 250 °C and 600 bar without acetic acid being formed. After we have added the catalyst the desired products are obtained at a high rate.

A *catalyst lowers the barrier* of activation of a reaction, i.e. it lowers the activation energy. When protons or Lewis acids are the catalysts this description seems accurate, as for instance in a Diels-Alder reaction (Figure 1.2):

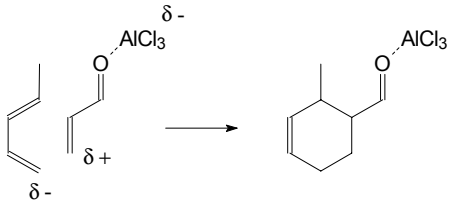

Figure 1.2. Lewis acid catalysis; the "base case"

The catalyst makes the dienophile more electrophilic. It lowers the energy level of the LUMO and the interaction between the LUMO of the dienophile and the HOMO of the diene increases. As a result the reaction becomes faster than the uncatalysed one. Accidentally it becomes also more regioselective. In this instance the catalysed reaction is very much the same as the uncatalysed reaction. Often this is not the case. In particular when the reagents are totally unreactive towards one another (ethene versus ethene, methanol versus CO, see above) the simple picture of a catalyst that lowers the reaction barrier is an oversimplification.

The following description is more general. A catalyst provides a more attractive reaction pathway for the reagents in order to arrive at the products. This new pathway may involve many steps and may be rather complicated. Imagine the direct reaction between methanol and CO. One can calculate what the most likely reaction pathway for the thermal reaction looks like using ab initio molecular orbital methods. It may well be that an almost complete dissociation of the methyl and hydroxyl bond is needed before CO starts interacting with the methanol fragments. (The temperature required for this reaction also allows the energetically more attractive formation of methane and CO_2!) The catalytic reaction involves the formation of methyl iodide, reaction of methyl iodide with a rhodium complex, reaction of the methyl rhodium fragment with co-ordinated CO, etc. which is not quite the simplest and most direct route one can imagine and yet it is the basis of a highly sophisticated catalytic process. The catalyst brings the reagents together in a reactive state. Summarising, *a catalyst provides a new reaction pathway* with a low barrier of activation, which may involve many intermediates and many steps. The sequence of steps we call the mechanism of the reaction. Mechanism also refers to the more detailed description of a reaction at the molecular bonding level. During the process, the catalytic cycle, the catalyst participates in many "complexes" all of which one can call "the" catalyst. It cycles continuously from one species to another. In this sense the catalyst itself remains unchanged during the catalytic conversion (Ostwald, page 1).

1.2 Homogeneous catalysis

Homogeneous catalysis, by definition, refers to a catalytic system in which the substrates for a reaction and the catalyst components are brought together in one phase, most often the liquid phase. More recently a narrower definition has become fashionable according to which homogeneous catalysis involves (organo)metallic complexes as the catalysts (strictly speaking an organometallic compound should contain a bond between a carbon atom and the metal, but this is not true for all catalysts to be discussed). As a shorthand notation it will also be used here, but it should be borne in mind that there are many interesting and important reactions employing homogeneous catalysts that are not (organo)metallic complexes. Examples of such systems or catalysts are:

- general acid and base catalysis (ester hydrolysis),
- Lewis acids as catalysts (Diels-Alder reactions),
- organic catalysts (thiazolium ions in Cannizzarro reactions),
- porphyrin complexes (epoxidations, hydroxylations),
- enzymatic processes,
- co-ordination complexes (polyester condensations).

Ligand effects are extremely important in homogeneous catalysis by metal complexes. One metal can give a variety of products from one single substrate simply by changing the ligands around the metal centre: see Figure

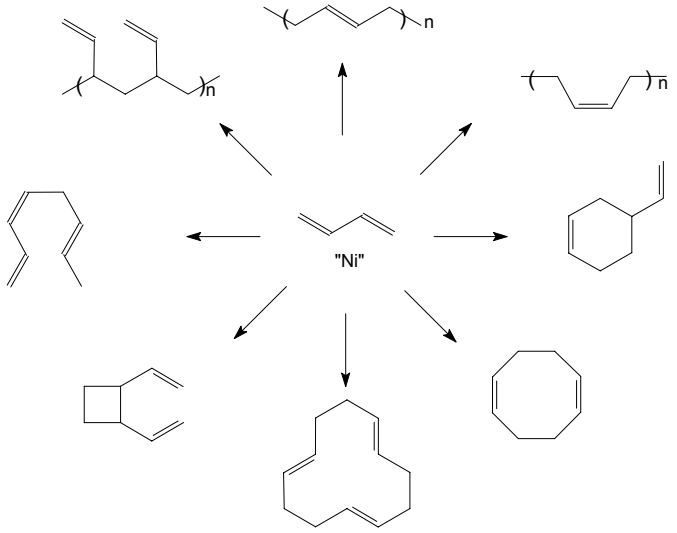

Figure 1.3. Effect of ligands and valence states on the selectivity in the nickel catalysed reaction of butadiene

1.3, showing the products that can be obtained from butadiene with various nickel catalysts (not shown). Polymers are obtained when allylnickel(II) complexes are used as catalysts and cyclic dimers and the all-*trans*-trimer are the product when nickel(0) is the catalyst precursor. Linear dimerisation requires the presence of protic species. Ligands are useful for the fine-tuning of the microstructures of polymers and oligomers. Cyclooctadiene is a commercial product, which is converted mainly to cycloctene. The all-*cis*-trimer is a commercial product as well, but this is made with the use of a titanium catalyst.

1.3 Historical notes on homogeneous catalysis

By far the oldest homogeneous catalysts are metallo-enzymes, although one might wonder whether a metal complex built into a high-molecular weight protein, encapsulated in a compartment of a cell is truly homogeneous. If the answer is positive it means that homogeneous catalysts are millions of years old! We will not go into them in detail here, but rather just mention a few, such as iron porphyrin complexes active for oxidation, zinc complexes for decarboxylation reactions and alcohol dehydrogenase, nickel complexes in hydrogenase enzymes for hydrogen activation, cobalt corrin (methylcobalamin) complexes for carbon-carbon bond formation, copper imidazole (from histidine) complexes in hemocyanin, etc [1]. One of the oldest in vitro uses of whole-cells (in contrast with isolated enzymes) is probably yeast for the fermentation of sugars to alcohol, but one cannot exclude the use of other mechanisms for the aging of materials that we do not know about today.

One might think that the oldest man-made catalysts were heterogeneous, but that may not be so. A very old catalytic process is the making of sulfuric acid via the so-called "lead chamber process" (~1750) in which nitrogen oxides oxidise sulfur dioxide to the trioxide and NO is re-oxidised by air to NO_2. Thus, NO_x is reoxidised by air and NO/NO_2 are the catalysts and since all reside in the gas phase this should be called homogeneous catalysis. From 1870 onwards a number of heterogeneous catalytic processes has been found and applied industrially [2]. The first industrially applied catalyst working in solution and employing organometallic intermediates is most likely mercury sulfate, which was used in the nineteen twenties for the conversion of acetylene to acetaldehyde. This involves the addition of water to acetylene and no oxidation is required. Industrially it is the predecessor of the Wacker chemistry, which uses ethylene for an oxidative conversion to acetaldehyde. This change came about when the coal based economy (coal to acetylene using electric arcs) changed to oil in the 1950's.

A second process that came on stream in the fifties is the oligomerisation of ethene using cobalt complexes, but the number of homogeneously catalysed

processes remained low in the sixties although four more processes came on stream, namely the nickel catalysed hydrocyanation (Dupont), the cobalt catalysed carbonylation of methanol (BASF), cobalt catalysed hydroformylation (Shell) (discovered already in 1938 Ruhrchemie), and the molybdenum catalysed epoxidation of propene (Halcon Corporation). Since the seventies the proportion of homogeneous catalysts has been increasing with success stories such as that of rhodium catalysed carbonylation of methanol (Monsanto), rhodium catalysed hydroformylation (Union Carbide Corporation using Wilkinson's findings), Shell's higher olefins process, asymmetric hydrogenation to L-DOPA (Monsanto), and ring-opening polymerisation of cyclooctene using tungsten metathesis catalysts (Huels).

The majority of the homogeneous processes were developed for bulk chemicals as only products having a sufficiently large volume could justify the expenditure needed for the development of totally new catalysts and the engineering involved. It was only in the nineties that applications in the fine chemicals area took off, utilising the research results of the bulk chemicals area and the large academic effort that had been set up in the meantime.

1.4 Characterisation of the catalyst

Before looking at the chemistry and the processes it is useful in this introduction to say a few words about the actual experimental techniques available in the laboratory. Organometallic complexes are most conveniently characterised by NMR spectroscopy (^{1}H, ^{31}P, ^{13}C, ^{195}Pt etc.) [3]. The same holds for the study of catalyst precursors or organometallic catalysts and intermediates. *In-situ* observation of a "catalyst" has associated problems: NMR spectroscopy requires relatively high concentrations and the species observed might not be pertinent to the catalytic process. The routinely used high-pressure NMR tube, made from sapphire and a titanium head and pressure valve, has the disadvantage that reactive systems involving gas consumption cannot be studied in a true in situ fashion. Suppose we have a pressure of 10 bar of H_2 or CO, leading to a concentration of respectively 20 or 100 mM of this gas in an organic solvent such as toluene. At this lower limit of catalyst concentration one turnover will consume all gas present in solution and diffusion from the gas phase will take hours, and moreover the total volume of the gas phase represents only enough gas for another 10 or 20 turnovers. Thus, in situ measurements of reacting systems with these tubes is hardly possible. Only in a few laboratories in the world equipment is available that allows good gas-liquid mixing and thus real *in situ* measurements [4]. The disadvantage of high concentrations remains.

IR spectroscopic measurements allow more practical, lower, catalyst concentrations than NMR spectroscopic measurements. More importantly, an

IR-cell can be used as an on-line detector connected to a reaction vessel. Both techniques play an important role in the study of the variation of the ligand environment of the catalytic complexes in a controlled manner. Both IR and NMR spectroscopy can be used at high pressure in dedicated tubes or cells. The specific advantages and disadvantages of both techniques are summarised below:

NMR	IR
high concentrations	low concentrations
high pressure	high pressure
when gas is consumed not in situ	in situ measurements
detailed structural information	less structural information

The disadvantage of gas consumption and limited replenishment may also occur for certain IR cells. When an autoclave is connected via pump and tubing to a high-pressure cell, the length of the connecting tube and the rate of circulation may prohibit the observation of the in situ species, because all gas has been consumed before the reactants reach the cell. Unforced stirring in an autoclave which contains the IR windows directly inside the cell may lead to the same problem. Internal reflectance IR spectroscopy is an elegant solution; the reflectance IR probe is mounted directly inside the autoclave [5]. However, a tenfold higher signal-to-noise ratio is obtained in the transmission mode. A drawing of a cell utilising transmission IR spectroscopy is shown in Figure 1.4. It has a very short time delay in the transport of liquid from the autoclave to the cell by a centrifugal pump and efficient mixing is accomplished in the autoclave [6].

Single-crystal X-ray determination, elemental analysis, and mass-spectroscopy are used for the characterisation of complexes and products. Cyclic voltammetry, EXAFS (Extended X-ray Absorption Fine Structure Spectroscopy), NMR, UV-vis spectroscopy, and IR can also be used to determine electronic properties of the ligands and their complexes [7].

The catalytic processes are monitored with the usual techniques such as gas-chromatography, liquid-chromatography, pressure or gas-flow registration, calorimetry [8], IR and UVvis spectroscopy, etc. Recently X-ray Absorption Fine Structure Spectroscopy (XAFS) has been used for the *in situ* identification of species present in a homogeneous catalyst system [9]. EXAFS data give information about the types and number of neighbouring atoms, the distance to these atoms, and the disorder in a particular coordination shell around the X-ray absorbing atom. New data analyses methods have led to improved and more reliable interpretations of EXAFS data [10]. Stop-flow methods with the simultaneous use of Time-Resolved EXAFS and UVvis spectroscopy give even

even more detailed data on the changes in a homogeneous catalyst while the catalytic reaction is progressing [11].

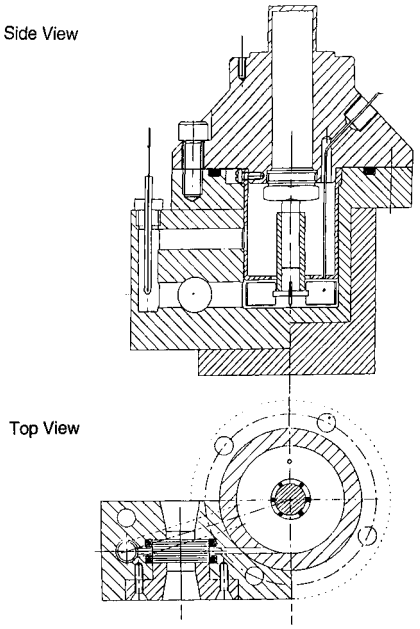

Figure 1.4. Transmission HP-IR cell for in situ measurements

1.5 Ligand effects

1.5.1 Phosphines and phosphites: electronic effects

The readers will be aware of the basic principles of bonding in organometallic complexes, especially the bonding of alkenes and carbon monoxide, and this will not be dealt with here. We will say a few words about ligands containing phosphorus as the donor element.

Phosphine based ligands have found widespread application not only in organometallic chemistry but also in industrial applications of homogeneous catalysis. *Alkyl phosphines* are strong bases, also towards protons, and as expected they are good σ-donor ligands. Organo*phosphites* are strong π-acceptors and they form stable complexes with electron rich transition metals. Probably they are also good σ-donors as they form stable complexes with high-valent metals as well. The metal-to-phosphorus bonding resembles that of metal-to-ethene and metal-to-carbon monoxide. The σ-donation using the lone pair needs no further clarification. The strong binding of phosphites to

especially low-valent metals suggests that π-back-bonding may be dominating in these complexes. The question arises as to which orbitals on phosphorus are responsible for π-back donation. The current view is that the anti-bonding σ*-orbitals of phosphorus to carbon (in the case of a phosphine) or to oxygen (in the case of a phosphite) play the role of the π-acceptor orbital on phosphorus [12].

The σ-basicity and π-acidity of phosphorus ligands has been studied in an elegant manner by looking at the stretching frequencies of the co-ordinated carbon monoxide ligands in complexes such as $NiL(CO)_3$ or $CrL(CO)_5$ in which L is the phosphorus ligand. Strong σ-donor ligands give a high electron density on the metal and hence a substantial back-donation to the CO ligands and lowered IR frequencies. Strong π-acceptor ligands will compete with CO for the electron back-donation and the CO stretch frequencies will remain high. Figure 1.5 illustrates this. Note that ligand orbitals are empty and the metal d-orbitals are filled.

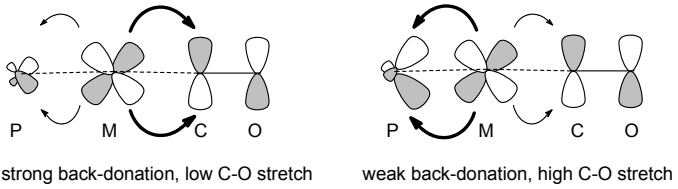

Figure 1.5. Electronic effects of ligands

The IR frequencies represent a reliable yardstick of the electronic properties of a series of phosphorus ligands toward a particular metal. The latter restriction is important, because it is clear that the proton basicity scale (considering a proton as a metal) is not the same as a metal phosphine stability series.

The electronic parameters of phosphine ligands may differ somewhat from one metal to another. When plotting a property of a series of metal complexes (such as stability constants, rate constants, spectral data) versus the electronic parameter of phosphorus ligands this is best done by using the electronic property as determined for the same metal. Strohmeier and Horrocks [13] compared phosphorus ligand properties by measuring the CO stretching vibrations in $CrL(CO)_5$. Tolman [7] has defined an electronic parameter for phosphorus ligands based upon the vibrational spectra of $NiL(CO)_3$; with $L=P(t\text{-}Bu)_3$ as the reference, the electronic parameter χ (chi) for the other ligands is simply defined as the difference in the IR frequencies of the symmetric stretches of the two complexes. The variability of the phosphorus

ligands is nicely reflected in the IR frequencies, which can be measured with sufficient accuracy to give different values for the relevant substituents. Carbon substituents give χ-values ranging from 0 to 20, phosphites are found in the range from 20 to 40, and halogen substituted compounds are found up to 59. For comparison, the ligands at the top of the range, such as PF_3, are as good electron acceptors as carbon monoxide or even better.

Some typical values are:

Ligand PR_3, R=:	χ-value:	IR frequency (A_1) of $NiL(CO)_3$ (in cm^{-1})
t-Bu	0	2056
n-Bu	4	2060
4-$C_6H_4NMe_2$	5	2061
Ph	13	2069
4-C_6H_4F	16	2072
CH_3O	20	2076
PhO	29	2085
CF_3CH_2O	39	2095
Cl	41	2097
$(CF_3)_2CHO$	54	2110
F	55	2111
CF_3	59	2115

When mixed phosphorus compounds are considered the sum of the individual contributions of the substituents can be used to calculate the χ-value of the ligand as was shown by Tolman. The χ_i-value for a single substituent R is simply 1/3 of the χ-value of the ligand PR_3. In extreme cases the additivity rule may not apply but as a first approximation it remains useful.

For rhodium complexes the IR stretch frequency of *trans*-$RhClL_2(CO)$ has been used [14].

1.5.2 Phosphines and phosphites: steric effects

Many attempts have been undertaken to define a reliable steric parameter complementary to the electronic parameter. Most often Tolman's parameter θ (theta) is used. Tolman proposed to measure the steric bulk of a phosphine ligand from CPK models in the following way. From the metal centre, located at a distance of 2.28 Å from the phosphorus atom in the appropriate direction, a cone is constructed which embraces all the atoms of the substituents on the phosphorus atom (see Figure 1.6).

The cone angle is measured, and these cone angles θ (simply in degrees) are the desired steric parameters. Several other methods have been proposed which have led to a modification of the series by Tolman. One particularly useful method is based on complex dissociation constants for ligands with equal electronic parameters [15]. Sterically more bulky ligands give less stable complexes. Within a series of similar ligands, e.g. aryl phosphites, this leads to a reliable yardstick. Crystal structure determinations have shown that in practice the angles realised in the structures are smaller than the θ-values would suggest. For example, two cis triphenylphosphine molecules may have a P–M–P angle as small as 95° whereas the θ-values would predict 145°. In reality intermeshing of the R-substituents leads to smaller effective cone angles. A recent search in the crystal structure database showed that in 39 divalent, square-planar palladium complexes the average P–Pd–P angle is 100.5° [16].

Ligands never form a perfect cone either and in some instances steric interactions nearby the metal may be important, while for other properties interactions more distant from the metal may dominate. This can be taken into account when the cone angle is determined. This point has been addressed in the procedure for determining the so-called solid angle, which utilises crystal structure data. The procedure involves the projection of all atoms of the ligand on the metal surface and the solid angle tells us how much of the surface is covered by this projection [17].

Thermochemistry has been used to determine heats of formation of metal-phosphine adducts. When electronic effects are small, the heats measured are a measure of the steric hindrance in the complexes; heats of formation decrease with increasing steric bulk of the ligand. Recent thermochemistry concerning ligand effects can be found in reference [18].

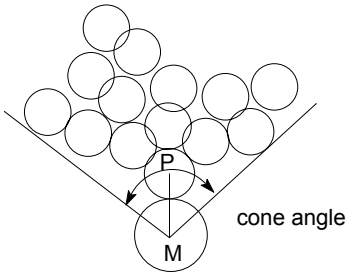

Figure 1.6. Tolman's cone angle

Some typical values are:

Ligand PR_3, R=:	θ-value:
H	87
CH_3O	107
n-Bu	132
PhO	128
Ph	145
i-Pr	160
C_6H_{11}	170
t-Bu	182
2-t-BuC_6H_4O	190
2-$(CH_3)C_6H_4$	194

An ideal separation between steric and electronic parameters is not possible: bending the ideal angles may be energetically more favourable for the overall energy of the complex than the "inflexible" CPK approach, but changing the angles will also change the electronic properties of the phosphine ligand. Bending the alkyl groups away from their ideal angles will destabilise their bonding σ-orbitals and lower the antibonding σ* orbitals, thus enhancing π-back donation. Both the χ- and θ-values should be used therefore with some reservation.

Recently several attempts have been undertaken to describe the steric properties of ligands using molecular mechanics and analysis of data taken from X-ray studies [28] and data-mining [19]. The AMS method [20], AMS = the accessible molecular surface, in which the effective contours of the ligands are calculated, resembles that of the calculation of accessible surface for enzymes. Crystallographic data have also been used to calculate and compare steric ligand properties, more in particular for bidentate ligands (solid angle (Ω) [21], pocket angle [22]).

1.5.3 Linear Free Energy Relationships

Quantitative use of steric and electronic parameters for rationalising or predicting properties of metal complexes and catalysts has received a great deal of attention, although the majority of studies on ligand effects in catalysis have been confined to simple plots or tabulations. As in physical organic chemistry, one might expect that quantification of electronic effects of substituents, as compared to steric effects, on reaction rates will be most successful. Indeed, the second order rate constants for substitution of carbonyl ligands by phosphines in metal complexes could be nicely quantitised using the half neutralisation potentials of the phosphines by Basolo [23]. Deviations were only found for very bulky ligands and this was of course ascribed to steric effects. Tolman proposed a simple equation to include both electronic and steric effects using

the χ- and θ-values (see below). Heimbach used higher order polynomials with χ- and θ-values as the parameters to describe reaction rates and selectivities, but such higher order equations reduce the insight [24]! Today extended "Tolman" equations are available mainly due to the work of Giering and Poë, which are highly accurate. In the following we will briefly introduce QALE, Quantitative Analysis of Ligand Effects, introduced and developed by Giering and coworkers [25].

The use of χ-values in a quantitative manner in linear free-energy relationships (LFER), the same way as Hammett, [26] Taft, [26] and Kabachnik [27] constants, for aromatics, aliphatics, and phosphorus compounds respectively, has no theoretical justification. LFER's express the logarithm of the rate or the equilibrium constant of a reaction as the product of a constant for a particular substituent and a constant for this particular reaction. In other words, it assumes a proportional change in free energy values for a range of reactions or states when the substituents are varied. As the reference for Hammett σ-constants the pK_a-values for substituted benzoic acids are used. Since the χ-values stem from IR frequencies rather than stability data or kinetic data, which involve directly free energies, strictly speaking such a direct translation is not allowed. Therefore it is striking that the methods to describe reactivities and stabilities for series of substituted complexes by the electronic parameters of the substituents multiplied by a parameter for the reaction have been very successful [28].

Tolman's equation includes steric effects and the quantifications of steric effects in LFER have also been useful. The equation reads:

$$\text{Property} = a + b(\chi) + c(\theta)$$

The values for χ and θ are as defined above and used as dimensionless numbers. "Property" as in Hammett relations should be the logarithm of a rate constant, equilibrium constant, etc. An important refinement for the steric contribution was made after the recognition that below a certain threshold of cone angles the property no longer changed and one should use the value 0 for c [29]. Above the threshold a linear relation was found. Thus, for each property a steric threshold θ_{th} was defined and the equation now reads:

$$\text{Property} = a + b(\chi) + c(\theta - \theta_{th})\lambda$$

where λ, the switching factor, reads 0 below the threshold and 1 above it. The electronic parameter has been refined as well and is replaced by two parameters, one for the σ-donicity (χ_d) and one for the π-acceptor property (π_p) [30]. This is in accord with our qualitative view on bonding in metal complexes. A third parameter was introduced, initially called "aryl effect", but

later it became clear that it was also needed in other instances, e.g. when chlorides are the substituents at phosphorus [31]. The "physical" origin of this parameter is not known.

$$\text{Property} = a(\chi_d) + b(\theta - \theta_{st})\lambda + c(E_{ar}) + d(\pi_p) + e$$

When one of the substituents at phosphorus is hydrogen another parameter was needed for $PZ_{3-i}H_i$, to account for the number i of hydrogen substituents giving the equation:

$$\text{property} = a(\chi_d) + b(\theta - \theta_{st})\lambda + c(E_{ar}) + d(\pi_p) + ei + f$$

This looks rather complicated, but the positive side is that the substituent parameter can also be used for other central atoms than phosphorus such as sulfur, silicon, nitrogen, carbon, etc.

One might wonder why cone angles obtained via the simple procedure suggested by Tolman, work so well. Often data from X-ray measurements show the same cone angle, but if they don't they are not necessarily more accurate in LFER, on the contrary. In the solid state other forces might lead to the observed cone angle and one does not have the faintiest idea what energy is associated with this distortion. Therefore any data taken from solution equilibria work much better, because in these instances the free energies needed for these distortions are included in the equilibria studied.

Since catalytic processes comprise several steps, the outcome of LFER may not be straightforward as the substituent effect on various rate or equilibrium constants occurring in the rate equation may be counteracting. The occurrence of inactive states for our catalyst may obscure the intrinsic acitivities we are interested in for our QALE studies. The preference of a catalyst to remain in a certain inactive or dormant state will strongly depend on ligand properties. Thus these effects have to be avoided or included in quantification studies of ligand substituent effects. For reactions having a simple rate equation, the evaluation of ligand effects with the use of methods such as QALE will augment our insight in ligand effects, a better comparison of related reactions, and a useful comparison between different metals. Most studies concern single steps or measurements of properties, but at least one catalytic study has been reported, *viz.* the asymmetric hydrosilylation of acetophenone in which the steroelectronic effect for the silane substrate was described [32].

1.5.4 Phosphines and phosphites: bite angle effects

Diphosphine ligands offer more control over regio- and stereoselectivity in many catalytic reactions; the stability of the bidentate co-ordination reduces the

number of species present compared to monodentate ligands that can form a range of species containing one to four ligands. Tolman's cone angle concept has been widely accepted for monodentate ligands, but extending its use to bidentate ligands appeared to be less straightforward. The major difference between mono- and bidentate ligands is the ligand backbone, a scaffold which keeps two phosphorus donor atoms at a specific distance (Figure 1.7). This distance is ligand specific and it is an important characteristic, together with the flexibility of the backbone. A standardised bite angle, with defined M–P bond lengths and a „metal" atom that does not prefer any specific P–M–P angle is a convenient way of comparing bidentate ligands [33].

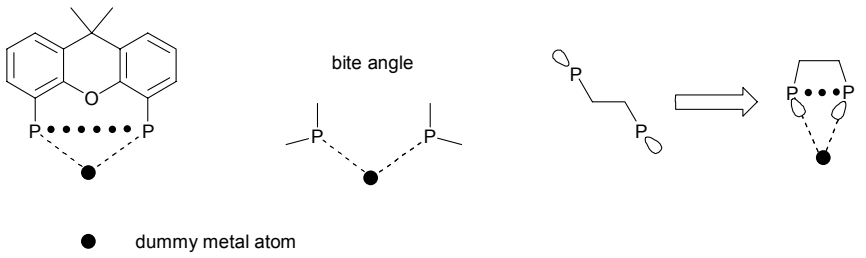

Figure 1.7. Definition of the bite angle

Of the large number of conformations free ligands can adopt, few contain the phosphorus atoms with the correct orientation to allow bidentate coordination to a single metal centre. The lone pairs of electrons have to point in the direction of the metal centre. The easiest way to find these conformations is the introduction of a dummy metal atom (Figure 1.7). If the same dummy-P bond length is used for all ligands, the calculated bite angles are a function of the non-bonded P...P distance. We will describe the „bite angles" obtained in this way as ligand bite angle or natural bite angle (Casey, [34]), as opposed to P–M–P „bite" angles measured in crystal structures.

The potential formation of different catalytic species has to be taken into account when a series of similar ligands are compared. With increasing ligand bite angles, the formation of dimeric *trans*-complexes becomes more likely, as for dppb [35]. Increasing flexibility of a ligand backbone, wrong orientation of phosphorus lone-pairs, and increasing steric bulk of the substituents raises the chance of an arm-off η^1-coordination.

Many examples show that the ligand bite angle is related to catalytic performance in a number of reactions. Early examples are the platinum-diphosphine catalysed hydroformylation [36] or palladium catalysed cross coupling reactions of Grignard reagents with organic halides [37]. In recent years, a correlation between ligand bite angles and catalyst selectivities has

been observed in rhodium catalysed hydroformylation [38], nickel catalysed hydrocyanation [39] and Diels-Alder reactions [40].

The P–M–P angle found in transition metal complexes is a compromise between the ligand's preferred bite angle and the one preferred by the metal centre. The former is mainly determined by constraints imposed by the ligand backbone and by steric repulsion between substituents on the phosphorus atoms and/or the backbone. Electronic effects seem to have a more indirect influence by changing the preferred metal-phosphorus bond length. The metal preferred bite angle, on the other hand, is mainly determined by electronic requirements, i.e. the nature and number of d-orbitals involved in forming the molecular orbitals. Other ligands attached to the metal centre can influence the bite angle if they are very bulky or if they have a strong influence on the metal orbitals (π-bonding ligands for example).

For the calculation of ligand bite angles, either molecular modelling or P...P distances determined from crystal structures can be used. Molecular modelling has been used to calculate „natural" bite angles, ligand bite angles calculated using a „rhodium" dummy atom and fixed Rh–P distances of 2.315 Å [41]. Bite angles are a function of the M–P bond length. In order to obtain a meaningful comparison between different ligands, the measured (or calculated) angles have to be standardised to one, defined M–P bond length. Standardised bite angles can be calculated from the P...P-distance (table 1).

Table 1.1. Diphosphines and their bite angles [33]

Ligand	X-ray values[a]	molecular modelling[b]
	P–M–P	β_n
dppm	71.7	
dpp-benzene	83.0	
dppe	85.0	78.1, 84.4 (70-95)
dppp	91.1	86.2
dppb	97.7	98.6
dppf	95.6	99.1
BINAP	92.4	
DIOP	97.6	102.2 (90-120)
Duphos(Me)	82.6	
BISBI	122.2	122.6 (101-148)[c]
		112.6 (92-155)
NORPHOS		123 (110-145)
Transphos		111.2
T-BDCP		107.6 (93-131)
DPEphos	102.5	102.2 (86-120)
Xantphos	107.1	111.7 (97-135)
DBFphos		131.1 (117-147)

[a] Standardized M–P distances from X-ray structures and angles recalculated.

[b] In brackets the flexibility range, i.e. accessible angles within 3 kcal/mol.

[c] Two conformations of backbone.

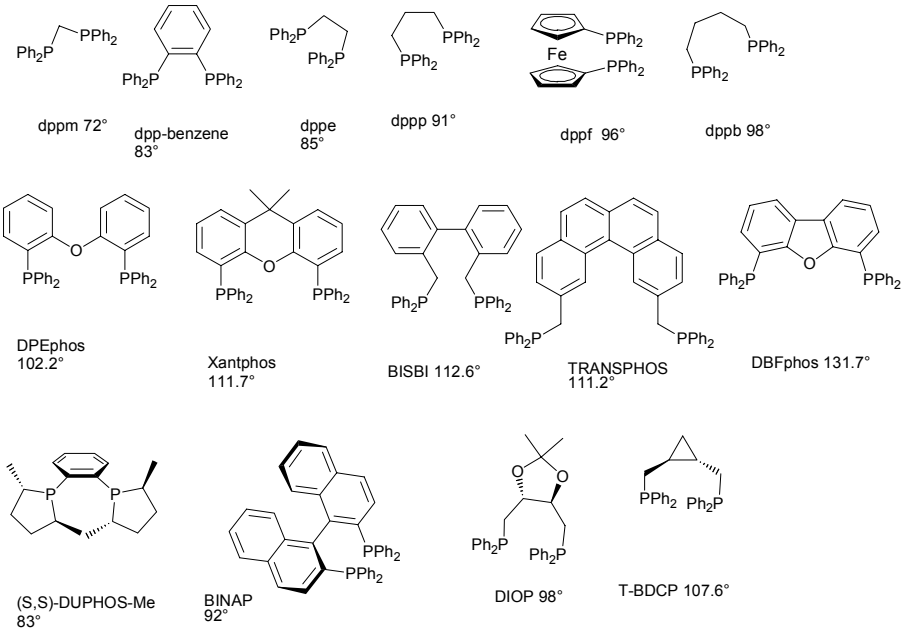

Figure 1.8. Bidentate ligands and their bite angles

With the aim of rationalizing the effect of (wide) bite angle diphosphines in catalytic reactions a distinction can be made between two different effects, both related to the bite angle of diphosphine ligands [42]:

The first one, which we will call *steric bite angle effect* is related to the steric interactions (ligand–ligand or ligand–substrate) generated when the bite angle is modified by changing the backbone and keeping the substituents at the phosphorus donor atom the same. The resulting steric interactions can change the energies of the transition states and the catalyst resting states, thus modifying the activity or selectivity of the catalytic system.

The second one, the *electronic bite angle effect* is associated with electronic changes in the catalytic centre when changing the bite angle [16]. It can be described as an orbital effect, because the bite angle determines metal hybridisation and as a consequence metal orbital energies and reactivity. This effect can also manifest itself as a stabilisation or destabilisation of the initial, final or transition state of a reaction. When the substituents at the phosphorus donor atom are kept the same while the bite angle is changed, the steric properties also change, unfortunately.

1.6 Ligands according to donor atoms

An overview of all ligands useful in catalysis is an impossible task and it would probably repeat what will follow in later chapters. Very briefly we will mention here the ligands most common in catalysts, although it should be borne in mind that the discovery of new catalysts continues, often using ligands that so far have been neglected. There has always been a strong emphasis on phosphorus containing ligands in homogeneous catalysis directed at organometallic catalysts, but in the last decades a large variety of donor groups has been added to this. In this brief summary we will refer to the chapters in which more can be found and whenever possible some general properties will be mentioned.

1.6.1 Anionic and neutral hydrocarbyl groups

Cyclopentadienyl ligands have become extremely important in catalysis for metal such as Ti, Zr, and Hf (Chapter 10) and in academic studies of related elements such as Ta. Ethylene polymerisation with the use of Cp_2TiCl_2 (alkylated with aluminium alkyl compounds) has been known for many decades, but the intensive interest in derivatives of these compounds started in the early 1980's following the discovery of MAO (methaluminoxane – see chapter 10) which boosted metallocene catalyst activities by several orders of magnitude. Commercial interest focussed on ethylene copolymers (LLDPE where more homogeneous comonomer incorporation resulted in greatly improved copolymer properties) and in enantiospecific polymerisations for propene, styrene, etc.

Aromatics occur as ligands in ruthenium complexes that are used for hydrogen transfer reaction, i.e. two hydrogen atoms are transferred from a donor molecule, e.g. an alcohol, to a ketone, producing another alcohol. Especially the enantiospecific variant has become important, see Chapter 4.4. The substitution pattern of the aromatic compound influences the enantioselectivity of the reaction.

In these ruthenium complexes the bond between aromatic and metal atom (ion) is very strong and no ligand-metal exchange occurs. In other instances the interaction between aromatic and metal ion can be very weak. For instance, when weakly coordinating anions are used together with Early-Transition Metal cations, these metal ions can be solvated by aromatics if no stronger ligands are present. An intramolecular stabilising aromatic group for titanium catalysts active in the trimerisation of ethene has been reported, see Chapter 9.3.

Aromatics have also been utilised as ligands in nickel complexes recently reported to be highly active in the addition (or vinyl-type) polymerisation of

norbornenes [43]. This class of catalyst is exemplified by (η_6-toluene)Ni(C_6F_5)$_2$ which is further described in chapter 10 (olefin polymerisation).

1.6.2 Alkoxy and imido groups as anionic ligands

Alkoxides and imido are used as anionic ligands in zirconium and titanium catalysts for the polymerisation of alkenes, sometimes as the only anions, but often in combination with cyclopentadienyl ligands. Imides linked to cyclopentadienyl groups form part of the single-site catalyst developed by Dow (Chapter 10) (Figure 1.9, **1**). In very different titanium catalysts, namely those used for epoxidation of alkenes, also alkoxide ligands are used (Chapter 14).

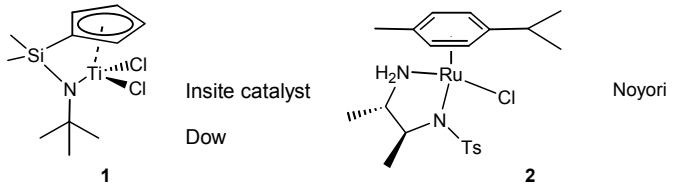

Figure 1.9. Amido ligands

Alkoxides connected to a neutral ligand, either a phosphine or an imine, are excellent ligands for divalent metal catalysts of nickel and palladium for alkene reactions, in which the second valence of the complex is made up by a hydrocarbyl group involved in a chain growth reaction (or hydride during the chain transfer process). Many of these nickel compounds are active as ethene oligomerisation catalysts. Alkoxides and amides feature also in hydrogen transfer catalysts where they may even play an active role in abstracting a proton from the alcohol substrate (Chapter 4.4, Figure 1.9, **2**).

While for main group elements of columns 1-3 the metal to oxygen and nitrogen bonds are much more stable, for transition metal complexes the differences between carbon centred and oxygen or nitrogen centred anions is much smaller, even more so at the right hand side of the periodic table. As a result many metal-to-hetero atom bonds participate in catalytic reactions leading to carbon-to-hetero atom bonds and it allows us to carry out a large part of our organometallic chemistry in the presence of water, alcohols, or amines.

1.6.3 Amines, imines, oxazolines and related ligands

Nitrogen ligands are the most donor functions in enzymes, the oldest "homogeneous" catalysts. Here they occur in imidazoles, porphyrins, binding to metals such as copper and iron, and they are involved in many oxidation reactions. Numerous mimics of these complexes are used in homogeneous

catalysis, such as oxidation of C–H bonds or oxidative coupling reactions of phenols [44].

Amines and pyridines as ligands are subjects of the oldest studies in coordination chemistry and catalysis. Pyridines were used already in "man-made catalysts" in hydrogenation catalysts based on copper one or two decades before phosphines (in platinum complexes) [45]. Amines, containing sp^3 hybridized nitrogen, is the analogue of phosphines. They are strong, hard s-donors compared to phosphines and stabilise high-valent metal complexes, for example tetravalent palladium and platinum [46]. Due to the smaller atomic radius of nitrogen the cone angles are larger than those of the corresponding phosphines (NMe_3 $\theta = 132°$, PMe_3 $\theta = 132°$, NEt_3 $\theta = 150°$, PEt_3 $\theta = 132°$) [47].

Nitrogen ligands, especially pyridine and imidazole ligands, are much more stable than phosphines. Pyridines are not prone to oxidation as phosphines, and other common decomposition pathways for phosphines such as phosphorus-to-carbon bond cleavage, phosphido formation, or hydrolysis of phosphites [48] (see also Chapter 2.12). Nitrogen ligands are therefore far preferred to phosphines in oxidation catalysis. The bonding characteristics of pyridine (and other sp^2 hybridised nitrogen centred ligands) and phosphorus donor ligands are very different; they are good σ-donors and poor π-acceptor ligands, but not to the extreme of amines. Like amines they stabilise higher valence states of metal complexes rather than low valence states. For example in divalent metal catalysis of palladium or nickel their behaviour may be very similar, but in catalytic reactions involving reductive eliminations leading to zerovalent complexes, the performance is different, phosphorus being the preferred one in this instance.

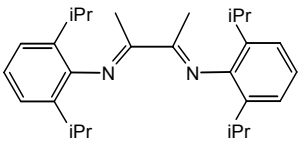

3

Figure 1.10. Diimine ligands

Diimines can be easily made from 1,2 diamines by condensing them with aldehydes [49] and in particular bulky aromatic aldehydes have led to a range of interesting new nickel and palladium catalysts for polymerisation of alkenes Brookhart, Du Pont [50] (Figure 1.10, **3**). Oxazolines have the added advantage compared to other imine-nitrogen based ligands that the asymmetric derivatives are readily accessible. The group of PyBox ligands (Figure 1.11) represents an example of the use of chiral oxazolines [51]. Another important new range of asymmetric catalysts are the bisoxazolines, **4**, and related structures [52].

Mono-oxazolines containing phosphine groups as the second donor atom, **5**, have also found wide application [53]. When the oxygen atom in oxazolines is replaced by a substituted nitrogen atom, one obtains imidazolines, **6**, which still contain the asymmetric carbon atom, but in addition offer the possibility of electronic variation via substitution at the amine-nitrogen atom [54]. The latter substituent might also be used for immobilisation through covalent linkages.

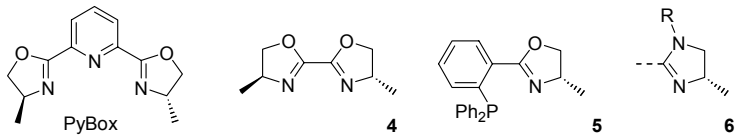

Figure 1.11. Bisoxazolines, phosphino-oxazolines, and imidazolines

1.6.4 Phosphines, phosphites, phosphorus amides, phospholes and related ligands

In section 1.5 under ligand effects we already had a close look at the properties of phosphine and phosphite ligands. By changing the substituents at phosphorus the steric and electronic properties can be changed over a very wide range. Electronically phosphorus ligands can be either strong σ-donors (e.g. t-Bu substituents) or strong π-acceptors (e.g. fluoroalkoxide substituents). Clearly the whole range in between is accessible by using mixtures of all possible groups. In addition to oxygen and carbon centred substituents one can also use nitrogen as the connecting atom which leads to amides, or, if mixed oxygen and nitrogen substituents are considered, amidites. Dialkylamino groups (Figure 1.10, **7**) are electronically similar to hydrocarbyl groups in phosphorus compounds (χ_i for Et_2N = 2.4 pyrolidines, best donors [7]). For nitrogen groups connected with electron-withdrawing acyl groups or sulfone groups the χ-value can be very high and thus these phosphorus amidites are good π-acceptor ligands (**9**) [55]. Pyrrole as a substituent at phosphorus also leads to a very electron-poor phosphorus ligand, **10** [56]. The advantage of nitrogen substituents compared to those of oxygen is that the steric hindrance near the metal centre in a metal complex can be more conveniently modified due to the presence of an extra linkage. In general phosphites and phosphorus amidites such as **8** are more easily made than phosphines, they allow a greater variation in structure and properties [57], they are less sensitive to oxidation, but they are often prone to hydrolysis. The rate of hydrolysis is strongly dependent on the precise ligand structure [48] and often a stable analogue can be found. Ligands of type **8** have become of great importance in recent years (Chapter 4.4).

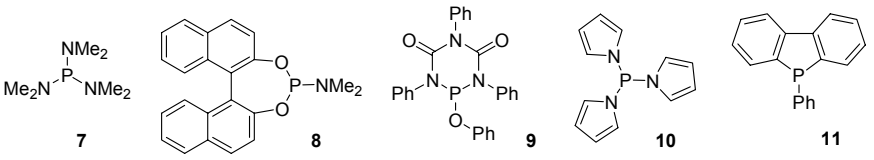

7 8 9 10 11

Figure 1.12. Phosphorus amidites, phopshorus pyrroles, and phospholes

A special type of phosphine is worth mentioning, viz. phospholes, the phosphorus analogues of pyrroles. Especially dibenzophosphole **11** has been used very often as a group similar to diphenylphosphine. Even though the atom count for dibenzophosphole is slightly lower (by 4 hydrogen atoms) it behaves usually as a slightly bulkier group because of its rigidity. The electronic property is also different, as its χ-value is higher. The synthetic applicability is somewhat restricted compared to Ph_2P, which is available both as the chloride and the phosphido anion, since phospholes are only available as the phosphido anion.

1.6.5 Carbenes, carbon monoxide

Carbenes are both reactive intermediates and ligands in catalysis. They occur as intermediates in the alkene metathesis reaction (Chapter 16) and the cyclopropanation of alkenes. As intermediates they carry hydrogen and carbon substituents and belong therefore to the class of Schrock carbenes. As ligands they contain nitrogen substituents and are clearly Fischer carbenes. They have received a great deal of attention in the last decade as ligands in catalytic metal complexes [58], but the structural motive was already explored in the early seventies [59].

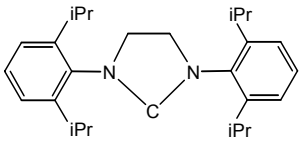

12

Figure 1.13. Carbene ligand

Recent successes are partly based on the use of aryl or bulky aryl substituents at the nitrogen atoms of the imidazolium rings. As ligands they are strong σ-donors (stronger than t-Bu_3P) and hardly π-acceptors, they are sometimes called "singlet carbenes".

Carbon monoxide is often both reactant and ligand. As a ligand it is a strong π-acceptor and a moderate σ-donor. By comparison of IR data one might say that its χ-value is around 55, i.e. similar to hexafluoroisopropyl phosphite.

Extending the comparison with the steric properties of phosphorus ligands, clearly CO is one of the smallest ligands available! The interesting feature of CO as a ligand of is that it can be studied by IR, and also *in situ* IR, in a frequency area that is transparent (1800–2200 cm^{-1}). A disadvantage is that in order to obtain concentrations in an organic liquid in the order of 0.1 M one needs pressures in the order of 10 bar.

1.6.6 Common anions

Anions often form part of the coordination or organometallic complex and their role should not be underestimated. In many cases they are reactants as well, e.g. in cross-coupling reactions (Chapter 13) in which a salt is formed as the second product and even in the simple series of halides its anion function toward the metal centre makes an enormous difference in catalytic behaviour. Halides and carboxylates bind strongly to the metal ions and thus their function as a ligand goes beyond doubt. Carboxylates connected to a phosphine moiety are found as ligands in the Shell process for ethene oligomerisation (Chapter 9). Iodides are important ingredients of methanol carbonylation chemistry and they form part of the ligand environment of the rhodium or iridium metal (Chapter 6).

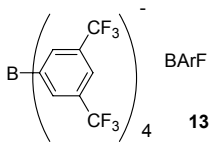

13

Figure 1.14. Example of a WCA

Weakly or non-coordinating anions (WCA, NCA) have received a great deal of attention and they are indispensable in homogeneous catalysis (WCA is the preferred term, because even the most weakly coordinating anions have been found to interact with positively charged metal ions). The cationic counter-ion obtained by using WCA's is readily accessible for the reactants. Especially in reactions involving alkenes (hydrogenations, carbonylations, polymerisations) the introduction of WCA's has led to many breakthroughs. In the early history of homogeneous catalysis the role of creating vacant sites at metal ions to facilitate alkene coordination was played by Lewis acids abstracting chloride ions from the catalyst precursor ("Ziegler catalysts"). The use of WCA's has led to much more control over the species formed in the reactor compared to the use of Lewis acids.

References

1 Reedijk J.; Bouwman, E. Ed. *Bioinorganic Catalysis*, 2nd edn., Marcel Dekker, Inc., New York, **1999**.

2 Moulijn, J. A.; van Leeuwen, P. W. N. M.; van Santen, R. A. Ed. Chapter 1 in *Catalysis, an integrated aspproach to homogeneous, heterogeneous and industrial catalysis.* **1993**, Elsevier, Amsterdam. Studies in Surface Science, Volume 79.

3 Roe, D. C.; Kating, P. M.; Krusic, P. J.; Smart, B. E. *Topics in Catalysis,* **1998**, *5*, 133.

4 Iggo, J. A.; Shirley, D.; Tong, N. C. *New J. Chem.*, **1998**, 1043. Van der Slot, S. C.; Kamer, P. C. J.; van Leeuwen, P. W. N. M.; Iggo, J. A.; Heaton. B. T. *Organometallics,* **2001**, *20,* 430. Cusanelli, A.; Frey, U.; Marek, D.; Merbach, A. E. *Spectroscopy Europe* **1997**, *9*, 22. Cusanelli, A.; Nicula-Dadci, L.; Frey, U.; Merbach, A. E. *Inorg. Chem.* **1997**, *36*, 2211.

5 Moser, W. R.; Papite, C. J.; Brannon, D. A.; Duwell, R. A.; Weininger, S. J. *J. Mol Cat.* **1987**, *41*, 271.

6 Van Rooy, A. Thesis, University of Amsterdam, **1995**.

7 Tolman, C. A. *Chem. Rev.* **1977**, *77*, 313.

8 Rosner, T.; Pfaltz, A.; Blackmond, D. G. *J. Am. Chem. Soc.* **2001***, 123*, 4621.

9 Tromp, M.; van Bokhoven, J. A.; van Haaren, R. J.; van Strijdonck, G. P. F.; van der Eerden, A. M. J.; van Leeuwen, P. W. N. M.; Koningsberger, D. C. *J. Am. Chem. Soc.* **2002***, 124*, 14814.

10 Koningsberger, D. C.; Mojet, B. L.; van Dorssen, G. E.; Ramaker, D. E. *Topics Catal.* **2000**, *10*, 143.

11 Tromp, M.; Sietsma, J. R. A.; van Bokhoven, J. A.; van Strijdonck, G. P. F.; van Haaren, R. J.; van der Eerden, A. M. J.; van Leeuwen, P. W. N. M.; Koningsberger, D. C. *Chem. Commun.,* **2003**, 128.

12 Marynick, D. S. *J. Am. Chem. Soc.* **1984***, 106*, 4064. Orpen, A. G.; Connelly, N. G. *J. Chem. Soc. Chem. Commun.* **1985**, 1310.

13 Strohmeier, W.; Müller, F. J. *Chem. Ber.* **1967***, 100*, 2812. Horrocks Jr., W. D.; Taylor, R. C. *Inorg. Chem.* **1963***, 2,* 723.

14 Van der Slot, S. C.; Duran, J.; Luten, J.; Kamer, P. C. J.; van Leeuwen, P. W. N. M. *Organometallics,* **2002***, 21,* 3873.

15 Trogler, W. C.; Marzilli, L. G. *Inorg. Chem.* **1975***, 14*, 2942.

16 van Leeuwen, P. W. N. M. ; Zuideveld, M. A.; Swennenhuis, B. H. G.; Freixa, Z.; Kamer, P. C. J.; Goubitz, K.; Fraanje, J.; Lutz, M.; Spek, A. L. *J. Am. Chem. Soc.* **2003***, 125,* 5523.

17 White, D.; Taverner, B. C.; Leach, P. G. L.; Coveille, N. J. *J. Comp. Chem.* **1993**, *36,* 1042.

18 Serron, S.; Nolan, S. P.; Moloy, K. G. *Organometallics,* **1996**, *15,* 4301.

19 Mingos, D. M. P. *Mod. Coord. Chem*. **2002**, 69.

20 Angermundt, K.; Baumann, W.; Dinjus, E.; Fornika, R.; Görls, H.; Kessler, M.; Krüger, C.; Leitner, W.; Lutz, F. *Chem. Eur. J*. **1997**, *3,* 755.

21 Hirota, M.; Sakakibara, K.; Komatsukazi T.; Akai, I. *Comput. Chem.* **1991**, *15*. 241; White, D.; Taberner, B. C.; Coville, N. J.; Wade, P. W. *J. Organomet. Chem.* **1995**, *495*, 41. White, D.; Taberner, B. C.; Leach, P. G. L.; Coville, N. J. *J. Organomet. Chem.* **1994**, *478*, 205. Xing-Fu, L.; Xi-Zhang, F.; Ying-Ting, X.; Hai-Tung, W.; Jie, S.; Li, L. *Inorg. Chim. Acta*, **1986**, *116*, 85. White, D.; Coville, N. J. *Adv. Organomet. Chem.* **1994**, *36*, 95.

22 Koide, Y.; Bott, S. G.; Barron, A. R. *Organometallics,* **1996**, *15*, 2213.

23 Schuster-Woldan, H. G.; Basolo, F. *J. Am. Chem. Soc.* **1966***, 88,* 1657. Thorsteinson, E. M.; Basolo, F. *J. Am. Chem. Soc.* **1966***, 88,* 3929.

24 Heimbach, P.; Bartik, T.; Boese, R.; Schenkluhn, H.; Szczendzina, G.; Zeppenfeld, E. *Zeitschr. Chem.* **1988***, 28*, 121.

25 Fernandez, A. L.; Prock, A.; Giering, W. P. *Organometallics,* **1996**, *15,* 2784. At the moment of writing this a website is available at which all information about QALE can be found: www.web.bu.edu/quale
26 Hansch, C.; Leo, A.; Taft, R. W. *Chem. Rev.* **1991***, 91*, 165.
27 Kabachnik, M. I. *Dokl. Chem. (Engl. transl.)* **1956***, 110*, 577.
28 Bunten, K. A.; Chen, L.; Fernandez 1, A. L.; Poe, A. J. *Coord. Chem. Rev.* **2002***, 233-234*, 41.
29 Dahlinger, K.; Falcone, F.; Poe, A. J. *Inorg. Chem.* **1986***, 25*, 2654. Golovin, M. N.; Rahman, M. M.; Belmonte, J. E.; Giering, W. P. *Organometallics* **1985***, 4*, 1981.
30 Liu, H. -. Y.; Eriks, E.; Prock, A.; Giering, W. P. *Organometallics* **1990**, *9*, 1758. Bartik, T.; Himmler, T.; Schulte, H. -G.; Seevogel, K. J. *J. Organomet. Chem.* **1984**, *272*, 29. Fernandez, A. L.; Reyes, C.; Prock, A.; Giering, W. P. *Perkin Trans 2* **2000**, 1033.
31 Wilson, M. R.; Woska, D. C.; Prock, A.; Giering, W. P. *Organometallics* **1993**, *12*, 1742.
32 Reyes, C.; Prock, A.; Giering, W. P. *J. Organomet. Chem.* **2003**, *671*, 13.
33 Dierkes, P.; van Leeuwen, P. W. N. M. *J. Chem. Soc. Dalton Trans.* **1999**, 1519.
34 Casey, C. P.; Whiteker, G. T. *Isr. J. Chem.* **1990**, *20*, 299.
35 Vogl, E. M.; Bruckmann, J.; Krüger, C.; Haenel, M. W. *J. Organomet. Chem.* **1996***, 520*, 249. Dekker, G. P. C. M.; Elsevier, C. J.; Vrieze, K.; van Leeuwen, P. W. N. M. *Organometallics,* **1992***, 11,* 1598.
36 Hayashi, T.; Kawabata, Y.; Isoyama, T.; Ogata, I. *Bull. Chem. Soc. Jpn.,* **1981***, 54*, 3438. Kawabata, Y.; Hayashi, T.; Ogata, I. *J. Chem. Soc., Chem. Commun.* **1979**, 462.
37 Hayashi, T.; Konishi, M.; Kumada, M. *Tetrahedron Lett.* **1979***, 21*, 1871. Hayashi, T. K. M.; Kobori, Y.; Kumada, M.; Higuchi, T.; Hirotsu, K. *J. Am. Chem. Soc.* **1984***, 106*, 158.
38 Casey, C. P.; Whiteker, G. T.; Melville, M. G.; Petrovich, L. M.; Gavney, J. A.; Powell, D. R. *J. Am. Chem. Soc.* **1992***, 114*, 5535 (corr. 10680). Kranenburg, M.; van der Burgt, Y. E. M.; Kamer, P. C. J.; van Leeuwen, P. W. N. M.; Goubitz, K.; Fraanje, J. *Organometallics,* **1995***, 14*, 3081. Yamamoto, K.; Momose, S.; Funahashi, M.; Ebata, S.; Ohmura, H.; Komatsu, H.; Miyazawa, M. *Chem. Lett.,* **1994**, 189.
39 Goertz, W.; Kamer, P. C. J.; van Leeuwen, P. W. N. M.; Vogt, D. *Chem. Commun.* **1997**, 1521. Kranenburg, M.; Kamer, P. C. J.; van Leeuwen, P. W. N. M.; Vogt, D.; Keim, W. *J. Chem. Soc. Chem. Commun.* **1995**, 2177.
40 Davies, I. W.; Gerena, L.; Castonguay, L.; Senanayake, C. H.; Larsen, R. D.; Verhoeven, T. R.; Reider, P. J. *Chem. Commun.* **1996**, 1753.
41 Casey, C. P.; Whiteker, G. T. *Isr. J. Chem.* **1990***, 30*, 299.
42 Freixa, Z.; van Leeuwen, P. W. N. M. *J. Chem. Soc., Dalton Trans.* **2003**, 1890.
43 Barnes, D. A.; Benedikt, G. M.; Goodall, B. L.; Huang, S. S.; Kalamarides, H. A.; Lenhard, S.; McIntosh, L. H., III; Selvy, K. T.; Shick, R. A.; Rhodes, L. F. *Macromolecules* **2003**, *36*, 2623.
44 A. S. Hay, H. S. Blanchard, G. F. Endres and J. W. Eustance, *J. Am. Chem. Soc.* **1959,** *82*, 6335. Gamez, P.; van Dijk, J. A. P. P.; Driessen, W. L.; Challa, G.; Reedijk, J. *Adv. Synth. Catal.* **2002***, 344,* 890.
45 Cramer, R. D.; Jenner, E. L.; Lindsey, R. V.; Stolberg, U. G.; *J. Am. Chem. Soc.* **1963***, 85*, 1691.
46 Canty, A. J. *Acc. Chem. Res.* **1992**, *25*, 83.
47 Brown, T. L.; Lee, K. J. *Coord. Chem. Rev.* **1993**, *128*, 89.
48 van Leeuwen, P. W. N. M. *Appl. Catal. A: General* **2001**, *212*, 61.
49 Vrieze, K.; van Koten, G. *Inorg. Chim Acta.* **1985**, *100*, 79.
50 Johnson, L. K.; Killian, C. M.; Brookhart, M. *J. Am. Chem. Soc.* **1995***, 117,* 6414. Ittel, S. D.; Johnson, L. K.; Brookhart, M. *Chem Rev.* **2000***, 100*, 1169.

51 Nishiyama, H.; Sakaguchi, H.; Nkamura, T.; Horihata, M.; Kondo, M. Itoh, K. *Organometallics,* **1989***, 8,* 846.
52 Lowenthal, R. E.; Abiko, A.; Masamune, S. *Tetrahedron Lett.* **1990**, *31*, 6005. Evans, D. A.; Woerpel, K. A.; Hinman, M. M.; Fad, M. M. *J. Am. Chem. Soc.* **1991**, *113*, 726. Müller, D.; Umbricht, G.; Weber, B.; Pfaltz, A. *Helv. Chim. Acta,* **1991**, *74*, 232. Bolm, C. *Angew. Chem., Int. Ed. Engl.* **1991**, *30*, 542.
53 Helmchen, G.; Pfaltz, A. *Acc. Chem. Res.* **2000**, *33*, 336.
54 Bastero, A.; Castillón, S.; Claver, C.; Ruiz, A. *Eur. J. Inorg. Chem.* **2001**, *12***,** 3009**.** Bastero, A.; Ruiz, A.; Claver, C.; Milani, B.; Zangrando, E. *Organometallics*, **2002**, *21,* 5820. Menges, F.; Neuburger, M.; Pfaltz, A. *Org. Lett.* **2002**, *4*, 4713.
55 Van der Slot, S. C.; Kamer, P. C. J.; Van Leeuwen, P. W. N. M.; Fraanje, J.; Goubitz, K.; Lutz, M.; Spek, A. L. *Organometallics* **2000***, 19*, 2504.
56 Moloy, K. G.; Petersen, J. L. *J. Am. Chem. Soc.* **1995***, 117*, 7696.
57 Peña, D.; Minnaard, A. J.; de Vries, J. G.; Feringa, B. L. *J. Am. Chem. Soc.* **2002**, *124*, 14553.
58 Trnka, T. M.; Grubbs, R. H. *Acc. Chem. Res.* **2001***, 34*, 18.
59 Cardin, D. J.; Cetinkaya, B.; Doyle, M. J.; Lappert, M. F. *Chem. Soc. Rev.* **1973***, 2*, 99.

Chapter 2

ELEMENTARY STEPS

Organometallic Chemistry

2.1 Creation of a “vacant” site and co-ordination of the substrate

The function of a catalyst is to bring the reactants together and lower the activation barrier for the reaction. To bring the reactants together a metal centre must have a vacant site. Metal catalysis begins, we could say, with the creation of a vacant site. For a homogeneous catalyst in a condensed phase this may be less easy than for a heterogeneous catalyst at the surface of a solid under high vacuum. In the condensed phase solvent molecules will always be co-ordinated to the metal ion and "vacant site" is an inaccurate description. Substrates are present in excess and so may be the ligands. Therefore, a competition in complex formation exists between the desired substrate and other potential ligands present in the solution. Often a negative order in one of the concentrations of the "ligands" present can be found in the expression for the rate of product formation. When the substrate co-ordinates strongly to the metal centre this may give rise to a zero order in the concentration of the substrate, i.e. saturation kinetics (c.f. Michaelis-Menten kinetics). Also, strong co-ordination of the product of the reaction may slow down or inhibit the catalytic process. These phenomena are very similar to desorption and adsorption in heterogeneous catalysis.

Another way of looking at the question of 'creation of a vacant site' and 'co-ordination of the substrate' is the classical way by which substitution reactions are described (Figure 2.1). Two extreme mechanisms are distinguished, an associative and a dissociative one. In the dissociative mechanism the rate-controlling step is the breaking of the bond between the metal and the leaving ligand. A solvent molecule occupies the open site, which is a phenomenon that does not appear in the rate equation. Subsequently the solvent is replaced by the

substrate in a fast step. In the associative process (S_N2) the displacement is a bimolecular process with simultaneous bond breaking of the ligand and bond formation of the metal and the substrate. In square planar complexes as found for many group 9 and 10 metals the associative process is most common.

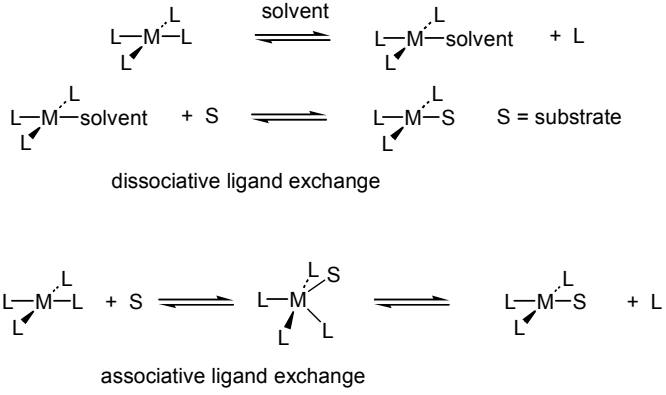

Figure 2.1. Dissociative and associative ligand exchange

It is useful to study the rate equations for the dissociative and associative displacement reactions.

2.2 Insertion versus migration

Insertion and migration refer to the process in which an unsaturated molecule inserts to a metal-anion bond. The two ways of describing this elementary step have been depicted in Figure 2.2 and 2.3 In the platinum complex shown an acetyl fragment is formed from a co-ordinated CO and a methyl group, both attached to platinum. Clearly, the two reacting groups should occupy positions cis to one another, otherwise the reaction cannot occur [1].

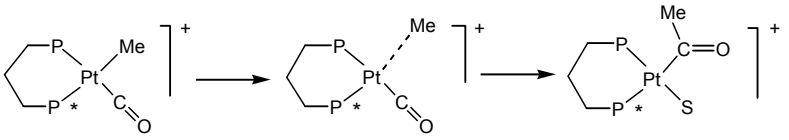

Figure 2.2. The insertion mechanism

The important difference between the insertion mechanism (2.2) and the migration mechanism (2.3) is the following. In the insertion mechanism carbon monoxide inserts into the metal methyl bond and the acyl bond formed takes

the position of the methyl group, i.e. the σ–bonded fragment retains its position trans to P*.

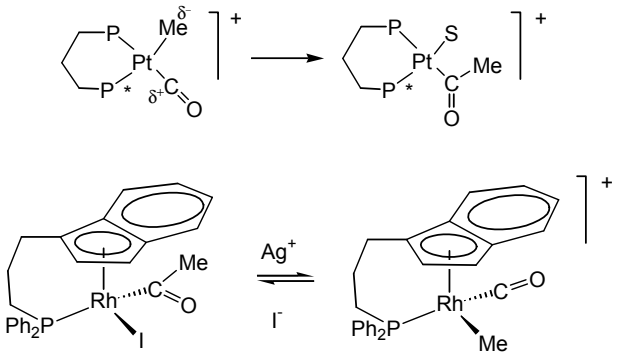

Figure 2.3. The migration mechanism

In the migration mechanism the methyl group migrates to the co-ordinated carbon monoxide and now the resulting acetyl group occupies the position cis to P*. There is convincing experimental evidence supporting the migration mechanism versus the insertion mechanism [see references in 2]. The mechanism shown in Figure 2.3 has been proven by NMR studies on diphosphine complexes of platinum containing slightly different phosphino groups such that they can be distinguished in the NMR spectrum of the alkyl and acyl species [3]. The rhodium complex shown proves the migration mechanism for a complex having a piano-stool structure [2]. Theoretical calculations also support the migration mechanism [4]: the **anionic** methyl group moves to the **positively** charged carbon atom (see δ charges in Figure 2.3). Hence migration is the most accurate description for this process. In the literature, however, the reaction is often referred to as "insertion". To do justice to the intimate details one also writes "migratory insertion".

There are several experiments that suggest that insertion is the actual process. Most systems studied are concerned with Mn and Fe as the metals, of which only recently new Fe complexes have become of interest from a catalytic point of view. In Figure 2.4 we have depicted a simple example for platinum. The most stable starting material shows the methyl group and the phosphine in cis positions, due to the trans influence. The same holds for the acetyl product. This might be explained as proof for an insertion reaction, but as the figure shows the migration may be preceded by an isomerisation or after the migration an isomerisation may take place. This is supported by the observation that such "asymmetric" ligands always undergo insertion reactions much more slowly than the symmetric ones. Thus, diphosphine complexes and bipyridine complexes give much faster reactions than the mixed phosphino-nitrogen

ligands [5]. In general, these experiments do not disprove the cis-migration mechanism, but presumably result from topomerisations of the intermediates or products [6].

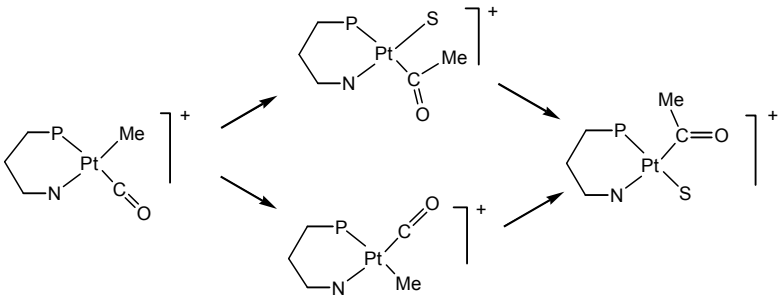

Figure 2.4. Effective insertion reaction

So far we have automatically presumed that the reacting carbon monoxide is co-ordinated to the metal. There is experimental evidence that methyl migration indeed occurs to co-ordinated CO. The classic proof stems from a relatively inert complex in which both the migration and the exchange of co-ordinated CO with free CO are slow. The reaction of $CH_3Mn(CO)_5$ in the presence of ^{13}C labelled free CO results in the formation of $CH_3(CO)Mn(CO)_4(^{13}CO)$ in which the labelled CO is present as co-ordinated carbon monoxide and not in the acetyl group (Figure 2.5). Hence, there is no direct reaction between the methyl manganese unit and the newly incoming carbon monoxide. There is, as yet, no proven example of an insertion of an uncomplexed unsaturated substrate into a metal-to-carbon σ–bond. In heterogeneous catalysis coordination of the substrates to the surface is known as the Langmuir-Hinshelwood mechanism, while the reaction of a gas-phase molecule with a fragment on the surface is named the Eley-Rideal mechanism.

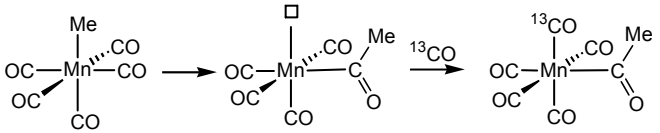

Figure 2.5. Disproval of "outersphere" insertion

A second important migration reaction involves alkenes instead of carbon monoxide. Figure 2.6 gives a schematic representation of a hydride that migrates to a co-ordinated ethene molecule *cis* to the hydride. The figure shows the hydride migration, which may result in an empty space in the co-ordination sphere of the metal. This co-ordinative unsaturation can be lifted in two ways:

firstly an agostic interaction with the β-hydrogens may occur, amply supported by theory and experiment [7]; secondly an incoming ligand may occupy the vacant site.

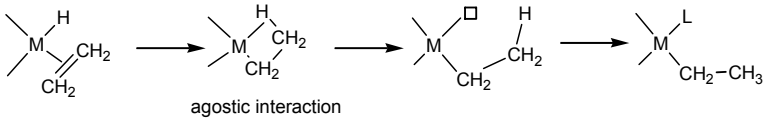

Figure 2.6. Hydride migration to ethene

If and how activation of a co-ordinated alkene takes place prior to migration is not always clear-cut. Co-ordinated alkenes are subject to π–backdonation and σ–donation and the overall outcome of the electron density cannot be predicted. Molecular orbital calculations at the Extended Hückel level [8] show that in many cases the co-ordinated alkene is not activated towards migration (i.e. nucleophilic attack) and it cannot be a priori predicted that rapid migration of the hydride will occur. Strong back-donation leads to more electron-rich alkenes, which makes them less susceptible for the attack of the nucleophilic migrating group. When an asymmetric bonding of the alkene is invoked, as shown in 2.7, a strong polarisation of the alkene will be the result. In this distorted structure the alkene is activated towards the hydride migration.

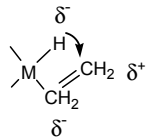

Figure 2.7. Charge distribution in a migration reaction

The migration reaction of hydrides to alkenes can be described as a 2+2 addition reaction. The reaction takes place in a *syn* fashion with respect to the alkene; the two atoms M and H add to the same face of the alkene (Figure 2.8). This has been unequivocally established by experiments. Later we will see reactions where this is not the case although the overall stoichiometry is the same for both types.

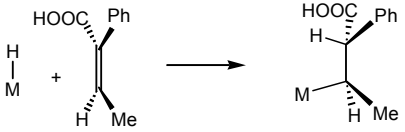

Figure 2.8. Syn-addition of a metal hydride

Thermodynamically the insertion of an alkene into a metal alkyl bond is much more favourable than the insertion of carbon monoxide into a metal alkyl bond. The latter reaction is more or less thermoneutral and the equilibrium constant is near unity under standard conditions. Insertion of alkenes into metal-carbon bonds is energetically favourable and usually irreversible. The energy gain is in the order of 80 $kJ.mol^{-1}$ when a double bond of an alkene is replaced by a single bond and a new single bond is formed in addition. The complexation energy is in the same order of magnitude or even larger for certain ligands. A rough estimate tells us that migration will lead to a loss of energy if indeed the complexation energy is high. It is therefore important that a new ligand enters the co-ordination sphere in order to stabilise the migration product.

If the new ligand enters the co-ordination sphere before the migration has been completed, this may show up in the kinetics of the insertion reaction. A second order behaviour of incoming ligand and complex would then be observed. This is indeed the case in a few examples that have been studied in detail [9]. Bergman observed a 70-fold increase in rate of a methyl migration in a molybdenum complex between reactions carried out in 2-methyl tetrahydrofuran and tetrahydrofuran (Figure 2.9). The unsubstituted THF gave the highest rate. The approach of 2-methyl tetrahydrofuran is more difficult.

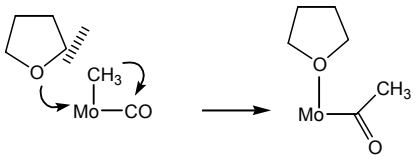

Figure 2.9. Incoming thf ligand enhancing migration

Formation of new σ–bonds at the cost of the loss of the π–bond of the alkene during alkene hydrogenation, polymerisation etc. makes the overall processes of alkenes thermodynamically feasible and the process is highly exothermic.

The metal hydride bond is stronger than a metal carbon bond and the insertion of carbon monoxide into a metal hydride is thermodynamically most often uphill. Alkene insertion into a metal hydride is thermodynamically allowed and often reversible.

In the article by Spencer and Orpen the degree of agostic interaction of the metal and the ethyl group depends on the steric parameters of the ligands (Figure 2.10). The sterically most hindered complex (ortho-xylene bridge, J=5220) is a β-agostic complex. The sterically less hindered complex is an ethene-hydride complex. The latter fragments require more space. The

σ-interaction of the Pt-H fragment competes with the Pt-P σ-interaction and as a result the coupling constant is now much smaller (2980 Hz).

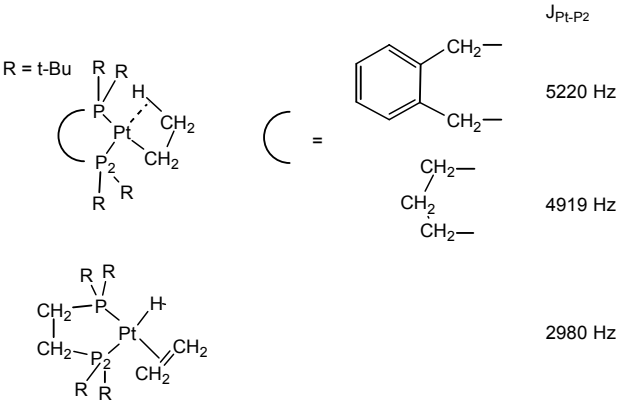

Figure 2.10. Agostic interaction during hydride migration

2.3 β-Elimination and de-insertion

The reverse reaction of the migration of η^1-bonded anionic groups to co-ordinated alkenes is called β-elimination (Figure 2.11). The migration reaction diminishes the total electron count of the complex by two, and formally creates a vacant site at the metal; β-elimination does the opposite. β-Elimination requires a vacant site at the complex (neglecting solvent co-ordination) and during the process the electron count of the complex increases by two electrons. The reaction resembles the β-elimination occurring in many organic reactions, but the difference lies in the intramolecular nature of the present process, as the eliminated alkene may be retained in the complex. In organic chemistry the reaction may well be a two-step process, e.g. proton elimination with a base followed by the leaving of the anion. In transition metal chemistry the availability of d-orbitals facilitates a concerted cis β-elimination.

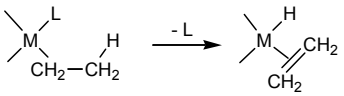

Figure 2.11. β-hydride elimination

Suppression of β-elimination is often a desirable feature. It can be achieved in several ways:

1. Maintain co-ordinative saturation. In a catalytic cycle this may be a counterproductive suggestion, since the next reaction in the catalytic cycle will also require a vacant site.
2. Selection of those metals where the metal alkyl complexes are stable with respect to hydride and liberated alkene. For the metals on the left-hand side of the periodic table, the Early Transition Metals and the Lanthanides, the alkyls are relatively stable. Therefore it is not surprising that the best alkene polymerisation catalysts are found amongst these metals.
3. Steric hindrance may hamper the correct stereochemistry required for β-elimination, and perhaps this can be used to stabilise our metal alkyl complex. In the modern polymerisation catalysts for polypropene this feature has actually been observed, which leads to higher molecular weight polymers. This now forms part of the design of new catalysts.

Instead of β-elimination one will also find the terms de-insertion and extrusion, especially for CO. The process is completely analogous because

1. a vacant site is needed for the reaction to occur,
2. the electron count of the metal increases by two during the de-insertion (provided that the carbon monoxide remains co-ordinated to the metal and solvent co-ordination is neglected).

Insertion takes place between a π–bonded fragment and a σ–bonded fragment in mutual cis-positions, as was described above. The de-insertion reaction can only proceed if there is a vacant site *cis* to the acyl group. The experiment outlined in Figure 2.12 proves this point. A manganese acetyl complex which is labelled with ^{13}C at the acyl carbonyl group was synthesised and heated to give de-insertion of CO. The result was that the only product formed contained the methyl substituent in a position *cis* to the labelled ^{13}C.

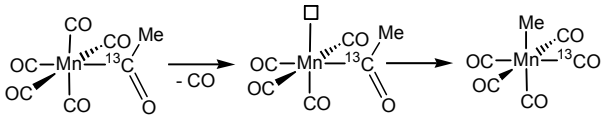

Figure 2.12. Migratory de-insertion

2.4 Oxidative addition

In an oxidative addition reaction a compound XY adds to a metal complex during which the XY bond is broken and two new bonds are formed, MX and MY. X and Y are reduced, and both will have a minus one charge (formally at least) and hence the formal oxidation state of the metal is raised by two. The co-ordination number of the metal also increases by two. While the electron

count around the metal complex actually increases by two, the *d*-electron count of the metal decreases by two (Figure 2.13).

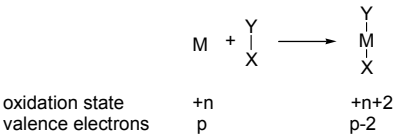

Figure 2.13. Formal representation of oxidative addition

The 16-electron square planar complex is converted into an octahedral 18-electron complex. In Figure 2.14 we have depicted the oxidative addition of methyl iodide to Vaska's complex (L=phosphine). Iodide ions accelerate the reaction and addition of an anion to the metal is the first step in that instance [10].

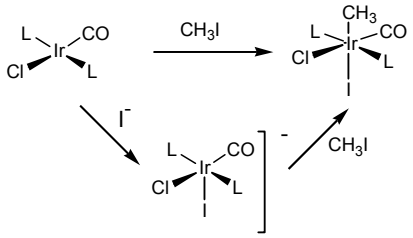

Figure 2.14. Oxidative addition

Electronic ligand effects are highly predictable in oxidative addition reactions; σ-donors strongly promote the formation of high-valence states and thus oxidative additions, e.g. alkylphosphines. Likewise, complexation of halides to palladium(0) increases the electron density and facilitates oxidative addition [11]. Phosphites and carbon monoxide, on the other hand, reduce the electron density on the metal and thus the oxidative addition is slower or may not occur at all, because the equilibrium shifts from the high to the low oxidation state. In section 2.5 more details will be disclosed.

The oxidative addition of **alkyl halides** can proceed in different ways, although the result is usually a trans addition independent of the mechanism. In certain cases the reaction proceeds as an S_N2 reaction as in organic chemistry. That is to say that the electron-rich metal nucleophile attacks the carbon atom of the alkyl halide, the halide being the leaving group. This process leads to inversion of the stereochemistry of the carbon atom (only when the carbon atom is asymmetric can this be observed). There are also examples in which racemisation occurs. This has been explained on the basis of a radical chain

mechanism. Indeed, radical scavengers have proven the presence of radicals by slowing down the reaction, and radical traps have demonstrated the expected ESR signals. The reaction sequence for the radical chain process reads as follows:

$$L_nM + R\bullet \rightarrow L_nRM\bullet$$
$$L_nRM\bullet + RX \rightarrow L_nRMX + R\bullet$$

The oxidative addition of acids is another instructive example. It resembles the reactions with alkyl halides and may result in an "amphoteric" hydride:

$$L_4Ni + H^+ \rightarrow L_4HNi^+$$

The starting material is an 18 electron nickel zero complex which is protonated forming a divalent nickel hydride. This can react further with alkenes to give alkyl groups, but it also reacts as an acid with hard bases to regenerate the nickel zero complex. Similar oxidative addition reactions have been recorded for phenols, water, amines, carboxylic acids, mineral acids (HCN), etc.

Oxidative additions involving **C-H bond breaking** have recently been the topic of an extensive study, usually referred to as C-H activation; the idea is that the M-H and M-hydrocarbyl bonds formed will be much more prone to functionalization than the unreactive C-H bond. Intramolecular oxidative additions of C-H bonds have been known for quite some time: see Figure 2.15. This process is named orthometallation or cyclometallation. It occurs frequently in metal complexes, and is not restricted to "ortho" protons. It is referred to as cyclometallation and is often followed by elimination of HX, while the metal returns to its initial (lower) oxidation state.

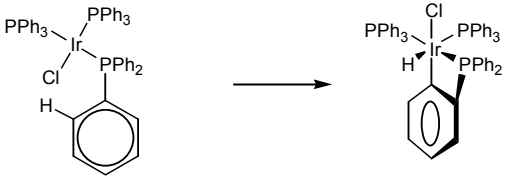

Figure 2.15. Orthometallation via C-H activation as oxidative addition

Oxidative addition involving **carbon-to-oxygen bonds** is of relevance to the catalysis with palladium complexes. The most reactive carbon-oxygen bond is that between allylic fragments and carboxylates. The reaction starts with a palladium zero complex and the product is a π-allylic palladium(II) carboxylate: Figure 2.16.

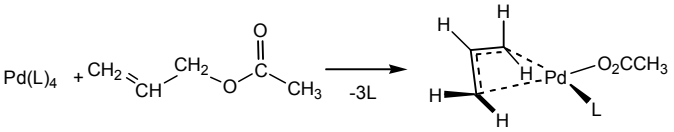

Figure 2.16. Oxidative addition of allyl acetate to Pd(0)

The point of interest is the "amphoteric" character of the allyl anion in this complex. On the one hand it may react as an anion, but on the other hand it is susceptible to nucleophilic attack by, for example, carbon centred anions. This has found widespread use in organic synthesis. The reaction with the anion releases a palladium zero complex and in this manner palladium can be employed as a catalyst.

Silicon hydrides can also oxidatively add to low-valent transition metal complexes forming a metal hydride silyl complex which can undergo subsequent insertion reactions. This elementary step forms the basis for the hydrosilylation process for alkenes and ketones.

The hydrosilylation process involves the following sequence of reactions:

- oxidative addition of a silicon hydride to a low-valent metal,

- complexation of an alkene,

- insertion of the alkene,

- reductive elimination.

The alkene "inserts" either in the metal hydride bond or in the metal silyl bond. The latter reaction leads to alkenylsilyl side products and also alkane formation may occur. Similar reactions have been observed for hydroboration, the addition of R_2BH to alkenes. (R_2 may be the catechol dianion).

2.5 Reductive elimination

Reductive elimination is simply the reverse reaction of oxidative addition: the formal valence state of the metal is reduced by two (or one in a bimetallic reaction), and the total electron count of the complex is reduced by two. While oxidative addition can also be observed for main group elements, this reaction is more typical of the transition elements in particular the electronegative, noble metals. In a catalytic cycle the two reactions always occur pair-wise. In one step the oxidative addition occurs, followed for example by insertion reactions, and then the cycle is completed by a reductive elimination of the product.

Reductive eliminations can be promoted by stabilisation of the low-valent state of the product. This means ligands that are good π-acceptors, bulky ligands, and ligands preferring bite angles more suited for tetrahedral than for square-planar complexes, when we deal with group 10 metals.

Reductive elimination of molecules with **carbon-carbon bonds** has no counterpart in oxidative addition reactions because the metal-carbon bonds energies are usually not large enough to compensate for the energy of the carbon-carbon bond, and secondly the carbon-carbon bond is much less reactive than a carbon-hydrogen bond or a dihydrogen bond due to repulsive interactions. Examples in the literature generally involve group 10 metals, e.g. Figure 2.17. In practice the reactions are less straight-forward than the one shown in Figure 2.17 and several other decomposition pathways are available.

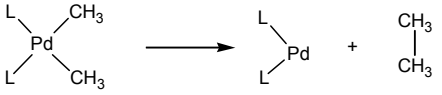

Figure 2.17. Reductive elimination leading to a C-C bond

When the reductive elimination involves a symmetric situation as in Figure 2.17, the process is most likely also symmetric, that is to say that the carbon-to-palladium bonds are being broken simultaneously with the making of the new carbon-to-carbon bond. In an asymmetric situation, for example a hydride group and a vinyl substituent at palladium, the elimination may have the character of a "migratory reductive elimination". The hydride starts to migrate as it were to the vinyl group, utilizing the antibonding olefinic bond (see for example [12]). The reductive elimination of aryl ethers from arylpalladium alkoxides has been described in the same way, having a Meisenheimer type intermediate [13], Figure 2.18. Elimination is "asymmetric" in that the carbon-to-palladium bond remains intact while oxygen-to-palladium is being broken and the carbon-to-oxygen bond is being formed. This detail should not be surprising, because when one looks at the reverse reaction, i.e. the oxidative addition of an aromatic halide to a palladium(0) complex, one would expect that palladium will attack the aryl halide at the electron deficient carbon atom carrying the halide atom. The putative intermediate is exactly the same as that presumed in the reductive elimination reaction. This mechanism for oxidative addition had already been proposed in 1971 [14]!

As outlined above, the reaction can be induced by the addition of *electron withdrawing* ligands; in this case electron-poor alkenes are very effective. Electronic effects of the ligands were introduced in section 2.4, for the oxidative addition. Another potential electronic effect is that of the bite angle. Square-planar, divalent palladium complexes will prefer P–Pd–P angles with values close to 90°, for example in the complexes shown in Figure 2.18. In the zerovalent complexes this angle may be considerably higher; for a tetrahedral product the angle may be 109°, and for a trigonal product even higher. Thus, if one would use a ligand with a "ligand preference" for wider bite angles, the

reductive elimination will be promoted, probably both kinetically and thermodynamically. In Chapter 11 we will come back to this [15].

When the steric repulsion between a *cis* bidentate and two substituents R and CN increases in a series of bidentate phosphine complexes of palladium, the rate of reductive elimination of R-CN increases by several orders of magnitude [16]. Actually, the steric effect and electronic effect are related and careful variation of only one property at a time is needed to distinguish between the two.

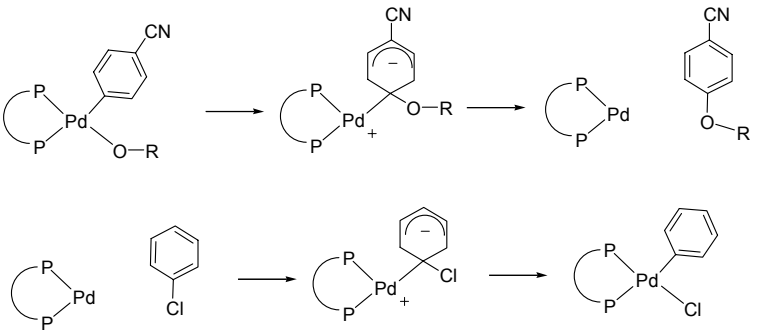

Figure 2.18. "Migratory" reductive elimination and oxidative addition

The reductive elimination/oxidative addition is of practical importance in catalytic cycles, for example the rhodium/methyl iodide catalysed carbonylation of methanol. In organic synthesis the palladium or nickel catalysed cross-coupling presents a very common example involving oxidative addition and reductive elimination. A simplified scheme is shown in Figure 2.19 [17].

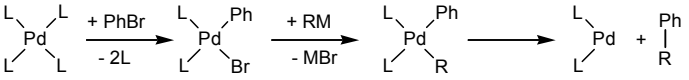

Figure 2.19. Palladium catalysed cross-coupling

2.6 α-Elimination reactions

α-Elimination reactions have been the subject of much study since the mid seventies mainly due to the pioneering work of Schrock. The Early Transition Metals are most prone to α-elimination, but the number of examples of the later elements is growing. A classic example is shown in Figure 2.20. In decomposition reactions of dimethyl metal complexes of palladium and nickel

one finds the formation of methane, which is also attributed to an α-elimination process. The methylidene complex is not observed in this instance.

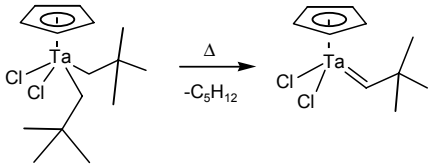

Figure 2.20. α–Elimination

Metal alkylidene complexes find application in the metathesis of alkenes, the cyclopropanation of alkenes (Grubbs, Schrock), Wittig type reactions, and the McMurry reaction. In suitable complexes α-elimination can occur twice yielding alkylidyne complexes. See Figure 2.21 for an example with tungsten.

Alkylidyne complexes can be used as catalysts for the metathesis of alkynes. For a classic review see Schrock [18].

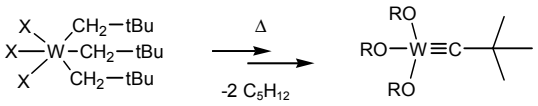

Figure 2.21. α-elimination leading to alkylidyne complex

2.7 Cycloaddition reactions involving a metal

Cycloaddition refers to a process of unsaturated moieties forming a metallacyclic compound. It is sometimes categorised under oxidative additions, but we prefer this separate listing. Examples of the process are presented in Figure 2.22. Metal complexes which actually have revealed these reactions are M = L_2Ni for reaction **a**, M = Cp_2Ti for reactions **b** and **c**, M = Ta for **d**, and M = $(RO)_3W$ for **e**. The latter examples involving metal-to-carbon multiple bonds have only been observed for early transition metal complexes, the same ones mentioned under α-elimination, 2.20.

In examples 2.22 **a** and **b** the metals increase their valence by two, and this is not just a formalism as indeed the titanium(II) and the nickel(0) are very electron rich metal centres. During the reaction a flow of electrons takes place from the metal to the organic fragments, which end up as anions. In these two reactions the metal provides two electrons for the process as in oxidative addition reactions. The difference between cycloaddition and oxidative addition is that during oxidative addition a bond in the adding molecule is being broken, whereas in cycloaddition reactions fragments are combined.

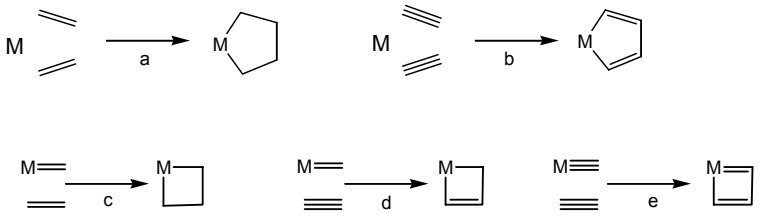

Figure 2.22. Cycloaddition reactions

For reactions 2.22 **c** and **d** the situation is slightly different. The formal valence of the metal increases in **c** and **d** with two units again when the alkylidene is considered as a two-electron neutral ligand. The two electrons donated by the metal in the "oxidative addition" process were already involved in the bonding of the alkylidene, and not present at the metal centre as a surplus non-bonding lone pair (cf. square planar d^8 complexes, or the above d^2 Ti and d^{10} Ni cases). The reaction of the alkylidyne in 2.22 **e** is a cycloaddition reaction for which other descriptions make little sense. Some textbooks regard alkylidenes as four-electron dianions; in this formalism the valence does not change during a cycloaddition. Three mechanisms can be proposed for the intimate reaction mechanism for **c-e**, analogous to the organic 2+2 cycloadditions:

a pericyclic (concerted) mechanism,
a diradical mechanism, and
a diion mechanism.

In view of the polarisation of the metal(+) carbon(-) bond an ionic intermediate may be expected. The retention of stereochemistry, if sometimes only temporarily, points to a concerted mechanism.

The reverse reaction of a cycloaddition is of importance for the construction of catalytic cycles. The retro-cycloadditions of reactions **a** and **b** in Figure 2.22 are not productive, unless the structures were obtained via another route.

For 2.22 **c-e** the following retro reactions can be envisaged leading to new products: see Figure 2.23.

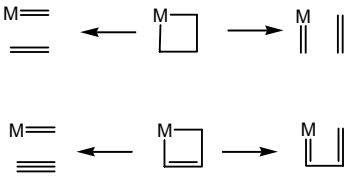

Figure 2.23. Retrocycloaddition

Reaction 2.22 **a** may be followed by various other reactions such as insertions, ß-eliminations or regular reductive eliminations (See Figure 2.24). The reductive elimination reaction is governed by the common rules given in the section on reductive elimination. The reaction shown has been observed for nickel complexes.

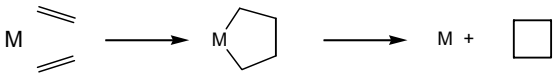

Figure 2.24. Cycloaddition followed by reductive elimination

2.8 Activation of a substrate toward nucleophilic attack

2.8.1 Alkenes

Co-ordination of an alkene to an electronegative metal (often it may carry a positive charge) activates the alkene toward attack of nucleophiles. After the nucleophilic attack the alkene complex has been converted into a σ–bonded alkyl complex with the nucleophile at the β-position. With respect to the alkene (in the "organic" terminology) the alkene has undergone *anti* addition of M and the nucleophile Nu, see Figure 2.25.

As indicated under section 2.2. the overall result is the same as that of an insertion reaction, the difference being that insertion gives rise to a *syn*-addition and nucleophilic attack to an *anti*-addition. Sometimes the two reaction types are called *inner sphere* and *outer sphere* attack. There is ample proof for the *anti* fashion; the organic fragment can be freed from the complex by treatment with protic acids and the organic product can be analysed [19]. Appropriately substituted alkenes will show the *syn* or *anti* fashion of the addition. The addition reaction of this type is the key-step in the Wacker-type processes catalysed by palladium.

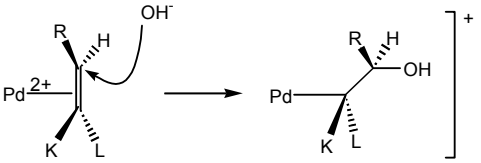

Figure 2.25. Nucleophilic attack to a co-ordinated alkene

The analogy with the addition of Br^+OH^- to alkenes seems appropriate. Whether or not an alkene will be activated by the metal toward nucleophilic attack is not clear as we are dealing with the counteracting influences of donation and back-donation. Experience tells us that we need positively charged rare earth metals or transition metals, and the late transition metals should not contain donor groups such as phosphines. In Figure 2.24 the depicted nucleophile is anionic, but Nu may also be a neutral nucleophile such as an amine. Often palladium salts in water without other donor ligands are the most active catalysts in Wacker-type reactions. There are many alkene complexes of middle and late transition elements which also undergo this type of reaction, e.g. M = Pt^{2+}, Hg^{2+}, Zn^{2+}, $FeCp(CO)^{2+}$.

2.8.2 Alkynes

Alkynes show the same reaction and again the product obtained is the *anti* isomer. After a suitable elimination from the metal the alkene obtained is the product of the *anti* addition. Earlier we have seen that insertion into a metal hydride bond and subsequent hydrogenation will afford the *syn* product. If we use BH_4^- as the nucleophile we can accomplish *anti* addition of a hydride. Thus, with the borohydride methodology and the hydrogenation route either isomer can be prepared selectively.

2.8.3 Carbon monoxide

Co-ordinated carbon monoxide is activated towards nucleophilic attack. Through σ-donation and π-back donation into the antibonding CO π^* orbitals the carbon atom has obtained a positive character. This makes the carbon atom not only more susceptible towards a migrating anion at the metal centre, but also for a nucleophile attacking from outside the co-ordination sphere. In this instance it is more difficult to differentiate between the two pathways. There are examples showing that the electrophilicity of the carbon atom can be further increased by the action of Lewis acids complexing to the oxygen atom of the co-ordinated CO.

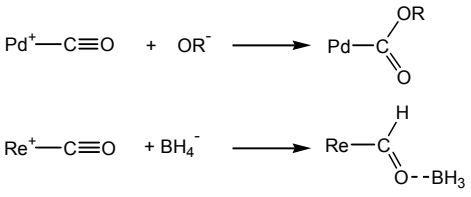

Figure 2.26. Nucleophilic attack at co-ordinated carbon monoxide

Figure 2.26 shows an alkoxide attack at co-ordinated CO giving a carboalkoxy complex, and a borohydride attack at co-ordinated CO in which the boron simultaneously acts as a Lewis acid. The BH_3 complexation now stabilises the formyl complex that would otherwise be thermodynamically inaccessible. So far the latter reaction has only been of academic interest in homogeneous systems (it may be relevant to heterogeneous systems though proof is lacking).

The nucleophilic attack by alkoxides, amines, and water is of great interest to homogeneous catalysis. A dominant reaction in syn-gas systems is the conversion of carbonyls with water to metal hydrides and carbon dioxide ("Shift Reaction"), see Figure 2.27.

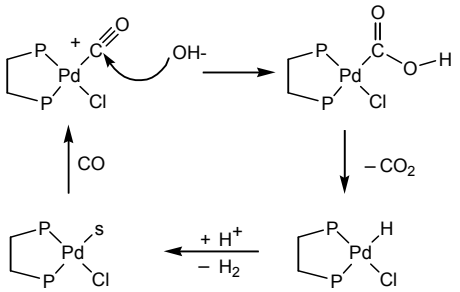

Figure 2.27. Hydroxide attack followed by elimination of CO_2

2.8.4 Other substrates

We have already reviewed the activation of alkenes, alkynes, and carbon monoxide towards nucleophilic attack. The heterolytic splitting of dihydrogen is also an example of this activation; it will be discussed in Section 2.10. The reaction of nucleophiles with silanes co-ordinated to an electrophilic metal can be regarded as an example of activation towards nucleophilic attack (Figure 2.28). Complexes of Ir(III) and Pd(II) give t.o.f. for this reaction as high as 300,000 mol.mol.$^{-1}$.h^{-1}.

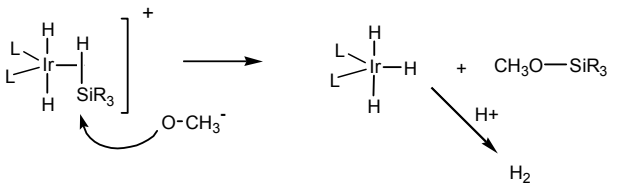

Figure 2.28. η^2-$HSiR_3$ complex, nucleophilic attack, and heterolytic splitting [20]

Recent advances include alkyl iodides as substrates that can be activated by metal complexation. Also π-allyl "anions", when co-ordinated to palladium, are activated toward attack by nucleophiles. This is very similar to the activation of co-ordinated alkenes and it shows the very high electrophilicity of palladium. The valence state of palladium, and/or the charge on palladium, and therefore also the ligands attached to it are very important:

- palladium(2+) surrounded by weak donors is a strong electrophile,
- palladium(0) reacts as a nucleophile with methyl iodide,
- palladium(2+) surrounded by nitrogen donor ligands and alkyl groups reacts as a nucleophile with methyl iodide! giving tetravalent palladium (Figure 2.29).

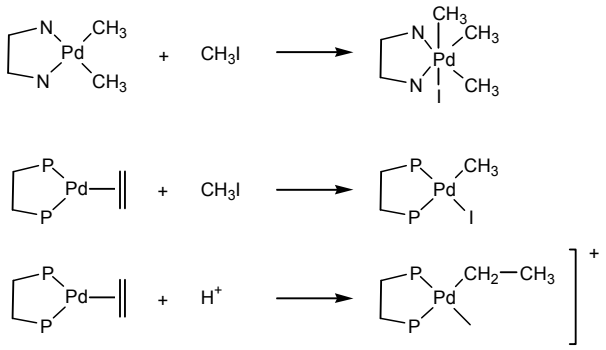

Figure 2.29. Palladium, the "chameleon" catalyst

There is obviously a relation with the classic activation of molecules by Lewis acids, but here we have confined ourselves to the activation of "soft" substrates by "soft" acids. Examples of "hard" acid activated reactions include Diels-Alder additions, nitrile solvolysis, ester solvolysis, ester formation, Oppenauer reactions etc (see Lewis acid catalysed reactions, 2.11).

2.9 σ-Bond metathesis

A reaction which is rather new and not mentioned in older textbooks is the so-called σ-bond metathesis. It is a concerted 2+2 reaction immediately followed by its retrograde reaction giving metathesis. Both late and early transition metal alkyls are prone to this reaction, but for d^0 early transition metals there is no other mechanism than σ-bond metathesis at hand. Many similar reactions such as the reaction of metal alkyls with other HX compounds could be described as if they would follow this pathway, but the use of the term σ-bond metathesis is restricted to those reactions in which one reacting species is a metal hydrocarbyl or metal hydride and the other reactant is a hydrocarbon or dihydrogen. In Figure 2.30 the reaction has been depicted.

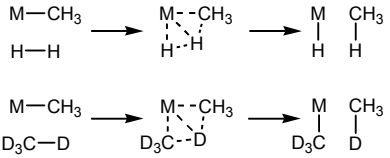

Figure 2.30. σ-bond metathesis

There are of course borderline cases; when the reacting hydrocarbon is acidic (as in the case of 1-alkynes) a direct attack of the proton at the carbanion can be envisaged. It has been proposed that acyl metal complexes of the late transition metals may also react with dihydrogen according to a σ-bond metathesis mechanism. However, for the late elements an alternative exists in the form of an oxidative addition reaction. This alternative does not exist for d^0 complexes such as Sc(III), Ti(IV), Ta(V), W(VI) etc. and in such cases σ-bond metathesis is the most plausible mechanism.

2.10 Dihydrogen activation

In the reactions above we have not explicitly touched upon the reactions of dihydrogen and transition metal complexes. Here the reactions that involve the activation of dihydrogen will be summarised, because they are very common in homogeneous catalysis and because a comparison of the various mechanisms involved may be useful. Three reactions are usually distinguished for hydrogen:

- oxidative addition (Figure 2.14),
- heterolytic cleavage, and
- σ-bond metathesis (see Figure 2.31).

Oxidative addition of dihydrogen commonly involves transformation of a d^8 square planar metal complex into a d^6 octahedral metal complex, or similar transformations involving $d^2 \rightarrow d^0$, $d^{10} \rightarrow d^8$ etc. The oxidative addition of

dihydrogen to low-valent metal complexes is a common reaction in many catalytic cycles. In spite of the high strength of the dihydrogen bond the reaction proceeds smoothly to afford cis dihydrido complexes. The bond energy of a metal hydrogen bond is in the order of 240 +/- 40 $kJ.mol^{-1}$ which is sufficient to compensate for the loss of the H-H bond (436 $kJ.mol^{-1}$). The hydride is formally charged with a minus one charge and this electron count gives dihydrogen the role of an oxidising agent! The classic example of oxidative addition to a d^8 metal complex is the reaction discovered by Vaska and Diluzio [21]:

$$\text{trans-IrCl(CO)(PPh}_3)_2 + H_2 \quad \rightarrow \quad \text{IrH}_2\text{Cl(CO)(PPh}_3)_2$$

In rhodium complexes the reaction has found widespread application in hydrogenation. In model compounds the reaction reads [22]:

$$\text{Rh(diphosphine)}_2^+ + H_2 \rightarrow \text{RhH}_2\text{(diphosphine)}_2^+$$

The reaction of a metal-dimer with H_2 can also be regarded as an oxidative addition reaction. For instance, a dimer of a d^7 metal complex reacts with dihydrogen to give two d^6 species. In this process dihydrogen also gives formally two hydride anions. A well-known example in the present context is the conversion of dicobaltoctacarbonyl into hydridocobalttetracarbonyl:

$$\text{Co}_2(\text{CO})_8 + H_2 \rightarrow 2\ \text{HCo(CO)}_4$$

In the past this was referred to as a homolytic reaction [23]. It is clear that it would be highly unlikely that dihydrogen would be split into a metal hydride and a highly energetic hydrogen radical; in this sense the term homolytic splitting is misleading.

Heterolytic cleavage of dihydrogen has been the topic of much study and discussion, but there are only very few cases in which clear proof has been obtained for the occurrence of a splitting of dihydrogen into a proton and a metal bonded hydride. In the ideal case the heterolytic splitting is catalysed by the metal ion and a base which assists in the abstraction of the proton. In this reaction there is no formal change in the oxidation state of the metal. The mechanism has been put forward for Ru(II) complexes which can react with dihydrogen according to:

$$\text{RuCl}_2(\text{PPh}_3)_3 + H_2 \rightarrow \text{RuHCl(PPh}_3)_3 + \text{HCl}$$

Ruthenium has a sufficient number of d-electrons to undergo oxidative addition of dihydrogen, which could then be quickly followed by reductive

elimination of HCl. Experimentally it is difficult to distinguish between the two pathways (vide infra). Stretching it a bit further, the heterolytic splitting reaction is also very close to a σ-bond metathesis except that the transition state would be very polar with chloride as one of the participating atoms in the 2+2 intermediate, and, formally, the heterolytic splitting reaction does not require a 2+2 transition state. Observations on dihydrogen complexes of ruthenium have thrown new light on the heterolytic splitting of dihydrogen [24]. They have shown that $CpRu(L)(\eta^2\text{-}H_2)^+$ reacts rapidly with NEt_3 as can be deduced from the dynamic ^1H NMR spectra which indicate a rapid exchange of the dihydrogen complex with its conjugate base, CpRu(L)(H) (Figure 2.31).

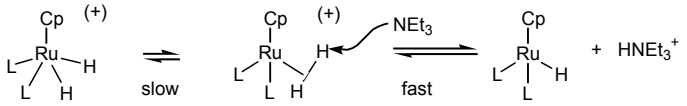

Figure 2.31. Heterolytic cleavage of dihydrogen

This reaction is much faster than the exchange with the corresponding dihydride complex. The present studies on dihydrogen complexes may lead to a better understanding of the heterolytic splitting of dihydrogen. Indeed, it seems reasonable that dihydrogen can be activated towards reaction with a base through complexation to a cationic complex.

There is another possible mechanism for heterolytic splitting of dihydrogen in which the base is coordinated to the metal. After the reaction the acid conjugate formed may stay on the metal or may leave the metal, as shall be the case for HCl and $HOOCCH_3$. This mechanism would be suitable for heterolytic splitting of dihydrogen on solid oxides. In Figure 2.32 one example has been depicted [25]. Throughout the process the platinum remains divalent.

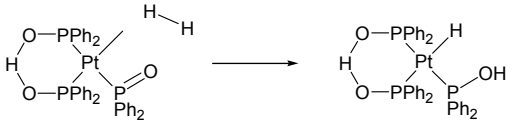

Figure 2.32. Heterolytic splitting of dihydrogen by a "base-metal" pair

2.11 Activation by Lewis acids

In section 2.8 we have discussed the activation of substrates towards nucleophilic attack by co-ordination of the fragment to a transition metal. Here we will describe a few examples of activation of reagents when complexed to Lewis acids. In organic textbooks one will find a variety of reactions catalysed by Lewis acids.

2.11.1 Diels-Alder additions

The Diels-Alder reaction is the reaction of a diene with a mono-ene to form a cyclohexene derivative, an important reaction for the construction of organic intermediates. One of its attractions is the atom efficiency of 100%, no by-products being formed. The mono-ene, or dienophile which may also be an alkyne, has a LUMO of low energy while the diene is usually electron rich with a high lying HOMO. The interaction of these two orbitals starts the reaction between the two molecules (Figure 2.33) [26].

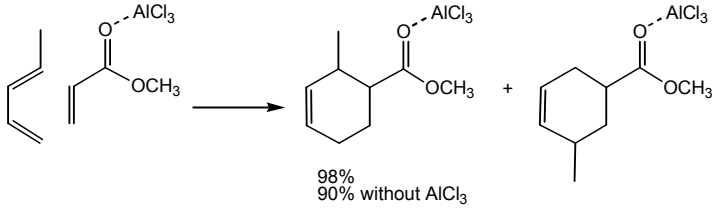

Figure 2.33. Lewis acid catalysed Diels-Alder reaction

The reaction can be accelerated by complexation of the dienophile to a Lewis acid which further lowers the level of the interacting LUMO [27]: Two regio-isomers are formed in the example shown, we shall not consider the stereochemistry. Typically in these systems governed by frontier orbitals, the reactions not only become much faster with a Lewis acid catalyst, but also more regioselective.

For these and similar reactions recently a variety of Lewis acidic aluminium, rare earth metals, and titanium alkoxides have been applied. Alkoxides have the additional advantage that they can be made as enantiomers using asymmetric alcohols which opens the possibility of asymmetric catalysis. Examples of asymmetric alcohols are bis-naphtols, menthol, tartaric acid derivatives [28]. Other reactions comprise activation of aldehydes towards a large number of nucleophiles, addition of nucleophiles to enones, ketones, etc.

2.11.2 Epoxidation

Alkenes can be transformed into epoxides by hydroperoxides and a catalyst, which often is a high-valent titanium or molybdenum complex acting as a Lewis acid. The mechanism is not clear in great detail; in Figure 2.34 a suggested mechanism is given. Coordination of the alkene to the metal prior to attack of the electrophilic oxygen is not considered as a necessary step.

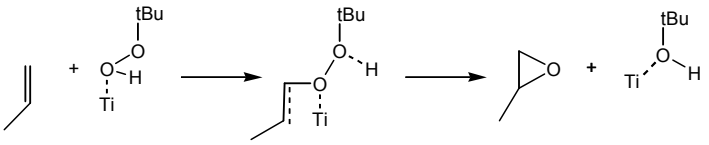

Figure 2.34. Epoxidation with Lewis acids

The key factor is the action of the metal on the peroxo group making one oxygen atom electrophilic. Whether or not the metal is bonded to carbon in the intermediate is not known, but also considered unlikely; naturally this will depend on the particular substrate and catalyst. Epoxidation will be discussed in Chapter 14, with special emphasis on asymmetric epoxidation with chiral metal catalysts.

2.11.3 Ester condensation

An application of industrial importance of Lewis acidic metal salts is the condensation of carboxylic diacids and diols to give polyesters. This is an acid catalysed reaction that in the laboratory is usually catalysed by protic acids. For this industrial application salts of manganese, nickel, or cobalt and the like are used. From a chemical point of view this chemistry may not be very exciting or complicated, the large scale on which it is being carried out makes it to an important industrial reaction [29].

2.12 Carbon-to-phosphorus bond breaking

The breaking of carbon-to-phosphorus bonds is by itself not a useful reaction in homogeneous catalysis. It is an undesirable side-reaction that occurs in systems containing transition metals and phosphine ligands and that leads to deactivation of the catalysts. Two reaction pathways can be distinguished, oxidative addition and nucleophilic attack at the co-ordinated phosphorus atom (Figure 2.35).

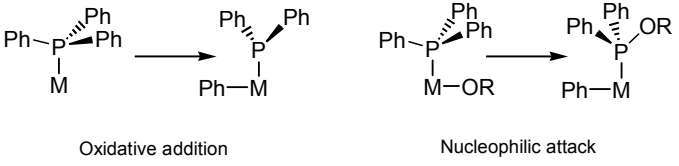

Figure 2.35. Phosphine decomposition

The importance of transition-metal mediated decomposition of ligands has been reviewed by Garrou [30] with an emphasis on oxidative addition as the mechanism.

Oxidative addition. The oxidative addition of a phosphine to a low valent transition metal can be most easily understood by comparing the Ph_2P-fragment with a Cl- or Br- substituent at the phenyl ring; electronically they are very akin, cf Hammett parameters and the like. The phosphido anion formed during this reaction will usually lead to bridged structures, which are extremely stable.

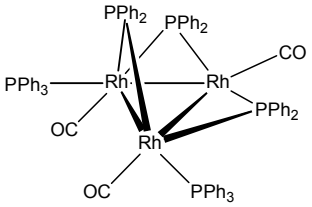

Figure 2.36. Decomposition product of $RhH(CO)(PPh_3)_3$

Thermal decomposition of $RhH(CO)(PPh_3)_3$, the well known hydroformylation catalyst, in the absence of H_2 and CO leads to a stable cluster shown in Figure 2.36 containing μ_2-PPh_2 fragments [31]. Under hydroformylation conditions also other products are found such as benzaldehyde, benzene, and diphenylpropylphosphine.

Cluster or bimetallic reactions have also been proposed in addition to monometallic oxidative addition reactions. The reactions do not basically change. Reactions involving breaking of C-H bonds have been proposed. For palladium catalysed decomposition of triarylphosphines this is not the case [32]. Likewise, Rh, Co, and Ru hydroformylation catalysts give aryl derivatives not involving C-H activation [33]. Several rhodium complexes catalyse the exchange of aryl substituents at triarylphosphines [34]:

$$R'_3P + R_3P \text{ --- (Rh) --> } R'R_2P \text{ etc}$$

These authors propose as the mechanism for this reaction a reversible oxidative addition of the aryl-phosphido fragments to a low valent rhodium species. A facile aryl exchange has been described for complexes $Pd(PPh_3)_2(C_6H_4CH_3)I$. The authors [35] suggest a pathway involving oxidative additions and reductive eliminations. The mechanism outlined below, however, can also explain the results of these two studies.

Nucleophilic attack. Current literature underestimates the importance of nucleophilic attack as a mechanism for the catalytic decomposition of phosphines, especially with nucleophiles such as acetate, methoxy, hydroxy and hydride (Figure 2.37). For examples of nucleophilic attack at co-ordinated phosphorus see references [36].

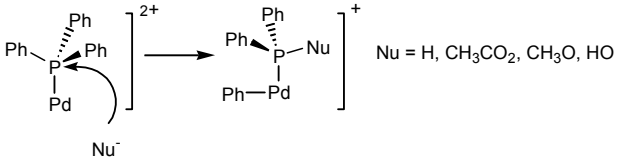

Figure 2.37. Phosphine decomposition via nucleophilic attack

Related to this is the mechanism for the catalytic oxidation of phosphines by water. This reaction plays a role in "catalysis in water" using water-soluble phosphine ligands.

More recently a variation of this mechanism was reported by Novak [37]. The mechanism involves nucleophilic attack at co-ordinated phosphines and it explains the exchange of aryl groups at the phosphine centres with the intermediacy of metal aryl moieties. After the nucleophilic attack the phosphine may dissociate from the metal as a phosphonium salt. To obtain a catalytic cycle the phosphonium salt adds oxidatively to the zerovalent palladium complex (Figure 2.38). *Note "where the electrons go".*

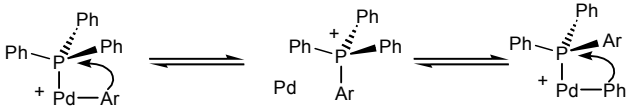

Figure 2.38. Aryl exchange via phosphonium compounds

A catalytic decomposition of triphenylphosphine has been reported [38] in a reaction involving rhodium carbonyls, formaldehyde, water, and carbon monoxide. The following reactions may be involved (Figure 2.39):

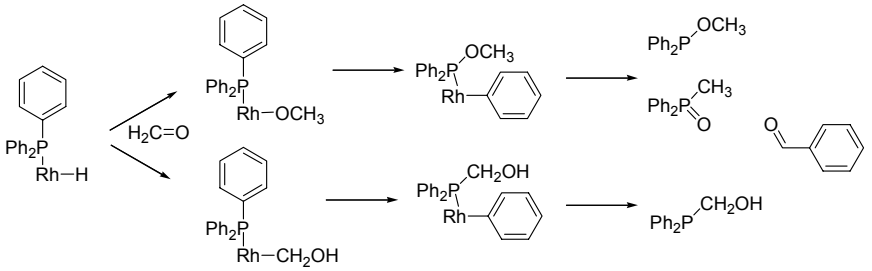

Figure 2.39. Catalytic decomposition of triphenylphosphine

Hydroformylation of formaldehyde to give glycolaldehyde is an attractive route from syn-gas toward ethylene glycol. The reaction is catalysed by rhodium arylphosphine complexes [39] but clearly phosphine decomposition is

one of the major problems to be solved before a catalyst can be applied commercially [40].

2.13 Carbon-to-sulfur bond breaking

While breaking of the carbon-to-phosphorus bond is a nuisance in catalysis with organometallic complexes, the breaking of carbon-to-nitrogen and -to-sulfur bonds is a desired reaction in the oil industry. Hydrodenitrification (HDN) and hydrodesulfurisation (HDS) are carried out on a large scale in order to remove nitrogen and sulfur from the fuel feedstocks.

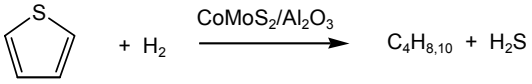

Figure 2.40. Hydrodesulfurisation

Catalysts are heterogeneous sulfided nickel (or cobalt) molybdenum compounds on a γ-alumina. The reaction has been extensively studied with substrates such as thiophene (Figure 2.40) as the model compound mainly with the aims of improving the catalyst performance. The mechanism on the molecular level has not been established. In recent years the reaction has also attracted the interest of organometallic chemists who have tried to contribute to the mechanism by studying the reactions of organometallic complexes with thiophene [41]. Many possible co-ordination modes for thiophene have been described.

As a second step in the reaction, following co-ordination, most authors propose an oxidative addition of the C-S fragments to the transition metal, similar to the reaction found for carbon-to-phosphorus bond breaking. Since the C-S bond is rather weak it is easy to break and indeed several model reactions can be found in the literature.

In order to get a catalytic cycle it is necessary that the metal sulfide intermediate can react with hydrogen to form the reduced metal complex (or compound) and H_2S. For highly electropositive metals (non-noble metals) this is not possible for thermodynamic reasons. The co-ordination chemistry and the oxidative addition reactions that were reported mainly involved metals such as ruthenium, iridium, platinum, and rhodium.

Studies on heterogeneous catalysts seem to invoke partial hydrogenation of thiophene prior to desulfurization [42]; the catalysts are also active hydrogenation catalysts. Recently evidence for a facile and selective desulfurisation of partly hydrogenated thiophene has been reported, the reaction of 2,5-dihydrothiophene on (110) molybdenum surfaces (Figure 2.41) [43].

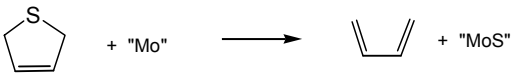

Figure 2.41. Desulfurisation of 1,5-dihydrothiophene

In organic chemistry this is called a retro-pericyclic reaction and it should indeed have a low barrier of activation. Under the high vacuum techniques applied, on clean surfaces, the reaction proceeds already below 140 K (the temperature at which desorption of the weakly co-ordinated butadiene is observed).

Advances can be found in references [35-44]. A model sequence of reactions for iridium is shown in Figure 2.42. Crucial to most mechanisms is the oxidative addition of the C-S moiety to the metal centre, for which many examples have been reported. The model reaction of 2.42 involves stepwise reactions with hydride and protons and is as yet stoichiometric [45].

Hydrodesulfurisation of thiophene must be accompanied by hydrogenation of double bonds otherwise there may exist thermodynamic constraints [46].

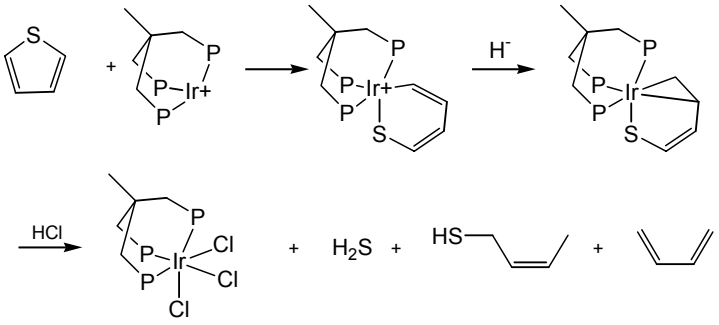

Figure 2.42. Oxidative addition of *thiophene* to iridium (I) followed by stoichiometric "desulfurisation" ref [39].

A catalytic example of C-S bond breakage in benzothiophene has been reported by Bianchini [47]. A catalytic desulfurisation was not yet achieved at the time as this is thermodynamically not feasible at such mild temperatures because of the relative stability of metal sulfides formed. Bianchini used a water-soluble catalyst in a two-phase system of heptane–methanol/water mixtures in which the product 2-ethylthiophenol is extracted into the basic aqueous layer containing NaOH. Figure 2.43 gives the reaction scheme and the catalyst. The 16-electron species Na(sulfos)RhH is suggested to be the catalyst. Note that a hydrodesulfurisation has not yet been achieved in this reaction because a thiol is the product. Under more forcing conditions the formation of H_2S has been observed for various systems.

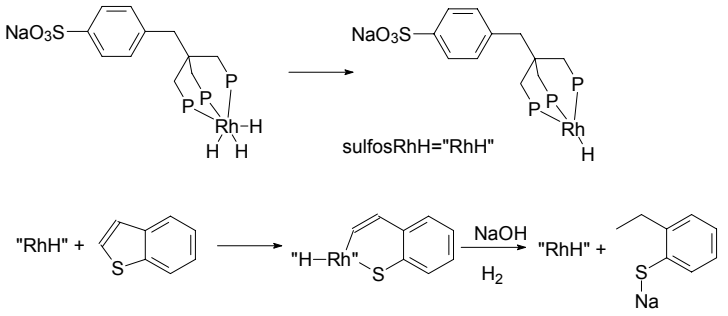

Figure 2.43. Catalytic C-S bond breaking

2.14 Radical reactions

Radical reactions play a role in many oxidation reactions. As we shall see later in the Wacker process the re-oxidation of palladium zero by dioxygen is catalysed by copper. It involves the two-electron transfer from palladium(0) to two copper(II) species giving palladium(II) and two copper(I) species. In heterogeneous oxidations electron transfer plays a key role and it often involves the non-stoichiometric transfer of electrons and oxygen to a solid catalyst. The solid catalyst acts as a reservoir for the redox species, a situation that cannot be easily realised in homogeneous systems. The mechanism according to which a solid can act as a reservoir for e.g. oxygen atoms during an oxidation reaction is referred to as the Mars-van Krevelen mechanism.

Co(III) and Mn(III) salts are used as initiators for the autoxidation of methylaromatics to carboxylic acids. The metal "radicals" assist in making the first organic radicals which will subsequently enter into the common catalytic autoxidation cycle for RH molecules:

$$RH + Co(III)^{3+} + Br^- \rightarrow R\bullet + Co(II)^{2+} + HBr$$

$$R\bullet + O_2 \rightarrow RO_2\bullet \text{ etcetera}$$

The actual schemes of these reactions are very complicated; the radicals involved may also react with the metal ions in the system, the hydroperoxide decomposition may also be catalysed by the metal complexes, which adds to the complexity of the autoxidation reactions. Some reactions, such as the cobalt catalysed oxidation of benzaldehyde have been found to be oscillating reactions under certain conditions [48].

A significant development of the last decade involving radicals and organometallic complexes is the “living” radical polymerisation. In a common radical polymerisation (see Atkins, page 910, 5th Ed.) the molecular weight

distribution of the product is broad due to a fast termination reaction of two reactive polymer chain end radicals. In order to obtain a "living" polymer system [49] the actual radical concentration has to be kept extremely low. This can be done by binding the growing chain, reversibly, to a halide radical (abstracted from a metal complex) or to stable organic radicals, with the use of compounds such as TEMPO. When organic "catalysts" are used the initiation is done in the usual way by a radical initiator, e.g. a peroxide thermally decomposing into two radicals.

TEMPO combines with the radical chain and keeps the concentration of the growing radical chain low, such that the recombination of radicals is suppressed. This type of radical polymerisation is called Atom Transfer Radical Polymerisation (ATRP). It has the properties of a living polymerisation, as the molecular weight increases steadily with time and one can make block polymers this way by adding different monomers sequentially.

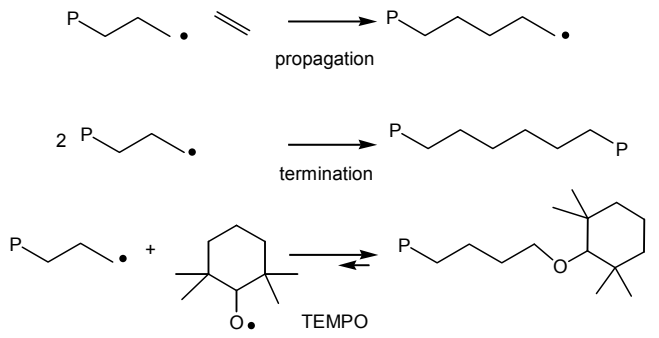

Figure 2.44. Hypothetical scheme for TEMPO controlled "living" radical polymerization

Alternatively metal complexes can be used. In all cases studied so far the metal complex provides, temporarily, a halogen radical to the chain, while the metal switches between oxidation states. An example is shown in Figure 2.45. Suitable metals are Ru(II)/Ru(III), Ni(II)/Ni(III) and Cu(I)/Cu(II). The ligands co-ordinated to the metal centre can be used to fine-tune the properties of the metal complex as has been shown for copper and dinitrogen and trinitrogen ligand systems by Matyjaszewski [49]. Initially several authors assumed that indeed the metal centre acted as the temporary radical trap, similar to TEMPO, but the current idea is that this is not the case. Nickel(II) bromide forms the initiating radical, and nickel(III) bromide provides the bromine radical to stop the growth of the radical chain. This way the concentration of the growing chains is kept low and the rate of the termination reaction (coupling of two growing chains, or hydrogen exchange between two chains) is suppressed. The molecular weight can be better controlled, but the overall rate becomes much

lower. This is one example out of many and this one uses a complex type extensively studied in the van Koten group [50]. The concentrations of the reagents are very critical; when the concentration of CCl_3Br is too high its adduct to the acrylate is obtained instead of a polymer. In this case the reaction is called Atom Transfer Radical Addition, in the example the Kharasch reaction.

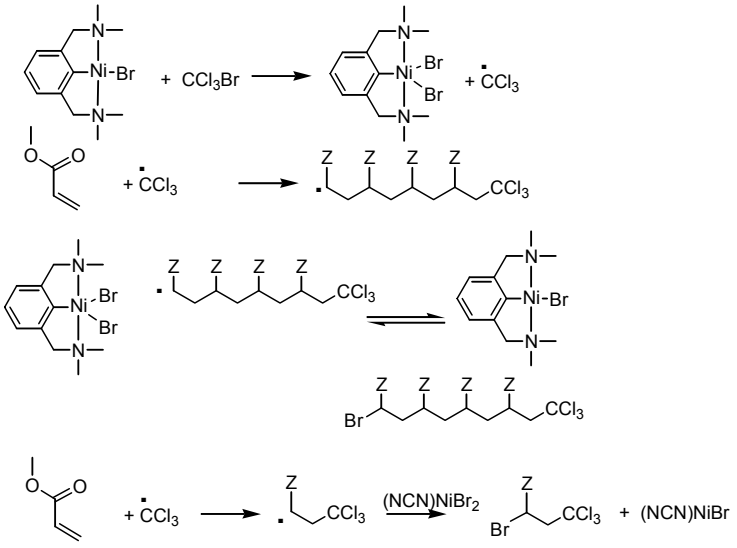

Figure 2.45. ATRP and Kharasch addition with nickel catalyst

References

1 Anderson, G. K.; Cross, R. J. *Acc. Chem. Res.* **1984**, *17*, 67. Mawby, R.J.; Basolo F.; Pearson, R.G. *J. Am. Chem. Soc.* **1964**, *86,* 5043. Noack, K.; Calderazzo, F. *J. Organometal. Chem.* **1967**, *10*, 101. Flood, T.C.; Jensen, J.E.; Statler, J.A. *J. Am. Chem. Soc.* **1981**, *103*, 4410.

2 Kataoka, Y.; Shibahara, A.; Yamagata, T.; Tani, K. *Organometallics* **2001**, *20*, 2431.

3 van Leeuwen, P. W. N. M.; Roobeek, C. F.; van der Heijden, H. J. *J. Am. Chem. Soc.* **1994,** *116*, 12117.

4 van Leeuwen, P. W. N. M.; Morokuma, K.; van Lenthe, J. H. Eds.; Theoretical Aspects of Homogeneous Catalysis; Kluwer Academic Publishers: Dordrecht, The Netherlands, **1995**. Maseras, F.; Lledós, A. Computational Modeling of Homogeneous Catalysis, Kluwer Academic Publishers: Dordrecht, The Netherlands, **2002**.

5 Dekker, G. P. C. M.; Buijs, A.; Elsevier, C. J.; Vrieze, K.; van Leeuwen, P. W. N. M.; Smeets, W. J. J.; Spek, A. L.; Wang, Y. F.; Stam, C. H. *Organometallics,* **1992***, 11*, 1937.

6 Lundquist, E. G.; Folting, K.; Huffman, J.C.; Caulton, K.G. *Organometallics* **1990**, *7*, 2254. García Alonso, F. J.; Llamazares, A.; Riera, V.; Vivanco, M.; Diaz M. R.; García Granda, S. *J. Chem. Soc. Chem. Commun.* **1991**, 1058.

7 Versluis, L.; Ziegler, T.; Fan, L. *Inorg. Chem.* **1990**, *29,* 4530. Brookhart, M.; Green, M. L. H. *J. Organomet. Chem.* **1983**, *250,* 395. Mole, L.; Spencer, J. L.; Carr, N.; Orpen, A. G. *Organometallics,* **1991**, *10,* 49. Conroy-Lewis, F. M.; Mole, L.; Redhouse, A. D.; Litster, S. A.; Spencer, J. L. *J. Chem. Soc. Chem. Commun.* **1991**, 1601.

8 Thorn D. L.; Hoffmann, R. *J. Am. Chem. Soc.* **1978**,*100*, 2079.

9 Bergman, R. *J. Am. Chem. Soc.* **1981**, *103,* 7028.

10 Hickey, C. E.; Maitlis, P. M. *J. Chem. Soc. Chem. Commun.* **1984**, 1609.

11 Amatore, C.; Jutand, A. *Acc. Chem. Res.* **2000**, *33*, 314.

12 Calhorda, M. J.; Brown J. M.; Cooley, N. A. *Organometallics,* **1991**, *10,* 1431.

13 Widenhoefer, R. A.; Buchwald, S. L. *J. Am. Chem. Soc.* **1998**, *120*, 6504.

14 Fitton, P.; Rick, E. A. *J. Organomet. Chem.* **1971**, *28,* 287.

15 Goertz, W.; Kamer, P. C. J.; van Leeuwen, P. W. N. M.; Vogt, D. *Chemistry, Eur. J.* **2001**, *7,* 1614.

16 Marcone, J. E.; Moloy, K. G. *J. Am. Chem. Soc.* **1998**, *120,* 8527.

17 Brown , J. M.; Cooley, N. A. *Chem. Rev.* **1988,** *88,* 1031.

18 Schrock, R. R. *Acc. Chem. Res.* **1979**, *12,* 98.

19 Bäckvall, J. E.; Åkermark B.; Ljunggren, S. O. *J. Am.Chem. Soc.* **1979**, *101,* 2411.

20 Luo, X.-L.; Crabtree, R. H. *J. Am. Chem. Soc.* **1989**, *111*, 2527.

21 Vaska, L. Diluzio, J. W. *J. Am. Chem. Soc.* **1962**, *84,* 679. Vaska, L. *Acc. Chem. Res.* **1968**, *1,* 335.

22 James, B. R.; Mahajan, D. *Can. J. Chem.* **1979**, *57,* 180.

23 Ungváry, F. *J. Metalorg. Chem.* **1972**, *36*, 363. Major, A.; Horváth, I. T.; Pino, P. *J. Mol. Catal.* **1988**, *45*, 275. Mirbach, M. F. *J. Metalorg. Chem.* **1984**, *265*, 205.

24 Chinn, M. S.; Heinekey, D. M. *J. Am. Chem. Soc.* **1990**, *112,* 5166.

25 Van Leeuwen, P. W. N. M.; Roobeek, C. F.; Wife, R. L.; Frijns, J. H. G. *J. Chem. Soc. Chem. Commun.* **1986**, 31.

26 Inuki, T. ; Kojima, T. *J. Org. Chem.* **1967**, *32*, 869, 872.

27 Fleming, I. *Frontier Orbitals and Organic Chemical Reactions*, Wiley, New York **1976**, p. 161.

28 Denmark, S. E.; Fu, J. *Chem. Rev.* **2003**, *103*, 2763. Ueki, M.; Matsumoto, Y.; Jodry, J. J.; Mikami, K. *Synlett* **2001**, 1889. Ishihara, K.; Kurihara, H.; Matsumoto, M.; Yamamoto, H. *J. Am. Chem. Soc.* **1998**, *120*, 6920. Reetz, M. T.; Kyung, S. H.; Bolm, C.; Zierke, T. *Chem. & Ind. (London)* **1986**, 824.

29 Ishihara, K.; Ohara, S.; Yamamoto, H. *Science* **2000**, *290*, 1140.

30 Garrou, P. E. *Chem. Rev.* **1985**, *85*, 171

31 Billig, E.; Jamerson, J. D.; Pruett, R. L. *J. Organomet. Chem.* **1980**, *192*, C49.

32 Goel, A. B. *Inorg. Chim. Acta,* **1984**, *84*, L25.

33 Sakakura, T. *J. Organometal. Chem.* **1984**, *267*, 171. Abatjoglou, A. G.; Billig, E.; Bryant, D. R. *Organometallics,* **1984**, *3*, 923.

34 Abatjoglou, A. G.; Bryant, D. R. *Organometallics,* **1984**, *3*, 932.

35 Kong, K-C.; Cheng, C-H. *J. Amer. Chem. Soc.* **1991**, *113*, 6313.

36 Kikukawa, K.; Takagi, M.; Matsuda, T. *Bull. Chem. Soc. Japan,* **1979**, *52*, 1493. Sisak, A.; Ungváry, F.; Kiss, G. *J. Mol. Catal.* **1983**, *18*, 223. Bouaoud, S-E.; Braunstein, P.; Grandjean, D.; Matt, D. *Inorg. Chem.* **1986**, *25*, 3765. Alcock, N.W.; Bergamini, P.; Kemp, T. J.; Pringle, P. G. *J. Chem. Soc. Chem. Commun.* **1987**, 235. van Leeuwen, P. W. N. M.; Roobeek, C. F.; Orpen, A. G. *Organometallics,* **1990**, *9*, 2179. The latter reference gives an example of a stoichiometric substitution of an aryl group by an alkoxide at platinum.

37 Goodson, F. E.; Wallow, T. I.; Novak, B. M. *J. Am. Chem. Soc.* **1997**, *119*, 12441.

38 Kaneda, K.; Sano, K.; Teranishi, S. *Chem. Lett.* **1979**, 82.
39 Chan, A. S. C.; Caroll, W. E.; Willis, D. E. *J. Mol. Catal.* **1983***, 19,* 377.
40 van Leeuwen, P. W. N. M. *Appl. Catal. A: General* **2001**, *212*, 61.
41 Chen, J.; Daniels, L. M.; Angelici, R. J. *J. Am. Chem. Soc.* **1990***, 112,* 199. Angelici, R. J. *Acc. Chem. Res.* **1988***, 21,* 387. Dong, L.; Duckett, S. B.; Ohman K. F.; Jones, W. D. *J. Am. Chem. Soc.* **1992**, *114,* 151. Bianchini, C.; Meli, A. *Acc. Chem. Res*. **1998**, *31*, 109. Chen, J.B.; Angelici, R. J. *Coord. Chem. Rev.* **2000***, 206,* 63.
42 Kraus, J.; Zdrazil, M. *React. Kinet. Catal. Lett.* **1977**, *6,* 45.
43 Liu, A.C.; Friend, C.M. *J. Am. Chem. Soc.* **1991***, 113,* 820.
44 Meyers, A.W.; Jones, W.D.; McClements, S.M. *J. Am. Chem. Soc.* **1995***, 117,* 11704. Vicic D.A.; Jones, W.D. *Organometallics,* **1997***, 16*, 1912.
45 Bianchini, C.; Meli, A.; Peruzzini, M.; Vizza. F.; Frediani, P.; Herrera, V.; Sánchez-Delgado, R. A. *J. Am. Chem. Soc.* **1993***, 115,* 2731.
46 Stull, D.E.; Westrum E.F.; Sinke, G.C. "The Chemical Thermodynamics of Organic Compounds," Wiley, New York, **1969.**
47 Bianchini, C.; Meli, A.; Oberhauser, W.; Vizza. F. *Chem. Commun*. **1999**, 671.
48 Colussi, A. J.; Ghibaudi, E.; Yuan, Z.; Noyes, R. M. *J. Am. Chem. Soc.* **1990***, 112*, 8660.
49 Matyjaszewski, K.; Patten, T. E.; Xia, J. *J. Am. Chem. Soc.* **1997***, 119,* 674. Matyjaszewski, K. *Macromol. Symp.* **2002**, *183*, 71. Matyjaszewski, K.; Xia. J. H. *Chem. Rev.* **2001***, 101*, 2921. Yamada, K.; Miyazaki, M.; Ohno, K.; Fukuda, T.; Minoda, M. *Macromolecules,* **1999***, 32,* 290. Matyjaszewski, K.; Goebelt, B.; Paik, H. –J.; Horwitz, C. P. *Macromolecules,* **2001***, 34*, 430.
50 Kleij, A. W.; Gossage, R. A.; Gebbink, R. J. M. Klein; Brinkmann, N.; Reijerse, E. J.; Kragl, U.; Lutz, M.; Spek, A. L.; van Koten, G. *J. Am. Chem. Soc.* **2000***, 122*, 12112. Granel, C.; Dubois, P.; Jérôme, R.; Teyssié, P. *Macromolecules,* **1996***, 29*, 8576.

Chapter 3

KINETICS

A conditio sine qua non for deciding on a mechanism

3.1 Introduction

Kinetics is one of the key issues of catalysis together with selectivity and catalyst stability. Chemical kinetics has been discussed in several dedicated works [1] and the readers will be aware of its basics [2]. In the following sections several commonly used concepts are mentioned such as steady state approximation, rate-determining step, determination of selectivity, and a few points of particular interest to catalysis will be high-lighted such as incubation.

3.2 Two-step reaction scheme

A catalytic reaction often consists of more than one step and therefore the expression for the rate for a reaction between two substrates A and B rarely takes the simple form of v=k[A][B]. At least one would assume that also the catalyst concentration [M] forms part of the equation. Thus more than one step is involved, each of which may be an equilibrium reaction. During the catalytic process the individual steps may not reach equilibrium and the competing rates determine the concentrations of each intermediate. While each individual reaction may obey a simple rate equation, the observed overall rate equation can be very complicated. What does the rate equation look like and how can it be expressed in measurable quantities is the question to be asked.

Suppose we have a simple reaction scheme consisting of two steps as shown in Figure 3.1. Reaction 1 is reversible and reaction 2 is irreversible. The rate of a sequence of two reactions can be expressed in an analytical fashion.

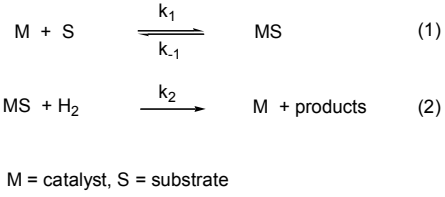

Figure 3.1. Two-step reaction scheme

$$v = k_2 [MS][H_2] \quad (3)$$

$$d[MS]/dt = 0 = k_1[M][S] - k_{-1}[MS] - k_2[MS]H_2] \quad (4)$$

$$[M_t] = [M] + [MS] \quad (5)$$

$$v = \frac{k_1 k_2 [M_t][S][H_2]}{k_1[S] + k_2[H_2] + k_{-1}} \quad (6)$$

Figure 3.2. A simple two-step catalytic reaction; steady-state approximation

It can be solved by the so-called Bodenstein or steady-state approximation. This approximation supposes that the concentration of the reactive intermediate, in this case MS, is always small and constant. For a catalyst, of which the concentration is always small compared to the substrate concentration, it means that the concentration of MS is small compared to the total M concentration. The rate of production of products for the scheme in Figure 3.1 is given by equation (3). Equation (4) expresses the steady state approximation; the amounts of MS being formed and reacting are the same. Equation (5) gives [M] and [MS] in measurable quantities, namely the total amount of M (M_t) that we have added. If we don't add this term, the nominator of equation (6) will not contain the term of k_1 and the approximations that follow cannot be carried out.

3.3 Simplifications of the rate equation and the rate-determining step

Often equation (6) from Figure 3.2 can be simplified, at least for part of the window of concentrations or pressures that are applied. The two simplest ones are a) reaction (1) is much slower than reaction (2), and b) reaction (2) is much slower than (1). The free-energy profiles for these two cases are depicted in Figure 3.3, respectively A and B. Case A implies that $k_2 >> k_{-1} >> k_1$ (concentrations omitted for the sake of simplicity). The rate equation simplifies

to $v=k_1[M][S]$. Reaction (1) is called the rate-determining step; as soon as SM has been formed via the slow forward reaction (1) it is converted to products. Note that the rate of reaction in this case is independent of the H_2 concentration. The catalyst in the reaction mixture occurs as complex M, which is called the resting state. In this instance the resting state is the state immediately preceding the rate-determining step. In addition the rate-determining step as defined here shows the highest barrier in the energy profile of the overall reaction scheme. As we will see, intuitively one might opt for a different definition and this often leads to confusion.

Case B is very common and can also be worked out easily. It is seen that the barriers for both the forward and backward reaction of (1) are much lower than the barrier for (2). We are dealing with a fast pre-equilibrium and a rate-determining reaction (2); k_1, $k_{-1} >> k_2$ (concentrations omitted). It is also referred to as Curtin-Hammett conditions in U.S. literature; it refers to the kinetics of a system of a number of rapidly equilibrating species or conformations, each one of which might undergo a different conversion, but all that counts is the global, lowest barrier, as that is the direction the system takes.

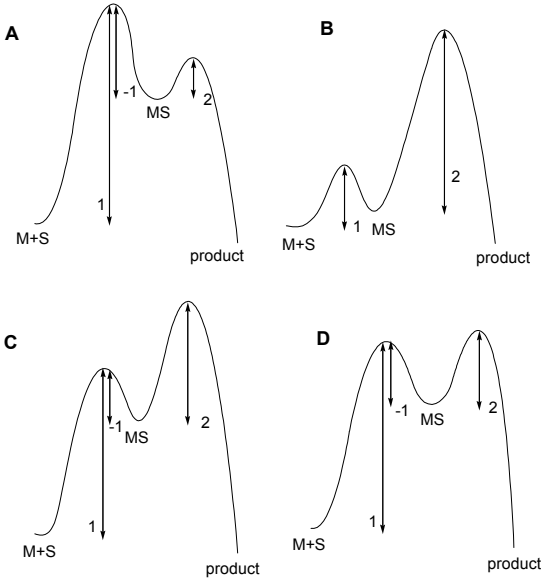

Figure 3.3. Typical free energy profiles

The rate equation is presented in equation (7). It can also be derived from $v = k_2[MS][H_2]$ when we substitute for [MS] the equilibrium fraction of the catalyst that occurs as MS. Note that we do not fulfil the Bodenstein approximation, but our general formula (6) is still valid. If the free energy of

MS is lower than that of M the system is in the regime of substrate saturation; addition of more S does not lead to a rate increase. The behaviour of the reaction rate in case B is typical of enzymes and in biochemistry this is referred to as Michaelis-Menten kinetics. The success of the application of the Michaelis-Menten kinetics in biochemistry is based on the fact that indeed only two reactions are involved: the complexation of the substrate in the pocket of the enzyme and the actual conversion of the substrate. Usually the exchange of the substrate in the binding pocket is very fast and thus we can ignore the term $k_2[H_2]$ in the denominator. Complications arise if the product binds to the binding site of the enzyme, product inhibition, and more complex kinetics result.

As mentioned above, for case **B** we can omit the k_2 term from the denominator and we obtain (for a metal catalyst example) equation (7) in Figure 3.4. This may not be immediately recognised as the characteristic equation one is used to in biochemistry. When one plots the rate versus the substrate concentration, equation (7) will lead to a curved line, provided that considerable substrate binding takes place. Using paper and pencil such a curved line is not amenable to further analysis and therefore Lineweaver and Burk introduced the well-known plot of the inverse rate versus the inverse of the substrate concentration, see equation (8), for a hydrogenation catalyst. If the hydrogen pressure is kept constant a plot of the 1/v versus 1/[S] gives a strait line in the graph from which k_2 and the equilibrium constant can be derived.

$$v = \frac{k_1 k_2 [M_t][S][H_2]}{k_1[S] + k_{-1}} \qquad (7)$$

$$\frac{1}{v} = \frac{1}{k_2 [M_t][H_2]} + \frac{k_{-1}}{k_1 k_2 [M_t][S][H_2]} \qquad (8)$$

Figure 3.4. Lineweaver-Burk expression for the metal catalysed reactions (1-2)

Case **C** in Figure 3.3 is instructive from the point of view of what one should call rate-determining. The barrier for reaction (2) is clearly the highest point in our profile and thus we will call this the rate-determining step. The reactive intermediate MS when formed in this scheme will like in **B** mainly return to M, but compared to **B** the formation of MS is much slower, because the barrier related with k_1 is very high. If one would carry out stoichiometric reactions to measure the rates of the individual steps or MO calculations to calculate the barriers, one will find that the barrier for the forward reaction (1) is higher than that for reaction (2). Nevertheless, we will say that reaction (2) is rate determining. The main part of the energy required to have the reaction

proceed is used for the formation of MS via reaction (1). The rate equation to be used is clearly equation 6, the one containing all terms.

Case **D** has been added to show an intermediate case for **A** and **C**. The barriers for k_{-1} and k_2 are taken more or less the same (note that the actual rate for (2) will also depend on the concentration of H_2). One can say in this instance that the rate-determining step is the forward reaction (1) and that the two rates leading from MS back or forward determine the proportion of MS that leads to product. Equation (9) obtained by omitting k_1 from the denominator in (6) underscores this.

$$v = k_1[M_t][S] \frac{k_2[H_2]}{k_2[H_2] + k_{-1}} \qquad (9)$$

Figure 3.5. Approximation for case **D**

The resting state of the catalyst, in the schemes chosen so far, has been a species at the beginning of the catalytic cycle. We will discuss one example, **E**, in which this is not the case.

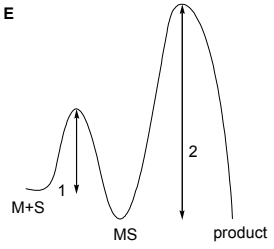

Figure 3.6. A resting state MS different from the starting catalyst M

In scheme **E** in Figure 3.6 it is seen that one of the intermediates (MS) has a lower energy than the starting complex M. This means that all M will be relatively quickly converted to MS and that all catalyst resides in the MS state. Step (2) is rate-determining and the rate equation for this catalytic system reduces to $v = k_2[M_t][H_2]$. Under these conditions the rate of reaction is independent of the concentration of the substrate S.

By way of exercise, let us summarise a few dependencies on concentrations using the simple reaction scheme used so far:

A: the order in S and M is one and the order in H_2 is zero;

B: the order in S is between zero and one, depending on the equilibrium and the relative value k_2, and the order in M is one, and the order in H_2 is one;

C and **D**: broken orders will be found in H_2 and S and a first order in M.

Note that in the elementary steps the reaction rates are first or second order and only in the overall equation they become complex. A negative order in one of the reagents means that a pre-equilibrium exists involving dissociation or substitution of L as shown in (10) and (11). The rate of reaction is now given by (12) containing a negative order in [L].

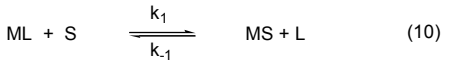

$$v = \frac{k_1 k_2 [M_t][S][H_2]}{k_1[S] + k_2[H_2] + k_{-1}[L]} \qquad (12)$$

Figure 3.7. Simple reaction scheme including substitution of L

If one would be able to derive from the experimental data an accurate rate equation like (12) the number of terms in the denominator gives us the number of reactions involved in forward and backward direction that should be included in the scheme of reactions, including the reagents involved. The use of analytical expressions is limited to schemes of only two reaction steps. In a catalytic sequence usually more than two reactions occur. We can represent the kinetics by an analytical expression only, if a series of fast pre-equilibria occurs (as in the hydroformylation reaction, Chapter 9, or as in the Wacker reaction, Chapter 15) or else if the rate determining step occurs after the resting state of the catalyst, either immediately, or as the second one as shown in Figure 3.1. In the examples above we have seen that often the rate equation takes a simpler form and does not even show all substrates participating in the reaction.

3.4 Determining the selectivity

Next to the "rate-determining step" we are interested in the step(s) determining the selectivity. In a multi-step reaction scheme the selectivity has been determined as soon as an irreversible step has occurred after the selectivity has been fixed in the fragment being formed. Often the step determining the selectivity will coincide with the rate-determining step, but this is not necessary as we will show. We can think of many variations and complicated systems, but we will refrain to only three. The first one has become known as the "major–minor" example from enantiospecific hydrogenation (see Chapter 4). Before the works by J. Halpern and J. M. Brown were published, the general guide for ligand design – be it successful or not – was to design a best fit between complex and substrate resembling the desired product. Thus, it was thought that if the substrate-to-metal-complex

adduct leading to the R-enantiomer were the most stable, the product of that reaction would be the R-enantiomer. For the first cases of rhodium-catalysed, enantiospecific hydrogenation that were studied in detail, this turned out to be wrong; the most stable intermediate ("major" isomer) reacted much more slowly than the less stable intermediate ("minor" isomer).

Since we have not discussed yet enantiospecific catalysis we will show a fictitious catalyst for the hydrogenation of an enone, which can undergo hydrogenation to an aldehyde (Figure 3.8, path a) or to allyl alcohol (path b), via respectively hydrogenation of the alkene or aldehyde function (such catalysts do exist). The complex of the metal with the η^2 bonded alkene is more stable than the aldehyde bonded complex. We assume that the two complexes are in fast equilibrium, but the alkene complex is the "major" species. If, however, the barrier for aldehyde hydrogenation is lower (path b), the product of this reaction is mainly allyl alcohol! The energy scheme is shown in Figure 3.8.

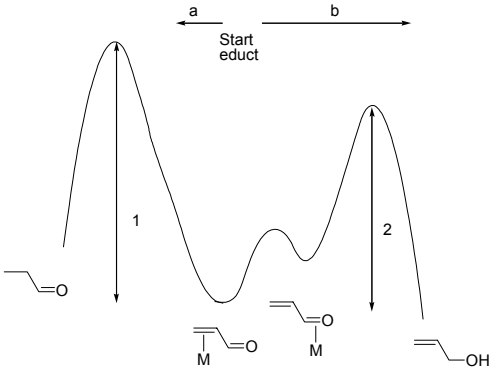

Figure 3.8. Major-minor species and selectivity

The major intermediate observed in solution is the alkene complex, but it interchanges rapidly with the aldehyde complex. The product formed according to this scheme is allyl alcohol, because the overall barrier 2 is lower than barrier 1 (above we named this Curtin-Hammett conditions). Barrier 2 is also the rate-determining step in this sequence.

A second scheme (Figure 3.9) shows how the selectivity can be determined before the rate-determining step occurs, provided that the selectivity-determining step is still irreversible. The ratio of the barrier 1a and 1b determines how much of products a and b will be formed. Subsequently, the resting states are occupied, but the backward barrier is higher than the forward barriers 2a and 2b. The barriers 2 form the rate-determining one! These are delicate balances and since the barriers are free energies it can be imagined that

if one of the steps is dependent on a concentration of a reagent, the relative heights of the barriers change.

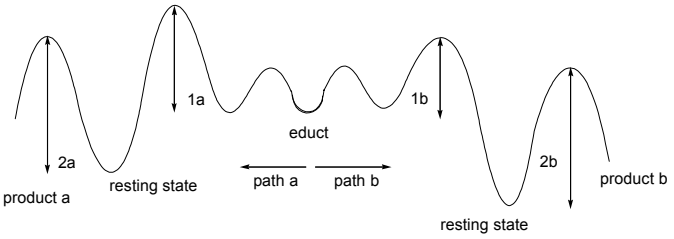

Figure 3.9. Selectivity is determined in steps 1, while steps 2 are rate-determining

The third case involves a determination of the selectivity in competing steps occurring *after* the rate-determining step has taken place, which is the same for both products. The rate equation only contains the rate-determining step and does not deal with the selectivity! Step 1 has the highest energy barrier and the intermediate now reacts via two pathways 2a and 2b to the two products a and b, for which the ratio is controlled by the heights of the energies indicated by arrows a and b.

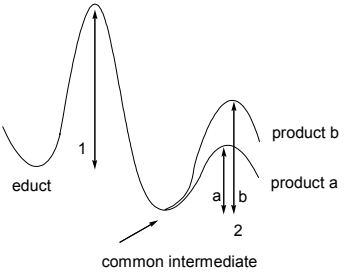

Figure 3.10. Selectivity determined after rate-controlling step

Thus we have seen a variety of possibilities, even for reaction schemes containing a small number of reactions. Before one can draw a mechanism, one needs to carry out kinetic measurements, but even then the mechanism may not be evident, as kinetics often allow more mechanistic interpretations.

3.5 Collection of rate data

The rate of a reaction and its dependency on the concentrations of the reactants can be measured in several ways. A simple method involves the measurement of the rate at zero to low conversion at different concentrations of one of the substrates, keeping the concentration of other substrates constant. The latter can be done by using an excess of the other substrates (e.g. tenfold excess), which means that we can assume that the concentrations of the latter ones are constant under so-called pseudo-first-order conditions. Secondly we can monitor the reaction rate over a longer period of time taking into account the change in concentration for this one substrate. Alternatively, one can monitor the concentrations of all species and analyse the results numerically.

As a reactor one can use

1) a batch reactor, in which at all times good mixing is applied and the concentrations monitored as described above, or
2) a plug-flow reactor, in which no mixing takes place and the residence time in the tube determines the degree of conversion, or
3) a CSTR, continuously stirred tank reactor, in which a steady state is obtained depending on the residence of the reagents in the vessel, which is also rapidly stirred so as to ensure that there are no concentration differences in the vessel.

If one of the reactants is a gas, sufficiently fast mixing of the gas into the liquid is needed. As mentioned in Chapter 1, a pressure of 25 bar of H_2 or CO, gives a concentration of 50 mM of this gas in an organic solvent and if the target is to obtain concentrations of the product in the order of moles per litre, considerable amounts of gas have to be absorbed. If gas transport is the limiting factor in the conversion of our starting material, we say the reaction is mass transport limited. Whether this occurs during rate measurements can be checked by measuring the rates versus the stirring rate. Mixing is sufficient if the rate does not increase further when the stirring rate is raised.

There are many ways to measure the concentrations of reacting species or species formed during the reaction, such as there are: gc, UV-visible spectroscopy, IR spectroscopy, refractometry, polarometry, etc. Conversion can be monitored by pressure measurements, gas-flow measurements, calorimetry, etc. Data are collected on a computer and many programmes are available for data analysis [3,4]. The two-reaction system described above can be treated graphically, if it fulfils either the Bodenstein or Michaelis-Menten criteria.

3.6 Irregularities in catalysis

At least two phenomena may lead to deviations in the kinetic behaviour of catalytic systems, namely incubation and catalyst decomposition. Incubation is said to occur when the catalytic reaction does not immediately start at the time all reagents have been put together. Roughly speaking, there may be two causes for this, 1) the catalyst has not been formed yet and 2) an impurity in the substrate causes temporarily a poisoning of the catalyst. Catalyst formation stands for a variety of reactions that may have to take place before the catalytic reaction can start. For example we start with a metal salt that has to be transformed into a hydride by either hydrogen or a reducing agent and this reaction is much slower than the catalysis that should take place. Or the catalyst precursor may have to lose one ligand before it can start the catalytic cycle. If a reaction of this type occurs, the kinetics will not correspond to one of the equations introduced above, because the concentration of the catalyst is not known and is growing over time.

Inhibition of a catalytic reaction by impurities present may take place and sometimes this may have a temporary character. If it is permanent one cannot be mistaken in the kinetic measurements. Impurities that are more reactive than the substrates to be studied may block the catalyst if they react according to a scheme like that of Figure 3.7. Only after all inhibitor has been converted the conversion of the desired substrate can start. Another type of deactivation that may occur is the formation of dormant states, which is very similar to inhibition. Either the regular substrate or an impurity may lead to the formation of a stable intermediate metal complex that does not react further. There are examples where such intermediates can be rescued from this dormant state for instance by the addition of another reagent such as dihydrogen (Chapter 10, dormant states in propene polymerisation).

Catalyst decomposition (“die-out”) during the catalytic reaction is a common phenomenon also distorting the kinetic measurements. If the decomposition reaction obeys a rate equation in a well-behaved manner, one can include the decomposition reaction in the kinetics, but usually one will prefer the use of a stable catalyst. Catalyst decomposition is an import issue in applied catalysis although it has received relatively little attention in literature as far as homogeneous catalysis is concerned [5].

References

1 Benson, S. W. *The Foundations of Chemical Kinetics*, McGraw-Hill, New York, **1960**. Masel, R. I. *Chemical Kinetics and Catalysis*, Wiley, New York, **2001**.
2 Atkins, P. W. *Physical Chemistry*, Oxford University Press, **1994**, 5th Ed. Chapters 25 and 26.
3 Merrill, J. C.; Spicer, L. D.; Brown, R.; Walling, C. *J. Chem. Educ.* **1975***, 52*, 528. Allendoerfer, R. D. *J. Chem. Educ.* **2003***, 80*, *110* and **2002***, 79*, 638. Rosner, T.; Le Bars, J.; Pfaltz, A.; Blackmond, D. G. *J. Am. Chem. Soc.* **2001***, 123*, 1848.
4 Search the web for KINSIM (for Windows).
5 Van Leeuwen, P. W. N. M. *Appl. Catal. A: General* **2001**, *212*, 61.

Chapter 4

HYDROGENATION

The success story of asymmetric catalysis

4.1 Wilkinson's catalyst

Homogeneously catalysed hydrogenation reactions are only of minor importance from an industrial viewpoint with the notable exception of asymmetric hydrogenation. A large part of today's general knowledge on homogeneous catalysis has been derived from the early studies on hydrogenation. Undoubtedly the most popular homogeneous catalyst for hydrogenation is Wilkinson's catalyst, $RhCl(PPh_3)_3$, discovered in the sixties [1]. The reaction mechanism, its dependence on many parameters, and its scope have been studied in considerable detail. Nowadays, with the availability of high-field NMR equipment, the results of such studies would give rise to much less controversy, but the discussions and debates in the 60's and 70's have certainly contributed to the fame of the catalyst. The commonly accepted reaction sequence reads as follows:

$$RhCl(L)_3 + S \rightleftharpoons RhCl(L)_2S + L$$

$$RhCl(L)_2S + H_2 \rightleftharpoons RhH_2Cl(L)_2S$$

$$RhH_2Cl(L)_2S + H_2C{=}CH_2 \rightleftharpoons RhH_2Cl(L)_2(H_2C{=}CH_2) + S$$

$$RhH_2Cl(L)_2(C_2H_4) + S \rightleftharpoons Rh(C_2H_5)Cl(L)_2S$$

$$RhH(C_2H_5)Cl(L)_2S \rightarrow H_3CCH_3 + RhCl(L)_2S$$

In this scheme L stands for triarylphosphines and S for solvent (ethanol, toluene). The alkene is simply ethene. The first step in this sequence is the dissociation of one ligand L which is replaced by a solvent molecule. Several

alternatives have been found involving, for instance, the formation of dimers from the unsaturated species. For simplicity we have chosen for Wilkinson's complex as the starting point in our cycle. As in many other cases the number of valence electrons switches during the cycle between two differing by two electrons; in this instance the valence electron counts switch between 16 and 18. A 14-electron count for the unsaturated species occurring at the beginning of the cycle has also been discussed.

After ligand dissociation an oxidative addition reaction of dihydrogen takes place. As usual this occurs in *cis* fashion and can be promoted by the substitution of more electron-rich phosphines on the rhodium complex. The next step is the migration of hydride forming the ethyl group. The "ligand effect" (the shorthand notation for the effect that systematic variation of the ligands has on a performance aspect of a catalyst) on the insertion/migration processes is not as clear as that on the redox processes. Reductive elimination of ethane completes the cycle. Obviously, the rate of this step can be increased by employing electron withdrawing ligands. Within a narrow window of aryl phosphines small changes in rates have been observed, which could indeed be explained along the lines sketched above. Strong donor ligands, however, stabilise the trivalent rhodium(III) chloro dihydride to such an extent that the complexes are no longer active.

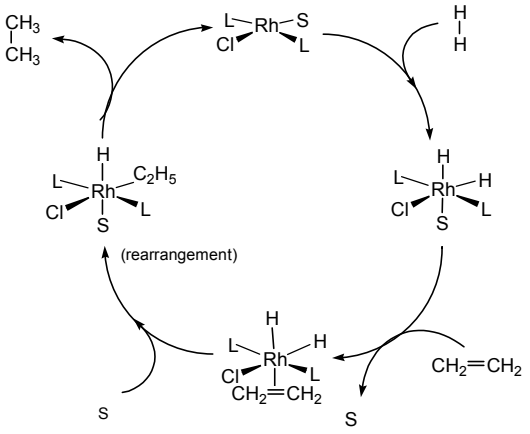

Figure 4.1. Wilkinson's hydrogenation cycle

Another way of representing catalytic cycles is shown in Figure 4.1. Note that the reactions have been drawn as irreversible reactions while most of them are actually equilibria. If one wants to derive kinetic equations, we strongly recommend the use of reaction sequences as shown on the previous page, because cycles such as 4.1 often lead to mistakes.

Many species have been observed in the solution in addition to those shown in 4.1, such as dimers $[RhCl(PPh_3)_2]_2$, $RhCl(PPh_3)_2$(olefin), dimers containing hydrides, etc., which indicates that the species actually observed may have little to do with the catalytic cycle. The reverse is also true; few of the species mentioned in scheme 4.1 can be observed and their existence is only known from the kinetic studies! The actual concentrations are far below the NMR detection level during the catalysis [2].

A ligand effect has been reported [3]. As mentioned above, the knowledge about "ligand effects" is limited. The following range of reactivities has been reported for the hydrogenation of cyclohexene:

Ligand:	Relative reactivity:
$(4\text{-}ClC_6H_4)_3P$	1.7
Ph_3P	41
$(4\text{-}CH_3C_6H_4)_3P$	86
$(4\text{-}CH_3OC_6H_4)_3P$	100

In view of the above remarks the explanation of the effect of the electronic parameter of the ligand requires a careful study of all systems, since so much of the rhodium is tied up in "parking places" that the effect of the ligand may not simply be the enhancement of the reactivity.

The results in the table suggest that, if we neglect changes in the concentrations of the inactive species caused by the changes in the ligand, the rate-determining step is the oxidative addition of dihydrogen.

4.2 Asymmetric hydrogenation

4.2.1 Introduction

Today many examples are known showing that tailor-made chiral metal complexes, comprising a metal atom bound to chiral organic ligands, can discriminate with high precision (energy differences exceeding 10 $kJ.mol^{-1}$) between enantiotopic atoms or faces of an achiral molecule. Many of these chiral complexes have also an interesting catalytic activity for the production of a broad range of enantiomerically pure compounds. As the chiral complexes can be synthesised in both hands, in principle, both enantiomers of a compound are accessible. (This is a clear distinction from enzymatically catalysed reactions, which produce only one enantiomer.)

The demand for enantiomerically pure compounds with a wanted biological activity is growing rapidly in fine-chemical synthesis. An obvious reason for

this development is that the *opposite* enantiomer of a chiral pharmaceutical or chemical has at best no activity, or worse, causes side effects.

"Prochirality". Planar molecules possessing a double bond such as alkenes, imines, and ketones, which do not contain a chiral carbon in one of the side chains, are not chiral. When these molecules coordinate to a metal a chiral complex is formed, unless the alkene etc. has C_{2V} symmetry. In other words, even a simple alkene such as propene will form a chiral complex with a transition metal. So will trans-2-butene, but cis-2-butene won't. If a bare metal atom coordinates to cis-2-butene the complex has a mirror plane, and hence the complex is not chiral. It is useful to give some thought to this and find out whether or not alkenes and hetero-alkenes form chiral complexes. One can also formulate it as follows: complexation of a metal to the one face of the alkene gives rise to a certain enantiomer, and complexation to the other face gives rise to the other enantiomer.

For tetrahedrally substituted carbon we have learned the well-known Cahn-Ingold-Prelog rules for the determination of the absolute chirality. For complexes of planar molecules to metals rules have been introduced to allow us to denote the faces of the planar molecule; they are called the *re* face and the *si* face. Usually this simple annotation is used, but we will see that in fact it is more complicated. Sometimes authors do not want to go through the trouble of "counting" *re* or *si* and say that Rh-H adds to the pro-S side of the alkene, meaning that after hydrogenation the S-enantiomer is formed during this particular enantiospecific hydrogenation (Crabtree, in his book on Organometallic Chemistry). This makes the annotation of the *face* of the alkene dependent on the reaction that it will undergo, whereas the alkene has two different faces, independent of the reaction it will undergo. Surely, epoxidation and hydrogenation will lead to a different CIP count in the product. If only one reaction is being considered, the "pro-S side" annotation works just as well.

In Figure 4.2 we have drawn how we can distinguish the two faces of an alkene, or rather the side of attack of a specific atom of the alkene. The arrow on the left approaches the lower carbon of the alkene and when looking from this viewpoint we "count" the weight of the three substituents the same way as in the CIP rules. We then see the order 1, 2, and 3 counter-clockwise, and we say that the arrow approaches the carbon atom from the *si* face. For simplicity we call this the *si* face of the alkene and in most cases this will do. If all four substituents at the alkene are different we can determine the *re/si* properties of both carbon atoms and these may be different! This results in the nomenclature that an alkene may have a *re,re* and *si,si* face or *re,si* and *si,re* face. Thus, in the latter case one has to indicate to which atom the label is referring. For any enantiospecific, catalytic reaction (hydrogenation, hydroformylation, polymerisation) it is very convenient to use the *re* and *si* indicators in the discussion.

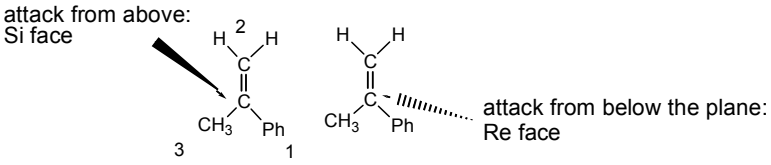

Figure 4.2. Re and Si faces of a 1,1-disubstituted substituted alkene

When a chiral metal complex forms a complex with a "prochiral alkene", either because it contains a chiral ligand or a chiral metal centre, the resulting complex is a diastereomer. Thus, a mixture of diastereomers can form when the chiral complex coordinates to both faces of the alkene. As usual, these diastereomers have different properties and can be separated. Or, more interestingly, in the catalytic reactions below, the two diastereomers are formed in different amounts and their reactivities are different as well.

4.2.2 Cinnamic acid derivatives

The asymmetric hydrogenation of cinnamic acid derivatives has been developed by Knowles at Monsanto [4]. The synthesis of L-dopa (Figure 4.3), a drug for the treatment of Parkinson's disease, has been developed and is applied on an industrial scale. Knowles received the Nobel Prize for Chemistry in 2001 together with Noyori (see below, "BINAP") and Sharpless (asymmetric epoxidation).

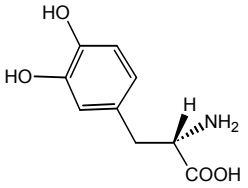

Figure 4.3. L-Dopa

The reaction is carried out with a cationic rhodium complex and an asymmetric diphosphine as the ligand, which induces the enantioselectivity ("cationic" is used exhaustively in literature to refer to metal salts containing weakly coordinating anions; we will also use the imperfect, colloquial expression "cationic"). Surprisingly, the reaction is not very sensitive to the type of diphosphine used, although it must be added that most ligands tested are bis(diphenylphosphino) derivatives and that the enantiomeric excesses obtained do show some variation. On the other hand the reaction is very sensitive to the type of substrate and the polar substituents are prerequisites for a successful asymmetric hydrogenation. Figure 4.4 shows the overall reaction.

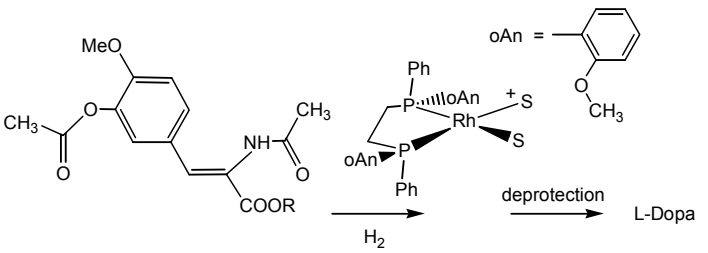

Figure 4.4. Synthesis of L-Dopa

The hydrogenation reaction is carried out with a substituted cinnamic acid. The acetamido group is of particular importance because it functions as a secondary complexation function in addition to the alkene functionality. In the first step the alkene co-ordinates to the cationic rhodium species (containing an enantiopure phosphine DIPAMP in Figures 4.4 and 4.5 with the chirality at phosphorus carrying three different substituents, Ph, o-An, CH_2) for which there are several diastereomeric structures due to:

- the asymmetry in the diphosphine ligand and the "prochirality" in the substrate (*re versus si)*,
- and the two co-ordination sites at rhodium.

The two co-ordination sites, however, are equivalent due to the C_2 symmetry of the diphosphine complex. This reduces the number of diastereomers from four to two. In Figure 4.5 the two enantiomeric intermediate alkene adducts have been drawn. Note that the faces are indicated by *si,si* and *re,re* because the configurations of two carbon atoms have to be assigned. After hydrogenation, only one chiral centre has formed at the α-carbon atom, because the β-carbon atom now carries two hydrogen atoms and thus does not form a chiral centre.

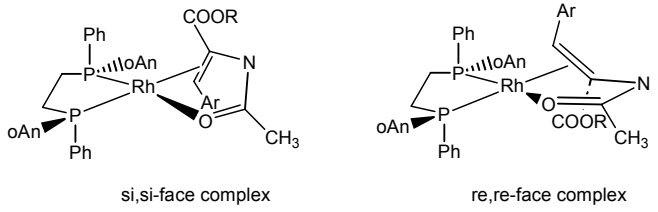

Figure 4.5. Diastereomeric alkene complexes with DIPAMP-Rh

One can try to figure out from the pictures how two diastereomeric intermediates are formed. It is more convenient to adopt a "formal" approach. We can explain the formation of enantiomers when a metal (even a bare Ag^+ ion would do) co-ordinates to our alkene substrate, and equally so the formation of diastereomers in Figure 4.5.

Ligand intermezzo. A large series of asymmetric ligands have been developed most of which having the asymmetric "centre" in the bridge rather than at the phosphorus atoms as is the case in DIPAMP, the ligand shown above for the L-dopa synthesis. Their synthesis is similar to the one developed by Kagan for DIOP (see Figure 4.6) starting from asymmetric acids which can be commercially obtained (tartaric acid in the case of DIOP) [5]. Crucial to the success of this family of ligands is the C_2 "propeller" type symmetry which divides the space around rhodium (or any metal) into four quadrants, two relatively empty and two filled ones (see Figure 4.7).

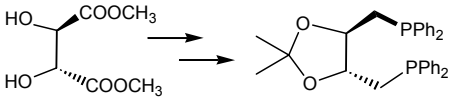

Figure 4.6. Structure and synthesis of DIOP

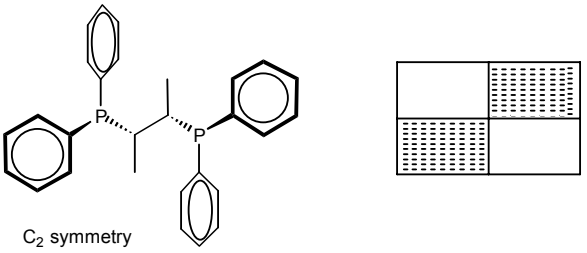

Figure 4.7. Front view of a chiral diphosphine and quadrant division

Two phenyl groups at one phosphorus of the chelating ring adopt an axial and an equatorial position. This explains the similarity of this large family of ligands in the enantioselective reactions, as all ligands divide the space in four quadrants as shown. Co-ordination of the dehydroalanine derivative (or enamides in general) will now take place such that the auxiliary donor atom coordinates to one site, and the phenyl substituted alkene will coordinate to the other site with the face that gives the least interaction of its substituents with the phenyl group of the ligand pointing into the same quadrant. This gives the predominant metal alkene adduct.

Not all diphosphine ligands adopt C_2 symmetry with respect to the four phenyl groups. For instance $Ph_2P(CH_2)_4PPh_2$, which lacks the constraints of DIOP in the ring in the C4-bridge, will not adopt a C_2-symmetry but most often it adopts a C_s-symmetry similar to a meso ligand having C_s symmetry (Figure 4.8). In this configuration two phenyl groups *cis* on the chelating ring will take axial (more or less) positions, and the two at the other face of the ring will assume equatorial positions. Even though there may be an asymmetric centre in

the backbone of a diphosphine, if it prefers this C_s "local" symmetry for the phenyl groups the enantiomeric character is not optimally passed on to the substrate coordinating to the C_s-diphos ligand-metal complex. Many crystal structures have been determined that support this view, as do molecular graphics (or molecular mechanics) for a broad range of ligands [6]. Fig. 4.8 shows the C_s-symmetric arrangement of the four phenyl groups in a diphosphine complex.

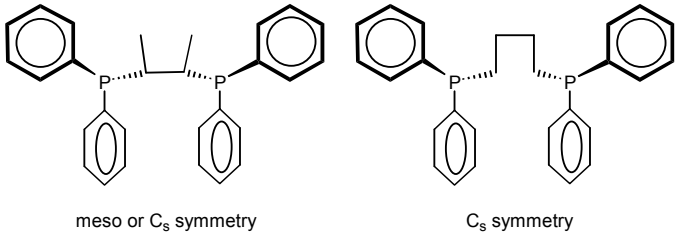

Figure 4.8. Front view of a "meso" diphosphine and C4 bridge ligand

Kinetics. Detailed studies by Halpern [7] and Brown [8] have revealed that the most stable intermediate of the two alkene adducts is (Figure 4.9) not the one that leads to the major observed enantiomeric product.

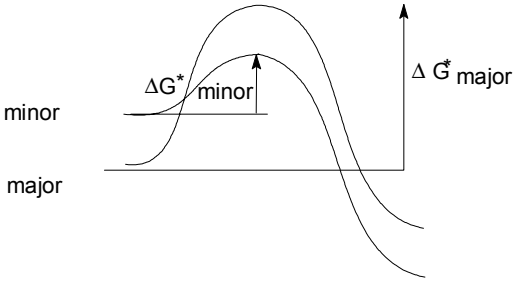

Figure 4.9. Minor species leading to dominant product route

This means that the less stable intermediate alkene complex reacts faster in the subsequent reactions. The next step in the hydrogenation sequence involves the oxidative addition of dihydrogen to the alkene complex (Figure 4.10).

The oxidative addition of H_2 is irreversible, and provided that no dissociation of the alkene occurs, this step determines the enantioselectivity. *<In general, one should realise, that the steps determining rate and selectivity need not be one and the same step of a reaction.>* Migration of the hydride locks the configuration of the enantiomeric centre; in general, this step may

also be reversible, and detailed studies are required in order to determine which is the rate-determining step and which one determines the enantioselectivity.

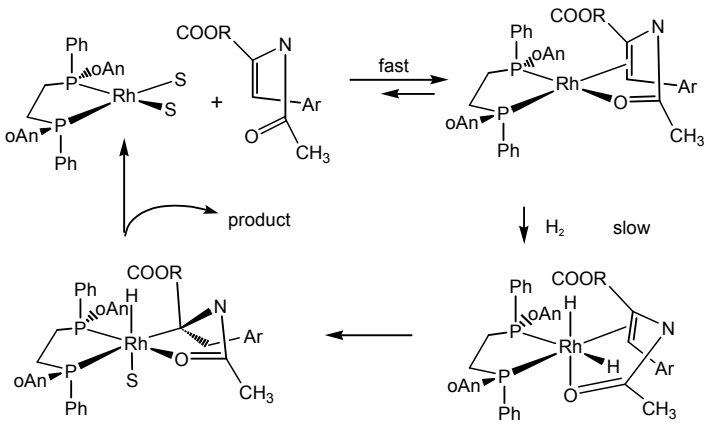

Figure 4.10. Asymmetric hydrogenation via major and minor alkene complex intermediate; only one diastereomer shown

In the examples studied, neither the dihydride intermediates nor the alkyl intermediates have been observed and therefore it seems reasonable to assume that addition of H_2 is also the rate-determining step. <*Since the latter is a bimolecular reaction and the other ones are monomolecular rearrangement reactions one cannot say in absolute terms that oxidative addition is rate-determining.*>

The example illustrates two points:

1. the intermediate alkene adduct observed in the NMR spectra is not the one leading to the major catalytic pathway,

2. enantioselectivity is determined in the first irreversible step after the enantio centre was formed which is not always the same as the rate-determining step.

The difference between this catalytic system and Wilkinson's catalyst lies in the sequence of the oxidative addition and the alkene complexation. As mentioned above, for the cationic catalysts the intermediate alkene (enamide) complex has been spectroscopically observed. Subsequently oxidative addition of H_2 and insertion of the alkene occurs, followed by reductive elimination of the hydrogenation product.

The enantioselectivity determining step. Above we learnt that the oxidative addition of hydrogen is the rate-determining step. This step is irreversible and it also determines the enantioselectivity. This complex could still epimerise via substrate dissociation, but apparently it does not and migratory insertion is faster than epimerisation. We remember that two diastereomeric intermediates are involved, the "major" and the "minor" species and the minor species is the

one leading to the product with high e.e. This is so, because the reaction of the minor product with dihydrogen is much faster than the reaction of the major species.

One might ask the question why a reaction involving such a small dihydrogen molecule can lead to such enormous differences in rate for the diastereomeric alkene adducts present (major and minor). Tentative answers were developed by Brown, Burk and Landis [9]. Their studies included the use of iridium instead of rhodium since the iridium hydride intermediates can be studied spectroscopically. Consider the oxidative addition in Figure 4.10.

The oxidative addition can take place from the top of the molecule (as shown), but it can also take place from the bottom, giving another diastereomeric intermediate that probably does not undergo migration. The two oxidative additions require *rotations in opposite directions* of the substrate with respect to the rhodium phosphine complex. The rotation required also depends on the geometrical isomer of the rhodium complex to be formed (alkene/amide *trans* or *cis* to phosphine; here we have chosen an amide *cis* to both phosphorus atoms). Both the major and the minor diastereomeric substrate complex require such a **rotation** upon oxidative addition.

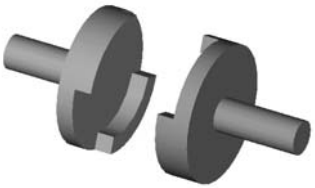

Figure 4.11. Clutches having a good fit

The formation of the two productive diastereomeric dihydrides may involve two different barriers for rotation. Thus, a very stable alkene-rhodium complex resulting from a very good fit of the substrate in the ligand-rhodium cavity, may lead to a more hindered rotation of the alkene upon oxidative addition [10]. Imagine the substrate clutched in the cleft of the C_2 ligand giving a staggered-like configuration, which leads to a strong fit resisting rotation. In the minor species, less stable, one could imagine a more eclipsed-like configuration, which will more easily rotate. The overall result of these energetics is hard to predict; molecular mechanics can only show us the energies of the intermediates, while kinetics (free energies of activation) are pivotal in determining the enantiospecificity. The pictures of the clutches show that if there is a good fit, they will resist rotation with respect to one another during oxidative addition.

Predicting chirality. The quadrant rules of phosphines (Figure 4.7) leads to a high predictive value in a wide range of diphosphines (see section 4.3), provided also that similar substrates are being considered. The cited literature in reference 9 gives ample support for this. Deciding on the position of the quadrants may not always be straightforward and may require crystallographic and molecular modelling studies. Our simplification of axial and equatorial substituents also may need refining, as substituents may adopt intermediate positions, maintaining though the C_2 symmetry determined by crowded and less crowded quadrants [11].

The enantioselectivity depends also on the structure of the enamide substrate, especially the α-substituent, as was already reported by Knowles. In a few substrates the enantioselectivity even reverses! These exceptions to the general rule have found explanation in electronic effects [12]. Knowles reported that an electron withdrawing substituent at the α-position was important in order to obtain a high enantioselectivity, see Figure 4.12 [13].

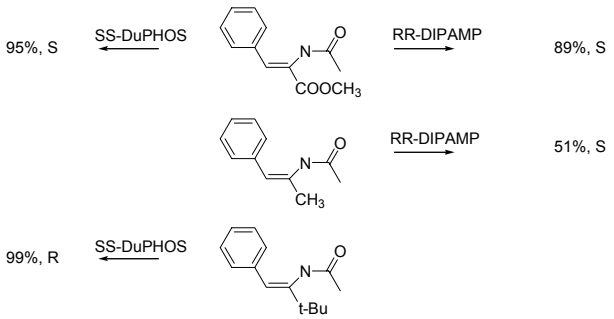

Figure 4.12. Influence of α-substituent on e.e.

When the α-substituent is an ester and (SS)-DuPHOS is used one obtained the S-enantiomer of the amide. An electron releasing group (t-butyl) in this instance completely reverses the chirality [14]! The explanation is that for electron-withdrawing α-substituents rhodium forms an α-alkyl bond, while for electron releasing α-substituents rhodium forms a β-alkyl benzylic bond as shown in Figure 4.13 [15].

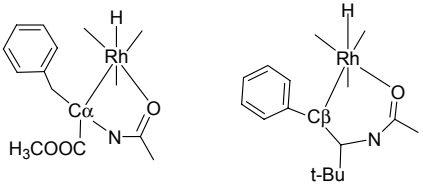

Figure 4.13. α- and β-alkyl hydrido rhodium intermediates

It should be noted that not the final stabilities, but rather the intermediates and transition states determine which isomer is formed. In the precursor alkene complex calculations show that already the respective α and β carbon atoms occupy the positions closest to the plane of coordination and that the respective barriers in both cases are indeed the lowest in the model studied [12].

4.2.3 Chloride versus weakly coordinating anions; alkylphosphines versus arylphosphines

One last remark concerning the two catalysts we have discussed in more detail, cationic rhodium catalysts and the neutral chloride catalyst of Wilkinson. The difference of the catalytic system discussed above from that of the Wilkinson catalyst lies in the sequence of the oxidative addition and the alkene complexation. The hydrogenation of the cinnamic acid derivative involves a cationic catalyst that first forms the alkene complex; the intermediate alkene (enamide) complex can be observed spectroscopically.

There are a few exceptions amongst the cationic complexes that also undergo oxidative addition of dihydrogen prior to alkene complexation. Alkylphosphines, raising the electron density on the rhodium cation, have been shown to belong to these exceptions, which seems logical [16]; electron-rich phosphine complexes can undergo oxidative addition of H_2 before the alkene coordinates to the rhodium metal.

4.2.4 Incubation times

Common precursors for the enantioselective hydrogenation with the use of "cationic" rhodium are the tetrafluoroborate salts of bis-alkadiene rhodium. As a solvent one often uses dichloromethane or methanol, in which tetrafluoroborate is indeed weakly or non-coordinating. The first alkadiene at rhodium is rapidly replaced in situ by the phosphorus ligands added.

4.3 Overview of chiral bidentate ligands

4.3.1 DuPHOS

Another type of useful ligands involves the so-called DuPHOS ligands developed by Burk at Dupont [17]. They consist of a variety of backbones and have the asymmetry in the phospholane ring. The DuPHOS ligands are extremely powerful and their fine-tuning by way of changing the backbone or, more importantly, the R-substituents on the phospholane ring has led to many successful applications. See Figure 4.12. Note the typical "propeller" C_2 symmetry.

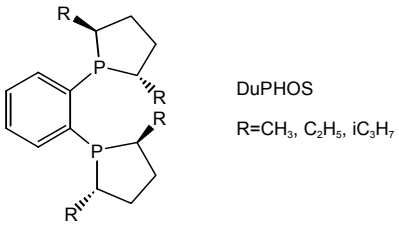

Figure 4.14. DuPHOS ligands

4.3.2 BINAP catalysis

During the first decade of asymmetric hydrogenation research (1970ties) all catalysts seemed to behave similarly, that is to say they all needed the amide auxiliary and all ligands were based on the same principles, containing a chiral bridge such as the famous DIOP ligand (Figure 4.6) or containing two chiral phosphorus atoms such as DIPAMP. In the meantime many new ligands have been developed, several of which are based on binaphthyl atropisomers. Axial (a)symmetry is the fourth way to introduce chirality in the ligand. One early example is BINAP (Figure 4.13). Applications of interest were, and still are, unsaturated precursors not containing a polar auxiliary ligand.

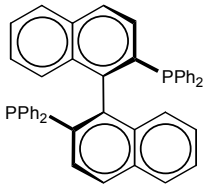

Figure 4.15. S-BINAP ligand

BINAP was introduced by Noyori [18]. It has been particularly explored for reduction with ruthenium catalysts. While the first generation rhodium catalysts exhibited excellent performance with dehydroamino acids (or esters), the second generation of hydrogenation catalysts, those based on ruthenium /BINAP complexes, are also highly enantioselective for other prochiral alkenes. An impressive list of rather complex organic molecules has been hydrogenated with high e.e.'s.

Firstly, the system will also hydrogenate enamides with high e.e., provided that the amide substituent and the one substituent at the other carbon are *cis* to one another. Secondly, the Ru(BINAP)$(RCO_2)_2$ catalyst gives enantioselective hydrogenation of acrylic derivatives, see the examples below for Naproxen and the like.

A third class of compounds that can be hydrogenated are ketones or aldehydes containing another polar group. The pressures used are high (50-100 bar H_2) but the enantioselectivities are excellent. The general reaction (R can be varied extensively) is shown in Figure 4.16. Since these ß-substituted ketones are easy to make, this method is extremely powerful for the synthesis of enantiomers. Furthermore, the catalyst is also very selective in the formation of diastereomers. An industrial application is shown below [19].

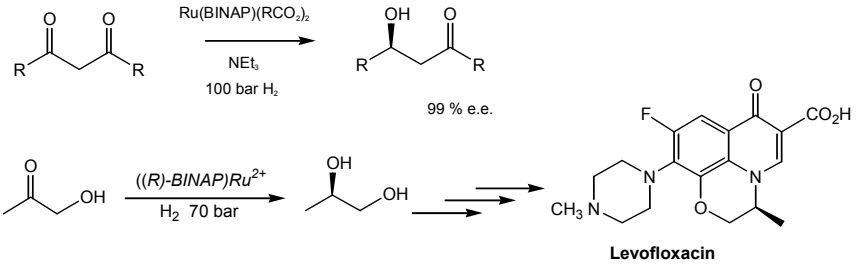

Figure 4.16. BINAP-Ruthenium hydrogenations of functionalised ketones

Applications. In the last decade a lot of research has been devoted to the development of catalytic routes to a series of asymmetric carboxylic acids that lack the acetamido ligand as additional functionality. In Figure 4.17 four are listed, which are important as anaesthetics for rheumatic diseases. Their sales in $ beat many bulk chemicals: the turnover of Naproxen (retail) in 1990 was $ 700 million for 1000 tons. S-Naproxen is now being produced by Syntex via resolution with a chiral auxiliary. The main patents from Syntex expired in the U.S. in 1993, the reason for a lot of activity to study alternative synthetic routes. Routes leading to an asymmetric centre are:

- asymmetric hydrogenation of an unsaturated acid,
- asymmetric carbohydroxylation of a styrene precursor,
- asymmetric hydroformylation of a styrene precursor and oxidation.

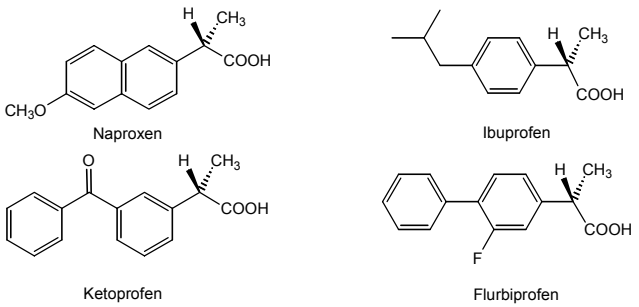

Figure 4.17. Pharmaceuticals of interest

Noyori using ruthenium complexes of the ligand BINAP has successfully accomplished asymmetric hydrogenation of molecules of this type. With this system a high enantioselectivity can be achieved (97%) albeit at rather high pressures (135 bar).

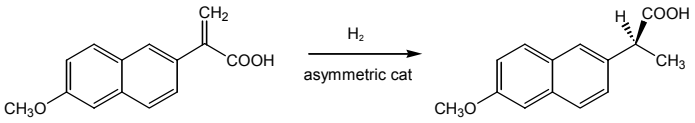

Figure 4.18. Monsanto route to S-Naproxen; hydrogenation step

Monsanto [20] reported a similar route using BINAP. This system operates at a much lower pressure. The starting material is the corresponding acetyl aromatic compound, which is reacted with CO_2 via an electrochemical reduction in 95% yield in a divided cell using a lead cathode and a sacrificial aluminium anode. The obtained aluminium salt is acidified and dehydrated to give the unsaturated (atropic type) acid precursor. This can be asymmetrically hydrogenated in methanol under 7 bar of H_2 with an enantiomeric excess of 98.5%. A turnover number of 3000 was reported. The reaction is shown in Figure 4.18. Other routes are available, for a review see Giordano [21].

4.3.3 Chiral ferrocene based ligands

The ligands discussed so far all contained C_2 symmetry. An important new class of ligands having C_1 symmetry was introduced by Togni [22] (see Figure 4.19). They can be easily made from an enantiomeric amine as the precursor in a few steps. Different substituents can be introduced at the phosphorus atoms. In addition to the chiral carbon atom the molecule has planar chirality as well. The chiral carbon atom is used to introduce the planar chirality, i.e. lithiation of the ferrocenyl amine takes place at a specific side of the amine at the ferrocene moiety.

Recently two new processes have come on stream utilising these ferrocene based chiral ligands [22]. The first one is the rhodium catalysed hydrogenation of an already chiral precursor for Biotin. A very high diastereoselectivity is obtained, 99%. The second example involves the asymmetric hydrogenation of an imine using an iridium catalyst. The enantioselectivity for the intermediate used for the production of Metolachlor is only 80%, but this is considered tolerable for an agrochemical (Figure 4.20). Nothing is known about the mechanisms of these reactions.

Asymmetric catalysis involving metal catalysed hydrogenations and isomerisations is becoming increasingly important in the production of pharmaceuticals, agrochemicals and flavours and fragrances. More examples of

asymmetric homogeneous catalysts used industrially can be found in the literature [23].

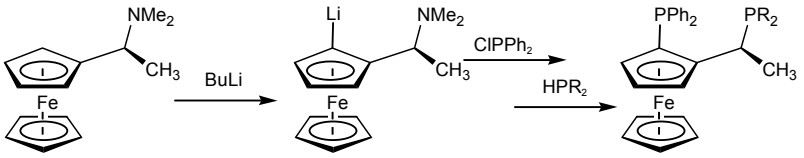

Figure 4.19. Ferrocene derived C_1 asymmetric chiral ligands

In summary, we have encountered five types of asymmetric phosphine ligands:
1. ligands containing a chiral phosphorus atom (DIPAMP),
2. ligands having a chiral backbone (DIOP),
3. ligands carrying chiral substituents on phosphorus (DuPhos),
4. atropisomeric ligands (BINAP), and
5. ligands having a planar asymmetry (JosiPhos).

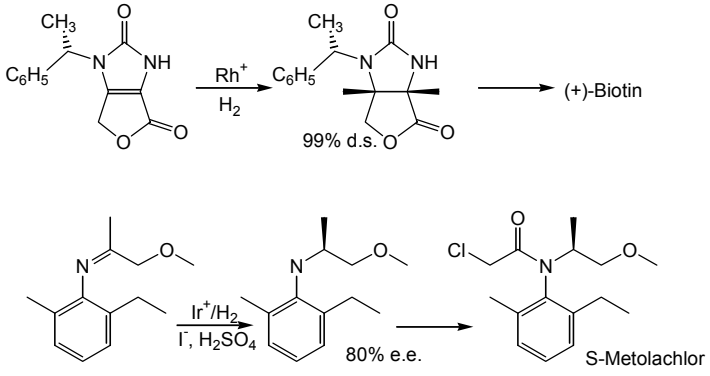

Figure 4.20. Commercialised asymmetric hydrogenations using ferrocene based ligands

4.4 Monodentate ligands

In the very early work on asymmetric hydrogenation research focussed on the use of monodentate phosphine ligands, preferably containing a chiral phosphorus atom as the chiral element. After the successful introduction of DIOP and DIPAMP it was soon realised that bidentate ligands containing a C_2 axis as the chiral element reduced the number of possible structures and thus simplified the planning and design of ligands. First of all, they would always

give *cis* donor complexes and therefore the two remaining, reacting entities, often involved in a migratory insertion reaction, will be forced to occupy *cis* positions as well. Secondly, the bridge between the two donors would enable the optimisation of the substituents at phosphorus, in such a way that effective chirality transfer can occur. However, there is no fundamental reason why either C_1 ligands or a proper combination of monodentates would not be able to give reactions with high enantioselectivity, even though the common view dictates that bidentates are most efficient.

The history of bidentates was preceded by some successes of monodentates, but these were soon overshadowed by DIPAMP. For instance Knowles reported first about the monodentate "homologues" of DIPAMP, which gave respectively 55% (PAMP) and 88% e.e. (CAMP) in the hydrogenation of 2-acetamidocinnamate [13,24] (Figure 4.21). Since 1999 a renaissance of monodentates has taken place.

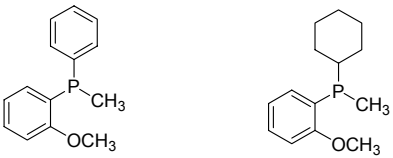

PAMP CAMP

Figure 4.21. Early examples of monodentate chiral ligands

Breakthroughs that took place around the year 2000 have shown, in contrast to the common view, that indeed chiral monodentate phosphorus ligands can also lead to high enantioselectivities in a number of asymmetric hydrogenations. In the years following, monophosphines, monophos-phonites, monophosphoramidites, and monophosphites have been successfully used in the enantioselective hydrogenation of α-dehydroamino acids and itaconic acid derivatives [25].

Phosphoramidites are probably the most versatile ligands in this series as in amidites the substituents at the nitrogen atom are in close proximity to the metal centre and also the substituents could carry chiral centres. In Figure 4.22 we have depicted the simplest derivative, named "Monophos", which is highly efficient for asymmetric hydrogenation but for a variety of other reactions as well. The ligand is much easier to make than most, if not all, chiral bidentate phosphine ligands and surely commercial applications will appear.

A DSM's Monophos sample-kit of ligands as developed by Feringa, de Vries, and co-workers is commercially available from Strem Chemicals (as well as various kits of Solvias ligands, such as Josiphos).

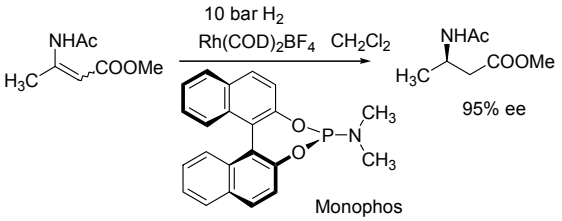

Figure 4.22. Monophos as monodentate ligand in rhodium catalysed asymmetric hydrogenation

In contrast to CAMP and PAMP, monomeric analogues of DIPAMP, the closest bidentate analogues of Monophos give a much slower reaction and a lower e.e. [26]! Thus, the structure of the complex containing two monodentates, even if one might assume that the smallest groups, i.e. the methyl groups at nitrogen, will point to the space in between the two ligands, is definitely not the same as that of a bidentate having the nitrogen atoms directed toward one another via the ethylene bridge, see Figure 4.23.

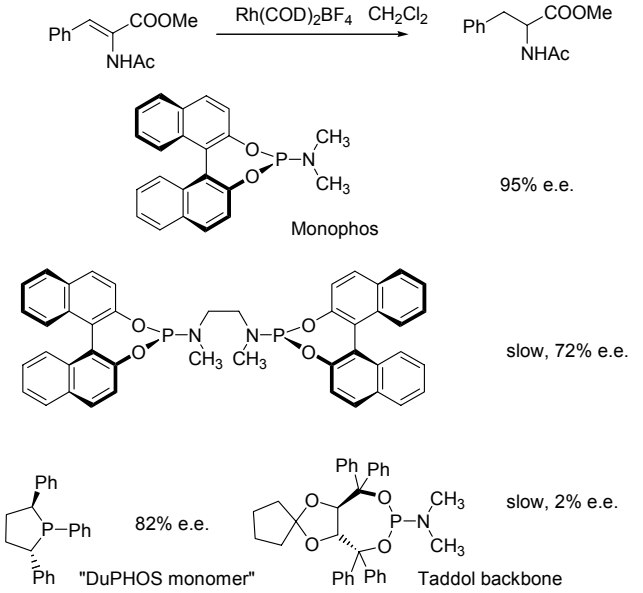

Figure 4.23. Related bisphosphorusamidite of Monophos and a TADDOL based amidite

The BINOL substituent seems to be crucial; firstly the related phosphites and phosphinites function just as well as the amidites, and secondly the bidentate BINOL based phosphorusamidite performs reasonably well compared to other groups. So far, all other substituents at oxygen, such as TADDOL, give low e.e.'s. As an indication that BINOL amidites are not

unique we added to Figure 4.23 a formal "monomer" of DuPHOS (Figure 4.14), reported by Fiaud, that also gives a good e.e., 82%, despite not yet being optimised for substituent effects [25].

4.5 Non-linear effects

The observation of non-linear effects (NLE) is a phenomenon regularly studied in asymmetric catalysis and we will discuss it briefly here. The possibility of such an effect during a chemical reaction was first considered and observed by Feringa and Wynberg [27]. Kagan discovered and explained the importance of non-linear effects in enantioselective, homogeneous catalysis or other reactions that involve chiral auxiliaries [28]. It is relevant to catalysts containing more than one monodentate ligand, or complexes that form dimers or oligomers. Assume, we have a chiral catalyst M^R that gives a product P^R with an e.e. of 100%, provided the optical purity of the catalyst is also 100%. If we now test a catalyst with an e.e. of only 50%, our product will also show an e.e. of 50%, because the two catalyst components M^R (75%) and M^S (25%) will have the same activity, and thus we produce P^R (75%) and P^S (25%) in the same ratio, and thus the e.e. of our product is 50%. A plot of the e.e. of the catalyst versus the e.e. of the product will be linear, curve **b** in Figure 4.24.

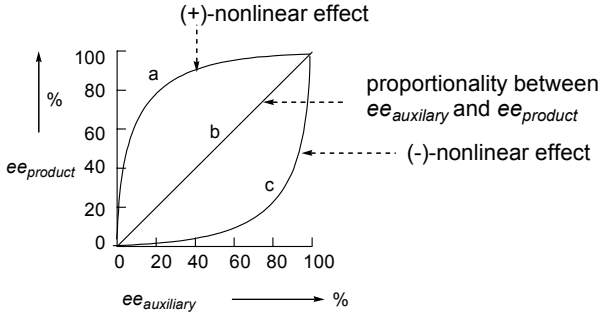

Figure 4.24. Non-linear effects in enantioselective catalysis

Now assume that our catalyst has the structure ML_2 and for the sake of simplicity the catalyst produces purely P^R if the two ligands are both L^R, in complex ML^R_2. In this case, if one now uses a mixture of enantiomers for the ligand a new situation arises as we form three complexes: ML^R_2, ML^S_2, and ML^RL^S. The racemic ones (RR and SS) have the same free energies, but the meso complex has a different free energy. When a ligand with an e.e. of 50% is used, with R as the major enantiomer, the stabilities of the two complexes determines how much of the racemic pair and how much of the meso complex will be formed. First, we keep it very simple, and assume that the meso is

extremely stable. In solution we will find 50% of ML^RL^S and 50% of ML^R_2. These two catalysts will also have different catalytic activities. If the meso complex would have zero activity, we would make pure P^R (!), even though our ligand has an e.e. of 50% only. Since we have less catalyst the rate will drop with the e.e. of the ligand, but at all times we would make an enantiomerically pure product [29]. This is called a positive non-linear effect (curve **a**, but the curve represents a less extreme situation). The reverse might also happen; if the meso complex is more active than the racemic complex, then the e.e. found in the product will be lower than the e.e. of L. This is called a negative non-linear effect (curve **c**). In practice the effects are never so severe. MonoPhos, for instance, shows a slight non-linear effect; a ligand e.e. of 50% gives a product having an e.e. of 60% in the hydrogenation of itaconic acid [26].

A similar situation can occur when the chiral complex (containing a chiral bidentate for instance) can form dimeric species. These dimers may either be the catalyst or just an inactive resting state. Since free energies and rate constants for "meso" and "racemic" dimeric species may differ, non-linear behaviour of e.e. of ligand versus e.e. of product can result.

L-699,392, Merck's drug for the treatment of chronic asthma, is an example of asymmetric amplification on an industrial scale (see Figure 13.19). The ketone reduction can be carried out stoichiometrically with a borane-(–)-α-pinene reagent. The terpene natural products are often mixtures of isomers and enantiomers. A reagent prepared from 98% optically pure (–)-α-pinene gives a product e.e. of 97%, but a reagent prepared from less expensive 70% optically pure (–)-α-pinene yields a product e.e. of 95%, which can be pushed to >99.5% by using an excess [30].

4.6 Hydrogen transfer

For fine-chemical applications the use of hydrogen pressure may be disadvantageous because of investment in high-pressure equipment and safety concerns and therefore other routes have been considered for hydrogenation of alkenes and ketones. For ketones and esters in the organic laboratory a variety of stoichiometric reductions are available, but the use of borohydridic and aluminium hydridic reagents on a large scale is not attractive either. The reason being the tedious or even dangerous work-up needed because occlusion of reactive hydrides occurs, as we also know from small-scale laboratory experiments.

Another method, in particular for the preparation of alcohols from ketones involves the transfer of hydrogen from a hydrogen donor. The classic example is the commercially applied Meerwein-Ponndorff-Verley reaction, which uses stoichiometric amounts of $Al(O^iPr)_3$ to produce acetone and the alkoxides of the alcohols desired [31]. The catalytic version of this reaction, employing

complexes of iridium, rhodium, ruthenium, etc. containing dinitrogen ligands has been known for many years and TON's up to one million have been reported [32]. The reaction scheme is presented in Figure 4.25.

The product is an equilibrium mixture and an excess of 2-propanol must be used to obtain high yields. Ammonium formate or formic acid have also been used as the hydrogen donor and now the reaction to the alcohol is complete, because the thermodynamics are more favourable and because CO_2 leaves the reaction medium.

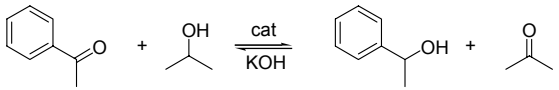

Figure 4.25. Hydrogen transfer reaction for 2-propanol and benzophenone

Since 1980 the interest in this reaction increased because enantiospecificity was introduced and much more valuable products could be made. A wide variety of ligands was tested, such as chiral dipyridines, phenanthrolines, diphosphines, aminoalcohols, bis-oxazolines, bis-oxazolines with a third donor atom in the centre, bis-thioureas, diamines, etc [33]. In 1981 the highest e.e. reported was still only 20%. For many years the best results were obtained with chiral diimines and phenanthrolines but e.e.'s were below 70% [34]. Pfaltz introduced bis-oxazolines for this reaction and obtained e.e.'s as high as 91% [35] in 1991.

The most important breakthrough was reported by Noyori in 1996 [36], which involved the use of a ruthenium complex containing a chiral, substituted amine and a cymene ligand, see Figure 4.26. Surprisingly the aromatic cymene moiety remains bonded to ruthenium throughout the catalytic cycle. In the following we will see that in the most likely mechanism the protons attached to the nitrogen atoms play an active role.

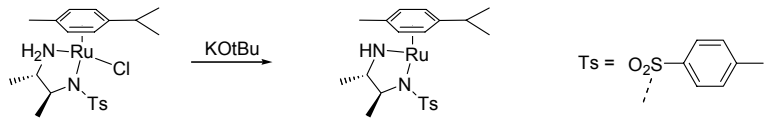

Figure 4.26. Noyori's H-transfer pre-catalyst and the reactive intermediate

Two mechanisms have been put forward, one involving β-hydride elimination and migratory insertion reactions, and the other one involving a direct, concerted transfer of the two hydrogen atoms from the alcohol donor to the reactive intermediate complex and vice versa donation to the ketone. Both pathways assume a heterolytic character for the overall transfer; this is to say

that the hydrogen atom at oxygen is transferred as a proton and the hydrogen atom bonded to carbon obtains a hydridic character in the transfer process. In Figure 4.27 the concerted mechanism as proposed by Noyori is shown [37]. Species **a** is a 16-electron species but the amides have the possibility to donate more electrons to ruthenium. The driving force to form the transient intermediate **b** is the hydrogen bond between the alcohol and the amide nitrogen atom. The steps on the left are simply the reverse of the steps on the right and thus we need only half of the reaction scheme, provided that we change the ketone or alcohol in the scheme. The peculiar feature of the mechanism is that the ketone substrate does not coordinate to the metal, as we are used to in organometallic mechanisms.

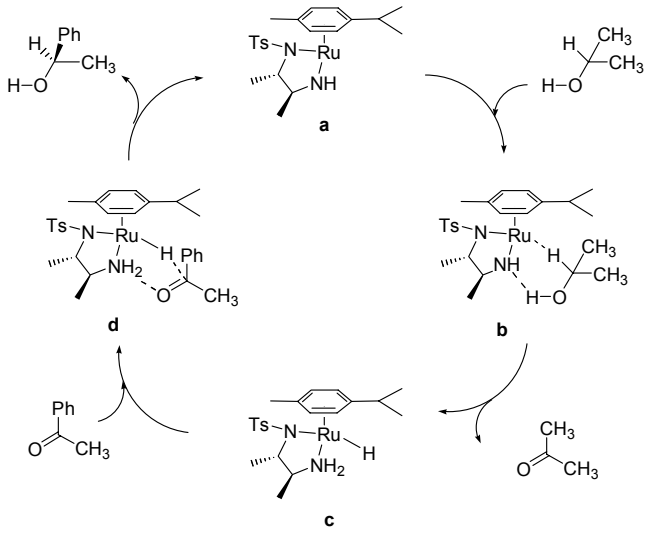

Figure 4.27. Concerted mechanism for hydrogen transfer from alcohol to complex and from complex to ketone

Such a heterolytic mechanism could also apply to the addition of dihydrogen to a metal centre, in which the base now is internal (part of the complex) rather than an external base, such as NEt_3 that attacks the activated dihydrogen molecule (Figure 2.31). This mechanism may operate in heterogeneous metal oxide catalysts and has perhaps been proposed a number of times in literature, but we are aware of only one example for a homogeneous catalyst (Figure 2.32) [38]. For the Noyori catalyst containing both a cymene ligand and a diamine (amine/amide) the number of electrons may exceed 18 when the ketone coordinates to the hydride intermediate, but this can be released by a slippage of the cymene to an η^2 binding mode instead of the η^6 conformation [39].

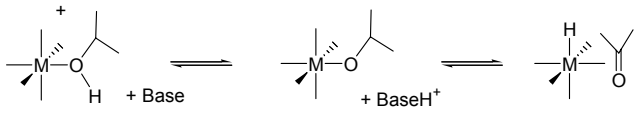

Figure 4.28. Simplified scheme for the hydride mechanism for hydrogen transfer

Clearly, in the related catalysts containing just simple bidentate phosphines, dipyridines, or bis-oxazolines the concerted, heterolytic transfer cannot take place in the same way, unless we invoke an alkoxide or other anion as the proton-receiving moiety. In Figure 4.28 we have presented a simplified scheme for the hydride/proton mechanism for hydrogen transfer using an "external" base.

A classic mechanism using metal dihydrides has been proposed initially [33]. This scheme can also account for hydrogen exchange in which alkanes and alkenes are the reactants and products. In this mechanism, both O-H and C-H hydrogen atoms of the alcohol are transferred to the metal, generating a metal dihydride species, most likely via an oxidative addition [40]. It has been shown that under basic conditions $RuCl_2(PPh_3)_3$ in 2-propanol is easily converted into $RuH_2(PPh_3)_3$. If a dihydride is an intermediate the two hydrogen atoms to be transferred become equivalent when they are hydrides.

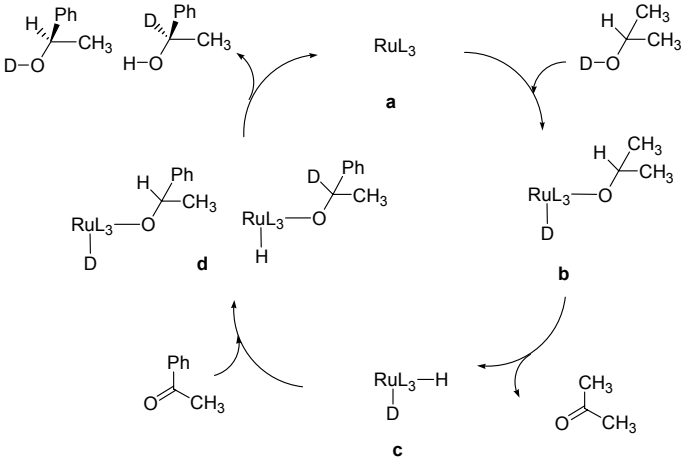

Figure 4.29. Dihydride mechanism for hydrogen transfer

Many experiments with alcohols containing O-deuterated or C-deuterated species have shown that in several, older catalysts indeed an exchange between these two positions occurs and that the hydrogen atoms originating from either carbon or oxygen in the alcohol "do not remember" from which atom they originate. Thus, as shown in Figure 4.29, *d*-O-2-propanol will give a mixture of

O-deuterated and C-deuterated phenetyl alcohol, perhaps with a slight deviation due to an isotope effect. This has indeed been observed. In other catalysts though, deuterium stemming from oxygen returns to the next oxygen atom. If the latter is observed, a Noyori type mechanism is proposed. We do not fully agree with this, because in a "Noyori type intermediate" exchange of hydrogen and deuterium might occur via a dihydrogen complex as shown in Figure 4.30. Partial reorganisation of this type may explain the many non-conclusive experiments in this chemistry. Also, in older catalysts more species may be present and other reactions leading to exchanges may occur.

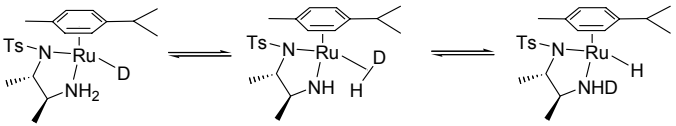

Figure 4.30. Dihydrogen complex interchanging H and D

A more recent isotope study has been conducted with the use of the actual Noyori catalyst by Casey and Johnson [41]. They studied the kinetic isotope effect by ^{1}H NMR spectroscopy at –10 to –30 °C for the reaction of d_6, d_7 (CH/OD and CD/OH), d_8 isotopically substituted propan-2-ol and 4-phenylbut-3-yn-2-none. The catalyst and the reaction are shown in Figure 4.31.

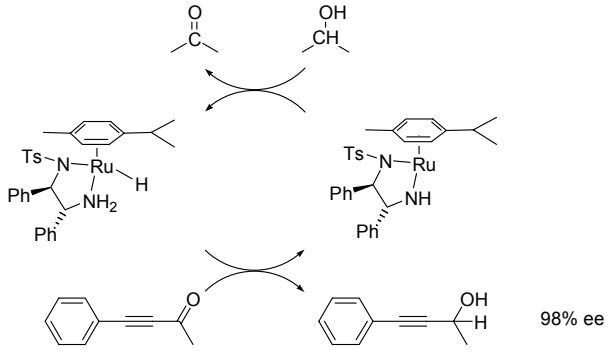

Figure 4.31. Catalyst used for determining the kinetic isotope effect

The isotope effects for transfer of hydrogen were 1.79 for transfer from OH to N and 2.86 for transfer from CH to ruthenium. The isotope effect for transfer of the doubly labelled material (d_8 2-propanol) was 4.88, within the experimental error. If the hydrogen atoms would be transferred in separate

steps, the overall isotope effect would have been close to either one of the two isotope effects observed, namely the one that is rate-determining. These isotope effects provide convincing evidence for a mechanism involving concurrent transfer of hydrogen from oxygen to nitrogen and from carbon to ruthenium.

A commercial application is as yet not known, but in view of the advantages compared to hydrogenation several companies have new processes in the development stage. In Chapter 13, Figure 13.19, an example is shown for the synthesis of Merck's drug for the treatment of chronic asthma: L-699,392, which involves two Heck reactions and one enantiospecific hydrogenation reaction with a stoichiometric asymmetric borohydride reagent (section 4.5) [30]. For the latter Noyori reported a catalytic hydrogen transfer reaction with 92% e.e. using triethylamine- formic acid and ruthenium as a catalyst [42].

References

1 Jardine, F. H.; Osborn, J. A.; Wilkinson, G.; Young, J. F. *Chem. Ind. (London)* **1965**, 560; *J. Chem. Soc. (A)* **1966**, 1711.
2 Halpern, J.; Okamoto, T.; Zakhariev, A. *J. Mol. Catal.* **1976**, *2*, 65. Halpern, J.; Wong, C. S. *J. Chem.Soc. Chem. Commun*. **1973**, 629.
3 O'Connor, C.; Wilkinson, G. *Tetrahedron Lett.* **1969**, *18*, 1375.
4 Knowles, W. S.; Sabacky M. J.; Vineyard, B. D. *Adv. Chem. Ser.* **1974**, *132,* 274.
5 Kagan, H. B.; Dang, T.-P. *J. Am. Chem. Soc.* **1972**, *94,* 6429.
6 Brown, J. M.; Evans, P. L. *Tetrahedron,* **1988**, *44,* 4905.
7 Halpern, J. *Science,* **1982**, *217,* 401; Chan, A. S. C.; Pluth, J. J.; Halpern, J. *J. Am. Chem. Soc.* **1980**, *102,* 5922.
8 Brown, J. M.; Chaloner, P. A. *J. Am. Chem. Soc.* **1980**,*102,* 3040.
9 Armstrong, S. K.; Brown J. M.; Burk, M. J. *Tetrahedron Lett.* **1993**, *34,* 879. Giovannetti, J. S.; Kelly C. M.; Landis, C. R. *J. Am. Chem. Soc.* **1993**, *115,* 4040. Kimmich, B. F. M.; Somsook E.; Landis, C. R. *J. Am. Chem. Soc.* **1998**, *120,* 10115. Landis C. R.; Brauch, T. W. *Inorg. Chim. Acta,* **1998**, *270,* 285. Feldgus, S.; Landis, C. R. *J. Am. Chem. Soc.* **2000**, *122,* 12714.
10 Kyba, E. P.; Davis, R. E.; Juri P. N.; Shirley, K. R. *Inorg. Chem.* **1981**, *20,* 3616.
11 Dahlenburg, L. *Eur. J. Inorg. Chem.* **2003**, 2733.
12 Feldgus, S.; Landis, C. R. *Organometallics,* **2001**, *20*, 2374.
13 Vineyard, B. D. Knowles, W. S.; Sabacky M. J.; Bachman, G. L.; Weinkauff, D. J. *J. Am. Chem. Soc.* **1977**, *99,* 5946.
14 Burk M. J.; Casy, G.; Johnson, N. B. *J. Org. Chem.* **1998**, *63,* 6084.
15 Gridnev, I. D.; Higashi, N.; Inamoto, T. *J. Am. Chem. Soc.* **2000**, *122,* 10486.
16 Gridnev, I. D.; Higashi, N.; Asakura, K.; Inamoto, T. *J. Am. Chem. Soc.* **2000**, *122,* 7183.
17 Burk M. J.; Feaster, J. E. *J. Am. Chem. Soc.* **1992**, *114,* 6266. Burk, M. J. *J. Am. Chem. Soc.* **1991**, *113,* 8518.
18 Miyashita, A.; Yasuda, A.; Takaya, H.; Toriumi, K.; Ito, T.; Souchi, T.; Noyori, R. *J. Am. Chem. Soc.* **1980**, *102,* 7932.
19 Noyori, R. *Acta Chem. Scand,* **1996**, *50*, 380.
20 Chan, A.S.C. US Patent 4,994,607 (to Monsanto) 1991. Chan, A. S. C.; Chen, C. C.; Yang, T. K.; Huang, J. H.; Lin, Y. C. *Inorg. Chim. Acta,* **1995**, *234,* 95.

21 Giordano, C.; Villa, M.; Panossian, S. Chapter 15 in Chirality in Industry, Ed. Collins, A. N.; Sheldrake G. N.; Crosby, J. **1992**, Wiley.
22 Togni, A. *Angew. Chem. Int. Ed. Engl.* **1996***, 35,* 1475. Blaser H.-U.; Spindler, F. *Top. Catal.* **1998***, 4,* 275. Togni, A.; Breutel, C.; Schnyder, A.; Spindler, F.; Landert, H.; Tijani, A. *J. Am. Chem. Soc.* **1994***, 116,* 4062.
23 Catalytic Asymmetric Synthesis, Ojima, I. Ed. VCH Publishers, New York **1993**. Asymmetric Catalysis in Organic Synthesis; Noyori, R. Ed. John Wiley and Sons, Inc. New York, **1994**.
24 Knowles, W. S.; Sabacky M. J.; Vineyard, B. D. *J. Chem. Soc. Chem. Commun.* **1972***,* 10.
25 Peña, D.; Minnaard, A. J.; de Vries, J. G.; Feringa, B. L. *J. Am. Chem. Soc.* **2002**, *124*, 14553. Komarov, I. V.; Börner, A. *Angew. Chem., Int. Ed.* **2001***, 40,* 1197. Guillen, F.; Fiaud, J.-C. *Tetrahedron Lett.* **1999**, *40*, 2939. Claver, C.; Fernandez, E.; Gillon, A.; Heslop, K.; Hyett, D. J.; Martorell, A.; Orpen, A. G.; Pringle, P. G. *Chem. Commun.* **2000**, 961. van den Berg, M.; Minnaard, A. J.; Schudde, E. P.; van Esch, J.; de Vries, A. H. M.; de Vries, J. G.; Feringa, B. L. *J. Am. Chem. Soc.* **2000**, *122*, 11539. Reetz, M. T.; Mehler, G. *Angew. Chem., Int. Ed.* **2000**, *39*, 3889.
26 Van den Berg, M.;p Minnaard, A. J.; Haak, R. M.; Leeman, M.; Schudde, E. P.; Meetsma, A.; Feringa, B. L.; de Vreis, A. H. M.; Maljaars. C. E. P.; Willans, C. E.; Hyett, D.; Boogers, J. A. F.; Hendrickx, H. J. W.; de Vries, J. G. *Adv. Synth. Catal.* **2003**, *345*, 308.
27 Wynberg, H.; Feringa, B. *Tetrahedron* **1976***, 32*, 2831.
28 Puchot, C.; Samuel, O.; Duñach, E. Zhao, S.; Agami, C.; Kagan, H. B. J. *Am. Chem. Soc.* **1986***, 108,* 2353. Girard, C.; Kagan, H. B. *Angew. Chem. Int. Ed. Engl.* **1998***, 37*, 2922.
29 D. G. Blackmond, *Acc. Chem. Res.* **2000***, 33*, 402. Blackmond, D. G. *Adv. Synth. Catal.* **2002***, 344*, 156.
30 King, A. O.; Corley, E. G.; Anderson, R. K.; Laresen, R. D.; Verhoeven, T. R.; Reider, P. J.; Xiang, Y. B.; Belley, M.; Leblanc, Y.; Labelle, M.; Prasit, P.; Zamboni, R. J. *J. Org. Chem.* **1993**, *58,* 3731.
31 De Grauw, C. F.; Peters, J. A.; van Bekkum, H.; Huskens, J. *Synthesis*, **1994**, 1007.
32 Camus, A.; Mestroni, G.; Zassinovich, G. *J. Organometal. Chem.* **1980***, 184,* C10.
33 Zassinovich, G.; Mestroni, G.; Gladiali, S. *Chem. Rev.* **1992**, *92,* 1051.
34 Gladiali, S.; Pinna, L.; Delogu, G.; De Martin, S.; Zassinovich, G.; Mestroni, G.; *Tetrahedron: Asymmetry,* **1990**, *1,* 635.
35 Müller, D.; Umbricht, G.; Weber, B.; Pfaltz, A. *Helv. Chim. Acta* **1991**, *74*, 232.
36 Fujii, A.; Hashiguchi, S.; Uematsu, N.; Ikariya, T.; Noyori, R. *J. Am. Chem. Soc.* **1996***, 118,* 2521.
37 Noyori, R.; Hashiguchi, S. *Acc. Chem. Res.* **1997**, *30*, 97.
38 Van Leeuwen, P. W. N. M.; Roobeek, C. F.; Wife, R. L.; Frijns, J. H. G. *J. Chem. Soc. Chem. Commun.* **1986**, 31.
39 Petra, D. G. I.; Reek, J. N. H.; Handgraaf, J.-W.; Meijer, E. J.; Dierkes, P.; Kamer, P. C. J.; Brussee, J.; Schoemaker, H. E.; van Leeuwen, P. W. N. M. *Chem. Eur. J.* **2000***, 6*, 2818.
40 Pàmies, O.; Bäckvall, J.–E. *Chem. Eur. J.* **2001**, *7,* 5051.
41 Casey, C. P.; Johnson, J. B. *J. Org. Chem.* **2003**, *68*, 1998**.**
42 Fujii, A.; Hashiguchi, S.; Uematsu, N.; Ikariya, T.; Noyori, R. *J. Am. Chem. Soc.* **1996***, 118,* 2521.

Chapter 5

ISOMERISATION

The way to menthol

5.1 Hydrogen shifts

Insertion and β-elimination. A catalytic cycle that involves only one type of elementary reaction must be a very facile process. Isomerisation is such a process since only migratory insertion and its counterpart β-elimination are required. Hence the metal complex can be optimised to do exactly this reaction as fast as possible. The actual situation is slightly more complex due to the necessity of vacant sites, which have to be created for alkene complexation and for β-elimination.

As expected, many unsaturated transition metal hydride complexes catalyse isomerisation. Examples include monohydrides of Rh(I), Pd(II), Ni(II), Pt(II), Ti(IV), and Zr(IV). The general scheme for alkene isomerisation is very simple; for instance it may read as follows (Figure 5.1):

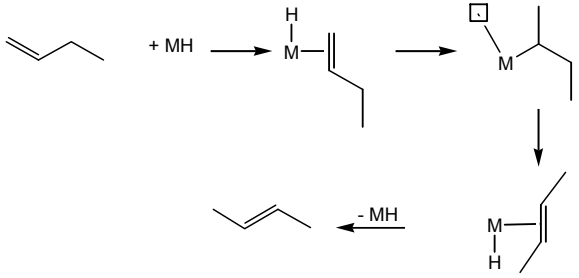

Figure 5.1. Simplified isomerisation scheme involving β-elimination

An excess of ligand, including CO, will often inhibit isomerisation. $HCo(CO)_4$, an unstable hydrido-carbonyl complex, belongs to the examples of catalysts also active in an atmosphere of CO. This is the only homogeneous catalyst being commercially applied, albeit primarily for its hydroformylation activity. Higher alkenes are available as their terminal isomers or as mixtures of internal isomers and the latter, the cheaper product, is mainly converted to aldehydes/alcohols by hydroformylation technology. Later we will see that the isomerisation reaction also plays a pivotal role in this system. Since 1990 several catalysts based on rhodium, platinum and palladium have been discovered that will also hydroformylate internal products to terminal aldehydes.

Isomerisation is also an important step in the DuPont process for making adiponitrile (Chapter 11) in which internal pentenenitriles must be converted to the terminal alkene. The catalyst is the same as that used for the hydrocyanation reaction, namely nickel(II) hydrides containing phosphite ligands.

Since the hydride based isomerisation is such a facile reaction it often occurs even when it is not desired. Thus, if hydrides play a role in the catalytic cycle and alkenes are present or formed during the reaction, isomerisation may represent an undesired side reaction. For instance in the Heck reaction (see Chapter 13) an alkene and a palladium hydride are formed and thus, if the alkene can isomerise, this may happen at the end of the cycle as a secondary process.

Another application of an isomerisation reaction can be found in the production of the third monomer that is used in the production of EPDM rubber, an elastomeric polymerisation product of Ethene, Propene and a Diene using vanadium chloride catalysts. The starting diene is made from vinylnorbornene via an isomerisation reaction using a titanium catalyst. The titanium catalyst is made from tetravalent salts and main group hydride reagents, according to patent literature.

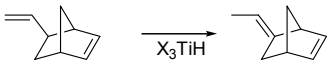

Figure 5.2. Isomerisation of vinylnorbornene by TiH species

Allylic mechanism. A second mechanism that has been brought forward involves the formation of allylic intermediates. The presence of a hydride on the metal complex is not required in this mechanism which can best be described as an oxidative addition of an "activated" C-H bond (i.e. an allylic hydrogen) to the metal. The allyl group can reconnect its hydrogen at the other end of the allyl group and the result is also a 1,3 shift of hydrogen. The allylic hydride variant is depicted in Figure 5.3. Another way of forming the allyl

metal intermediate involves a heterolytic splitting: a base abstracts H^+ from the co-ordinated alkene. This is a common method for the formation of π–allyl palladium complexes from Pd(II) salts, alkenes and a base. The mechanism in Figure 5.4 is the same as that shown in Figure 5.3 except for the temporary storage of the hydrogen atom which is now a proton while in the former case it is a hydride.

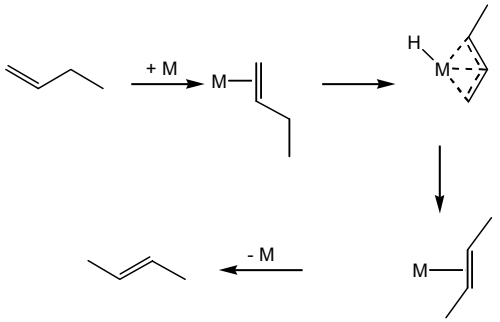

Figure 5.3. Simplified allylic isomerisation scheme

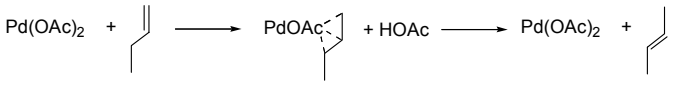

Figure 5.4. Palladium(II) acetate as an isomerisation catalyst

This reaction is very slow as the synthesis of palladium complexes via this route also requires elevated temperatures. Thus, the formation of hydrides that function as the isomerisation catalysts always remains a likely possibility.

5.2 Asymmetric Isomerisation

An important application of an isomerisation is found in the Takasago process for the commercial production of (-)menthol from myrcene. The catalyst used is a rhodium complex of BINAP, an asymmetric ligand based on the atropisomerism of substituted dinaphthyl (Figure 5.5). It was introduced by Noyori [1].

BINAP has been extensively used for the asymmetric hydrogenation, transfer hydrogenation and isomerisation of double bonds using both ruthenium and rhodium complexes.

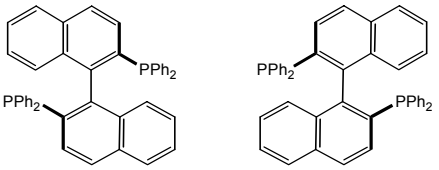

Figure 5.5. The two enantiomers of BINAP

The synthesis of menthol is given in the reaction scheme, Figure 5.6. The key reaction [2] is the enantioselective isomerisation of the allylamine to the asymmetric enamine. It is proposed that this reaction proceeds via an allylic intermediate, but it is not known whether the allyl formation is accompanied by a base-mediated proton abstraction or hydride formation.

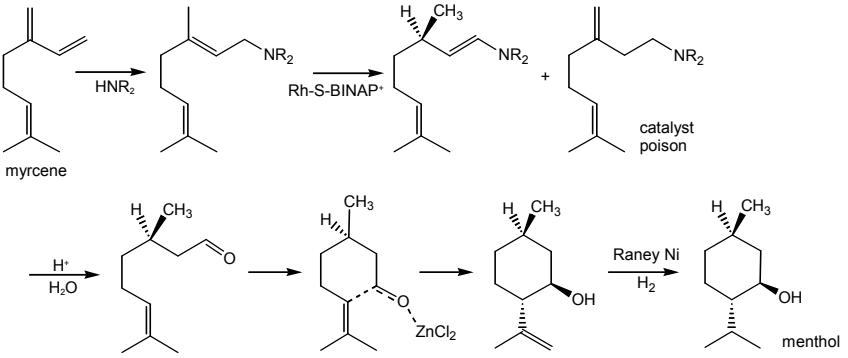

Figure 5.6. The Takasago process for (-)menthol

This is the only step that needs to be steered to the correct enantiomer, since the other two stereocentres are produced in the desired stereochemistry with the route depicted. Of the eight possible isomers only this one (1R,3R,4S) is important. After the enantioselective isomerisation the enamine is hydrolysed. A Lewis acid catalysed ring closure gives the menthol skeleton. In the six-membered ring of the intermediate all substituents can occupy an equatorial position and thus this intermediate is strongly favoured. In a subsequent step the isopropenyl group is hydrogenated over a heterogeneous Raney nickel catalyst.

Asymmetric catalysis involving metal catalysed hydrogenations and isomerisations is becoming increasingly important in the production of pharmaceuticals, agrochemicals and flavours and fragrances. More examples of asymmetric homogeneous catalysts used are found in reference [3].

Industrial practice. Both the ligand, S-BINAP, and rhodium are rather expensive (both ≈ € 50-150 per gram) and the turnover per mole of catalyst

should be high, > 50,000 [3]. A substantial amount of process work was needed in order to achieve an acceptable turnover-number (TON). Without pre-treatment the TON is only 100. When the substrate was treated with Vitride (sodium bis(2-methoxyethoxy)aluminium hydride) the TON raised to 1000. Removal of an amine isomer (catalyst poison, see Figure 5.6) was essential (TON 8,000). A tenfold increase was obtained by using a ligand to rhodium ratio of 2 instead of 1. Recovery with small losses eventually gave turnover numbers of 400,000. The method was commercialised in 1984. The main part of the annual production of 11,800 tonnes (1998) [4] is still obtained from the natural source, *Méntha arvensis*. The oil obtained from the glandular hairs contains, like in many plants of the Labiatae family, a wide variety of terpene-derived substances (menthol, menthol esters, menthone, pinenes, R,S-limonene, carvone), including other substances such as for example 3-octanone and 3-octanol. The aromatised form of menthol is thymol, a major constituent of thyme oil. The related pulegone (*Méntha pulegium*, pennyroyal oil) is a poison and its level in food is kept below 20 ppm.

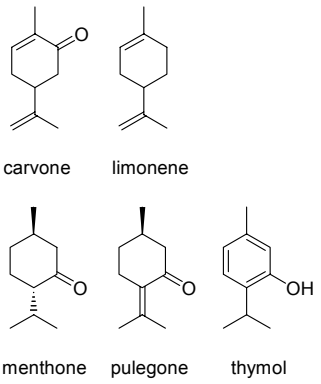

Figure 5.7. Méntha arvensis

5.3 Oxygen shifts

The isomerisation of allyl and propargylic alcohols involves the 1,3-shift of an oxygen atom rather than a hydrogen atom. Isomerisation of allyl alcohols can be catalysed by a variety of metal oxo complexes and in this instance the reaction does not involve metal carbon bonds as we will see. One could imagine that allylic metal species can participate in isomerisation of allylic compounds, but for the alcohols themselves this is not an easy reaction. In chapter 13 reactions of allyl acetates and the like, which are more prone to

formation of metal allyl species, will be discussed. A shift of oxygen from carbon-1 in an allyl alcohol to carbon-3 will lead in most cases to an equilibrium and since substrate and product are very much alike this reaction cannot be pushed to completion by removing the product selectively, for instance. By producing silyl ethers or borate esters it appeared possible to shift the equilibrium and acceptable yields have been reported.

The mechanism for allyl alcohol isomerisation has been studied and the presence of alkoxy and oxo groups in the metal catalyst seems to be essential [5]. Not only vanadium, but also rhenium and molybdenum analogues are catalyst for this reaction. The mechanism is depicted in Figure 5.8. The substituents at oxygen can be alkyl groups or silyl groups.

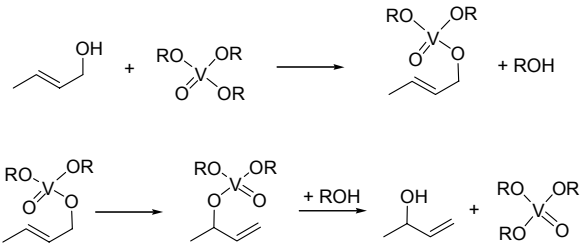

Figure 5.8. Mechanism of allyl alcohol isomerisation

If the alkene is an alkyne instead, we are dealing with a propargylic alcohol and now the thermodynamics are more favourable and the product is an enone. Commercial application is found in the production of citral from dehydrolinalool via vanadium-catalysed isomerisation (Figure 5.9). Note that the last step involves a transfer of hydrogen as well when the enol rearranges to the aldehyde!

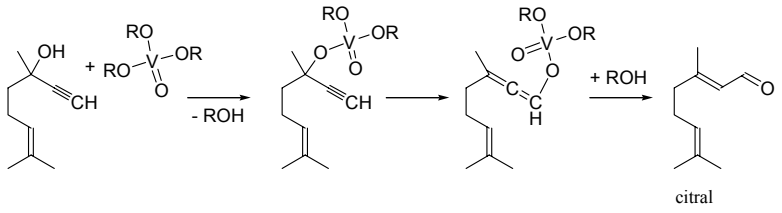

Figure 5.9. Citral from dehydrolinalool

References

1 Miyashita, A.; Yasuda, A.; Takaya, H.; Toriumi, K.; Ito, T.; Souchi, T.; Noyori, R. J. *Am. Chem. Soc.* **1980***, 102,* 7932.

2 Tani K.; Yamagata, Y.; Tatsuno, Y.; Yamagata, Y.; Tomita, K.; Agutagawa, S.; Kumobayashi, H.; Otsuka, S. *Angew. Chem. Int. Ed. Engl.* **1985***, 24,* 217.

3 Akutagawa, S. Chapter 16 in *Chirality in Industry,* Ed. Collins, A. N.; Sheldrake, G. N.; Crosby, J. **1992**, Wiley.

4 Clark, G. S. *Menthol, Perfumer & Flavorist*, **1998**, *23*, 33.

5 Chabardes, P.; Kuntz, E.; Varagnat, J. *Tetrahedron,* **1977***, 33,* 1775. Belgacam, J.; Kress, J.; Osborn, J. A. *J. Am. Chem. Soc.* **1992***, 114,* 1501. Bellemin-Laponnaz, S.; Le Nuy, J. P.; Osborn, J. A. *Tetrahedron. Lett.* **2000***, 41*, 1549. Bellemin-Laponnaz, S.; Le Nuy, J. *C. R. Chimie,* **2002**, *5,* 217.

Chapter 6

CARBONYLATION OF METHANOL AND METHYL ACETATE

Another textbook example

6.1 Acetic acid

Monsanto developed the rhodium-catalysed process for the carbonylation of methanol to produce acetic acid in the late sixties. It is a large-scale operation employing a rhodium/iodide catalyst converting methanol and carbon monoxide into acetic acid. At standard conditions the reaction is thermodynamically allowed,

$$CH_3OH + CO \rightarrow CH_3COOH \qquad \Delta G = -75 \text{ kJ mol}^{-1}$$

but without a catalyst, as so many carbonylation reactions, it would not take place at all.

Other methods for the preparation of acetic acid are partial oxidation of butane, oxidation of ethanal –obtained from Wacker oxidation of ethene–, bio-oxidation of ethanol for food applications, and we may add the same carbonylation reaction carried out with a cobalt catalyst or an iridium catalyst. The rhodium and iridium catalysts have several distinct advantages over the cobalt catalyst; they are much faster and far more selective. In process terms the higher rate is translated into much lower pressures (the cobalt catalyst is operated by BASF at pressures of 700 bar). For years now the Monsanto process (now owned by BP) has been the most attractive route for the preparation of acetic acid, but in recent years the iridium-based CATIVA process, developed by BP, has come on stream.

The two catalyst components are rhodium and iodide. Under the circumstances CO and water reduce RhI_3 to monovalent rhodium. A large

excess of iodide is present. Under the reaction conditions methanol and the iodide component form methyl iodide. Rhodium is present as the anionic species $RhI_2(CO)_2^-$. The mechanism reads (reactions 1 and 5 are equilibria):

$$CH_3OH + HI \rightleftharpoons CH_3I + H_2O \quad (1)$$

$$CH_3I + RhI_2(CO)_2^- \rightarrow CH_3RhI_3(CO)_2^- \quad (2)$$

$$CO + CH_3RhI_3(CO)_2^- \rightarrow CH_3C(O)RhI_3(CO)_2^- \quad (3)$$

$$CH_3C(O)RhI_3(CO)_2^- \rightarrow RhI_2(CO)_2^- + CH_3COI \quad (4)$$

$$CH_3COI + H_2O \rightleftharpoons CH_3COOH + HI \quad (5)$$

The percentage of the selectivity in methanol is in the high nineties but the selectivity in carbon monoxide may be as low as 90%. This is due to the shift reaction:

$$CO + H_2O \rightarrow H_2 + CO_2 \quad (6)$$

The mechanism of the shift reaction in this catalyst system involves the attack of hydroxide anion at coordinated carbon monoxide, forming a metallacarboxylic acid. Elimination of CO_2 gives a rhodium hydride species that can react with the proton stemming from water to give dihydrogen. Rhodium may be either Rh(I) or Rh(III) as the valence of the metal does not change during this process.

Thus, while water is an indispensable ingredient for the "organic" cycle (1 and 5), a high concentration of water causes the major loss of one of the feedstocks. Water is also made in situ together with methyl acetate from methanol and acetic acid. Not only water, but also HI is the cause of by-product formation:

$$CH_3RhI_3(CO)_2^- + HI \rightarrow CH_4 + RhI_4(CO)_2^- \quad (7)$$

$$RhI_2(CO)_2^- + 2\ HI \rightleftharpoons H_2 + RhI_4(CO)_2^- \quad (8)$$

Reactions 7 and 8 involve oxidation of rhodium(I) to rhodium(III). Reaction 8 can also be written as an oxidative addition of I_2 (formed thermally from 2 HI) to the Rh(I) complex. Rhodium(III) iodide (for convenience written as an anionic carbonyl complex) may precipitate from the reaction medium. It has to be converted to rhodium(I) again. This is done in the acetic acid process by water and carbon monoxide.

The mechanism for the reduction of rhodium(III) by CO and H_2O to give rhodium(I) again starts the same way as that for reaction (6), but now, if it

concerns Rh(III), after the hydride formation reductive elimination of HX occurs.

Other companies (e.g. Hoechst, now Celanese) have developed a slightly different process in which the water content is low in order to save CO feedstock [1]. In the absence of water it turned out that the catalyst precipitates. Also, the regeneration of rhodium(III) is much slower. The formation of the trivalent rhodium species is also slower because the HI content is much lower when the water concentration is low. The water content is kept low by adding part of the methanol in the form of methyl acetate. Indeed, the shift reaction is now suppressed. Stabilisation of the rhodium species and lowering of the HI content can be achieved by the addition of iodide salts (Li, ammonium, phosphonium, etc). Later, we will see that this is also important in the acetic anhydride process. High reaction rates and low catalyst usage can be achieved at low reactor water concentration by the introduction of tertiary phosphine oxide additives [1].

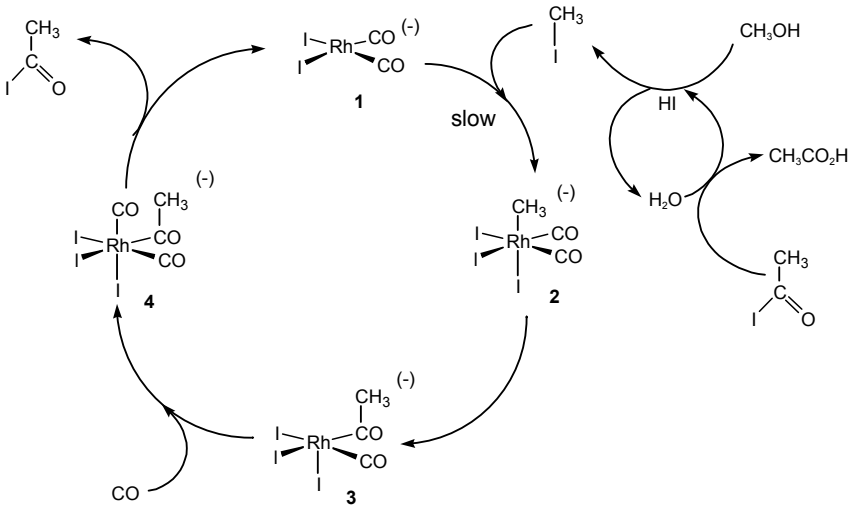

Figure 6.1. Monsanto carbonylation of methanol

Figure 6.1 shows the reaction sequence in the "cyclic" fashion. After the oxidative addition to form **2**, methyl migration takes place to give **3**. The coordination sphere of **3** is completed by another molecule of CO to give **4,** which undergoes reductive elimination of acetyl iodide while regenerating **1**. Acetyl iodide reacts with water in the "organic" cycle to give acetic acid and hydrogen iodide. One could imagine a direct attack of water at the acetyl group of **4** as the reaction producing acetic acid. There is no evidence for either mechanism as the kinetics for this part of the cycle do not show up in the rate

equation; in palladium chemistry it has been found that such a direct reaction is slow and ester or acid formation occurs via a reductive elimination type process (Chapter 12).

Kinetics and the isolation of intermediates

The rate-determining step in this process is the oxidative addition of methyl iodide to **1**. Within the "operating window" of the process the reaction rate is independent of the carbon monoxide pressure and independent of the concentration of methanol. The methyl species **2** formed in reaction (2) cannot be observed under the reaction conditions. The methyl iodide intermediate enables the formation of a methyl rhodium complex; methanol is not sufficiently electrophilic to carry out this reaction. As for other nucleophiles, the reaction is much slower with methyl bromide or methyl chloride as the catalyst component.

In situ IR studies [2] reveal the presence of $RhI_2(CO)_2^-$ only, as is to be expected since after the addition of MeI all steps are fast. Until 1991, the methyl-rhodium complex **2** had never been observed. Maitlis and co-workers [3], however, realised that the intramolecular migration reaction is a first order reaction while the oxidative addition is second order in Rh and MeI. The latter reaction can therefore be enhanced relative to the former by raising the concentrations. When the oxidative addition is carried out at 5–35 °C in neat MeI the methyl adduct $MeRh(CO)_2I_3^-$ can be observed both in IR and NMR spectroscopy. The IR data could be confirmed with ^{13}C NMR at –60 °C with $^{13}CH_3I$ and ^{13}CO. Two equivalent carbonyls are observed with a rhodium–carbon coupling constant of 60 Hz. The methyl carbon signal at –0.65 ppm shows a typical rhodium coupling constant of 14.7 Hz. (Figure 6.2). Furthermore, the kinetics of the reaction were measured. The kinetic data are in agreement with those found for the overall reaction under the conditions where the catalysis is carried out ($\Delta H^{\ddagger}$ 63 kJ mol^{-1} and $\Delta S^{\ddagger}$ –59 J mol^{-1} K^{-1}).

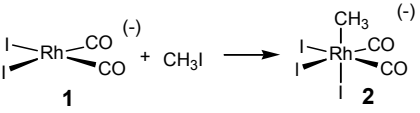

^{13}C NMR: two equivalent carbons with J_{Rh-C} = 60 Hz

^{13}C NMR: methyl group with J_{Rh-C} = 14 Hz at δ = -0.6 ppm

Figure 6.2. NMR data for the methyl intermediate **2** in the Monsanto process [3]

The CATIVA process

Other metals are also active under similar conditions using the same iodide based chemistry: iridium, nickel, and palladium have been described. BP has announced [4] that an improved process became operative in 1996 using

iridium (or a combination of iridium and another metal, usually ruthenium). The new system shows high rates at low water concentrations. The catalyst system exhibits high stability allowing a wide range of process conditions and compositions to be accessed without catalyst precipitation. In 2003 four plants are in operation using this new catalyst.

Indeed, in general the oxidative addition to iridium [5] is much faster than that to the corresponding rhodium complexes. Also the equilibrium is on the side of the trivalent state. Thus, as expected reaction (2) is much faster for iridium. In itself this does not mean that the iridium catalyst is therefore faster than the rhodium catalyst. As we have learnt before, the reductive elimination may be slower for iridium. Apparently, this situation has not yet been reached. Migration is now the slowest step [6]. This seems to be a common phenomenon for third row metals. For platinum complexes also the migration reactions are slower than those for palladium. In third row metals the metal-to-carbon σ-bonds are stronger, more localised, and more covalent than those in second-row metal complexes (a relativistic stabilisation of the Ir–CH_3 bond). One can imagine that a more diffuse, electron-rich, σ-bonded hydrocarbyl migrates more easily. Quantum-mechanical calculations based [7] on DFT showed indeed that the free energies of activation for the migration reaction are 116.3 kJ.mol^{-1} (Ir) and 72.2 kJ.mol^{-1} (Rh), in good agreement with the experimental estimates at 128.5 kJ.mol^{-1} (Ir) and 81.1 kJ.mol^{-1} (Rh).

In contrast to the rhodium process the most abundant iridium species, the catalyst resting state, in the BP process is not the Ir(I) iodide, but the product of the oxidative addition of MeI to this complex.

Two distinct classes of promoters have been identified for the reaction: simple iodide complexes of zinc, cadmium, mercury, indium, and gallium, and carbonyl complexes of tungsten, rhenium, ruthenium, and osmium. The promoters exhibit a unique synergy with iodide salts, such as lithium iodide, under low water conditions. Both main group and transition metal salts can influence the equilibria of the iodide species involved. A rate maximum exists at low water conditions, and optimisation of the process parameters gives acetic acid with a selectivity in excess of 99% based upon methanol. IR-spectroscopic studies have shown that the salts abstract iodide from the ionic methyl-iridium species and that in the resulting neutral species the migration is 800 times faster (Figure 6.3) [8].

The levels of liquid by-products formed are a significant improvement over those achieved with the conventional high water rhodium based catalyst system and the quality of the product obtained under low water concentrations is exceptional [4].

Transition metal complexes added might also play a role in aiding the reduction of iridium(III) species, but no evidence for this has been reported.

The catalyst, the way it is operated, is about 25% faster than the Monsanto rhodium catalyst. In addition, it was assumed that the oxidative addition is no longer rate-determining and that now the migration of the methyl group to the co-ordinated carbon monoxide is rate-determining (Figure 6.3).

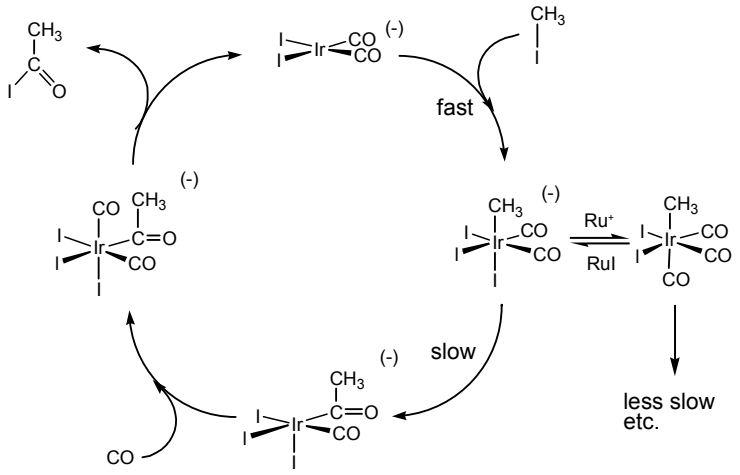

Figure 6.3. BP's CATIVA process

6.2 Process scheme Monsanto process

The rate equation for the Monsanto process under process conditions reads:

$$v = k\,.[Rh\,I_2(CO)_2^-].[CH_3I]$$

The two catalyst components are rhodium and iodide, which can be added in many forms. A large excess of iodide may be present. Rhodium is present as the anionic species $RhI_2(CO)_2^-$. Typically the rhodium concentration is 10 mM and the iodide concentration is 1.5 M, of which 20% occurs in the form of salts. The temperature is about 180 °C and the pressure is 50 bar. The methyl iodide formation from methanol is almost complete, which makes the reaction rate also practically independent of the methanol concentration. In other words, at any conversion level (except for very low methanol levels) the production rate is the same. For a continuous reactor this has the advantage that it can be operated at a high conversion level. As a result the required separation of methanol, methyl acetate, methyl iodide, and rhodium iodide from the product acetic acid is much easier.

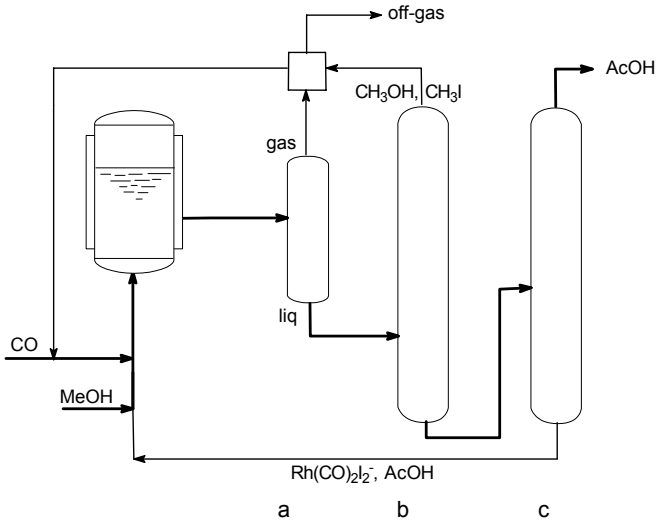

Figure 6.4. Process scheme Monsanto a= depressurisation, b= light ends removal, c= acetic acid distillation

For the separation of acetic acid from the catalysts components two routes can be envisaged: (i) removing the product as a gas from the reactor (stripping) or (ii) removing the liquid mixture from the high pressure reactor, releasing the pressure and accomplishing a distillation in a second vessel. The latter process scheme is presented in Figure 6.4. The liquid product mixture is taken to a depressuriser. The light ends are distilled off and recycled. An off-gas stream removes the carbon dioxide and methane formed. The product acetic acid is distilled off and the bottom of this column containing acetic acid, iodide, rhodium and heavy ends is fed back into the reactor.

Stripping has the technical advantage that the expensive rhodium catalyst remains in the reactor and the disadvantage that the least volatile component (acetic acid) has the lowest concentration of all components in the gas removed by stripping. Distillation as a separation method has the advantage that acetic acid is the most abundant component in the liquid, but now rhodium will be circulated in the system and will remain in the bottom of the distillation unit and it should not precipitate anywhere!

For a process it is very attractive if the reaction rate is independent of the concentrations of the educts. The conversion rate is constant over a wide range of concentrations, and the high rate is retained at a high conversion level. This means that distillation is carried out with a liquid with a very high product content.

Reactor materials. One drawback that could be mentioned is the high corrosivity of iodide. Hydrogen iodide is very corrosive, but the presence of iodide salts makes it even worse. Carbon monoxide will also react with many metals under the reaction conditions (30 bar of CO, 180 °C). Hastelloy-C is an inert material which is used in the laboratory. For the actual plants titanium cladded reactors have been mentioned as a possible solution.

Safety aspects. The toxicity of carbon monoxide, methyl iodide, and heavy metals is well known. The safety precautions to be taken for working with CO and high pressures are well recognised. It should be borne in mind that the MAC value for a "common" substance such as acetic acid is extremely low.

6.3 Acetic anhydride

In many applications acetic acid is used as the anhydride and the synthesis of the latter is therefore equally important. In the 1970's Halcon (now Eastman) and Hoechst (now Celanese) developed a process for the conversion of methyl acetate and carbon monoxide to acetic anhydride. The process has been on stream since 1983 and with an annual production of several 100,000 tons, together with some 10–20% acetic acid. The reaction is carried out under similar conditions as the Monsanto process, and also uses methyl iodide as the "activator" for the methyl group.

The reaction scheme follows that of the Monsanto process except for the "organic" cycle, in which acetic acid replaces water, and methyl acetate replaces methanol (Figure 6.5):

$$CH_3COOCH_3 + HI \rightleftharpoons CH_3COOH + CH_3I \quad (9)$$

$$CH_3COI + CH_3COOH \rightleftharpoons CH_3COOOCCH_3 + HI \quad (10)$$

Reaction (9) generates methyl iodide for the oxidative addition, and reaction (10) converts the reductive elimination product acetyl iodide into the product and it regenerates hydrogen iodide. There are, however, a few distinct differences [2,9] between the two processes. The thermodynamics of the acetic anhydride formation are less favourable and the process is operated much closer to equilibrium. (Thus, before studying the catalysis of carbonylations and carboxylations it is always worthwhile to look up the thermodynamic data!!!) Under standard conditions the ΔG values are approximately:

$$MeOAc + CO \rightarrow Ac_2O \qquad -10.5\ kJ.mol^{-1}$$

$$MeOH + CO \rightarrow AcOH \qquad -75\ kJ.mol^{-1}$$

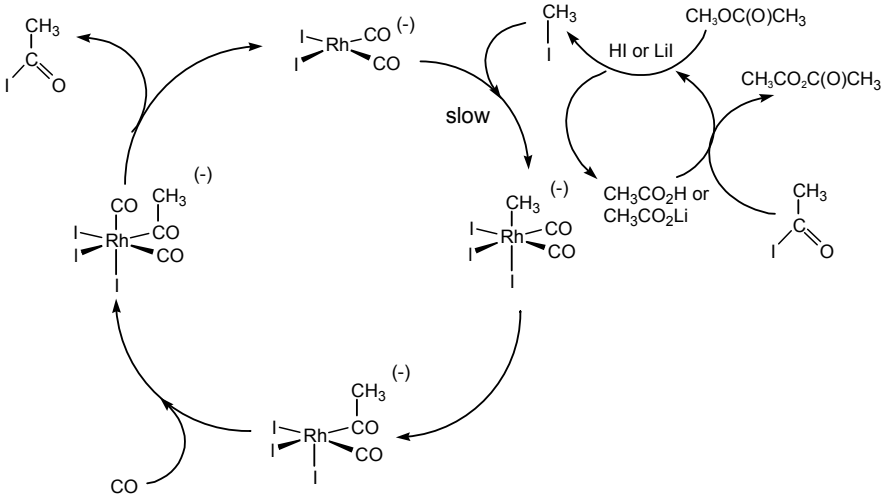

Figure 6.5. Eastman carbonylation of methyl acetate

Two more differences are:

(i). in the Eastman process 5% of H_2 is added to the carbon monoxide, and

(ii). the addition of cations such as Li^+ or Na^+ is necessary.

Re (i). If the reaction is run in the absence of H_2 it has an initiation period of 15 to 90 minutes at 180 °C at 50 bar. The activation energy measured is higher in the absence of dihydrogen (114 kJ.mol^{-1}). In the presence of dihydrogen the incubation is absent, and the activation energy is 63 kJ/mol, which is the same as that of the Monsanto process. (ΔH = 60.5 kJ.mol^{-1}, ΔS = –27 eu). The IR spectrum of the reaction mixture under operating conditions shows the characteristic absorptions of the $Rh(CO)_2I_2^-$ anion at 2055 and 1984 cm^{-1}. In the absence of hydrogen another absorption at 2100 cm^{-1} is also recorded which is assigned to the anion of trivalent rhodium, $Rh(CO)_2I_4^-$, and which disappears with the addition of hydrogen.

Not only does the initiation require hydrogen, but also later in the reaction it may be necessary to reduce rhodium(III) to rhodium(I), since methyl-rhodium(III) is being formed continuously in the reaction:

$$CH_3RhI_3(CO)_2^- + HI \rightarrow CH_4 + RhI_4(CO)_2^- \quad (11)$$

This protonation may, besides the desired CO insertion, also form inactive trivalent rhodium iodides. In the Monsanto acetic acid process the addition of the reducing agent H_2 is not required for two reasons:

- In the Monsanto acetic acid process (not in the Hoechst version) there is a lot of water present through the equilibrium between CH_3OH and HI

(reaction (1) in the scheme), which may act as a reducing agent directly with CO,

- or H_2 is formed in situ via a shift reaction.

Water also causes a change in the reaction medium, which may be advantageous. A drawback of the reducing medium in the Eastman process is that in addition to acetic anhydride, the by-product ethylidene diacetate is formed, $CH_3CH(AcO)_2$. This can be thermally decomposed to vinyl acetate and acetic acid, or it can be reduced to ethyl acetate, which in the recycle would lead eventually to propionic acid.

Re (ii). The "salt effect" is more intriguing. At low lithium concentrations (lithium is the most effective cation) the reaction is first order in the salt concentration and zero order in rhodium, methyl iodide, and carbon monoxide. The rate steeply increases with the lithium concentrations. At high lithium concentrations the rate dependencies equal the Monsanto process, i.e. first order in rhodium and methyl iodide, and zero order in CO. The metal salts are involved in two reactions:

$$AcI + MOAc \rightleftharpoons Ac_2O + MI \qquad (12)$$

$$MeOAc + MI \rightleftharpoons MeI + MOAc \qquad (13)$$

Reaction (12) ensures that acetyl iodide is converted to the product, because in the case that M=H the equilibrium lies to the left. The second reaction (13) is slow, and the equilibrium shifts to the right with decreasing size of the cation. With lithium as the cation, this reaction has the highest rate and it is most complete. (Li^+, K=0.388, k=8 $l.mol^{-1}.h^{-1}$; Na^+, K=0.04, k=2.6). Hence, this combination of reactions necessitates the use of LiI instead of HI, and it adds a third cycle to the reaction scheme, namely the lithium cycle, which must generate MeI. (In Figure 6.5 the “acid” cycle and the “salt’ cycle are drawn as two coinciding cycles). At low concentrations this cycle may be rate-determining.

The overall reaction represents an all syn-gas route to acetic acid and acetic anhydride. At present, in Europe, syn-gas is being produced from natural gas, but eventually it will represent a route from coal, the future feedstock for syn-gas.

6.4 Other systems

6.4.1 Higher alcohols

From the methanol process we already learnt that propionic acid is one of the by-products. It stems from the formation of ethanal, which is hydrogenated

to ethanol and this is carbonylated to propionic acid. In the cobalt process it is made in considerable quantities. Nevertheless, there exists no process for making higher homologues of acetic acid, which may reflect both the market situation and the absence of a good process.

A comparative study [10] into the Rh-catalysed carbonylation of ROH (R = Me, Et, Pr) shows that in all cases, the reaction rate is 1st order in both [Rh] and added [HI] and independent of CO pressure. The only Rh species observed by IR under catalytic conditions was **1**. The rates of carbonylation decreased in the stated order of R, with relative rates of 21:1:0.47, respectively at 170 °C. This order of the R-groups and the large differences between them is a common feature for organic reactions of this type. All the data are consistent with rate-determining nucleophilic attack by the Rh complex anion on the corresponding alkyl iodide.

6.4.2 Phosphine-modified rhodium catalysts

Oxidative addition to complex **1** is the slowest and rate-determining step in the reaction scheme and also it is a singular step, involving the conversion of the catalyst resting state to a more reactive **2**. An obvious way to obtain a faster catalyst is the substitution of carbonyl ligands in **1** by electron-donating phosphines, as organometallic chemistry tells us this variation never fails. Indeed, several variants that are indeed faster are known [11], but none of them has found application.

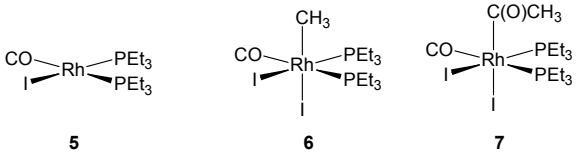

Figure 6.6. Phosphine modified rhodium catalyst for AcOH synthesis

Under mild conditions catalyst **5**, $[RhI(CO)(PEt_3)_2]$, is 1.8 times faster than **1** in the carbonylation of methanol in the presence of CH_3I and water at 150 °C [12]. The reaction is first order in $[CH_3I]$ and zero order in CO pressure. Stoichiometric studies show that the rate of oxidative addition of CH_3I to **5** is 57 times faster than to **1** at 25 °C. **6** can be isolated and characterised. In CH_2Cl_2, **7** reductively eliminates CH_3COI. **5** reacts with CO to give $[RhI(CO)_2(PEt_3)_2]$. The phosphine complex degrades to **1** during the course of the reaction. Catalyst degradation occurs via $[RhHI_2(CO)(PEt_3)_2]$, formed by oxidative addition of HI to **5**, which reacts further with HI to give $[RhI_3(CO)(PEt_3)_2]$ from which $[Et_3PI]^+$ reductively eliminates and is hydrolysed to give Et_3PO.

Bidentate phosphines perform somewhat better as regards stability, because less free phosphine is present due to the higher complex binding constants. In a related reaction the $Rh(CO)_2(acac)Ph_2P(CH_2)_3PPh_2$ catalyst gives high rates (100-200 turnovers h^{-1}) and selectivities in the reductive carbonylation of methanol to acetaldehyde, which is comparable to the best cobalt catalysts, but at a much lower temperature (140 °C) and pressure (70 bar) [13]. Compounds **8** and **9** have been identified as intermediates, but the stability during long reaction times has not been reported [14]. Unsaturated complex **8** possesses a distorted five-coordinate geometry that is intermediate between square pyramid and trigonal bipyramidal structures.

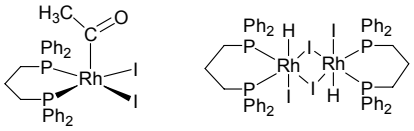

8 **9**

Figure 6.7. Identified intermediates for catalyst based on dppp

Rhodium complexes of unsymmetrical diphosphines of the type $Ph_2PCH_2CH_2PAr_2$, Ar = F substituted Ph groups, are also good catalysts and they seem to be longer-lived catalysts than the symmetrical ones under the conditions of the industrial process [15]. In situ IR studies show that the ligands are indeed coordinated to the metal during the catalysis. Since the major species observed contain the diphosphine ligand and because they perform better than the ligand free species, it is clear that we are dealing with a "ligand accelerated" process. It is not clear why the unsymmetric ligands are better than the symmetric ones.

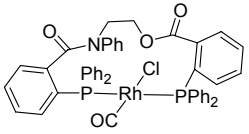

Figure 6.8. Complex with trans ligand for the carbonylation of methanol

As bidentates seemed to give more stable complexes, and because *trans* configurations seemed to be favoured by some of the monodentates, Thomas and Süss-Fink investigated the use of ligands that are bidentate and can coordinate in a *trans* fashion [11,16]. This has led to the development of new diphosphines based on condensation reactions of 2-diphenylphos-phinobenzoic acid with aminoalcohols or diols, reminiscent of the wide bite angle ligands used by Trost for the asymmetric allylic alkylation (Chapter 13.2). The best

ligand found is the one shown in Figure 6.8, the catalyst formed with this ligand is about twice as fast as the phosphine-free system. The compound does indeed form *trans* complexes with Rh(CO)Cl. In addition complexes have been isolated in which ligands of this type form bidentate *trans* spanning positions on a rhodium dimer, which is not surprising because such halide bridged dimers are bent and the *trans* positions across the dimer span about the same distance as trans positions across a monomer. From the two-dimensional pictures it would seem that the ligand may also behave as a *cis* bidentate ligand and further experiments with rigid trans ligands are needed to provide further evidence.

Hemi-labile phosphine ligands carrying an ether function, ester function or thioether as the second, labile donor-group have shown to be very good ligands for the rhodium-catalysed carbonylation of methanol [13,17]. Carbonylation of methanol occurs at unusually low temperature and pressure with cis-$RhCl(CO)_2Ph_2P(CH_2)_2P(O)Ph_2$, the mono-oxide of dppe as the ligand! The square planar complex $RhCl(CO)Ph_2P(CH_2)_2P(O)Ph_2$ was also observed, but the catalytic activity was ascribed to complexes in which the ligand acts as a monodentate. The reason why this complex is so active is not fully understood and surely testing of such hemi-labile ligands in catalytic reactions utilising cationic complexes seems worthwhile.

We will briefly mention a few more examples of such hemi-labile ligands and their complexes. Complex **10** (Figure 6.9) is an example of a phosphine-ether ligand, which undergoes methyl migration after oxidative addition of CH_3I to afford the acyl complex **11** containing two Rh-O bonds. Heating **11** in the presence of CO results in the reductive elimination of AcI, which upon hydrolysis is transformed to AcOH [18].

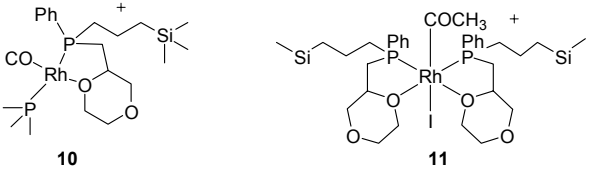

Figure 6.9. Phosphino-ethers as ligands

Rhodium complexes of the type $(MeO)_2P(O)CH_2CH_2P(Ph)_2RhL_3$ exhibit excellent catalytic properties in the carbonylation of methanol to acetic acid [19]. Rhodium(I) carbonyl complexes containing phosphino-thiolate and phosphino-thioether ligands are four times as active in catalysing the carbonylation of MeOH to AcOH as **1** [20]. Steric and electronic effects on the reactivity of rhodium and iridium complexes containing P-S, P-P, and P-O ligands have been studied, again showing the favourable effects of donor ligands on the rhodium systems [21]. Doubts remain about the long term

effects and stability of the phosphine complexes. Complex **12** cis-[RhI(CO)($Ph_2PCH_2P(S)Ph_2$)] (Figure 6.10) is eight times more active than **1** for the carbonylation of methanol at 185 °C; the X-ray crystal structure of the analogous cis-[RhCl(CO)($Ph_2PCH_2P(S)Ph_2$)] was reported together with in situ spectroscopic evidence in the catalytic cycle [22]. A more detailed study of **12** showed that indeed oxidative addition is faster, but that in this instance the migratory insertion was also accelerated due to a steric effect [23].

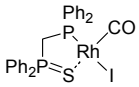

12

Figure 6.10. Phosphino-sulfide ligand

6.4.3 Other metals

Several nickel catalysts for the carbonylation of methanol have been reported, including an IR study [24]. The carbonylation of MeOH to form MeOAc and HOAc was studied using phosphine modified NiI_2 as the metal catalyst precursor. The reaction was monitored using a high pressure, high temperature, in situ Cylindrical Internal Reflectance FTIR reactor [25].

The reaction of alcohols with CO can also be catalysed by palladium iodides, and various ligands or solvents. Acetic acid is prepared by the reaction of MeOH with CO in the presence of a catalyst system comprising a palladium compound, an ionic iodide compound, a sulfone solvent at conditions similar to those of the rhodium system (180 °C, 60 bar), and, in some cases, traces of a nickel-bipyridine compound were added. Sulfones or phosphine oxides play a stabilising role in preventing metal precipitation [26]. Palladium(II) salts catalyse the carbonylation of methyl iodide in methanol to methyl acetate in the presence of an excess of iodide, even without amine or phosphine co-ligands; platinum(II) salts are less effective [27].

Catalysts based on palladium or nickel are much less stable than those based on rhodium or iridium as they are prone to metal formation. The reaction can be carried out in the absence of strong donor ligands needed for the stabilisation of tetravalent palladium. Thus, it seems likely that the catalyst switches between the zerovalent and divalent state and the electron count and geometry of palladium or nickel intermediates (NiL_4 = 18e, $NiMeIL_2$ = 16e) on the one hand and rhodium or iridium intermediates (Rh(I) = 16e, Rh(III) = 18e) on the other hand may be different. At high methanol concentration the rate of the palladium system is higher than that of rhodium, but the rate drops when the reaction progresses, which points to different kinetics [26].

References

1 Hallinan, N.; Hinnenkamp, J. *Chem. Ind.* **2001**, *82* (Catalysis of Organic Reactions), 545.

2 Morris, D. E.; Tinker, H. B. *Rev. Sci. Instrum.* **1972**, *43*, 1024.

3 Haynes, A.; Mann, B. E.; Gulliver, D. J.; Morris, G. E.; Maitlis, P. M. *J. Am. Chem. Soc.* **1991**, *113,* 8567. Haynes, A.; Mann, B. E.; Morris, G. E.; Maitlis. P. M. *J. Am. Chem. Soc.* **1993**, *115,* 4093.

4 C&EN, March 3, 1997. Jones, J. H. *Platinum Met. Rev.* **2000**, *44,* 94.

5 Ellis, P. R.; Pearson, J. M.; Haynes, A.; Adams, H.; Bailey, N. A.; Maitlis, P. M. *Organometallics,* **1994**, *13,* 3215. Griffin, T. R.; Cook, D. B.; Haynes, A.; Pearson, J. M.; Monti, D.; Morris, G. E. *J. Am. Chem. Soc.* **1996**, *118,* 3029.

6 Sunley, G. J.; Watson, D. J. *Catal Today* **2000**, *58,* 293. Ghaffar, T.; Charmant, J. P. H.; Sunley, G. J.; Morris, G. E.; Haynes, A.; Maitlis, P. M. *Inorg. Chem. Commun.* **2000**, *3,* 11.

7 Cheong, M.; Schmid, R.; Ziegler, T. *Organometallics,* **2000**, *19,* 1973.

8 Wright, A. P. Abstracts of Papers, 222nd ACS National Meeting, Chicago, IL, U. S. August 26-30, **2001** CATL-044. *Chem. Abstr*. AN **2001**:637430.

9 Zoeller, J. R.; Agreda, V. H.; Cook, S. L.; Lafferty, N. L.; Polichnowski, S. W.; Pond, D. M. *Catalysis Today,* **1992**,*13,* 73.

10 Dekleva, T. W.; Forster, D. *J. Am. Chem. Soc.* **1985**, *107*, 3565. Forster, D.; Dekleva, T. W. *J. Chem. Educ.* **1986**, *63*, 204.

11 Thomas, C. M.; Süss-Fink, G. *Coord. Chem. Rev.* **2003**, *243,* 125.

12 Rankin, J.; Benyei, A. C.; Poole, A. D.; Cole-Hamilton, D. J. *J. Chem. Soc., Dalton Trans*. **1999**, 3771.

13 Moloy, K. G.; Wegman, R. W. *Adv. Chem. Ser. (Homogeneous Transition Met. Catal. React.),* **1992**, *230,* 323.

14 Moloy, K. G.; Petersen, J. L. *Organometallics* 1995*, 14*, 2931.

15 Carraz, C.-A.; Orpen, A. G.; Ellis, D. D.; Pringle, P. G.; Ditzel, E. J.; Sunley, G. J. *Chem. Commun.* **2000**, 1277.

16 Thomas, C. M.; Mafua, R.; Therrien, B.; Rusanov, E.; Stoeckli-Evans, H.; Süss-Fink, G. *Chem. Eur. J.* **2002**, *8,* 3343.

17 Wegman, R. W.; Abatjoglou, A. G.; Harrison, A. M. J. Chem. Soc., Chem. Commun. **1987**, 1891.

18 Lindner, E.; Glaser, E. *J. Organomet. Chem.* **1990**, *391*, C37.

19 Freiberg, J.; Weigt, A.; Dilcher, H. *J. Prakt. Chem./Chem.-Ztg* **1993**, *335*, 337. For related phosphino-phosphonates see: Bischoff, S.; Weigt, A.; Miessner, H.; Luecke, B. *Energy Fuels* **1996**, *10*, 520.

20 Dilworth, J. R.; Miller, J. R.; Wheatley, N.; Baker, M. J.; Sunley, J. G. *J. Chem. Soc., Chem. Commun.* **1995**, 1579. For more P-S ligands see: Das, P.; Konwar, D.; Dutta, D. K. *Indian J. Chem., Sect. A: Inorg., Bio-inorg., Phys., Theor. Anal. Chem.* **2001**, *40A*, 626.

21 Gonsalvi, L.; Adams, H.; Sunley, G. J.; Ditzel, E.; Haynes, A. *J. Am. Chem. Soc.* **2002**, *124*, 13597.

22 Baker, M. J.; Giles, M. F.; Orpen, A. G.; Taylor, M. J.; Watt, R. J. *J. Chem. Soc. Chem. Comm*. **1995**, 197.

23 Gonsalvi, L.; Adams, H.; Sunley, G. J.; Ditzel, E.; Haynes, A. *J. Am. Chem. Soc*. **1999**, *121*, 11233.

24 Inui, T.; Matsuda, H.; Takegami, Y. *J. Chem. Soc., Chem. Commun.* **1981**, 906-7. Wang, X.; Jia, Z.; Wang, Z. *J. Nat. Gas Chem.* **1992**, *1*, 65. Liu, T. C.; Chiu, S. J. *Ind. Eng. Chem. Res.* **1994**, *33*, 488. Kelkar, A. A.; Ubale, R. S.; Deshpande, R. M.; Chaudhari, R. V. *J. Catal.* **1995**, *156*, 290.

25 Moser, W. R.; Marshik-Guerts, B. J.; Okrasinski, S. J. *J. Mol. Catal. A: Chem.* **1999***, 143*, 57.
26 van Leeuwen, P. W. N. M.; Roobeek, C. F. (to Shell). EP133331: 1985; *Chem. Abs.102,* 205749.
27 Yang, J.; Haynes, A.; Maitlis, P. M. *Chem. Comm.* **1999**, 179.

Chapter 7

COBALT CATALYSED HYDROFORMYLATION

The old workhorse

7.1 Introduction

Functionalisation of hydrocarbons from petroleum sources is mainly concerned with the introduction of oxygen into the molecule. Roughly speaking, two ways are open: oxidation and carbonylation. Oxidation is the preferred route for aromatic acids, acrolein, maleic anhydride, ethene oxide, propene oxide, and acetaldehyde. Hydroformylation (older literature and technical literature refer to the "oxo" reaction) is employed for the large-scale preparation of butanal and butanol, 2-ethylhexanol, and detergent alcohols (Figure 7.1). Butanal and butanol are used in many applications as a solvent, in esters, in polymers etc. The main use of 2-ethylhexanol is in phthalate esters that are softeners (plasticisers) in PVC. The catalysts applied in hydroformylation are based, as in methanol carbonylation, on cobalt and rhodium. We will see that the cobalt catalyst resembles the one described for the methanol carbonylation process, but the rhodium one is distinctly different from the Monsanto catalyst sharing with it only the propensity for a fast migratory insertion of carbon monoxide.

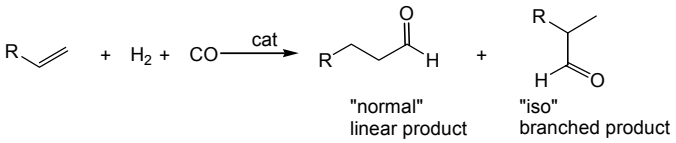

Figure 7.1. The hydroformylation reaction

7.2 Thermodynamics

Thermodynamics of hydroformylation and hydrogenation of propene at standard conditions are as follows:

$H_2 + CH_3CH{=}CH_2 + CO \rightarrow CH_3CH_2CH_2C(O)H$

ΔG	63	–138	–117 (l)	$= -42$ kJ.mol^{-1}
ΔH	21	–109	–238	$= -150$ kJ.mol^{-1}

$H_2 + CH_3CH{=}CH_2 \rightarrow CH_3CH_2CH_3$

ΔG	63	–25	$= -88$ kJ.mol^{-1}
ΔH	21	–105	$= -126$ kJ.mol^{-1}

At higher temperatures the entropy loss becomes more important and ΔG will be less negative.

The thermodynamically favoured product of a hydroformylation reaction is not the aldehyde but the alkane. Yet the product is the aldehyde because "kinetic" control occurs.

The reaction is highly exothermic. Thus, if the reaction is conducted under adiabatic conditions the temperature rises and ΔG approaches zero, at which point the reaction reaches equilibrium and the temperature will not increase further, preventing further escalation!

7.3 Cobalt catalysed processes

The hydroformylation of alkenes was accidentally discovered by Roelen while he was studying the Fischer-Tropsch reaction (syn-gas conversion to liquid fuels) with a heterogeneous cobalt catalyst in the late thirties. In a mechanistic experiment Roelen studied whether alkenes were intermediates in the "Aufbau" process of syn-gas (from coal, Germany 1938) to fuel. He found that alkenes were converted to aldehydes or alcohols containing one more carbon atom. It took more than a decade before the reaction was taken further, but now it was the conversion of petrochemical hydrocarbons into oxygenates that was desired. It was discovered that the reaction was not catalysed by the supported cobalt but in fact by $HCo(CO)_4$ which was formed in the liquid state.

A key issue in the hydroformylation reaction is the ratio of linear and branched product being produced (Figure 7.1). Scientifically it is an interesting question how the linearity can be influenced and maximised by influencing the kinetics and changing the ligands. The catalytic cycle for the formation of linear aldehyde is shown in Figure 7.2. The first processes for

hydroformylation were based on cobalt carbonyl complexes. The only ligand present is carbon monoxide. We have omitted the geometry of the cobalt complexes.

For the sake of clarity only the route to linear product has been shown. The first step is the replacement of a carbon monoxide ligand by an alkene. Indeed, a negative order in CO pressure has been reported while the rate is proportional to the alkene concentration. Alkene complexation may be a one-step associative process via a 20-electron intermediate, as shown, or more likely a two-step dissociative process. In the next step migration of the hydride ion gives an alkyl cobalt complex, which may be either linear (as shown in Figure 7.1) or branched. An incoming carbon monoxide occupies the vacant site. The next move is the migration of the alkyl to a co-ordinated carbon monoxide to give an acyl complex. Up to here all reactions should be written as potential equilibria. In the last step dihydrogen reacts with the acyl complex to form the aldehyde product and to regenerate the starting complex hydrido cobalt carbonyl. In cobalt-catalysed hydroformylation the last step is often rate-determining.

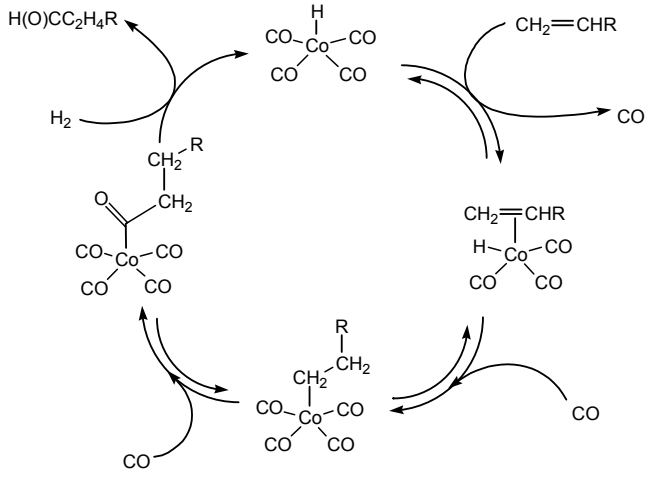

Figure 7.2. Mechanism of the cobalt catalysed hydroformylation

The last reaction of the catalytic cycle has been the subject of much controversy. Two reactions may lead to the product:

$$HCo(CO)_4 + RC(O)Co(CO)_4 \longrightarrow RCOH + Co_2(CO)_8 \qquad (1)$$

$$RC(O)Co(CO)_4 + H_2 \longrightarrow RCOH + HCo(CO)_4 \qquad (2)$$

The latter reaction might involve an oxidative addition, rapidly followed by a reductive elimination, or alternatively it might involve a σ–bond metathesis

reaction. Experimentally this distinction will be difficult to verify. The two schemes, a bimetallic reaction or a direct reaction with dihydrogen, give rise to different kinetics. For both schemes experimental evidence has been reported and both mechanisms may be operative depending on the exact conditions [1].

Recently proof has been reported for a heterometallic bimolecular formation of aldehyde from a manganese hydride and acylrhodium species [2]. Phosphine free, rhodium carbonyl species show the same kinetics as the cobalt system, i.e. the hydrogenolysis of the acyl-metal bond is rate-determining. Addition of hydridomanganese pentacarbonyl led to an increase of the rate of the hydroformylation reaction. The second termination reaction that takes place according to the kinetics under the reaction conditions (10-60 bar, 25 °C) is reaction (3). The direct reaction with H_2 takes place as well, but it is slower on a molar basis than the manganese hydride reaction.

$$HMn(CO)_5 + RC(O)Rh(CO)_4 \longrightarrow RCOH + MnRh(CO)_9 \quad (3)$$

This reaction includes loss of CO prior to reaction of the rhodium fragment and the manganese fragment to form more reactive, electron deficient species, which we have omitted from the reaction equation.

7.4 Cobalt catalysed processes for higher alkenes

In Chapter 8 we will discuss the hydroformylation of propene using rhodium catalysts. Rhodium is most suited for the hydroformylation of terminal alkenes, as we shall discuss later. In older plants cobalt is still used for the hydroformylation of propene, but the most economic route for propene hydroformylation is the Ruhrchemie/Rhône-Poulenc process using two-phase catalysis with rhodium catalysts. For higher alkenes, cobalt is still the preferred catalyst, although recently major improvements on rhodium (see Chapter 8) and palladium catalysts have been reported [3].

The higher alkene feed (C_{10-14}) for the production of detergent alcohols is either a product from the wax-cracker (terminal and internal alkenes) or the by-product of the ethene oligomerisation process (internal alkenes). In the near future a feed from high-temperature Fischer-Tropsch may be added to this. The desired aldehyde (or alcohol) product is the linear one and the cobalt catalyst must therefore perform several functions:

- the internal alkenes must be isomerised to the terminal ones (in the thermodynamic mixture only a very small amount of terminal alkene will be present),
- the hydroformylation catalyst must have a very strong preference for the terminal carbon atoms in order to obtain an acceptable (60-80%) percentage of linear products.

In general the activity of transition metal complexes for alkene isomerisation is low in the presence of carbon monoxide, but $HCo(CO)_4$ is an exception to this rule. Depending on conditions, full equilibration of the alkene isomers is obtained.

Under the reaction conditions $HCo(CO)_4$ is an effective isomerisation catalyst. The linear-to-branched ratio obtained is the same for terminal and internal alkenes. This means that alkene addition or insertion is definitely not rate-determining in this system. 1-Alkenes, but also internal alkenes, are rapidly isomerised to the thermodynamic mixture of terminal and internal alkenes. Nevertheless the aldehyde product may consist of as much as 70% linear product, which indicates a very strong selectivity for hydroformylation at the terminal carbon atom. Kinetically this can be explained by a faster or preferential formation of the 1-alkyl group or a faster migration of the 1-alkyl group. The preference for hydroformylating *terminal* carbon atoms seems to be extremely high. The activity for 1-alkenes is much higher than that for internal alkenes; the reaction may be a thousand times faster. It is relatively difficult to study this in detail because the alkenes are rapidly isomerised! Deuteration studies have demonstrated a complete scrambling of deuterium and hydrogen at high temperatures.

In the first few minutes of a batch reaction using 1-alkenes an extremely fast reaction therefore may take place, which is the direct hydroformylation of 1-alkene, but after an equilibration to the internal isomers has taken place the reaction slows down considerably.

Figure 7.3 gives an overview of the reactions involved in the hydroformylation of internal alkenes to linear products. It has been suggested that cobalt, once attached to an alkene, "runs" along the chain until an irreversible insertion of CO occurs. Thus, the alkene does not dissociate from the cobalt hydride during the isomerisation process. There is no experimental support for a clear-cut proof for this mechanism. In alkene polymerisation reactions this type of "chain running" has been actually observed.

Perhaps by using partly deuterated feeds one can design an experiment to find proof for the "chain running" mechanism in the reaction below.

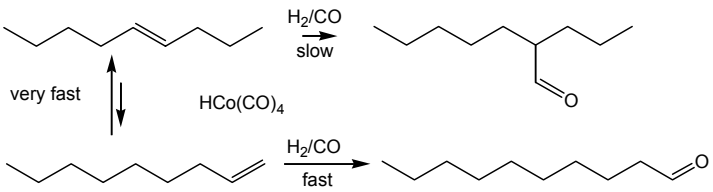

Figure 7.3. Hydroformylation of internal alkenes

7.5 Kuhlmann cobalt hydroformylation process

In the following sections a few typical processes will be described. An example of a cobalt catalysed hydroformylation reaction for **higher** alkenes is the Kuhlmann process (now Exxon process), for which the flow-scheme –a liquid/liquid separation– is shown in Figure 7.4. In this process the hydroformylation is done in one, organic phase consisting of alkene and aldehyde. The reactor is often a loop reactor or a reactor with an external loop to facilitate heat transfer.

A liquid/liquid separation of product and catalyst is done in separate vessels after the reaction has taken place. The reaction mixture is sent to a gas separator and from there to a counter current washing tower (a simple phase separator is shown in the figure) in which the effluent is treated with aqueous Na_2CO_3. The acidic $HCo(CO)_4$ is transformed into the water soluble conjugate base $NaCo(CO)_4$. The product is scrubbed with water to remove the traces of base. The oxo-crude goes to the distillation unit.

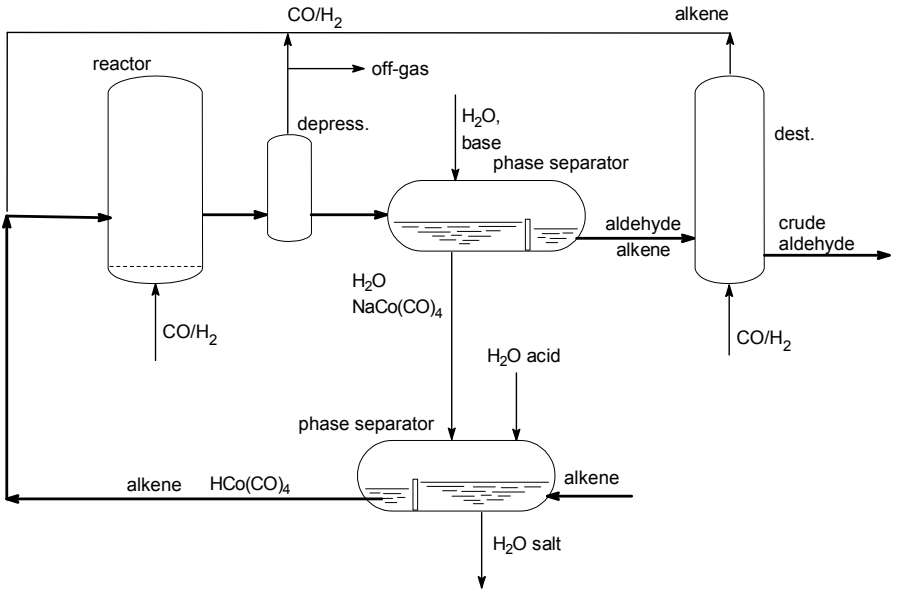

Figure 7.4. Kuhlmann hydroformylation process

The basic solution in water containing $NaCo(CO)_4$ is treated with sulphuric acid in the presence of syn-gas and $HCo(CO)_4$ is regenerated. This can be extracted as is shown in the drawing from water into the substrate, alkene. The catalyst is returned to the reactor dissolved in the alkene. Compared to other schemes (BASF, Ruhrchemie) the elegant detail of the Kuhlmann process is

that the cobalt catalyst is not decomposed via (partial) oxidation but is left in the system as the tetracarbonylcobaltate.

7.6 Phosphine modified cobalt catalysts: the Shell process

In the sixties it was recognised that ligand substitution on the cobalt carbonyl complex might influence the performance of the catalyst. Tertiary alkyl phosphines have a profound influence:

- the reaction is a hundred times slower [4,5],
- the selectivity to linear products increases,
- the carbonyl complex formed, $HCoL(CO)_3$, is much more stable, and
- the catalyst acquires activity for hydrogenation.

A process based on this catalyst has been commercialised by Shell [6]. An efficient ligand reported is 9-eicosyl-9-phosphabicyclononane (Figure 7.5) [7]. The long C-20 chain is needed to obtain a phosphine with a high boiling point.

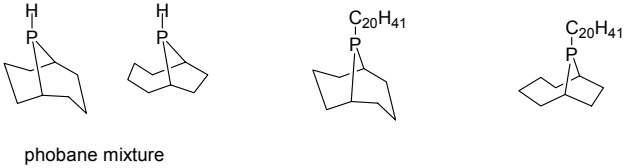

Figure 7.5. A ligand reported by Shell for Co hydroformylation

As a result of the higher stability the process can be (and must be!) operated at lower pressure (25-100 bar versus 200-300 bar for $HCo(CO)_4$). The higher stability can be explained by the electron donation of the phosphine to the electron deficient cobalt carbonyl thus strengthening the Co-CO bonds. The phosphine complex is less active than the tetracarbonyl complex and therefore the reaction is carried out at higher temperatures (170 °C versus 140 °C). The temperature is "dictated" by the rate required; the high pressures in the tetracarbonyl system are needed to prevent decomposition of the carbonyls to metal and CO.

The linearity of the product of the Shell process is higher, 75-90% versus 60-70% for the non-ligand modified process. The reason for this is not entirely clear; on steric grounds one might expect that the linear alkyl and acyl complexes are more stable leading to a higher linearity. Electronically the effects on rate and selectivity cannot be easily rationalised.

The hydrogenation activity is an added advantage of this route, since most of the hydroformylation-products are converted to the alcohols anyway. Concurrent with the hydrogenation of aldehyde to alcohol, however, hydrogenation of alkene feedstock to alkane occurs, which may be as high as 15% under certain conditions (versus 2-3% for the non-ligand-modified

process). This is a considerable loss that has to be counterbalanced economically by the higher linearity of the product.

Process description.

The hydroformylation of both higher and lower alkenes is carried out with a phosphine complex $HCo(CO)_3L$. In this system the catalyst also remains intact as in the Kuhlmann process. The phosphine is a high boiling trialkylphosphine (sensitive towards oxidation) that ensures that during the distillation of the product from the heavy ends the catalyst remains in the bottoms phase of the distillation. This mixture of heavy ends and catalyst is recycled to the reactor. Compared to the other cobalt-catalysed processes the flow scheme looks simple, see Figure 7.6. The catalyst is subjected to forcing conditions during the distillation. Furthermore, the reactor is several times larger because this catalyst is much slower. To limit the hydrogenation of alkenes the reaction can be done in stages; in the first reactor the partial pressure of hydrogen is lower and in the last reactor the partial pressure is higher, to ensure hydrogenation of aldehyde to alcohol. The product of propene can be either butanol or 2-ethylhexanol. The dimerisation of butanal can be done in the hydroformylation reactor and hence in this instance base must be added. This aldol condensation also leads to the formation of heavy ends, which requires a bleed stream.

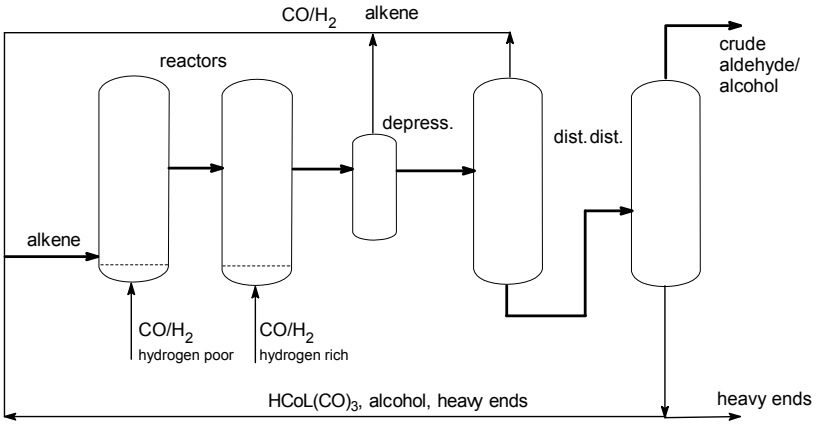

Figure 7.6. Flow scheme of the Shell process

7.7 Cobalt carbonyl phosphine complexes

7.7.1 Carbonyl species

A whole range of cobalt complexes has been observed under syn-gas pressure. The actual complexes formed will depend strongly on the conditions.

A wide range of temperatures (25–200 °C), pressures (1–300 bar), and concentrations has been used and therefore comparison must be done with great care with consultation of the original literature. We will restrict ourselves to a few instructive examples, some general observations and comments. The complexes are shown in Figure 7.7 (L is a phosphine).

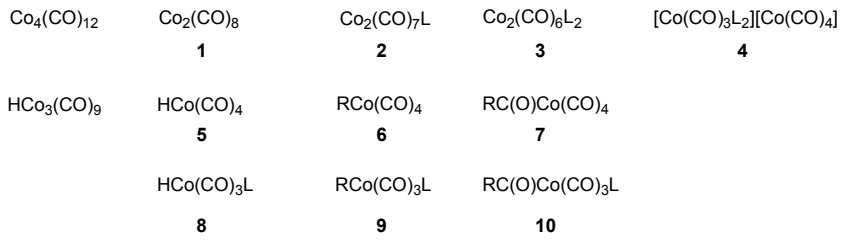

Figure 7.7. Examples of complexes involved in cobalt hydroformylation

The tetranuclear and trinuclear clusters will only be observed at low pressures [8], but all other species are very common under hydroformylation conditions. Complex **4** is an ionic complex that is formed in polar solvents [9] and even hexa-solvated, divalent cobalt species may form as the cation. Under practical conditions both the dimers and the hydrides are observed, thus depending on the hydrogen pressure there will be more or less of the hydride present.

The reaction conditions chosen for the in situ IR studies are often much milder (25–100 °C, 100 bar) than the process conditions (140 °C, 250 bar), which may not affect the equilibria, as the higher pressure compensates for the higher temperature. The relative rate, however, of isomerisation of 1-alkenes may increase dramatically between room temperature and 140 °C.

Most authors agree that upon addition of alkene to an equilibrium mixture of **1** and **5**, the ratio changes considerably, favouring the dimeric species **1**. Van Boven [1] explained this by assuming that the major aldehyde-forming step is the bimetallic elimination mechanism, involving **5** and **7**, shown in equation (1) (actually most of van Boven's work is concerned with phosphine complexes, which makes it more complicated as we will see below). Mirbach [1] essentially found the same, but his analysis showed that the major productive pathway is still maintained by species **7** in its reaction with dihydrogen, equation (2), section 7.3. Occasionally a reaction according to equation (1) occurs, which forms the unreactive dimer **1**. Most data point to a slow regeneration of **5** from dihydrogen and **1**. Thus, dicobaltoctacarbonyl becomes an important resting state, or rather a dormant state, in the catalytic process.

We have illustrated this mechanism in Figure 7.8. The major species observed are shown in the boxes and one can derive that species 1 will build up

to a certain dynamic "equilibrium" value. The explanation is not meant to hold for each system as it is only valid in certain windows of operation, but it is instructive for a general understanding.

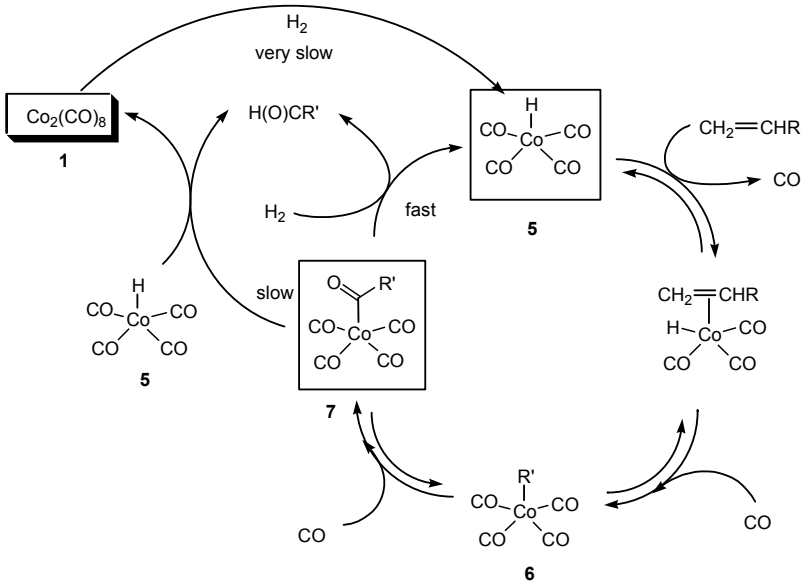

Figure 7.8. Cobalt carbonyl mechanism after Mirbach [1]

Cyclohexene reacts much more slowly than hex-1-ene (80 °C, 100 bar, Mirbach [1]), which is related to the slower insertion of internal alkenes and the absence of 1-alkene isomerisation under these conditions. As less acylcomplex **7** is formed per unit of time, the rate of formation of dimer **1** will also decrease. Since the rate of regeneration of **5** from **1** and H_2 remains the same during the cyclohexene hydroformylation, the dimer concentration will be lower. This was indeed observed. Even if the rate-determining step would no longer be the hydrogenolysis, but for instance the alkene complexation + insertion reaction, the rate of the system may retain a positive response to higher pressures of hydrogen. This will be due to a favourable shift in the equilibrium between **5** and **1** or, more likely, a faster regeneration of **5** from **1**, both due to the higher pressure of H_2.

Interestingly, the exchange of cobalt between **1** and **5** is extremely rapid according to NMR measurements above 100 °C and roughly seven orders of magnitude faster than hydroformylation, but this does not involve exchange with H_2 [10]! The mechanism turned out to be dissociation of the dimer into two radicals $\bullet Co(CO)_4$, which subsequently exchanges a hydrogen atom with **5**, $HCo(CO)_4$ at extremely high rates. The Co-Co bond dissociation energy for **1** is

only 80 kJ.mol^{-1}. Exchange of CO is of the same order of magnitude. Thus we are dealing with a highly dynamic system that only once in a while will carry out a hydroformylation cycle!

It is likely that the saturated complex $Co_2(CO)_8$ loses one molecule of CO to give unsaturated $Co_2(CO)_7$ before reacting with H_2. In spite of the extremely fast exchange of free CO with coordinated CO the regeneration of $HCo(CO)_4$ remains a slow process.

7.7.2 Phosphine derivatives

Monophosphines. The use of phosphines in cobalt-catalysed hydroformylation was first reported by Slaugh from Shell Development in the sixties [6]. Tributylphosphine was reported as a selective and active ligand, but the phobane based derivatives seem much more effective (Figure 7.5) [7]. Alkylphosphine are strong electron donors and thus dissociation of carbon monoxide is retarded, which leads to more stable catalysts, but also much slower catalysts. Carbonyl complexes **1** and **5** may be some 100–200 times more active than complexes **3** and **8** containing an alkylphosphine ligand [4]. Arylphosphines do not seem to be very effective ligands and there may be two reasons for this. First, they are weaker electron donors and form less stable complexes in the competition with CO. Weaker ligands give more carbonyl species and thus should give a faster reaction, but this only holds for high pressures needed to stabilise the phosphine free complexes. Secondly, arylphosphines quickly decompose at higher temperatures. It was demonstrated that at 190 °C a fast phosphorus-carbon bond cleavage occurs leading to arenes, arylalkyls or aryl aldehyde derivatives [11]. The more electron withdrawing the aryl group was, the faster the decomposition was. Alkylphosphines are therefore the preferred ligands.

Slaugh arrived at the following order of activity (195 °C, 36 bar):

$Ph_2EtP > PhBu_2P > Bu_3P > Et_3P > PhEt_2P > Cy_3P$

The linear : branched ratio was as follows:

$Bu_3P > Et_3P = PhEt_2P = Cy_3P = PhBu_2P > Ph_2EtP$, ranging from 5.5 to 3.

One should be aware that the rate data are especially prone to variation. We have already seen that 1-alkenes are hydroformylated at a much higher rate, but at the same time they are rapidly isomerised to the much less reactive internal alkenes. This together with the highly exothermic reaction may result in low reproducibility. The results will thus strongly depend on the experimental procedures and how carefully they were executed.

Ligand effects in a series of tertiary phosphines $L=P(C_3H_6OCH_3)_3$, PBu_3, $P(C_2H_4CO_2CH_3)_3$, and $P(C_2H_4CN)_3$ has been studied using the complexes $Co_2(CO)_6(L)_2$ as the catalyst precursor [12]. For a 1 : 1 ligand to cobalt ratio the results were the same for all ligands and the percentage of linear products

amounted to 60% (40 bar H_2, 5 bar CO, 150 °C). When the ligand : cobalt ratio was increased to 10, the linearity increased to 90% but the rate was rather impractical. Perhaps, bis-phosphine complexes are formed, which are electron-rich and only slowly dissociate a molecule of CO.

High-pressure in-situ NMR spectroscopy have been reported about reactions of carbon monoxide with cobalt complexes of the type, $[Co(CO)_3L]_2$. For L=P(n-C_4H_9)$_3$, high pressures of carbon monoxide cause CO addition and disproportionation of the catalyst to produce a catalytically inactive cobalt(I) salt with the composition $[Co(CO)_3L_2]^+[Co(CO)_4]^-$. Salt formation is favoured by polar solvents [13].

A very effective monodentate ligand was already introduced in Figure 7.5 containing the phobane moiety. It can be made from PH_3 by radical addition to 1,5-cyclooctadiene, which gives two isomers, a 1,5 and a 1,4 bridged phosphabicyclononane ("phobane"). The two isomers have different properties and can be separated via their bis(hydroxymethyl)phosphonium salts [14]. A long C-20 chain is connected to phobane, also via a radical mechanism. The deprotonated form of phobane has also been used for obtaining other substituted ligands.

Another group of bicyclic aliphatic phosphines has been introduced by Sasol [15]. Their ligands are based on addition of PH_3 to limonene (the R-enantiomer). A mixture of two diastereomeric compounds is obtained due to the two configurations of the methyl group at the C-4 position (Figure 7.9). The Lim-H compounds obtained can be functionalised at the phosphorus atom with the usual radical reactions with alkenes or substitution reactions of their conjugate bases formed after treatment with BuLi with electrophiles.

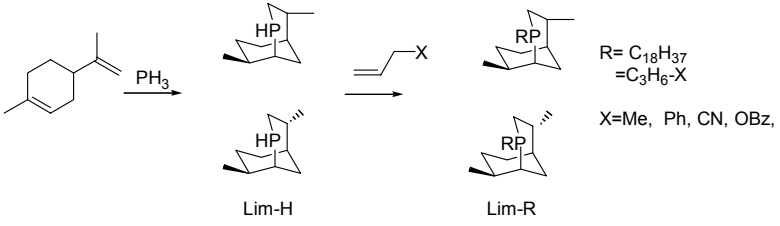

Figure 7.9. Lim ligands developed by Sasol; position of R group not defined

The phobane derivatives (Figure 7.5) contain two secondary hydrocarbyl groups and are therefore relatively bulky, comparable to (i-Pr)$_2$P-n-alkyl ligands. The Lim ligands contain two primary alkyl groups, but the branching at the other positions may compensate for this and it may still behave as a bulky ligand. Electronically the alkyl groups are strong donors, but it is expected that the steric strain caused by the ring systems raises the χ-value of the ligands (i.e. makes them better π-acceptors). The differences observed in oxidation and

quaternisation of the two phobane isomers and the two Lim diastereomers shows that the different ring structures lead to slightly different acid-base properties for each pair.

Subtle electronic effects were also observed for the Sasol ligands, as in the series X = CN, Ph, OBz, Me a decrease in the rate of reaction was found while the linearity followed the reverse trend; the better donor gives the highest linear to branched ratio (4.9, very similar to the best Shell catalyst; 170 °C, 85 bar). As the authors remarked, this is not an intrinsic ligand effect on the reaction; it is a measure of the amount of phosphine-free catalyst **5** that is present in the equilibrium. Thus the weaker donor ligands give more **5** and thus a higher rate and a lower l:b ratio. This was supported by IR and NMR measurements.

Diphosphines. The use of dppe in cobalt catalysed hydroformylation was reported by Slaugh [16], but compared to PBu_3 it had little effect on the rate and the selectivity of the cobalt carbonyl catalyst. Thus, it seemed that even a bidentate aryl phosphine was relatively inert toward cobalt carbonyls under hydroformylation conditions. In stoichiometric reactions of $HCo(CO)_4$ or $Co_2(CO)_8$ and dppe a chelate complex was obtained [17]. $Bu_2P(CH_2)_4PBu_2$ gives a 7-membered ring chelate, but in hydroformylation it behaves as PBu_3 and most likely acts as a monodentate ligand under CO pressure.

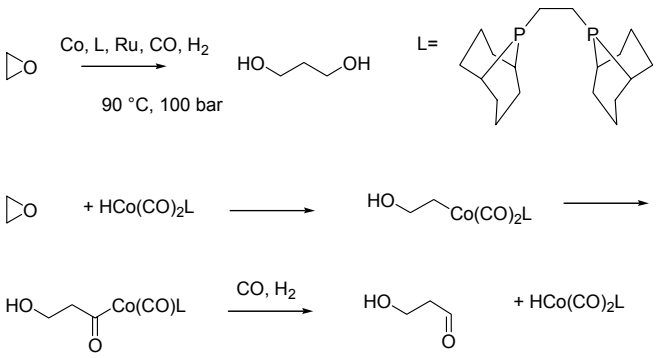

Figure 7.10. Ethylene oxide to 3-hydroxypropanal; only one isomer shown for L

Alkyldiphosphines turned out to be very useful in a different reaction, namely the carbonylation/hydrogenation of ethylene oxide to give 1,3-propanediol also using cobalt catalysts. Interestingly, the ligand contains two phobane units bridged by 1,2-ethenediyl. The process was commercialised by Shell [18].

Most likely the cobalt catalyst is $HCo(CO)_2(L)$, which has a very electron rich metal centre and dissociation of CO does not occur under the reaction conditions. The first step is a reaction of the cobalt hydride with ethylene oxide forming a hydroxyethylcobalt species, which does not require dissociation of

CO! Subsequently a migratory insertion will take place. Oxidative addition of H_2 will be faster at the electron rich metal centre and thus the aldehyde will form. Hydrogenation takes place at ruthenium (added as $Ru_3(CO)_{12}$) as indeed catalyst systems containing cobalt only are known to give 3-hydroxypropanal as the product.

References

1 Van Boven, M.; Alemdaroglu, N. H.; Penninger, J. M. L. *Ind. Eng. Chem. Prod. Res. Dev.* **1975**, *14,* 259. Major, A.; Horváth, I. T.; Pino, P. *J. Mol. Catal.* **1988**, *45,* 275. Mirbach, M. F. *J. Organometal. Chem.* **1984**, *265,* 205. Azran, J.; Orchin, M. *Organometallics,* **1984**, *3,* 197.

2 Li, C.; Widjaja, E.; Garland, M. *J. Am. Chem. Soc.* **2003***, 125*, 5540.

3 Drent, E.; Budzelaar, P. H. M. *J. Organomet. Chem.* **2000***, 593*, 211.

4 Slaugh, L. H.; Mullineaux, R. D. *J. Organomet. Chem.* **1968***, 13,* 469.

5 Crause, C.; Bennie, L.; Damoense, L.; Dwyer, C. L.; Grove, C.; Grimmer, N.; van Rensburg, W. J.; Kirk, M. M.; Mokheseng, K. M.; Otto, S.; Steynberg, P. J. *Dalton Trans.* **2003**, 2036**.**

6 Slaugh, L. H.; Mullineaux, R. D. *U.S. Pat.* 3,239,569 and 3,239,570, **1966** (to Shell)*; Chem. Abstr.* 1**964**, *64,* 15745 and 19420.

7 Van Winkle, J. L.; Lorenzo, S.; Morris, R. C.; Mason, R. F. *U.S. Patent*, 3,420,898, **1969**. *U.S. Appl.* 1965-443703; *Chem. Abstr.* 1**967**, *66,* 65101.

8 Tannenbaum, R.; Bor, G. *J. Organomet. Chem*. **1999**, *586*, 18. Fachinetti, G.; Balocchi, L.; Secco, F.; Venturini, M. *Angew. Chem. Int. Ed. Engl*. **1981**, *20*, 204.

9 Andreetta, A.; Montrasi, G.; Ferrari, G. F.; Pregaglia, G. P.; Ugo, R. *Nouveau J. Chim*. **1978**, *2*, 463. Kramarz, K. W.; Klingler, R. J.; Fremgen, D. E.; Rathke, J. W. *Catalysis Today* **1999**, *49*, 339.

10 Klingler, R. J.; Rathke, J. W. *J. Am. Chem. Soc.* **1994**, *116,* 4772.

11 Dubois, R. A.; Garrou, P. E. *Organometallics,* **1986**, *5,* 466.

12 Rosi, L.; Bini, A.; Frediani, P.; Bianchi, M.; Salvini, A. *J. Mol. Catal. A: Chem.* **1996***, 112*, 367.

13 Rathke, J. W.; Klingler, R. J.; Chen, M. J.; Gerald, R. E., II; Kramarz, K. W. *Chemist*, **2003**, *80*, 9.

14 Downing, J. H.; Gee, V.; Pringle, P. G. *Chem. Commun*. **1997**, 1527.

15 Steynberg, J. P.; Govender, K.; Steynberg, P. J. *WO Patent,* 2002014248, **2002**.

16 Cannel, L. G.; Slaugh, L. H.; Mullineaux, R. D. Ger. Pat. 1,186,455 (priority date 1960, to Shell); *Chem. Abstr.* **1965**, *62*, 16054.

17 Kagan, Yu. B.; Butkova, O. L.; Korneeva, G. A.; Shishkina, M. V.; Zvezdkina, L. I.; Bashkirov, A. N. *Neftekimiya,* **1983***, 23,* 77 (*Chem. Abstr.* **1983***, 99*, 405143).

18 Slaugh, L. H.; Weider, P. R.; Arhancet, J. P.; Lin, J.-J. (to Shell) PCT Int. Appl. **1994**, WO 9418149 (*Chem. Abstr.* **1995***, 122*, 231194).

Chapter 8

RHODIUM CATALYSED HYDROFORMYLATION

Bite angles and selectivity

8.1 Introduction

Since Shell's report on the use of phosphines in the cobalt catalysed process, which included preliminary data for the use of rhodium as well [1], many industries started to apply phosphine ligands in rhodium catalysed processes [2]. While alkylphosphines are the ligands of choice for cobalt, they lead to slow reactions when applied in rhodium catalysis. In the mid-sixties the work of Wilkinson showed that arylphosphines should be used for rhodium and that even at mild conditions active catalysts can be obtained [3]. The publications were soon followed by those of Pruett, in which phosphites were introduced (Figure 8.1) [4].

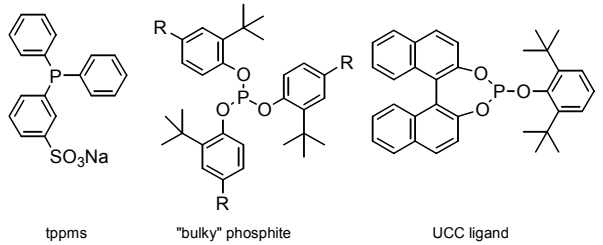

tppms "bulky" phosphite UCC ligand

Figure 8.1. Structures of ttpms, van Leeuwen's "bulky phosphite", and a highly stable, bulky phosphite from UCC

As a result, the second-generation processes used rhodium as the metal. The first rhodium-catalysed, ligand-modified process came on stream in 1974 (Celanese) and more were to follow in 1976 (Union Carbide Corporation) and in 1978 (Mitsubishi Chemical Corporation), all using triphenylphosphine (tpp). The UCC (now Dow) process has been licensed to many other users and it is

often referred to as the LPO process (Low Pressure Oxo process). Not only are rhodium catalysts much faster – which is translated into milder reaction conditions –, but also their feedstock utilisation (or atom economy) is much better than that of cobalt catalysts. For example, the cobalt-alkylphosphine catalyst may give as much as 10% of alkane as a by-product. Since the mid-seventies the rhodium catalysts started to replace the cobalt catalysts in propene and butene hydroformylation. For detergent alcohol production though, even today, the cobalt systems are still in use, because there is no good alternative yet for the hydroformylation of internal higher alkenes to mainly linear products.

The third generation process concerns the Ruhrchemie/Rhône-Poulenc process utilizing a two-phase system containing water-soluble rhodium-tppts in one phase and the product butanal in the organic phase. The process has been in operation since 1984 by Ruhrchemie (or Celanese, nowadays). The system will be discussed in section 8.2.5. Since 1995 this process is also used for the hydroformylation of 1-butene.

In the late sixties phosphites have also been considered as candidate ligands for rhodium hydroformylation, but tpp turned out to be the ligand of choice. A renewed interest in phosphites started in the eighties after van Leeuwen and co-workers had discovered the peculiar effect of bulky monophosphites giving very high rates [5]. Bryant and co-workers at Union Carbide have expanded this work enormously, first by making more stable bulky monophosphites [6], later by focusing on diphosphites, which gave in a number of cases very high regioselectivity [7]. There is only one relatively small commercial application of "bulky monophosphite" by Kuraray for the hydroformylation of 3-methylbut-3-en-1-ol [8]. A large amount of research has been devoted to diphosphites in the last decade aiming at a variety of applications. The results will be discussed in section 8.4.

Diphosphines have also become very popular ligands since the late eighties in rhodium hydroformylation, e.g. Eastman's BISBI. The two-phase system underwent considerable improvements involving diphosphines [9].

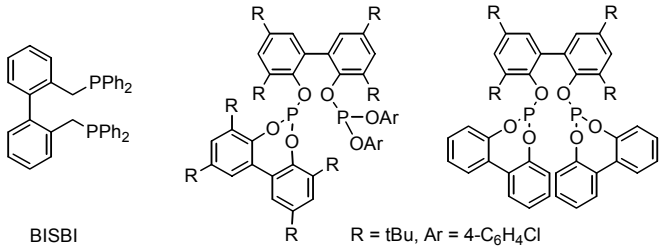

Figure 8.2. Eastman's BISBI and typical diphosphites from Union Carbide Corporation

In recent years the interest in hydroformylating higher alkenes with catalysts other than cobalt has increased. Platinum and palladium based catalysts have been studied and the results of the latter [10] seem very promising. Platinum has been known for many years to have a high preference for the formation of linear products, but ligand decomposition hampers applications [11].

A ligand with great potential for hydroformylation of higher, terminal alkenes is monosulfonated triphenylphosphine, tppms, that was studied by Abatjoglou, also at Union Carbide [12] (section 8.2.6). In this system hydroformylation is carried out in one phase that is worked up afterwards by adding water, which gives two phases to separate catalyst and product.

The fourth generation process for large-scale application still has to be selected from the potential processes that have been "nominated". In the chapters to follow several of these candidates will be discussed. The fourth generation will concern higher alkenes only, since for propene hydroformylation there are hardly wishes left [13]. Many new phosphite-based catalysts have been reported that will convert internal alkenes to terminal products [6,7,14] and recently also new diphosphines have been reported that will do this [15,16,17].

Asymmetric rhodium catalysts are discussed in section 8.6. The most interesting ligand discovered for asymmetric hydroformylation is undoubtedly BINAPHOS, introduced by Takaya [18], but certain diphosphites also give high enantioselectivities [19,20].

Ligand design for fine chemical applications has been very limited and usually the ligands designed for large-scale applications are also tested for more complicated organic molecules. Tpp has been the workhorse in fine chemicals hydroformylation ever since Wilkinson's first examples [21,22], but also bulky phosphite [5], tppts and tppms [23] turned out to be very useful, and also diphosphites have been studied [24].

8.2 Triphenylphosphine as the ligand

8.2.1 The mechanism

In Figure 8.3 the well-known mechanism, as first proposed by Heck [25], has been depicted. It corresponds to Wilkinson's so-called dissociative mechanism [3]. The associative mechanism involving 20-electron intermediates for ligand/substrate exchange will not be considered. For PPh_3 as the ligand a common starting complex is $RhH(PPh_3)_3CO$, complex **1**, which under 1 bar of carbon monoxide forms the complexes **2ee** and **2ae**, containing two phosphine ligands in equatorial positions (denoted **ee** throughout the

scheme) or one in an apical position and the other ligand in an equatorial position (complexes denoted **ae**). Brown [26] found a preference for the **ee** isomer of the hydride complex. Dissociation of either equatorial L or equatorial CO from **1** or **2** leads to the square-planar intermediates **3c** and **3t**, which have phosphines in *cis* or *trans* configurations respectively. Preferential dissociation of equatorial ligands from trigonal bipyramids is normally observed. Complexes **3** associate with ethene to give complexes **4**, again in two isomeric forms **ae** and **ee**, having a hydride in an apical position and ethene coordinating in the equatorial plane.

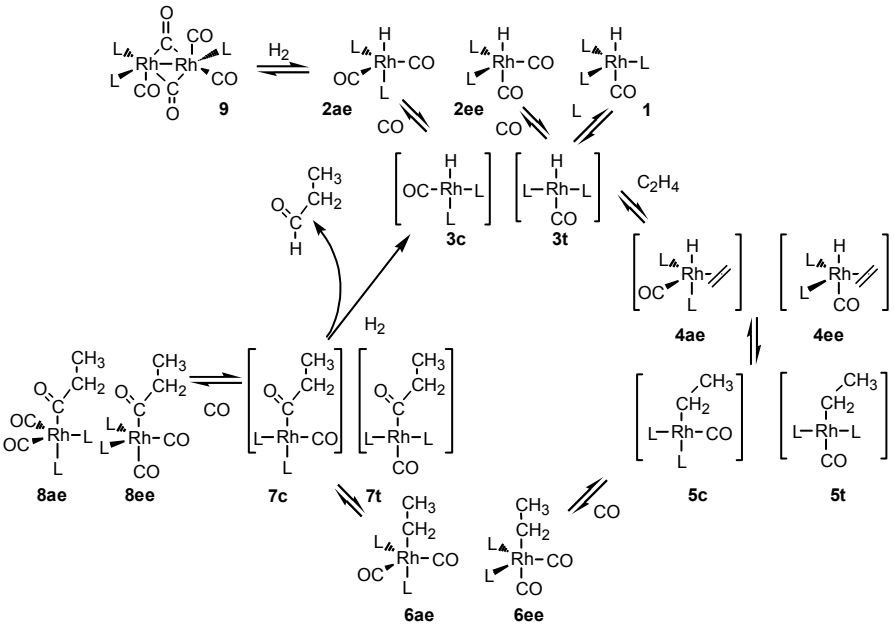

Figure 8.3. Simplified mechanism for hydroformylation of ethene (L = PPh3)

While four-coordinate species rhodium **3c** have never been observed, the analogous four-coordinate complex *trans*-$Rh(PCy_3)_2(CO)H$ has been isolated and structurally characterized [27]. In addition, magnetization transfer experiments indicate that both **1** and **2** are in equilibrium with free PPh_3 [26]. These results are highly suggestive of the formation of the four-coordinate complex **3** by phosphine dissociation from **1** and **2**. The complexes not observed experimentally (for PPh_3 and alkylrhodium) are shown in brackets in Figure 8.3.

Although the complexes shown in Figure 8.3 contain at least two coordinated PPh_3 ligands, a large body of indirect evidence suggests the influence of equilibria involving catalytically active species containing a single

coordinated phosphine ligand. Such monophosphine species were initially invoked to explain the positive effect on the regioselectivity in hydroformylation that is typically seen with increasing P:Rh ratios (see 8.2). The ^{31}P NMR magnetization transfer experiments described by Brown [26] also indicate that PPh_3 dissociation from the RhL_2 complex **2** occurs, albeit at a significantly lower rate than the corresponding PPh_3 dissociation from tris-phosphine complex, **1**. When very bulky phosphite ligands are used, NMR spectra have revealed the presence of monoligated species $Rh[P(OAr)_3](CO)_3H$ [5].

It has not been established experimentally whether alkene complexation is reversible or not; in the scheme we have drawn all steps except the hydrogenolysis at the end as reversible. Experiments with the use of deuterated substrates suggest that alkene coordination and insertion into the Rh-H bond can be reversible processes, certainly when the pressures are low. Complex **4** undergoes a migratory insertion to give square-planar alkyl complexes **5c** and **5t**, which are respectively *cis* or *trans*. In the absence of CO, the 16-electron complexes containing aryl groups or alkyl groups without ß-hydrogen atoms can be isolated as mixtures of *cis* and *trans* isomers [28]. Complex **5** can undergo ß-hydride elimination, thus leading to isomerisation when higher alkenes are used, or it can react with CO to form trigonal bipyramidal complexes **6**. Thus, under low pressure of CO more isomerisation may be expected. At low temperatures (< 70 °C) and a sufficiently high pressure of CO (> 10 bar) the insertion reaction is usually irreversible and thus at this point also the regioselectivity of hydroformylation of 1-alkenes is determined.

Complexes **6** undergo the second migratory insertion in this scheme to form the acyl complexes **7**. Complexes **7** can react either with CO to give the saturated acyl intermediates **8**, which have been observed spectroscopically, or with H_2 to give the aldehyde product and the unsaturated intermediates **3**. The reaction with H_2 involves presumably oxidative addition and reductive elimination, but for rhodium no trivalent intermediates have been observed. For iridium the trivalent intermediate acyl dihydrides have been observed [29]. The Rh-acyl intermediates **8** have also been observed [26] and due to the influence of the more bulky acyl group, as compared to the hydride atom in **2e** and **2a**, isomer **8ae** is the most abundant species.

At low hydrogen pressures and high rhodium concentrations, formation of dirhodium species such as **9** becomes significant. Since several of the studies of the Wilkinson group were carried out under such conditions, formation of di-rhodium species was very relevant to their chemistry. Not only did they report the formation of the orange dirhodium species of type **9**, they also observed the formation of red dirhodium species containing two carbon monoxide molecules less than **9**. A dirhodium complex **9** containing three molecules of PPh_3 was fully characterized [30]. Regeneration of rhodium hydrides from dormant

rhodium species formed by impurities is another cause for the positive rate response to raising the H_2 pressure. Note that in Figure 8.3 not all reagents have been depicted in the scheme for the sake of simplicity.

8.2.2 Ligand effects and kinetics

Steric and electronic properties of a ligand can drastically influence the rate and selectivity of the hydroformylation reaction. A systematic study though is absent for several reasons. For monodentate ligands a systematic study is impeded by the variety of complexes that may be involved at the various stages of the catalytic cycle. Secondly, $RhH(PPh_3)_3CO$ was used as the precursor in several studies, while aiming at the study of the effect of ligands added. Use of this procedure without removal of the liberated PPh_3 leads most likely to mixed phosphine complexes, which complicates interpretations. Thirdly, complexes of type **1** were often used without the addition of free ligand, which is needed to ensure a high equilibrium concentration of **1** or **2**. Other complications arise from the use of different experimental conditions. As we shall see in section 8.2-4 changes in temperature, concentrations and pressure can significantly influence rate and regioselectivity. For these reasons, studies which are performed under conditions outside those typically used for hydroformylation (10–30 bar, temperature 70–120 °C, [Rh] = $\approx 10^{-3}$ M, [alkene] = 0.1–2 M, [L] depending on complex stability) can result in conclusions that are not particularly relevant. Impurities in one of the feedstocks often led to oxidation of the phosphine ligand. Another source of erroneous results is the use of rhodium chloride (and the like) as the precursor, while it has been known for a long time that this leads to only partial conversion to hydrido species [3]. When discussing selectivities, one often does not take into account isomerisation. In addition, many interesting effects have been published only in patents and these results are less accessible than journal articles.

Thus, we are facing an impossible task to summarize the "ligand effect" for monodentate phosphines (and phosphorus ligands) and to give credit to the numerous contributions. For the sake of didactics we will present a few rules of thumb, which at this point will not be fully exemplified by literature data, but which will be supported when diphosphines are discussed in section 8.3.

Electronic effects.

Electron donating ligands, such as alkylphosphines, lead to slower catalysts and as result they require higher temperatures [31]. In recent years it has been shown that triethylphosphine gives turnover numbers of 700 $mol.mol^{-1}.h^{-1}$ for 1-hexene and very high turnover numbers for ethene at 120 °C and 40 bar. Hydroformylation with this catalyst may take place via a different mechanism. As a secondary solvent-dependent reaction hydrogenation to alcohols takes place [31c]. Arylphosphines containing electron-withdrawing substituents give

a faster catalytic reaction than triphenylphosphine [32,33,34]. Phosphites can give faster catalysts than phosphines [35,36], but this is certainly not true for all cases. A recent study in supercritical CO_2 also shows that electron withdrawing arylphosphines form more active catalysts [37], but the low concentrations of $RhHL_3(CO)$, in the absence of extra L added, and the relatively high concentration of CO in the supercritical medium may lead to excessive dissociation of the phosphine ligand. Dibenzophospholes are more electron-withdrawing than diphenylphosphino groups and without exception the former lead to faster catalysts [26,38,15,39]. In general, ligand effect studies are hard to compare, because for a particular ligand the rates may differ by at least an order of magnitude, depending on the concentration of rhodium, ligand and CO.

Most of the authors cited agree on the explanation; electron-withdrawing ligands lead to a decrease of the back-donation to carbon monoxide and thus to a weaker binding of the carbonyls. This will affect the formation of species **3** and **7**, such that their rate of formation, or their equilibrium concentration increases. Alkene complexation, giving complexes **4**, may also be accelerated or become more favoured thermodynamically. Migratory insertions are not particularly sensitive to electronic properties of the ligand [21 and references therein], but it is important to remember that oxidative addition will be slowed down when electron-withdrawing ligands are used.

Steric effects.

More sterically demanding ligands will favour the formation of species containing a low number of ligands L and therefore more CO ligands. A high proportion of CO ligands also leads to electron poor rhodium species and thus to enhanced dissociation of CO. For phosphites this effect has been clearly observed [40] as will be discussed in section 8.4.

In spite of the industrial importance of the rhodium-PPh_3 catalyst, very few data have been published on the kinetics of the hydroformylation reaction and the data known are often contradictory. Early mechanistic work by Wilkinson (at < 1 bar) demonstrated the inhibitory effect of increased CO and PPh_3 concentrations on 1-hexene hydroformylation [21]. Increased Rh and alkene concentrations were observed to lead to higher catalytic rates. Wilkinson also observed an accelerated hydroformylation rate caused by increasing H_2 pressure, which is most likely an artefact of inactive dirhodium species formed under "non-standard", low-pressure conditions. We will argue that under "standard" catalytic conditions the reaction is first order in the concentration of alkene, first order in the rhodium concentration, zero order in hydrogen, and the reaction shows a negative order in ligand concentration (phosphine or carbon monoxide, or both). The most detailed, early study is the report by Cavalieri d'Oro et al.[41] from Montedison. They found the following expression for the rate:

$$v = k\,[C_3H_6]^{0.6}\,[PPh_3]^{-0.7}\,[CO]^{-0.1}\,[Rh]^{1}\,[H_2]^{0}$$

(conditions 90–110 °C, p(CO) = 1–25 bar, p(H_2) = 1–45 bar, [PPh_3] = 0.05–5 M, [Rh] = (0.5–7).10^{-3} M, PPh_3/Rh = 300:1 to 7:1, [propene]$_{t=0}$ = 2–7 M)

They reported an overall apparent activation energy of 84 kJ.mol^{-1} for the process. The important features of this kinetic study are the zero order dependence in dihydrogen, the negative order in PPh_3 ligand (and CO), and the positive order in alkene concentration. Under "standard" conditions (T = 70–120 °C, CO = 5–25 bar, H_2 = 5–25 bar, Rh ≈ 1 mM, alkene = 0.1 – 2 M), i.e. the "industrial operating" conditions, chosen by many workers in the field, this rate equation seems a good starting point for arylphosphine modified catalysts.

The observed *order in propene* concentration is less than one, which might point to saturation kinetics. Indeed, high concentrations were used, but perhaps the non-ideal behaviour of propene (critical temperature 94 °C) plays a role in this. Under similar conditions for 1-hexene and 1-octene a neat first order behaviour in alkene has been observed using Rh-PPh_3 catalysts [36, 42].

At *high PPh_3 concentrations*, where the catalyst resting state is $(PPh_3)_3Rh(CO)H$, phosphine dissociation must occur to form the coordinatively unsaturated intermediates **3c** and **3t**. This dissociation is suppressed by increased PPh_3 concentration, which serves to reduce the concentration of active Rh species in the catalytic cycle.

At *lower PPh_3 concentrations* where the predominant resting state observed by in situ studies is $(PPh_3)_2Rh(CO)_2H$, species **3c** and **3t** are formed by CO dissociation, which is likewise inhibited by increased CO concentration. Consistent with this mechanism is the recent determination that dissociation/association of CO is reversible and faster than hydroformylation for arylphosphines (see 8.3). An inverse order in CO pressure and a zero order dependency on H_2 pressure was reported by several authors [32,42,43]. Under "standard" conditions, we propose that the best starting point for the kinetics is an equation of the type:

$$Rate(type-I) = \frac{A[alkene][Rh]}{B+[L]}$$

(the constants A, B do not refer to specific rate constants;

[L] is proportional to [PPh_3] and [CO]).

Two possible scenarios exist which are consistent with this rate equation. Rate determining *alkene coordination* by **3c** and **3t** followed by rapid alkene insertion into the Rh-H bond is one possibility. An equally valid alternative explanation for the observed kinetics involves rate determining migratory

insertion of alkene into Rh-H preceded by fast, reversible alkene coordination. In both cases, the concentrations of coordinatively unsaturated **3c** and **3t** are influenced by PPh_3 and CO concentrations.

The kinetics at moderate PPh_3 concentrations are in agreement with a catalyst resting state of $RhH(PPh_3)_2(CO)_2$ and a transition state of composition $RhH(PPh_3)_2(CO)$(alkene). At very high PPh_3 concentrations, the likely resting state is $RhH(PPh_3)_3(CO)$ and a transition state of composition $RhH(PPh_3)_2(CO)$(alkene) is again likely. The set of rate-limiting reactions are dissociation of CO (or PPh_3), complexation of alkene, and migratory insertion. Dissociation/association of CO is reversible and faster than hydroformylation for arylphosphines (see 8.3). Complexation of alkene is most likely reversible, although there are no experimental data on this process. Theoretical studies [44] indicate that complexation of CO or ethene to species **3** (Figure 8.3) has a low barrier. For migratory insertion of ethene into the metal-hydride an early transition state was found, involving a re-organization of the complex. This means that steric hindrance will play a crucial role and especially the rotation of the alkene from the in-plane coordination to a perpendicular coordination mode contributes to the barrier.

Several articles in the literature are in disagreement with the kinetics presented above, even textbooks, but the present view is that the majority of hydroformylation systems obeys the above rate law [45]. The cause of the reported deviations is the presence in many systems of dimer **9** (for whatever reason), which gives indeed rise to a higher rate when the hydrogen pressure is raised [46]!

For carbonyl systems and bulky phosphite systems, the resting state of the catalysts (for 1-alkenes) is the acylrhodium species of type **8** and thus, the reaction with dihydrogen is rate limiting [47,48]. The approximate rate equation is given below for type–II kinetics. We would like to stress that type-II kinetics is the exception rather than the rule.

$$Rate(type-II) = \frac{C[H_2][Rh]}{D+[CO]}$$

8.2.3 Regioselectivity

The regioselectivity of the catalysts based on PPh_3 has been extensively studied (see review [45]). The regioselectivity of 1-alkene hydroformylation varies from 70 to 96 % for the linear aldehyde. The highest selectivity is obtained at high concentrations of PPh_3, or even liquid PPh_3, and low pressures of CO. Isomerisation should be considered as well, as this forms an “escape” route for the branched alkyl intermediate leading to internal alkene isomers

instead of branched aldehyde. Since the activity of most phosphine catalysts for internal alkenes is low, the apparent linearity of the aldehyde product is high, but the overall selectivity to linear aldehyde may be low. This will be discussed further in 8.3.

Clearly, the number of phosphines coordinated to rhodium, along with the stereochemistry at Rh, determines the regioselectivity. At high PPh_3 concentrations, the resting state of the catalyst is **1** (Figures 8.3 and 8.4) and at moderate concentrations the resting state is a mixture of **2ae** and **2ee**. Wilkinson [3] and Andreetta [41] suggested that species **3** give high linear to branched ratios (20:1), and that at moderate phosphine concentrations square planar intermediates **10**, containing only one phosphine are formed, which would lead to low linear to branched ratios (4:1) (see Figure 8.4).

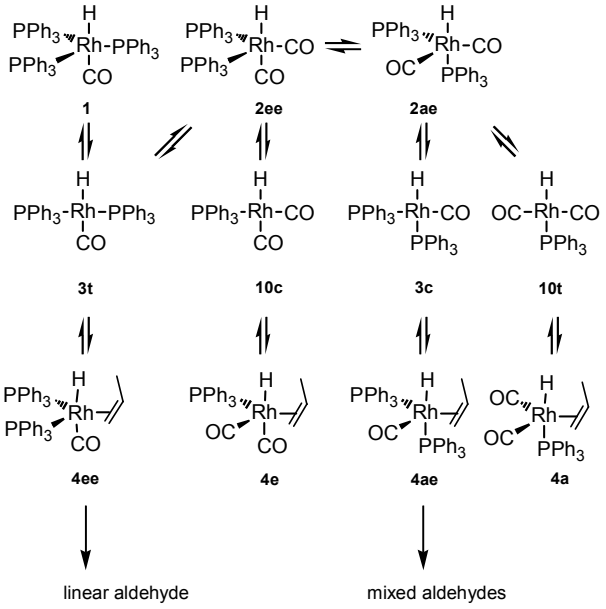

Figure 8.4. Scheme with intermediates involved in determining regioselectivity

Dissociation of PPh_3 from **1** gives **3t**, dissociation of CO from **2ee** also gives **3t**, while dissociation of CO from **2ae** will give **3c**. Dissociation of PPh_3 from **2** gives the isomers **10t** and **10c**. The use of diphosphines such as dppe and dppp gives modest linear-branched ratios and their putative intermediates **3** must have *cis* structure **3c**. Therefore, **3c** is not a likely intermediate for the *selective* hydroformylation. For linear-branched ratios of 4:1 we don't have to invoke mono-phosphine species of type **10**, as already structure **3c** suffices for the production of moderate l:b ratios (3/1). In conclusion, the species leading to

high linearity is the *trans* species **3t**, while **3c**, **10cb,** and **10t** all lead to low l:b ratios.

8.2.4 Process description, rhodium-tpp

LPO process. Propene hydroformylation can be done with a rhodium triphenylphosphine catalyst giving a linearity ranging from 60 to 96 % depending on the phosphine concentration. At very high phosphine concentration the rate is low, but the linearity achieves its maximum value. The commercial process (Union Carbide Corporation, now Dow Chemicals) operates presumably around 30 bar, at 120 °C, at high triphenylphosphine concentrations, and linearities around 92%. The estimated turnover frequency is in the order of only 300 mol(product).mol^{-1}(Rh).h^{-1}. Low ligand concentrations, with concomitant low linearities (70%), will give turnover frequencies in the order of 5–10,000 at 10 bar and 90 °C.

In the presence of carbon monoxide this rhodium catalyst has no activity for hydrogenation and the selectivity based on starting material is virtually 100%. The butanal produced contains no alcohol and can be converted both to butanol and to other products as desired.

The low-pressure oxo process was developed by Union Carbide Corporation, based on the Wilkinson patents. Temperature and pressure have to be controlled very carefully because the linearity strongly depends on these parameters. Ligand and rhodium (300 ppm) are very sensitive to impurities and the feed must be very thoroughly purified. In the initially applied process the rhodium catalyst was retained in the reactor, apart from a small purification cycle required for the removal of heavy ends and catalyst decomposition products that slowly build up. The gases are led into the reactor at the bottom via a sprinkler. The product aldehyde was removed with the gases by "stripping". The alkene conversion per pass is estimated to be 30%, and the propene is recycled. The small catalyst recycle is necessary because slow decomposition of the ligand occurs. Triphenylphosphine decomposes in the rhodium-catalysed process to a phenyl fragment and a diphenylphosphido fragment. Diphenylphosphide forms very stable, though inactive rhodium complexes. Impurities in the feed may also cause the formation of inert rhodium complexes. A general disadvantage is that the by-products remain in the catalyst phase.

In today's plants the product is taken out of the reactor as the liquid mixture containing the catalyst and distillation is done in a separate distillation vessel, see Figure 8.5.

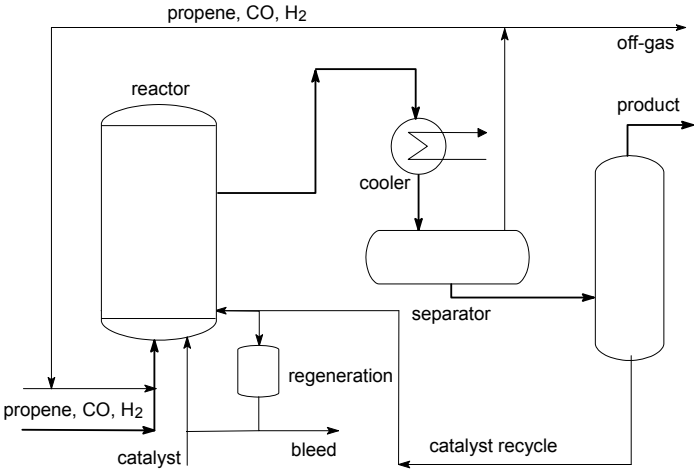

Figure 8.5. LPO process scheme with removal of product in liquid phase

8.2.5 Two-phase process, tppts: Ruhrchemie/Rhône-Poulenc

In 1986 a new process came on stream employing a two-phase system with rhodium in a water phase and the substrate and the product in an organic phase. For propene this process is the most attractive one at present. The catalyst used is a rhodium complex with a sulphonated triarylphosphine, which is highly water-soluble (in the order of 1 kg of the ligand "dissolves" in 1 kg of water). The ligand, tppts (Figure 8.6), forms complexes with rhodium that are most likely very similar to the ordinary triphenylphosphine complexes (i.e. $RhH(CO)(PPh_3)_3$).

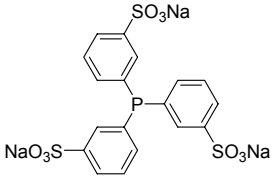

Figure 8.6. Tppts

The tppts process has been commercialised by Ruhrchemie (now Celanese), after the initial work conducted by workers at Rhône-Poulenc, for the production of butanal from propene. Since 1995 Hoechst (now Celanese) also operates a hydroformylation plant for *1-butene*. The partly isomerised, unconverted butenes are not recycled but sent to a reactor containing a cobalt catalyst. The two-phase process is not suited for higher alkenes because of the

low solubility of higher alkenes in water and the first-order dependency of the rate on alkene concentration.

Process description. In the reactor (Figure 8.7) the three phases (water+catalyst // butanal+propene // syn-gas+propene) are mixed vigorously to ensure transfer of the reacting gases to the catalyst. The heat of reaction is used for the distillation of the product (for our convenience the heat exchanger was drawn as a separate unit, but of course reactor/ heat exchanger/ distillation unit can be integrated). Subsequently the mixture is depressurised and the two-phase liquid mixture is led to a settler tank for phase separation. Experiments in laboratory glassware show that a very neat and fast separation of the two phases occurs. We know that in a common organic synthesis this is often not the case. The separation of a water-layer and an organic solvent layer often leads to an inseparable "interphase" between water and organic solvent.

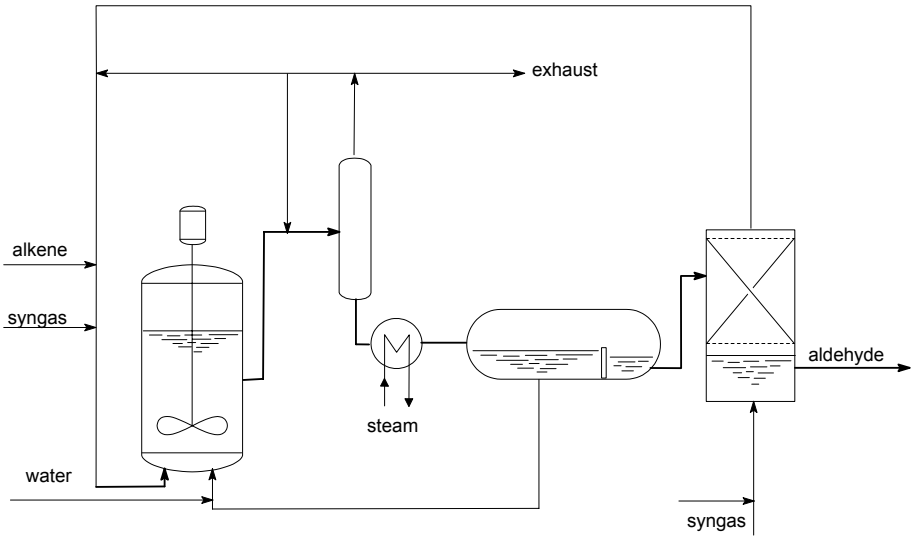

Figure 8.7. Ruhrchemie/Rhône-Poulenc process

Hoechst-Ruhrchemie (now Celanese) reported that no detectable losses of rhodium occur. We assume that propene is stripped from the aldehyde product and finally distillation of the aldehyde is conducted to separate the branched (8%) and linear product (92%). Note that the amounts of water lost in the aldehyde phase have to be replaced. Note also that by-products arising from aldol condensation, if any, are separated from the catalyst together with the product. These heavy ends end up in the bottom of the product distillation, which is advantageous, as the bottom can be sent to an incinerator. In processes such as the Shell process (Figure 7.6), the heavy end is a mixture of

decomposition products, condensation products, and catalyst components, which are recycled. The build-up of the impurities requires a bleed-stream, from which the catalyst has to be removed.

8.2.6 One-phase catalysis, two-phase separation

The two-phase process described above is an ideal process in terms of separation of all components and stability. It cannot be used, however, for higher alkenes, not even 1-alkenes. The reason for this is the extremely low solubility of higher alkenes in water; for instance the solubility of 1-octene is 1000 times lower than that of propene. Actually, it is not known whether the reaction takes place at the heterogeneous interface of water and the organic layer or in the homogeneous water phase with dissolved propene. Intimate mixing is needed, both for the "heterogeneous" reaction and for the homogeneous reaction to accelerate transportation. Since the reaction rate has a first order dependency on the alkene concentration, it is obvious that two-phase catalysis using water is not a viable option for higher alkenes. One might use micellar or vesicular systems containing the catalyst, in which the substrate has a higher solubility than in water, but even then the rates are still moderate, probably because transport of alkene through the water layer remains slow [49]. Another interesting technique is the immobilisation of the aqueous catalyst on a silica surface (supported aqueous phase catalysts, SAPC) [50], but this has not reached widespread application either. SAPC is always faster than a two-phase system or directly immobilised system [51] and in one case Mortreux found that SAPC for methyl acrylate was even faster than the homogeneous counter part [52].

High rates for higher alkenes can only be obtained if the concentration of the alkene is high. This means that the reaction must be carried out in one phase, which is an apolar medium. In the second step, rhodium complex, unconverted alkene, and aldehyde product must be separated. For high boiling products and temperature sensitive rhodium complexes distillation is not an attractive solution. Union Carbide Chemicals (now Dow Chemical) introduced a catalyst extraction method, applied after the hydroformylation has taken place. We discuss this method here, also because the scope may be broader than that of hydroformylation only. The ligand used is both soluble in water and semi-polar solvents. The solvent in the hydroformylation reactor is N-methyl-pyrrolidone. The latter is miscible both with water and with apolar feedstocks and products. After the hydroformylation reaction water is added and a liquid-liquid separation takes place, and the rhodium-ligand complex goes to the polar phase and the organics to the organic layer. It is important that all rhodium is retained in the aqueous phase, but the separation of the "organics" in such mixtures containing N-methyl-pyrrolidone will not be

perfect and may require several more extractions. This is an easy procedure on a large-scale, continuous operation. Potential ligands for this type of processes are shown in Figure 8.8, tppms and DPBS; the latter seems the most stable one [53]. The process can be used for a broad range of higher alkenes [54].

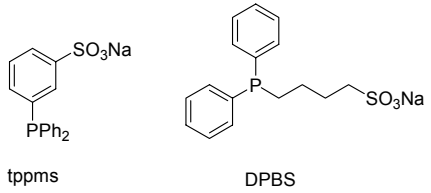

Figure 8.8. Ligands for one-phase catalysis, two-phase extraction

In 2001 Sasol announced the commercialisation of a Rh-catalysed hydroformylation technology, licensed from Kvaerner (Davy McKee), for conversion of Sasol's Fischer-Tropsch 1-alkenes to detergent alcohols, on 120 kt/a scale [55] that is probably using this technology.

8.3 Diphosphines as ligands

It was known that diphosphines such as dppe and dppp gave catalysts with a low preference for linear product in the rhodium-catalysed hydroformylation [45]. Important breakthroughs were reported in the late eighties with BISBI **11** (see Figure 8.9) and the predecessors of Xantphos (vide infra) all showing a high regioselectivity for the formation of linear aldehydes [39]. Propene was hydroformylated by Eastman Chemicals using BISBI under "standard" conditions in a vapour stripped reactor. The aldehyde product shows a high linearity (l:b = 30). For comparison, other ligands known until then gave much lower linearities as shown in Table 8.1, taken from their work and other sources.

Improved variations were described in a later patent [39]. Instead of diphenylphosphino groups dibenzophosphole groups were used, which often leads to an increase in rate and selectivity. The rate of reaction was accelerated by high propene pressures, hinting at the common rate equation for hydroformylation under "standard" conditions. Under optimised conditions (i.e. low CO pressure) l:b ratios as high as 288 were obtained for propene.

Table 8.1. Hydroformylation results using BISBI and other ligands [33,39,56]

Ligand	Bite angle	Rate (mol.mol^{-1}.h^{-1})	Ratio l:b
12	126	2550	2.6–4.3
BISBI, **11**	113/120	3650	25
13	107	3200	4.4–12
DIOP [also 56]	102	3250	4.0–8.5
dppf [also 33]	99	3800	3.6–5
dppp	91	600	0.8–2.6
dppe	85		2.1
PPh_3[a]		6000	2.4

Conditions: syn gas pressure 16 bar, [Rh] = 1.5 mM, ligand/Rh = 2.4, 95–125 °C, solvent 2,2,4-trimethyl pentane-1,3-diolmonoisobutyrate (Texanol), propene pressure 5 bar. Other sources used different conditions and alkenes.

[a] [Rh] = 0.7 mM, ligand/Rh = 124.

Examination of molecular models of metal complexes of BISBI indicates that the chelate bite angle is much greater than 90°, the most common bite angle for bidentate ligands [57]. The work quoted so far, and the results shown in Table 8.1 led to the speculation that ligands with wider bite angles may perhaps have a fortuitous effect on the l:b ratio in the hydroformylation of 1-alkenes. However, at this time of date few chelating diphosphines had been proven by X-ray crystallography to be capable of adopting large bite angles. To identify ligands with wide bite angles Casey and Whiteker [58] introduced the concept of the "natural bite angle" (See Chapter 1.5.4).

Extending the speculations presented in Section 8.2 for PPh_3 and its rhodium complexes one expected that BISBI would coordinate in a bis-equatorial fashion (**14**) in $RhH(L\text{-}L)(CO)_2$, thus leading to **3t** only when dissociation of a CO molecule takes place (due to strain in the backbone **3t** might not be completely trans). NMR and IR spectroscopy proved [57] that the structure of complexes **11** indeed contained the two phosphorus atoms in the equatorial plane and hydrogen in one of the apical positions (**14**, Figure 8.9).

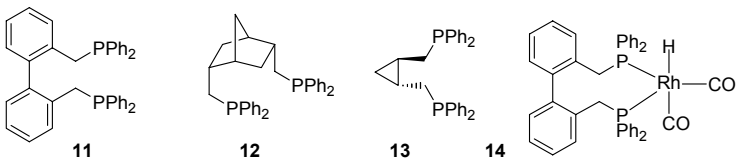

Figure 8.9. Wide bite angle ligands

Yamamoto and Casey separately reported that 2,5-dppm-nor **12** (Figure 8.9) while having a wide natural bite angle (126°) [59], gave an unexpectedly low l:b ratio of only 2.6. This result was attributed to its inability to form stable

chelates. Molecular mechanics calculations show that the rhodium chelate complex of **12** has 12 kcal more strain than the free ligand; in contrast, BISBI and dppe chelates are less than 3 kcal more strained than the free ligands. In designing new wide bite angle ligands, it is suggested that the extra strain imposed by chelation should be calculated so as to determine whether the new ligand would form a stable chelate.

It was concluded from the data in Table 8.1 that apparently wider bite angles and thus a bis-equatorial coordination mode of a diphosphine lead to high l:b ratios, although the reason for this was not understood in detail.

8.3.1 Xantphos ligands: tuneable bite angles

Readily available backbones for tuneable wide bite angles turned out to be those based on xanthene and related compounds (Figure 8.10). The diphosphines derived from these cover a range of angles from 102 to 121° (or 126° for cyclic substituents). Key feature of these ligands is the oxygen ether atom in the bridge that prevents metallation and that in neutral rhodium hydrides does not participate in the coordination to the metal. By changing the fragment in the back of the molecule (C_1, C_2, N, S) the bite angle can be easily tuned. The natural bite angles are shown in Figure 8.10 and Table 8.2.

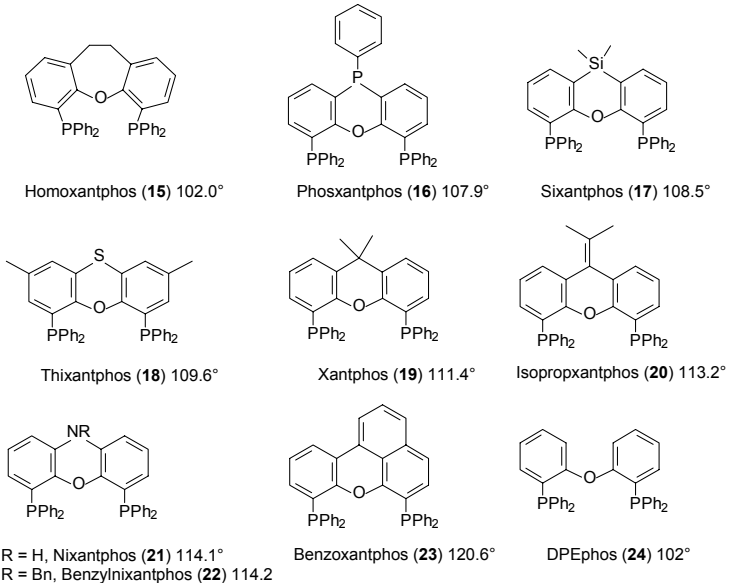

Figure 8.10. Xantphos type ligands and their calculated β_n values

Hydroformylation. The hydroformylation results for the series **15–24** are shown in Table 8.2 [60]. From the table one can see that the selectivity for linear aldehyde increases with wider bite angles. For ligands **15–19** the l:b ratio increases, but at higher bite angles the effect levels off.

Table 8.2. Hydroformylation of 1-octene using Xantphos ligands[a]

ligand	β_n, deg	**ee:ae**[d]	l:b ratio[b]	% lin. ald.[b]	% isomer.[b]	tof[b,c]
15	102.0	3:7	8.5	88.2	1.4	37
16	107.9	7:3	14.6	89.7	4.2	74
17	108.5	6:4	34.6	94.3	3.0	81
18	109.6	7:3	50.0	93.2	4.9	110
19	111.4	7:3	52.2	94.5	3.6	187
20	113.2	8:2	49.8	94.3	3.8	162
21	114.1	7:3	50.6	94.3	3.9	154
22	114.2	8:2	69.4	94.9	3.7	160
23	120.6	6:4	50.2	96.5	1.6	343

[a] Conditions: $CO/H_2 = 1$, $P(CO/H_2) = 20$ bar, ligand/Rh = 5, substrate/Rh = 637, [Rh] = 1.00 mM, number of experiments = 3. In none of the experiments was hydrogenation observed. [b] Linear over branched ratio, percentage linear aldehyde, percent isomerisation to 2-octene, and turnover frequency were determined at 20% alkene conversion. [c] Turnover frequency = (mol of aldehyde) (mol of Rh)$^{-1}$ h^{-1}. [d] Calculated from J_{P-H} NMR data.

The rate of reaction increases with increasing bite angle (with the exception of ligands **20–22**) as one might expect since two phosphines with a small bite angle are a better donor pair than two phosphines having a wider bite angle. The stronger donation by the phosphines leads to more back-donation to CO and thus stronger bonding of CO.

Ligand **23**, which will adopt a flattened conformation compared with the other ligands, gives an interesting result in that a low isomerisation rate is observed. Ligand **15** assumes a local C_2 type symmetry, in contrast to the other ligands all having C_s symmetry. Ligand **24**, the diphosphine made from diphenyl ether, is a substitute for **15** as it has the same small bite angle of 102°. It gives a moderate linear branched ratio of 6.7 but no isomerisation [53] at a pressure of 10 bar.

Three X-ray crystal structures of (L–L)Rh(CO)H(PPh_3) (L–L = **18, 22, 23**) were determined and all structures reveal distorted trigonal bipyramidal complex geometries with all the phosphines occupying equatorial sites. The observed P-Rh-P angles for ligands **18**, **22** and **23** in the crystal structures are 111.7º, 110.2º and 109.2º respectively, which is the reverse of the calculated natural bite angles! The observed bite angles are within the flexibility ranges calculated for the ligands. The bite angle of approximately 110º found in all three crystal-structures is probably the result of stereoelectronic interactions between the diphosphine and the large triphenylphosphine ligand.

Electronic effects. To study the nature of the electronic effect in the rhodium diphosphine catalysed hydroformylation, a series of thixantphos **18** ligands with varying basicity was synthesized **25–30** (Figure 8.11). In this series of ligands, steric differences are minimal so purely electronic effects could be investigated.

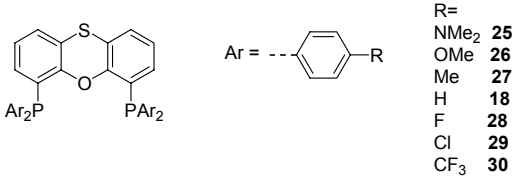

Figure 8.11. Substituted thixantphos ligands

The X-ray crystal structure of (**26**)Rh(CO)H(PPh_3) is very similar to the previous ones. The P-Rh-P bite angle is 109.3°. The small difference in observed bite angles confirms the assumption based on molecular mechanics that *p*-substitution on the aryl rings has only minor steric effects. The better donor prefers a smaller bite angle. A noticeable difference is found in the Rh-CO distance. The decreased Rh-CO bond length for the *p*-CH_3O-thixantphos complex (1.86 Å) compared to the thixantphos complex (1.89 Å) is a result of increased back-bonding of rhodium to the carbonyl ligand.

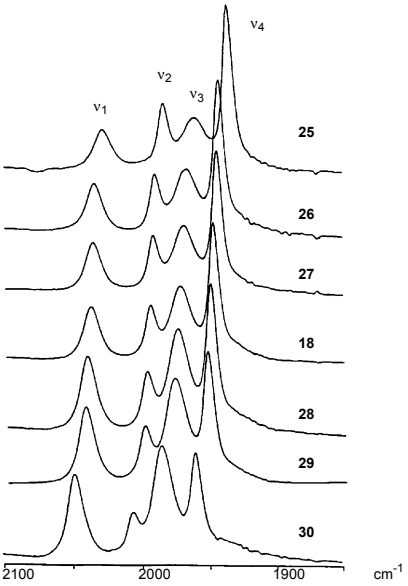

Figure 8.12. IR spectra of complexes RhH(ligand)CO (ligand = **25–30, 18**)

In situ IR spectra. Unambiguous evidence for the presence of **ee** and **ae** complex isomers was supplied by HP-IR spectroscopy. The spectra of the (diphosphine)$Rh(CO)_2H$ complexes all showed four absorption bands in the carbonyl region (Figure 8.12).

In an effort to assign the bands to **ee** and **ae** isomers the (thixantphos)$Rh(CO)_2D$ complex was measured for comparison. Upon H/D exchange, only ν_1 and ν_3 shift to lower wavenumbers (respectively 18 and 14 cm^{-1}), and therefore, these two bands are assigned to the carbonyl frequencies of the **ee** complex. The two bands that do not shift, ν_2 and ν_4, belong to the **ae** complex. From the disappearance of a low-frequency shoulder upon H/D exchange, it can be concluded that one of the rhodium hydride vibrations is partly hidden under ν_4.

During hydroformylation the IR spectra of the rhodium species (diphosphine)$Rh(CO)_2H$ for ligands **26**, **18**, and **30** do not change. The respective **ee**:**ae** equilibria are not influenced, and no other carbonyl complexes are observed; thus these are the catalyst's resting state. The coupling constants in the NMR spectra reflect the equilibria between **ae** and **ee** species.

Hydroformylation results in Table 8.3 show that, with the exception of ligands **28** and **30**, the rate of the reaction increases with decreasing phosphine basicity. An explanation for the deviant behaviour of **28** and **29** can be that catalyst formation is incomplete or deactivation of the catalyst occurs. Decreasing phosphine basicity facilitates CO dissociation from the (diphosphine)$Rh(CO)_2H$ complex and enhances alkene coordination to form the (diphosphine)Rh(CO)H(alkene) complex, and therefore, the reaction rate increases.

Table 8.3. Electronic effects in hydroformylation using thixantphos derivatives

ligand	χ_i	**ee:ae**	l:b	2-octene, %	nonanal, %	t.o.f.
25	1.7	47:53	44.6	4.8	93.1	28
26	3.4	59:41	36.9	5.3	92.1	45
27	3.5	66:34	44.4	4.7	93.2	78
18	4.3	72:28	50.0	4.9	93.2	110
28	5.0	79:21	51.5	5.7	92.5	75
29	5.6	85:15	67.5	6.9	91.7	66
30	6.4	92:8	86.5	6.8	92.1	158

1-octene, 80 °C, 20 bar of 1:1 CO/H_2, 1.0 mM rhodium (diphosphine/Rh = 5)

While the l:b ratio increases with the χ-value, no electronic effect of the ligands on the selectivity for linear aldehyde is observed. The selectivities for linear aldehyde are all between 92 and 93%. The increase in l:b ratio with decreasing phosphine basicity can be attributed completely to an increased tendency of the branched alkyl rhodium species to form 2-octene instead of

branched aldehyde (Figure 8.13). The increasing electrophilicity of the rhodium centre leads to a higher reactivity of the rhodium alkyl species toward CO dissociation and β-hydrogen elimination. The total amount of all other products (branched aldehyde and 2-octene) is 7–8% for all ligands.

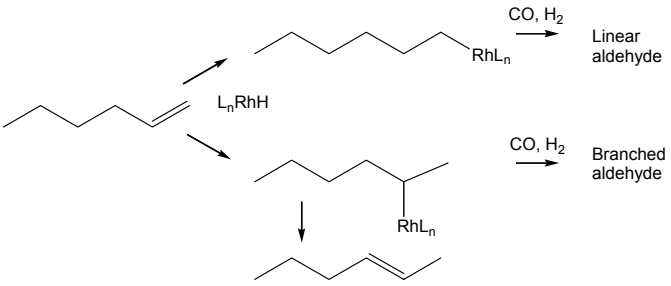

Figure 8.13. Competition between 2-hexene formation and branched aldehyde formation

It was found that CO exchange in (diphosphine)Rh(CO)$_2$H complexes proceeds via the dissociative pathway [60]. The decay of the carbonyl resonances of the (diphosphine)Rh(^{13}CO)$_2$H complexes indeed followed simple first-order kinetics. The experiments with ligand **20** at different ^{12}CO partial pressure show that the rate of CO displacement is independent of the CO pressure. Furthermore, the rate is also independent of the (diphosphine)Rh(^{13}CO)$_2$H complex concentration, as demonstrated by the experiments with ligand **18**. It can therefore be concluded that CO dissociation for these complexes obeys a first-order rate-law and proceeds by a purely dissociative mechanism.

It was found that the CO dissociation rate at 80 ºC is about 100 times as fast as the hydroformylation reaction. It is not likely that increasing the bite angle would lower the activation energy for alkene coordination. Increasing the bite angle results in increased steric congestion around the rhodium centre and consequently in more steric hindrance for the alkene entering the coordination sphere. What kind of electronic effect the widening of the bite angle has on the activation energy for alkene coordination is unclear, since it depends on the bonding mode of the alkene. Rhodium to alkene back-donation is promoted by narrow bite angles, while alkene to rhodium donation is enhanced by wide bite angles [61].

Internal alkenes. Dibenzophosphole- and phenoxaphosphino substituted xantphos ligands **31** and **32** [62] (Figure 8.14) show a high activity and selectivity in the rhodium catalysed linear hydroformylation of 1-octene (l:b = > 60). More importantly, ligands **31** and **32** exhibit an unprecedented high activity and selectivity in the hydroformylation of trans 2- and 4-octene to linear nonanal.

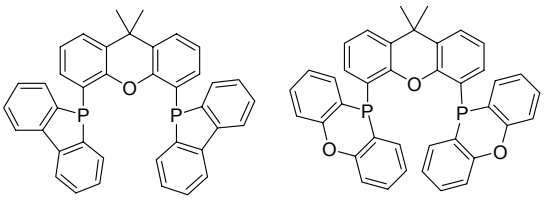

31 **32**

Figure 8.14. Ligand structures

Table 8.4. Hydroformylation of 2- and 4-octene[a,d]

Ligand	Substrate	l:b ratio[b]	% linear ald	t.o.f[c].
PPh_3	2-octene	0.9	46	39
31		9.5	90	65
32		9.2	90	112
PPh_3	4-octene	0.3	23	2
31		6.1	86	15
32		4.4	81	20

[a] [Rh] = 1.0 mM, Rh:P:octene = 1:10:673. [b] l:b Ratio includes all branched aldehydes.

[c] Turnover frequencies were calculated as (mol aldehyde)(mol catalyst)$^{-1}$(h)$^{-1}$ at 20–30% conversion. [d] 120 °C and p = 2 bar.

They constitute the first rhodium phosphine modified catalysts for such a selective linear hydroformylation of internal alkenes. The extraordinary high activity of **32** even places it among the most active diphosphines known. Since large steric differences in the catalyst complexes of these two ligands are not anticipated, the higher activity of **32** compared to **31** might be ascribed to very subtle bite angle effects or electronic characteristics of the phosphorus heterocycles.

The high l:b ratios of ligands **31** and **32** are in good agreement with earlier observations that diphosphines with natural bite angles close to 120° give very selective catalysts. The calculated bite angles are largely due to the interference of the rigid substituent rings at phosphorus. Table 8.4 shows the activities and selectivities achieved for internal alkenes. To enhance the rate of isomerisation and to prevent hydroformylation of the internal alkenes, a relatively high temperature and low pressure were used. The dissociation rate of CO from the resting state (**32**)$RhH(CO)_2$ was very fast, several times faster than that found for diphenylphosphino Xantphos ligands [60]. Thus larger (natural) bite angles promote the formation of four-coordinate species, as may be expected. For the same reason they will enhance isomerisation, since this involves a competition between CO association and β-hydrogen abstraction by the vacant site [16,17].

8.4 Phosphites as ligands

8.4.1 Electronic effects

Aryl phosphites were among the first ligands that were extensively studied. The results obtained with triphenylphosph**ine** and triphenyl phosph**ite** are strikingly similar at low ligand concentrations. At higher ligand metal ratios phosphites may retard the reaction. The electronic and steric properties of the phosphite have a large effect on the rate and selectivity of the reaction.

The results of the early work by Pruett and Smith [4] together with two more recent data [63], are summarised in Table 8.5. We have added the χ- and θ-values in this overview, which were not yet known when the catalytic work was reported.

Table 8.5. Hydroformylation with rhodium phosphite and phosphine catalysts

Ligand R_3P R=	χ-value	θ-value	linearity of product %
n-Bu	4	132	71
n-BuO	20	109	81
Ph	13	145	82
PhO	29	128	86
2,6-$Me_2C_6H_3O$	28	190	47
4-Cl-C_6H_4O	33	128	93
CF_3CH_2O	39	115	96
$(CF_3)_2CHO$	51	135	55

(conditions: 90 °C, 7 bar CO/H_2 = 1:1, substrate heptene-1, ligand/rhodium varies from 3:1 to 20:1, or [L]=3–20 mM) (from ref [4]; last two entries from ref [63])

One general trend that emerges from the table is that ligands with high χ-values give a higher selectivity toward linear products. In addition more isomerisation is obtained; unfortunately this is often neglected in the reports. Preferably one would like to have also values for the absolute rates in addition to the selectivities, but since these are lacking a detailed explanation of the results is not always possible.

The trend towards higher linearities breaks down at two instances; one involves a rather bulky ligand with a θ-value of 190°, the other one involves hexafluoroisopropyl phosphite that has a very high χ-value. Both give rise to unstable rhodium carbonyl complexes either for steric reasons (vide infra) or for electronic reasons. The χ-value of hexafluoroisopropyl phosphite is very high indeed and it is thought that this value of 51 means that electronically it is very similar to CO, i.e. a strong electron acceptor. Hence, the propensity of its

mixed carbonyl hydride rhodium complexes to lose CO is likely to be similar to the rather unstable $HRh(CO)_4$.

8.4.2 Phosphites: steric effects

Very bulky phosphite ligands (see Figure 8.1, 8.15) yield unstable rhodium complexes. The cone angle of o-t-Bu-phenyl phosphite, **33**, is as high as 180° and the complex formed with rhodium has the formula $HRh(CO)_3L$; apparently there is not enough space for the co-ordination of a second phosphite (Figure 8.14). In a trigonal bipyramidal complex there would be room for two bulky ligands at the two axial positions but this would leave an equatorial position for a σ-bonded hydride, which is undesirable. The mono-ligand complex cannot be isolated and has only been observed under a pressure of CO and H_2 [64].

This complex easily looses CO, which enables co-ordination of a molecule of alkene. As a result the complexes with bulky phosphite ligands are very reactive towards otherwise unreactive substrates such as internal or 2,2-dialkyl 1-alkenes. The rate of reaction reaches the same values as those found with the triphenylphosphine catalysts for monosubstituted 1-alkenes, i.e. up to 15,000 mol of product per mol of rhodium complex per hour at 90 °C and 10–30 bar. When 1-alkenes are subjected to hydroformylation with these monodentate bulky phosphite catalysts an extremely rapid hydroformylation takes place with turnover frequencies up to 170,000 mole of product per mol of rhodium per hour [65]. A moderate linearity of 65% can be achieved. Due to the very fast consumption of CO the mass transport of CO can become rate determining and thus hydroformylation slows down or stops. The low CO concentration also results in highly unsaturated rhodium complexes giving a rapid isomerisation of terminal to internal alkenes. In the extreme situation this means that it makes no difference whether we start from terminal or internal alkenes.

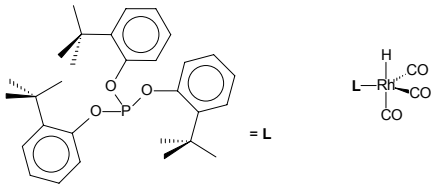

33

Figure 8.15. Bulky phosphite and its rhodium complex

Since hydroformylation of internal alkenes is also relatively fast with this catalyst the overall linearity obtained may become rather low (20–30%). This explains the low linearity of a non-optimised reaction using a similar bulky-phosphite R = 2,6-$Me_2C_6H_3O$ quoted in Table 8.5.

A comment about metal-ligand ratio. Many authors in the field of homogeneous catalysis suffice to state the ligand-to-metal ratio (L/M) in their reports on catalysis. This is common practice even amongst experienced people. In general this is not enough; the absolute values of the concentrations are as important as the ratio. Consider the following exercise. The catalytically active complex is involved in the following equilibrium:

$$HM(CO) + L \rightleftharpoons HM(L) + CO$$

The selective and fast catalyst species we want is HM(L) *and we have determined that at a certain pressure we need a twenty-fold excess of* L *in order to have 95 % of* M *in the* M(L) *state.*

The concentration of M = 10^{-3} *molar. Suppose we want to reduce the concentration of* M *to* 10^{-5}. *When we calculate the equilibrium constant from the first example and then calculate the required concentration of L at* M= 10^{-5} *molar we find the following rule of thumb: if an excess of L is needed, keep [L] the same and lower [M] only!*

8.5 Diphosphites

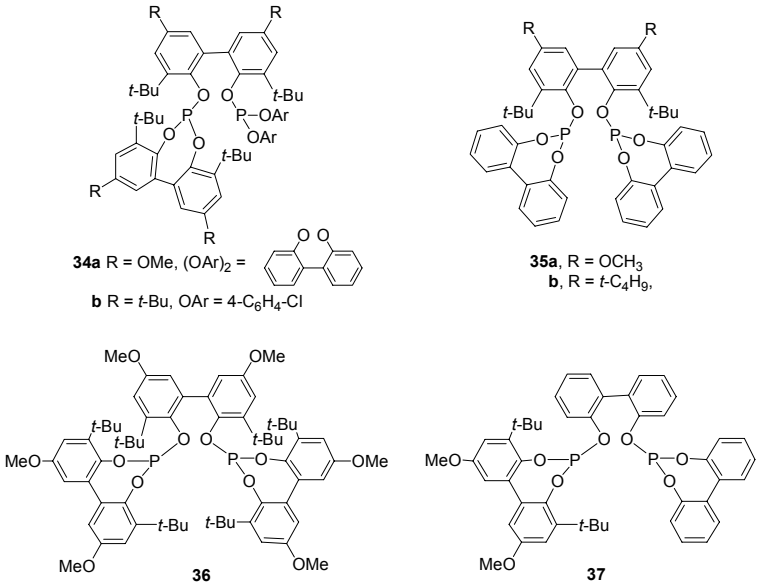

Figure 8.16. Typical examples of UCC diphosphites

The diphosphites are an interesting class of ligands. Union Carbide Corporation has exploited the effect of higher rates of bulky phosphites [5] by taking *bi*dentates, which give higher linearities than monodentate bulky phosphites (Figure 8.16) [6,7]. Certain diphosphites were found to give very high linearities even when internal alkenes were used. All major companies have since the late 1980's carried out research on diphosphite catalysts.

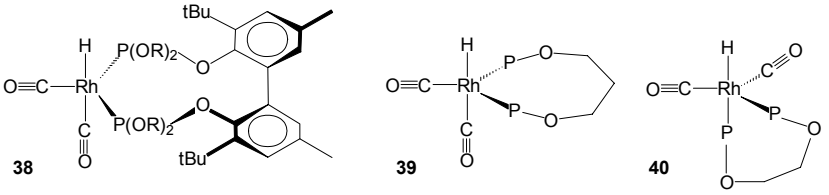

Figure 8.17. Diphosphite rhodium complexes **38**, **39**, and **40**

Their preparation is often very easy and a large variety is accessible. As for phosphines, the co-ordination mode depends on the length of the bridge. Bridges consisting of five atoms (OC_3O) (**39**), as in Xantphos (C_2OC_2), and bridges of six atoms (**38**) give complexes containing bis-equatorial co-ordination. Complexes of ligands having only four atoms in the bridge (OC_2O) show equatorial-axial co-ordination (**40**) (Figure 8.17).

Complexes containing equatorial-axial ligands always give low selectivity. Complexes giving high selectivity to linear aldehydes always contain bis-equatorially co-ordinating ligands (wide bite angles). The reverse is not true, since many complexes having the desired structure still give low selectivities.

Phosphite complex **38** is a typical example of the new generation catalysts. The NMR characteristics include a small coupling constant J_{P-H}, (< 30 Hz), and if the two phosphorus atoms are inequivalent, a large J_{P-P} coupling constant (250 Hz). Complex **40** shows the opposite: one large and one small coupling constant J_{P-H}, (180 and –30 Hz), and, if the two phosphorus atoms are inequivalent, a small J_{P-P} coupling constant (< 80 Hz). At room temperature the complexes of type **40** are extremely fluxional and in fact the proton spectrum shows a triplet (doubled due to ^{103}Rh, spin 1/2) due to the averaged coupling constants of the two phosphorus nuclei. The details of chemical shifts and coupling constants are now well known and can be used for the determination of the solution structures [66]. One crystal structure of a complex having structure **38** has been published [67].

Table 8.6. Hydroformylation using rhodium bulky diphosphite catalysts[a]

Ligand	T, °C	p CO/H_2 bar	Ratio CO/H_2	Alkene	Isom. %	Rate,[b] mol. (mol Rh)$^{-1}$. h^{-1}	l:b
34a [c]	70	2.5	1:2	1-Butene		2400	50
34a [c]	71	6.7	1:2	"		730	35
36 [c]	70	7	1:2	"		160	6.3
37 [c]	70	4.3	1:1	Propene		280	1.2
36 [c]	70	4.3	1:1	"		20	2.1
35a [c]	74	4.5	1:1	"		402	53
35a [d]	80	20	1:1	1-octene	18	3600	>100
35b [d]	80	20	1:1	1-octene	27	6,120	51
34b [d]	80	20	1:1	1-octene	n.d.	3375	19

[a] Conditions: 0.1–1 mM Rh, L/Rh = 10–20, [alkene] = 0.5–1 M in toluene. [b] Initial rate. [c] [6,7]. [d] [67]. N.d. = not detected.

From Table 8.6 it is seen that the ligand structure has a very large effect on the rate and regioselectivity of the reaction, often in an unpredictable way. In general ligands that coordinate in an **a-e** give low linearities, but an **e-e** coordination mode is not a guarantee for high linearities. Even for internal alkenes such as butene-2 linearities above 70% have been reported [6,7]. Various other, functionalised alkenes have been subjected to hydroformylation including methyl 3-pentenoate, which involved an isomerisation to obtain the linear product. The linear C-6 aldehyde-ester chain can be converted either to adipic acid or caprolactam, important nylon constituents. This opens a route to these products starting from butadiene with high atom economy, which could replace the present route starting from cyclohexene/cyclohexane by oxidation, a less clean route.

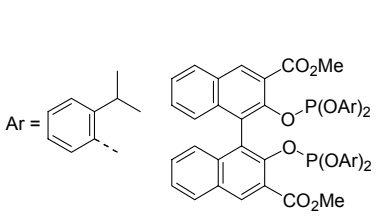

41

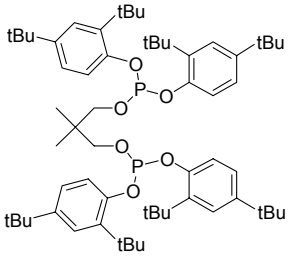

42

Figure 8.18. DSM-DuPont ligands and Mitsubishi ligand

DuPont and DSM have patented the use of ligand **41** (Figure 8.18) for the hydroformylation of methyl 3-pentenoate to linear product [68]. Instead of *t*-butyl groups on the bridge they use electron-withdrawing ester groups, while the remaining substituents are monophenols, rather than diols or bisphenols. The necessary isomerisation to the linear alkene prior to hydroformylation reaction is probably promoted by the electron-withdrawing ester groups. They were able to obtain high selectivity for the linear aldehyde, providing a useful intermediate to nylon-6 feedstocks. Comparable selectivity up to 97% was reported for the hydroformylation of 2-hexene.

The efficacy of monophenols containing bulky substituents was first described in the patents from Mitsubishi Chemical Corporation [69] (**42**, Figure 8.17). They report high yields of aldehyde (> 90%) for the hydroformylation of 1-alkenes with high linearities. The l:b ratios are generally above twenty using this ligand.

8.6 Asymmetric Hydroformylation

8.6.1 Rhodium catalysts: diphosphites

Asymmetric hydroformylation of alkenes is potentially an important reaction for the synthesis of chiral aldehydes as intermediates in drug synthesis, although we are not aware of an industrial application as yet. Square planar complexes of platinum containing chiral diphosphines have been for a long time the catalysts of choice for this reaction [70]. The bidentate ligands used were usually diphosphines developed for asymmetric hydrogenation, which are also square planar complexes. For many years the enantiomeric excesses obtained using rhodium and these diphosphines as the catalyst have been below 60%. Rhodium hydroformylation requires trigonal bipyramids and one can imagine that the steric constraints in the latter are different from those in square planar complexes. If the alkene coordinates in the equatorial plane, the interaction of the substrate with the bidentate is weaker than in a square planar intermediate, certainly if the bidentate phosphine is also positioned in the equatorial plane. Results for phosphine ligands in combination with rhodium are still moderate, but in the nineties two new types of ligands have led to high e.e.'s, namely diphosphites and phosphine-phosphite ligands.

Most popular as the substrate for studying asymmetric hydroformylation has been styrene, which might also form linear aldehyde.

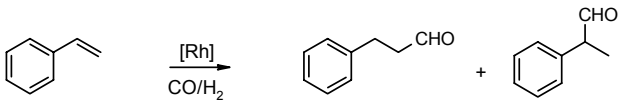

Figure 8.19. Styrene hydroformylation

The first reports on asymmetric hydroformylation using diphosphite ligands revealed no asymmetric induction [71]. In 1992, Takaya et al. published the results of the asymmetric hydroformylation of vinyl acetate (e.e.=50%) with chiral diphosphites [72]. In 1992, an important breakthrough appeared in the patent literature when Babin and Whiteker at Union Carbide reported the asymmetric hydroformylation of various alkenes with e.e.'s up to 90%, using bulky diphosphites derived from homochiral (2R,4R)-pentane-2, 4-diol (see Figure 8.20). Van Leeuwen et al. studied the influence of the bridge length, bulky substituents and cooperativity of chiral centres on the performance of the catalyst [73,74].

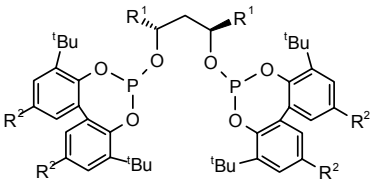

43

Figure 8.20. Chiral diphosphite **43**

Optically active diols are useful building blocks for the synthesis of chiral diphosphite ligands. Chiral diphosphites based on commercially available optically active 1,2 and 1,4-diols, 1,2:5,5-diisopropylidene-D-mannitol, L-α,α,α,α-tetramethyl-1,3-dioxalan-4,5-dimethanol and L-diethyl tartrate, were first used in the asymmetric hydroformylation of styrene [75].

When the bridging backbone consists of three carbon atoms often high e.e.'s can be obtained. Indeed, the starting hydride complexes contained the bidentate ligand in the trigonal plane and since the ligands are very bulky one might expect that the rotations needed for hydride migration might lead to different rates. When the backbone consists of two carbons, the ligand adopts **a-e** co-ordination and low e.e.'s were obtained. Ligands having four carbon atoms in the bridge lead to the desired **e–e** conformation, but e.e.'s are disappointingly low. Thus the same phenomena are observed as previously, when we discussed the bidentate phosphites in their use for high linearity.

Sugar backbones have been used many times, and indeed, when a three-carbon bridge is involved good e.e.'s may be obtained [76].

An interesting phenomenon concerns the introduction of atropisomerism in the bisphenol substituents (Figure 8.21). Due to steric hindrance one of the isomers will be preferentially formed and thus it seemed worthwhile to enforce certain combinations of chirality, i.e. backbone and substituent chirality.

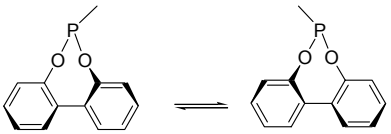

Figure 8.21. Atropisomerism in bisphenol moieties

For the bisnaphthol ligands a matched and mismatched combination was found; it turned out that the matched combination, giving the highest e.e., was also the most stable one. The same occurred when bisphenols were used, as accidentally the most stable ones are the ones that gave highest e.e.'s. The e.e.'s also increased with the steric bulk, but an optimum was reached when $SiMe_3$ groups were used (Figure 8.22) [77].

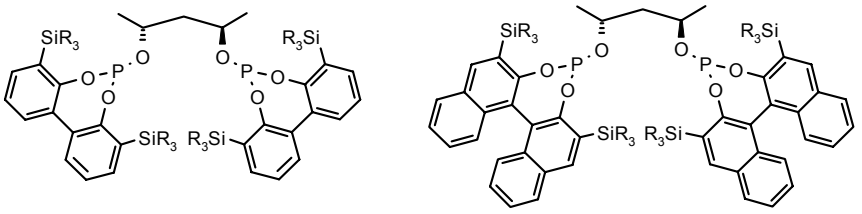

44a (R = Me)
44b (R = Et)
44c (R = *tert*-Bu Me_2)

45a (R = Me)
45b (R = Et)
45c (R = *tert*-Bu Me_2)

Figure 8.22. Bisphenol and bisnaphthol pentane-2,4-diol diphosphites

8.6.2 Rhodium catalysts: phosphine-phosphite ligands

The most important ligand for asymmetric hydroformylation is BINAPHOS (**46**, Figure 8.23), synthesized by Takaya and Nozaki. Also for other reactions it turned out to be a highly efficient ligand. The phosphine-phosphite ligand was expected to combine the high enantioselectivity obtained with diphosphines such as BINAP in asymmetric hydrogenation with the apparently efficient coordination of the phosphite moiety [78]. The Rh(I) complex of C_1-symmetric (R,S)-BINAPHOS provided much higher enantioselectivities than

either C_2 symmetric diphosphine ligands or diphosphite ligands, *viz.* more than 90% e.e. for a wide variety of both functionalised and internal alkenes [78,79,80,81].

A range of structural combinations has been reported. In the structures presented in Figure 8.23 the first R/S indicator refers to the binaphthyl (biphenyl) bridge and the second to the bisnaphthol (bisphenol) moiety. Thus for **48**, which lacks the bisphenol chirality, we write in the table (R,--), and for **50**, which contains a non-chiral biphenyl bridge, we write (--,R).

For all ligands the absolute configuration of the product obtained is the same as that of the absolute configuration of the binaphthyl (biphenyl) bridge. Thus, it seems that the binaphthyl bridge directs the position of the diphenylphosphino fragment. Remarkably, the best combination is formed when the absolute configurations for the binaphthyl and bisnaphthol moieties are opposite (i.e. S,R or R,S diastereomers). Enantioselectivities were much lower with (R,R)-ligands. R,R diastereomer **46** still gives the R-aldehyde in excess, but the e.e. is low (26%).

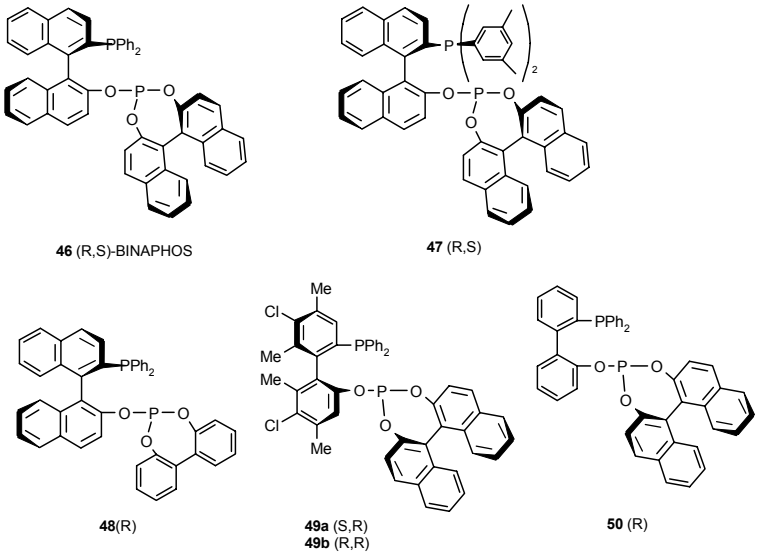

Figure 8.23. (R,S) BINAPHOS and related ligands

The results obtained for ligands **48** and **50,** which contain only one fixed stereocentre, are interesting and very informative about the system. Ligand **48**-(R,--), in which only the binaphthyl bridge has a predetermined absolute configuration R, leads to an e.e. of 83% (R-aldehyde), which is quite close to the value of 94% for (R,S)-BINAPHOS. This suggests that in the formation of the complex the binaphthyl bridge controls the conformation of the bisphenol

moiety so that the final conformation is (R,S). Likewise, **50**-(--,R) gives 69% e.e. of the S-aldehyde, which suggests that the complex formed assumes an (S,R) conformation, since now the R-bisnaphthol induces the formation of an S-diphenyl bridge. The control by the binaphthyl bridge in **48** is somewhat more efficient than that of the bisnaphthol moiety in **28**.

In the free ligand **50** a slight preference for the S,R diastereomeric conformation is observed, but in the complexes the preference for the S,R or R,S conformation is very strong, as is concluded from the NMR spectra and the catalytic results. In the free ligands with R,S configurations the through-space coupling constants between the two phosphorus nuclei are always larger than those in R,R ligands. This shows that in R,S ligands the ligand has a natural tendency to bring the donor atoms into close proximity. When an excess of R,R and R,S ligands with respect to rhodium is present, the latter give the most stable complexes and they are formed prevalently in the mixtures. In diphosphites, the bisphenol configurations were also observed to be controlled by the backbone and the most stable configurations lead to the highest e.e.'s in hydroformylation catalysis [75,78].

Table 8.7. Asymmetric hydroformylation of styrene using ligands **46**–**50**

Ligand	T ºC	CO/H_2 bar/bar	Time h	Conversion (%)	b/l	% e.e. (Absolute configuration)
46 (S,R)	60	50/50	43	>99	88/12	94 (S)
46 (R,S)	80	50/50	16	>99	86/14	89 (R)
46 (R,S)	60	10/90	40	>99	88/12	92 (R)
46 (R,R)	60	50/50	38	>99	86/14	25 (R)
47 (R,S)	60	50/50	37	>99	90/10	85 (R)
48 (R,--)	60	50/50	43	>99	91/9	83 (R)
49 (S,R)	60	50/50	42	>99	90/10	94 (S)
49 (R,R)	60	50/50	40	95	92/8	16 (R)
50 (–,R)	60	50/50	40	98	89/11	69 (S)

Styrene 20 mmols in benzene. [Rh] = 0.010mmol. L = 0.040 mmol. The e.e.'s were determined by GLC analysis of the corresponding 2-arylpropionic acids derived by Jones oxidation of the products

The spectroscopic data of phosphine-phosphite complexes show slight differences between the (R,S) and (S,R) complexes on the one hand and the (R,R) and (S,S) complexes on the other. In the latter compounds the data are less clear-cut, which could be due to structural deviations of the monohydride complexes from an ideal trigonal bipyramid or to equilibria between isomers. The two **ea** isomers cannot be distinguished by IR spectroscopy as their absorptions tend to coincide [82].

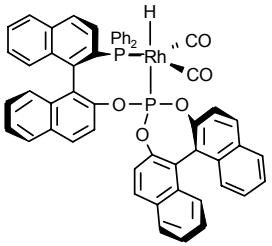

Figure 8.24. $RhH(CO)_2$(BINAPHOS) complex

^{31}P NMR spectroscopy shows that the complex [$RhH(CO)_2$(R,S-**46**)] is a single species at 60 ºC and 25 ºC in toluene-d_8 under 1 bar of CO. No apical-equatorial interchange was observed at any temperature. The unique dissymmetric environment in a single catalytically active species created by the phosphine-phosphite seems to be an important factor in the high enantioselectivity obtained.

References

1 Slaugh, L. H.; Mullineaux, R. D. U.S. Pat. 3,239,569 and 3,239,570, **1966** (to Shell)*; Chem. Abstr.* 1**964**, *64,* 15745 and 19420. *J. Organomet. Chem.* **1968**, *13*, 469.

2 Onoda, T. *ChemTech*. **1993**, Sept. 34.

3 Young, J. F.; Osborn, J. A.; Jardine, F. A.; Wilkinson, G. *J. Chem. Soc. Chem. Comm.* **1965**, 131. Evans, D.; Osborn, J. A.; Wilkinson, G. *J. Chem. Soc. (A)*, **1968**, 3133. Evans, D.; Yagupsky, G.; Wilkinson, G. *J. Chem. Soc. A* **1968**, 2660.

4 Pruett, R. L.; Smith, J. A. *J. Org. Chem.* **1969**, *34*, 327. (b) Pruett, R. L.; Smith, J. A. S. African Pat. 6804937, 1968 (to Union Carbide Coorporation); *Chem. Abstr.* **1969**, *71*, 90819.

5 van Leeuwen, P. W. N. M.; Roobeek, C. F. *J. Organometal. Chem.* **1983**, *258,* 343; Brit. Pat. 2,068,377, US Pat. 4,467,116 (to Shell Oil); *Chem. Abstr.* **1984**, *101*, 191142. Jongsma, T.; Challa, G.; van Leeuwen, P. W. N. M. *J. Organometal. Chem.* **1991**, *421*, 121. van Rooy, A.; Orij, E. N.; Kamer, P. C. J.; van Leeuwen, P. W. N. M. *Organometallics*, **1995**, *14*, 34.

6 Billig, E.; Abatjoglou, A. G.; Bryant, D. R.; Murray, R. E.; Maher, J. M. U.S. Pat. 4,599,206 **1986** (to Union Carbide Corp.); *Chem. Abstr.* **1989**, *109,* 233177.

7 Billig, E.; Abatjoglou, A. G.; Bryant, D. R. U.S. Pat. 4,769,498, U.S. Pat. 4,668,651; U.S. Pat. 4748261, **1987** (to Union Carbide Corp.); *Chem. Abstr.* **1987**, *107*, 7392r.

8 Yoshinura, N.; Tokito, Y. Eur. Pat. 223,103, **1987 (**to Kuraray).

9 Aqueous Phase Organometallic Catalysis-Concepts and Applications, eds. B. Cornils and W. A. Herrmann, Wiley-VCH, Weinheim, **1998**.

10 Drent, E.; Jager, W. W. U.S. Pat. 5,780,684, **1998** (to Shell); *Chem. Abstr.* **1998**, *129*, 137605.

11 Hayashi T.; Kawabata Y.; Isoyama T.; Ogata, I. *Bull. Chem. Soc. Jpn*. **1981**, *54*, 3438.

12 Abatjoglou, A. G.; Bryant, D. R.; Peterson, R. R. U.S. Pat. 5,180,854) **1993** (to Union Carbide Corp.; *Chem. Abstr.* **1991**, *113*, 80944.

13 Wiebus, E.; Cornils, E. *Chem. Ing. Tech.* **1994**, *66*, 916; Cornils, B.; Wiebus, E. *ChemTech,* **1995**, *25*, 33,; Cornils, B.; Wiebus, E. *Recl. Trav. Chim. Pays-Bas,* **1996**, *115*, 211.

14 van Leeuwen, P. W. N. M.; Roobeek, C. F. Brit. Pat. 2 068 377, **1980** (to Shell); *Chem. Abstr.* **1984**, *101*, 191142.

15 van der Veen, L. A.; Kamer, P. C. J.; van Leeuwen, P. W. N. M. *Angew. Chem. Int. Ed. Engl.* **1999**, *38*, 336.
16 Klein, H.; Jackstell, R.; Wiese, K.-D.; Borgmann, C.; Beller, M. *Angew. Chem. Int. Ed.* **2001**, *40*, 3408.
17 Selent, D.; Hess, D.; Wiese, K. D.; Rottger, D.; Kunze, C.; Borner, A. *Angew. Chem. Int. Ed. Engl.* **2001**, *40*, 1696.
18 Sakai, N.; Mano, S.; Nozaki, K.; Takaya, H. *J. Am. Chem. Soc.* **1993**, *115*, 7033.
19 Babin, J. E.; Whiteker, G. T. U.S. Pat. 5,360,938 **1994** (to Union Carbide Corp.); *Chem. Abstr.* **1995**, *122*, 186609.
20 Buisman, G. J. H.; Kamer, P. C. J.; van Leeuwen, P. W. N. M. *Tetrahedron: Asymmetry*, **1993**, *4*, 1625. Diéguez, M.; Pamies, O.; Ruiz, A.; Castillon, S.; Claver, C.; *Chem. Eur. J.* **2001**, *7*, 3086.
21 Brown, C. K.; Wilkinson, G. *J. Chem. Soc. (A)* **1970**, 2753.
22 Eilbracht, P.; Bärfacker, L.; Buss, C.; Hollmann, C.; Kitsos-Rzychon, B. E.; Kranemann, C. L.; Rische, T.; Roggenbuck, R.; Schmidt, A. *Chem. Rev.* **1999**, *99*, 3329.
23 Grosselin, J. M.; Mercier, C.; Allmang, G.; Grass, F. *Organometallics,* **1991**, *10*, 2126. Mercier, C.; Chabardes, P. *Pure Appl. Chem.*, **1994**, *66*, 1509. Haber, S.; Kleiner, H.-J. WO 9705104, 1997 (to Hoechst); *Chem. Abstr.* **1997**, *126*, 199349.
24 Cuny, G. D.; Buchwald, S. L. *J. Am. Chem. Soc.* **1993**, *115*, 2066.
25 Heck, R. F. *Acc. Chem. Res.* **1969**, *2*, 10.
26 Brown, J. M., Kent, A.G. *J. Chem. Chem. Soc. Perkin Trans. II*, **1987**, 1597.
27 Freeman, M. A.; Young, D. A. *Inorg. Chem*. **1986**, *25*, 1556.
28 Dahlenburg, L.; Mirzaei, F.; Yardimcioglu, A. *Z. Naturforsch.***1982**, *37b*, 310.
29 Deutsch, P. P.; Eisenberg, R. *Organometallics*, **1990**, *9*, 709.
30 Chan, A. S. C.; Shieh, H. S.; Hill, J. R. *J. Chem. Soc., Chem. Commun.* **1983**, 688.
31 (a) Oswald, A. A.; Hendrikse, D. E.; Kastrup, R.V.; Irikura, K.; Mozeleski, E. M.; Young, D. A. *Phosphorus and Sulfur,* **1987**, *30,* 237. (b) Oswald, A. A.; Merola, J. S.; Mozeleski, E. J.; Kastrup, R.V.; Reisch, J. C. *Adv. Chem. Series* **1981**, *104*, 503. (c) MacDougall, J. K.; Simpson, M. C.; Green, M. J.; Cole-Hamilton, D. J. *J. Chem. Soc. Dalton Trans.* **1996**, 1161. (d) Lawrenson, M. J. (to B.P.) UK Patent, 1,254,222 and 1,284,615; *Chem. Abstr.* **1972***, 76*, 33787 and **1972***, 77*, 125982.
32 Moser, W. R.; Papite, C. J.; Brannon, D. A.; Duwell, R. A.; Weininger, S. J. *J. Mol Cat.* **1987**, *41*, 271.
33 (a) Unruh, J. D.; Christenson, J. R. *J. Mol Cat.* **1982**, *14*, 19. (b) Unruh, J. D.; Segmuller, B. E.; Chupa. G. R.; Pryor, K. E. (to Hoechst Celanese) U.S. Patent 5,567,856; *Chem. Abstr.* **1996**, *125,* 328099.
34 Buhling, A.; Kamer, P. C. J.; van Leeuwen, P. W. N. M. *J. Mol. Catal. A: Chemical*, **1995**, *98*, 69.
35 Janecko, H.; Trzeciak, A. M.; Ziolkowski, J. J. *J. Mol. Cat.* **1984**, *26*, 355.
36 van Rooy, A.; de Bruijn, J. N. H.; Roobeek, C. F.; Kamer, P. C. J.; van Leeuwen, P. W. N. M. *J. Organomet. Chem.* **1996**, *507*, 69.
37 Palo, D. R.; Erkey, C. *Organometallics*, **2000**, *19*, 81.
38 (a) Hayashi, T.; Tanaka, M.; Ogata, I. *J. Mol. Catal.,* **1979**, *6*, 1. (b) Hjortkjaer, J.; Toromanova-Petrova, P. *J. Mol. Cat.* **1989**, *50*, 203. (c) Neibecker, D.; Réau, R. *J. Mol. Catal.,* **1989**, *53*, 219.
39 (a) Devon, T. J.; Phillips, G. W.; Puckette, T. A.; Stavinoha, J. L.; Vanderbilt, J. J. (to Texas Eastman) U.S. Patent 4,694,109, **1987**; *Chem. Abstr.* **1988**, *108*, 7890. (b) Devon, T. J.;

Phillips, G. W.; Puckette, T. A.; Stavinoha, J. L.; Vanderbilt, J. J. (to Texas Eastman) U.S. Patent 5,332,846, **1994**; *Chem. Abstr*. **1994**, *121*, 280,879.

40 Van Leeuwen, P. W. N. M.; Roobeek, C. F. *J. Organomet. Chem.***1983**, *258,* 343.

41 (a) Cavalieri d'Oro, P.; Raimondo, L.; Pagani, G.; Montrasi, G.; Gregorio, G.; Andreetta, A. *Chim. Ind. (Milan),* **1980**, *62*, 572. (b) Gregorio, G.; Montrasi, G.; Tampieri, M.; Cavalieri d'Oro, P.; Pagani, G.; Andreetta, A. *Chim. Ind. (Milan),* **1980**, *62*, 389.

42 Strohmeier, W.; Michel, M. *Z. Phys. Chem.Neue Folge,* **1981**, *124*, 23 (in German).

43 Evans, D.; Osborn, J. A.; Wilkinson, G. *J. Chem. Soc. (A)*, **1968**, 3133.

44 (a) Musaev, D. G.; Morokuma, K. *Adv. Chem. Phys.* **1996**, *95*, 61. (b) Musaev, D. G.; Matsubara, T.; Mebel, A. M.; Koga, N.; Morokuma, K. *Pure Appl. Chem.* **1995**, *67*, 257. (c) Van der Veen, L. A.; Boele, M. D. K.; Bregman, F. R.; Kamer, P. C. J.; van Leeuwen, P. W. N. M.; Goubitz, K.; Fraanje, J.; Schenk, H.; Bo, C. *J. Am. Chem. Soc.* **1998**, *120*, 11616.

45 Van Leeuwen, P. W. N. M.; Claver, C. Eds. *Rhodium Catalyzed Hydroformylation,* Kluwer Acad. Publ. **2000**, Dordrecht.

46 Castellanos-Paéz, A.; Castillón, S.; Claver, C.; van Leeuwen, P. W. N. M.; de Lange, W. G. J. *Organometallics*, **1998**, *17*, 2543. Divekar, S. S.; Deshpande, R. M.; Chaudhari, R. V. *Catal. Lett.*. **1993**, *21*, 191.

47 Heil, B.; Marko, L. *Chem. Ber.* **1968**, *101*, 2209. Feng, J.; Garland, M. *Organometallics,* **1999**, *18*, 417.

48 Jongsma, T.; Challa, G.; van Leeuwen, P. W. N. M. *J. Organometal. Chem.* **1991**, *421*, 121. van Rooy, A.; Orij, E. N.; Kamer, P. C. J.; van Leeuwen, P. W. N. M. *Organometallics*, **1995**, *14*, 34.

49 Schreuder Goedheijt M.; Hanson, B. E., Reek, J. N. H.; Kamer, P. C. J.; van Leeuwen, P. W. N. M. *J. Am. Chem. Soc.* **2000**, *122*, 1650.

50 Arhancet, J. P.; Davis, D. E., Merola, J. S.; Hanson, B. E. *Nature*, **1989**, *339*, 454.

51 Sandee, A. J.; Slagt, V. F.; Reek, J. N. H.; Kamer, P. C. J.; van Leeuwen, P. W. N. M. *Chem. Commun.* **1999**, 1633.

52 Fremy, G.; Monflier, E.; Carpentier, J.-F.; Castanet, Y.; Mortreux, A.; *Angew. Chem. Int. Ed. Engl.* **1995**, *34*, 1474.

53 Abatjoglou, A. G.; Bryant, D. R.; Peterson, R. R., Eur. Pat. Appl. 350922, **1989**; U.S. Pat. 5,180,854, 1993 (to Union Carbide); *Chem. Abstr.* **1990**, *113*, 80944.

54 Abatjoglou, A. G.; Peterson, R. R.; Bryant, D. R., in "*Catalysis of Organic Reactions*" (Malz, R. E., Ed.), Chem. Ind. *68*, Dekker, New York, **1996**, pp 133-139.

55 *Chem. Eng. News*, **1999**, 18 Oct., p. 20. Betts, M. J.; Dry, M. E.; Geertsema, A.; Rall, G. J. H., Int. PCT Pat. Appl. WO 97/01521 **1997** (to Sastech, Sasol Chemicals Europe); *Chem. Abstr*. **1997**, *126*, 173362.

56 Consiglio, G.; Botteghi, C.; Salomon, C.; Pino, P. *Angew. Chem.* **1973**, *85*, 665.

57 Casey, C. P.; Whiteker, G. T.; Melville, M. G.; Petrovich, L. M.; Gavney, J. A., Jr.; Powell, D. R. *J. Am. Chem. Soc*. **1992**, *114*, 5535.

58 Casey, C. P.; Whiteker, G. T. *Isr. J. Chem.* **1990**, *30*, 299.

59 Casey, C. P.; Paulsen, E. L.; Beuttenmueller, E. W.; Proft, B. R.; Matter, B. A.; Powell, D. R. *J. Am. Chem. Soc.* **1999**, *21*, 63. Yamamoto, K.; Momose, S.; Funahashi, M.; Miyazawa, M. *Synlett.* **1990**, 711.

60 Kranenburg, M.; van der Burgt, Y. E. M.; Kamer, P. C. J.; van Leeuwen, P. W. N. M. *Organometallics*, **1995**, *14*, 3081. van der Veen, L. A.; Keeven, P. H.; Schoemaker, G. C.; Reek, J. N. H.; Kamer, P. C. J.; van Leeuwen, P. W. N. M.; Lutz, M.; Spek A. L. *Organometallics*, **2000**, *19*, 872.

61 Tatsumi, K.; Hoffmann, R.; Yamamoto, A.; Stille, J. K. *Bull. Chem. Soc. Jpn.* **1981**, *54*, 1857.

62 van der Veen, L. A.; Kamer, P. C. J.; van Leeuwen, P. W. N. M. *Organometallics*, **1999***, 18*, 4765. van der Veen, L. A.; Kamer, P. C. J.; van Leeuwen, P. W. N. M. *Angew. Chem. Int. Ed. Engl.* **1999***, 38*, 336.
63 Van Leeuwen, P. W. N. M.; Roobeek, C. F. *J. Organomet. Chem.* **1983**, *258,* 343. Van Leeuwen, P. W. N. M.; Roobeek, C. F. Brit. Pat. 2 068 377, **1980** (to Shell); *Chem. Abstr.* **1984**, *101*, 191142.
64 Jongsma, T.; Challa, G.; van Leeuwen, P. W. N. M. *J. Organometal. Chem.* **1991**, *421*, 121.
65 Van Rooy, A.; Orij, E. N., Kamer, P. C. J.; Van den Aardweg, F.; Van Leeuwen, P. W. N. M. *J. Chem. Soc., Chem. Commun.* **1991**, 1096. Van Rooy, A.; Orij, E. N.; Kamer, P. C. J.; Van Leeuwen, P. W. N. M. *Organometallics,* **1995**, *14*, 34.
66 van Leeuwen, P. W. N. M.; Buisman, G. J. H.; van Rooy, A.; Kamer, P. C. J. *Rec. Trav. Chim. Pays-Bas,* **1994***, 113*, 61.
67 van Rooy, A.; Kamer, P. C. J.; van Leeuwen, P. W. N. M.; Goubitz, K.; Fraanje, J.; Veldman, N.; Spek, A. L. *Organometallics,* **1996**, *15*, 835.
68 Burke, P. M.; Garner, J. M.; Tam, W.; Kreutzer, K. A.; Teunissen, A. J. J. M. WO 97/33854, 1997, (to DSM/Du Pont); *Chem. Abstr.* **1997**, *127*, 294939.
69 Sato, K.; Kawaragi, Y.; Takai, M.; Ookoshi, T. US Pat. 5,235,113, EP 518241 (to Mitsubishi)*; Chem. Abstr.* **1993**, *118*, 191183. Sato, K.; Karawagi, J.; Tanihari, Y. Jpn. Kokai Tokkyo Koho JP 07,278,040 (to Mitsubishi)*; Chem. Abstr.* **1996**, *124*, 231851.
70 Consiglio, G. *Catalytic Asymmetric Syntheses*, I. Ojima editor VCH Publishers, New York, **1993**. Agbossou, F.; Carpentier, J. F.; Mortreux, A. *Chem. Rev.* **1995**, *95*, 2485. Gladiali, S.; Bayón, J .C.; Claver, C. *Tetrahedron Asymmetry,* **1995**, *7*, 1453.
71 Wink, J. D.; Kwok ,T. J. ; Yee A. *Inorg. Chem*. **1990**, *29*, 5007
72 Sakai, N.; Nozaki, K.; Mashima, K.; Takaya, H.*Tetrahedron . Asymmetry*, **1992**, *3*, 583.
73 Babin, J. E.; Whiteker, G. T. *PCT Int. Appl.* **1993**, WO 9303839 (to UCC). *Chem. Abstr.* **1993**, *119*, 559872.
74 Buisman G. J. H., Vos, E. J.; Kamer, P. C. J.; van Leeuwen, P. W. N. M. *J. Chem. Soc. Dalton Trans.* **1995**, 409.
75 Buisman, G. J. H.; Kamer, P. C. J.; van Leeuwen, P. W. N. M.; *Tetrahedron Asymmetry*, **1993**, *4,* 1625.
76 Diéguez, M.; Ruiz, A.; Claver, C. *Dalton Trans.* **2003**, 2957.
77 Buisman, G. J. H.; van der Veen, L. A.; Klootwijk,: de Lange, W. G. J.; Kamer, P. C. J.; van Leeuwen, P. W. N. M.; Vogt D. *Organometallics*, **1997**, 16, 2929.
78 Sakai, N.; Mano, S.; Nozaki, K.; Takaya, H.; *J. Am. Chem. Soc*. **1993**, *115*, 7033.
79 Sakai, N.; Nozaki, K.; Takaya, H. *J. Chem Soc. Chem. Comm.* **1994**, 395.
80 Higashijima, T.; Sakai, N.; Nozaki, K.; Takaya, H. *Tetrahedron Letters,* **1994**, *35*, 2023.
81 Horiuchi, T.; Ohta, T.; Nozaki, K.; Takaya, H. *Chem Comm.* **1996**, 155. Horiuchi T.; Ohta, T.; Shirakawa, E.; Nozaki, K.; Takaya, H. *J. Org. Chem*. **1997**, *62*, 4285.
82 Deerenberg, S.; Kamer, P. C. J.; van Leeuwen, P. W. N. M. *Organometallics*, **2000**, *19*, 2065.

Chapter 9

ALKENE OLIGOMERISATION

How selective can it be

9.1 Introduction

1-Alkenes, or linear α-olefins as they are called in industry, are desirable starting materials for a variety of products. Polymers and detergents are the largest end-uses. We mention a few applications:

C_4	polybutylene
C_{6-8}	comonomers in HDPE, LLDPE, synthetic esters
C_{6-10}	alcohols (hydroformylation) as phthalates for PVC plasticisers
C_{8-10}	as trimers in synthetic lub-oils
C_{10-14}	after hydroformylation, detergents
C_{14-16}	sulphates and sulfonates in detergents

Industrially, alkenes are obtained by:

[1] *Thermal cracking of wax*. From thermal cracking a thermodynamic mixture might have been expected, but the wax-cracker product contains a high proportion of 1-alkenes, the kinetically controlled product. Still, the mixture contains some internal alkenes as well. For several applications this mixture is not suitable. In polymerisation reactions only the 1-alkenes react and in most cases the internal alkenes are inert and remain unreacted. For the cobalt catalysed hydroformylation the nature of the alkene mixture is not relevant, but for other derivatisations the isomer composition is pivotal to the quality of the product.

[2] *Paraffin dehydrogenation*. Paraffin dehydrogenation gives exclusively internal alkenes.

[3] *Alcohol dehydration*. Other routes to linear higher alcohols are available such as the reduction of fatty acids and an aluminium based oligomerisation of ethene followed by oxidation. The higher alcohols are used as such or they are dehydrated to make 1-alkenes.

[4] *Ethene oligomerisation.* In view of the above limitations there is a demand for a process that selectively makes linear 1-alkenes. Three processes are available, two based on aluminium alkyl compounds or catalysts and one on nickel catalysts. The aluminium processes use aluminium in a stoichiometric fashion and they produce a narrow molecular weight distribution (a Poisson distribution, *vide infra*).

[5] *Fischer-Tropsch*. Oct-1-ene is produced as one of the many products in the conversion of syn-gas and isolated by careful distillations and extractions of the mixture by Sasol.

The ethene-based processes give only even-numbered alkenes (including the one making alcohols) while the other two processes produce both odd and even numbered alkenes. In the last two decades there has been a trend to close down wax cracking alkene plants, and the products are now increasingly derived from ethene. Note that ethene is also a cracker product.

9.2 Shell-Higher-Olefins-Process

Many transition metal hydrides will polymerise ethene to polymeric material or, alternatively, dimerise it to butene. Fine-tuning these catalysts to produce a mixture of predominantly C_8 to C_{20} oligomers is not trivial. Nickel complexes have been extensively studied by Wilke and co-workers for their activity as alkene oligomerisation catalysts. In the late sixties Keim and co-workers at Shell [1] discovered a homogeneous nickel catalyst which selectively oligomerises ethene to higher homologues (Figure 9.1). This is not a structure that has been observed, but the putative initiator (of each chain) that is prepared in situ from nickel zero and the functionalised carboxylic acid.

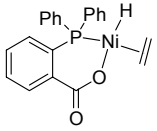

Figure 9.1. An example of a SHOP catalyst

9.2.1 Oligomerisation

The catalyst is prepared in a pre-reactor from nickel salts with boron hydrides as the reductant under a pressure of ethene and then ligand is added.

Polar solvents such as alcohols are used for the dissolution of the catalyst. The catalyst solution and ethene are led to the reactor, a stirred autoclave, which is maintained at 80-120 °C and 100 bar of ethene (Figure 9.2).

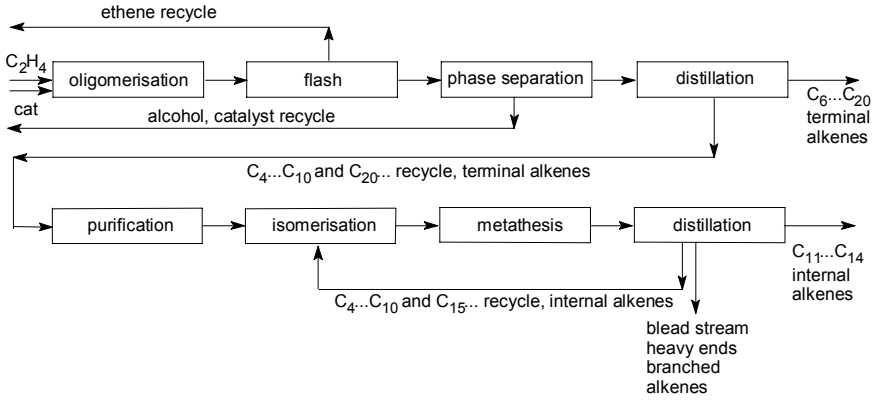

Figure 9.2. Simplified flow scheme of SHOP process

The nickel catalyst in the oligomerisation step. The product distribution of the oligomerisation is determined by two competing reactions, chain growth versus chain termination. Essential for a good catalyst performance are the soft neutral ligand and the mono-anionic ligand in *cis* position, leaving room for either hydride or an alkyl as the other anionic ligand and ethene also in mutual *cis* disposition. This catalytic system has been developed by Shell and in the seventies two commercial units came on stream. Since then many variations based on the ligand requirements described above have been added to the literature. Also other nickel based processes have been developed and successfully applied.

According to the specification by Shell the product contains only 3% of internal or branched alkenes. This is an important feature of the process. The ethene pressure has to be maintained at a high level, compared with the butene concentration, in order to obtain preferential insertion of ethene with respect to butene. Insertion of the latter leads to branched products. Another peculiar property of this catalyst is that it has very little activity for isomerisation under the conditions. Obviously this is also very important because the goal is making terminal alkenes.

Figure 9.3 pictures the oligomerisation reaction: Ni is an abbreviation for the nickel-ligand moiety, k_g stands for the rate of the growth reaction, and k_t for the rate of the termination reaction. These rate constants are the same for all intermediate nickel alkyls, except perhaps for the first two or three members of the sequence owing to electronic and steric effects. Interestingly, a simple kinetic derivation leads to an expression for the product distribution. One can

start this derivation by stating that for each nickel alkyl intermediate, the ratio of the growth fraction and the termination fraction is the same, because the rates for these two reactions are the same at each "intersection". Hence, in words, the summation of all moles of products <n+2 and higher> divided by the molar quantity of product <n> has the ratio k_g/k_t at each "intersection". The rates are indicated by two constants k_g and k_t, which is a simplification, because the actual rates may also contain concentration terms of ethene (especially for k_g), or concentration terms of reagents that aid the β-elimination. However, these will be the same for each intermediate alkyl nickel complex and therefore can be omitted. From the summations we can derive that the molar ratio of two successive alkenes is constant, i.e. each alkene concentration is a certain, constant fraction of the preceding alkene; this ratio we will call γ. The result is a so-called geometric or Schulz-Flory distribution. The expressions are given in Figure 9.3.

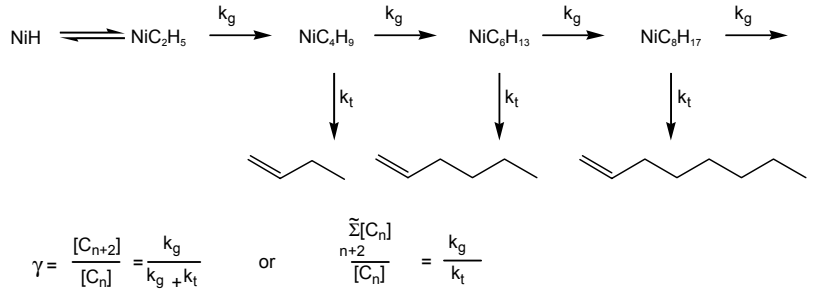

Figure 9.3. Geometric oligomer distribution

This means that the maximum amount of oligomers within a certain range can be calculated by this expression. For the synthesis of detergent alkenes this means that only half or less of the alkenes produced fall within the desirable range of useful materials, i.e. C_6 through C_{20} compounds.

In Figures 9.4 and 9.5 [2] we have depicted the product distributions (weight % and mol % of each oligomer indicated by number of carbon atoms) for two different γ-values. The effect of small changes in the ratios of the two rates turns out to be very large. Clearly, the curve for the mol % follows the expected geometric distribution; each next fraction is obtained by multiplication of the previous one by the γ-value. When the γ-value becomes close to unity, a distribution typical of a polymer is obtained. The curve of the weight percentage is obtained by multiplication of the mol fractions with their respective molecular weights, summation of the total weight and taking the percentage for each oligomer. On the right-hand side of the graphs the γ-values are given together with the total percentage of the product in the range C_6-C_{20}.

In practice this range is somewhat smaller. Hence the selectivity to "desired" product is in the order of only 50 %!

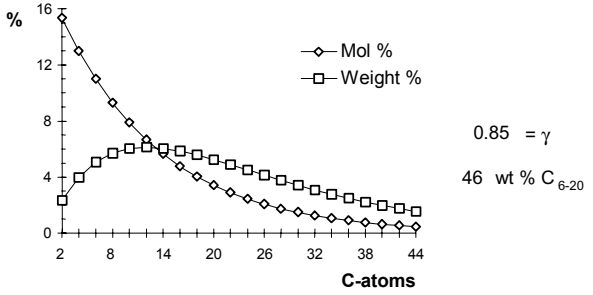

Figure 9.4. Typical Schulz-Flory distribution for γ=0.85

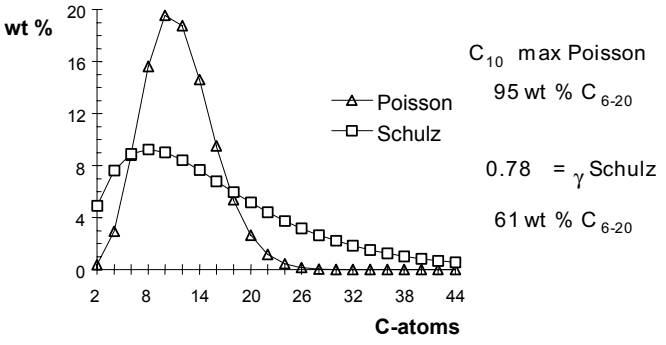

Figure 9.5. Comparison of Poisson and Schulz-Flory distribution, see text

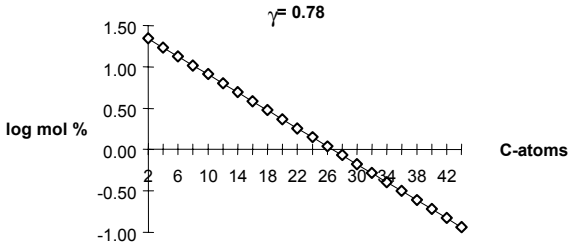

Figure 9.6. Logarithmic plot of the mol % fraction of oligomers versus carbon number in a Schulz-Flory distribution

A logarithmic plot of the mol fraction (or the number of moles) versus the carbon number will give a straight line (Figure 9.6). The logarithmic plot of the

molar amounts of oligomers produced is a convenient check on the product distribution of an oligomerisation reaction.

The graph in Figure 9.5 shows weight percentages for the Poisson distribution together with the Schulz-Flory distribution for respectively five moles of ethene per growing centre (Poisson mechanism) and a Schulz-Flory distribution for a γ-value equal to 0.78. We see that the selectivity to the desired products increases enormously for a Poisson distribution. Now 95 % of the weight of the products falls within the desired range. Therefore, a large research effort has been conducted to find processes that would lead to a distribution of this type. As mentioned above, the aluminium process does indeed give a Poisson distribution of the oligomers (or more precisely, aluminium alkyls), but only ONE chain is produced per "catalyst" per cycle. Any catalytic system, involving chain transfer and a constant ratio of k_g and k_t, will produce a Schulz-Flory distribution, as the kinetic derivation has indicated.

Process control. As mentioned before, the product distribution is highly sensitive to the γ-value. For an industrial process it is extremely important to control the γ-value with high precision. A slight deviation will give another product distribution and the huge recycle streams change accordingly. Therefore a range of variables requires strict control:

- the temperature; note that the reaction is highly exothermic,
- ethene concentration
- but-1-ene concentration
- composition of the medium
- catalyst activity
- process operation; e.g. mixing, settling of the two phases, pressure release, cooling.

The sensitivity of the product distribution for small changes of these parameters can also be exploited to our advantage; the product distribution can be easily adjusted to changes of the demand for certain oligomers, but only within the limits of Schulz-Flory distributions!

9.2.2 Separation

The product alkenes are insoluble in the alcohol and phase separation takes place. After settling, the alcohol layer goes to a regeneration unit. The alkene layer is washed and ethene is recycled to the reactor. The products are distilled and the desired fractions are collected.

9.2.3 Purification, isomerisation, and metathesis

The lower alkenes and the heavy alkenes must be "disproportionated" to give the full range of alkenes. In the second part of the process the higher and

the lower alkenes are converted into internal detergent olefins via a combination of isomerisation and metathesis reactions. Direct metathesis of the higher and lower 1-alkenes is not productive, since metathesis of e.g. C_{22} and C_4 1-alkenes would give ethene and an internal C_{24}, which is not an improvement. To this end the light and heavy alkenes are sent to an isomerisation reactor after having passed a purification bed, a simple absorbent to remove alcohol and ligand impurities. The isomerised mixture is then passed over a commercial molybdenum metathesis catalyst (CoMox), also a fixed bed reactor, to give a broad mixture of internal alkenes, containing 10-20% in the range desired. The product now is a mixture of internal, linear alkenes. The light and heavy alkenes of this mixture are again recycled, and eventually all material leaves the isomerisation/metathesis plant as internal C_{11-14} alkenes. This "by-product" constitutes a large part of the production, and only half of the production or less amounts to the more valuable 1-alkenes. Branched alkenes are not metathesised by the catalyst used. In spite of the high selectivity of the oligomerisation reaction, the recycled branched alkenes build up in the isomerisation-metathesis units, until they reach a level as high as 50%. A bleed stream of the heavies controls the amount of branched material and the amount of (continuously growing) polymers. After distillation the C_{11-14} fraction of internal alkenes (±15%) is used as a feedstock for alcohol production via cobalt hydroformylation catalysts. The light and heavy products are recycled.

The typical size of a Shell process plant described here is 250-350,000 tons per year. The total production of higher olefins via this and similar routes is estimated to be 2 million tons annually. A large part of the alkenes are produced for “captive” use, i.e. for use by the producing company itself.

9.2.4 New catalysts

In the last decade several new catalyst systems have been studied. In the seventies many catalysts related to the nickel system of Shell have been studied. Typically they all contain a bidentate ligand carrying a negative charge. Since the discovery of the new titanium and zirconium metallocene catalysts for the polymerisation of alkenes (see next chapter), the same systems have also been tested for the oligomerisation of ethene. Earlier in this chapter we mentioned the aluminium-based method in which aluminium is used in a stoichiometric fashion; at each triethylaluminium three chains of oligomers grow exhibiting a Poisson distribution. Catalytic systems lead to a much broader Schulz-Flory distribution. Mixed catalysts have been reported in which the chain growth takes place at a fast zirconium catalyst, after which the chain is transferred to an aluminium atom. Depending on the kinetics, a variety of molecular weight distributions can be obtained. These will not be discussed here.

A more recent development comprises the use of iron and cobalt containing pyridinediimine ligands. Extremely fast catalysts were reported simultaneously by the groups of Brookhart and Gibson, and workers at Dupont, (Figure 9.7) [3]. Turnover frequencies as high as several millions per hour were recorded! This is a totally unexpected development showing that a new combination of ligand and metal can lead to surprises. Since the first reports many industries have started investigations in this area. Catalyst activities are very high, and a separation of catalyst and product in a two-phase system as in SHOP may not be needed. The molecular weight distribution though will still require the isomerisation/metathesis sequence as in the Shell Higher Olefins Process. Purification of the initial product before entering this isomerisation/metathesis recycle can probably be skipped, but the content of branched alkenes should be very low.

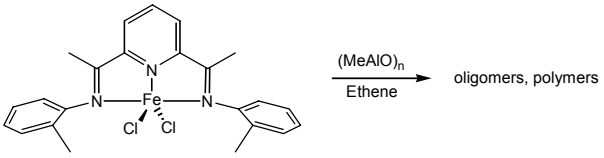

Figure 9.7. Example of a new catalyst for ethene oligomerisation and polymerisation

The mechanism for the new iron based catalyst is basically the same as for nickel: a series of insertions followed by β–hydride-elimination. Initiation for iron (with aluminium alkyls) is different from the nickel catalyst (oxidative addition of the phosphinoacid to produce a hydride). It has not been published yet whether the product of this reaction has the same high quality as SHOP with regards to branching and isomerisation (both should be low). A higher degree of substitution at the aryl groups leads to highly active polymerisation catalysts.

A typical feature of the new cobalt and iron catalysts is that the molecular weight does not depend on the pressure of ethene. The polymerisation rate goes up if the pressure is increased but the molecular weight distribution remains the same. This phenomenon has been observed for more catalysts, but we will discuss the concept here. We have presumed that the SHOP catalyst gives higher molecular weights when the pressure is increased, because the rate of propagation increases and the unimolecular rate of β-hydride elimination remains the same, thus the ratio of k_g/k_t increases. For a catalyst showing the alternative behaviour (no dependence on ethene concentration) we conclude that both the rate of insertion and the chain termination have a first order dependency on the concentration of ethene. In Figure 9.8 we propose how this works.

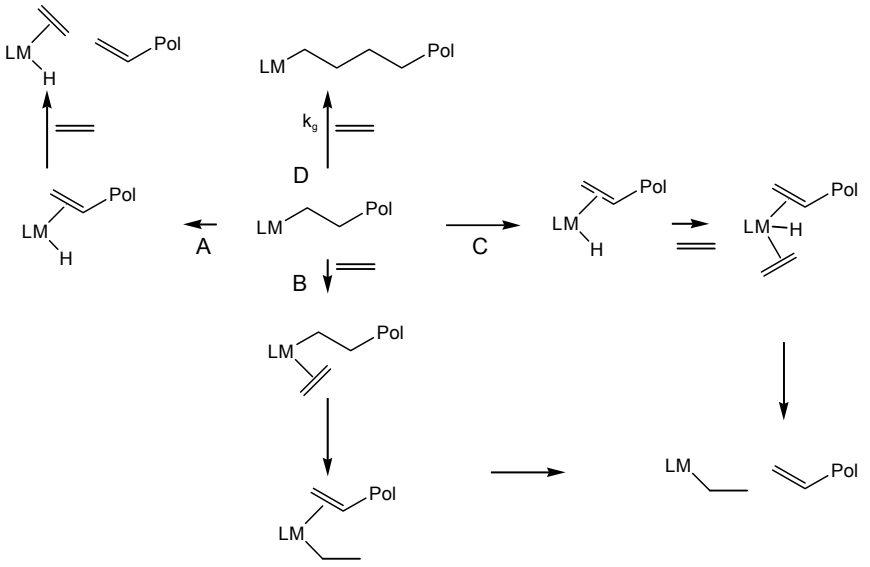

Figure 9.8. Possible chain transfer pathways and propagation

In Figure 9.8 path D is the propagation pathway and the arrow indicates that this reaction is fast and first order in ethene concentration. Pathways A, B, and C are the chain termination (transfer) pathways. Reaction A is slow and independent of the ethene concentration. This is the situation we have presumed for SHOP. B and C represent two possibilities we cannot distinguish; in B we see a slow reaction of the complex with ethene, followed by a fast, direct transfer of hydrogen from the polymer chain to ethene, forming the new growing ethyl chain. Path C shows a fast β-hydride elimination and a slow reaction with ethene leading also to the alkene terminated polymer chain and the new ethyl metal initiator. Thus, in B and C we observe a first order dependence in ethene concentration for the chain transfer process. Since the propagation is also first order in ethene the rate of production will increase, but the molecular weight distribution remains the same.

A fourth mechanism for chain transfer involves the transfer of the polymer chain to the large excess of aluminium alkyls present. This has also been observed. Since the reaction rate for this process depends on the concentration of the aluminium compound, the molecular weight distribution now also depends on the latter concentration. For oligomer production this is only relevant when a very large excess of aluminium alkyls is present.

For hafnium this has been reported previously [4]. A large excess of aluminium, a hafnium catalyst not undergoing β-hydride termination but smoothly inserting ethene molecules, and a fast exchange between the two metals leads to a desirable Poisson distribution.

9.3 Ethene trimerisation

Another, highly selective oligomerisation reaction of ethene should be mentioned here, namely the trimerisation of ethene to give 1-hexene. Worldwide it is produced in a 0.5 Mt/y quantity and used as a comonomer for ethene polymerisation. The largest producer is BP with 40 % market share utilizing the Amoco process, formerly the Albemarle (Ethyl Corporation) process. About 25 % is made by Sasol in South Africa where it is distilled from the broad mixture of hydrocarbons obtained via the Fischer-Tropsch process, the conversion of syn-gas to fuel. The third important process has been developed by Phillips.

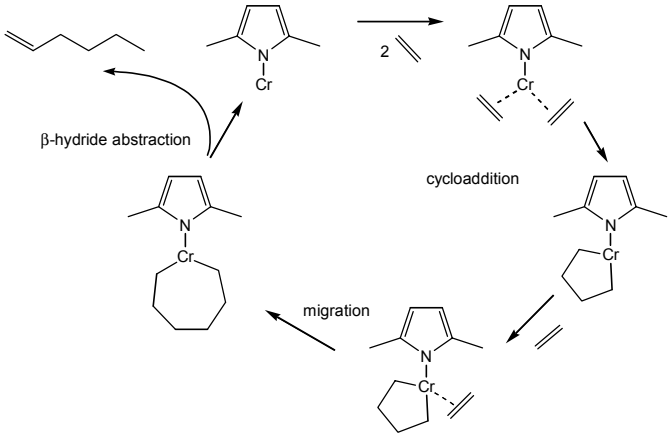

Figure 9.9. Mechanism for the trimerisation of ethene using chromium catalysts

Most catalysts are based on chromium that has been studied for this purpose since the mid-seventies, probably started by Union Carbide Corporation. Chromium is the metal of the Phillips ethene polymerisation catalysts and presumably it was discovered accidentally that under certain conditions 1-hexene was obtained as a substantial by-product. Neither the precise catalytic cycle nor the intermediate complexes or precursors are known. It is generally accepted that an alkyl aluminium compound first reduces the chromium source and that coordination of two molecules of ethene is followed by cyclometallation, giving a chromocyclopentane. During the cyclometallation the valence of chromium goes up by two and thus a starting valence of either one or zero seems reasonable. This cyclic mechanism explains why such high selectivity is obtained [5].

The Phillips process uses a threefold excess of 2,5-dimethylpyrrole, a chromium salt, and an excess of an alkyl aluminium compound [6]. In Figure 9.9 we have drawn only one ligand per chromium, but we do not know the

composition of the catalyst. We estimate that more pyrroles may be bound to the chromium atom, in a fashion not known! The salts present may also coordinate to the metal [7].

The first steps involve coordination and cycloaddition to the metal. Insertion of a third molecule of ethene leads to a more instable intermediate, a seven-membered ring, that eliminates the product, 1-hexene. This last reaction can be a β-hydrogen elimination giving chromium hydride and alkene, followed by a reductive elimination. Alternatively, one alkyl anion can abstract a β-hydrogen from the other alkyl-chromium bond, giving 1-hexene in one step. We prefer the latter pathway as this offers no possibilities to initiate a classic chain growth mechanism, as was also proposed for titanium [8]. The byproduct observed is a mixture of decenes (!) and not octenes. The latter would be expected if one more molecule of ethene would insert into the metallocycloheptane intermediate. Decene is formed via insertion of the product hexene into the metallo-cyclopentane intermediate followed by elimination.

In the Amoco process the stabilizing ligand could well be a triphosphine, as patents report the complex $PrP(C_2H_4PEt_2)_2CrCl_3$ as the precursor [9]. Metal to ligand ratio is one. The reported selectivitity is higher than 99 %. A related ligand having P-N-P donor groups, $R_2P(CH_2)_2NH(CH_2)_2PR_2$, is also highly effective [10]. Organometallic chromium compounds that might be related to the Amoco catalyst have been reported in the literature, but note that they were made (1987-1988) before the Amoco invention (1992-1998). They were only tested as polymerisation catalysts (!) and were slow catalysts for this reaction (Figure 9.10). From the trivalent chromium compound on the left one could abstract one methyl anion, thus creating a reactive, unsaturated species, which can undergo the insertion of the third molecule of ethene. The divalent chromium compound shown on the right is diamagnetic [11].

Figure 9.10. Examples of alkyl chromium phosphine complexes

Chromium complexes of ligands of the type $Ar_2PN(Me)PAr_2$ (Ar = ortho-methoxy-substituted aryl group), on activation with MAO, are extremely active and selective catalysts for the trimerisation of ethylene [12]. Using the ligand shown in Figure 9.11 rates as high as 1 ton of 1-hexene per gram of chromium per hour have been achieved. The same ligands were used successfully in the

catalysis with palladium and nickel in respectively carbonylation chemistry and ethene polymerisation.

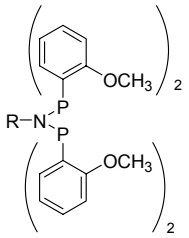

Figure 9.11. Ligand for use as a chromium catalyst for the trimerisation of ethene

Triazacyclohexane also gives rise to very active catalysts with the use of chromium [13] as do ligands of the type $RS(CH_2)_2NH(CH_2)_2SR$ [14]. The latter coordinate in a meridional fashion, while the former can only coordinate in a facial fashion. Recently examples using cyclopentadienyl titanium complexes [15] and tantalum have been reported [16]. The diversity of the chromium systems and the new metal systems show that very likely more catalysts will be discovered that are useful for this reaction, including 1-octene producing catalysts! (1-octene is in high demand as a comonomer for ethene polymerisation for certain grades of polyethylene).

While the identity of the chromium complexes has not yet been established, the titanium catalyst is generated in situ from a well-defined precursor and the proposed structure of the catalyst seems very likely [15]. The catalyst is made from $Cp'TiCl_3$ and MAO or from $Cp'Ti(CH_3)_3$ and $[PhHNMe_2][B(C_6F_5)_4]$ where Cp' represents a cyclopentadienyl group having an aryl group connected to it. Most likely a cationic cyclopentadienyl species is formed, stabilised by arene coordination, as the arene ring was found to be indispensable (Figure 9.12). The generation of the titanacyclopentane involves formally a switch between Ti(II) and Ti(IV). The reductive eliminations in the scheme may actually be direct reactions leading to an alkene complex, rather than a β-hydride elimination followed by a reductive elimination, as mentioned above for chromium.

For several of these ligands the reaction is first order in ethene and thus it was suggested that the insertion of ethene in the titanacyclopentane ring is the rate-determining step, as was also found for the triazacyclohexane catalyst [13]. Turnover numbers of the titanium catalyst are very high, but since some of the chromium catalysts have a second order dependency in ethene a comparison cannot be made; at higher pressure these chromium catalysts will be more effective [7,17].

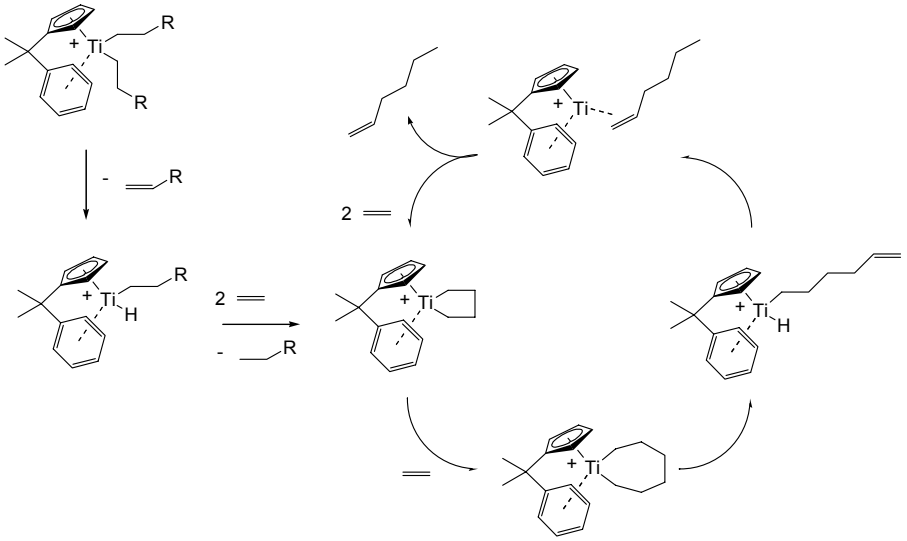

Figure 9.12. Titanium catalyst for ethene trimerisation [15]

9.4 Other alkene oligomerisation reactions

Dimersol

Many alkene oligomerisation reactions have been studied, but here we will confine ourselves to a few that have been commercialised. They will not be discussed in detail because the mechanisms are all basically the same, although not known in detail for many of them. *Dimersol* ® is the trade name for mixtures of propene, propene/butene or butene dimers obtained by the process developed by IFP. Mixtures of butenes are dimerised in a similar fashion and the octenes are hydroformylated to give alcohols suitable for dinonyl phthalates, used as plasticisers in PVC. Dimersols and trimersols are used as additives for gasoline [18]. The preparation for the catalyst involves a Ziegler procedure (i.e. the in situ preparation of a catalyst by reduction of a transition metal salt with an alkyl aluminium compound) using a nickel salt, triethylaluminium, and a phosphine ligand. Alternatively, butadiene may be added to make a π-crotyl nickel complex first, as is often done in polymerisation experiments. The most likely mechanism involves a nickel hydride species, as in the SHOP reaction, but cyclometallic species have also been proposed, as in Figure 9.9. With the use of PMe_3 as the ligand mainly methylpentenes are obtained, whereas the more bulky $PEt(t\text{-}Bu)_2$ gives mainly dimethylbutenes [19].

The process is run in a CSTR without solvent at 50 °C. The reaction is highly exothermic and heat is removed via external circulation. To ensure high

conversion in a once-through process a plug-flow reactor is added. At the end of the reactor the catalyst is quenched with ammonia, and the inorganic components are removed by washing with aqueous caustic soda and water [20]. In order to make heptenes from propene and butanes, the much more reactive propene is added in portions at various stages in a sequence of reactors.

Cyclododecatriene

1,5,9-cyclododecatriene is made industrially from butadiene via trimerisation using titanum catalysts, obtained via a Ziegler procedure. The product is the cis-trans-trans isomer (Figure 9.13). It is converted (via hydrogenation and oxidation) to nylon-12 intermediates. Zerovalent nickel gives the all *trans* isomer if the reaction is carried out in the absence of ligands or when small phosphites are used as the ligand. More bulky phosphite ligands give rise to 1,5-cyclooctadiene [21]. In a commercial application this is converted to cyclooctene, which is used in ring-opening metathesis polymerisation (Chapter 16). For both metals the most likely carbon-carbon bond-forming step involves a cyclometallation. For nickel such π-allylic intermediates have been characterised.

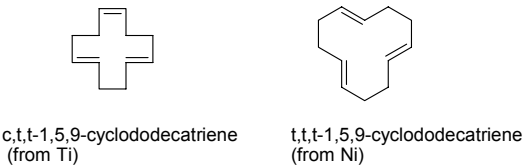

Figure 9.13. 1,5,9-cyclododecatriene isomers

Vinylnorbornene (ethylidenenorbornene)

Norbornadiene and ethene can be codimerised to give vinylnorbornene, which is isomerised to ethylidenenorbornene with the same nickel or titanium hydride catalyst (Figure 9.14).

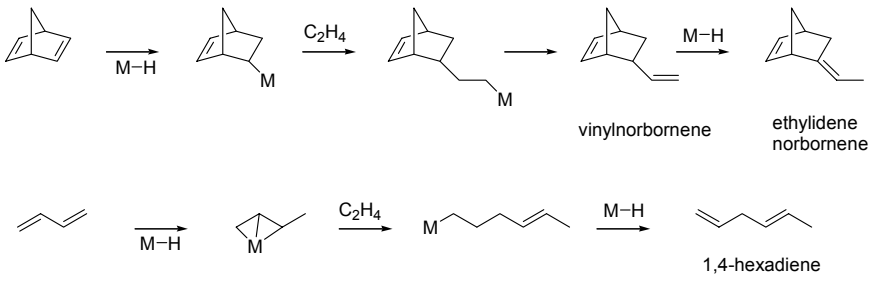

Figure 9.14. Diene-ethene codimerisation

1,4-Hexadiene

Industrially this diene is made the same way as ethylidenenorbornene from butadiene and ethene, but now isomerisation to 2,4-hexadiene should be prevented as the polymerisation should concern the terminal alkene only. In both systems nickel or titanium hydride species react with the more reactive diene first, then undergo ethene insertion followed by β-hydride elimination. Both diene products are useful as the diene component in EPDM rubbers (ethene, propene, diene). The nickel hydride chemistry with butadiene represents one of the early examples of organometallic reactions studied in great detail [22] (Figure 9.14).

References

1 van Zwet, H.; Keim, W. US 3,635,937 (to Shell) 1972. *Chem. Abstr.* **1971***, 75,* 110729a.

2 For convenience of the calculation we included a value for ethene (2, in the graphs); this value has no practical meaning.

3 Small, B. L.; Brookhart, M.; Bennett, A. M. A. *J. Am. Chem. Soc.* **1998***, 120,* 4049 and 7143. Small, B. L.; Brookhart, M. *Macromolecules,* **1999***, 32,* 2120. Britovsek, G. J. P.; Gibson, V. C.; Kimberly, B. S.; Maddox, P. J.; McTavish, S. J.; Solan, G. A.; White, A. J. P.; Williams, D. J. *Chem. Commun.* **1998**, 849. Britovsek, G. J. P.; Gibson, V. C.; Mastroianni, S.; Oakes, D. C. H.; Redshaw, C.; Solan, G. A.; White, A. J. P.; Williams, D. J. *Eur. J. Inor. Chem.* **2001**, 431.

4 Samsel, E. G.: US 5,597,937 (to Albemarle Corp) 1997.

5 Briggs, J. R. *Chem. Commun.* **1989**, 674 and U.S. Patent 4,668,838 (to Union Carbide Corp.) 1987. *Chem. Abstr.* **1987***, 107*, 578604.

6 Hogan, J. P.; Banks, R. L. (Phillips Petroleum Co) US 2,825,721, 1958. Hogan, J. P. *J. Poly. Sci. A* **1970**, *8*, 2637.

7 Yang, Y.; Kim, H.; Lee, J.; Paik, H.; Jang, H. G. *Appl. Catal. A-Gen.* **2000**, *193,* 29.

8 Blok, A. N. J.; Budzelaar, P. H. M.; Gal, A. W. *Organometallics* **2003***, 22*, 2564.

9 Wu, F. J. (Amoco Corp.) US 5,744,677 and US 5,811,618. *Chem. Abstr.* **1998***, 129*, 262005 and **1995**, *123*, 35775.

10 McGuinness, D. S.; Wasserscheid, P.; Keim, W.; Englert, U.; Dixon, J. T.; Grove, C. *Chem. Commun.* **2003**, 334.

11 Gardner, T. G.; Girolami, G. S. *J. Chem. Soc., Chem. Commun*. **1987**, 1758. Hermes, A. R.; Morris, R. J.; Girolami, G. S.; *Organometallics,* **1988***, 7,* 2372.

12 Carter, A.; Cohen, S. A.; Cooley, N. A.; Murphy, A.; Scutt, J.; Wass, D. F. *Chem. Commun*. **2002**, 858. Cooley, N. A.; Green, S. M.; Wass, D. F.; Heslop, K.; Orpen, A. G.; Pringle, P. G. *Organometallics,* **2001**, *20*, 4769.

13 Kohn, R. D.; Haufe, M.; Kociok-Kohn, G.; Grimm, S.; Wasserscheid, P.; Keim, W. *Angew. Chem. Int. Ed.* **2000**, *39*, 4337.

14 McGuinness, D. S.; Wasserscheid, P.; Keim, W.; Morgan, D.; Dixon, J. T.; Bollmann, A.; Maumela, H.; Hess, F.; Englert, U. *J. Am. Chem. Soc.* **2003***, 125,* 5272.

15 Deckers, P. J. W.; Hessen, B.; Teuben, J. H. *Angew. Chem. Int. Ed.* **2001**, *40*, 2516 and *Organometallics* **2002***, 21*, 5122.

16 Andes, C.; Harkins, S. B.; Murtuza, S.; Oyler, K.; Sen, A. *J. Am. Chem. Soc.* **2001**, *123,* 7423.

17 Manyik, R. M.; Walker, W. E.; Wilson, T. P. *J. Catal.* **1977**, *47*, 197.

18 Chauvin, Y.; Hennico, A.; Leger, G.; Nocca, J. L. *Erdöl, Erdgas, Kohle,* **1990***, 106,* 309.

19 Bogdanovic, B.; Biserka, H.; Karmann, H. G.; Nussle, H. G.; Walter, D.; Wilke, G. *Ind. Eng. Chem.* **1970**, *62*, 34.
20 Chauvin, Y.; Gaillard, J. F.; Quang, D. V.; Andrews, J. W. *Chem. Ind. (London U.K.)* **1974**, 375.
21 Bogdanovic, B.; Heimbach, P.; Kroner, M.; Wilke, G. *Liebigs Ann. Chem.* **1969***, 727,* 143.
22 Tolman, C. A. . *J. Am. Chem. Soc.* **1970***, 92,* 6777.

Chapter 10

ALKENE POLYMERISATION

In pursuit of stereoregularity

10.1 Introduction to polymer chemistry

In this chapter we will discuss a few topics in the area of alkene polymerisations catalysed by homogeneous complexes of early and late transition metals (ETM, LTM). One of the main research themes for the ETM catalysts has been the polymerisation of propene, while industries have also paid a lot of attention to metallocenes giving LLDPE (linear low-density polyethylene, for thinner plastic bags). In less than a decade a completely new family of catalysts has been developed which enables one to synthesise regioselective and stereoselective polymers of a wide variety of monomers. These new catalysts are starting to find application on industrial scale, but as yet only reports on commercialisation of (branched) polyethylene and polystyrene have appeared.

Making polymers is an important application of catalysis and this chapter serves as an introduction to more advanced works in this area [1]. Before starting we need to know a few things about polymers, which we will very briefly summarise below.

Synthesis. Polymers can be made by condensation reactions and by addition polymerisations. An example of the former is the condensation of diols and diesters forming polyesters; all molecules are involved in the steady growth of species of higher molecular weight. Addition polymerisation involves the reaction of initiating species with monomers thus building up this limited number of growing polymer molecules in an excess of monomers. Four types of addition reactions can be distinguished for organic monomers [2]:

- radical polymerisation (and living radical polymerisation, see page 46),
- anionic polymerisation,
- co-ordination polymerisation, and
- cationic polymerisation.

Transition metal complexes play a key role in co-ordination polymerisation.

Polymer molecular properties. Making a polymer of high quality is much more complicated than making butanal, for example, because the material properties of a polymer depend heavily on a number of molecular properties. For example, 1% of mistakes in a propene polymer chain can spoil the properties of a polymer completely (crystallinity for instance), while 10% of a by-product in a butanal synthesis can be removed easily by distillation. PVC contains only 0.1% defects as allylic and tertiary chlorides and this necessitates the use of a large package of stabilisers!

During the preparation the following properties of the polymer have to be tuned:

regioselectivity,
cis- or trans-isomerism, (in polybutadienes)
stereoselectivity,
molecular weight, M_w: weight average molecular weight,
M_n: number average molecular weight,
molecular weight distribution; a measure of this is the ratio of M_w/M_n, called the polydispersity.

Also used as a measure for molecular weights, especially by polymer chemists [2], are "number average degree of polymerisation" and the "weight average degree of polymerisation", P_w and P_n. Here we will use M_w and M_n. They are defined as follows:

$$\overline{M_n} = \frac{\Sigma N_i M_i}{\Sigma N_i} \qquad \overline{M_w} = \frac{\Sigma W_i M_i}{\Sigma W_i}$$

The number average molecular weight is the average molecular weight as we would define in daily life, *viz.* the sum of the numbers of molecules with a certain molecular weight multiplied by that molecular weight, and divided by the total number of molecules.

The weight average molecular weight is the sum of the weights of the molecules times the molecular weight divided by the total weight. A simple example may illustrate the usefulness of the entity M_w. Suppose we have one mole of a polymer with a molecular weight of 1 million in which we dissolve 100 moles of a solvent of molecular weight 100. The number average molecular weight of this mixture will be approximately 1 million divided by 101, i.e. ~10,000. A pure material that would have this molecular weight would be an adhesive, a sticky glue-like material. This number would say very little about the material that we actually have: a tough high MW material with a few solvent molecules dissolved in it (1% by weight). The weight average molecular weight will give us the molecular weight of the fraction that dominates our mixture, i.e. the M_w will be almost 1 million. Hence M_w is more

realistic than M_n. The dispersity, $M_w/M_n = 100$, gives us an idea about the very broad molecular weight distribution of this polymer mixture.

Physical properties to be controlled by these molecular factors include:

melting point, T_m (only the crystalline part shows a melting point)
crystallisation temperature,
glass transition temperature, T_g
strength,
modulus, (describes the relation between stress and deformation)
crystallinity,
viscosity of the molten polymer, and
morphology of the polymer particles.

Applications. Next to fuels, polymers are the organic chemicals produced on the largest scale. They find application as:

plastics	PE, PP, PS, PVC
fibres,	nylons, polyesters
rubbers,	IPR (isoprene rubber), BR (butadiene rubber), SBR (styrene-butadiene rubber)
coatings,	PMMA (polymethyl methacrylate),
resins, and adhesives.	

On a smaller scale many new functional polymers are produced having valuable properties for electrical, optical or magnetic applications. There exist numerous metal catalysed processes and we will discuss only a few to explain basic concepts using both examples from bulk polymers and fine chemical, high-value polymers.

10.1.1 Introduction to Ziegler Natta polymerisation

The titanium catalyst for the stereoselective polymerisation of propene to isotactic polymer was discovered by Natta in the mid fifties [3], applying the Ziegler catalyst. Soon after its discovery it has been turned into commercial exploitation and today isotactic polypropylene is one of the most important commodity polymers with a worldwide annual production of 20 M tons. Polymers with side-groups, of which polypropylene (PP) is the simplest one, may possess stereoregularity in the arrangement of these side-groups, i.e. methyl groups for PP. For example, if all methyl groups are oriented toward the same direction when we have stretched the polymer chain, we say the polypropene is isotactic (see Figure 10.1) (for the proper definition, see page 196). If the methyl groups are alternatingly facing to the front and the back, we say the polymer has a syndiotactic microstructure. Random organisation of the methyl groups (not shown) is found in atactic polymers. The stereoregularity of a polymer has an enormous influence on the properties of the polymer. Isotactic PP is the well-known semicrystalline material that we all know (e.g. in car

bumpers), while atactic PP is a rubber-like material with a glass-transition temperature (0–20°C) that has been used in chewing gum and carpets. The degree of isotacticity determines the "melting point" of the polymer. Isotactic PP with less than one mistake per 200 inserted monomers melts at 166 °C.

The catalyst and the concomitant technology have undergone drastic changes over the years. The titanium catalysts can be prepared by the interaction of $TiCl_4$ and alkylaluminium compounds in a hydrocarbon solvent.

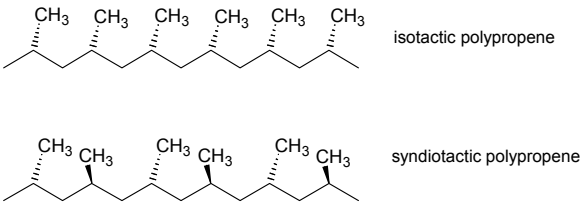

Figure 10.1. Microstructures of polypropylene

This reaction can be carried out with numerous variations to give a broad range of catalysts. It is a heterogeneous high-surface $TiCl_3$ material of which the active sites contain titanium in an unknown valence state. It is quite likely that alkyltitanium groups at the surface are responsible for the co-ordination polymerisation. In more recent catalysts titanium supported on magnesium salts are used [4,5].

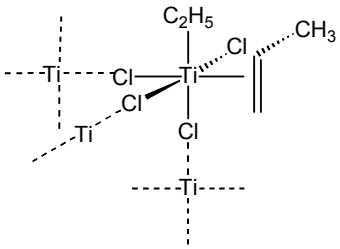

Figure 10.2. Cossée-Arlman mechanism

The Cossée-Arlman mechanism. The mechanism proposed for the polymerisation on solid titanium chloride catalysts is essentially the same for all catalysts and it is usually referred to as the Cossée-Arlman mechanism [6]. Titanium is hexa-coordinated in the $TiCl_3$ (or supported catalysts) by three bridging chloride anions (indicated by dashed Ti atoms), one terminal chloride anion, and one terminal chloride that is replaced by an alkyl group by the alkylating agent (Et_2AlCl or Et_3Al), and a vacancy that is available for propene co-ordination (see Figure 10.2). This simple picture yields an asymmetric titanium site, but by considering the lattice surface four bridging chlorides may

also lead to an asymmetric site. There was little doubt about the basic chemistry, i.e. alkylation of the metal followed by co-ordination of propene and migration of the alkyl group and/or insertion of propene. On the basis of Extended Hückel calculations Cossée proposed that migration rather than insertion occurs.

Propene can insert in three ways, which are presented in Figure 10.3. For titanium and zirconium the main mechanism is the 1,2 mode of insertion (note that we say insertion. although the "intimate" mechanism is a migration!). The other two modes are responsible for mistakes in the polymer chain.

The mechanism for 3,1-insertion involves a 2,1-insertion, a β-hydride elimination at carbon-3, and re-insertion giving a metal-carbon-3 bond.

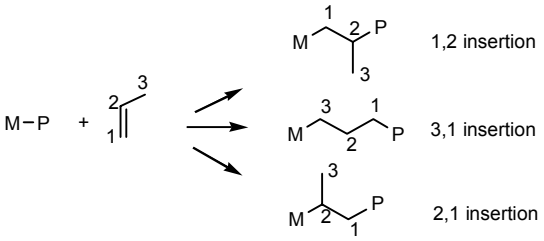

Figure 10.3. Insertion modes

In Cossée's view, one way or another, the ***site*** controls the way a propene molecule inserts; by doing so in a very controlled manner one can imagine that a stereoregular polymer will form. Site control would seem obvious, since different catalysts give different stereospecifities (reality is more complicated as we will see). The asymmetry of the site regulates the mode of co-ordination of the propene molecule, or in other words it steers the direction the methyl group will point to. We will not go into detail of the mechanism of the heterogeneous reaction as there is, relative to the homogeneous catalysts, a considerable amount of speculation involved. In section 10.2 we will discuss the homogeneous catalysts and the stereochemistry of the polymerisation reaction, but first we will have a closer look at the control of the enantiospecifity.

Site control versus chain-end control. Over the years two mechanisms have been put forward as being responsible for the stereo-control of the growing polymer chain: firstly the site-control mechanism and secondly the chain-end control mechanism. In the site control mechanism the structure of the catalytic site determines the way the molecule of 1-alkene will insert (enantiomorphic site control). Obviously, the Cossée mechanism belongs to this class. As we have seen previously, propene is prochiral and a catalyst may attack either the *re*-face or the *si*-face. If the catalyst itself is chiral as the one drawn in Figure 10.2, a diastereomeric complex forms and there may be a preference for the

formation of particular diastereomer and the rates of insertion for the two diastereomers may be different. If the catalyst adds to the same face of each subsequent propene molecule, we say isotactic PP is formed (a definition proposed by Natta; when each chiral carbon atom obtained after propene insertion has the same absolute configuration, *isotactic* polymer is formed). Thus, we see that stereoregular polymerisation is concerned with asymmetric catalysis and indeed the way the problems are tackled these days have much in common with asymmetric hydrogenation and related processes (Chapters 4 and 5). *Note that in asymmetric hydrogenation the catalyst contains only one enantiomer of the ligand, while in polymerisation reaction the racemic catalyst mixtures are almost invariably used.*

When we look more closely at the intermediate polymer chain we see an alternative explanation emerging. After the first insertion has taken place a stereogenic centre has been obtained at carbon 2, see Figure 10.4. Co-ordination with the next propene may take place preferentially either with the *re*-face or the *si*-face, with the methyl group pointing up or down, as displayed in Figure 10.4.

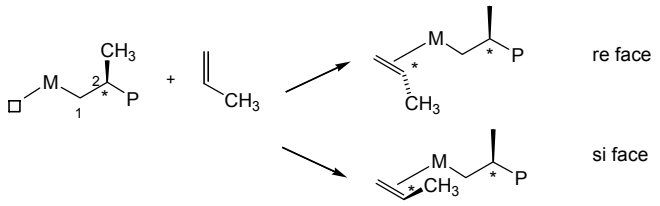

Figure 10.4. Simple model showing enantiomorphic chain-end control

Summarising, in the chain-end control mechanism the last monomer inserted determines how the next molecule of 1-alkene will insert. Several Italian schools [7] have supported the latter mechanism. What do we know so far? Firstly, there are catalysts not containing a stereogenic centre that do give stereoregular polymers. Thus, this must be chain-end controlled. Secondly, whatever site-control we try to induce, the chain that we are making will always contain, by definition, an asymmetric centre. As we have mentioned above, the nature of the solid catalysts has an enormous influence on the product, and this underpins the Cossée site-control mechanism. Thus both are operative and both are important. Occasionally, chain-end control alone suffices to ensure enantiospecifity.

10.1.2 History of homogeneous catalysts

We will discuss some of the recent advances in the area of alkene polymerisations catalysed by homogeneous complexes of zirconium and

titanium. One of the main research themes for these catalysts has been the polymerisation of propene. In less than a decade during the eighties a completely new family of catalysts has been developed which enables one to synthesise regioselective and stereoselective polymers of a wide variety of monomers.

From the early days on there has been an interest in homogeneous catalysts for the polymerisation of propene and ethene. It was thought that in a homogeneous system all metal atoms (titanium, chromium) could in principle participate in the catalytic process and, activity and stereospecificity, MW, dispersity, and morphology being the same, the low level of catalyst needed would make its removal unnecessary. In a homogeneous system, the molecular weight distribution might be much narrower and could be controlled at will. Drawbacks were also envisaged such as morphology of the powder to be formed and stereocontrol. For stereocontrol in heterogeneous systems, the $TiCl_3$ lattice seemed to play an important role and stereocontrol was not considered to be an easy task in a homogeneous catalyst. Polymerisation of ethene with homogeneous catalysts has been known since the very early days of Ziegler catalysis (Figure 10.5. Breslow [8]), but these catalysts failed to polymerise propene and only dimerisation of propene (to 2-methyl-pentene-1) was observed. Bis-cyclopentadienyltitanium dichloride is alkylated with diethylaluminium chloride and the cation formed co-ordinates to ethene followed by multiple insertions.

Using the catalyst shown in Figure 10.5 propene leads to dimerisation only. The difference in behaviour between ethene and propene is explained by the hydrogen at a tertiary carbon that is formed using propene, which undergoes β-hydride elimination.

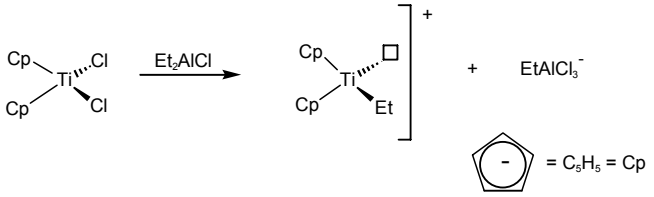

Figure 10.5. The first homogeneous metallocene catalyst for ethene polymerisation

Twenty years later Reichert [9] and Breslow [10] discovered that the addition of small amounts of water to the alkylaluminum chloride co-catalysts resulted in a one to two orders of magnitude increase in ethylene polymerization activity. In the 1980s the first reports appeared concerning the homogeneous stereospecific polymerisation, but they received relatively little attention because in the same period the first highly active, supported,

heterogeneous titanium catalysts were reported and the industrial interest in the more risky field of homogeneous catalysts diminished.

The development of the new family of homogeneous catalysts based on biscyclopentadienyl Group 4 metal complexes for the stereoselective polymerisation of alkenes is mainly due to Kaminsky, Ewen and Brintzinger. The first breakthrough came from the laboratory of Sinn and Kaminsky who had been studying the interaction of zirconium and aluminium alkyls for a couple of years. In 1980 they [11] reported on an extremely fast homogeneous catalyst for the polymerisation of ethene formed from the interaction of $Cp_2Zr(CH_3)_2$ and $(CH_3AlO)_n$ (the aluminium compound, named alumoxane or aluminoxane, was obtained from the reaction of trimethylaluminium and traces of water that were accidentally present; nowadays alumoxanes, abbreviated as MAO, are commercially available). At 8 bar of ethene and 70 °C an average rate of insertion of ethene was reported amounting 3.10^7 mole of ethene per mole of zirconium complex per hour! It was this increase in order by several orders of magnitude which elevated metallocenes from academic curiosities to contenders for commercialization. With propene this catalyst led to completely atactic polymer [12].

Ewen was the first to report the synthesis of stereoregular propene polymers with soluble Group 4 metal complexes and alumoxane as the co-catalyst [13]. He found that Cp_2TiPh_2 with alumoxane and propene gives isotactic polypropene. This catalyst does not contain an asymmetric site that would be able to control the stereoregularity. A stereo-block-polymer is obtained, see Figure 10.6. Formation of this sequence of regular blocks is taken as a proof for the chain-end control mechanism.

The explanation for the existence of a stereo-block polymer is that after a "mistake" this mistake will "propagate" as the chain end controls the stereochemistry of the new centre to be formed. Thus after the mistake has occurred, the polymer switches the stereochemistry from s to r.

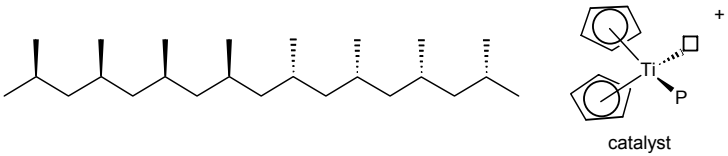

Figure 10.6. Stereo-block catalyst, Ewen [6]

Note that the catalyst of Figure 10.6 contains the same titanium part as that of Figure 10.5, but that they differ in the aluminium Lewis acid and anions formed. The use of diethylaluminium chloride (DEAC, the common initiator for heterogeneous titanium catalysts) gave propene dimerisation only. This

dramatic impact of the activator or anion should perhaps be even more emphasized!

Using an intrinsically chiral titanium compound (rac ethylene-bis-indenyl *titanium* dichloride, Figure 10.7), first described by Brintzinger [14], Ewen [13] obtained polypropene that was in part isotactic. Subsequently Kaminsky and Brintzinger have shown that highly isotactic polypropene can be obtained using the racemic *zirconium* analogue of the ethylene-bis(indenyl) compound [15].

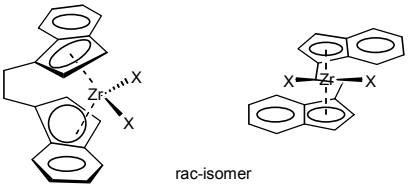

Figure 10.7. Bis-indenyl Group 4 metal catalysts for making isotactic polypropylene

Modification of the cyclopentadienyl ligands has led to a very rich chemistry and today a great variety of microstructures and combination thereof can be synthesised as desired including isotactic polymer with melting points above 160 °C, syndiotactic polypropene [16], block polymers, hemi-isotactic polymers etc.

Fundamental studies have led to a detailed insight into the mechanism of the polymerisation and the control of the microstructure through the substituents on the cyclopentadienyl ligands. The nature of the catalyst has been the topic of many studies and it is generally accepted that it is a cationic Cp_2ZrR^+ species [17]. For a survey of these studies and the dominant effects playing a role the reader is referred to recent contributions by Ewen [18] and Erker [19]. The first requirement for obtaining an active catalyst is to ascertain the formation of cationic species. Secondly, the metallocene (or related ligand) must have the correct steric properties. In the present chapter we will summarise a few of the features that play a role in determining the microstructure; the field is still in development and obviously the definitive answer to several questions has not been given yet.

Another, independent development involves vanadium catalysed propene polymerisation leading to syndiotactic polypropylene [20], see 10.2.1.

10.2 Mechanistic investigations

10.2.1 Chain-end control: syndiotactic polymers

As we have seen above polymerisation of all “prochiral” alkenes produces a new stereogenic centre for each monomer inserted. In a site-controlled

polymerisation the chiral catalyst site (and the mutual positions of the co-ordinating alkene and the migrating alkylgroup) determine how the next alkene will be incorporated. When chain-end control occurs, the chiral centre in the chain - i.e. the one stemming from the previous alkene inserted - determines the stereochemistry of the next alkene that will insert. When the catalyst does not contain a stereogenic centre, any resulting stereospecifity of the polymerisation must result from chain-end control.

Achiral catalysts derived from vanadium sources and DEAC [$VCl_4/AlCl(C_2H_5)_2$ or $V(acac)_3/AlCl(C_2H_5)_2$], developed by Doi and co-workers, are the best known examples giving syndiotactic polymers [20]. Termination experiments have proven that this polymerisation involves a 2,1 insertion instead of the expected, more common 1,2 insertion. This is to say that the intermediate vanadium alkyl contains a branched or secondary alkyl group, although one would expect that a primary alkyl in this ionic complex is more stable. Direct observation has not yet been achieved, but the termination experiments unequivocally prove that the reacting species is a secondary alkyl vanadium complex, also after presumed equilibration of the living polymer before it is made to react with a terminating agent such as I_2. There still is the possibility of a very fast equilibrium between the primary and secondary alkyl, the latter being far more reactive in the termination reaction. This chain-end control occurs only at very low temperatures, as in the titanium case for isotactic polymer, studied by Ewen.

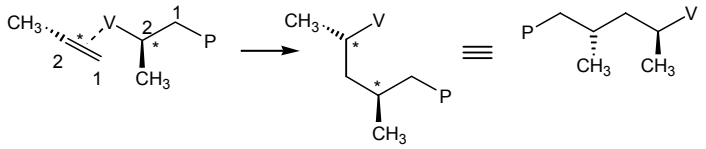

Figure 10.8. Chain end control through 2,1 insertions leading to syndiotactic polymer

Figure 10.8 shows the important features. On the left we see the growing polymer chain containing a vanadium ion at carbon-2 of the last inserted propene. Carbon-2 is enantiotopic (chiral); according to the Cahn-Ingold-Prelog convention it has the R configuration. Co-ordination of the following ("prochiral") propene molecule will create another chiral centre. As we have seen before the metal can either co-ordinate to the *re* or the *si* face of propene. Hence, we can either form a *si*-R or a *re*-R diastereomer. The figure shows the *si*-R diastereomer. The free energies of these diastereomeric precursors or intermediates will of course be different, and so will be the free energies of activation of the formation of the alkene adduct (shown on the left) and that of the insertion reaction. Thus, there can be a preference to form either *si*-R or a

re-R. After the insertion we see that the two last chiral centres have opposite absolute configurations, i.e. by definition syndiotactic polymer is formed.

The detailed kinetics determine how this happens precisely. We don't know whether the complexation reaction or the insertion reaction is rate-determining. Theoretical work on insertion reactions of early-transition metal catalysts indicates that the complexation is rate determining and that the migration reaction has a very low barrier of activation. If the complexation is irreversible, it also determines the enantioselectivity.

The formal part explains the origin of the enantiospecificity, but it does not explain which type of tacticity one might expect. The following explanation is speculative and oversimplified but it seems to work. Two simple assumptions explain why a syndiotactic polymer is obtained. Firstly, the growing chain assumes a conformation in which the two largest groups, being the polymer chain and the vanadium complex, are trans to one another in the chain end formed by the last two carbon atoms. (see Fig 10.8, the polymer chain is arranged in such a way that it lies in the plane of the figure; the double bond of the propene to be inserted also lies in the plane with its substituents in a plane perpendicular to the plane of the figure; the methyl groups above or below the plane of the figure are drawn in the usual manner). Secondly, the insertion of propene takes place via a migration mechanism reminiscent of a 2+2 addition. The methyl group of the propene to be inserted and the one of the previously inserted propene molecule will assume positions leading to a minimum of steric interaction (see Fig 10.8).

Before the next insertion can take place (not shown) the molecule in the middle of Figure 10.8 has to rearrange. Since the two largest groups attached to the last inserted propene are now in mutual syn positions the chain must be rotated around the vanadium-to-carbon bond and the newly formed C–C-bond in order to obtain the more stable trans configurations at all linkages, i.e. the chain being stretched as it is usually represented. In this way the structure shown on the right is obtained. When this procedure is repeated a couple of times we see that indeed a syndiotactic microstructure is formed. Molecular mechanics calculations support this explanation [21,14]; when 2,1 insertion occurs the growing polymer will tend to form a syndiotactic microstructure.

10.2.2 Chain-end control: isotactic polymers

By the same token, 1,2 insertion gives an isotactic microstructure. If the methyl group of the previously inserted molecule is upwards, the methyl group of the next molecule will be pointing downwards (see Figure 10.9, Catalyst: $Ti(Cp)_2Ph_2$; the polymer chain is arranged in such a way that it lies in the plane of the figure; the double bond of the propene to be inserted also lies in the plane with its substituents in a plane perpendicular to the plane of the figure; the

methyl groups above or below the plane of the figure are drawn in the usual manner).

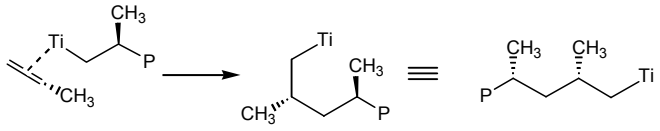

Figure 10.9. Chain-end control through 1,2 insertions leading to isotactic polymers

The interaction may not be quite as strong as in the case of 2,1 insertion discussed above, but there will always be a tendency of the growing chain to arrive at an isotactic stereochemistry when 1,2 insertion occurs. One example of chain-end control leading to isotactic polymer was reported by Ewen [13] using Cp_2TiPh_2/alumoxane as the catalyst. The stereoregularity increased with lower temperatures; at –45 °C the isotactic index as measured on pentads amounted to 52 %. The polymer contains stereoblocks of isotactic polymer. At 25 °C the polymerisation gives almost random 1,2 insertion and an atactic polymer is formed.

10.3 Analysis by ^{13}C NMR spectroscopy

10.3.1 Introduction

The analysis of the products using high resolution ^{13}C NMR has greatly contributed to the mechanistic insight and distinction between the various catalysts. A few examples will serve as an illustration of this point. The chemical shift of the methyl side groups in polypropylene depends on the local stereoregularity of the polymer. As usual we consider the stretched chain. A methyl group can "see" whether their nearest neighbours are pointing in the same or the opposite direction. In fact the chemical shift of the methyl group, given the present status of our ^{13}C NMR technique, undergoes small shifts depending on the position of two neighbours in each direction. Since this is a local effect, only the relative position of the methyl group is our concern. The relation between two adjacent methyl groups is indicated with *m* (meso) or *r* (racemic) which means that with respect to the stretched chain they are on the same side (*m*) or on opposite sides (*r*), see Figure 10.10. Thus a sequence of five methyl groups can be distinguished; we say the analysis is based on pentads. If our NMR resolution had been less powerful and could only distinguish the position of the two nearest neighbours, our analysis would have been based on triads.

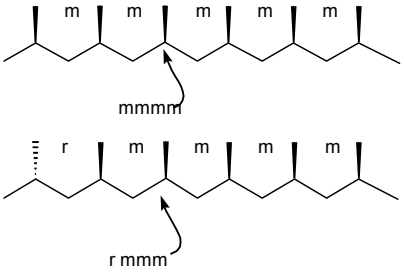

Figure 10.10. m and r pentad relationships

Hence, a syndiotactic polymer consists of a sequence of *r* relationships, whereas the isotactic polymer consists of purely *m* relationships. With two adjacent *m* stereocentres, *mm*, we say that we are dealing with a triad of methyl groups with an isotactic stereochemistry. As mentioned above, we cannot only tell the stereochemical relation with the two nearest neighbours (the *mm, mr, and rr* triads), but we can also deduce the relation with the two next ones from the chemical shifts observed. In other words, with ^{13}C NMR we are able to distinguish pentads of methyl groups, i.e. we can distinguish from the NMR spectrum for example a sequence *rmmm* from a sequence *mmmm*. We can expect ten different pentads in atactic polymer. Coincidentally two of these have the same chemical shift and hence in NMR analysis of atactic propene polymers nine signals are observed, in three groups of three peaks each.

Statistical analysis is important and relatively easy. Suppose we have a fully atactic polymer which we analyse for the triad content for isotactic polymer. Only three methyl resonances due to triads are observed, and the statistical ratio of *mm, rr,* and *mr* is 1:1:2. Thus even in the atactic polymer our isotactic content is 25%! Pentad analysis, however, would give only 8% *mmmm* isotactic content! Especially for catalysts with low enantiospecificity it is worthwhile keeping this in mind.

The *r* and *m* nomenclature needs one further comment, though it may be *confusing*. By definition, an isotactic polymer is built from units containing the same absolute configuration. This can be ascertained in the growing chain by applying the Cahn-Ingold-Prelog rules while the heavy atom is still there. In terms of the pentad relationships this leads to *mmmm* pentads. Yet, *m* refers to *meso* as we have just seen, which indicates the presence of a mirror plane and therefore *opposite absolute* configurations. The explanation is that in the finished polymer we cannot determine the absolute configuration any more and indeed in between two side groups we find locally a mirror plane mirroring the adjacent methyl groups. The same story applies to the syndiotactic polymers that are constructed from alternating absolute configurations at the catalyst site and yet the relation between neighbouring methyl groups is *r* from *racemic*.

10.3.2 Chain-end control

Control by the catalytic site and control by the growing chain can be easily distinguished from one another by studying the "mistakes" as they occur in the ^{13}C NMR spectrum. When a chain-end control mechanism is operative the NMR spectra of the errors made will tell us that this is indeed the mechanism. If in a sequence of isotactic insertions one mistake is made the next propene that comes in will be directed by the previous one and the "mistake" will persist in the growing chain. Hence, after a block having all methyl groups pointing to one direction, a block will form having the methyl groups pointing to the other side of the growing chain (Figure 10.11).

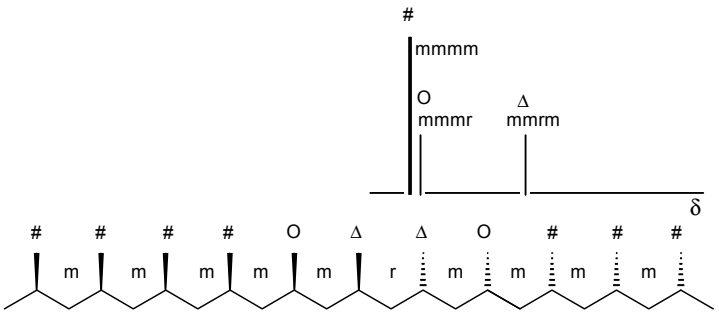

Figure 10.11. Single mistake during a chain-end controlled isotactic polymerization and schematic ^{13}C NMR spectrum of the methyl region (assuming that chain continues in "m" mode)

Above we mentioned the results reported by Ewen [13] who found that Cp_2TiPh_2/alumoxane gives a polypropene with isotactic stereoblocks. Naturally, this achiral catalyst can only give chain-end control as it lacks the necessary chiral centre for site control. In the ^{13}C NMR the stereoblocks can be clearly observed as they lead to the typical 1:1 ratio of *mmmr* and *mmrm* absorptions in addition to the main peak of *mmmm* pentads. These are two simple examples showing how the analysis of the ^{13}C NMR spectra can be used for the determination of the most likely mechanism of control of the stereochemistry. Obviously, further details can be obtained from the statistical analysis of the spectra and very neat examples are known [18].

10.3.3 Site control mechanism

In a system with site control ideally the mistake leads to a single odd insertion in the chain: the site enforces for instance the growth of an isotactic chain with all *m* configurations and after one mistake has occurred it will return to producing the same configurations. In other words, an isospecific catalyst will produce a polymer chain with all methyl groups pointing towards us (as in

Fig 10.12), but when a mistake occurs **one** methyl group will be pointing backwards. Let us look at the result in the ^{13}C NMR spectrum. In the polymer chain this gives a series of *m* relationships interrupted by two *r* configurations. In the NMR spectrum this gives rise to three new peaks belonging to *mmmr, mmrr,* and *mrrm* in a 2:2:1 ratio. (See Figure 10.12).

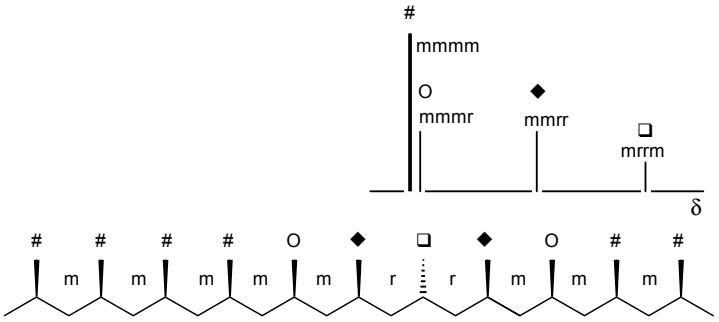

Figure 10.12. Single mistake during a site-controlled isotactic polymerization and schematic ^{13}C NMR spectrum of the methyl region.

Single site versus multiple sites; homogeneous vs heterogeneous catalysts. A general difference between the products of the homogeneous catalysts on the one hand and the heterogeneous catalysts on the other hand has been noted for the initial results of the metallocene catalysts in the mid-eighties. Measurement of the overall isotactic index of the products of the homogeneous catalysts revealed that polymers with isotactic indices as high as 96% still have a melting point of only 140 °C, whereas the products of heterogeneous catalysts with such isotactic indexes show melting points of 160–6 °C. The molecular weight distribution for the homogeneous catalyst was very narrow, M_w/M_n=1.8, as is to be expected from a homogeneous catalyst and the molecular weight may be as high as 300,000 [22], strongly decreasing upon raising the temperature. For a heterogeneous catalyst this value may be as high as 7.

The solution to the problem of the low melting point reads as follows. The commercial heterogeneous catalysts contain, in spite of their high degree of optimisation, different sites, one group producing polymer with a high isotactic index (99+%) and another group of sites producing a small amount of atactic polymer. Hence a mixture of two polymers is formed of which the melting point is determined by the isotactic component. The homogeneous catalyst, on the other hand, contains ideally only one type of site that produces one polymer with often a somewhat lower isotactic index. While the isotactic index may look very promising the melting point may be disappointing since all the errors made occur in the main chain of the product giving a lower melting point. Subsequently, improved homogeneous catalysts have been synthesised which

also give polypropene melting points above 160 °C and isotactic indices of 99.7% [23].

10.4 The development of metallocene catalysts

10.4.1 Site control: isotactic polymers

Until 1984 no well defined homogeneous catalysts were known based on Group 4 metals that would polymerise propene. Many attempts had been undertaken using bis(cyclopentadienyl)metal dichlorides in combination with the co-catalysts most popular in heterogeneous Ziegler-Natta polymer catalysis such as $(C_2H_5)_3Al$ and $(C_2H_5)_2AlCl$. At most dimerisation of propene was observed. The first breakthrough involved the use of alumoxane $(CH_3AlO)_n$ as the co-catalyst. Apparently a large excess of this compound combines the desired Lewis acidity with sufficient alkylating power in order to generate the catalytically active species. The structure of the catalyst has been proven to be a cationic species $Cp_2M\text{-}R^+$ (M = Ti, Zr, Hf) by Jordan, Turner, and others [24]. The second important breakthrough was how to build a chiral centre into the Group 4 metallocene. Substituted chiral metallocene complexes had already been reported in 1982 by Brintzinger [14]. A combination of Group 4 complexes with these ligands and alumoxane led to the first homogeneous, site-controlled, isotactic polymerisations of propene (M=Ti [15], M=Zr [22]).

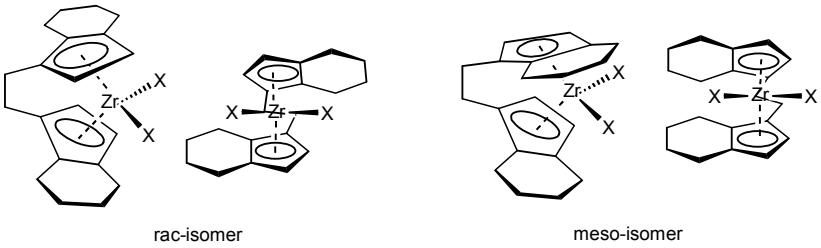

Figure 10.13. Structure 1,2-ethanediyl-tetrahydroindenyl-ZrX_2

The basic structure of the new catalysts is depicted in Figure 10.13. Zirconium is tetrahedrally surrounded by two cyclopentadienyl ligands and two chlorides. The latter two ligands are not essential as they are replaced before the polymerisation can start by an alkyl group (e.g. CH_3 from methylalumoxane) and by a solvent molecule thus generating the required cationic species. The two cyclopentadienyl anions are linked together by a bridge, here an ethane bridge, and extended with an organic moiety which renders the molecule its chirality. In the example of Figure 10.13 a 1,2-ethane bridged bis(1,1-tetrahydroindenyl) dianion has been drawn. Two compounds are

obtained when this complex is synthesised, the rac-isomer mixture and the meso-isomer. Often they can be separated by crystallisation. The sterically less hindered rac-isomers may be formed in excess. The isomers can only interchange by breaking of a cyclopentadienyl-metal bond and reattaching the metal at the other face of the cyclopentadienyl ligand. This process is very slow compared to the rate of insertion reactions with propene.

The rac-isomers have a twofold axis and therefore C_2-symmetry. The meso-isomer has a mirror plane as the symmetry element and therefore C_s-symmetry. For polymerisation reactions the racemic mixture can be used since the two chains produced by the two enantiomers are identical when begin- and end-groups are not considered. Note: When catalysts of this type are to be used for asymmetric synthesis, e.g. as Lewis acids in Diels-Alder reactions, separation of the enantiomers is a prerequisite [25].

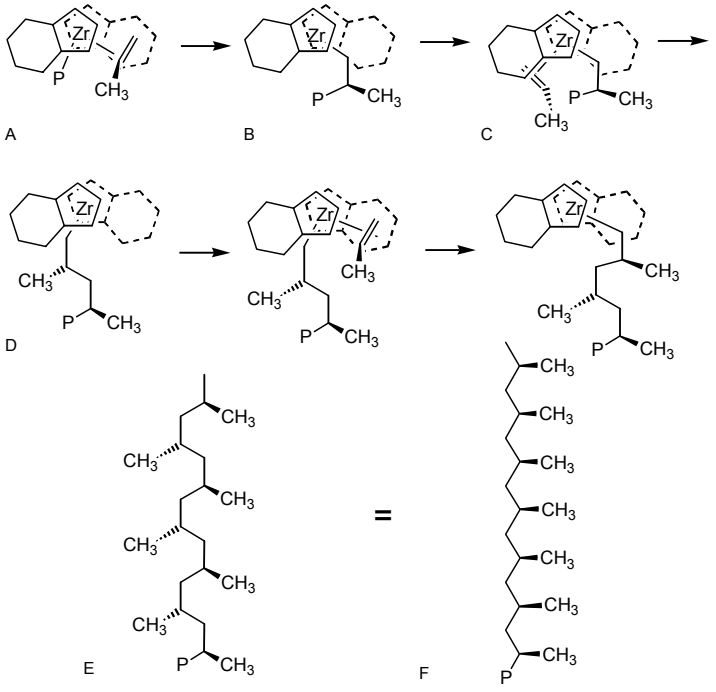

Figure 10.14. Simplified view of site-controlled isotactic polymerization

To start the polymerisation the X atoms in Fig 10.13 are replaced by a growing alkyl chain and a co-ordinating propene molecule. Co-ordination of propene introduces a second chiral element and several diastereomers can be envisaged. The step-by-step regulation of the stereochemistry by the site can be most clearly depicted by drawing the molecule as shown in Figure 10.14, a

simplified picture neglecting interaction of polymer chain and indenyl ligand. Here we have taken the plane of the paper identical to the plane determined by Zr and the two X atoms of Figure 10.13 or in other words the plane bisecting the two cyclopentadienyl planes. Propene co-ordinates in a π-fashion to zirconium with the two alkene carbons situated in the plane. The migratory insertion reaction can be described as a 2+2 addition and, as was found experimentally, following 1,2 regioselectivity. This eliminates two diastereomers, the ones stemming from 2,1 insertion. For the 1,2 insertion two possible structures remain, one with the methyl group pointing up (Figure 10.14 A) and one with the methyl group below the plane, not shown. The methyl group above the plane (drawn in full) will clearly be favoured. If we accept that the transition state resembles the co-ordination complex, the stereochemistry of the insertion product follows from structure A → B. The alkyl group has migrated to the other co-ordination site of the complex. The question that remains is: What will be the relation between the next insertion and the one that we have just described?

The next molecule of propene will co-ordinate onto the complex with the methyl group pointing downwards, C, migration of the new alkyl anion gives D with the stereochemistry shown. When this process is repeated several times, forming the polymer carbon chain in the plane of the figure, structure E is obtained. From this structure we cannot immediately deduce what the microstructure is, since the polymer chain is not stretched as shown before (Figure 10.1). By rotating carefully around the bonds indicated we obtain from E the isotactic stereochemistry, F. Hence, the experimentally found isotactic stereochemistry with rac-bis(indenyl) derived complexes can be explained with a very simple set of pictures.

The formal view. The formal view is much simpler. The racemic catalysts have a twofold axis and therefore C_2-symmetry. Both sites of the catalysts will therefore preferentially co-ordinate to the same face (be it *re* or *si*) of propene. Both sites will show the same enantiospecificity; the twofold axis converts one site in the other one. Subsequently, insertion will lead to the same enantiomer. According to the definition of Natta, this means that isotactic polymer will be formed. If the chain would move from one site to the other without insertion of a next molecule of propene, it will continue making the same absolute configuration at the branched carbon atom. Hence, no mistake occurs when this happens.

When the chain is transferred from one zirconium atom to another, there is a 50% chance in the racemate that the chain will continue to grow producing the opposite absolute configuration.

If the zirconium complex racemises once in a while a blocky isotactic polypropylene will be obtained.

10.4.2 Site control: syndiotactic polymers

The explanation given so far sounds very reasonable, but further evidence is welcome. An elegant experiment was carried out by Ewen [13], which supports the mechanism. It involves the use of isopropyl(1-fluorenyl-cyclopentadienyl) ligands as shown in Figure 10.15 (Ewen used a compound with an isopropyl bridge at the back side). This complex has no chirality (i.e. the dichloride precursor) and one might expect no tacticity in the propene polymer product. The catalyst was found to give syndiotactic polymer. If the fluorenyl group is below the plane, propene co-ordination at both left and right hand side sites will occur with the methyl group above the plane (Figure 10.16, A, C). A series of migratory insertions of the alkyl group to propene molecules with their methyl substituents pointing up lead to the chain E. Stretching the chain leads to structure F which clearly has a syndiotactic arrangement of the substituents along the chain. This is an important result, since hitherto it was thought that syndiotactic polymers could only be obtained via 2,1 insertion controlled by the stereochemistry of the chain-end.

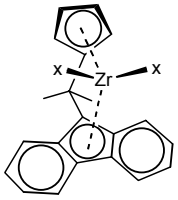

Figure 10.15. Cyclopentadienyl-fluorenyl metal catalyst

The formal view. The fluorenyl-cyclopentadienyl complex contains a mirror plane. The two sites are therefore mirror images. One site co-ordinates to the *re*-face of propene, the other site to the *si*-face of propene. One site will therefore be enantiospecific for making R configured carbon atoms and the other site for S configured carbon atoms. This alternation of configuration leads to a syndiotactic polymer.

When the chain migrates from one site to the other without insertion we obtain two stereocentres of the same absolute configuration and our pentad analysis will show one meso (m) *in the series of* (r) *relationships.*

If one 1,2-insertion occurs with the "wrong" stereochemistry we obtain two m *relationships in the series of* (r) *relationships.Thus several types of mistakes can be distinguished from the* ^{13}C *NMR analysis.*

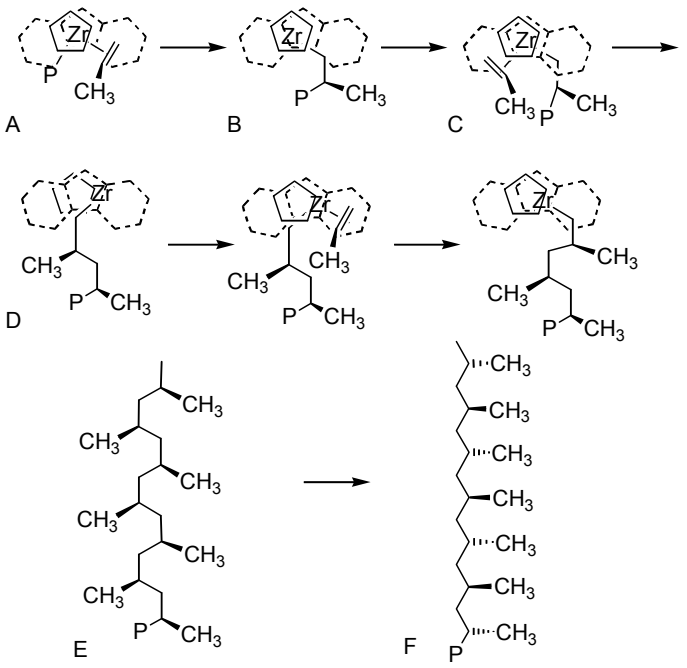

Figure 10.16. Simplified view for syndiotactic polymer formation at a C_s symmetric catalyst

Errors. Errors can be introduced in several ways, for the bis-indenyl as well as for the fluorenyl-cyclopentadienyl complexes:

- 1,2 insertion with the methyl group pointing to the sterically more hindered direction,
- 2,1 insertion (with two orientations),
- 2,1 insertion followed by isomerisation (3,1 insertion),
- alkyl migration without insertion in the fluorenyl complex, and
- alkyl exchange between metals.

Impurities in the zirconium precursor complex can also lead to lower tacticities. The activities of complexes may differ several orders of magnitude and therefore the results can be distorted considerably by impurities. With the present knowledge one can estimate to what extent impurities will distort the results. For example it was found that the presence of the meso-isomer in a bis(indenyl)ethane type catalyst may sometimes produce only little of the atactic isomer. The meso-isomer containing one alkyl group and a propene co-ordinated to the vacant site will have no preference for the methyl group pointing up or down, regardless the position of the chain. The two sites, however, will show a great difference towards propene co-ordination, one being very open and the other being strongly sterically hindered. The hindrance at one site may be such that this site is virtually blocked for propene co-

ordination and as a result the rate of propene polymerisation of such a catalyst may be very low.

10.4.3 Double stereoselection: chain-end control and site control

So far we have looked at chain-end control and site control if they were independent. As already mentioned, a site-control-*only* mechanism does not exist. Since we are, by definition, making a chiral chain-end and since chain-end control does occur as found in achiral catalyst systems, site control must be accompanied by chain-end influences, or a(n) (a)symmetric site may amplify specific chain end influences. Recent results have shown that this is indeed the case [18,19,21,26]. The simple explanation given above has to be modified. We limit ourselves to two issues, (a) the stereochemistry of the co-ordinating propene and (b) reinforcement of the two mechanisms.

(a) Molecular mechanics calculations [27] and thorough analysis of the substituent effect on the statistical distribution of microstructure defects indicate that firstly the polymer chain assumes the energetically most favourable position with respect to the (asymmetric) site. For the fluorenyl-cyclopentadienyl ethane ligand this means that the chain will occupy the empty space at the cyclopentadienyl face. Subsequently the incoming propene will direct its methyl group into the most favourable direction which is now the fluorenyl side of the catalyst. This *reverses* the propene orientation given in Figure 10.16 A, C. It does not fundamentally change the explanation because *all* propene molecules will orient themselves into the same direction. For the present purposes Figures 10.15 and 10.16 are sufficient and we have not attempted to redraw the structures with the polymer chains included; the experts will prefer to treat this problem with molecular mechanics and computer graphics in a more sophisticated manner. According to Corradini this reversion of the propene orientation also holds for the $TiCl_3$ catalyst. In Figure 10.17 we have shown the orientation of propene in the heterogeneous catalyst. The front left is called the blocked side by Cossée, as this is where the bulk crystal lattice is situated. In the back there is free space and the polymer chain will be in this free space (exposed side, Cossée). As a result the methyl group will be on the most hindered side of titanium (in the absence of polymer), directed by the methyl group of the previously inserted monomer, as in the chain-end controlled mechanism (Figure 10.9). [In Figure 10.17 we have not drawn the crystal lattice, but indicated the blocked and exposed side].

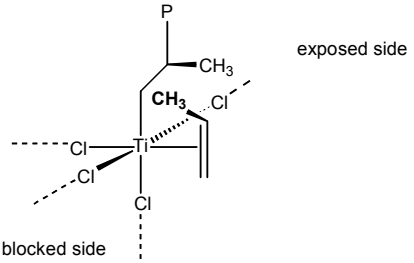

Figure 10.17. Corradini's active site on asymmetric α-$TiCl_3$ surface

(b) This brings us to double stereoselection and reinforcement of the mechanisms. If the site (a)symmetry will control the orientation of the chain, and if then the orientation of the incoming propene is controlled by both the chain and the site, the highest stereoselection is obtained when the two influences reinforce one another. For 1,2 insertion this can be done most effectively for isotactic polymerisation, since chain-end control "naturally" leads to isotactic polymer and this we can reinforce by site control with ligands of the bis(indenyl)ethane type. The chain-end influence of short chains is smaller than that of longer polymer chain; indeed the isotactic index at the very beginning of the chain was found to be lower than that in the polymer. It may also be inferred that making syndiotactic polymer via a 1,2 insertion mechanism on Ti or Zr complexes is indeed more difficult than making an isotactic polymer, because the two mechanisms now play a counterproductive role.

Important: The reinforcement was proven experimentally by the analysis of the stereoregularity of short chains. The enantioselectivity appeared to be very low for single insertions of propene in small alkyl chains. Thus, if the "controlling" polymer chain is absent, the site control is poor [28].

Numerous papers have appeared on further detailed studies of the mechanism, including chain transfer mechanisms, epimerization of the stereocenter shortly after its formation, the role of agostic interactions, etc. A special issue of Chemical Reviews gives a complete overview [29].

10.5 Agostic interactions

Elegant studies by Bercaw and Brintzinger using an isotopic labeling technique developed by Grubbs revealed that alkene insertion can be assisted by agostic interactions in many metallocene polymerization systems [30]. These studies depict a detailed view of the mechanism of stereoselection using chiral metallocenes for alkene polymerization. One of the α-hydrogens of the growing chain forms an agostic, extra link with the metal centre. The agostic

interaction can occur in the ground and in the transition state, or in the latter only. This rigidifies the transition state for alkene insertion and thus increases the stereoselectivity. Complete transfer of the α-hydrogen to the metal atom leads to a hydrido-alkylidene metal complex that can undergo a cycloaddition reaction with the incoming alkene, forming a metallacyclobutane. This gives ring-opening with the hydride to give the new chain; this is the so-called Green-Rooney mechanism [31]. The leading proposals for the mechanism are the direct insertion (Cossée-Arlman) and the transition-state agostic interaction. Figure 10.18 summarises the various mechanisms.

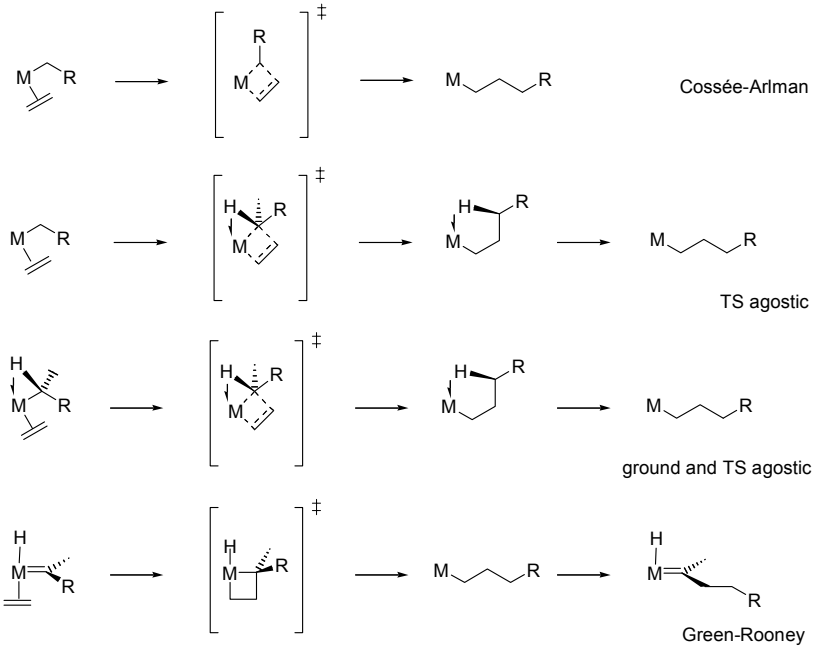

Figure 10.18. Mechanisms for alkene insertion

After insertion according to the α-agostic TS mechanisms a γ-hydrogen agostic interaction will exist (many X-ray structures suggest that β-agostic structures will be the resting state of such compounds). We can distinguish between the two leading mechanisms via deuterium isotope effects. If the insertion proceeds with the assistance of an agostic α-hydrogen, this step should exhibit a secondary isotope effect when hydrogen is replaced by deuterium. The technique involves replacement of one α-hydrogen by a deuterium label. The metal alkyl complex has a preference for the formation of the agostic interaction with the hydride and thus the stereochemistry of the insertion product can tell us whether or not agostic interactions played a role.

10.6 The effect of dihydrogen

Recently many subtle effects of the ligand structure, concentrations of alkene, and conditions on the polymerisation have been reported to have significant effects on molecular weight, regioselectivity, branching, stereoselectivity or enantioselectivity, incorporation of other monomers, chain transfer, etc. Often these subtle effects can be understood from the mechanism, or they contribute to the understanding of the detailed processes going on.

One particular example is both of industrial importance and fundamentally very interesting: the effect of the hydrogen pressure. In the actual, commercial processes using (as yet) heterogeneous catalysts *dihydrogen* is used as the reagent to control the molecular weight.

Another way of controlling the molecular weight would be β-*elimination*. This is a monomolecular process, in its simplest form, which can be enhanced by raising the temperature. For the control of a process this is disadvantageous, certainly for a highly exothermic process which might have runaway character. Furthermore, the product would contain unsaturated end-groups which are sensitive to oxidation and could further insert into growing chains affording branched copolymers.

The control of the molecular weight via a reagent to be added is much more convenient. Dihydrogen gives saturated end-groups thus solving the additional problems as well. Two leading groups in this field discovered two further, peculiar advantages of the use of dihydrogen as a chain transfer agent, Chadwick at Shell for heterogeneous catalysts, and Busico for the metallocene catalysts [32,33]:

- the rate increases upon the application of dihydrogen, and
- the selectivity increases (the melting point of the polymer increases),
- while naturally the molecular weight is depressed. Therefore this can only be useful for catalysts that give high molecular weight polymers.

How the groups unravelled this phenomenon is an interesting detective story but for our purposes it is more convenient to progress directly to the conclusion. In Figure 10.19 we outlined the two modes of insertion that can occur, 1,2 and 2,1 insertion. The latter often leads to isomerisation via β-elimination and re-insertion, which will lower the stereoregularity. Another outcome, especially for catalysts that show little or no β-elimination would be to continue the polymerisation resulting in an error in the chain and hence a lower melting point of the polypropene.

It turns out that the insertion of a next molecule of propene in the branched alkyl metal complex is much slower than the insertion of propene in a regular chain formed after a 1,2 insertion. In several catalysts studied this leads to a situation in which a great deal of the catalyst sites are "dormant", i.e. the metal is tied up in unreactive secondary alkyl metal complexes. If eventually an

insertion does occur it leads to an error in the chain. By admitting dihydrogen in such a system the unreactive secondary alkyl metal complexes are removed by the reaction with dihydrogen, which is of course less hampered by the steric hindrance of the alkyl group.

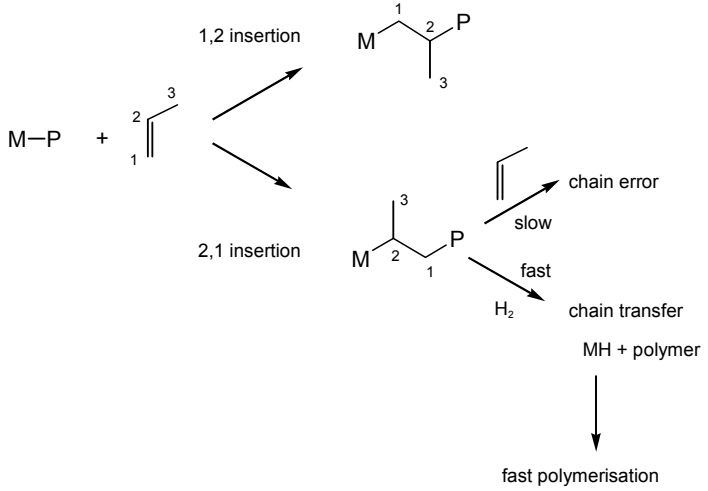

Figure 10.19. Effect of dihydrogen on rate and stereoselectivity

The metal hydride formed will start a new fast growing polymer chain. Thus,

1. the molecular weight is lowered somewhat,
2. the overall activity increases, and
3. the number of errors in the chains diminishes.

Another way to recover the catalyst from the dormant site is the copolymerisation of ethene, but this is slower and less attractive than the use of hydrogen. Furthermore the use of ethylene inevitably results in the formation of propylene-ethylene copolymers with all the consequent effects on polymer properties.

10.7 Further work using propene and other alkenes

In addition to propene and ethene many other alkenes (higher alkenes, styrenes, cyclic alkenes) have been polymerised with these new catalysts and a great variety of new polymers and oligomers have been synthesised including plastic materials with melting points as high as 500 °C, novel rubber materials etc. Several new polymers can now be made by catalyst design. Basically, the concepts developed by Cossée and his contemporaries have not changed, but today we have the tools to design the catalysts that may give the desired

polymer. Stereoselectivity and molecular weight may not be high enough in some instances, but the achievements are impressive. A 1-cyclopentadienyl,-2-indenyl-ethane ligand gives alternatingly insertion in an isotactic and an atactic fashion giving a hemitactic polymer as is to be expected (Figure 10.20).

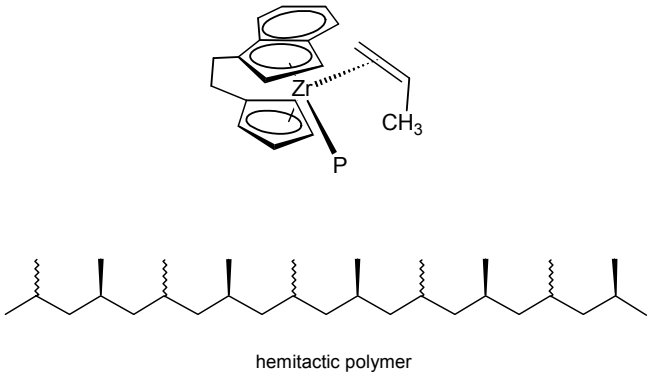

Figure 10.20. Cyclopentadienyl-indenyl zirconium catalyst for hemispecific polymerisation

One could also imagine a complex that at one site will insert only one certain type of alkene due to high steric constraints (e.g. ethene) and a second alkene at the other site thus giving an alternating copolymer that may even contain stereoregularity, thus obtaining for instance an alternating norbornene/ethene copolymer [34].

Here we have discussed only very few of the many ligands that have been studied. Many variations of substituents at the cyclopentadienyl ligand have been studied, and there are more to come as well as variation in the structure of the bridge, the anions, and the central metal. In summary, the toolbox is quite extensive; prediction of properties of new polymers to be made can guide the catalysis research in the design of new catalysts.

Structure-performance relationships for bis-indenyl catalysts. An interesting study about substituent effects in bisindenyl zirconium catalysts was published by Spaleck [35], Figure 10.21. By changing the substituents on the rings one could influence the rate of reaction, the molecular weight and the isotacticity. This has not been analysed in detail yet, but it is to be expected that the effects we have discussed above can explain these exciting results. Thus, for instance the position of the growing chain can be such that β-hydride elimination is retarded in one case and thus higher molecular weights are obtained. Likewise 2,1 insertion can be lower in certain catalysts and thus a higher active and more selective catalyst is obtained. Most interestingly, the three properties of importance, rate, molecular weight, and isotacticity can reach the highest values in one and the same catalyst! The “response” of these

systems to the presence of dihydrogen has not been reported and we must refrain from detailed explanations.

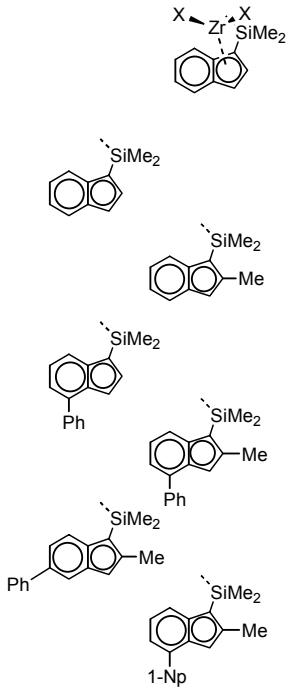

	rate	mol-weight	tacticity
	kg PP. mmol^{-1} Zr.h^{-1}	MW. 10^{-3}	% mmmm
	190	36	82
	99	195	88
	48	42	86
	775	729	95
	63	188	78
	875	920	99.1

Figure 10.21. Influence of substituents on zirconium catalysts (Spaleck, [35])

Many of the older bis-indenyl catalysts are less selective at higher temperatures, which was ascribed initially to a lower selectivity of the insertion reaction itself. More recent work by Busico, based on deuteration studies and again based on very detailed and elegant analysis of ^{13}C NMR spectra of the polymers, has shown that in fact epimerisation of the growing alkyl chain occurs via a series of β-hydride eliminations and re-insertion reactions [36] involving even tertiary alkyl zirconium species.

If this is the case and if the rate of polymerisation increases with the propene concentration, the latter influences the tacticity.

The use of deuterium labels in propene can help to establish the epimerisation of the intermediate alkyl species.

Constrained geometry catalysts. One of the very few applications of metallocene or single site catalysts at this moment (2003) involves the so-called constrained geometry catalyst, developed by Dow. It is a titanium complex containing only one cyclopentadienyl ring and a small amido ligand, thus creating a very open site (Figure 10.22) [37]. The ligand was first reported by

Bercaw and Okuda [37]. The catalyst is used for the copolymerisation of ethene and 1-octene, giving long-branched polyethylene, which has attractive polymer properties: narrow MWD, high conversion, no extractables, good blending, easy processing, and more! The narrow molecular weight distribution is typical of well-behaved, homogeneous catalysts. The high conversion means that the catalyst is stable at the high temperature used (>130 °C). It is a high temperature solution process with much shorter residence times than the gas-phase process. "No extractables" means that the lower molecular weight products insert into growing polymer chains, which makes sense because also octene-1 is efficiently inserted. The easy processing is caused by the long chain branching; branching leads to less entanglements in spite of the high molecular weight.

Ultra-High-Molecular-Weight PE is difficult to synthesize (since chain transfer must be almost entirely suppressed) and thus for these extremely strong materials other catalysts are needed. Figure 10.22 shows the Dow catalyst based on titanium(IV) and a competing catalyst developed by DSM based on titanium(III).

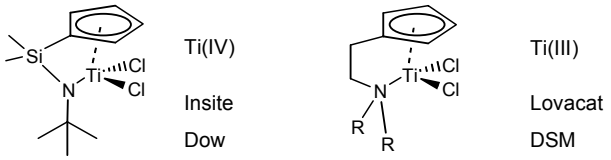

Figure 10.22. Dow's constrained geometry catalyst "Insite" and DSM's "Lovacat"

Syndiotactic Polystyrene. Syndiotactic polystyrene is an interesting material because it has a T_g of 95 °C and a T_m of 260 °C [38]. Polystyrene made via radical polymerisation may show some syndiotacticity, but its heat distortion temperature is too low to allow its use in important applications requiring temperatures around 120 °C or higher, such as medical equipment which requires sterilization or hot water storage containers. Idemitsu and Dow have reported titanium-based catalysts such as the one shown in Figure 10.23. We presume that the mechanism is a chain-end controlled "2,1" insertion.

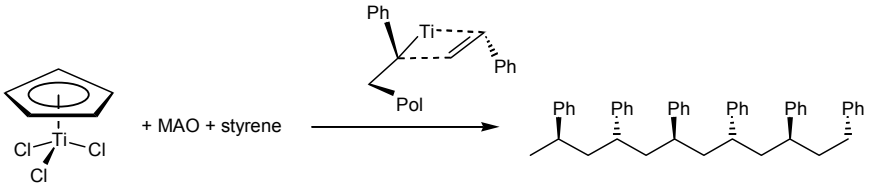

Figure 10.23. Syndiotactic, chain-end controlled polystyrene catalyst

Syndiotactic and Cossée type isotactic PP. Bercaw et al. [39] designed a catalyst that has C_s symmetry and indeed gives syndiotactic polypropene (Figure 10.24, left-hand side structure). Clearly, like the catalyst by Ewen (Figure 10.15, fluorenyl-cyclopentadienyl), the C_s catalyst leads to syndiotactic polypropene as by virtue of the symmetry each insertion on the left or right hand side is one anothers mirror image and thus leads to alternatingly R and S absolute configurations at the saturated carbon atom formed.

Interestingly, the analog shown on the right-hand side, carrying a large chiral group at the central carbon atom in the front of the molecule, leads to a predominantly isotactic polymer molecule. This catalyst has C_1 symmetry. The explanation is that after each insertion the growing polymer chain moves to the sterically less encumbered side of the complex. Thus, the insertion takes place such that each time the same absolute chiral conformation is produced, i.e. an isotactic polymer is obtained. This is a model for the initial Cossée proposal for the mechanism for making isotactic polymer; he also suggested that a "back skip" of the polymer chain was necessary to make sure that the next propene molecule would feel the same environment as the previous one thus giving isotacticity.

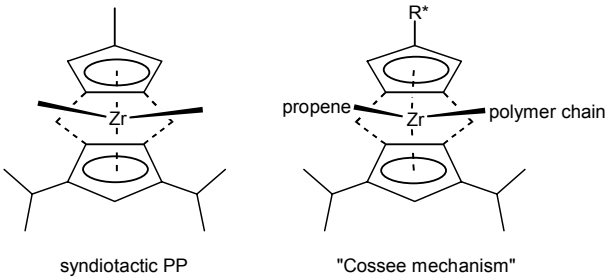

Figure 10.24. Bercaw catalysts for syndiotactic polymer and isotatic polymer

Alternating block polymers of PP. Let's have a look at the two catalyst precursors shown in Figure 10.25. The left-hand one is a complex possessing C_2 symmetry, which should give isotactic PP in the propene polymerisation, since by enantiomorphic site control this gives rise to isotactic polymer. Likewise, the isomer shown on the right-hand side, should give atactic polymer because it has C_s symmetry. Interestingly, the two isomers can interconvert via a rotation type mechanism and in this particular case the isomerising rotation is slower than the rate of polymerisation. Thus, the catalyst will produce for some time an atactic polymer and then switch to the other isomer and produce the isotactic polymer. Atactic and isotactic blocks will form. As a polymer this will have properties (essentially an elastomer) distinct from those of regular *syndio*

or *isotactic* nature, thus illustrating the power of the design component in these new homogeneous catalysts [40].

"Site isomerisation" also occurs in heterogeneous systems [41]. A certain blockiness of the polymer tells us that this phenomenom is taking place.

When the rate of polymerisation is dependent on the propene concentration, but site isomerisation is not, the concentration of propene effects the properties of the polymer. A faster polymerisation will lead to a higher stereospecificity in the polymer.

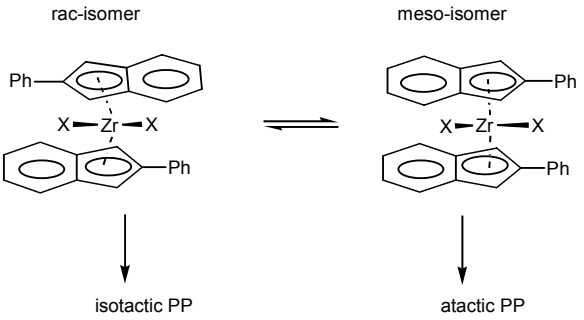

Figure 10.25. Waymouth's catalyst giving blocks of atactic and isotactic polymer

Norbornene-ethene copolymers. In 1996 Ticona (Mitsui and the former Hoechst) announced the commercial production of copolymers of norbornene and ethene using titanium metallocene catalysts (Figure 10.26). The new material was called Topas™ and was meant for optical applications. It is a random copolymerisation and several grades can be obtained [42]. Many attempts have been made to obtain a perfectly alternating material (also using palladium and nickel catalysts) as this material has a good balance of properties (other than being rather brittle) finding application in CD-roms and the like.

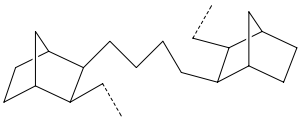

Figure 10.26. Norbornene-ethene "Topas" polymers

10.8 Non-metallocene ETM catalysts

Substituted cyclopentadienyl ligands are extremely effective for a variety of polymerisation reactions, but they are not unique. Both from a point of view of scientific interest and from a patent point of view, in attempts to acquire one's

own position, numerous other anionic ligands have been screened and found to give active catalysts for polymerisation reactions. Complexes of titanium and zirconium containing phenoxides, amides, and many other anions have been discovered that are active catalysts [43]. An important example are the so-called FI catalysts developed by Fujita and co-workers at Mitsui Chemicals [44]. FI stands for Fenokishi-Imin, Japanese for phenol-imine, or Fujita group Invented! It is an example of a successful "transfer" of a ligand system from late transition metal catalysis, more in particular Group 10 metals, to Group 4 metal complexes. A common feature of many ligands important in alkene polymerisation catalysts of nickel is that they are *cis* bidentates and carry one minus charge, see for example the SHOP ligand (Chapter 9), which is the first one of this type that was discovered and applied. In nickel catalysis, taking place in the square plane, only one ligand is needed, but for group 4 metals we need two, both to make up the charge and to occupy four of the six coordination sites in an octahedral complex. The two remaining sites are for the growing chain and alkene coordination, and an overall plus one charge is obtained. A typical FI catalyst precursor is shown in Figure 10.27.

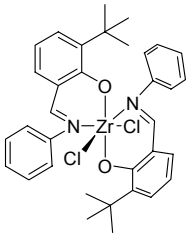

Figure 10.27. Example of FI catalyst

Phenol-imines are easy to prepare and many ligands have been tested. The dichloride precursors can be converted into the active species in the usual way as reported for metallocene catalysts. Astonishingly high turnover numbers were measured for ethene polymerisation, 65,000 s^{-1} bar^{-1}. Titanium catalysts containing fluorinated aryl groups give a living polymerisation of ethene with $M_n > 400{,}000$ and a polydispersity $M_w/M_n < 1.2$. Propene as the substrate leads to monodisperse, *syndiotactic* polypropylene, with *rr* diads up to 98%. The syndiotactic nature is peculiar as the catalyst precursor has C_2 symmetry. The mechanism implies a 2,1 insertion and chain-end control. Six-membered rings containing a metal ion (titanium in this instance) are not flat and it is thought that perhaps dynamic ring isomerisation plays a role in the enhancement of the syndiospecific reaction. Because of its living character one can also make block copolymers of ethene and propene. Also products of lower molecular weight can be produced.

10.9 Late transition metal catalysts

In the last decade an enormous revival of late transition catalysts for the polymerisation of alkenes has taken place [45] (remember that the first discovery of Ziegler for ethene polymerisation also concerned *nickel* and not titanium). The development of these catalysts is due to Brookhart in collaboration with DuPont (Figure 10.28) [46]. Detailed low-temperature NMR studies have revealed the mechanism of the reaction [47]. Interestingly, the resting state of the catalyst is the ethene-metal-alkyl complex and not the metal-alkyl complex as is the case for the ETM catalysts. For ETM catalysts the alkene complex intermediates are never observed. Thus, the migratory insertion is the rate-determining step (the "turnover limiting step", in Brookhart's words) and the reaction rate is independent of the ethene concentration.

Increased steric bulk of the diimine aryl substituents leads to faster reactions! This is because the ground state of the resting state is destabilised relative to the transition state and the barrier to insertion thus becomes lower.

Another typical feature of these catalysts is the socalled "chain walking". Prior to insertion of the next ethene molecule a series of β-hydride elimination and re-insertions can take place, which looks like a metal atom running along the chain. Insertion of ethene in a secondary alkyl chain leads to the formation of branches. During the isomerisation process palladium can even cross tertiary carbon atoms, since "branches on branches" are obtained.

When the ethene pressure is raised the number of branches decreases, while the productivity of the catalyst remains the same (the reaction is zero order in ethene pressure). Chain walking requires an open site at the metal and obviously the competition between ethene complexation and chain walking determines the number of branches formed.

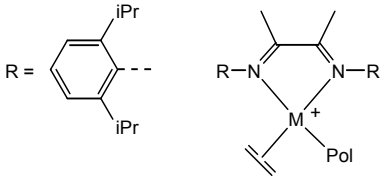

Figure 10.28. Brookhart's ethene polymerisation catalysts, M=Pd, Ni

Highly branched ethene-methyl acrylate polymers. The cationic palladium diimine complexes are remarkably tolerant towards functional groups, although the rates decrease somewhat when polar molecules are added. In ETM catalysis addition of polar molecules or monomers kills the catalyst and therefore it was very interesting to see what the new palladium catalysts would do in the presence of polar monomers. Indeed, using methyl acrylate a copolymerisation

is obtained [48], but the methyl acrylate molecules are not incorporated in the chain. Instead they form the terminals of the branches (Figure 10.29). After insertion of an acrylate no insertion of ethene or acrylate occurs due to the relative stability of this species. Chain walking occurs and insertion takes place at the secondary alkyl formed.

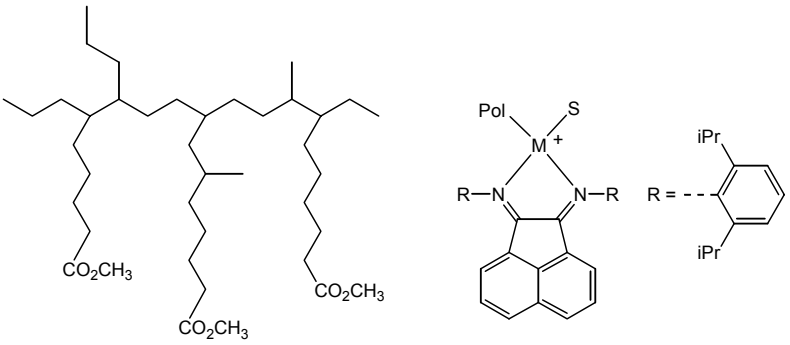

Figure 10.29. Ethene-acrylate copolymers and the catalyst, M=Pd, Ni

Du Pont has published a huge number of compounds and polymerisation reactions in a series of patents. The commercialisation is being actively pursued [46].

Tridentate ligands for cobalt and iron catalysts. The catalysts discussed earlier in the section on ethene oligomerisation can also be used for making polymers, provided that they are suitably substituted. In Figure 10.30 we have depicted such a catalyst, substituted with isopropyl groups at the aryl substituents on the imine group, as in Brookhart's catalysts [49]. The initiation is now carried out by the addition of MAO to a salt of the cobalt or iron complexes. The catalysts obtained are extremely active, but they cannot be used for polar substrates.

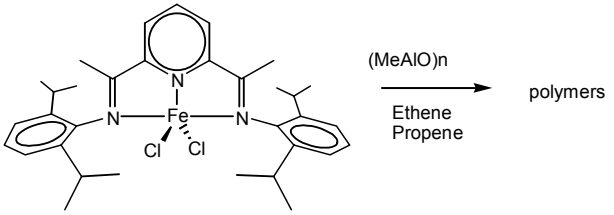

Figure 10.30. New iron catalyst for ethene polymerisation

Norbornene high-value added polymers

As said in the introduction there are many more polymers than can be discussed within the limits of this chapter, but we want to add just one example of a group of high-value polymers that is made using the same principles of coordination polymerisation as shown above for the commodity polymers. We mentioned metallocene catalysts that can be used to copolymerise ethene and norbornene to give Topas™ type products.

One can imagine that homopolymers of norbornene can lead to a variety of stereoregularities and we have drawn a few in Figure 10.31 to give an impression without the intention of being exhaustive and neglecting the nomenclature.

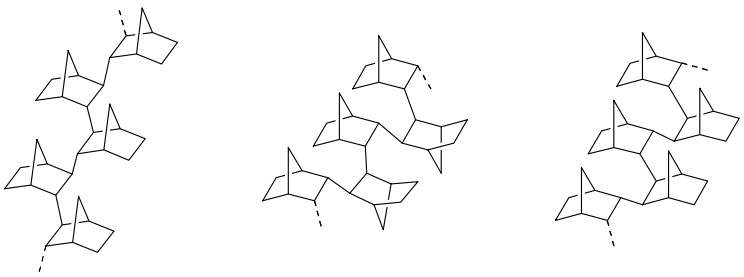

Figure 10.31. Examples of stereoregular homopolymers of norbornene

Following pioneering work by Sen [50] and Risse [51] in the 1980's, B.F. Goodrich launched a new family of amorphous norbornene-based polymers aimed at a number of microelectronic applications. The polymers are high-priced specialties (up to €6,000 per kg). These new polymers were made possible by a breakthrough in the area of single component catalysts based on Group 10 (Ni and Pd) transition metals [52]. These catalysts are characterised by their ability to:

- Produce norbornene homopolymers having ultra-high glass transition temperatures (Tg = 355-390 °C) that can be tailored by copolymerization with 5-alkylnorbornenes.
- Produce polymers with molecular weights exceeding 2,000,000 down to oligomers by a chain transfer mechanism with 1–alkenes.
- Polymerise and copolymerise norbornenes bearing functionality (carboxylic acid esters, ethers, anhydrides, etc.).

Each of these polymers exploit the ability of the group 10 metal catalysts used to tolerate functional groups and to copolymerise norbornene monomers bearing esters etc. into the polymer backbone. In the case of low-k dielectric polymers (Avatrel™) low levels (2-10 mol %) of 5-triethoxysilylnorbornene are used to impart good adhesive properties, the remaining 90+% of the monomer being a 5-alkylnorbornene. The alkylnorbornene is selected to tailor

the glass transition temperature of the polymer and to impart toughness into the product. Other polymers concern optical applications such as wave-guides and photolithographic applications, primarily deep UV (193 nm) positive photo-resists. A variety of substituted norbornenes is easily accessible via well known Diels-Alder additions of functionalised alkenes to cyclopentadiene.

The catalyst is a simple "naked" divalent palladium or nickel complex, containing no other ligands than alkenes (Figure 10.32). Both give extremely fast polymerisations of norbornenes, nickel usually being the fastest catalyst. They give different microstructured polymers as can be deduced from the ^{13}C and ^{1}H NMR spectra. Molecular weights are high, because a β-hydride elimination is not feasible in the rigid metal-alkyl structure. The molecular weight can be lowered by adding 1-decene, as after insertion of a linear alkene β-hydride elimination can take place.

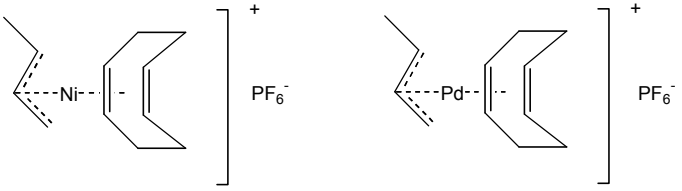

Figure 10.32. Typical "naked" nickel and palladium catalysts

The glass transition temperature in the polymer containing a few percent of 5-triethoxysilanenorbornene for dielectric applications can be lowered by increasing the amount of 5-decylnorbornene (see Figure 10.33).

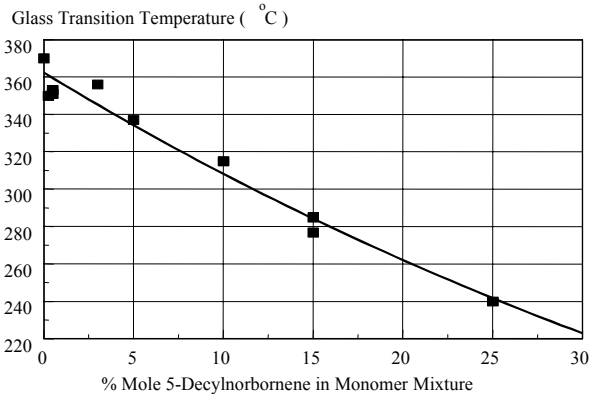

Figure 10.33. Effect of polymer composition on glass transition temperature

References

1 *Ziegler Catalysts*. Fink, G., Mülhaupt, R., Brintzinger, H. H., Eds.; Springer: Berlin, **1995**.
2 Challa, G. *Polymer Chemistry, an Introduction.* Ellis Horwood series in Polymer Science, Kemp, T. J.; Kennedy, J. F. Eds. **1993,** New York.
3 McMillan, F. M. *The Chain Straighteners: Fruitful Innovation. The Discovery of Linear and Stereoregular Polymers*. **1981**, The Macmillan Press Ltd. London, U.K.
4 van der Ven, S. "Polypropylene and other polyolefins: polymerization and characterization", Elsevier Science Publishers, New York, **1990**.
5 Goodall, B. L. "Polypropylene: Catalysts and Polymerization Aspects" in [3], Chapter 1, p. 1-125.
6 Cossée, P. *J. Catal.* **1964***, 3*, 80. Arlman, E. J. *J. Catal.* **1964***, 3*, 89. Arlman, E. J.; Cossée, P. *J. Catal.* **1964***, 3*, 99.
7 Allegra, G. *Makrom. Chem.* **1971**, *145,* 235.
8 Breslow, D. S.; Newburg, N. R. *J. Am. Chem. Soc.* **1957***, 82*, 5072.
9 Reichert, K. H.; Meyer, K. R. *Makromol. Chem.,* **1973***, 169*, 163.
10 Long, W. P.; Breslow, D. S. *Justus Leibigs Ann. Chem*., **1975**, 463.
11 Sinn, H.; Kaminsky, W.; Volmer H.-J.; Woldt, R. *Angew. Chem., Int. Ed. Engl.* **1980***, 19,* 390.
12 Sinn H.; Kaminsky, W. *Adv. Organometal. Chem.* **1980***, 18*, 99.
13 Ewen, J. A. *J. Am. Chem.Soc.* **1984***, 106,* 6355.
14 Wild, F. R. W. P.; Zsolnai, L.; Huttner, G.; Brintzinger, H. H. *J. Organomet. Chem.* **1982***, 232,* 233.
15 Kaminsky, W.; Külper, K.; Wild, F. R. W. P.; Brintzinger, H. H. *Angew. Chem. Int. Ed. Engl.* **1985***, 24*, 507.
16 Ewen, J. A. *J. Am. Chem. Soc.* **1988***, 110*, 6255.
17 Jordan, R. F.; LaPointe, R. E.; Bajgur, C. S.; Echols, S. F.; Willett, R. J. Am. Chem. Soc., 1987, 109, 4111. Hlatky, G. G.; Turner, H.W.; Eckman, R. R. *J. Am. Chem. Soc.,* **1989***, 111*, 2728.
18 Ewen, J. A.; Elder, M. J.; Jones, R. L.; Haspeslagh, L.; Atwood, J. L.; Bott, S. G.; Robinson, K. *Makrom. Chem., Makrom. Symp.,* **1991**, *48/49*, 253.
19 Erker, G.; Nolte, R.; Aul, R.; Wilker, S.; Krüger, C.; Noe, R. *J. Am. Chem. Soc.,* **1991***, 113,* 7594.
20 Takegami, Y.; Suzuki, T. *Bull. Chem. Soc. Jpn.* **1969**, *42,* 848. Zambelli, A.; Natta G.; Pasquon, I. *J. Polymer Sci.,* **1963**, *C4,* 411. Doi, Y.; Suzuki, S.; Nozawa, F.; Soga, K.; Keii, T. in "Catalytic Polymerization of Olefins", Keii, T.; Soga, K. Eds., Kodanska, Tokyo (**1998**) p 439.
21 Corradini, P.; Busico, V.; Cavallo, L.; Guerra, G.; Vacatello M.; Venditto, V. *J. Mol. Catal.* **1992**, *74,* 433.
22 Kaminsky, W.; Külper, K.; Wild F. R. W. P.; Brintzinger, H. H. *Angew. Chem. Int. Ed. Engl.* **1985**, *24*, 507.
23 Mise, T.; Miya S.; Yamazaki, H. *Chem. Lett.* **1989**, 1853.
24 Jordan, R. F.; LaPointe, R. E.; Bajgur, C. S.; Echols, S. F.; Willett, R. *J. Am. Chem. Soc.* **1987**, *109,* 4111.
25 Bondar, G. V.; Aldea, R.; Levy, C. J.; Jaquith, J. B.; Collins, S. *Organometallics* **2000***, 19*, 947.
26 Corradini, P.; Guerra, G.; Vacatello M.; Villani, V. *Gazz. Chim. Ital.* 1988, **118,** 173. Waymouth, R.; Pino, P. *J. Am. Chem. Soc.,* 1990, *112,* 4911.
27 Cavallo, L. Guerra, G.; Vacatello, M.; Corradini, P. *Macromolecules,* **1991**, *24,* 1748.

Cavallo, L.; Guerra, G.; Oliva, L.; Vacatello, M.; Corradini, P. *Polym. Commun.,* **1989**, *30,* 17.
28 Sacchi, M. C.; Barsties, E.; Tritto, I.; Locatelli, P.; Brintziger, H. H.; Stehling, U. *Macromolecules,* **1997**, *30*, 3955.
29 *Chem. Rev*. **2000**, *100*, Frontiers In Metal-Catalyzed Polymerization, Gladysz, J. A. Ed. issue nr 4, pp. 1167-1682.
30 Piers, W. E.; Bercaw, J. E. *J. Am. Chem. Soc.* **1990***, 112,* 9406. Krauledat, H.; Brintzinger, H. H. *Angew. Chem., Int. Ed. Engl.* **1990***, 29*, 1412. Grubbs, R. H.; Coates, G. W. *Acc. Chem. Res*. **1996***, 29*, 85.
31 Ivin, K. J.; Rooney, J. J.; Stewart, C. D.; Green, M. L. H.; Mahtab, R. *J. Chem. Soc. Chem. Commun.* **1978**, 604.
32 Chadwick, J. C.; Miedema A.; Sudmeijer, O. *Macromol. Chem. Phys.* **1994**, *195,* 167. Corradini, P.; Guerra, G.; Vacatello, M.; Villani, V. *Gazz. Chim. Ital*., **1988**, *118*, 173. Busico, V.; Cipullo, R.; Chadwick, J. C.; Modder J. F., Sudmeijer, O. *Macromolecules,* **1994**, *27*, 7538.
33 Busico, V.; Cipullo, R. Corradini, P. *Makromol. Chem., Rapid Commun.* **1992**, *13,* 15.
34 Kaminsky, W.; Beulich, I.; Arndt-Rosenau, M. *Macromol. Symp.* **2001***, 173*, 211.
35 Spaleck, W.; Küber, F.; Winter, A.; Rohrmana, J.; Bachmann, B.; Antberg, M.; Dolle, V.; Paulus, E. F. *Organometallics,* **1994**, *13*, 954. Toto, M.; Cavallo, L.; Corradini, P.; Moscardi, G.; Resconi, L.; Guerra, G. *Macromolecules,* **1998**, *31*, 3431.
36 Busico, V.; Brita, D.; Caporaso, L.; Cipullo, R.; Vacatello, M. *Macromolecules,* **1997***, 30*, 3971.
37 Shapiro, P. J.; Bunel, E.; Schafer, W. P. *Organometallics,* **1990***, 9*, 867. Okuda, J. *Chem. Ber.* **1990***, 123*, 97. Stevens, J. C.; Timmers, F. J.; Rosen, G. W.; Knight, G. W.; Lai, S. Y. EP 416815 (to Dow) **1991**. Van Beek, J. A. M.; Van Doremaele, G. H. J.; Gruter, G. J. M.; Arts, H. J.; Eggels, G. H. M. R. PCT Int. Appl. WO 9613529 (to DSM) **1996**. *Chem. Abstr*. **1996**, *125*, 435053.
38 Ishihara, N.; Seimiya, T.; Kuramoto, M.; Uoi, M. *Macromolecules* **1986***, 19*, 2464. Tomotsu, N.; Ishihara, N.; Newman, T. H.; Malanga, M. T. *J. Mol. Catal. A: Chem.* **1998***, 128,* 167.
39 Herzog, T. A.; Zubris, D. L.; Bercaw, J. E.; *J. Am. Chem. Soc.* **1996**, *118,* 11988.
40 Brintzinger, H. H.; Fischer, D.; Mulhaupt, R.; Rieger, B.; Waymouth, R. M. *Angew. Chem. Intl. Ed. Engl.* **1995***, 34*, 1143. Waymouth, R. *Science* **1995***, 267*, 217.
41 Chadwick, J. C. *Macromolecular Symposia,* **2001***, 173*, 21 and references therein, especially V. Busico.
42 Data sheets concerning Topas from Hoechst. 9. Cherdron, H.; Brekner, M-J.; Osan, F. *Angew. Makromol. Chem.* **1994***, 223*, 121.
43 Van de Linden, A.; Schaverien, C. J.; Meijboom, N.; Ganter, C.; Orpen, A. G. *J. Am. Chem. Soc.* **1995***, 117*, 3008. Capachione, C.; Proto, A.; Ebeling, H.; Mülhaupt, R.; Möller, K.; Spaniol, T. P.; Okuda, J. *J. Am. Chem. Soc.* **2003,** *125,* 4964.
44 Matsui, S.; Fujita, T. *Catal. Today,* **2001***, 66,* 63. Makio, H.; Kashiwa, N.; Fujita, T. *Adv. Synth. Catal.* **2002***, 344*, 477.
45 *Late Transition Metal Polymerization Catalysis*. Rieger, B.; Saunders, L.; Kacker, S.; Striegler, S.; Eds. **2003**, Wiley-VCH Verlag GmbH, Weinheim, Germany.
46 Johnson, L. K.; Killian, C. M.; Brookhart, M. *J. Am. Chem. Soc.* **1995***, 117,* 6414. Ittel, S. D.; Johnson, L. K.; Brookhart, M. *Chem Rev.* **2000***, 100*, 1169.
47 Svejda, S. A.; Johnson, L. K.; Brookhart, M. *J. Am. Chem. Soc.* **1999***, 121,* 10634.
48 Johnson, L. K.; Mecking, S.; Brookhart, M. *J. Am. Chem. Soc.* **1996***, 118*, 267. Mecking, S.; Johnson, L. K.; Wang, L.; Brookhart, M. *J. Am. Chem. Soc.* **1998***, 120,* 888.

49 Britovsek, G. J. P.; Gibson, V. C.; Mastroianni, S.; Oakes, D. C. H.; Redshaw, C.; Solan, G. A.; White, A. J. P.; Williams, D. J. *Eur. J. Inor. Chem.* **2001**, 431. Britovsek, G. J. P.; Bruce, M.; Gibson, V. C.; Kimberley, B. S.; Maddox, P. J.; Mastroianni, S.; McTavish, S. J.; Redshaw, C.; Solan, G. A.; Stromberg, S.; White, A. J. P.; Williams, D. J. *J. Am. Chem. Soc.* **1999***, 121*, 8728. Small, B. L.; Brookhart, M. *Macromolecules,* **1999***, 32,* 2120. Mecking, S. *Angew. Chem. Int. Ed.* **2001***, 40*, 534.

50 Sen, A.; Lai, T. W. *Organometallics,* **1982***, 1,* 415. Sen, A.; Lai, T. W.; Thomas, R. R. *J. Organomet. Chem.* **1988***, 358*, 567.

51 Mehler, C.; Risse, W. *Makromol. Chem., Rapid Commun.* **1991***, 12*, 255. Seehof, N.; Mehler, C.; Breunig, S.; Risse, W. *J. Mol. Catal.,* **1992***, 76*, 219.

52 Goodall, B. L.; Benedikt, G. M.; McIntosh, L. H. III; Barnes, D. A. Rhodes, L. F. *Proc. Am. Chem. Soc. Div. Polym. Mat.: Sci. Eng.,* **1997***, 75*, 56. Goodall, B. L.; Benedikt, G. M.; Jayaraman, S.; McIntosh, L. H. III; Barnes, D. A. Rhodes, L. F.; Shick, R. A. *Polym. Prep., Am. Chem. Soc. Div. Polym. Chem.* **1998***, 39*, 216. Goodall, B. L. Encyclopedia of Materials: Science and Technology, Elsevier Science Ltd., **2001**, 1959-1963. Barnes, D.A.; Benedikt, G. M.; Goodall, B. L.; Huang, S. S.; Kalamarides, H. A.; Lenhard, S.; McIntosh, L. H.; Selvy, K. T.; Shick, R. A.; Rhodes, L. F. *Macromolecules*, **2003**, *36*, 2623. Goodall, B. L.; Benedikt, G. M.; Mcintosh, L. H., III; Barnes, D. A.; Rhodes, L. F. (to B. F. Goodrich Company) **1996**, USP 5,569,730. *Chem. Abstr.* **1996***, 125*, 701934.

Chapter 11

HYDROCYANATION OF ALKENES

The early days of steric and electronic effects

11.1 The adiponitrile process

The transition metal catalysed addition of HCN to alkenes is potentially a very useful reaction in organic synthesis and it certainly would have been more widely applied in the laboratory if its attraction were not largely offset by the toxicity of HCN. Industrially the difficulties can be minimised to an acceptable level and we are not aware of major accidents. DuPont has commercialised the addition of HCN to butadiene for the production of adiponitrile [ADN, $NC(CH_2)_4CN$], a precursor to 1,6-hexanediamine, one of the components of 6,6-nylon and polyurethanes (after reaction with diisocyanates). The details of the hydrocyanation process have not been released, but a substantial amount of related basic chemistry has been published. The development of the ligand parameters χ and θ by Tolman formed part of the basic studies carried out in the Du Pont labs related to the ADN process [1].

Addition of HCN to acetone to form the cyanohydrin is still the main route to methyl methacrylate. Hydrocyanins can be converted to amino acids as well. The nitrile group can be easily converted to amines, carboxylic acids, amides, etc. Addition to aldehydes and activated alkenes can be done with simple base, but addition to unactivated alkenes requires a transition metal catalyst. The methods of HCN addition have been discussed by Brown [2].

First we will describe the hydrocyanation of ethene as a model substrate. The catalyst precursor is a nickel(0) tetrakis(phosphite) complex which is protonated to form a nickel(II) hydride. Actually, this is an oxidative addition of HCN to nickel zero. In Figure 11.1 the hydrocyanation mechanism in a simplified form is given: the basic steps are the same as for butadiene, the actual substrate, but the complications due to isomer formation are lacking.

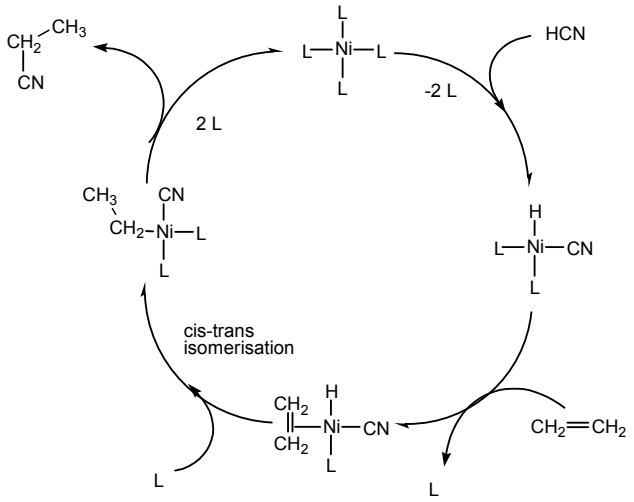

Figure 11.1. Simplified scheme for hydrocyanation

The basic steps are well known: after oxidative addition of HCN, we find coordination of ethene, migratory insertion of ethene into the nickel hydride bond, and reductive elimination of ethyl cyanide (propanenitrile). More detailed studies by Du Pont's McKinney and Roe [3] have shown that the productive cycle involves the reductive elimination by the process shown in Figure 11.2.

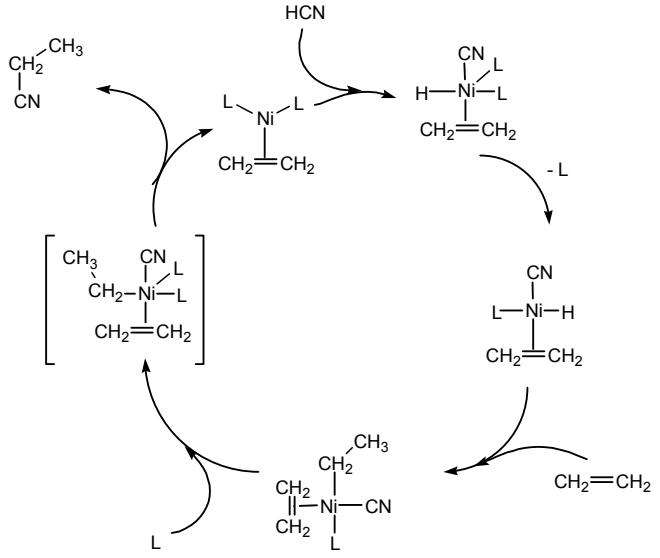

Figure 11.2. The mechanism found by McKinney

Reductive elimination takes place after association of an electron-withdrawing phosphite ligand with the nickel ethyl cyanide complex. The cycle of Figure 11.1 is not productive, at least under the conditions that were studied. Association of this type is not uncommon and has been observed in more instances; an electron-withdrawing ligand accelerates the reductive elimination (see below). Figure 11.2 presents the scheme according to the findings of Roe and McKinney. The intermediate observed at –40 °C by ^{1}H, ^{31}P, and ^{13}C NMR spectroscopy is $(C_2H_4)L(CN)(C_2H_5)Ni$ (L=P(O-o-tolyl)$_3$). This intermediate reacts with L in a rate-determining step to produce propanenitrile and $(C_2H_4)L_2Ni$ which oxidatively adds HCN and regenerates the intermediate. The five-coordinate species drawn in brackets in Figure 11.2 was not observed directly, but the kinetics indicated that the process is first order in the four-coordinate complex and first order in the concentration of free ligand.

When a large excess of ligand is used, as in the actual process, the system becomes more complicated and species such as $(C_2H_4)L_3Ni$, $HNi(CN)L_3$, and NiL_4 are also observed. The activation parameters of the reaction are: $\Delta G^{\#}$(–40 °C)= 17 kcal/mol, $\Delta H^{\#}$= 9 kcal.mol^{-1}, $\Delta S^{\#}$= –34 cal.mol^{-1}.K^{-1}. The negative entropy of activation is consistent with the formation of a five-coordinate species. The reason for the associative character of the reductive elimination is two-fold:

1. the addition of one more phosphite ligand reduces the electron density at nickel disfavouring the divalent state, and
2. the resulting species after elimination will contain 14 electrons instead of only 12 which leads to a higher stability.

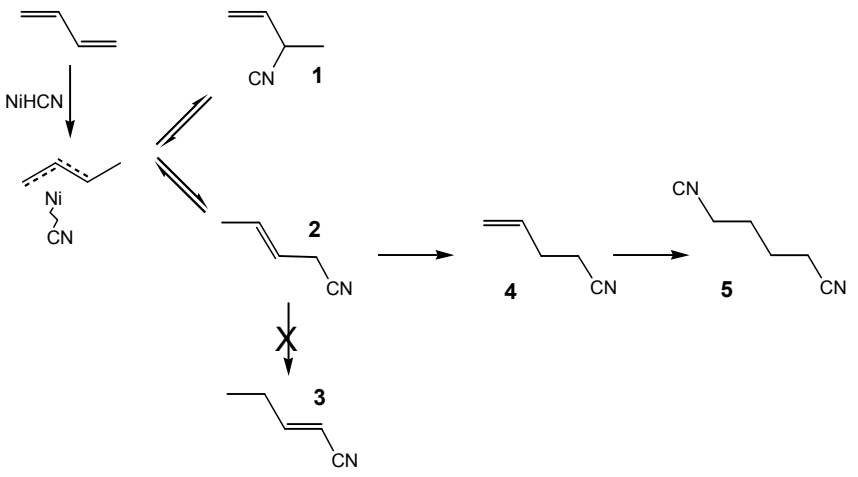

Figure 11.3. Hydrocyanation of butadiene

For example, reductive elimination of benzonitrile from $(Et_3P)_2Pd(CN)Ph$ is promoted by the addition of triethyl phosphite [4], addition of benzoquinone promotes reductive eliminations in palladium chemistry (Chapter 12), etc., but in all cases different roles can be envisaged, such as simple ligand exchange.

Hydrocyanation of butadiene is more complicated than that of ethene; it requires two hydrocyanation steps and several isomers can be observed. The isomers obtained in the first step of the HCN addition to butadiene are shown in Figure 11.3. The addition first leads to compounds **1** and **2**, in a 1:2 ratio, but they equilibrate to a favourable 1:9 ratio via the retro-reaction. The retro reaction involves a C-C bond breaking reaction, which is rare, but in this case the intermediate is a π-allyl species and a stable, anionic cyanide group. Electron-rich nickel species (Ni-dippe) can cleave aromatic nitrile C-C bonds [5].

In order to obtain adiponitrile, **2** should isomerize to **4**, and not to the thermodynamically more stable **3** (stabilised by the energy of conjugation). The thermodynamic ratio is **2**:**3**:**4** = 20:78:1.6 [6]. The isomerization of **2** to **4** happens to be favorably controlled by the kinetics of the reactions; the reaction **2** to **4** reaches equilibrium, but the reaction **2** to **3** does not. Note that the nickel complex not only is responsible for the addition of HCN but that it is also capable of catalysing selectively the isomerisation. The final step is the addition of HCN to **4** to give **5**, adiponitrile.

Often Lewis acids are added to the system as a cocatalyst. It could be envisaged that Lewis acids enhance the cationic nature of the nickel species and increase the rate of reductive elimination. Indeed, the Lewis acidity mainly determines the activity of the catalyst. It may influence the regioselectivity of the catalyst in such a way as to give more linear product, but this seems not to be the case. Lewis acids are particularly important in the addition of the second molecule of HCN to molecules **2** and **4**. Stoichiometrically, Lewis acids (boron compounds, triethyl aluminium) accelerate reductive elimination of RCN ($R=CH_2Si(CH_3)_3$) from palladium complexes $P_2Pd(R)(CN)$ (P_2= e.g. dppp) [7]. This may involve complexation of the Lewis acid to the cyanide anion, thus decreasing the electron density at the metal and accelerating the reductive elimination.

It was found [8] that the Lewis acidity plays only a minor role in the regioselectivity when $R_3Sn^+SbF_6^-$ Lewis acids were used, and that sterically more bulky Lewis acids strongly favour the formation of adiponitrile. This was also found for another series of Lewis acids: $B(C_6H_5)_3$, 96%; $ZnCl_2$, 82%; $AlCl_3$, 50%. When the steric bulk around the nickel complex increases the coordination of 4-pentenenitrile is preferred to coordination of 3-pentenenitrile, and secondly, as in hydroformylation with PPh_3 (Union Carbide system), the formation of a linear alkyl from 4-pentenenitrile is more favourable than the

formation of the branched alkyl species. This steric effect has also been reported for the hydrocyanation of propene by Druliner et al. [9].

Catalyst decomposition. When the reaction is carried out in the laboratory decomposition of the catalyst is observed, which leads to nickel(II) formation. It can be suppressed by adding the HCN needed step-wise and not all at once at the beginning of the reaction [10].

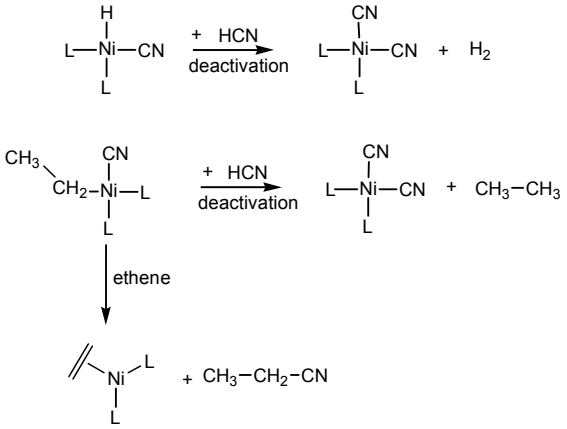

Figure 11.4. Catalyst deactivation

Deactivation can take place if the intermediate hydride or alkyl species react with HCN. The result is the formation of nickel dicyanides, which cannot be reconverted to active species. We think that Lewis acids, in addition to promoting reductive elimination, may also have a retarding effect on this reaction, see Figure 11.4, as a more positively charged nickel species will react more slowly with protons. On the other hand, though, stronger acids are formed as a result of the interaction of HCN with the Lewis acids.

11.2 Ligand effects

From the above model studies we concluded that the reductive elimination is the slow step in the process. It was thought until recently that only phosphites lead to active catalysts and even today very few phosphines have been reported as ligands, which supports the mechanistic studies. Reductive elimination can be promoted by the use of ligands that stabilise the zero-valent state of the metal. In this instance that means phosphorus ligands having high χ-values. That is why phosphites are better ligands than phosphines. We can use phosphites having higher χ-values than aryl phosphites, viz. fluoro-substituted alkyl phosphites. This does indeed lead to faster catalysts [11].

Another approach would be destabilisation of the square-planar geometry of the divalent state and stabilisation of the tetrahedral geometry of the zerovalent state by means of the bite angle. The ligands shown in Figs. 8.10 and 11.5 fulfil this requirement. The large natural bite angle of 110–120° will enhance the reductive elimination. Indeed, even diphosphines having large bite angles can provide active catalysts [10], see Fig. 11.5. Electron withdrawing groups further enhance the reactivity in the wide bite angle ligands [12].

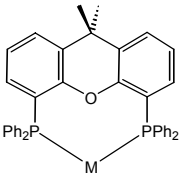

Figure 11.5. Ligands with large bite angles promoting reductive elimination in nickel and palladium complexes.

Diphosphites containing aryl groups and having wide bite angles combine the two effects and they provide good catalysts [13]. Chiral diphosphinites based on glucose backbones gave active catalysts [14]. The ligands used in this study by RajanBabu are shown in Figure 11.6. The substrates were styrene and other vinyl aromatics (Fig.11.7). The products of these reactions are precursors for the anti-inflammatory drugs of the naproxen and ibuprofen type.

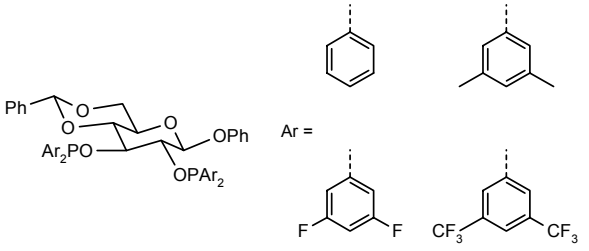

Figure 11.6. Diphosphinite ligands for asymmetric hydrocyanation [14]

The enantioselectivity increases dramatically when the ligands contain electron-withdrawing P-aryl substituents. Electron-donating substituents on the substrate give the highest ee (91% for 6-methoxy-2-vinylnaphthalene in apolar solvents). Mechanistic studies at room temperature have shown that at low concentration of HCN nickel zero species are the resting states, but at higher concentrations of HCN η^3-benzyl nickel cyanide species were also observed.

The enantioselectivity is determined in an irreversible step after the chiral atom has been formed. Deuteration experiments have shown that styrene

insertion and deinsertion is reversible under the reaction conditions. Therefore it would seem that the enantioselectivity is determined by the rates of the two reductive eliminations and the concentrations of the two diastereomers. For the faster systems this may change for an enantioselective insertion of styrene.

The diphosphinite ligands containing a four-atom bridge presumably have a wide bite angle, but the clearest example of bite angle effects is that of phosphines, which give no activity when small bite angles are applied. The starting point of this study was that orbital effects of the wide bite angle would accelerate the reductive elimination and indeed the effect of the bite angle was very clear. Figure 11.7 shows a simplified scheme. The reductive elimination can take two routes, either a reaction with HCN or a reaction with styrene. The latter seems more likely and instead of styrene as the electron withdrawing ligand also a second phosphine ligand might add.

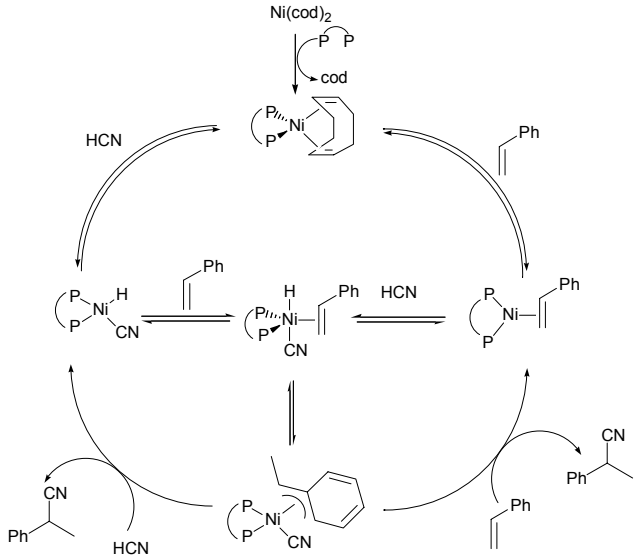

Figure 11.7. Simplified scheme for hydrocyanation of styrene

The results obtained indicate that diphosphines with natural bite angles close to 105º show high activities (Table 11.1). In contrast, when "classical" diphosphine ligands (79º < β < 96º) were used, no activity was detected, and formation of $Ni(P–P)(CN)_2$ was observed. The strong "peaking" at bite angles around 105° might involve a second reason, namely the acceleration of the decomposition reaction with HCN when ligands are used that prefer square planar complexes. Thus, the intermediary benzylic cyanide complexes undergo either reaction with HCN or reductive elimination. If reaction with HCN occurs, the effect is irreversible as inactive $L_2Ni(II)CN_2$ is formed.

Table 10.1. Nickel-catalysed hydrocyanation of styrene, using diphosphine ligands.[a]

Ligand	β(°)	% yield[b]	% branched
PPh_3	-	0	-
dppe	79	<1	40
dppp	87	4-11	ca. 90
dppb	99	3-8	92-95
BINAP	85	4	29
DPEphos	101	35-41	88-91
Sixantphos	105	94-95	97-98
Thixantphos	106	69-92	96-98
Xantphos	109	27-75	96-99

[a] Data from reference [12]. Reaction conditions: Styrene/Ni= 28.5, HCN/Ni= 17.5, [Ni]= 73.3 mM, T= 60 °C, t= 18 h. [b] Yields are based on HCN. Maximum yields based on styrene are 61%.

Moloy studied the effect of the bite angle on the stoichiometric reductive elimination of RCN from ($R=CH_2Si(CH_3)_3$) from palladium complexes $P_2Pd(R)(CN)$ from a range of ligands including dppe, dppp, and DIOP [15]. In this series a 10^4-fold rate increase was found! As in the Xantphos series the substitution at phosphorus are essentially identical and therefore they concluded that the kinetic ordering is attributable to changes in chelate size, increased bite angles, increased flexibility, all enhancing the reductive elimination.

Although most authors prefer a "bite angle effect" [16] and the orbital effect seems logical, there is no hard proof for it and the possibility remains that in fact the increasing steric demand of the ligand while the bite angle widens enforces reductive elimination. Thus, experiments are needed, with the use of ligands that have small bite angles but larger steric bulk. For methoxycarbonylation reactions of alkenes with palladium catalysts these experiments have been done, and for this reaction it has been shown that steric bulk is more important than the bite angle per se (see Chapter 12 and [16]).

References

1 McKinney, R. J. in *Homogeneous Catalysis*, Parshall, G. W. ed. Wiley, New York, **1992**, p.42.
2 Brown, E. S. *Aspects of Homogeneous Catalysis*, Vol. 2, Reidel, Dordrecht, **1974**, p. 57.
3 McKinney, R. J.; Roe, D. C. *J. Am. Chem. Soc*. **1986**, *108*, 5167.
4 Favero, G.; Gaddi, M.; Morvillo, A.; Turco, A. *J. Organometal. Chem.* **1978**, *149,* 395.
5 Garcia, J. G.; Brunkan, N. M.; Jones, W. D. *J. Am. Chem. Soc.* **2002**, *124*, 9547.
6 McKinney, R. J. *Organometallics*, **1985**, *4*, 1142.
7 Huang, J. K.; Haar, C. M.; Nolan, S. P.; Marcone, J. E.; Moloy, K. G. *Organometallics*, **1999**, *18*, 297.
8 McKinney, R. J.; Nugent, W. A. *Organometallics*, **1989**, *8*, 2871.

9 Tolman, C. A.; Seidel, W. C.; Druliner, J. D.; Domaille, P. J. *Organometallics,* **1984**, *3*, 33.
10 Goertz, W.; Keim, W.; Vogt, D.; Englert, U.; Boele, M. K. D.; van der Veen, L. A.; Kamer, P. C. J.; van Leeuwen, P. W. N. M. *J. Chem. Soc. Dalton Trans*. **1998**, 2981.
11 van Leeuwen, P. W. N. M.; Roobeek, C. F. $(CF_3CH_2O)_3P$ (χ=39) and $((CF_3)_2CHO)_3P$ (χ=51) with palladium catalysts, **1975**, unpublished.
12 Kranenburg, M.; Kamer, P. C. J.; van Leeuwen, P. W. N. M.; Vogt, D.; Keim, W. *J. Chem. Soc. Chem. Commun.* **1995**, 2177. Goertz, W.; Kamer, P. C. J.; van Leeuwen, P. W. N. M.; Vogt, D. *Chem. Commun.* **1997**, 1521. 103.
13 Baker, M. J.; Harrison, K. N.; Orpen, A. G.; Pringle, P. G.; Shaw, G. *J. Chem. Soc. ,Chem. Commun.,* **1991**, 803. Baker, M. J.; Pringle, P. G. *J. Chem. Soc. Chem. Commun.* **1991**, 1292. Wilson, T.; Kreutzer, K. A. PCT Int. Appl. WO 95 14,659 (to DuPont) **1995**. *Chem. Abstr.* **1995**, *123,* 286288.
14 Casalnuovo, A. L.; RajanBabu, T. V.; Ayers, T. A.; Warren, T. H. *J. Am. Chem. Soc.* **1994***, 116*, 9869.
15 Marcone, J. E.; Moloy, K. G. *J. Am. Chem. Soc.* **1998**, *120*, 8527.
16 Freixa, Z.; van Leeuwen, P. W. N. M. *Dalton Trans.* **2003**, 1890.

Chapter 12

PALLADIUM CATALYSED CARBONYLATIONS OF ALKENES

Polyketones, oligomers, and methyl propanoate

12.1 Introduction

In this chapter we will discuss some aspects of the carbonylation catalysis with the use of palladium catalysts. We will focus on the formation of polyketones consisting of alternating molecules of alkenes and carbon monoxide on the one hand, and esters that may form under the same conditions with the use of similar catalysts from alkenes, CO, and alcohols, on the other hand. As the potential production of polyketone and methyl propanoate obtained from ethene/CO have received a lot of industrial attention we will concentrate on these two products (for a recent monograph on this chemistry see reference [1]). The elementary reactions involved are the same: formation of an initiating species, insertion reactions of CO and ethene, and a termination reaction. Multiple alternating (1:1) insertions will lead to polymers or oligomers whereas a stoichiometry of 1:1:1 for CO, ethene, and alcohol leads to an ester.

12.2 Polyketone

12.2.1 Background and history

Thermoplastics with high-performance properties are in increasing demand [2]. The present products (e.g. aromatic polyketones, polyesters, polyamides, polyacetals, polyolefin specialities) span a wide range of performance and production costs. Relevant properties comprise strength, toughness, wear resistance, chemical resistance, heat resistance, UV stability, etc. Applications include a variety of automotive components, gears, fittings, containers, fibres, packaging, etc. In the last decades much effort has been devoted to the

development of such high-performance plastics that might be produced at lower costs.

In addition the ketone group can be modified easily to give ranges of new polymers, such as polyalcohols, polyamines or polyimines. The feasibility of these chemical modifications has been demonstrated, but the properties of these new polymers have not yet been established in great detail. Insertion of styrene, propene, and higher homologues opens the possibility of stereoregular polymers, another new group of polymers.

Copolymerization of ethene and carbon monoxide has been known for a long time. The first product was made via radical polymerisations [3]. These polymers had low molecular weights and the incorporation of CO was usually lower than required for a perfect alternation of ethene and CO. Besides, high pressures were required. Coordination polymerisation for ethene/CO was discovered by Reppe [4] using nickel cyanide catalysts (this was even before the Ziegler invention of ethene polymerisation!). The molecular weights were very low and in addition to the polymers diethylketone and propanoic acid were produced. The first palladium catalyst (phosphine complexes of $PdCl_2$) producing an alternating polymer of CO and ethene (Figure 12.1) was reported in 1967 [5]. The rates were promising (300 g/g Pd/hr) but the conditions were harsh (250 °C, 2000 bar). Similar palladium catalysts were used by Union Oil and Shell [6,7]. High molecular weights were achieved and the potential of the semi-crystalline high-melting polymer was recognised. The polymers made, however, contained a considerable amount of catalyst (often as black palladium metal) and this was deleterious to the stability of the polymer during processing. One might think that the polymers are inherently unstable due to intra and intermolecular condensation reactions, or due to UV sensitivity, but later this turned out to be not the case. Hence, considerably more active catalysts were needed.

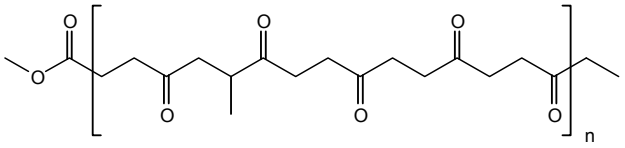

Figure 12.1. Ethene/CO alternating copolymer showing propene incorporation and methanol as chain transfer agent

It was Ayusman Sen [8] who discovered in 1982 that the use of weakly coordinating anions and phosphines as the ligands together with palladium yielded much more stable and active catalysts for the formation of polyketone from CO and ethene in alcoholic solvents. Cationic palladium-$(triphenylphosphine)_2(BF_4)_2$ gave a mixture of oligomers having methoxy ester

and ethylketone end-groups in moderate yields. In 1984 Drent [9] reported that cationic palladium complexes containing chelating bidentate diphosphine ligands produced alternating polymers of ethene and CO with 100% selectivity, high molecular weight, and yields up to several kg per g of palladium per hour. The process conditions are relatively mild, 30-60 bar and 80-100 °C. Now one was able to produce perfectly alternating polymers with melting points of ~260 °C containing only ppm quantities of palladium. Subsequently, it was shown that other alkenes could be copolymerised in a random fashion; when a terpolymer of ethene, propene and CO is made the resulting polymer possesses a lower melting point. The monodentate phosphine catalysts are several orders of magnitude slower (4 g precipitate.g^{-1} Pd.h^{-1}). Drent's discovery made the commercial production of aliphatic polyketone polymers economically attractive. Since the end of 1996 a commercial unit was on stream in the U.K. (20,000 ton/annum), but it was closed in 2000.

In the meantime improved nickel catalysts have also been developed by workers from Du Pont employing phosphinocarboxylic acids as the ligands [10]. Interestingly, the catalysts used here are similar to the nickel-ligand complexes used by Shell for their commercial ethene oligomerization process. Similar catalysts for making polyketone have also been patented by Keim et al. [11].

The unique properties of the polymer are outlined by Ash [2]. Aliphatic polyketones exhibit a desirable combination of strength, stiffness, and impact resistance over a broad range of temperatures. The polymers undergo unusually high elongation before yielding. In addition they show excellent friction and wear properties. The chemical resistance is also very high. The melt processing temperature of the ethene/CO polymer would be well above 260 °C. The first polymer that aroused commercial interest was an ethene/propene/CO terpolymer having a melting point of 220 °C, below that of the ethene/CO polymer.

12.2.2 Elementary steps: initiation

The mechanistic issues to be discussed are the initiation modes of the reaction, the propagation mechanism, the perfect alternation of the polymerisation reaction, chain termination reactions, and the combined result of initiation and termination as a process of chain transfer. Where appropriate, the regio- and stereoselectivity should be discussed as well. A complete mechanistic picture cannot be given without a detailed study of the kinetics. The material published so far on the kinetics comprises only work carried out at temperatures of –82 to 25 °C, which is well below the temperature of the catalytic process.

Initiation. The polymerisation reaction is efficiently catalysed by complexes of the type PdX_2(L-L) (L-L is a chelating bidentate phosphorus or nitrogen ligand -coordinating in a cis fashion-, X is a weakly or non-coordinating anion) in methanol as the solvent. Suitable ligands are dppe, dppp and dppb and both triflic and p-toluenesulfonic acid provide suitable anions in methanol. The catalyst can be made in situ by dissolving palladium acetate and adding ligand and a strong acid. When methanol is the solvent there is no need to create an active palladium alkyl initiator. In aprotic solvents such as dichloromethane on the other hand, palladium must be methylated with e.g. $Sn(CH_3)_4$ to provide an active catalyst [12]. Hydride formation is a likely initiation pathway in methanol for which at least three routes can be envisaged. Reaction (1) in Figure 12.2 shows the attack of water (hydroxide) at coordinated carbon monoxide, which after elimination of carbon dioxide gives palladium hydride **3**. A Wacker type reaction as shown in (2) also leads to the formation of **3**. Hydride elimination from palladium methoxy species **5** is another mechanism for the formation of hydride **3**. Formaldehyde and methanol are in equilibrium with dimethoxymethane and water under the reaction conditions. Hydrides are also efficient initiators as their insertion reactions with alkenes are extremely fast. These initiation reactions are collected in Figure 12.2.

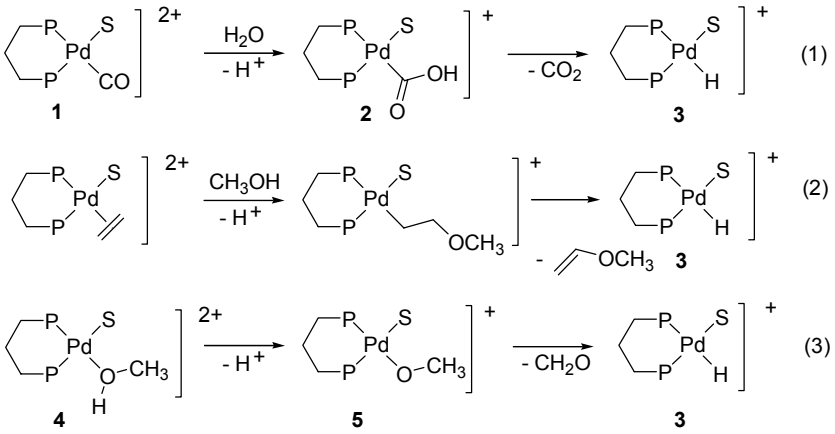

Figure 12.2. Palladium hydride formation from divalent palladium and CO and ethene in the presence of water or methanol as initiation reaction (P=PPh_2)

A fourth route to make palladium hydride species involves the use of dihydrogen and divalent palladium salts. The reaction is a heterolytic cleavage of dihydrogen with palladium and a base (equation 4, Figure 12.3). Oxidative addition of an acid to a palladium(0) species generates hydride **3**, also a useful initiation or regeneration reaction (equation 5, Figure 12.3). The reverse of reaction (5) can occur as a continuation of reaction 4, converting hydride

species **3** to palladium(0). Clearly, in a too basic a solution the base would react with the cationic palladium hydride species by abstracting a proton thereby forming a palladium(0) species, which is inactive in polymerisation reactions.

When carbon monoxide is bubbled through a methanol solution of (dppp)Pd(triflate)$_2$ a carbomethoxy-palladium species is formed, which can undergo insertion of alkenes and hence this is a feasible alternative initiation route to chain-growth polymerisation (Figure 12.4) [13]. To ensure a clean formation of the carbomethoxy species, however, exclusion of water is a prerequisite. If during the preparation water was present the formation of a palladium hydride complex (dppp)PdH$^+$ was observed (reaction (1), Figure 12.2).

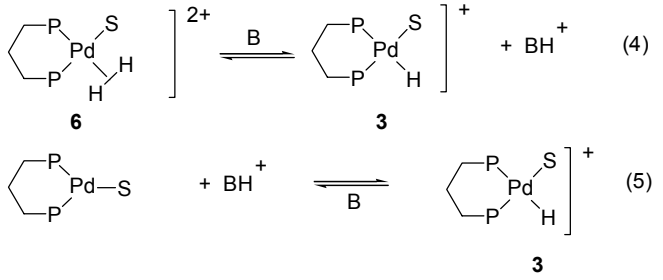

Figure 12.3. Hydrogen as the source for hydride formation (4) and oxidative addition /reductive elimination related to hydride formation (5)

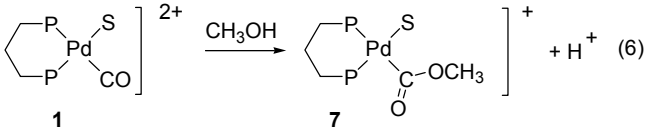

Figure 12.4. Carbomethoxy-palladium formation

In the absence of methanol or dihydrogen a palladium(II)alkyl species can be used as the initiating species, if not, the reaction may not start. Clearly, this alkyl complex is only the initiator and may not be regenerated during the polymerization process. There are two important ways for making a mono-alkylpalladium complex, 1) by monoalkylation via a metathesis reaction of a divalent palladium salt and an alkylating reagent, and 2) protonation of a dimethylpalladium complex with an acid, Figure 12.5.

Alkylation of a complex such as L_2PdCl_2 will in many instances lead to double alkylation or a mixture of monoalkyl and dialkyl complexes. A convenient alkylating agent giving purely monomethylpalladium turned out to be tetramethyltin, which has been widely used [12,14], reaction (7), Figure

12.5. The second popular way for generating an alkylpalladium species is the protonation of a bis-ligand-dimethylpalladium complex **10** using an acid that consists of protonated base and a weakly coordinating anion (WCA), reaction (8) [15]. The conjugate base is for example diethyl ether, which is a very weak ligand towards palladium and does not disturb the catalysis. A well-known example of a weakly coordinating anion is BArF, the structure of which is given in Figure 12.5. The resulting species **9** containing a cis-coordinating bidentate diphosphine is not very stable and usually it is generated in situ below room temperature. Adding another phosphine ligand can stabilise it; two phosphine ligands in cis positions of the methyl group ensure the formation of a stable complex.

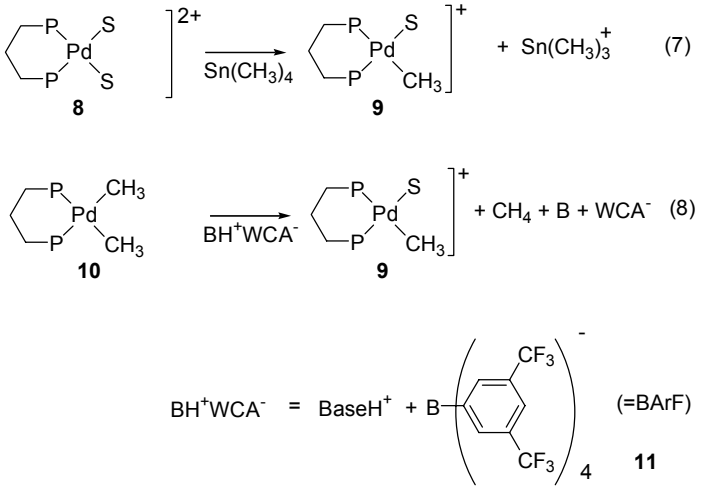

Figure 12.5. Palladium-monomethyl formation

12.2.3 Elementary steps: migration reactions

Insertion of carbon monoxide and alkenes into metal-carbon bonds is one of the most important reaction steps in homogeneous catalysis. It has been found for insertion processes of platinum [16] that the relative positions of the hydrocarbyl group and the unsaturated fragment must be *cis* in the reacting complex [17]. The second issue concerns the stereochemical course of the reaction, insertion versus migration as discussed in Chapter 2.2.

Accidentally, one proof for the migration mechanism stems from the polyketone model work and we will present it here. When the two "dents" of the bidentate ligand are only slightly inequivalent, be it sterically or electronically, this would allow the identification of the sites during migration or insertion. In order to do this we need two phosphorus ligands that are very

similar ligands but having well separated NMR frequencies. In Figure 12.6 we show the system fulfilling this criterion viz. 1,3-bis-phosphinopropenes (1-diphenylphosphino-2-t-butyl-3-dicyclohexylphosphinoprop-1-ene) both for platinum as for palladium complexes [18]. Actually a mixture of the two isomers ("cis" and "trans") was observed which reacted with different rates to the acetyl metal products.

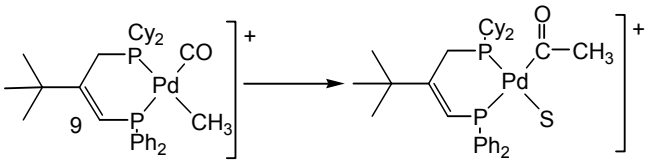

Figure 12.6. Proof for migration mechanism

Thus, in platinum and palladium complexes the insertion process of CO into metal-to-carbon σ-bonds involves a migration of the hydrocarbyl group to the unsaturated CO ligand. The least stable geometric isomers react faster than the more stable isomer, in accord with theoretical studies on this subject [19] and the findings for P∩N ligands (Chapter 2.2 [20]). When a series of migrations is required for a reaction, e.g. polyketone formation where the growing chain moves from one site to the other and vice versa, the migration mechanism implies that the fastest catalysts should be those that contain symmetric diphosphines or bipyridines [21] as has indeed been found.

Nitrogen ligands have a strong tendency to form five-coordinate complexes with platinum and palladium. The migration reaction in complexes with bipyridine type ligands might well involve five-coordinate species. Detailed kinetic measurements and spectroscopic characterisation were carried out by the group of Brookhart [22]. So far, very little is known about the involvement of an incoming ligand during the migration reaction. Recent theoretical studies by Ziegler indicate that at least for early transition metal complexes this is an essential element of the detailed mechanism. This will influence the kinetics of the polymerisation.

Rates of insertion of CO. The rate of CO insertion in the Pd-CH_3 bond has been studied by Dekker, Vrieze, van Leeuwen et al. [23] for the complexes (P-P)Pd(CH_3)Cl (P-P = dppe, dppp, dppb, dppf) and the ionic complexes $[(P\text{-}P)Pd(CH_3)(CH_3CN)]^+SO_3CF_3^-$. The rate was found to decrease in the order dppb ≈ dppp > dppf for the neutral chloro complexes with half-life times ranging from 18 to 36 minutes at 235 K and 25 bar of CO. The dppe complex reacted much more slowly with a half-life time of 170 minutes at 305 K. The rate of carbonylation of the Pd-CH_3 bond in the ionic triflate complexes was at least 10 times higher than those of the analogous neutral complexes, the order

being dppb ≈ dppp ≈ dppf > dppe with half-life times < 1.5 minutes at 235 K except for the dppe complex for which a half-life time of 2.5 minutes was measured. Carbonylation of the ionic PPh_3-coordinated complex [(dppp)Pd $(CH_3)(PPh_3)]^+SO_3CF_3^-$ was at least 2.5 times slower than that of the analogous CH_3CN-coordinated cationic complex. The rate differences agree qualitatively well with the overall rate of polymerisation found for dppe, dppp, and dppb [9], but this may be accidental as the CO insertion is not the rate limiting step under most conditions. Most likely the rate-determining step is alkene insertion.

The data for the insertion rate of CO into a palladium-methyl bond for dppp as the ligand has been studied with considerably more precision by Brookhart and co-workers [24]. The kinetics were studied in the temperature range between 191 and 210 K for a reaction similar to that of Figure 12.6, i.e. the starting material was the CO adduct of the methylpalladium(dppp)$^+$BArF$^-$ complex. A $\Delta G^{\#}$ of ~ 62 kJ.mol^{-1} was observed and since $\Delta S^{\#}$ was close to zero, a half-life time of ~10 s is calculated for the CO-adduct at 235 K, much shorter than the value for dppe given above (150 s).

The catalytic studies [9] and these model studies have shown that the bite angle and backbone flexibility of the ligand strongly influence the rate of migration in methyl-palladium complexes. There are several examples that seem to point to a rate-enhancing effect obtained by replacing the two-carbon bridge by a three- or four-carbon bridge in 1,n-diphenylphosphinoalkanes:

(a) the platinum catalysed hydroformylation of alkenes [25],

(b) the palladium catalysed CO/ethene copolymerization [vide infra],

(c) the palladium catalysed methoxy-carbonylation of styrene [26], and

(d) alkyl to vinyl migration in a palladium catalysed carbon-carbon bond formation [27].

It should be emphasized that this is only true within a series of diphenylphosphino ligands, i.e. the phenyl substituents are retained in the series.

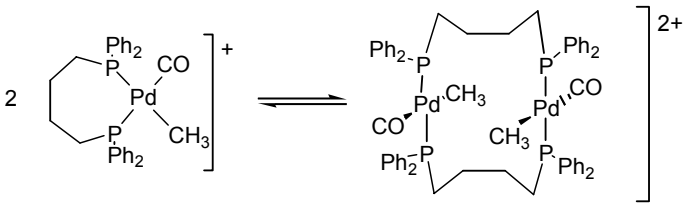

Figure 12.7. Example of dimer formation with dppb

When the bite angle becomes too wide, as for dppb, the behaviour of the catalytic systems of palladium may also be different. When ligands have large

bite angles and are relatively bulky their catalytic performance resembles that of monodentate ligands, that is to say that ethyl propanoate ester formation takes place rather than copolymerization. Yet in palladium complexes they may act as bidentate ligands, see Figure 12.7 or bimetallic species may form [23,28]. On the contrary, when the bridge contains only one atom between the phosphorus atoms (CH_2, dppm, or NCH_3), the narrow bidentate leads to a very fast polymerisation catalyst, provided that they contain bulky substituents, as dppm itself was a poor catalyst in methanol [29]. We will return to this later when discussing propanoate formation versus polymer formation. Like dppb, dppm ligands can also lead to bimetallic complexes and with an additional bridging atom they form A-frame complexes [30].

Insertion of alkenes. Alkene insertions have also been widely studied and many insertion products have been isolated [31]. Alkene insertions follow a migratory mechanism in the palladium and platinum square planar complexes with diphosphine ligands [18].

The study of alkene insertions in complexes containing diphosphine ligands turned out to be more complicated than the study of the CO insertion reactions [13]. When one attempts to carry out insertion reactions on acetylpalladium complexes decarbonylation takes place. When the reaction is carried out under a pressure of CO the observed rate of alkene insertion depends on the CO pressure due to the competition between CO and ethene coordination. Also, after insertion of the alkene into the acetyl species β-elimination occurs, except for norbornene or norbornadiene as the alkene. In this instance, as was already reported by Sen [8,27] a *syn* addition takes place and in this "strained" skeleton no β-elimination can take place. Therefore most studies on the alkene insertion and isolation of the intermediates concern the insertion of norbornenes [21,32]. The main product observed for norbornene insertion into an acetyl palladium bond is the exo species (see Figure 12.8).

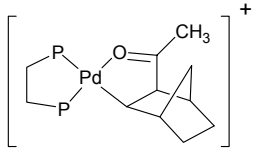

Figure 12.8. Exo species formed after norbornene insertion

Strain and steric properties of the alkenes determine the rate of insertion. The carbomethoxy complex (dppp)PdC(O)OCH_3^+ turned out to be less reactive than the corresponding acetyl-palladium (dppp)Pd$C(O)CH_3^+$, which was ascribed to the higher nucleophilicity of the acetyl group as compared to the carbomethoxy group.

In spite of the difficulties mentioned above, Brookhart and co-workers succeeded in measuring the barrier for ethene insertion into (dppp)PdC(O)CH_3^+ at 160 K, starting from the ethene adduct, generated at still lower temperatures, in the absence of CO. The barrier measured ($\Delta G^{\#}$) amounted to only 51.4 kJ/mol, i.e. the reaction is faster than the insertion of CO in an ionic alkylpalladium complex. The barrier of insertion of ethene into a palladium methyl species or palladium ethyl species was higher, at ~ 67 kJ/mol at ~ 233 K. As for the CO insertion described above, these values concern the barriers in "preformed" ethene adducts; at higher temperatures the overall barrier will be higher, because alkene coordination will be disfavoured by entropy and competition with CO and solvent. Formation of CO adducts will also be less favourable at higher temperatures.

Alternating insertions. The reaction proceeds via a perfectly alternating sequence of carbon monoxide and alkene insertions in palladium-carbon bonds (Figure 12.1). Several workers have shown the successive, stepwise insertion of alkenes and CO in an alternating fashion. In catalytic studies this was demonstrated by Sen, Nozaki, and Drent etc. In particular the work of Brookhart [15,22] and Vrieze/van Leeuwen [12,13,14,20,23,32] is relevant for stepwise mechanistic studies. The analysis of final polymers shows that also in the final product a perfect alternation is obtained. It is surprising that in spite of the thermodynamic advantage of alkene insertion versus CO insertion nevertheless exactly 50% of CO is built in.

The insertion of CO is in many instances thermodynamically unfavourable; the thermodynamically most favourable product in hydroformylation and carbonylation reactions of the present type is always the formation of low or high-molecular weight alkanes or alkenes, if chain termination occurs via β-hydride elimination). The decomposition of 3-pentanone into butane and carbon monoxide shows the thermodynamic data for this reaction under standard conditions. Higher pressures of CO will push the equilibrium somewhat to the left.

$$CH_3CH_2C(O)CH_2CH_3 \rightarrow CH_3CH_2CH_2CH_3 + CO$$

$$\Delta G \quad -135\ (g) \qquad -17\ (g) \qquad -137\ (g) = -19\ kJ/mol$$

Insertion of CO is therefore always kinetically controlled. When an alkyl palladium species has formed, the open site will be occupied by a coordinating CO molecule. Carbon monoxide coordinates more strongly to palladium than ethene, even when the palladium centre is cationic. The reason for this is steric; the "cone angle" of ethene is much larger than that of CO and the steric hindrance in the ethene complex is therefore much larger. If the barriers of activation for the insertion processes of ethene and CO are of the same order of

magnitude insertion of CO will take place. For CO this insertion may be reversible and only after an insertion of ethene has taken place the CO insertion has led to chain growth.

The acyl complex formed will, by the same token, also preferentially coordinate to CO instead of ethene. Double insertions of CO do not occur because this is thermodynamically even more unfavourable, and in addition the migration of more electronegative groups to CO is usually slower. An "occasional" co-ordination of ethene now leads to insertion of ethene and thus a perfect alternation of the two monomers occurs. After insertion of ethene a very stable intermediate is formed as a result of the intramolecular coordination of the ketone group. Many intermediates of this structure have been isolated. It can be imagined that during the migration of the acyl group to ethene a stabilising interaction of the acyl oxygen with palladium facilitates the reaction. The thermodynamic driving force for the overall reaction is the conversion of ethene into an alkyl chain (~ 84 kJ/mol).

Quantitative data for the difference in complexation of ethene and CO to hydrocarbylpalladium(dppp)$^+$ were reported by Brookhart and co-workers [15,33]. The equilibrium between CO and ethene coordination amounts to about 10^4 at 25 °C. Multiplied by the concentrations of the two gases and the two individual rate constants for the insertion they calculated that the ratio of CO insertion versus ethene insertion is about 10^5 in an alkyl-palladium intermediate under Curtin-Hammett conditions, that is to say fast exchange of coordinated CO and ethene ligands compared to insertion reactions. Figure 12.9 summarises this.

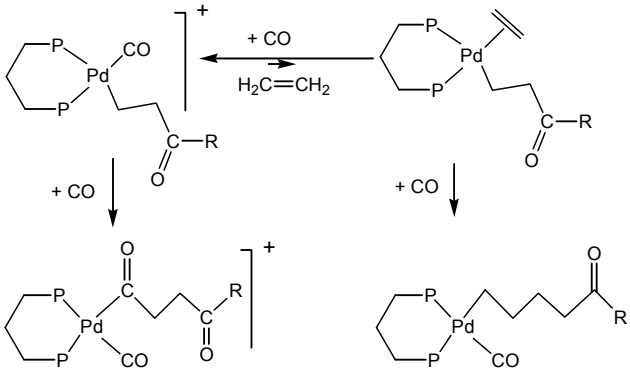

Figure 12.9. Curtin-Hammett kinetics for ethene/CO insertion

12.2.4 Elementary steps: chain termination, chain transfer

The common chain termination reactions comprise β-hydrogen elimination (9), protonation of an alkylpalladium complex (10), and nucleophilic attack at an acylpalladium complex (11) (Figure 12.10). The resulting hydride and methoxy complexes start a new chain via insertion of a molecule of ethene or CO respectively. Actually, MeOH is the chain transfer agent in the last two reactions. Other chain transfer reagents can also be used and they lead to different end groups.

In the simplest case, excluding β-hydrogen elimination (9), each route (10) and (11) leads to polymer chains or oligomers containing one ester (E) and one ketone (K) end group, KE polymers. When reactions (10) and (11) occur at comparable rates, which accidentally seems to be the case in several catalyst systems, there is formation of EE and KK polymers in addition to KE polymers. This is so because the growing chain does not "remember" whether it started from a hydride or a methoxy group and thus a distribution of chain ends will be obtained in between EE:KE:KK = 0.25:0.5:0.25 and 0:1:0 depending on the ratio of the rates of (10) and (11) [9].

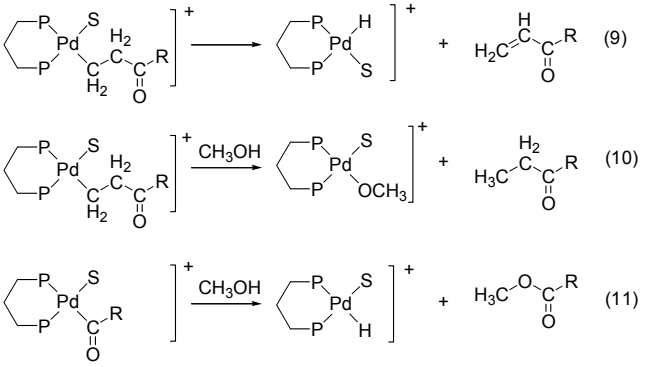

Figure 12.10. Chain transfer mechanisms

Deviations from an average K:E=1:1 have been observed, because the intermediate palladium species Pd^{2+} or PdH^{+} can be reduced or oxidised respectively to one another leading to an excess of K or E chain ends, or even one type of chain end only [9]. Chain termination ratios also depend on the phase in which the chain end resides, liquid phase or solid phase, as higher oligomers precipitate [34].

Formally, equation (10) involves a protonation of the alkyl chain, which is not a very fast reaction at the cationic palladium centre, as is also apparent from the stability of methylpalladium cations, which can be generated selectively

from dimethylpalladium complexes and acid without further reaction at low temperature [15,22,33]. At room temperature the half-life time of $[(dppp)Pd(CH_2C(CH_3)_3)(CH_3CN)]^+[CF_3SO_3]^-$ in CD_3OD with a tenfold excess of CF_3COOH is one hour [35]; methyl platinum complexes containing electron-withdrawing diphosphines survive strong acids for several days [36]. For a number of model compounds it has been shown [37, 38] that reaction of compounds containing a γ-keto group such as shown in reactions (12) and (13) with CH_3OD or D_2O form a ketone having the deuterium atom in the β-position (relative to palladium) instead of the expected α-position (relative to palladium), which has been explained by an enolate mechanism (Figure 12.11, equations 12-13). These elimination and re-insertion reactions are often very fast in palladium chemistry and they also occur in Heck and Wacker type reactions (Chapters 13 and 15).

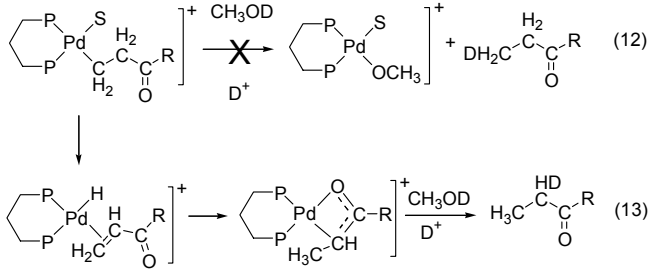

Figure 12.11. Enolate formation and protonation in chain transfer

As in alkene polymerizations, dihydrogen can also be used as a chain transfer agent in polyketone formation. The reaction is depicted as a hydrogenolysis or σ-bond metathesis reaction (reaction (14) in Figure 12.12), but it can also be described as a heterolytic cleavage of dihydrogen followed by reductive elimination (equations 15-16). Reaction of acid and palladium(0) regenerates palladium hydride. Interestingly, under most conditions no aldehyde end groups are formed, although the proper choice of ligand, halide anions, and solvent does give a hydroformylation of alkenes, in which a reaction of acyl end groups with dihydrogen must occur [39].

Water and carbon monoxide can produce dihydrogen in situ (shift reaction), as has been shown in the synthesis of diethylketone (pentan-3-one) from ethene, CO and water in the presence of palladium(II) salts, triphenylphosphine and acids [37]. Ether chain ends have been observed in some polymerization reactions [40] and low molecular weight products can also contain an ether moiety as an end group. Most likely ether chain ends are not formed by attack of alcohol at coordinated ethene in a Wacker type reaction, since this is usually followed by fast β-hydride elimination. Instead we propose that a palladium-

catalysed attack of alcohols at enones resulting from β-hydride elimination; the catalysed Michael reaction has been observed in separate experiments [41].

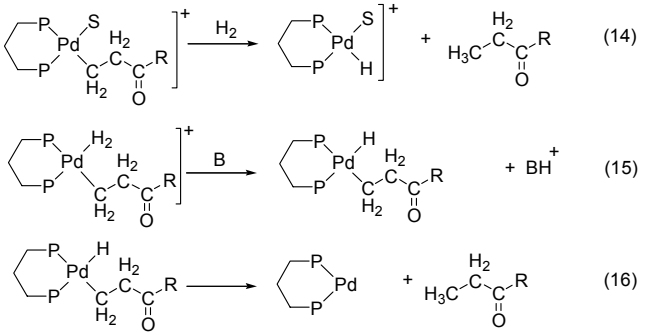

Figure 12.12. Dihydrogen as chain transfer agent

When chain transfer is very fast, the reaction observed is the alkoxycarbonylation of ethene, which is nothing but a perfect chain transfer after the insertion of just two monomers. In recent years several very fast catalysts for this reaction have been reported as we will see in the next section. The first effective catalysts reported by Sen [8] ($Pd(BF_4)_2$ and PPh_3) also give relatively fast chain transfer as the Flory-Schulz constant for their product was only 0.3–0.4 (see Chapter 9.2.1 on oligomerisation) and the product is an oligomer rather than a polymer.

12.2.5 Elementary steps: ester formation as chain termination

The formation of ester via reaction (11) of Figure 12.10 deserves some further attention as it is not one of the elementary steps discussed in Chapter 2. One possible mechanism is the direct, outer-sphere attack of an alcohol or alkoxide at the acyl carbon atom, similar to the reaction of acid halides and alcohols (17-18 in Figure 12.13). This reaction is accessible for both *cis* and *trans* diphosphine complexes **12** and **13**. Since monophosphines give mainly *trans* acyl complexes **13**, not suited for insertion reactions, they were thought to have a preference for making esters or low molecular weight products. *Trans* complexes do form esters in reactions with alcohols or alkoxides, but this does not give direct information about the mechanism [42,43,44].

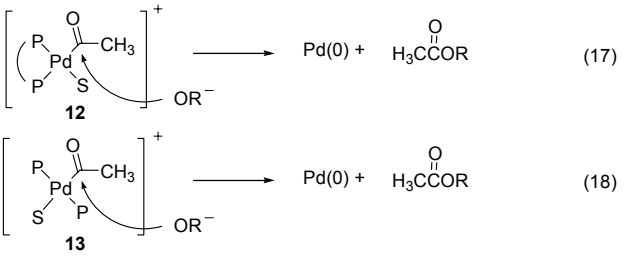

Figure 12.13. Ester formation by direct attack of alcohol

Bidentate diphosphines that give esters (see next section) were thought to react also via a *trans* intermediate, which may be formed for certain bidentates either due to the bridge length (dppb, Figure 12.7) or steric bulk of the substituents [45]. After reactions (17-18) have taken place, a palladium(0) complex remains that has to undergo oxidative addition of acid to regenerate an active hydride species. Under the reaction conditions very often palladium(0) complexes will undergo dimerisation and oxidative addition of one proton per dimer, forming the very stable dimers of type **18** (21, Figure 12.15).

The second mechanism involves the oxidative addition of methanol to the divalent acylpalladium complex **14** (19, Figure 12.14). This reaction has the only advantage that the new hydride initiator is formed in one step, but apart from this it is an unlikely reaction. Oxidative addition of alcohols is only known for electron-rich zerovalent palladium complexes [46].

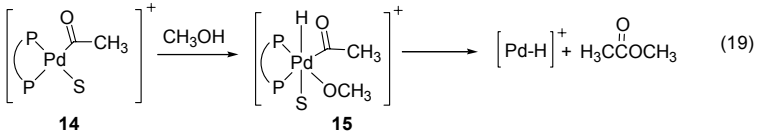

Figure 12.14. Ester formation via oxidative addition

The last possibility for ester formation (20, Figure 12.15) comprises the reductive elimination of esters from acyl-alkoxy-palladium complexes **17**, formed by deprotonation of the alcohol adducts **16**. Clearly, it requires *cis* coordination of the alkoxide and acyl fragment. Since monodentates have a preference for ester formation, it was thought that this mechanism was very unlikely.

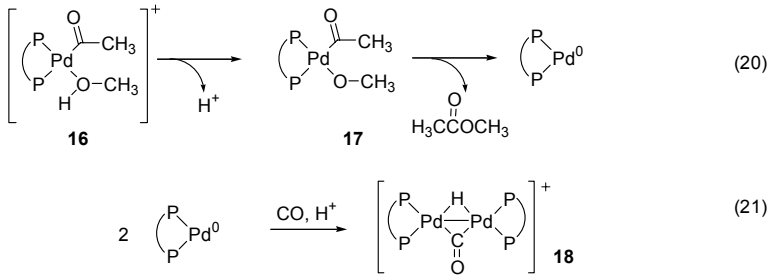

Figure 12.15. Ester formation via reductive elimination

Surprisingly, it was found, that acyl complexes containing rigid, *trans* coordinating ligands do not undergo alcoholysis [42]! For example, one of the ligands not able to form cis complexes is SPANphos [47], shown in Figure 12.16. The acetyl-palladium complex of this ligand did not undergo alcoholysis when methanol was added, thus showing that *cis* coordination is a prerequisite for ester formation.

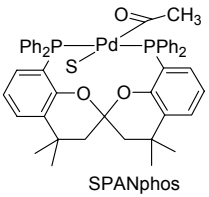

Figure 12.16. Trans enforced coordination for acetyl-palladium in SPANphos complex

It was concluded that a *trans* complex has to rearrange to a *cis* intermediate, which then will undergo reductive elimination. In a *trans* complex neither insertion reactions nor termination reactions take place! The sequence for a trans complex is shown in Figure 12.17. The group Z may be an ether oxygen atom in the ligand (or an iron atom if the bridge is ferrocene), or it may be a solvent molecule. The reductive elimination can be viewed as an intramolecular nucleophilic attack of the methoxy group on the acyl carbon atom. Palladium(0) dimerises with a proton and CO to give the orange dimer **18**.

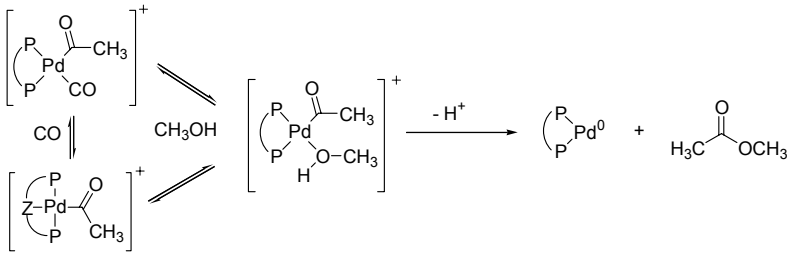

Figure 12.17. The mechanism of ester formation

These reductive eliminations occur for instance also in cross-coupling reactions where they are particularly effective when one of the partners of the reductive elimination has an sp^2-hybridised carbon atom bonded to the metal. A theoretical analysis of the reductive elimination of propene from *cis*-$(PH_3)_2Pd(CH_3)(CH{=}CH_2)$ shows that the best description for this reaction is a migration of the methyl group to the sp^2-carbon of the vinyl unit [48].

The formation of the C-X bond in hetero-cross coupling reactions is thought to proceed via a migration of the hetero atom to the aryl group, which develops a negative charge, which is π-stabilised by mesomeric interaction with acceptor substituents. Both for this reductive elimination and its reverse (oxidative addition) resonance-stabilised Meisenheimer complexes have been proposed [42,49,50,51]. This stabilised structure is depicted in Figure 12.18.

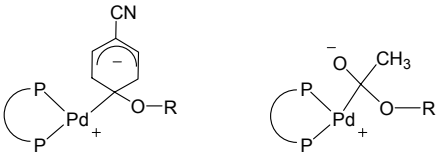

Figure 12.18. Mechanism for "migratory" reductive elimination

The acyl carbon atom is also sp^2-hybridised, much more electrophilic than an aryl carbon atom, and highly stabilised by the structure where the negative charge is on the oxygen atom (Figure 12.18). The acyl oxygen atom may, as in acid catalysed alcoholysis of esters, be protonated, before or after the formation of the new carbon-oxygen bond.

12.3 Ligand effects on chain length

12.3.1 Polymers

Numerous ligands have been tested in polyketone catalysis, but unfortunately very few clear data on the relationship between structure of the ligand and the influence on reaction rates and molecular weight have been published. We will start the discussion with the classic study of the effect of the bridge of the bidentate phosphine ligand on the rate and the molecular weight of the product [9]. A series of α–ω–bis-diphenylphosphinoalkanes was studied, with the alkane ranging from methane (dppm) to hexane (dpp-hexane, Table 12.1). The initial observations led to a rule of thumb that fast polymerisation catalysts required bidentate ligands with a 1,3-propanediyl bridge and that carbomethoxylation was favoured using monodentate ligands. The ligands having the methanediyl and hexanediyl bridge probably form different complexes that are not active. We will consider only the bridges ranging from 2 to 5 carbon atoms. We have added to this published table two columns containing k_g and k_t, as defined in Chapter 9.

As a measure for the growth rate we have simply taken the overall observed rate of production. This may not be the intrinsic rate of each catalyst, as part of the catalyst may be in an inactive state. The effect of the ligand bridge on the rate is moderate, but distinct. The effect on the number averaged molecular weight is much larger! The approximate value of the rate of termination (chain transfer in this instance) is shown in the last column.

Table 12.2. Effect of chain length of ligand bridge on rate and M_n [9][a]

Ligand	Rate, k_g mol.mol^{-1}.h^{-1}	DP,[b] ñ	k_t,[c]
dppm	1	2	
dppe	1000	100	10
dppp	6000	180	33
dppb	2300	45	52
dpp-pentane	1800	6	360
dpp-hexane	5	2	

[a] Conditions: palladium tosylate and diphosphine 0.7 mM in methanol, 84 °C, 45 bar CO/ethene. Rate = mol of CO per mol of Pd per hour.

[b] Average degree of polymerization in $H(C_2H_4CO)_n)OCH_3$ measured by NMR.

[c] k_t = rate of termination

Note that these rates are not true rate constants as these overall rates will contain concentration and pre-equilibria parameters. Nevertheless, longer bridges, and thus wider bite angles lead to a relative increase in the rate of chain transfer. Ester formation for the wide bite angle ligands were assigned to the formation of *trans* complexes as mentioned above.

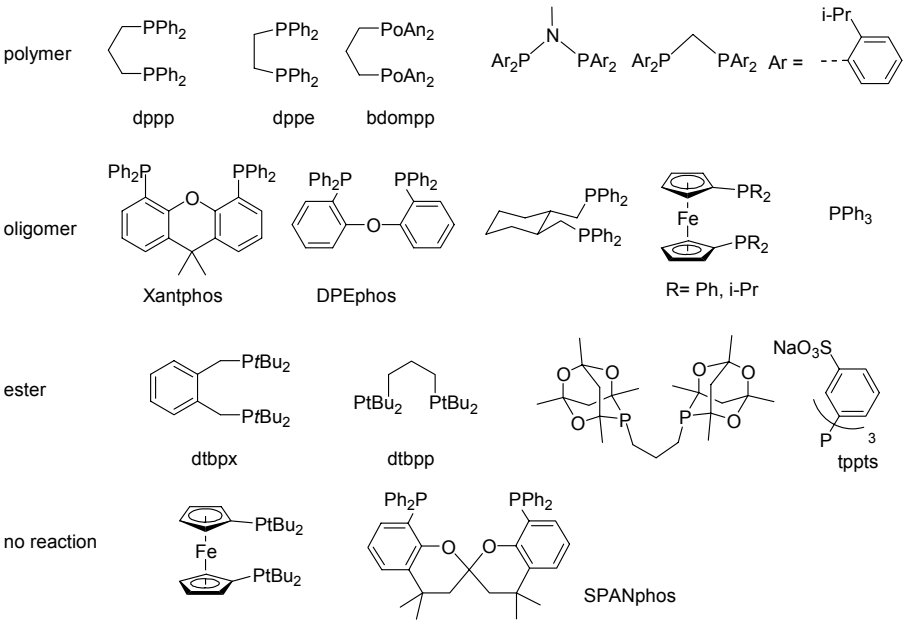

Figure 12.19. Ligand effects in the reaction of ethene, CO, MeOH and palladium(II) catalysts

For a long time the best ligand for making the commercial copolymer of ethene, propene, and CO was "bdompp", which contains a 1,3-propanediyl bridge and the phenyl groups with o-MeO substituents, anisyl groups, (bdompp= 1,3-bis(di-*o*-methoxyphenylphosphino)propane, Figure 12.19). An interesting discovery of recent years was that even ligands having a bridge consisting of only one carbon atom or one nitrogen atom could lead to fast catalysts giving high molecular weight polymer, provided that the substituents on phosphorus are bulky, substituted phenyl groups and that non-protic solvents are used [52]. Typical ligands leading to polymer are shown at the top of Figure 12.19.

Table 12.2 shows the polymerisation results for ligands of the structure $((2\text{-}R\text{-}C_6H_4)_2)P)_2NMe$ (see Figure 12.19). Reactions of entries 1-5 were carried out in dichloromethane. Initiation has to be done by adding an alkylating or arylating agent (in this case $B(C_6F_5)_3$ that transfers a C_6F_5 group), as there is no

water or methanol that can take care of this. It is seen that the productivity of the catalysts increases enormously when the steric bulk increases.

Table 12.3. Polymerisation results of ligand $((Ar_2)P)_2NMe$ [29]

Entry	Ligand, R=	Yield	Rate	$M_n.10^{-3}$	PDI
1	H	0.4	-	-	-
2	OMe	12.0	2300	43	2.4
3	Me	7.7	1650	113	2.5
4	Et	10.4	1900	179	3.6
5	i-Pr	17.0	5200	355	2.5
6	i-Pr, in MeOH	0.2	-	9	2.1

Conditions: 50 bar CO and C_2H_4, 70 °C, 3 h, in CH_2Cl_2, using $B(C_6F_5)_3$ as initiator or HBF_4 in entry 6, $Pd(OAc)_2$ and one equivalent of ligand, yield in g, rate in $m(CO).m(Pd)^{-1}.h^{-1}$. Propene incorporation omitted. Ligands see Figure 12.19.

For entries 3-5 the increase in molecular weight observed can be assigned to the increase in the rate of insertion and the rate of termination remains practically the same. An increase of the rate of polymerisation with the steric bulk of the ligand is usually ascribed to the destabilisation of the alkene adduct while the energy of the transition state remains the same. As a chain transfer reaction presumably β-hydride elimination takes place or traces of water might be chain transfer agents. Chain transfer does occur, because a Schulz-Flory molecular weight distribution is found (PDI ≈ 2, see Table 12.2). Shorter chains are obtained with a polar ortho substituent (OMe, entry 2) and in methanol as the solvent, albeit that most palladium is inactive in the latter case.

The combined views of Table 12.1 and Table 12.2 show that neither the bite angle nor the flexibility of the ligand bridge determines the rate of the growth process, but the *steric bulk* of the ligand. Quantitative measures of the ligands such as cone angle, solid angle etc as discussed in Chapter 1 may be useful.

It is important to note that in methanol as the solvent the reaction is much slower and also the molecular weight is much lower. Apparently a major part of the palladium complex occurs in an inactive state and the termination reaction is relatively accelerated by methanol. This suggests that ester formation is the dominant chain transfer mechanism in methanol, although β-hydride elimination will still occur.

12.3.2 Ligand effects on chain length: Propanoate

Another surprising result was that several bidentate ligands, including ligands with a 1,3-propanediyl bridge reported by Shell, give selectively and in a very fast reaction methyl propanoate [45,53,54] and thus the initial idea that monodentates are the best ligands for making ester had to be abandoned. At first it was thought that these bulky ligands easily lead to the formation of trans-

coordinated, oligomeric diphosphine complexes, which could explain the results [45]. For the bidentate ligand systems the possibility was mentioned that one phosphine moiety might dissociate from the palladium centre. Catalyst systems and conditions for the two reactions are very similar and thus it is the ligand that causes the change in growth versus termination. The best ligand for methyl propanoate formation is probably dtbpx (see Figure 12.19) for which a process is being developed by Lucite (formerly part of ICI).

Alkoxycarbonylation has been known for a long time, but the rates and selectivities of the new catalysts are outstanding. The mechanism of the alkoxycarbonylation reaction catalysed by palladium has been the topic of research for many years [55]. Stepwise reactions had shown the feasibility of two mechanistic pathways, shown in Figure 12.20, but kinetic studies and in situ observations on catalytic systems were lacking.

The "carbomethoxy" cycle starts with the attack of a methoxy group at a coordinated carbonyl group or a migratory insertion of CO in a palladium methoxy bond. Any type of methoxy species will have a low concentration in the acidic medium of the reaction. In Figure 12.20 many details of these reactions, discussed above in section 12.2, have been omitted and only a short-hand notation is presented. Subsequently insertion of ethene takes place. It is known from stoichiometric experiments that both reactions are relatively slow. In the final step a formal protonation takes place, which as we saw before, may actually involve enolate species.

The "hydride" cycle starts with palladium hydride and a fast migratory insertion of ethene. Insertion of CO is also a fast reaction, enhanced by the preferential coordination of CO with respect to ethene. The product is formed by reaction of propanoylpalladium with methanol which coordinates to palladium cis to the acyl group. A palladium zero complex may form that regenerates palladium hydride via an oxidative addition with a proton.

There is a lot of evidence and general agreement that the catalytic cycle of the new, fast catalysts starts with a palladium hydride species [45,56], with perhaps one exception [57].

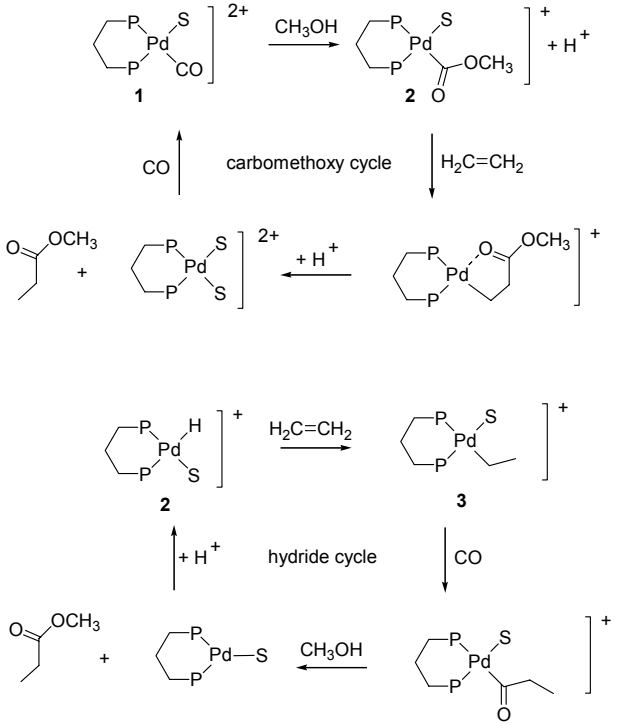

Figure 12.20. The two mechanisms for methoxycarbonylation

Now we will try to answer the question why at very large cone angles the *cis* bidentate ligands give ester formation rather than polymer. Initially, increasing steric bulk leads to faster polymerisation, but at some point it is overtaken by the termination reaction giving propanoates.

In Figure 12.17 we have seen that the ester formation takes place in a *cis* complex containing an alcohol group and acyl group *cis* to one another. The ester forms by deprotonation of the alcohol and a migratory reductive elimination of the ester. From many stoichiometric reactions it is known that reductive elimination of ester from an acyl-alkoxide-palladium species occurs practically without barrier [58]. If the reaction can indeed be described as a reductive elimination, this has important consequences for the impact of steric factors, as reductive elimination is strongly enhanced by increasing the steric bulk of the ligand environment. An illustrative example involving palladium chemistry is the influence of a bidentate ligand on the reductive elimination of an alkyl cyanide from (diphosphine)PdR(CN) as studied by Marcone and Moloy [59]. They found that the reductive elimination for these compounds increased by orders of magnitude when the bite angle was increased. Since all ligands used contain diphenylphosphino groups, the bite angle in this instance

is equivalent to the cone angle, or steric bulk of the ligand. The effect on the reductive elimination is much more pronounced than effects found on the rates of polymerisation.

The resting state of the propanoate catalysts may well be an acyl complex [60,61], while the attack of alcohol at the acylpalladium complex is considered to be the rate-determining step. It is probably more precise to say that fast pre-equilibria exist between the acyl complex and other complexes *en route* to it and that the highest barrier is formed by the reaction of alcohol and acylpalladium complex. The precise course of the reaction is still not known; presumably deprotonation of the coordinating alcohol and the migratory elimination are concerted processes, accelerated by the steric bulk of the bidentate ligand. Tóth and Elsevier showed that the reaction of an acetylpalladium complex and sodium methoxide is very fast and occurs already at low temperature to give methyl acetate and a palladium(I) hydride dimer [46].

Sen *et al* have shown that changing the reaction medium of the copolymerization reaction from methanol to higher alcohols (ethanol, *t*-butanol) increased the molecular weight of the copolymer produced [8]. Milani has shown that the molecular weight in styrene-CO copolymerization increases when 2,2,2-trifluoroethanol is used instead of methanol [62]. Thus, the alcohol has a distinct effect on the rate of the termination reaction, at least relative to the rate of propagation. With dichloromethane as the solvent polymers with a molecular weight higher than those in methanol are obtained. Also in stoichiometric reactions of acetylpalladium complexes the order of decreasing reactivity of alcohols is [42]:

$$MeOH > EtOH > i\text{-}PrOH > t\text{-}BuOH > CF_3H_2OH$$

12.3.3 Ligand effects on chain length: Oligomers

We have seen above that palladium complexes containing very bulky bidentate ligands give esters and those with relatively small ligands give polymer. As we are dealing with a competition between chain growth and chain termination it is no surprise that there is a group of ligands with intermediate steric bulk that will give oligomers. A few examples are shown in Figure 12.19. The regular *cis* bidentates fall in this class, but several ligands, such as Xantphos, DPEphos and triphenylphosphine need some further comment. All three ligands form both *cis* and *trans* complexes and the rates of reaction are considerably lower than those of *cis* bidentate complexes. Insertion rates are low because a *cis* coordination is needed and only the proportion that occurs in the *cis* isomer undergoes reactions. The *cis* complexes, though, have relatively

large cone angles! Thus the ester formation from the acyl intermediates will be fast and low-molecular weight material should form.

It is interesting to compare the product distributions obtained with DPEphos and PPh_3 under similar conditions in methanol. The Flory-Schulz constant (growth factor) for DPEphos is ~ 0.1 and that for PPh_3 was reported to be ~ 0.33 [8]. The resting state for PPh_3 is also the trans complex, which has to rearrange to the cis complex before it can undergo insertion reactions of substrates or undergo a chain termination. The respective bite angles of the two complexes are 103° (DPEphos) and 100.5° (cis-$(PPh_3)_2$) [42] and thus similar results may be expected.

When the *t*-butyl groups in dtbpp [53] or dtbpx [45] are replaced by the smaller *i*-propyl groups both systems give oligomers instead of methyl propanoate at high rates. When the 1,3-propanediyl bridge in dtbpp is replaced by a 1,2-ethanediyl bridge the accessibility of the catalyst for ethene increases such that in the reaction of ethene, CO, MeOH, and H_2 pentan-3-one was formed at extremely high rates instead of methyl propanoate, the product of the more bulky ligand [53].

Figure 12.19 shows a few more ligands with typical results. Tppts, tris-sulfonated triphenylphosphine, forms *trans* complexes as resting state in water and the product of the catalytic reaction is the ester, while triphenylphosphine gives oligomers. The *trans* isomer is inactive and the transient *cis* isomer contains a rather bulky pair of ligands and thus it gives methyl propanoate [63]. Sulfonated Xantphos versus Xantphos shows the same behaviour, as sulfonated Xantphos also gives methyl alkanoates [64]. Trans ligands such as SPANphos and bis(di-t-butylphosphino)ferrocene give no reaction at all, demonstrating that they are strictly *trans*-coordinating ligands and their complexes undergo neither insertion reactions nor termination reactions. This is a rather rare phenomenon in palladium catalysis, since every ligand will show some activity toward one or another product!

In the above we have seen that very subtle changes in steric and electronic properties of the ligands can influence the rates of insertion and chain transfer reactions. Especially the rates of change transfer span a range of many orders of magnitude; there may be five orders of magnitude between the alcoholysis rates of systems based on bdompp and dtbpx.

12.4 Ethene/propene/CO terpolymers

So far we have only discussed catalysts based on diphosphine ligands with a focus on ethene. We should mention that the ligands that are most effective for this reaction are also capable of making terpolymers of ethene, propene and CO. This is important because the commercially interesting polymers must contain a few percent of propene in order to lower the melting point to around

220 °C. The high melting point of pure ethene/CO (265 °C) gives decomposition and formation of brown, furanised polymers in the melt, which makes processing in extruders impossible.

The insertion rate of propene is about twenty times lower than that of ethene, and thus the propene concentration has to be relatively high in order to obtain a few percent of incorporation in the terpolymer [2,9].

12.5 Stereoselective styrene/CO copolymers

For making polymers based on styrene and carbon monoxide diphosphine ligands such as dppp are of no use, as they give unsaturated monoketones in a slow reaction in tetrahydrofuran [65]. The main product is 1,5-diphenylpent-1-en-3-one (Figure 12.21), which apparently forms via insertion of styrene into a palladium-hydride bond as a primary hydrocarbyl group, followed by insertion of CO, insertion of another styrene molecule giving a secondary hydrocarbyl. The latter is highly prone to β-hydride elimination and gives the enone product rather than insertion of a second molecule of CO. The second insertion might lead to a benzylic species, which are known to undergo slow insertion reactions. The unsaturated product is formed even when 40 bar of H_2 is present, showing that the tendency to β-hydride elimination is very large indeed.

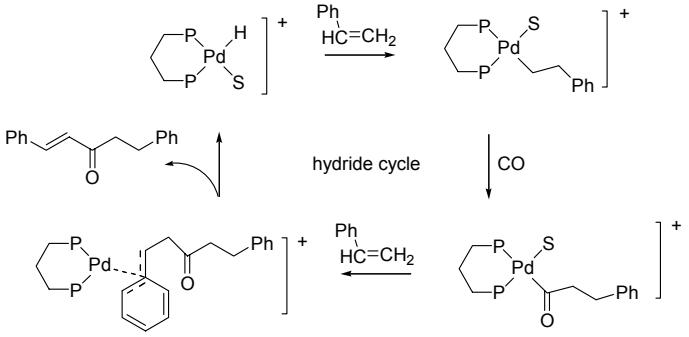

Figure 12.21. Formation of 1,5-diphenylpent-1-en-3-one

Interestingly, simple bidentate nitrogen ligands such as 2,2-bipyridine and phenanthroline give good results, both in terms of yield and molecular weight, provided that quinone is added to the methanol solvent [66]. A wide range of bidentate nitrogen ligands has been applied in regio- and stereospecific copolymerisation of styrene and CO. While many data have been collected, it remains unclear why only nitrogen ligands (and thioethers, also weak ligands!) lead to polymerisation catalysts. The instability of palladium hydrides bearing nitrogen ligands is a key issue. Firstly, this might explain why β-hydride elimination does not occur, as it is thermodynamically not attractive! Secondly,

after β-hydride elimination does happen, the highly unstable hydride decomposes to give palladium metal, which is indeed frequently observed in reactions of styrene with these catalysts. This explains the necessity of quinone in this system; quinone stabilises palladium(0) complexes and together with acid it can reoxidise zerovalent palladium back to divalent palladium!

The latter reaction is highly important in palladium chemistry and it is shown here in Figure 12.22.

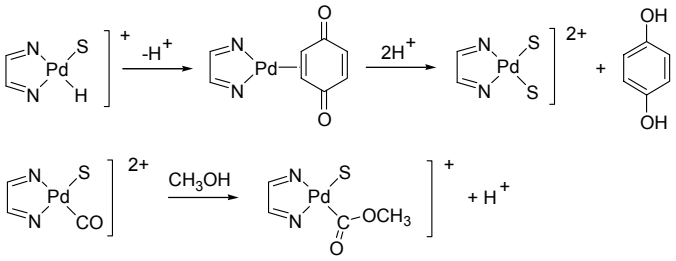

Figure 12.22. The role of quinone

Palladium(0) forms a complex with quinone that is now electron rich and can be protonated to give hydroquinone and palladium(II). The latter can start a new cycle via a carbomethoxy species after reaction with methanol and CO (c.f. reaction (6), Figure 12.4). Thus we have formally switched from a hydride initiator to a carbomethoxy initiator species. Addition of quinone to a non-active or moderately active palladium system is a diagnostic tool that tells us whether zerovalent palladium is involved as an inactive state. Likewise, one might add dihydrogen to a system to see whether palladium(II) salts need to be converted to a hydride to reactivate our dormant catalyst.

The styrene/CO polymers formed with palladium complexes of diimine ligands indeed contain ester and alkene end groups [65,66,67]. Slightly more ester end groups than alkene groups are formed, showing that in addition to β-hydride elimination some termination via methanolysis of acylpalladium chain ends occurs.

The polymers are highly regioregular, because always the electronically stabilised benzylic intermediates are formed (we avoid the indication 1,2 or 2,1 insertion, because formally styrene would be called 1-phenylethene, and thus our nomenclature for 1,2 or 2,1 insertion is the reverse of that for propene!). More surprising is that even the use of ligands having C_{2v} symmetry (i.e. they are non-chiral) a stereoregular polymer is obtained, with a prevailing syndiotactic structure containing 90% *u* dyads, or 80% *uu* triads. Clearly, when achiral C_{2v} ligands are used and a high percentage of *uu* triads is obtained, the polymerisation must be chain-end controlled.

The meaning of the notation *uu* should be explained. As there is never a (local) mirror plane or twofold axis expressing the relationship between two or three units in alkene/CO polymers, *meso* and *rac* cannot be applied. Instead one uses *u* and *l,* for *unlike* and *like. Unlike* means that two subsequent centres have different absolute configurations, thus they form a *syndiotactic* polymer, while *like* means that they have the same configuration and thus they form an *isotactic* polymer (see Figure 12.23).

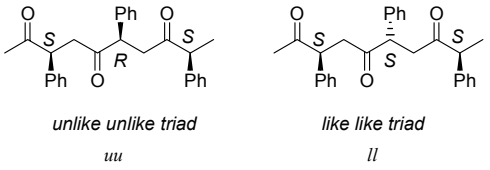

Figure 12.23. Stereochemistry in styrene-CO copolymer units

As the distance between the phenyl group of the coordinated styrene monomer and the phenyl group of the previously inserted one was thought to be relatively large, Drent and Budzelaar assumed that perhaps the chain would bend back to the palladium centre via coordination of the ketone group. Considering computer graphics and assuming a perpendicular arrangement of the acyl group the distance between previous alkene and next alkene is not very large and the weak interaction of ketone-palladium may not to be needed. Neither the back-bending nor the distant interaction can explain the exact stereochemical outcome.

The use of C_2 symmetric ligands changes the stereochemical outcome and now an isotactic polymer is produced [68,69,70]. Note in Figure 12.23 that in isotactic polymer the phenyl groups are at alternating sides of the stretched chain, which differs from polyolefins. Furthermore, unlike polypropylene, the isotactic polymer chain can be intrinsically chiral, because each unit –$CH_2CHPhC(O)$– is chiral. Even ideal structures of polypropylene are not chiral, because one can draw a mirror plane through each CH_2 or $CH(CH_3)$ group (for isotactic polymer), and a C_2 axis through a CH_2 group or a mirror plane through a $CH(CH_3)$ (for syndiotactic polymer) and thus the polymer molecules are not chiral (we disregard the end groups, the only ones making a difference, but this small chiral contribution is ineffective). If enantiomerically pure ligands are used for making isotactic polyketones only one enantiomer of the polymer may be obtained. In syndiotactic or atactic polymers the contributions of R and S units will cancel the optical activity, even though there is not a symmetry operation annihilating the chirality.

An effective group of ligands for obtaining isotactic polymer are C_2 symmetric bisoxazolines [68]. Since C_{2v} symmetric ligands gave syndiotactic

polymer via enantiospecific chain-end control, it is clear that for C_2 symmetric ligands enantiospecific site control must be the mechanism. Naturally, as we have seen in Chapter 10 for poly-alkenes, C_2 symmetric ligands create the same chirality at each site where the insertion may take place and the product is isotactic if site control is more effective than control by the chain. It can be imagined that the substituent (R=Me, iPr) at the oxazoline ring directs the aryl group of styrene such that an isotactic polymer is formed, irrespective the site we are looking at, because of the C_2 symmetry. An example of a catalyst giving polymer with main-chain chirality is shown in Figure 12.24.

The length of the oligomer chain plays a role in the stereospecificity, the presence of a few units in the initiating chain leads to an increase in diastereoselectivity, as was also found for growing propene oligomers. Thus, the hindrance between chain and metal catalyst contributes to the orientation of the phenyl substituent of the incoming styrene molecule.

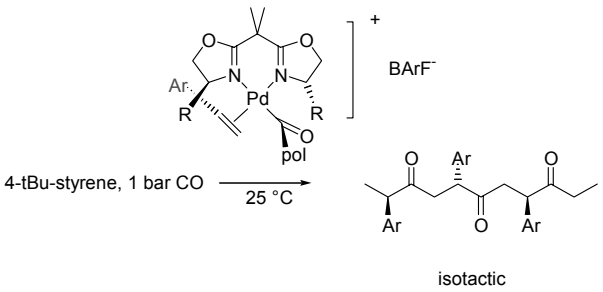

Figure 12.24. Chiral bisoxazoline complexes giving chiral 4-tBu-styrene/CO copolymers

At low temperature the polymerisation reaction for this system is living and a Poisson distribution rather than a Schulz-Flory one is obtained. This leads to the possibility of making a special type of block copolymers. The first block was grown with the bisoxazoline ligand yielding an isotactic block [71]. Subsequently, the ligand was replaced by the more strongly coordinating bipyridine which gave a syndiotactic block and a stereoblock polyketone was obtained (usually a block copolymer consists of two or more blocks of two different monomers lending different properties to the two blocks).

When the reaction is carried out with a racemic mixture of complexes, the product is a racemic mixture of the isotactic polymers. It was of interest to see what would happen if, after formation of a chiral block with one enantiomer of the bisoxazoline ligand, an equivalent of the other enantiomer was added. It was found that an excess of ligand changes the tacticity completely and the second block was syndiotactic! In these diimine palladium complexes exchange of ligand is relatively fast and it can often be observed on the NMR time scale as a broadening in the ^{1}H NMR spectra. The process may well be associative.

The explanation for the formation of syndiotactic polymer when ligand exchange occurs is as follows. After an insertion has led to the expected site-controlled stereo centre in the polymer chain, an exchange of ligand occurs and apparently the complex containing the other ligand enantiomer is more stable (or leads to a faster next insertion reaction), thereby producing the next stereo centre in the polymer chain with the opposite stereochemistry, and this way we form a syndiotactic polymer (or an atactic polymer [72]). When the reaction is carried out with an excess of enantiopure ligand the isotacticity is retained.

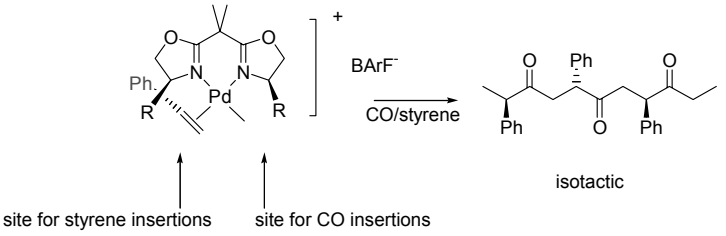

Figure 12.25. C_s meso ligands leading to isotactic copolymer

C_s ligands, the authors expected [72], should lead to syndiotactic polymer, because the mirror plane of the complex enhances insertions leading to alternation of the absolute configuration formed, similar to propene polymerisation and C_s meso ligands (chapter 10). One might expect that chain-end control and site control are strengthening the effect of one another and high stereoselectivities for syndiotactic polymer should be obtained. This is not the case and instead an isotactic polymer was found! If, however, an ideal alternating polymerisation would take place, CO will insert at one site, and styrene will always insert at the other, one and the same site. Styrene will always "see" the same enantiospecific site and thus an isotactic polymer should form, see Figure 12.25 for a simple representation. Rotation of the meso ligand reverses the stereochemistry and although this rotation is often fast compared to the rate of polymerisation, the isotacticity found contradicts this for this system. An excess of the meso ligand does lead to syndiotactic polymer showing the effect of ligand exchange or excess ligand induced rotation.

References

1 Sen, A. *Catalytic Synthesis of Alkene-Carbon Monoxide Copolymers and Cooligmers*. Catalysis by Metal Complexes, Volume 27. Kluwer AP, Dordrecht, **2003**.
2 Ash, C. E. *J. Mater. Educ.* **1994**, *16*, 1.
3 Brubaker, M. M. U.S. Patent 2,495,286, **1950**.
4 Reppe, W.; Magin, A. U.S. Patent 2,577,208, **1951**. *Chem. Abstr.* **1952**, *46*, 6143.
5 Gough, A. British Pat. 1,081,304, 1967; *Chem. Abstr*. **1967**, *67*, 100569.

6 Fenton, D. M. U.S. Pat. 3,530,109, 1970; *Chem. Abstr*. **1970**, *73*, 110466; U.S. Pat. 4,076,911, 1978; *Chem. Abstr*. **1978**, *88,* 153263.
7 Nozaki, K. U.S. Pat. 3,689,460, 1972; *Chem. Abstr*. **1972**, *77*, 152860; U.S. Pat. 3,694,412, 1972; *Chem. Abstr*. **1972**, *77*, 165324; U.S. Pat. 3,835,123, 1974; *Chem. Abstr*. **1975**, *83*, 132273.
8 Sen, A.; Lai, T. W. *J. Am. Chem. Soc*. **1982**, *104*, 3520. Lai, T. W.; Sen, A. *Organometallics* **1984**, *3*, 866. Sen, A.; Brumbaugh, J. S. J. *Organomet. Chem.* **1985**, *279*, C5. Sen, A. *ChemTech* **1986**, 48.
9 Drent, E. Eur. Pat. Appl. 121,965, 1984; *Chem. Abstr.* **1985**, *102,* 46423. Drent, E. *Pure Appl. Chem.* **1990**, *62,* 661. Drent, E. Eur. Pat. Appl. 229408, 1986; *Chem. Abstr.* **1988**, *108*, 6617. Drent, E. Eur. Pat. Appl. 399617, 1990; C*hem. Abstr.* **1991**, *114*, 165108. Drent, E.; van Broekhoven, J. A. M.; Doyle, M. J. *J. Organomet. Chem.* **1991**, *417*, 235. Drent, E.; Budzelaar, P. H. M. *Chem. Rev.* **1996**, *96,* 663.
10 Klabunde, U.; Tulip, T. H.; Roe, D. C.; Ittel, S. D. *J. Organomet. Chem.* **1987**, *334*, 141.
11 Driessen, B.; Green, M. J.; Keim, W. Eur. Pat. Appl. 470,759, 1992. *Chem. Abstr*. **1992**, *116*, 152623. Keim, W.; Maas, H.; Mecking, S. *Z. Naturforsch.* **1995**, *50b*, 430.
12 van Leeuwen, P. W. N. M.; Roobeek, C. F. Eur. Pat. Appl. 380,162, 1989. Van Leeuwen, P. W. N. M.; Roobeek, C. F.; Wong, P. K. Eur. Pat. Appl. 393,790, 1990; *Chem. Abstr*. **1991**, *114*, 103034.
13 Dekker, G. P. C. M.; Elsevier, C. J.; Vrieze, K.; van Leeuwen, P. W. N. M. *J. Organomet. Chem.* **1992**, *430*, 357.
14 Rülke, R. E.; Han, I. M.; Elsevier, C. J.; Vrieze, K.; Van Leeuwen, P. W. N. M.; Roobeek, C. F.; Zoutberg, M. C.; Wang, Y. F.; Stam, C. H. *Inorg. Chim. Acta,* **1990***, 169*, 5.
15 Shultz, C. S.; Ledfort, J.; DeSimone, J. M.; Brookhart, M. *J. Am. Chem. Soc.* **2000***, 122*, 6351.
16 Anderson, G. K.; Cross, R. J. *Acc. Chem. Res.* **1984**, *17*, 67.
17 Mawby, R.J.; Basolo F.; Pearson, R.G. *J. Am. Chem. Soc.* **1964**, *86,* 5043. Noack, K.; Calderazzo, F. *J. Organometal. Chem.* **1967**, *10*, 101. Flood, T.C.; Jensen, J.E.; Statler, J.A. *J. Am. Chem. Soc.* **1981**, *103*, 4410.
18 van Leeuwen, P. W. N. M.; Roobeek, C. F.; van der Heijden, H. *J. Am. Chem. Soc.* **1994**, *116*, 12117. van Leeuwen, P. W. N. M.; Roobeek, C. F.; *Recl. Trav. Chim. Pays-Bas*, **1995**, *114*, 61.
19 Koga, N.; Morokuma, K. *Chem. Rev*. **1991**, *91*, 823. Versluis, L.; Ziegler, T.; Baerends, E. J.; Ravenek, W. *J. Am. Chem. Soc.* **1989**, *111*, 2018. Axe, F. U.; Marynick, D. S. *J. Am. Chem. Soc.* **1988**, *110*, 3728. Berke, H.; Hoffmann, R. *J. Am. Chem. Soc.* **1978**, *100*, 7224.
20 Dekker, G. P. C. M.; Buijs, A.; Elsevier, C. J.; Vrieze, K.; van Leeuwen, P. W. N. M.; Smeets, W. J. J.; Spek, A. L.; Wang, Y. F.; Stam, C. H. *Organometallics,* **1992***, 11*, 1937.
21 de Graaf, W.; Boersma, J.; van Koten, G. *Organometallics* **1990**, *9,* 1479. Rülke, R. E.; Han, I. M.; Elsevier, C. J.; Vrieze, K.; van Leeuwen, P. W. N. M.; Roobeek, C. F.; Zoutberg, M. C.; Wang, Y. F.; Stam, C. H. *Inorg. Chim. Acta* **1990**, *169*, 5. Markies, B. A.; Wijkens, P.; Boersma, J.; Spek, A. L.; van Koten, G. *Recl. Trav. Chim. Pays-Bas* **1991**, *110*, 133.
22 Brookhart, M.; Rix, F. C.; DeSimone, J. M.; Barborak, J. C. *J. Am. Chem. Soc.* **1992**, *114*, 5894.
23 Dekker, G. P. C. M.; Elsevier, C. J.; Vrieze, K.; van Leeuwen, P. W. N. M. *Organometallics*, **1992**, *11*, 1598.
24 Ledford, J.; Shultz, C. S.; Gates, D. P.; White, P. S.; DeSimone, J. M.; Brookhart, M. *Organometallics*, **2001**, *20*, 5266. Shultz, C. S.; Ledford, J.; DeSimone, J. M.; Brookhart, M. *J. Am. Chem. Soc.* **2000**, *122,* 6351.

25 Kawabata, Y.; Hayashi, T; Ogata, I. *J. Chem. Soc. Chem. Commun.* **1979**, 462. Kawabata, Y.; Hayashi, T; Isoyama, T.; Ogata, I. *Bull. Chem. Soc. Jpn.* **1981**, *54*, 3438.
26 Sugi, Y.; Bando, K. *Chem. Lett.* **1976**, 727.
27 Brumbaugh, J. S.; Whittle, R. R.; Parvez, M.; Sen, A. *Organometallics* **1990,** *9*, 1735. Yamamura, M.; Moritani, I.; Murahashi, S.I. *Chem. Lett.* **1974**, 1423.
28 Dekker, G. P. C. M.; Elsevier, C. J.; Vrieze, K.; van Leeuwen, P. W. N. M. *Organometallics*, **1992**, *11,* 1598. Sanger, A. R. *J. Chem. Soc. Dalton Trans.* **1979**, 1971. Scrivanti, A.; Botteghi, C.; Toniolo, L.; Berton, A. *J. Organomet. Chem.* **1988***, 334,* 261. Knight, J. G.; Doherty, S.; Harriman, A.; Robins, E. G.; Betham, M.; Eastham, G. R.; Tooze, R. P.; Elsegood, M. R. J.; Champkin, P.; Clegg, W. *Organometallics*, **2000,** *19*, 4957.
29 Dossett, S. J.; Gillon, A.; Orpen, A. G.; Fleming, J. S.; Pringle, P. G.; Wass, D. F.; Jones, M. D. *Chem. Commun.,* **2001**, 699.
30 Balch, A. L. In *Homogeneous Catalysis with Metal Phosphine Complexes*; Pignolet, L. H. Ed., Plenum: New York, **1983**; pp 167-213.
31 Vetter, W. M.; Sen, A. *J. Organomet. Chem.* **1989**, *378*, 485. Catellani, M.; Chiusoli, G. P.; Castagnoli, C. *J. Organomet. Chem.* **1991**, *407*, C30. Li, C. S.; Cheng, C. H.; Liao, F. L.; Wang, S. L. *J. Chem. Soc., Chem. Commun.* **1991**, 710. Ozawa, F.; Hayashi, T.; Koide, H.; Yamamoto, A. *J. Chem. Soc., Chem. Commun.* **1991**, 1469. Markies, B. A.; Rietveld, M. H. P.; Boersma, J.; Spek, A. L. van Koten, G. *J. Organomet. Chem.* **1992**, *424*, C12.
32 van Asselt, R.; Gielens, E. E. C. G.; Rülke, R. E.; Elsevier, C. J. *J. Chem. Soc., Chem. Commun.* **1993**, 1203 and *J. Am. Chem. Soc.* **1994**, *116*, 977.
33 Rix, F. C.; Brookhart, M.; White, P. S. *J. Am. Chem. Soc.* **1996**, *118,* 4746.
34 Mul, W. P.; Drent, E.; Jansens, P. J.; Kramer, A. H.; Sonnemans, M. H. W. *J. Am. Chem. Soc.* **2001**, *123*, 5350.
35 Zuideveld, M. A.; Kamer, P. C. J.; van Leeuwen, P. W. N. M. *Organometallics* **2004***, 23*.
36 Houlis, J. F.; Roddick, D. M. *J. Am. Chem. Soc.* **1998***, 120,* 11020. Bennett, B. L.; Hoerter, J. M.; Houlis, J. F.; Roddick, D. M. *Organometallics* **2000**, *19*, 615.
37 Zudin, V. N.; Chinakov, V. D.; Nekipelov, V. M.; Rokov, V. A.; Likholobov, Y. I.; Yermakov, Y. I. *J. Mol. Catal.* **1989***, 52*, 27.
38 Zuideveld, M. A.; Kamer, P. C. J.; van Leeuwen, P. W. N. M.; Klusener, P. A. A.; Stil, H. A.; Roobeek, C. F. *J. Am. Chem. Soc.* **1998**, *120*, 7977.
39 Drent, E.; Jager, W. W. U.S. Pat. 5,780,684, **1998** (to Shell); *Chem. Abstr.* **1998**, *129*, 137605. Drent, E.; Budzelaar, P. H. M. *J. Organomet. Chem.* **2000***, 593*, 211.
40 Jiang, Z.; Sen, A. *Macromolecules*, **1994**, *27*, 7215.
41 Miller, K. J.; Kitagawa, T. T.; Abu-Omar, M. M. *Organometallics,* **2001***, 20*, 4403.
42 van Leeuwen, P. W. N. M.; Zuideveld, M. A.; Swennenhuis, B. H. G.; Freixa, Z.; Kamer, P. C. J.; Goubitz, K.; Fraanje, J.; Lutz, M.; Spek, A. L. *J. Am. Chem. Soc.* **2003**, *125*, 5523.
43 Verspui, G.; Papadogianakis, G.; Sheldon, R. A. *J. Chem. Soc., Chem. Commun.* **1998**, 401. Verspui, G.; Schanssema, F.; Sheldon, R. A. *Angew. Chem. Int. Ed.* **2000***, 39*, 804.
44 Del Rio, I.; Claver, C.; Van Leeuwen, P. W. N. M. *Eur. J. Inorg. Chem.* **2001**, 2719.
45 Clegg, W.; Eastham, G. R.; Elsegood, M. R. J.; Heaton, B. T.; Iggo, J. A.; Tooze, R. P.; Whyman, R.; Zacchini, S. *Organometallics,* **2002***, 21*, 1832. Knight, J. G.; Doherty, S.; Harriman, A.; Robins, E. G.; Betham, M.; Eastham, G. R.; Tooze, R. P.; Elsegood, M. R. J.; Champkin, P.A.; Clegg, W. *Organometallics* **2000**, *19*, 4957. Clegg, W.; Eastham, G. R.; Elsegood, M. R. J.; Tooze, R. P.; Wang, X. L.; Whiston, K. *Chem. Commun*. **1999**, 1877.
46 Portnoy, M.; Milstein, D. *Organometallics* **1994**, *13*, 600. Zudin, V. N.; Chinakov, V. D.; Nekipelov, V. M.; Likholobov, V. A.; Yermakov, Y. I. *J. Organomet. Chem.* **1985**, *289*, 425.

47 Freixa, Z.; Beentjes, M. A.; Batema, G. D.; Dieleman, C. B.; van Strijdonck, G. P. F.; Reek, J. N. H.; Kamer, P. C. J.; van Leeuwen, P. W. N. M. *Angew. Chem. Int. Ed.* **2003,** *42*, 1284.
48 Calhorda, M. J.; Brown, J. M.; Cooley, N. A. *Organometallics,* **1991***, 10*, 1431.
49 Widenhoefer, R. A.; Buchwald, S. L. *J. Am. Chem. Soc.* **1998***, 120*, 6504.
50 Mann, G.; Baranano, D.; Hartwig, J. F.; Rheingold, A. L.; Guzei, I. A. *J. Am. Chem. Soc.* **1998***, 120*, 9205.
51 Fitton, P.; Rick, E. A. *J. Organomet. Chem.* **1971***, 28,* 287.
52 Dossett, S. J. PCT Int. Appl. WO 9737765, 1997 (to BP Chemicals). *Chem. Abstr.* **1997**, *127*, 319387. Dossett, S. J.; Gillon, A.; Orpen, A. G.; Fleming, J. S.; Pringle, P. G.; Wass, D. F.; Jones, M. D. *Chem. Commun*. **2001**, 699.
53 Drent, E.; Kragtwijk, E. Eur. Pat. EP 495,548, 1992 (to Shell). Pugh, R. I.; Drent, E. *Adv. Synth. Catal.* **2002**, *344***,** 815**.**
54 Pugh, R. I.; Drent, E.; Pringle, P. G. *Chem. Commun.* **2001**, 1476.
55 Portnoy, M.; Frolow, F.; Milstein, D. *Organometallics* **1991**, *10*, 3960. Milstein, D. *Acc. Chem. Res.* **1988***, 21*, 428. Milstein, D.; Stille, J. K. *J. Am. Chem. Soc.* **1979***, 101*, 4981. Fenton, D. M. *J. Org. Chem.* **1973**, *38*, 3192. Knifton, J. *J. Org. Chem.* **1976**, *41*, 2885. Tsuji, J. *Organic Synthesis with Palladium Compounds*, Springer-Verlag, New York, **1980**. Heck, R. F. *Palladium Reagents in Organic Synthesis,* Academic Press, New York, **1985**.
56 Vavasori, A.; Cavinato, G.; Toniolo, L. *J. Mol. Catal. A: Chem.* **2001***, 176*, 11.
57 Methyl methacrylate may form an exception, although this is still subject to debate. Methyl methacrylate is made from propyne via methoxycarbonylation and the initiation is thought to take place at a carbomethoxypalladium species. Drent, E.; Arnoldy, P.; Budzelaar, P. H. M. *J. Organomet. Chem.* **1993**, *455*, 247. Kron, T. E.; Terekhova, M. I.; Noskov, Yu. G.; Petrov, E. S. *Kinet. Catal.* **2001**, *42,* 182. Drent, E.; Arnoldy, P.; Budzelaar, P. H. M. *J. Organomet. Chem.* **1994**, *475*, 57. Keijsper, J. J.; Arnoldy, P.; Doyle, M. J.; Drent, E. *Recl. Trav. Chim. Pays-Bas* **1996**, *115*, 248. Scrivanti, A.; Beghetto, V.; Campagna, E.; Zanato M.; Matteoli, U. *Organometallics*, **1998**, *17*, 630.
58 Tóth, I.; Elsevier, C. J. *J. Chem. Soc., Chem. Commun.* **1993**, 529.
59 Marcone, J. E.; Moloy, K. G. *J. Am. Chem. Soc.* **1998**, *120*, 8527.
60 Del Rio, I.; Claver, C.; Van Leeuwen, P. W. N. M. *Eur. J. Inorg. Chem.* **2001***,* 2719.
61 Noskov, Y. G.; Petrov, E. S. *Kinet. Catal.* **1997**, *38*, 520.
62 Milani, B.; Anzilutti, A.; Vicentini, L.; Sessanta o Santini, A.; Zangrando, E.; Geremia, S.; Mestroni, G. *Organometallics* **1997**, *16*, 5064.
63 Papadogianakis, G.; Verspui, G.; Maat, L.; Sheldon, R. A. *Catal. Lett.* **1997***, 47,* 43.
64 Schreuder Goedheijt, M.; Reek, J. N. H.; Kamer, P. C. J.; van Leeuwen, P. W. N. M. *Chem. Commun*. **1998**, 2431.
65 Pisano, C.; Mezzetti, A.; Consiglio, G. *Organometallics* **1992***, 11*, 20.
66 Drent, E. Eur. Pat. Appl. 229,408, **1988** (to Shell). *Chem. Abstr.* **1988**, *108,* 6617.
67 Busico, V.; Corradini, P.; Landriani, L.; Trifuoggi, M. *Makromol. Chem. Rapid Commun*. **1993**, *14*, 261. Barsacchi, M.; Consiglio, G.; Medici, L.; Petrucci, G.; Suter, U. W. *Angew. Chem. Int. Ed.* **1991**, *30*, 989.
68 Brookhart, M.; Wagner, M. I.; Balavoine, G. G. A.; Haddou, H. A. *J. Am. Chem. Soc.* **1994**, *116*, 3641.
69 Bartolini, S.; Carfagna, C.; Musco, A. *Macromol. Rapid Commun.* **1995***, 16,* 9.
70 Reetz. M. T.; Haderlein, G.; Angermund, K. *J. Am. Chem. Soc.* **2000**, *122*, 996.
71 Brookhart, M.; Wagner, M. I.. *J. Am. Chem. Soc.* **1996**, *118*, 7219.
72 Gsponer, A.; Milani, B.; Consiglio, G. *Helv. Chim. Acta,* **2002**, *85,* 4074.

Chapter 13

PALLADIUM CATALYSED CROSS-COUPLING REACTIONS

The new workhorse for organic synthesis

13.1 Introduction

The making of carbon-to-carbon bonds from carbocations and carbanions is a straightforward and simple reaction. Easily accessible carbanions are Grignard reagents RMgBr and lithium reagents RLi. They can be conveniently obtained from the halides RBr or RCl and the metals Mg and Li. They are both highly reactive materials, for instance with respect to water. *The thermodynamic driving force for the formation of such reactive materials and their subsequent reactions is the formation of metal halides.*

The reactions of these carbon centred anions with polar compounds such as esters, ketones, and metal chlorides are indeed very specific and give high yields. The reaction of Grignard reagents with alkyl or aryl halides, however, is extremely slow giving many side-products, if anything happens at all. Note that this is also the key to the success of preparing Grignard type reagents(!), otherwise the partially formed RMgBr would react with the starting material RBr still present to give the "homocoupled" R-R. Exceptions are allylic and benzylic halides which react very fast amongst themselves during their synthesis. The Grignard reagents of this structure require specific practical procedures otherwise the homocoupled species are formed.

Reactions that can be expected for the reaction of an alkyl halide and a metal alkyl are depicted in Figure 13.1. The reaction may require several days at room temperature or may proceed in a few minutes, depending on the nature of the species. Many by-products may be formed. First a metal-halide exchange may occur. The resulting exchange products can give coupling products as well. Secondly, elimination reactions instead of C-C coupling can occur. Also, a radical reaction may take place. In summary, the yield and selectivity of this simple reaction will be surprisingly low. Only if a Grignard reagent is used in a

coupling reaction with compounds that contain electrophilic carbon atoms, such as esters, ketones, and hetero-atom halides, the direct use of Grignard reagents (and related reagents) leads to high coupling efficiencies.

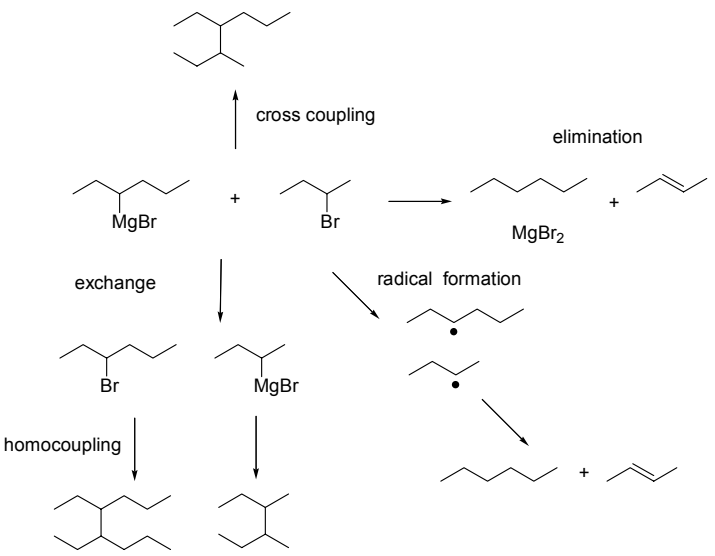

Figure 13.1. Products formed in a coupling reaction of a Grignard reagent and an alkyl halide

Thus, this reaction was of limited practical value until the transition metal catalysed cross-coupling reaction became known. Ever since, the "cross-coupling" reaction has found wide application in organic synthesis both in the laboratory and in industry. One might state that in any multi-step sequence for making an organic chemical, one of the steps involves a transition metal catalysed coupling reaction! The transition metal catalysts are usually based on palladium and sometimes nickel. In addition to organomagnesium and organolithium a great variety of organometallic precursors can be used. Also, many precursors can serve as starting materials for the carbocation. Last but not least, the ligand on the transition metal plays an important role in determining the rate and selectivity of the reaction. Here we will present only the main scheme and take palladium as the catalyst example, although many more metals have been found to be very useful. The reactions to be discussed are: allylic alkylation, Heck reaction, cross-coupling, and Suzuki reaction, a variant of the latter. Initially the cross-coupling chemistry focussed on carbon-to-carbon bond formation but in the last decade it has become also extremely useful for making carbon-to-heteroatom bonds. The organyl halide (or other anion used) involves in general an aryl, vinyl, or allylic species.

13.2 Allylic alkylation

The palladium-catalysed allylic alkylation has become a very important tool for organic chemists. It has been developed largely by Trost [1]. The allylic substitution in simple allylpalladium chloride was published by Tsuji [1]. At present there are numerous examples in the literature. The reagents used are all very mild and are compatible with many functional groups. The method has been applied in the synthesis of many complex organic molecules [2]. During the reaction a new carbon-carbon bond is formed and the resulting molecule still contains a double bond that might be used for further derivatisation. This is not the place to review all these reactions and we will concentrate on the simple model reactions.

The reaction starts with an oxidative addition of an allylic compound to palladium(0) and a π-allyl-palladium complex forms. Carboxylates, allyl halides, etc. can be used. In practice one often starts with divalent palladium sources, which require in situ reduction. This reduction can take place in several ways, it may involve the alkene, the nucleophile, or the phosphine ligand added. One can start from zerovalent palladium complexes, but very stable palladium(0) complexes may also require an incubation period. Good starting materials are the π-allyl-palladium intermediates!

At first we will consider triphenylphosphine L as the ligand, but in practice many other ligands are used as large ligand influences have been detected. If the ligands are L and X, as shown in Figure 13.2, the allyl fragment becomes "asymmetric" as a result of the different *trans* influences of X and L. The carbon atom *cis* to L (when L=phosphine) has more sp^3 character, while the other two carbon atoms adopt more sp^2 character and form a bond with double bond character. In brackets the π–σ bonding mode is depicted in Figure 13.2.

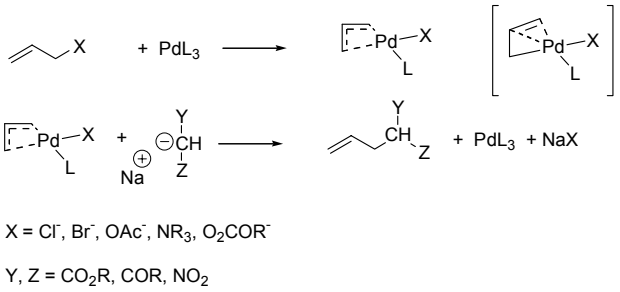

Figure 13.2. Palladium catalysed allylic alkylation

Formally, the allyl group is an anion in this complex, but owing to the high electrophilicity of palladium, the allyl group undergoes attack by nucleophilic reagents, especially soft nucleophiles. After this attack, palladium(0) "leaves" the allyl group and the product is obtained. (We say "leaves", because indeed in

terms of organic chemistry palladium(0) is a good "leaving group", taking the electrons with it). Palladium zero can re-enter the cycle and hence the reaction is catalytic in palladium. As a side-product a salt is formed. For small-scale industrial applications it is no problem to make salts in stoichiometric amounts. The un-catalysed reaction would produce the same amount of salt, but the aim is to make the catalytic reaction more selective and faster. The mechanism and a few examples of reagents are shown in Figure 13.2.

Regioselectivity can be high in this reaction and depends on the ligand used. Ligand effects can ensure substitution at the allylic carbon carrying one or two carbon substituents, or just the reverse. When a diphosphine ligand is used and a hexenyl group instead of the allyl group substitution occurs mainly at the terminal carbon, see Figure 13.3. Steric and electronic effects are opposing in this reaction. Sterically, attack at the unsubstituted carbon is favoured (linear product), but the substituted carbon is electronically favoured (the asymmetric, branched product), because it is more electrophilic. Electronic differentiation can also result from steric distortions brought about by the ligand.

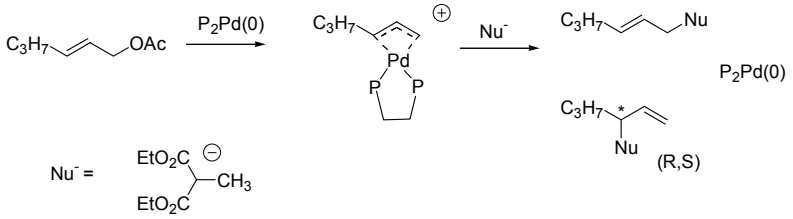

Figure 13.3. Regioselectivity in allylic alkylation

Nucleophilic attack at the substituted carbon atom (Figure 13.3) leads to chiral products. The enantioselective application of this reaction has received wide-spread attention in the last decade, after the important developments reported by Trost, using C_2 symmetric diphosphines, and the introduction of C_1 chiral ligands for this reaction by Helmchen, Pfaltz, and Williams. The stereochemistry of π-allylpalladium complexes is complicated and a source of errors. The π-allyl group can undergo two types of rearrangements: (1) a left-right interchange (called π-rotation) during which the palladium atom remains bonded to the same face of the allyl group, but the trans influences reverse, (2) a π–σ reaction during which a σ-bond is formed at one end and the face of the π-alkene part that co-ordinates to palladium changes. The π-rotation reaction is depicted in Figure 13.4. Mechanistically, it often involves the association with another nucleophilic ligand, which facilitates rotation in the quasi five-co-ordinate species. The two compounds are enantiomers, but note that the absolute configuration of the terminal carbon atoms remains the same during the rotation.

Figure 13.4. The π-rotation reaction in π-allylpalladium compounds

The π–σ reaction is shown in Figure 13.5, with the allyl groups now positioned behind the palladium atom. The first reaction shows the formation of a σ-bond at the unsubstituted carbon of the η^3-butenyl group, the fastest rearrangement in this complex. The alkene group dissociates and reattaches to palladium at the opposite face via rotation around the sp^3 C1-C2 bond. The absolute configuration at the substituted carbon atom is now reversed. In the second reaction the σ-bond is formed at the substituted carbon atom and after reattachment the allyl group again points into the other direction. The absolute configuration of the carbon atom is retained, as we did not break any bond of carbon-A (Figure 13.5), and the CIP rules give the same result. It is seen that the methyl substituent has moved from a *syn* position into an *anti* position and we have obtained another isomer of the complex. For the dimethyl substituted allylpalladium complex we see that any π–σ reaction will reverse the absolute configuration of one carbon atom and interchange *syn* and *anti* groups at the other carbon. The latter interchange also occurred in the first reaction, but since both substituents here were hydrogen atoms it was not productive. These reactions can be nicely studied in ^{1}H NMR line-broadening measurements. Note that in a mixed *syn-anti* complex both carbon atoms have the same absolute configuration.

This is interesting for enantiospecific reactions, because attack at either carbon atom leads to the same enantiomer!

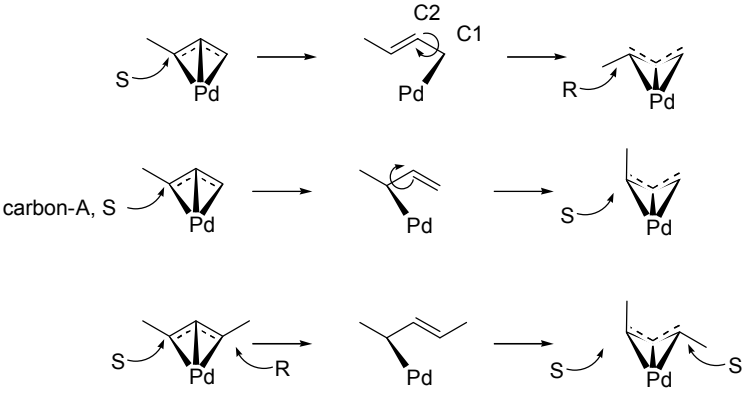

Figure 13.5. Examples of π–σ reactions (R and S denote absolute configurations)

The model substrate studied most often in enantiospecific catalysis is the symmetrically 1,3-diphenyl substituted allylpalladium complex shown in Figure 13.6. The hindrance that the two phenyl substituents at carbons 1 and 3 of the allyl fragment experience from the metal-ligand complex, is different under the influence of the C_2 chiral ligand. Without the C_2 chiral ligand, carbon atoms 1 and 3 are mirror images; palladium is attached to the "local" *re* and *si* face. The C_2 chiral ligand makes the carbon atoms 1 and 3 diastereotopic, i.e. they are chemically different. The steric distortion can create an electronic difference between the two carbon atoms, giving rise to a π–σ bonding mode, as mentioned above for X-L substituted palladium complexes. As a result one specific carbon atom (carbon-1 in Figure 13.6) undergoes selective attack by the nucleophile. This way a chiral compound is obtained. This charge control, or rather nucleophilicity control, will be especially important if the substitution reaction has an early transition state.

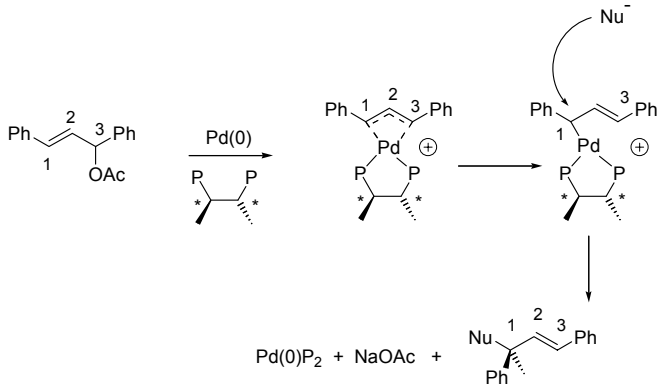

Figure 13.6. Asymmetric Allylic Alkylation, AAA

The interesting aspect of the C_2 symmetric ligand is that the mode of coordination of the allyl group with central carbon-2 pointing up or down is indifferent to the outcome, because these two structures are one and the same. Note that attack at carbon-1 gives one enantiomer, while attack at carbon-3 gives the opposite enantiomer. As mentioned above, in a *syn-anti* complex carrying two identical substituents, such as the phenyl groups shown here, carbon atom-1 and carbon atom-3 have the same absolute configuration and thus attack at both atoms leads to the same enantiomer. This presents another interesting approach to enantioselectivity in allyl compounds.

Mechanistic explanations are still subject to debate. It is well known that π-allylpalladium compounds may show distortions such that one end of the allyl group assumes a σ-character, while the other part assumes a π-character. The differentiation between C-1 and C-3 is due to the different steric interaction

with the C_2 symmetric ligand; the resulting Pd-C distances lead to a σ–π character in the allyl moiety. If the attack were a pure S_N2 attack, the nucleophile reacts at the σ-carbon atom, as has been argued, but one can also imagine that the attack takes place at the most electrophilic carbon atom, which is the one having the highest π-character. In P-N ligands, where we can easily differentiate the carbon atoms in the complex, the attack is known to proceed at the carbon atom having π-character (see below).

A great variety of ligands have been used. Trost [3] has been especially successful using chiral bidentate phosphines with a very wide bite angle (110°), see Figure 13.7. A variety of chiral 1,2-diamines connected to 2-diphenylphosphinobenzoic acid were used. These ligands "embrace" the metal and thus exert a steric influence on the allyl group. Even substrates carrying small substituents can now be enantiospecifically substituted.

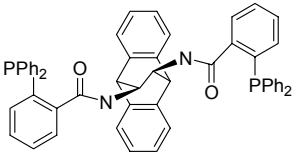

Figure 13.7. One of Trost's ligands for AAA

Realising that the bite angle was important in these ligands, a chiral ligand in the Xantphos series has been developed [4], which contains the phospholane moiety discovered by Burk as the chiral entity (Fig. 13.8). This ligand turned out to be very useful in several common allylic substitution reactions (1,3-dimethylallyl, 1,3-diphenylallyl, cyclohex-2-ene-1-yl) and kinetic resolution.

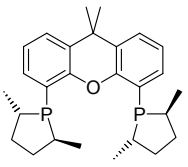

Figure 13.8. A Xantphos based chiral bidentate ligand

In this paper [4] the authors propose that the catalyst's resting states, the isomeric and diastereomeric π-allyl complexes, may not be important. Often rapid equilibria exist in π-allylpalladium complexes (Figures 13.4 and 13.5) and the transition state of any of these in the product-forming reaction determines the stereochemical outcome (Curtin-Hammett conditions). During the nucleophilic attack the allyl group undergoes a rotation, eventually forming a π-complex containing the alkene product. It was concluded that the steric

interactions associated with the synchronous events of nucleophilic attack and rotation are responsible for the chiral recognition [5]. This mechanism involves a late transition state as opposed to the electronically controlled reaction mentioned above.

The mechanism is illustrated in Figure 13.9. Nucleophilic attack leads to rotation and formation of the π-alkene complex. The left-hand structure will undergo a counter clockwise rotation and experience large steric hindrance. The clockwise rotation on the right leads to a much more favourable situation.

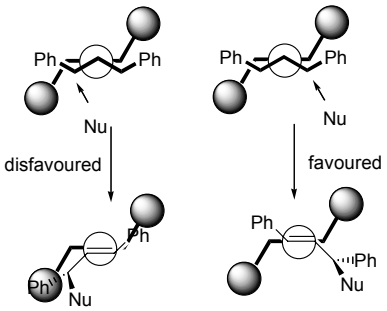

Figure 13.9. The rotation mechanism; spheres referring to steric hindrance by ligand [5]

Another interesting feature is that of kinetic resolution. The starting 1,3-diphenylallylic halide or acetate is a racemic mixture. Its reaction with palladium zero is exactly the reverse of the product forming reaction, which means that also during the oxidative addition of the acetate to the chiral ligand complex of palladium(0) the reaction may be enantiospecific. (Since the acetate leaving group and the attacking nucleophile are not the same, there will be differences in the reaction profiles.) If one enantiomer reacts faster than the other, the remaining starting material becomes enriched in one enantiomer. This is called kinetic resolution and it has been observed for this reaction [4,5].

When the allyl group is part of a cyclic structure, a π–σ reaction cannot take place to epimerise one of the chiral carbon atoms; after having formed the π–σ intermediate, the same π–face comes back-on to palladium. Thus, if we start from a racemic cyclic alkenyl acetate mixture, racemisation at the complex is blocked and the product will also be a racemate at 100% conversion. Kinetic resolution is still an option to obtain chiral product and starting material. Nevertheless high ee's were obtained when cyclic alkenyl acetates were used.

The explanation given is that allyl transfer takes place from palladium(II) to a palladium(0) species [6], which changes the face co-ordinated to palladium! See Figure 13.10. If now a chiral diphosphine is present, one of the routes for nucleophilic attack may be faster and selectively only one enantiomer may form [4].

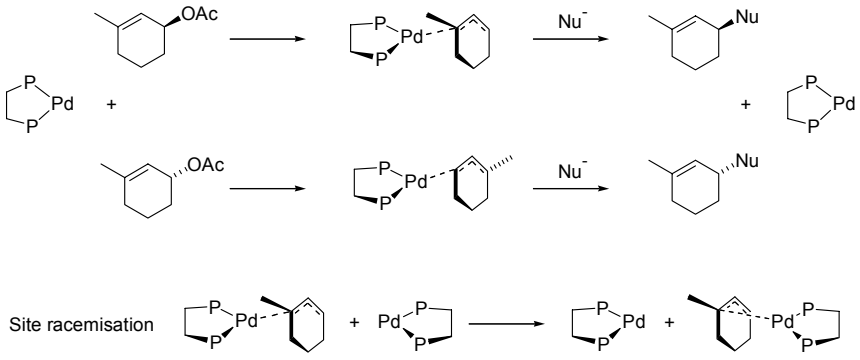

Figure 13.10. Cyclic allyl complexes and their reactions

For η^3-cyclohex-2-en-1-ylpalladium complexes the situation is different, because the allyl fragment has a plane of symmetry and the substrate is "symmetrised" during the addition reaction. Using chiral ligands one can obtain enantioselectivity (Fig. 13.11) and for a C_2 symmetric bidentate ligand this will always be the case. Note that π-rotation leaves the molecule unchanged, because of the C_2 axis in the ligand. The allyl group has C_S symmetry (it does not contain a chiral element) and thus the total complex forms only one enantiomer, when an optically pure ligand is used.

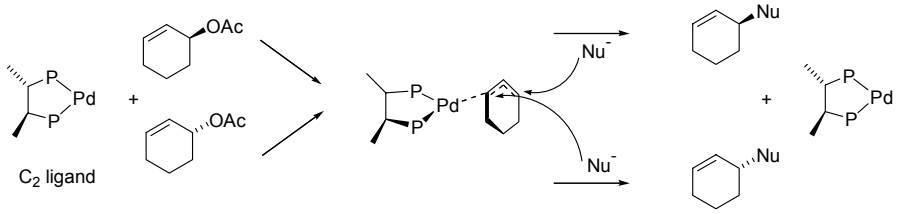

Figure 13.11. Enantioselection in cyclohex-2-en-1-yl substitution

For C_1 bidentate ligand systems there may be exceptions to this explanation, which have been called memory effects [7]. That is to say, the cyclohex-2-en-1-ylpalladium complex "remembers" whether it was formed from the R or the S isomer of the starting acetate! Thus the R enantiomer is transformed preferably into the R product (neglecting changes in the atom counting in the CIP rules), and the same for S, because the reaction sequence involves two reversions of configuration.

The C_1 bidentate ligand system may be as simple as a chiral monophosphine and a chloride ion, as shown in Figure 13.12. Suppose that in a P-X ligand system the nucleophilic attack takes place at the position trans to the phosphine, then we expect on the basis of micro reversibility that also the

attack of palladium at the cyclohex-2-ene-1-yl acetate will take place in such a fashion that the leaving acetate is positioned trans to the phosphine ligand. Thus, the nucleophile will enter at the same carbon, from the same outer sphere direction and thus the absolute configuration of the substrate will be retained. There is one further complication in this system, and that is that the system is not indifferent to π-rotation; allyl "up" and allyl "down" are different isomers, usually called *endo* and *exo*, with reference to some part of the ligand if this is a bidentate (e.g. for the P-N ligands shown in Figure 13.14). If *exo* and *endo* isomers would have the same energies the retention mechanism would cancel. The steric interaction can be increased to such an extent that one pathway will dominate and a memory effect may be observed.

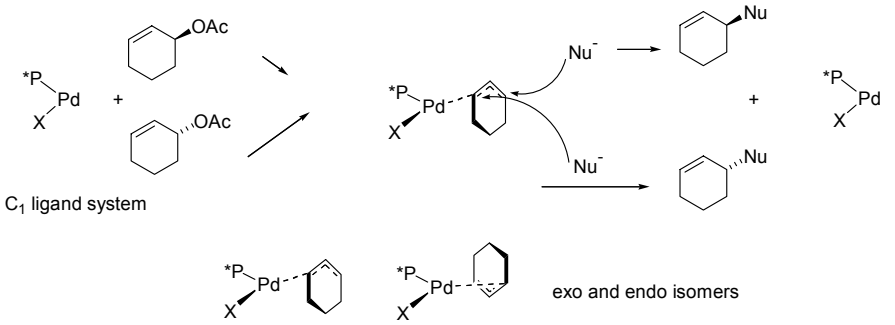

Figure 13.12. Example of a memory effect in AAA

An enormous variety of ligands have been applied to AAA, too many to mention. We will mention only two more groups of ligands, bisoxazolines and PHOX ligands. Bisoxazolines have been studied and reviewed by Pfaltz [8]. They are also C_2 symmetric bidentate ligands (Fig. 13.13) and the R-group can be easily varied to search for optimal rates and ee's.

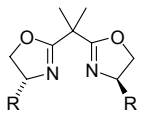

Figure 13.13. Chiral bisoxazoline ligands

The benefits of C_2-symmetry are due to the reduction of the number of possible catalyst-substrate isomers that may form, and the number of enantiospecific pathways (Helmchen, Pfaltz [9]). As they reasoned, there is no fundamental reason why a C_2-symmetric ligand is superior *qualitate qua* to a C_1-symmetric ligand. Two different co-ordinating ligands (P-X as shown above, or P-N, discussed here) could lead to more control, as the attack may

always take place *trans* to the phosphorus atom for instance, thus reducing the number of possibilities. To this end Helmchen, Pfaltz, and Williams introduced successfully the PPh_2-phenyl-oxazoline (PHOX) ligands [9]. In the phosphite variant the difference in trans effect is even more pronounced [10].

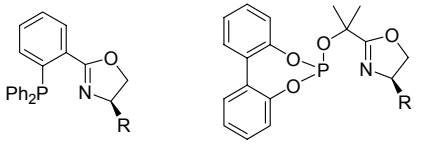

Figure 13.14. Phosphino-oxazoline ligands, PHOX

The PHOX ligands can be varied by changing the substitution at phosphorus, the oxazoline ring, and the bridge and thus a high variety can be made available. They have been applied to many catalytic reactions leading to high ee's with the appropriate substitution pattern.

Industrial applications of AAA on a large scale seem to be lacking, which is surprising for such a versatile reaction. In laboratory syntheses it is often used and the model reaction with 1,3-diphenylprop-2-en-1-yl is probably the most studied reaction in asymmetric syntheses for testing new ligands!

13.3 Heck reaction

A reaction related to cross-coupling reactions is the Heck reaction [11]. The reaction was first reported by Mizoroki [12]. We will confine ourselves to the basic scheme of the reaction, since again numerous variations have been reported [13]. The reaction involves the coupling of aryl halides (pseudo halide, vinyl halide) with alkenes in the presence of a base. Owing to the latter, as in the cross-coupling reaction, one equivalent of salt is formed. In the base case, the Heck reaction produces substituted styrenes. It is attractive that the Heck reaction does not involve Grignard type reagents and thus it allows the presence of groups reactive towards Grignard reagents such as esters, acids, ketones, etc.

The reaction starts with the oxidative addition of an aryl halide (Cl, Br or I) to palladium zero. The next step is the insertion of an alkene into the palladium carbon bond just formed. The third step is β-hydride elimination giving the organic product and a palladium hydrido halide. The latter reductively eliminates HX, which reacts with base to give a salt (Figure 13.15).

The atom economy of the cross-coupling reaction and the Heck reaction for making styrene from bromobenzene and vinyl bromide (cross), and bromobenzene and ethene (Heck) respectively are in favour of the Heck reaction, as that produces only one equivalent of salt.

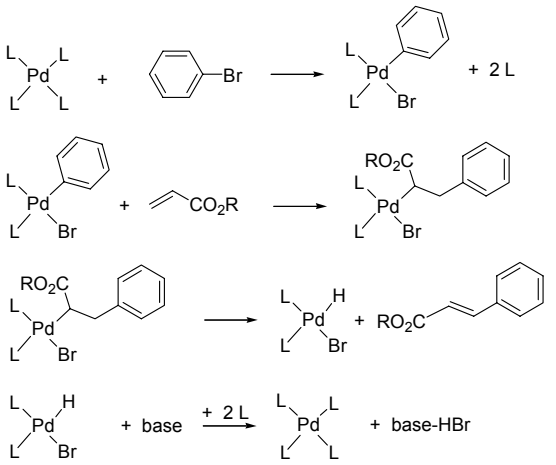

Figure 13.15. Mechanism of the Heck reaction

Sometimes the halide is replaced by non-coordinating anions such as $O_3SCF_3^-$. The advantage is that the palladium centre is now much less saturated and more positively charged (and hence more reactive) during the alkene co-ordination and insertion steps.

Ligand effects in Heck reactions

A new development comprises the use of catalysts containing bulky ligands, especially for the Heck reaction [14,15]. Beller reported the use of tri-*o*-tolylphosphine, which gave a very active catalyst. This ligand forms a metallated species as shown in Figure 13.16. Initially it was thought that the metallated species played a crucial role, but today's view is that it is a convenient precursor for a palladium(0) complex containing a bulky monodentate ligand [16] rather than a complex that mechanistically would lead to palladium(IV) species.

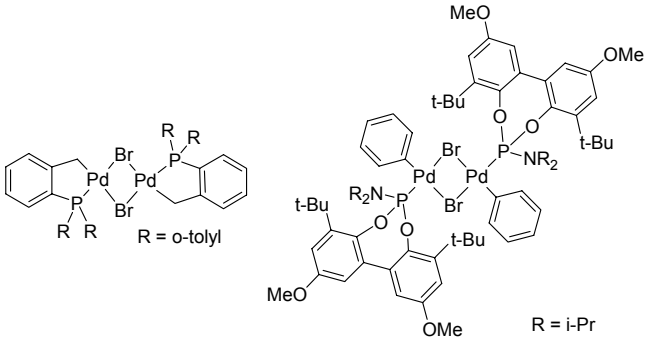

Figure 13.16. New catalysts for the Heck reaction [15]

While the sequence of steps for the Heck reaction remains the same for many catalysts, the kinetics may vary enormously and also the detailed composition of all intermediates may vary in the type and number of ligands. It had often been assumed that the oxidative addition is the slowest step and that may well be true for many systems based on PPh_3; definitely for aryl chlorides it seems to be the rule.

A study of the effect ligand properties has led to unexpected findings. A series of phosphines, phosphites and phosphorus amidites were screened for their activity while both steric and electronic properties were changed. A very active catalyst is the amidite complex shown in Figure 13.16 [15]. Bulky phosphites and amidites turned out to give the fastest catalysts, even twice as fast as the *o*-tolylphosphine system. When electron-poor ligands give the fastest catalyst, it is obvious that the oxidative addition of the aryl halide is no longer the slow step of the reaction, as electron-poor donor ligands will slow down this step. The substituents on the phosphite or phosphoramidite are preferentially ortho-t-butyl substituted phenols or bisphenols. The bulky ligands have in common that they do not form saturated, square-planar $ArPdBr(L)_2$ complexes, as smaller ligands would do, but instead they form halide-bridged dimers, which easily dissociate to give coordinatively unsaturated species. The latter reacts in a fast reaction with alkenes.

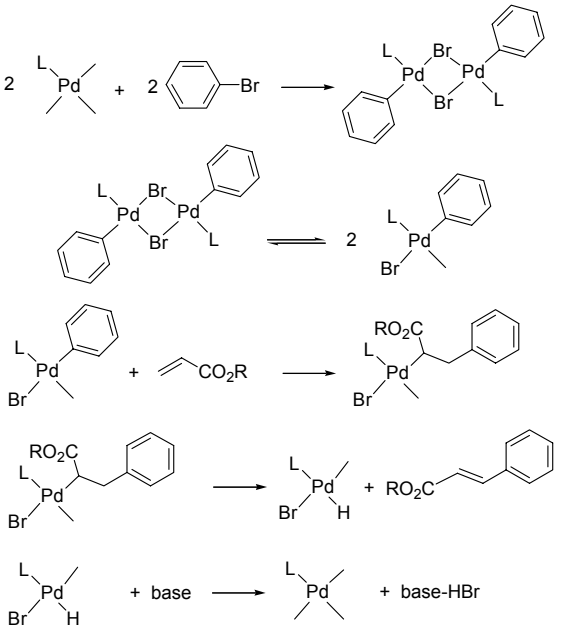

Figure 13.17. Mechanism of the Heck reaction for bulky ligand systems [15]

The resting state of this catalytic system was found to be the dimer shown. The migratory insertion is the rate-determining step and not the oxidative addition of aryl halide to a palladium zero species, see Figure 13.17. These kinetics were found for phenyl iodide; phenyl bromide already showed less clear-cut kinetics indicating that the oxidative addition is somewhat slower now. The system shown in Figures 13.16-17 gives at least half a million turnovers.

Thus, for each ligand, each anion, condition, concentrations, etc. the kinetics may be different and it is worthwhile to study this, rather than rely on general statements. Simple methods are satisfactory sometimes, but more accurate methods are available and have been applied successfully to the Heck reaction [17].

The rate equation for the reaction scheme in Figure 13.17 shows a zero order dependence in aryl iodide and base, a first order in alkene, and a square root order in the palladium concentration. We can conclude from this that either the complexation of acrylate to palladium or its insertion in the palladium-aryl bond is rate-determining.

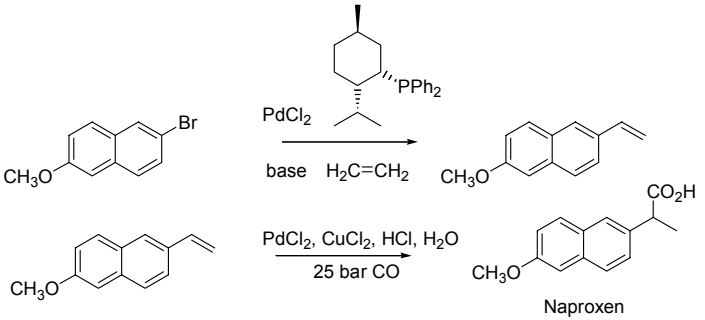

Figure 13.18. Albemarle's route to Naproxen

A *phosphine-free* version of the Heck reaction carried out in water has been reported by Beletskaya [18]. Simple $Pd(OAc)_2$ and Na_2CO_3 can be used for the coupling of a variety of aryl bromides and acrylic acid or styrene. The amount of catalyst used was in the order of 1%, but perhaps this can be lowered considerably. Other phosphine-free systems with the use of DMF as the solvent were reported by Buchwald [19]. In this instance trisubstituted alkenes were obtained. Usually somewhat higher temperatures are used for phosphine-free systems (100 °C). One could imagine that alkenes might serve as the ligand for zerovalent palladium and the polar solvent acts as the ligand toward divalent palladium. Recycling of a phosphine-free catalyst has been reported [20]. The catalyst is precipitated at the end of the reaction on a silica or carbon support and it is redissolved in the next run by the addition of a weakly oxidising

reagent such as iodine. In addition to all elegant ligand modified catalysts, there might also be scope for a simple ligand-free catalyst!

Industrial applications of the Heck reactions.

Several important industrial applications of the Heck reactions are known. The world's largest producer of Naproxen is Albemarle and they make Naproxen using two homogeneously catalysed steps, a Heck reaction and a palladium catalysed hydroxycarbonylation. The last step is carried out using palladium without chiral ligand and the enantiomers obtained are separated, see Figure 13.18.

In Figure 13.19 we have shown a route to L-699,392 published by Merck involving three steps based on homogeneous catalysts, *viz*. two Heck reactions and one asymmetric hydrogen transfer reaction, making first an alcohol and subsequently a sulphide [21]. Stoichiometric reductions for the ketone function have been reported as well [22] and the Heck reaction on the left-hand side can be replaced by a classic condensation reaction. L-699,392 is used in the treatment of asthma and related diseases.

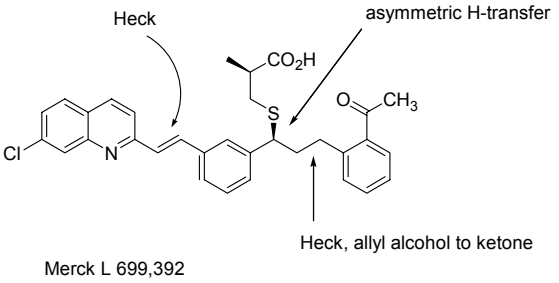

Figure 13.19. A combination of homogeneous catalysts to make a medicine

The use of cyclic alkenes as substrates or the preparation of cyclic structures in the Heck reaction allows an asymmetric variation of the Heck reaction. An example of an intermolecular process is the addition of arenes to 1,2-dihydrofuran using BINAP as the ligand, reported by Hayashi [23]. Since the addition of palladium-aryl occurs in a *syn* fashion to a cyclic compound, the β-hydride elimination cannot take place at the carbon that carries the phenyl group just added (carbon 1), and therefore it takes place at the carbon atom at the other side of palladium (carbon 3). The "normal" Heck products would not be chiral because an alkene is formed at the position where the aryl group is added. A side-reaction that occurs is the isomerisation of the alkene. Figure 13.20 illustrates this, omitting catalyst details and isomerisation products.

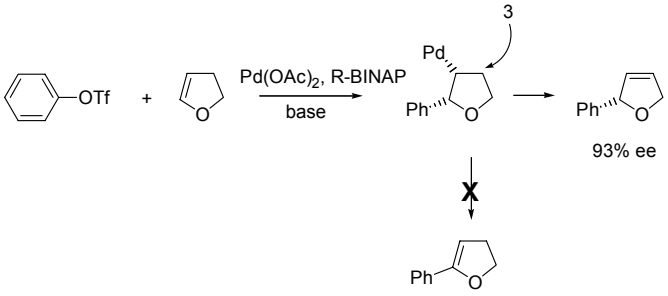

Figure 13.20. Asymmetric, intermolecular Heck reaction [23]

The reaction is carried out with aryl triflates and other details such as solvent and base used are also important. Intramolecular additions of aryl halides or triflates to alkenes in a side-chain leading to cyclic compounds have been reported by Overman [24]. Rather complicated ring structures can be made stereospecifically. While initially BINAP seemed the best ligand for this conversion, the number of useful ligands is increasing [25].

13.4 Cross-coupling reaction

As mentioned above (Section 13.1), the coupling of carbocations and carbanions (or their formal precursors) was of little practical value until the transition-metal-catalysed cross-coupling became available. The "cross-coupling" reaction has found wide application in organic synthesis both in the laboratory and in industry. Here we will present only the main scheme and use palladium as the example. Figure 13.21 gives the general scheme of the palladium catalysed cross-coupling reaction. Note that many variations on this scheme have been published, but here we are only concerned with the basics of this extremely useful chemistry.

We can start with palladium(II) or palladium(0), but for the mechanistic explanation the latter is more convenient (a practical starting material, as always in this chemistry, is the putative intermediate $L_2PhPdBr$). For palladium zero the cycle starts with oxidative addition of an aryl halide (PhBr in Figure 13.21) and a square planar Pd(II) complex is formed. Subsequently the inorganic bromide reacts with the Grignard or lithium alkyl reagent (here 2-BuMgBr) in the so-called *trans*-metallation reaction giving a diorganyl-palladium complex and magnesium dibromide. The third reaction that occurs is the reductive elimination leading to the organic "cross-coupling" product and the palladium(0) catalyst in its initial state.

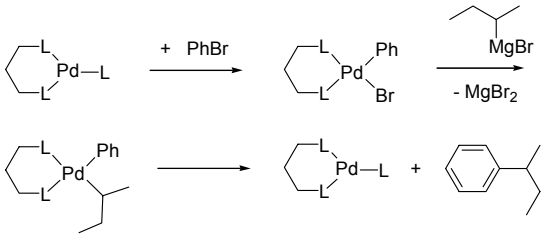

Figure 13.21. Palladium catalysed cross-coupling

Depending on the conditions, the ligand, the metal, the organic groups, and the main group metal the reaction can be very selective and fast. Numerous variations have been published. Not many kinetic studies have been carried out, or at least they have not been published. It is conceivable that all three reactions can be rate determining:

- *oxidative addition*, industrially it would be attractive to use chlorides instead of bromides or iodides and then indeed the oxidative addition is rate determining; when iodides are used this is not the case,
- *trans-metallation (or trans-alkylation),* industrially the use of Grignard or lithium reagents is most attractive since other organometallics are usually prepared via these as intermediates; trans-metallation using reactive magnesium or lithium compounds is fast compared to the previous reaction,
- *reductive elimination,* this can also be strongly influenced by the nature of the ligands, hydrocarbyl groups, electron-withdrawing additives etc.; most often this reaction is fast for sp^2 hydrocarbyl groups.

Side reactions are: exchange of organic groups, followed by "homo" coupling, β-hydrogen elimination with alkene formation, isomerisation followed by coupling, or benzene formation and alkene liberation. Examples are shown in Figure 13.22.

Suppose that the oxidative addition is the slowest reaction in the system. One can then minimise the occurrence of the un-catalysed reactions between the aryl halide and the Grignard reagent by keeping the concentration of the Grignard reagent very low.

The cross coupling reaction is applied industrially in the synthesis of alkyl-aryl compounds that are used in liquid crystals (Merck has hundreds of patents on this topic!) and that are used as chemicals in agriculture. For fine chemical synthesis the route that is actually being used is not announced in the literature. Judging from the number of patents on coupling reactions (including the Heck reaction discussed in the following paragraph) the industrial interest is large.

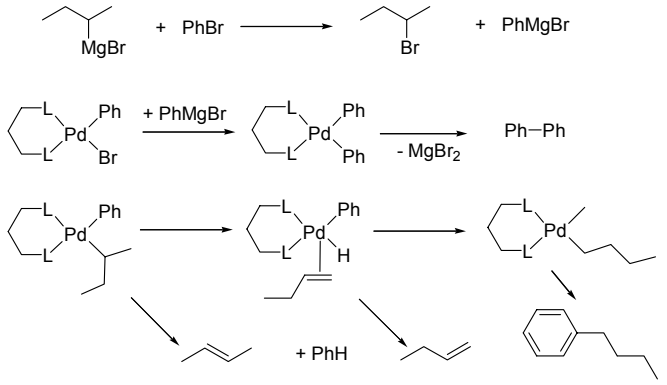

Figure 13.22. Side-products in the cross-coupling reaction

Industrial applications of the cross-coupling

One industrial application has been reported in detail by Giordano [26], Figure 13.23. It concerns the synthesis of Diflunisal, a non-steroidal anti-inflammatory drug. Sales price is around € 300 / kg and a few hundred tons are made worldwide per annum.

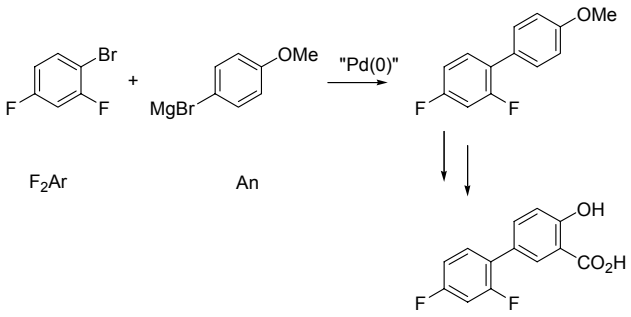

Figure 13.23. Synthesis of Diflunisal

A very pure product is required. The palladium content may not exceed 10 ppm and the impurities should be below 0.1 %. Classical syntheses as the Ullmann reaction cannot be applied because they give a lot of by-products.

Two steps are critical: the cross-coupling itself, and making the Grignard of 4-bromoanisole. Zambon has spent ~ 10 man-year on the optimisation of the cross-coupling reaction! In the following we summarise the results.

The Grignard is made from 4-bromoanisole, Mg (3 % excess), I_2 catalyst, in tetrahydrofuran (3 M), at 70 °C. The major problem is the formation of the "homo"coupled product during the Grignard synthesis. Up to 6% of 4,4'-dimethoxybiphenyl may be formed. The amount depends on the type of

magnesium that was used. The impurities found were Cu (10–100 ppm), Fe (30–300 ppm), Ni (5–10 ppm), and Mn (35–400 ppm). It turned out that high yields of the desired Grignard could only be obtained if the metal impurities for all these metals are at the lowest levels of the ranges indicated. It is not surprising that the transition metals are active; in this reducing medium they will be low-valent and undergo oxidative addition and then catalyse a cross-coupling reaction!

The next step is the coupling of the Grignard reagent with 1,3-difluoro-4-bromobenzene using $Pd(PPh_3)_4$ (0.1%) as the catalyst. The Grignard is added to a solution of the bromide. Substantial amounts of homocoupled 4,4'-dimethoxybiphenyl are formed when the Grignard is added too fast to the solution of the bromide. The following may explain this (Fig. 13.24):

Figure 13.24. Slow addition of Grignard suppresses homo-coupling

If oxidative addition is the slowest step in the reaction sequence, the concentration of the aryl bromide should be maximised. If the metallation reaction at palladium, replacing the bromide ion by the anisyl group is relatively fast, the concentration of the Grignard may be kept low. Side reactions are all due to reactions of the Grignard reagent anisyl magnesium bromide. Indeed, the reaction is operated in such a way that there is hardly any Grignard reagent in the solution. It is added over a period of 4 hours at the concentrations reported (3 M Grignard). It turned out that higher temperatures gave the best results. In practice a temperature of 85 °C is being used.

The catalyst is generated in situ from palladium acetate and triphenyl phosphine. The total turnover is more than 3000. The selectivity to cross-product is > 99%. The yield is > 96%. The reaction is run in 12 m^3 stainless steel and glass-lined reactors.

Further information about the organic reactions involved:

- the starting material for difluorobromobenzene is difluoroaniline that is converted to the bromide via diazotation,

- the methoxy group is removed by refluxing in HBr/AcOH,
- the carboxylic acid group is introduced via a base catalysed reaction with CO_2.

In literature no general agreement exists on the rate-determining step of the cross-coupling reaction, even though in the above example clearly the oxidative addition is the slowest step. This will of course depend on the system used and the palladium(0) species formed. It has been found that association of anions with Pd(0) makes palladium more susceptible to oxidative addition and thus the processes occurring in a medium that changes while the reaction progresses are complex [27]. Since aryl chlorides are much less reactive, in many instances the oxidative addition seems to be rate-determining. Aryl chlorides do react, however, when alkyl phosphines are used as the ligands [28] as now the oxidative addition becomes faster.

13.5 Heteroatom-carbon bond formation

From the recent advances the heteroatom-carbon bond formation should be mentioned. As for the other reactions in Chapter 13 the amount of literature produced in less than a decade is overwhelming. Widespread attention has been paid to the formation of carbon-to-nitrogen bonds, carbon-to-oxygen bonds, and carbon-to-sulfur bonds [29]. The thermodynamic driving force is smaller in this instance, but excellent conversions have been achieved. Classically, the introduction of amines in aromatics involves nitration, reduction, and alkylation. Nitration can be dangerous and is not environmentally friendly. Phenols are produced via sulfonation and reaction of the sulfonates with alkali hydroxide, or via oxidation of cumene, with acetone as the byproduct.

The cross-coupling alternative yields halide salts as co-products. During the preparation of aryl halides from the aromatic ring and dihalogen also one equivalent of halide salt is produced and thus there is further room for improvement if we could directly substitute a hydrogen atom by the hetero atoms mentioned!

The basic scheme for carbon-nitrogen bond formation using palladium catalysts containing an arbitrary bidentate ligand is depicted in Figure 13.25. Fairly strong bases are used, such as NaO*t*-Bu, KO*t*-Bu, Cs_2CO_3, etc. The reaction rates, selectivities and yields are highly dependent on substrates, ligands used, solvent, base, and reaction conditions. Instead of aryl halides one can also use triflates. In the oldest precedents of this reaction tin amides were used as the amide source rather than alkali metal amides [30]; it is through the work of Hartwig and Buchwald [29] in the last decade that the reaction has received such widespread attention.

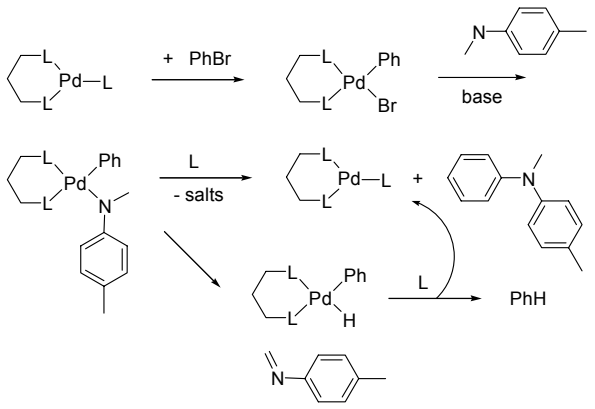

Figure 13.25. Carbon-nitrogen bond formation

Both monodentate phosphines such as PPh_3, P*t*-Bu_3, P*o*-Tol_3, and many other bulky monodentates [31,32,33], and bidentate phosphine ligands such as BINAP, dppf [31,34] can be very effective depending on the substrates. In some cases ligands having wide bite angles are the ligands of choice such as DPEphos and Xantphos [35,36]. Typical monodentate ligands are shown in Figure 13.26. Aryl halides containing electron withdrawing groups often give higher yields [31], which might be explained at first sight by assuming an acceleration of the oxidative addition reaction. Since this step is not rate determining, the explanation is different, see below.

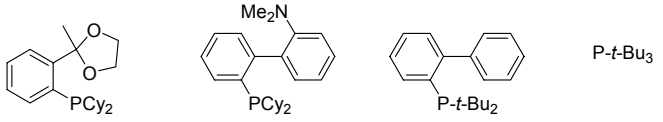

Figure 13.26. Typical, effective monodentate ligands

The carbon-oxygen bond formation follows the same pathway. For both nitrogen-carbon and oxygen-carbon bond formation, a competing reaction is β-hydride elimination (if a hydride is present at the heteroatom fragment), which lowers the yield and the "reduced" arene is obtained after reductive elimination. Reductive elimination of the C-N or C-O fragments should be faster than β-hydride elimination in order to avoid reduction of the aryl moiety. The side-reaction is shown at the bottom of Figure 13.25.

The kinetics of cross coupling reactions are usually complicated, as one might expect. We have learnt that the yields and selectivities strongly depend on the reaction conditions, which change considerably during the reaction: (a) the metal is involved in metal-ligand equilibria, (b) the amount of base present

change during the reaction because one of the reagents is a base, (c) ligand may decompose during the reaction, and (d) salts are being formed during the reaction. Even the minimum number of reactions to be considered (oxidative addition, halide replacement, reductive elimination) is known to depend heavily on all these factors! Therefore the study of just one step may be more informative.

As an example we have chosen the reductive elimination of arylamines from arylpalladium amide complexes studied by Driver and Hartwig [37]. Since the overall carbon-nitrogen bond formation seems slower than carbon-carbon bond forming reactions, we conclude that oxidative addition is most likely not the slowest, rate-determining step in the process. That leaves either amide formation, or the reductive elimination as the slowest step. Partial amide formation, as a pre-equilibrium before reductive elimination takes place, might also be considered [36]. Driver and Hartwig prepared a series of arylpalladium amide complexes and studied the rate of the reductive elimination reaction [31]. The bidentate ligand used was dppf, while PPh_3 was used as the monodentate model ligand.

Reductive elimination from dppf complexes of palladium as shown in Figure 13.27 appeared to be independent of the concentration of added PPh_3. The elimination occurs directly from the four-coordinate species. Furthermore the reductive elimination increased with the electron withdrawing nature of the substituents on the aryl ring. Resonance effects dominate over inductive effects, which is typical of an attack of the nitrogen donor to the sp^2 carbon atom of the aryl group. The overall reactivity of the amido groups was diarylamido < arylamido < alkylamido. This trend clearly shows that electron-donating groups accelerate reductive elimination [37]. Thus, the amido group acts as a nucleophile towards the electrophilic aryl group, as shown in Figure 13.26. The intermediate can probably be best described as a Meisenheimer complex (Figures 12.14, 13.27) [38]. Similar effects were observed for the reductive elimination of aromatic ethers and thioethers.

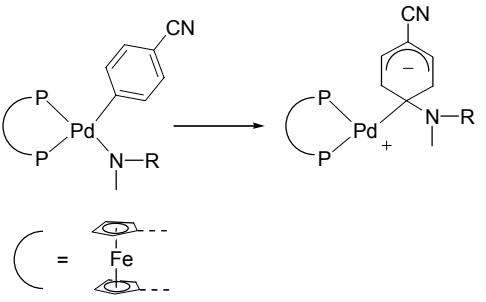

Figure 13.27. Mechanism of reductive elimination aryl-N

Monodentate phosphines, when present at low concentrations, lead to dimeric complexes as shown in Figure 13.28. The kinetics now show that dissociation of the dimer takes place before the reductive elimination. Reductive elimination from three-coordinate species is a well known phenomenon. This may be valid especially for electron-rich donor ligands. Reductive elimination also takes place at a variety four-coordinate complexes: (1) electron-rich and bulky (via a three-coordinate species?), (2) bidentate ligands with wide bite angles, and (3) electron-withdrawing bidentate ligands. Reductive elimination has been observed as an associative process, in which case the fifth ligand is an electron-withdrawing species.

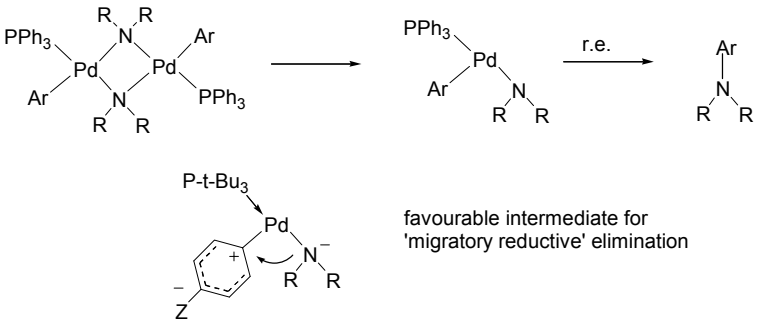

Figure 13.28. Reductive elimination from dimeric species

Reductive elimination of the dimeric species shows a half order in palladium concentration, proving that indeed dissociation of the dimer occurs prior to product formation. A bulky monodentate ligand, which is also a strong donor ligand leads to a favourable situation for a "migratory reductive" elimination; (1) A bulky ligand prefers the formation of mono-ligand complexes, (2) *trans* to the aryl group we find no donor group and thus the aromatic carbon atom becomes more electrophilic, and (3) the strong donor *trans* to the amide nucleophile enhances the nucleophilicity of the migrating nitrogen (Figure 13.28).

Such three-coordinate species, containing halides instead of the more reactive amides or alkoxides, have been isolated and identified by X-ray crystallography. The bromide and iodide indeed were found *trans* to the phosphine ligand (P*t*-Bu_3 and P*t*-Bu_2Ad, Ad = adamantyl) [39]. The complexes react indeed with diphenyl amine in the presence of base to give the reductive elimination products. One might speculate that bulky bidentate ligands dissociate "one arm" first, before undergoing the same reaction! Kinetic studies cannot exclude whether this takes place or not. Interestingly, this mechanism would also have a strong bearing on the issues discussed in Section 12.3 concerning the rate of ester formation from palladium acyl species, and thus the

molecular weight determination in the synthesis of polyketone versus methyl propionate.

13.6 Suzuki reaction

Worth mentioning is the use of less reactive organometallic derivatives of tin and boron. These reagents do not react with water, but they are still able to alkylate palladium bromide intermediates. As mentioned above, their formation does involve one more step, because they are made via Grignard type reagents. The coupling reaction using tin organometallics is referred to as a "Stille" coupling. The reagent based on boron was introduced by Suzuki [40] and the coupling reaction carries his name. The boronic ester derivative is made from trimethyl borate and an aryl anion reagent followed by hydrolysis of the two remaining methyl groups. This phenylboronic acid is soluble in water and the coupling reaction can even be carried out in water. It is compatible with many organic substituents such as esters, ketones, alcohols, etc. which would prohibit the use of Grignard reagents in coupling reactions. See Figure 13.29 for a scheme of the Suzuki coupling.

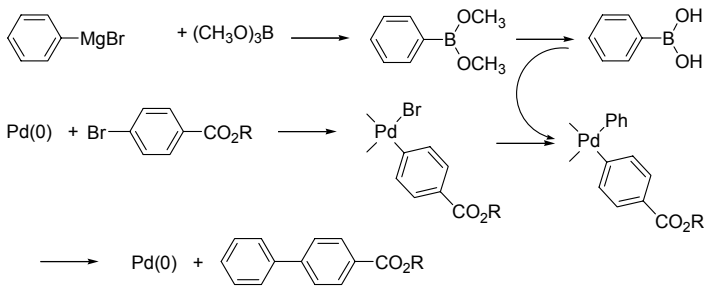

Figure 13.29. Suzuki cross-coupling reaction

As in the Heck reaction, bulky phosphorus ligands with a large variety of structures, especially bulky phosphites, lead to extremely high turnover numbers. Metallated ligand complexes are excellent precursors to this reaction, as reported by Bedford [41], and turnover numbers of millions were obtained. An example is shown in Figure 13.30. At these micromolar concentration levels of palladium and phosphite in refluxing toluene, traces of water may lead to hydrolysis of the phosphites and phosphinites (e.g. Ph_2POAr, Ar = 2,4-$tBu_2C_6H_3$) used. It has been shown that partially hydrolysed phosphites of the type $(RO)_2POH$ work just as well in a number of cases [42], as does *t*-Bu_2POH as reported by Li [43]. Therefore, in the very high activity catalysts, hydrolysis during activation of the catalyst precursor plays a definite role. Besides, in view

of the very low concentrations, complexation constants must be very high for these ligands!

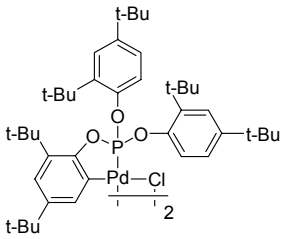

Figure 13.30. Metallated precursor [41] for the Suzuki reaction

Aryl chlorides as the substrate

Aryl chlorides are much cheaper reagents than aryl bromides, they cause less waste in weight and therefore they are preferred to the latter in cross-coupling chemistry. Aryl chlorides, though, are much less reactive than bromides or iodides and until 1998 only activated aryl chlorides could be used in metal-catalysed coupling chemistry. Activated aryl chlorides include for instance pyridyl chlorides, or aryl chlorides containing electron-withdrawing substituents. Since the introduction of electron-rich, bulky, monodentate ligands by Buchwald [44] and Fu [45] in this chemistry the scope of the reactions has extended enormously. Examples of the ligands used are shown in Figure 13.26.

Heterocyclic carbene ligands are strong σ-electron donors with properties close to those of for instance PCy_3. They form active catalysts with palladium for the Suzuki reaction of non-activated substrates [46]. The ligands IMes and Ipr are shown in Figure 13.31. It would seem that mono-ligand species are needed, very similar to bulky, electron-rich monophosphines.

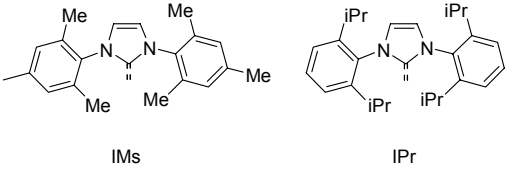

Figure 13.31. IMes and IPr carbene ligands for Suzuki catalysts

Application of the Suzuki cross-coupling reaction

In Figure 13.32 we have shown an example of the Suzuki reaction as applied by Clariant and Zeneca for the preparation of a pharmaceutical intermediate. These biaryls are precursors for the "sartan" type drugs used for

blood pressure regulation. Clariant uses tppts as the ligand and Zeneca sterically hindered alkylphosphines.

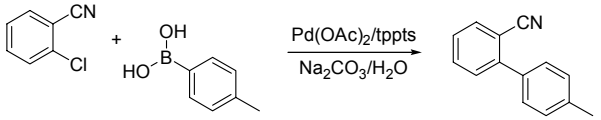

Figure 13.32. Example of industrially applied Suzuki coupling reaction

The Suzuki coupling is used for the preparation of a drug called Losartan, see Figure 13.33 [47]. The reaction is carried out in THF in the presence of water and K_2CO_3 as the base. The trityl (Tr) group is used as a protecting group which is removed after the coupling reaction with acid. The oxidative addition was found to be the rate-determining step in this system. The authors assumed, in accord with older literature, that arylboronic acid reacts with hydroxide ions to give $ArB(OH)_3^-$ which is much more reactive toward electrophilic attack than arylboronic acid itself.

Other applications might involve the synthesis of substituted alkylarenes useful as liquid crystalline materials. Liquid crystalline materials often contain bi-aryls or cyclohexylaryls and these can also made via one of the coupling reactions discussed above.

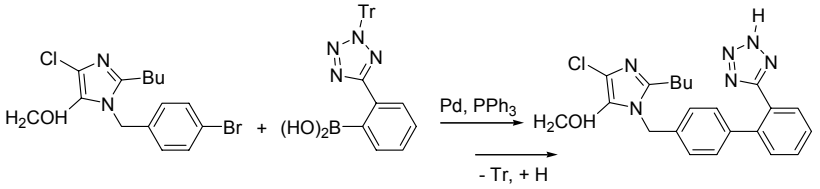

Figure 13.33. Synthesis of Losartan [47]

References

1 Trost, B. M.; Verhoeven, T. R. Eds. Wilkinson, Able, Stone, Comprehensive Organometallic Chemistry, **1982**, Vol. 8, 799. Tsuji, J.; Takahashi, H.; Morikawa, M. *Tetrahedron Letters*, **1965**, 4387.

2 Trost, B. M.; Crawley, M. L. *Chem. Rev.* **2003,** *103,* 2921.

3 Trost, B. M.; Van Vranken, D. L.; Bingel, C. *J. Am. Chem. Soc.* **1992***, 114*, 9327 and *Angew. Chem Int. Ed.* **1995***, 34*, 2386.

4 Dierkes, P.; Ramdeehul, S.; Barloy, L.; De Cian, A.; Fischer, J.; Kamer, P. C. J.; van Leeuwen, P. W. N. M.; Osborn, J. A. *Angew. Chem. Int. Engl. Ed.* **1998***, 37*, 3116.

5 Ramdeehul, S.; Dierkes, P.; Aguado, R.; Kamer, P. C. J.; van Leeuwen, P. W. N. M.; Osborn, J. A. *Angew. Chem. Int. Engl. Ed.* **1998**, *37*, 3118. Trost, B. M.; Toste, F. D. *J. Am. Chem. Soc.* **1999**, *121*, 4545.
6 Keinan, E.; Sahai, M.; Roth, Z.; Nudelman, A.; Herzig. J. *J. Org. Chem.* **1985**, *50*, 3558. Granberg, K. l.; Bäckvall, J. E. *J. Am. Chem. Soc.* **1992**, *114*, 6858.
7 Lloyd-Jones, G. C.; Stephen, S. C. *Chem. Eur. J.* **1998**, *4*, 2539.
8 Pfaltz, A. *Acc. Chem. Res.* **1993**, *26,* 339. Williams, J. M. J. *Synlett*. **1996**, 705.
9 Helmchen, G.; Pfaltz, A. *Acc. Chem. Res.* **2000**, *33,* 336.
10 Prétôt, R.; Pfaltz, A. *Angew. Chem. Int Ed.* **1998**, *37*, 323.
11 Heck, R. F.; Nolley, J. P. *J. Org. Chem.* **1972**, *37*, 2320.
12 Mizoroki, T.; Mori, K.; Ozaki, A. *Bull. Chem. Soc. Jpn.* **1971**, *44*, 581.
13 Cabri, W.; Candiani, I. *Acc. Chem. Res.* **1995**, *28*, 2. Brown, J. M.; Hii, K. K. *Angew. Chem. Int Ed.* **1996**, *35*, 657.
14 Beller, M.; Riermeijer, T. H.; Haber, S.; Kleiner, H. J.; Herrmann, W. A. *Chem. Ber.* **1996**, *129*, 1259. Ohff, M.; Ohff, A.; van der Boom, M.; Milstein, D. *J. Am. Chem. Soc.* **1997**, *119*, 11687.
15 van Strijdonck, G. P. F.; Boele, M. D. K.; Kamer, P. C. J.; de Vries, J. G.; van Leeuwen, P. W. N. M. *Eur. J. Inorg. Chem*. **1999**, 1073.
16 Louie, J.; Hartwig, J. F. *Angew. Chem. Int. Ed.* **1996**, *35,* 2359.
17 Rosner, T.; Le Bars, J.; Pfaltz, A.; Blackmond, D. G. *J. Am. Chem. Soc.* **2001**, *123*, 1848.
18 Bumagin, N. A.; Bykov, V. V.; Sukhomlinova, L. I.; Tolstaya, T. P.; Beletskaya, I. P. *J. Organomet. Chem.* **1995,** *486,* 259.
19 Gürtler, C.; Buchwald, S. L. *Chem. Eur. J.* **1999**, *5,* 3107.
20 de Vries, A. H. M.; Parlevliet, F. J.; Schmieder-van de Vondervoort, L.; Mommers, J. H. M.; Henderickx, H. J. W.; Walet, M. A. M.; de Vries, J. G. *Adv. Synth. Catal.* **2002,** *344,* 996.
21 Shinkai, I.; King A. O.; Larsen, R. D. *Pure & Appl. Chem.* **1994**, *66*, 1551. Larsen, R. D.; Corley, E. G.; King, A. O.; Carroll, J. D.; Davis, P.; Verhoeven, T. R.; Reider, P. J.; Labelle, M.; Gauthier, J. Y; Xiang, Y. B.; Zamboni, R. J. *J. Org. Chem.* **1996**, *61*, 3398.
22 King, A. O.; Corley, E. G.; Anderson, R. K.; Laresen, R. D.; Verhoeven, T. R.; Reider, P. J.; Xiang, Y. B.; Belley, M.; Leblanc, Y.; Labelle, M.; Prasit, P.; Zamboni, R. J. *J. Org. Chem.* **1993,** *58,* 3731.
23 Ozawa, F.; Kubo, A.; Hayashi, T. *J. Am. Chem. Soc.* **1991**, *113,* 1417.
24 Ashimori, A.; Overman, L. E. *J. Org. Chem.* **1992,** *57,* 4571.
25 Deng, W.-P.; Hou, X.-L.; Dai, L.-X.; Dong, X.-W. *Chem. Commun.* **2000**, 1483. Imbos,R.; Minnaard, A. J.; Feringa, B. L. *Dalton Trans*. **2003**, 2017.
26 Giordano, C. Peñiscola Meeting Cataluña Network on Homogeneous Catalysis, **1995**. Giordano, C.; Coppi, L.; Minisci, F. (Zambon Group S.p.A.), Eur. Pat. Appl. **1992**, EP 494419, *Chem. Abstr.* **1992**, *117*, 633603.
27 Amatore, C.; Jutand, A. *Acc. Chem. Res.* **2000**, *33*, 314.
28 Littke, A. F.; Fu, G. C. *Angew. Chem. Int. Ed.* **2002**, *41,* 4176.
29 Paul, F.; Patt, J.; Hartwig, J. F. *J. Am. Chem. Soc.* **1994**, *116*, 5969. Guram, A. S.; Rennels, R. A.; Buchwald, S. L. *Angew. Chem. Int. Ed. Engl.* **1995**, *34*, 1348. Driver M. S.; Hartwig, J. F. *J. Am. Chem. Soc.* **1996**, *118,* 7217. Paul, F.; Patt, J.; Hartwig, J. F. *Organometallics* **1995**, *14*, 3030. Wolfe, J. P.; Wagaw, S.; Buchwald, S. L. *J. Am. Chem. Soc.* **1996**, *118*, 7215. Hartwig, J F. *Acc. Chem. Res.* **1998**, *31,* 852.
30 Kosugi, M.; Kameyama, M.; Migita, T. *Chem. Lett.* **1983,** 927.
31 Driver, M. S.; Hartwig, J. F. *J. Am. Chem. Soc.* **1997**, *119,* 8232.

32 Aranyos, A.; Old, D. W.; Kiyomori, A.; Wolfe, J. P.; Sadighi, J. P.; Buchwald, S. L. *J. Am. Chem. Soc.* **1999***, 121,* 4369.
33 Bei, X.; Guram, A. S.; Turner, H. W.; Weinberg, W. H. *Tetrahedron Lett.* **1999,** *40,* 1237.
34 Sadighi, J. P.; Harris, M. C.; Buchwald, S. L. *Tetrahedron Lett.* **1998,** *39,* 5327.
35 Yin, J.; Buchwald, S. L. *Org. Lett.* **2000**, *2*, 1101. *J. Am. Chem. Soc.* **2002***, 124,* 6043.
36 Guari, Y.; van Strijdonck, G. P. F.; Boele, M. D. K.; Reek, J. N. H.; Kamer, P. C. J.; van Leeuwen, P. W. N. M. *Chem. Eur. J.* **2001***, 7,* 475.
37 Driver, M. S.; Hartwig, J. F. *J. Am. Chem. Soc.* **1997***, 119,* 8232.
38 Widenhoefer, R. A.; Zhong, H. A.; Buchwald, S. L. *J. Am. Chem. Soc.* **1997***, 119,* 6787.
39 Stambuli, J. P.; Bühl, M.; Hartwig, J. F. *J. Am. Chem. Soc.* **2002***, 124,* 9346.
40 Miyaura, N.; Suzuki, A. *Chem. Rev.* **1995***, 95,* 2457. Suzuki, A. *J. Organomet. Chem.* **1999,** *576,* 147.
41 Bedford, R. B.; Welch, S. L. *Chem. Commun.* **2001,** 129. Albisson, D. A.; Bedford, R. B.; Lawrence, S. E.; Scully, P. N. *Chem. Commun.* **1998,** 2095.
42 Bedford, R. B.; Hazelwood, S. L.; Limmert, M. E.; Brown, J. M.; Ramdeehul, S.; Cowlwy, A. R.; Coles, S. J.; Hursrhouse, M. B. *Organometallics* **2003***, 22*, 1364.
43 Li, G. Y.; *J. Org. Chem.* **2002**, *67,* 3643.
44 Old, D. W.; Wolfe, J. P.; Buchwald, S. L. *J. Am. Chem. Soc.* **1998***, 120,* 9722.
45 Littke, A. F.; Fu, G. C. *Angew. Chem. Int. Ed. Engl.* **1998***, 37*, 3387.
46 Zhang, C.; Huang, J.; Trudell, M. L.; Nolan, S. P. *J. Org. Chem.* **1999***, 64,* 3804. Fürstner, A.; Leitner, W. *Synlett* **2001**, 290.
47 Smith, G. B.; Dezeny, G. C.; Hughes, D. L.; King, A. O.; Verhoeven, T. R. *J. Org. Chem.* **1994***, 59,* 8151.

Chapter 14

EPOXIDATION

Large scale commodities and small scale beauties

14.1 Ethene and Propene oxide

Epoxidation of alkenes (Figure 14.1) is a powerful reaction for the introduction of oxygen in hydrocarbons.

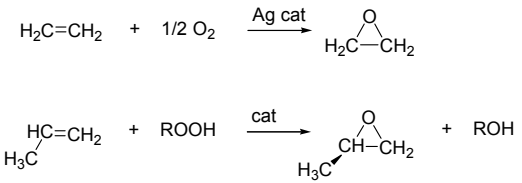

Figure 14.1. Catalytic epoxidation of alkenes

Oxygen can be used for the epoxidation of ethene over a silver catalyst, but for all other alkenes further oxidation occurs when the source of oxygen is dioxygen. On the heterogeneous silver catalyst dioxygen is absorbed both as diatomic oxygen and monoatomically, in a dissociative fashion. An important feature is probably that the chemisorption of oxygen is relatively weak on the silver surface. The mechanism involves the electrophilic attack of mono-oxygen on the π-electrons of ethene. An important issue is the suppression of further oxidation, as well as the transfer of the heat in this highly exothermic reaction (1300 $kJ.mol^{-1}$). Industrially this reaction is carried out at high temperature (250 °C, 15 bar of which 2/3 are inert gases) in bundles of tubular reactors. Ethene oxide is converted mainly to ethylene glycol for use in anti-freeze liquids and polyesters. Smaller outlets (still bulk chemicals) comprise glycol ethers, polyurethanes, and polyethylene glycols.

Higher alkenes, even propene, must be oxidised to their epoxides with the use of hydroperoxides. As catalysts one can use high-valent titanium or molybdenum complexes acting as a Lewis acid, including heterogeneous analogues. The mechanism is not clear in great detail; in Figure 14.2 a suggested mechanism is given.

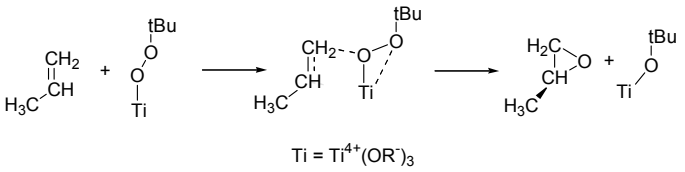

Figure 14.2. Epoxidation with Lewis acids and hydroperoxides

The key factor is the action of the metal on the peroxo group making one oxygen atom electrophilic. Whether or not the metal is bonded to the alkene in the intermediate is not known; if so, this will depend strongly on the particular substrate and the catalyst. Later, in the discussion of the dihydroxylation reaction we will come back to this (section 14.3.2). In the example shown in Figure 14.2 the second product is t-butanol stemming from t-butylhydroperoxide (industrially prepared from isobutane and dioxygen).

Ethylbenzene is oxidised to its hydroperoxide and this hydroperoxide is used for the epoxidation of propene. The resulting phenetylalcohol is dehydrated to give styrene (the major source of styrene industrially is the direct dehydrogenation of ethylbenzene). Such a coupled production of two products might seem ingenious, but it is not very attractive commercially as the two products must be produced in the stoichiometry given rather than in the ratio dictated by the market (it is called the SMPO process, Styrene Monomer, Propylene Oxide process). The weight ratio is about 2:1. The scheme is shown in Figure 14.3. The catalyst may be an immobilised complex of titanium (Shell) or molybdenum and in a homogeneous system also titanium tetraisopropoxide (Arco/ Atlantic Richfield) is used.

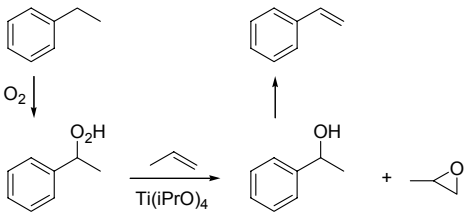

Figure 14.3. The SMPO process

14.2 Asymmetric epoxidation

14.2.1 Introduction

Epoxides are interesting starting materials for further derivatisation. In most instances the reaction will lead to the formation of mixtures of enantiomers (that is when the alkenes are prochiral, or when the faces are enantiotopic). Four important reactions should be mentioned in this context:

- the Katsuki-Sharpless epoxidation of allylic alcohols,
- the Jacobsen asymmetric epoxidation of alkenes,
- the Sharpless asymmetric hydroxylation of alkenes with osmium tetroxide, and
- the Jacobsen enantioselective ring-opening of symmetric epoxides (for example cyclohexene oxide).

It should be added that many other groups have contributed to the pre-developments of these inventions and also to later developments. All four reactions find wide application in organic synthesis. The Sharpless epoxidation of allylic alcohols finds industrial application in Arco's synthesis of glycidol, the epoxidation product of allyl alcohol, and Upjohn's synthesis of disparlure (Figure 14.4), a sex pheromone for the gypsy moth. The synthesis of disparlure starts with a C_{13} allylic alcohol in which, after asymmetric epoxidation, the alcohol is replaced by the other carbon chain. Perhaps today the Jacobsen method can be used directly on a suitable C_{19} alkene, although the steric differences between both ends of the molecules are extremely small!!

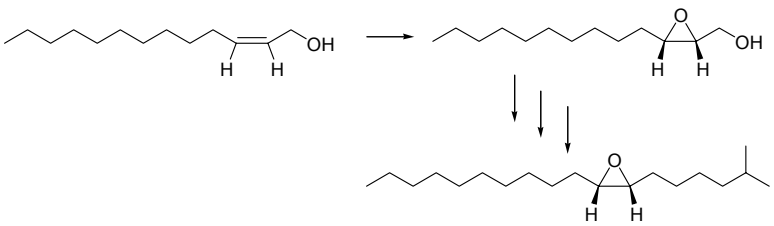

Figure 14.4. Disparlure

14.2.2 Katsuki-Sharpless asymmetric epoxidation

An important breakthrough in asymmetric epoxidation has been the Katsuki-Sharpless invention [1]. The reaction uses a chiral Ti(IV) catalyst, t-butylhydroperoxide as the oxidant and it works only for allylic alcohols as the substrate. In the first report titanium is applied in a stoichiometric amount. The chirality is introduced in the catalyst by reacting titanium tetra-isopropoxide

with one molecule of a simple tartrate ester, made from the natural product tartaric acid. The reaction is shown in Figure 14.5.

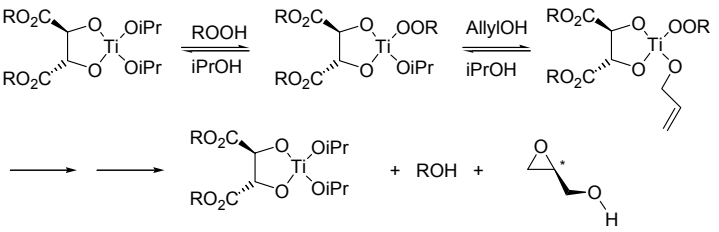

Figure 14.5. Katsuki-Sharpless asymmetric epoxidation

The kinetics of the reaction have been studied [2]. A first order has been found in the concentrations of the titanium catalyst, t-butylhydroperoxide, and the allylic alcohol. The reaction is slowed down by 2-propanol, or more accurately, it has an inverse second order in 2-propanol. Thus, the kinetic equation reads:

$$\upsilon = k_{\text{obs}} \frac{[\text{Ti}][\text{ROOH}][\text{allyl}-\text{OH}]}{[2-\text{PrOH}]^2}$$

This in accordance with the mechanism shown in Figure 14.5. In a pre-equilibrium two 2-propoxide anions are replaced by a tertiary-butylperoxy anion and an allyloxy anion, as follows clearly from the kinetic equation. This intermediate has a very low concentration and has not been observed directly. From here on we can only speculate on the interactions leading to a preferred attack on either of the enantiotopic faces of the alkene.

The kinetic equation rules out the possibility that an oxo species is generated first from hydroperoxide and titanium, which then reacts further with allyl alcohol. At the least, it would be highly coincidental to find these kinetics (the distinct formation of oxo species has been invoked in osmium-catalysed oxidations, as we will see in Chapter 14.3).

The enantioselectivity is not very sensitive to the nature of the allylic alcohol. By contrast, titanium and tartrates are essential to the success. This catalyst components combination is unique; note the difference with the L-Dopa asymmetric hydrogenation, which can be carried out with hundreds of C_2-chiral diphosphines, even monophosphines, but with a limited number of substrates only.

Water has a deleterious effect on the e.e. of the reaction and molecular sieves 4A were added to the reaction mixture, which changed the system from stoichiometric to catalytic [3]. Water and hydroxide are much stronger ligands toward titanium than alcohols and alkoxides, and thus it should be excluded

from the dichloromethane solvent. Furthermore, water may form during the reaction from the alcohols present. The reaction is rather slow, also because it is carried out at –20 °C for obtaining the highest e.e.

The catalyst structure is more complicated than indicated above. Both in solution and in the solid state the catalyst [4] (or closely related analogues) has a dimeric structure. In addition to the four alkoxides, an ester group coordinates to each titanium atom. One of the tartrate alkoxide oxygen atoms functions as a bridging ligand and in this way a six-coordinated, dimeric species is obtained. The dimeric structure is retained during the catalysis as appears from the kinetic studies (first order in Ti concentration), MW determinations, and NMR studies. This opens the possibility of binuclear catalysis, but Sharpless prefers a mechanism in which only one metal is involved. The dimeric structure having C_2-symmetry is shown in Figure 14.6 on the left.

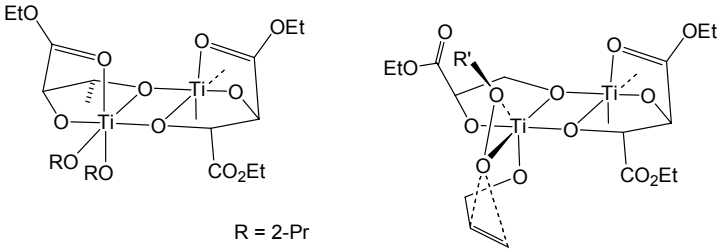

Figure 14.6. Dimeric titanium catalyst (RO and CO_2Et groups omitted from upper part)

Dimerisation and ester coordination restricts the number of sites available for alkoxides to two only, while maintaining a comparatively Lewis-acidic titanium centre, as needed for the reaction. In the dimer, the methine protons, alkoxide groups, and ester groups are inequivalent, but they show a rapid exchange on the ^{1}H NMR timescale at room temperature, as the $\Delta G^{\ddagger}$ for the process is only 64 kJ.mol^{-1}. This process is much faster than the catalytic reaction, but due to the C_2-symmetry of the tartaric esters the resulting structures of the dimers are the same.

Sharpless suggested that the hydroperoxide will coordinate at the equatorial site of one of the titanium cations, as depicted on the right-hand side of Figure 14.6, such that the prospective alkoxide oxygen atom (OR') can migrate to the axial position created by the leaving ester group while the terminal oxygen of the peroxide attacks the alkene. Nevertheless, the two dimer parts do play a role as is evident from the non-linear effect that has been found. The enantiopure dimer is a more reactive catalyst than the racemic dimer and apparently the allyloxy substrate experiences an influence of the titanium fragment to which it is not connected directly.

We speculate that a 1,2-s-*cis* configuration of the allyl alcohol as drawn in the figure will most readily undergo the electrophilic attack. The transition state involves a spiro conformation of the Ti-O-O ring and the O-C-C ring according to DFT calculations [5]. The s-*cis* structure with attack at the alternative face of the alkene moiety would lead to a stronger steric repulsion with the ester group in the right of the drawing, below the Ti_2-O_2 plane. Altogether, this leads to the observed 2S-allylalcohol epoxide when R,R-tartrate is used. In this fashion small groups such as ethyl carboxylic esters in β-positions at considerable distance from the reactive centre can induce such enormous e.e.'s (> 98%). It was found that Z-substituted allylic alcohols reacted much more slowly that E-substituted substrates. In the sketched structure of Figure 14.6 a substituent at the Z position will also interact with the ester group at the "spectator" titanium atom. This is an oversimplified picture as in all probability more species will occur in the media, depending on reactants, substrates and conditions.

Cinnamyl alcohols substituted at the para carbon atom lend support to the mechanism in which the rate-determining step is the attack of the electrophilic oxygen atom; the rate increases with the electron donicity of X, see Figure 14.7 [2].

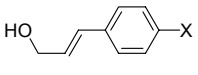

X=	relative rate
NO_2	0.4
H	1.0
Cl	1.2
CH_3O	4.4

Figure 14.7. Electronic effects in asymmetric epoxidation of cinnamyl alcohols

A common issue in "oxene" transfer from metal to an alkene is that of radical intermediates. We will not go into that here, but only hint to this phenomenon. The transfer of oxygen can be a concerted process in which the oxene starts forming a bond with both carbon atoms simultaneously, as we have assumed in the above, or the oxygen atom concentrates its attack on just one carbon atom, in which case a radical might form. In particular work with the use of *cis*- and *trans*-stilbene may demonstrate this. Addition to *cis*-stilbene in a concerted fashion will lead to the *cis* oxirane, but intermediacy of a radical (a stabilised benzylic radical) will give the more stable *trans* product. This has been important in iron and manganese porphyrin catalysed oxidations of alkenes with the use of a variety of oxidising agents. Figure 14.8 shows one possible explanation, the formation of a radical pair. This matter has been subject of extensive study and various mechanisms may be operative [6].

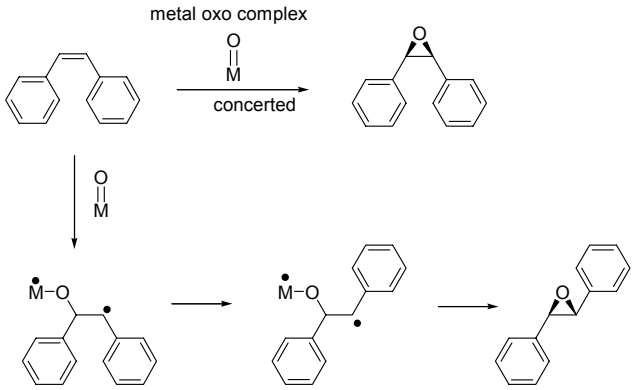

Figure 14.8. Radical versus concerted oxene transfer

ARCO has developed a process for both enantiomers of glycidol based on the Sharpless epoxidation (Figure 14.5) using the more stable and readily available cumylhydroperoxide instead of tert-butylhydroperoxide [7]; the process has been considered for commercial application.

14.2.3 The Jacobsen asymmetric epoxidation

A large assortment of metal complexes of porphyrins, salens (see below), phthalocyanins etc. has been studied as oxidation and epoxidation catalysts with either dioxygen or oxygen donors as the oxidant. As oxygen donors one has used hydrogen peroxide, hydroperoxoides, iodosobenzene (PhIO), NaOCl (bleach), peracids, pyridine-N-oxides, and the like. Typically in these systems the oxygen donor generates a high-valent metal-oxo complex, and subsequently the electrophilic oxo atom is transferred to the hydrocarbon substrate.

Although the Sharpless catalyst was extremely useful and efficient for allylic alcohols, the results with ordinary alkenes were very poor. Therefore the search for catalysts that would be enantioselective for non-alcoholic substrates continued. In 1990, the groups of Jacobsen and Katsuki reported on the enantioselective epoxidation of simple alkenes both using catalysts based on chiral manganese salen complexes [8,9]. Since then the use of chiral salen complexes has been explored in a large number of reactions, which all utilise the Lewis acid character or the capacity of oxene, nitrene, or carbene transfer of the salen complexes (for a review see [10]).

Salen stands for the tetradentate, dianionic ligands bis(salicylidene)-ethylenediamines (not the formal name either!), which form extremely stable complexes with a large variety of metals. Their basic structure and the simplified reaction equation for epoxidation is given in Figure 14.9.

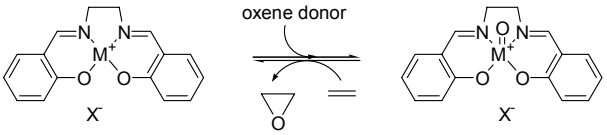

Figure 14.9. Salen structure and epoxidation reaction [10]

Metal salen complexes can adopt non-planar conformations as a result of the conformations of the ethane-1,2-diyl bridge. The conformations may have C_s or C_2 symmetry, but the mixtures are racemic. Replacement of the ethylenediamine linker by chiral 1,2-diamines leads to "chiral" distortions and a C_2 chiral symmetry of the complex due to the half-chair conformation of the 5-membered ring of the chelate. Depending on substitution at the axial positions of the salen complex, the symmetry may be reduced to C_1, but as we have seen before in diphosphine complexes of rhodium (Chapter 4) and bisindenyl complexes of Group 4 metals (Chapter 10) substitution at either side leads to the same chiral complex. Figure 14.10 sketches the view from above the complex and a front view.

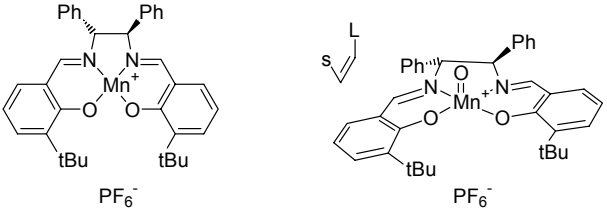

Figure 14.10. Chiral manganese salen complex

In the picture at the right we see that one half of the salen ligand is bent upwards and the other half is bent downward. Preferably the alkene approaches the metal-oxo moiety from the left as there is more space on this side. The side-on approach was first proposed by Groves as part of his studies on enantioselective epoxidation using porphyrin complexes [11]. Bulky substituents at the salicyl ring are crucial to the success as they direct the bulkier group of the alkene to the back of the complex. This can be readily imagined for *cis*-alkenes, as has been drawn, and indeed enantioselectivities are found to be much higher for *cis* alkenes than for *trans* alkenes. For *cis*-β-methylstyrene (1-phenylprop-1-ene) an e.e. of 84% was reported [9] with the use of iodosomesitylene as the oxene donor, while *trans*-β-methylstyrene gave an *e.e.* of 20% only.

The successful application of manganese salen complexes is illustrated in Figure 14.11. In the catalyst used large 2-phenylnaphthyl-1 substituents have

been introduced, while the salicyl benzene ring has also been replaced by a naphthyl moiety. In the ethane-diyl backbone methyl substituents are added at the 3 and 5 positions of the aryl ring. This shows the versatility of the "modular" approach, which is very common today in catalyst design and screening [12]. The aryl groups at the ethanediyl bridge occupy equatorial sites, but note that the analogue having a carboxylic acid group has the opposite absolute configuration and hence should give the opposite enantiomers. It does not give opposite enantiomers, however, which is assigned to the axial position the group assumes as a result of its complexation to the metal [13]. This is reminiscent of the ester complexation in the Sharpless catalyst.

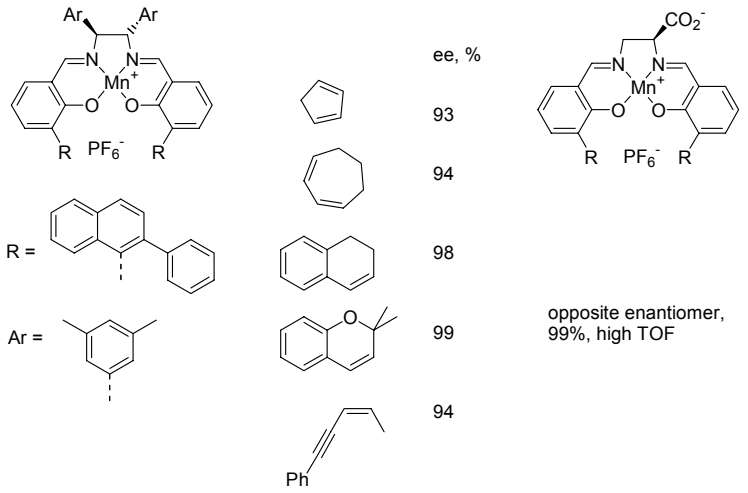

Figure 14.11. Examples of asymmetric epoxidation

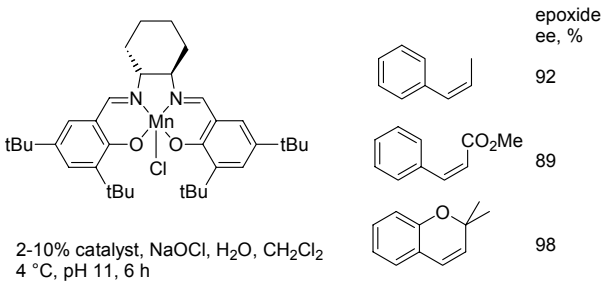

Figure 14.12. Jacobsen's catalyst

Chiral *trans*-cyclohexane-1,2-diamine was used as the bridging diamine and this led to a successful catalyst [14], often referred to as Jacobsen's catalyst (Figure 14.12). The oxidising agent is household bleach (!) diluted and buffered

at high pH. The substrate is dissolved in dichloromethane and the reaction is carried out as a two-phase reaction, the same procedure as is commonly used in metalporphyrin oxidation. The extra t-butyl groups compared to Figure 14.10 led to a further improvement of the performance of the catalyst.

We will conclude this section with a general note on the mechanisms of the asymmetric epoxidations developed by Jacobsen, Katsuki, including the work of Groves and others on porphyrin catalysis. According to experimental and theoretical studies, in this chemistry the "lock-and-key" mechanism seems to prevail. That is to say that most likely the transition state complex with the lowest energy as deduced from models and calculations, is also the one that leads actually to the enantiomer formed. Thus, the most favourable intermediate we construct, is the one leading to the product. Remember, that for asymmetric hydrogenation (rhodium diphosphine, enamide substrates) this was not the case. There we learnt about the "major-minor" issue, meaning that the minor, least stable intermediate, was the one that led to the favoured product. One should keep in mind that we discussed those examples to show the concepts and the results should not be generalised too readily for the whole areas! The transfer of an oxene atom to an alkene does seem more amenable to modelling than a multi-step, asymmetric hydrogenation reaction.

14.3 Asymmetric hydroxylation of alkenes with osmium tetroxide

14.3.1 Stoichiometric reactions

About a decade after the discovery of the asymmetric epoxidation described in Chapter 14.2, another exciting discovery was reported from the laboratories of Sharpless, namely the asymmetric dihydroxylation of alkenes using osmium tetroxide. Osmium tetroxide in water by itself will slowly convert alkenes into 1,2-diols, but as discovered by Criegee [15] and pointed out by Sharpless, an amine ligand accelerates the reaction (Ligand-Accelerated Catalysis [16]), and if the amine is chiral an enantioselectivity may be brought about.

Hydroxylation of alkenes by high-valent metal oxides occurs in two steps, firstly the formation of a metal dialkoxylate (or metallate ester) and secondly the hydrolysis of this species to a 1,2-diol and the low-valent metal hydroxide. The amine plays a role in the first step, the formation of the osmate ester, and Criegee added pyridine to OsO_4 to accelerate the reaction.

The stoichiometric process can be made catalytic when the latter is reoxidised to the high-valent species. The schematic process is portrayed in Figure 14.13. In older literature, the commonest oxidant used in stoichiometric reactions is potassium permanganate ($KMnO_4$), but in the last decades the focus

has been on OsO_4, especially since the discovery of enantioselective, catalytic variants.

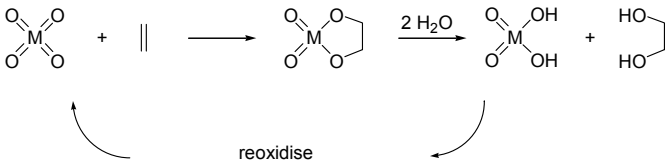

Figure 14.13. Schematic dihydroxylation of alkenes by metal oxo complexes

The stoichiometric enantioselective reaction of alkenes and osmium tetroxide was reported in 1980 by Hentges and Sharpless [17]. As pyridine was known to accelerate the reaction, initial efforts concentrated on the use of pyridine substituted with chiral groups, such as *l*-2-(2-menthyl)pyridine but e.e.'s were below 18%. Besides, it was found that complexation was weak between pyridine and osmium. Griffith and coworkers reported that tertiary bridgehead amines, such as quinuclidine, formed much more stable complexes and this led Sharpless and coworkers to test this ligand type for the reaction of OsO_4 and prochiral alkenes.

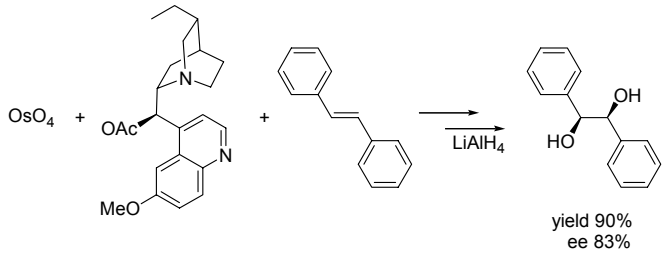

Figure 14.14. Asymmetric addition of OsO_4/dihydroquinine to *trans*-stilbene

In Figure 14.14 we have depicted the most striking result from the 1980 paper involving *trans*-stilbene as the substrate and dihydroquinine acetate. After addition the osmate ester was decomposed by reduction with $LiAlH_4$, a common procedure in the early days, to give the *threo*-diol. A diastereomer of the ligand, dihydroquinidine acetate, gave similar e.e. but the opposite enantiomer. The enantioselectivity was 83%.

The catalyst is a combination of a chemo-catalyst and a natural product taken from the cinchona alkaloids giving amazing results. In phosphine catalysed asymmetric catalysis these types of structures are lacking, as nature does not produce phosphines (!) and the phosphines used in the early years of development of asymmetric homogeneous catalysis lacked the complexity of

cinchona alkaloids. Cinchona species are trees indigenous to tropical South America. The bark contains a high percentage of alkaloids, amongst them quinine, quininidine, and cinchonidine [18]. Quinine and cinchonine (isolated in 1820!) are well known for their use as anti-malaria drugs. Hydrogenation of the vinyl group gives the dihydro derivatives mentioned above (Figure 14.15).

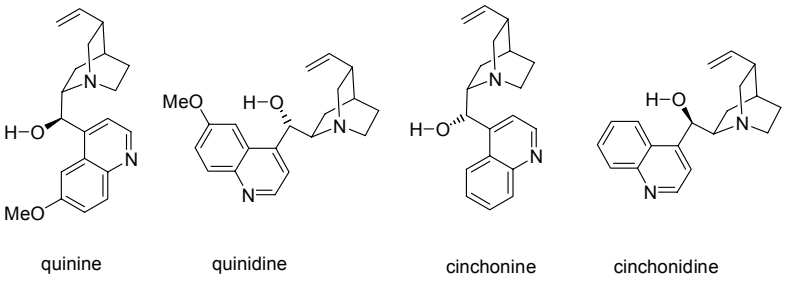

Figure 14.15. Structures of some alkaloids from Cinchona bark

For (E)-1-phenylpropene the e.e. was 48%, but for the (Z) isomer the e.e. was 26% only. This remained a general feature of the reaction: *cis*- alkenes give moderate results (note that (Z)-stilbene would give a non-chiral *meso*-product).

Several other enantiospecific dioxyosmylations have been published since and we will mention only one before turning to the catalytic results. Corey and co-workers used C_2-symmetric amines and obtained the chiral 1,2-diols in high yields and high e.e.'s after reductive work-up for a wide range of *trans*-alkenes [19], see a few examples in Figure 14.16. The reaction was extremely fast and can be carried out at –90 °C (2h ~90% yield) showing the high efficacy of the diamine in accelerating the addition.

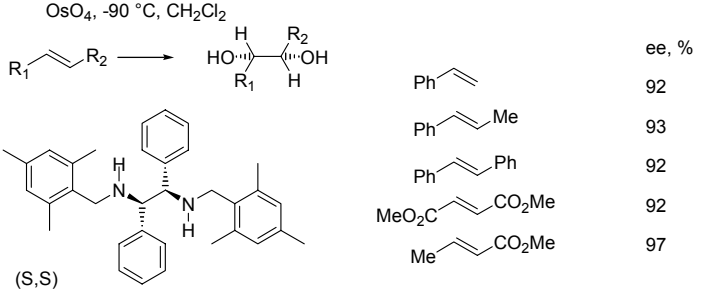

Figure 14.16. Corey's C_2-symmetric diamines in asymmetric dihydroxylation

These results show that bridgehead amines are not a requisite and secondly that bidentate ligands can also be used successfully. Molecular modelling is

relatively easy for C_2-symmetric ligands, as one can nicely see the four quadrants in which the ligand divides the space around osmium tetroxide, two empty quadrants, and two filled quadrants by the mesityl groups. Complexation of a *cis*-diamine to osmium leads to an octahedral complex that contains two axial and two equatorial oxygen atoms. The equatorial ones are likely more electron rich than the axial ones, and therefore it was assumed that at least one axial oxygen atom should be involved in the electrophilic attack to the alkene, the other one necessarily being an equatorial one.

Assuming this 3+2 addition (O=Os=O + C=C) and attack at axial-equatorial oxygen atoms the stereochemical outcome of the reaction could be predicted correctly for *trans*-alkenes. Attack at two equatorial oxygens would predict the wrong stereoisomer. As for the titanium-catalysed epoxidation a "lock-and-key" mechanism is proposed, which seems in this instance very well justified, as the addition is a one-step process governed by steric factors (and electronic factors for the axial versus equatorial issue). A simplified drawing in Figure 14.17 gives the favoured addition.

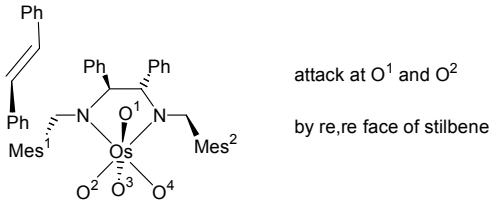

Figure 14.17. Stilbene addition in Corey's osmium complex

Attack from the bottom or the top leads to the same possibilities because of the C_2-symmetry. Attack at O^1-O^4 from above is severely hindered by mesitylene-2 and the same mesitylene will favour addition with the *re,re* face at the O^1-O^2 atoms. This attack (and the symmetry related O^3-O^4 positions) will produce the *S,S*-diastereomer of the diol found experimentally.

The mode of addition of alkene to osmium tetroxide has been the subject of debate, since initially it was thought that a 2+2 reaction occurred and that the metal atom was involved (Os=O + C=C) [17,20]. This gives a metallaoxetane that subsequently will have to rearrange to a metalla-dioxolane, see Figure 14.18. For clarity the amine has been omitted. Computational chemistry is fully in support of the 3+2 mechanism, which has a much lower barrier than the 2+2 mechanism for osmium. Amine complexation lowers the addition only slightly in the calculations, while its accelerating function in catalysis has been well recognised as we mentioned above [21].

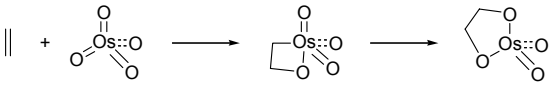

Figure 14.18. The 2+2 mechanism for alkene addition to OsO_4

Initially, it was thought more likely that the electron poor metal atom would be involved in the electrophilic attack at the alkene and also the metal-carbon bond would bring the alkene closer to the chiral metal-ligand environment. This mechanism is analogous to alkene metathesis in which a metallacyclobutane is formed. Later work, though, has shown that for *osmium* the actual mechanism is the 3+2 addition. Molecular modelling lends support to the 3+2 mechanism, but also kinetic isotope effects support this (KIEs for ^{13}C in substrate at high conversion). Oxetane formation should lead to a different KIE for the two alkene carbon atoms involved. Both experimentally and theoretically an equal KIE was found for both carbon atoms and thus it was concluded that an effectively symmetric addition, such as the 3+2 addition, is the actual mechanism [22] for osmium.

14.3.2 Catalytic reactions

Preliminary studies on catalytic osmylation were reported by Kokubo and co-workers who used bovine serum albumin, OsO_4, and t-butylhydroperoxide as the oxidant. Turnover numbers up to 40 and an e.e. for 2-phenylpropene of 68% was achieved [23]. Apparently the protein binds to osmium via nitrogen donors, but as different sites may be available this may lower the e.e.

Sharpless' stoichiometric asymmetric dihydroxylation of alkenes (AD) was converted into a catalytic reaction several years later when it was combined with the procedure of Upjohn involving reoxidation of the metal catalyst with the use of N-oxides [24] (N-methylmorpholine N-oxide). Reported turnover numbers were in the order of 200 (but can be raised to 50,000) and the e.e. for *trans*-stilbene exceeded 95% (after isolation 88%). When dihydriquinidine (*vide infra*) was used the opposite enantiomer was obtained, again showing that quinine and quinidine react like a pair of enantiomers, rather than diastereomers.

The AD has been developed into an extremely useful reaction, and Sharpless states that probably its synthetic utility surpasses that of titanium tartrate-catalysed asymmetric epoxidation [16], since the range of substrates is much larger for AD.

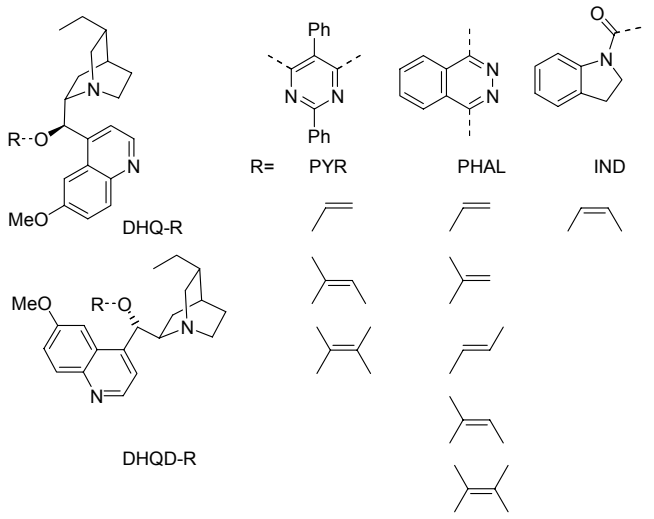

Figure 14.19. Ligand structures as developed by Sharpless and preferred substrates

Step by step, AD was converted into a very practical protocol and the most convenient oxidant found was $K_3Fe(CN)_6$ in t-BuOH/H_2O and a variety of R groups (replacing H in the free alkaloid, or acetate in the first generation of catalysts), each having an optimum performance for different substitution patterns of the alkene substrates (see Figure 14.19). Especially "PHAL" (1,4-phthalazinediyl) as a connector, see Figure 14.19, binding two alkaloid molecules was extremely effective as the second generation catalyst. Two convenient catalyst mixtures are available producing opposite diastereomers. The active amine catalyst component is abbreviated as $(DHQ)_2PHAL$ (AD-mix-α) or $(DHQD)_2PHAL$ (AD-mix-β). In this "dimeric" catalyst only one osmium tetroxide binds two one bridge-head nitrogen atom in the U-shaped cavity that the molecule forms.

The nitrogen ligand accelerates the addition step by orders of magnitude, but since the hydrolysis of the osmate esters becomes rate-determining the maximum effect of this acceleration is usually not obtained in the catalytic system. Since the addition to unmodified OsO_4 is so much slower, the rate of the ligand-free complex is low and substoichiometric amounts of amine (versus Os) can be used. Various co-reagents have been tested and identified which can accelerate the hydrolysis step, for example $MeSO_2NH_2$ [25].

Air or dioxygen can be used as an oxidant with non-chiral DABCO to give a low cost catalyst for dihydroxylation of alkenes into racemic mixtures; dihydroquinidine modified catalysts with the air variant give lower e.e.'s than the AD-mix catalysts [26].

14.4 Jacobsen asymmetric ring-opening of epoxides

Symmetric epoxides such as cyclohexene oxide would be an interesting source of chiral compounds if we were able to open the epoxide ring in an enantioselective fashion. Epoxides will bind to Lewis acids and the use of chiral Lewis acids might lead to enantioselective ring-opening. Nugent reported that chiral Lewis acids of zirconium complexes with S,S,S-triisopropylamine catalysed the enantioselective ring-opening of *meso*-epoxides by azidotrimethylsilane with an e.e. of 93% for the product of cyclohexene oxide [27] in moderate turnover numbers.

Jacobsen reasoned that there might be a relationship between the final stage of an epoxidation process and the binding of an epoxide to a Lewis acid. Thus, the question was, will chiral salen complexes do the job. Indeed, it was found that salen complexes containing chromium(III) or cobalt(III) catalyse the asymmetric ring opening of epoxides. The catalyst structure (see Figure 14.20) is the same as that used for epoxidation shown in Figure 14.12.

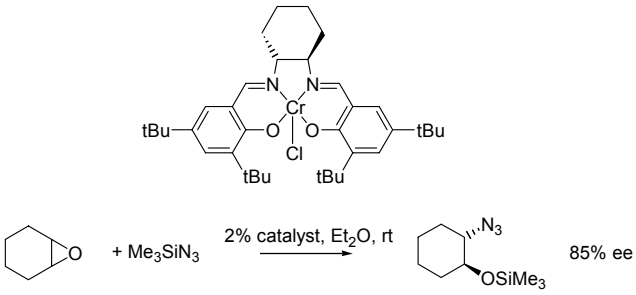

Figure 14.20. Jacobsen's catalyst in enantioselective ring opening of epoxide

A variety of *meso*-epoxides could be selectively ring-opened this way with e.e.'s as high as 97% [28]. The azides can be converted to 1,2-amino alcohols, which are very desirable synthetic intermediates. Surprisingly, the mechanism of the ARO (asymmetric ring-opening) was more complicated than expected [29]. First, it turned out that the chloride ion in Cr-salen was replaced by azide. Secondly, water was needed and HN_3 rather than Me_3SiN_3 was the reactant nucleophile. Thirdly, the reaction rate was found to be second order in catalyst concentration, minus one in epoxide (cyclopentene oxide), and zero order in HN_3 [30].

The second order in catalyst points to the involvement of two chromium salen molecules in the transition state complex. Therefore several dimeric species were synthesised; with suitable linkers the dimeric catalysts gave reaction rates that were one or two orders of magnitude higher than that of the monomeric catalyst. Trimeric species gave still higher reaction rates! The

negative order in substrate can perhaps be explained by a "sandwiching" up to the level of saturation of one substrate molecule in an aggregate, which becomes inactive when a second molecule of epoxide is complexed in this catalyst unit. The zero order for azide was explained by its rate-determining transfer from one chromium centre to the other, holding the epoxide.

Ring-opening by azide and the subsequent work-up is not ideal from a point of view of safety and costs and ring-opening by other nucleophiles is attractive. Furthermore, the use of *meso* compounds restricts the use of the catalyst to a small number of substrates and useful products.

Jacobsen and co-workers discovered that cobalt salen is a good catalyst for the carboxylic acid ring-opening reaction and the serendipitous discovery was made that, when using benzoic acid as the nucleophile for non-*meso* epoxides, a 1,2-diol was generated as a by-product with high enantioselectivity [31]. Diols can only be produced when water is present and the important finding therefore is the hydrolysis reaction taking place with high enantioselectivity. Thus a hydrolytic kinetic resolution was found with the use of trivalent cobalt salen complexes in the presence of a slight excess of water. The remaining epoxide enantiomer also has a high e.e.. We show only one example in Figure 14.21, namely for propene oxide. The ratio of the rates of the two enantiomers of propene oxide is around 500, showing an amazingly large influence of just one methyl group [32]. The e.e. in remaining epoxide and diol exceeded 98%! Larger groups than methyl lead to e.e.'s in excess of 99%.

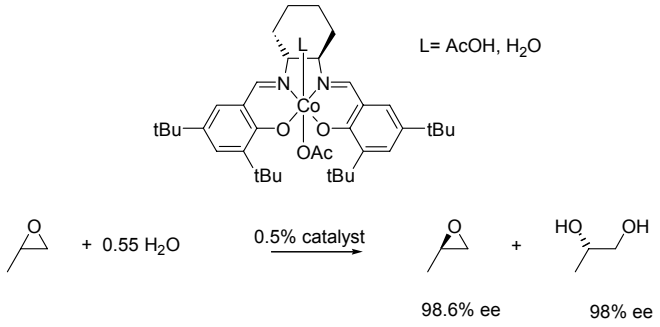

Figure 14.21. HKR for propene oxide

Covalent attachment chiral Co(salen) complexes to polystyrene and silica gave efficient and highly enantioselective catalysts for the hydrolytic kinetic resolution (HKR) of terminal epoxides, including epichlorohydrin. These systems provide practical solutions to difficulties with the isolation of reaction products from the HKR. Removal of the supported catalyst by filtration and repeated recycling was demonstrated with no loss of reactivity or enantioselectivity. The immobilised catalysts have been adapted to a

continuous flow process for the generation of reaction products in high yield and e.e.. Mechanistic studies showed a dramatic correlation between the degree of catalyst site-isolation and reaction rate indicating that also for these cobalt catalysts a cooperative bimetallic mechanism occurs [33].

14.5 Epoxidations with dioxygen

Even though epoxidation reactions with the use of hydrogen peroxide and hydroperoxides are attractive cost-wise and from an environmental point of view, there remains a quest for the use of dioxygen, as it is still cheaper and there might be not even the coproduction of alcohol or water. Such catalytic systems do exist, but in practice there always remains the danger of hydroperoxide formation in such a system and subsequent reactions, either of radical-chain nature or catalysed ones of the types we have seen above in sections 14.1–14.3. Sometimes aldehydes are added on purposes to generate peracids that are the oxidising species with the coproduction of carboxylic acid. Here we will confine ourselves to just one example, namely ruthenium porphyrins [34]. The intriguing property of substituted ruthenium porphyrin is that the dioxide functions as an oxo donor in oxidation reactions and that it can be regenerated with dioxygen. The chemistry of ruthenium porphyrin with dioxygen is complex and depends on substitution of the porphyrin ring and the solvent as well. In their reactions with dioxygen, as many metal porphyrins do, ruthenium porphyrin forms dimers of the type L*Ru*(III)-O-O-*Ru*(III)L (where *Ru* stands for ruthenium porphyrin).

Introduction of mesityl groups at the porphyrin ring can prevent the formation of the dimeric products and the reaction with dioxygen now leads to ruthenium(VI)-dioxo complexes of TMP (tetramesitylporphyrin) [35]. The *trans*-Ru(VI)O_2-TMP species can catalyse the epoxidation of alkenes as well as whole range of other oxidation reactions. After transfer of one oxygen atom to an organic substrate Ru(IV)O-TMP is formed, which disproportionates to an equilibrium of *Ru*O_2 and *Ru*(II):

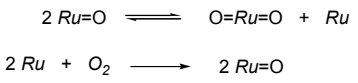

Figure 14.22. Trans-Ru(VI)-TMP-dioxo complex

Epoxidation of *cis*-β-methylstyrene and *trans*-β-methylstyrene produce the epoxides with retention of configuration [36]. The reaction is first order in styrene and *Ru*O_2 and the reaction is faster when the styrene molecules contain electron donating substituents. This shows that the oxo attack at the alkene is an electrophilic attack [37]. Epoxidation of 1-alkenes gives aldehyde as the

byproduct and ruthenium-TMP is deactivated by the formation of the ruthenium-TMP carbonyl complex. By ^{13}C labelling studies it was shown that the carbonyl group stems from the aldehyde side-product [38]; for ruthenium complexes it is not unusual that they find ways to decompose aldehydes and form carbonyl complexes. Formation of aldehydes may invoke several other mechanisms such as radical reactions or ion formation [39]. Asymmetric variants have also been reported, mainly for systems utilising other oxygen donors than dioxygen [34].

It is realised that both ruthenium and the substituted porphyrins are expensive catalyst components for industrial applications. Both turnover frequencies and turnover numbers are modest. Nevertheless it remains an interesting option to use dioxygen directly in epoxidation reactions.

References

1 Katsuki, T.; Sharpless, K. B. *J. Am. Chem. Soc*. **1980**, *102*, 106.
2 Woodard, S. S.; Finn, M. G.; Sharpless, K. B. *J. Am. Chem. Soc*. **1991**, *113*, 106. Finn, M. G.; Sharpless, K. B. *J. Am. Chem. Soc*. **1991**, *113*, 113.
3 Hanson, R. M.; Sharpless, K. B. *J. Org. Chem.* **1986**, *51*, 1922.
4 Pederson, S. F.; Dewan, J. C.; Eckman, R. R.; Sharpless, K. B. *J. Am. Chem. Soc*. **1987**, *109*, 1279.
5 Wu, Y.-D.; Lai, D. K. W. *J. Org. Chem.* **1995**, *60*, 673.
6 Dolphin, D.; Traylor, T. G.; Xie, L. Y. *Acc. Chem. Res.* **1997**, *30,* 251. Ostovic, D.; Bruice, T. C. *Acc. Chem. Res.* **1992**, *25,* 314. Groves, J. T.; Quinn, R. *J. Am. Chem. Soc*. **1985**, *107*, 5790. Meunier, B. *Chem. Rev.* **1992**, *92,* 1411.
7 W.P. Shum and M.J. Cannarsa, *Chirality in Industry II*, eds. A.N. Collins, G.N. Sheldrake and J. Crosby, J. Wiley & Sons, New York, 1997, p 363-380.
8 Zhang, W.; Loebach, J. L.; Wilson, S. R.; Jacobsen, E. N. *J. Am. Chem. Soc*. **1990**, *112*, 2801.
9 Irie, R.; Noda, K.; Ito, Y.; Matsumoto, N.; Katsuki, T. *Tetrahedron Lett.* **1990**, *31,* 7345.
10 Katsuki, T. *Adv. Synth. Catal.* **2002**, *344,* 131.
11 Groves, J. T.; Myers, R. S. *J. Am. Chem. Soc*. **1983**, *105*, 5791.
12 Mikame, D.; Hamada, T.; Irie, R.; Katsuki, T. *Synlett* **1995**, 827. Sasaki, H.; Irie, R.; Hamada, T.; Suzuki, K.; Katsuki, T. *Tetrahedron* **1994**, *50,* 11827.
13 Ito, Y. N.; Katsuki, T. *Tetrahedron Lett.* **1998**, *39,* 4325.
14 Jacobsen, E. N.; Zhang, W.; Muci, A. R.; Ecker, J. R. *J. Am. Chem. Soc*. **1991**, *113*, 7063.
15 Criegee, R. *Justus Liebigs Ann. Chem.* **1936**, *522,* 75, cited in [16].
16 Berrisford, D. J.; Bolm, C.; Sharpless, K. B. Iangew. *Angew. Chem. Int. Ed. Engl.* **1995**, *34,* 1059.
17 Hentges, S. G.; Sharpless, K. B. *J. Am. Chem. Soc*. **1980**, *102*, 4263.
18 www.rain-tree.com/quinine.htm
19 Corey, E. J.; DaSilva Jardine, P.; Scott, V.; Yuen, P-.W.; Connel, R. D. *J. Am. Chem. Soc*. **1989**, *111*, 9243.
20 Sharpless, K. B.; Teranishi, A. Y.; Bäckvall, J.-E. *J. Am. Chem. Soc*. **1977**, *99*, 3120.
21 Deubel, D. V.; Frenking, G. *Acc. Chem. Res.* **2003**, *36,* 645.
22 Corey, E. J.; Noe, M. C.; Grogan, M. J. *Tetrahedron Lett.* **1996**, *37,* 4899. DelMonte, A. J.; Haller, J.; Houk, K. N.; Sharpless, K. B.; Singleton, D. A.; Strassner, T.; Thomas, A. A. *J. Am. Chem. Soc*. **1997**, *119*, 9907.

23 Kokubo, T.; Sugimoto, T.; Uchida, T.; Tanimoto, S.; Okano, M. *J. Chem. Soc. Chem. Commun.* **1983**, 769.
24 VanRheenen, V.; Kelly, R. C.; Cha, D. Y. *Tetrahedron Lett.* **1976**, *17,* 1973.
25 Sharpless, K. B.; Amberg, W.; Bennani, Y. L.; Crispino, G. A.; Hartung, J.; Jeong, K.-S.; Kwong, H.-L.; Morikawa, K.; Wang, Z.-M.; Xu, D.; Zhang, X.-L. *J. Org. Chem.* **1992**, *57,* 2768.
26 Döbler, C.; Mehltretter, G. M.; Sundermeier, U.; Beller, M. *J. Am. Chem. Soc*. **2000**, *122*, 10289.
27 Nugent, W. A. *J. Am. Chem. Soc*. **1992**, *114*, 2768.
28 Martinez, L. E.; Leighton, J. L.; Carsten, D. H.; Jacobsen, E. N. *J. Am. Chem. Soc*. **1995**, *117*, 5897.
29 Jacobsen, E. N. *Acc. Chem. Res.* **2000**, *33,* 421.
30 Hansen, K. B.; Leighton, J. L.; Jacobsen, E. N. *J. Am. Chem. Soc*. **1996**, *118*, 10924.
31 Jacobsen, E. N.; Kakiuchi, F.; Konsler, R. G.; Larrow, J. F.; Togunaga, M. *Tetrahedron Lett.* **1997**, *38*, 773.
32 Schaus, S. E.; Brandes, B. D.; Larrow, J. F.; Tokunaga, M.; Hansen, K. B.; Gould, A. E.; Furrow, M. E.; Jacobsen, E. N. *J. Am. Chem. Soc.* **2002***, 124*, 1307.
33 Annis, D. A.; Jacobsen, E. N. *J. Am. Chem. Soc.* **1999**, *121*, 4147.
34 Ezhova, M. B.; James, B. R. in "*Advances in Catalytic Activation of Dioxygen by Metal Complexes",* Ed. Simándi, L. S. Volume 26, Catalysis by Metal Complexes, Kluwer Academic Publishers, Dordrecht, 2003.
35 James, B. R. *Chem. Ind.* (Marcel Dekker) **1992**, *47,* 245. Camenzind, M. J.; James, B. R.; Dolphin, D. *J. Chem. Soc. Chem. Commun.* **1986**, 1137. Groves, J. T.; Ahn, K. -H. *Inorg. Chem.* **1987**, *26,* 3831.
36 Groves, J. T.; Quinn, R. *J. Am. Chem. Soc.* **1985**, *107*, 5790.
37 Groves. J. T. *Proc. 8th Int. Symp. on Homog. Catal.* Amsterdam, **1992**, K-6.
38 Seyler, J. W.; Fanwick, P. E.; Leidner, C. R. *Inorg. Chem.* **1992**, *31,* 3699.
39 Bruice, T. C. *Aldrichim. Acta* **1988**, *21,* 87. Ostovic, D.; Bruice, T. C. *Acc. Chem. Res.* **1992**, *25,* 314.

Chapter 15

OXIDATION WITH DIOXYGEN

The largest ...

15.1 Introduction

Oxidation with dioxygen is an important reaction as dioxygen is the cheapest and most abundant source of oxygen atoms, even more so when air can be used as the oxidant. Introduction of oxygen in petrochemical feedstocks is crucial in the manufacturing of chemicals. Large-scale chemicals made via oxidative routes include ethylene oxide (Chapter 14.1), styrene (Chapter 14.1), acetic acid, phenol, maleic anhydride, adipic acid, phthalic acid, and acetaldehyde. The latter two examples will be discussed in this chapter. Acetic acid is made via partial combustion of butane, but there is also a syn-gas route as we have seen in Chapter 6. There are several routes to phenol; the one involving oxidation uses cumene ($iPrC_6H_5$), which is converted to its hydroperoxide via a radical chain reaction and decomposed to acetone and phenol. Maleic anhydride is made via oxidation of butane or benzene with the use of a heterogeneous vanadyl pyrophosphate catalyst.

Adipic acid ($HO_2C(CH_2)_4CO_2H$), one of the components of nylon-6,6, is the product of the sequence benzene–cyclohexe/ane/–cyclohexanol/one via hydrogenation and radical catalysed air-oxidation with cobalt initiators, very similar to phthalic acid to be discussed below. The last step to adipic acid is carried out with nitric acid in a stoichiometric reaction. This gives large amounts of nitrogen oxides (N_2O) as by-product [1], which have to be removed from the off-gases. There is a demand for better catalytic or enzymatic routes. A catalytic alternative that has been studied is the double hydroxycarbonylation of butadiene with palladium, iridium, and rhodium catalysts. A catalytic direct oxidation of cyclohexene also reduces the number of steps and by-products; as yet this route uses hydrogen peroxide as the oxidant [2]. A glucose-based biocatalytic route has also been described [3].

Selective oxidation with the use of air or dioxygen remains a major challenge, even for such simple compounds as methanol, phenol, higher alcohols, which are all made via large detours. The production of detergent alcohols requires a large number of steps (cracking of alkanes, oligomerisation of ethene, metathesis of alkenes, hydroformylation, hydrogenation!). The route starting from fatty acid esters requires fewer steps. Still, these optimised detours have reached an impressive atom and energy economy, which makes it hard for new routes to compete. Furthermore, large investments are involved in these bulk chemicals and timing is an important factor in renovation.

15.2 The Wacker reaction

Acetaldehyde is the product of the Wacker process. At the end of the fifties oxidation of ethene to ethanal replaced the addition of water to acetylene, because the acetylene/coal-based chemistry became obsolete, and the ethene/petrochemistry entered the commercial organic chemicals scene. The acetylene route involved one of the oldest organometallics-mediated catalytic routes started up in the 1920s; the catalyst system comprised mercury in sulfuric acid. Coordination of acetylene to mercury(II) activates it toward nucleophilic attack of water, but the reaction is slow and large reactor volumes of this toxic catalyst were needed. An equally slow related catalytic process, the zinc catalysed addition of carboxylic acids to acetylene, is still in use in paint manufacture.

Ethanal is only used as an intermediate to acetic acid and its derivatives and in the near future production of ethanal will be replaced by other routes based on methanol and syn-gas to give acetic acid and acetic anhydride. Vinyl acetate can also be made via syn-gas routes, but the major producer in Europe employs a direct Wacker route with a heterogeneous palladium catalyst (former Hoechst: ethene, acetic acid –from syn-gas–, and oxygen).

The Wacker-Hoechst process has been studied in great detail and in all textbooks it occurs as *the* example of a homogeneous catalyst system illustrating nucleophilic addition to alkenes. Divalent palladium is the oxidising agent and water is the oxygen donor according to the equation:

$$Pd^{2+} + H_2O \rightarrow Pd(0) + 2\,H^+ + \text{“O”}$$

The overall reaction reads:

$$C_2H_4 + 1/2\,O_2 \rightarrow CH_3CHO \qquad \Delta H = -244\ \text{kJ.mol}^{-1}$$

Including the palladium component the reaction reads:

$$C_2H_4 + Pd^{2+} + H_2O \rightarrow Pd(0) + 2\,H^+ + CH_3CHO$$

The reaction is highly exothermic as one might expect for an oxidation reaction. The mechanism is shown in Figure 15.1. Palladium chloride is the catalyst, which occurs as the tetrachloropalladate in solution, the resting state of the catalyst. Two chloride ions are replaced by water and ethene. Then the key-step occurs, the attack of a second water molecule (or hydroxide) to the ethene molecule activated towards a nucleophilic attack by co-ordination to the electrophilic palladium ion. The nucleophilic attack of a nucleophile on an alkene coordinated to palladium is typical of "Wacker" type reactions.

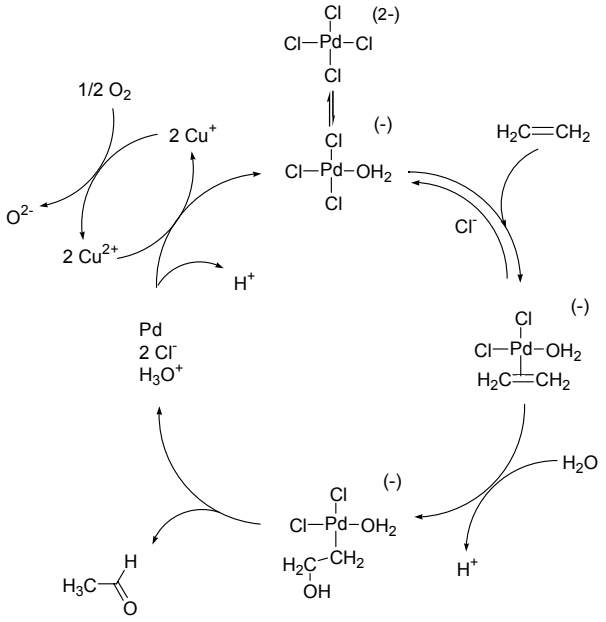

Figure 15.1. Reaction sequence of the Wacker reaction

The nucleophilic attack of the water or hydroxide species takes place in an *anti* fashion; i.e. the oxygen attacks from outside the palladium complex and the reaction is not an insertion of ethene into the palladium oxygen bond. This has been demonstrated in a model reaction by Bäckvall [4]. The reaction studied was the Wacker reaction of dideuterio-ethene (*cis* and *trans*) in the presence of excess of LiCl, which is needed to form 2-chloroethanol as the product instead of ethanal. The latter product would not reveal the stereochemistry of the attack! Note that all of the mechanistic work has been carried out, necessarily, on systems deviating in one aspect or another from the real catalytic one. The outcome depends strongly on the concentration of chloride ions [5].

The rate equation of the Wacker process reads as follows:

$$v = k[PdCl_4^{2-}][C_2H_4][H_3O^+]^{-1}[Cl^-]^{-2}$$

The tetrachloropalladate is the resting state of the catalyst and in a fast pre-equilibrium the crucial intermediate is formed. Note that we only have the kinetic data to support this hypothesis. The intermediate formed by the hydroxide attack is 2-hydroxyethylpalladium. After a rearrangement of the hydroxyethyl group, acetaldehyde (ethanal) forms and palladium zero is the reduced counterpart.

The literature disagrees about the rate-determining step of the Wacker process; this may be the β-hydroxyethyl formation, or a step following this e.g. the loss of another chloride ion (hence the strong inhibiting effect of high chloride concentrations). From that intermediate onwards all processes are fast and kinetics do not learn what might be happening.

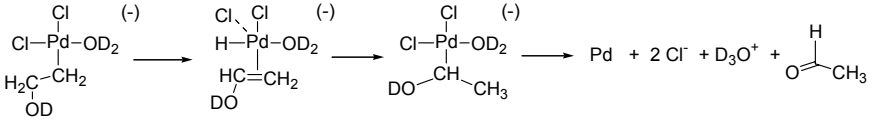

Figure 15.2. The Wacker reaction in D_2O

Studies in deuterated water have shown that the hydroxyl proton does not end up in the ethanal formed. The decomposition of the 2-hydroxyethyl is not a simple β-elimination to palladium hydride and vinyl alcohol, which then isomerises to ethanal. Instead, the four protons stemming from ethene are all present in the initial ethanal product [6] (measured at 5 °C in order to suppress deuterium/hydrogen exchange in the product) and most authors have therefore accepted an intramolecular hydride shift as the key-step of the mechanism (see Figure 15.2). There remains some doubt as to how the hydride shift takes place.

In its stoichiometric form, the reaction had been known since the beginning of the 20th century. Direct reoxidation of palladium by oxygen is extremely slow. The invention of Smidt (Wacker Chemie) involved the intermediacy of copper in the re-oxidation of palladium:

$$2\ Cu^{2+} + Pd(0) \rightarrow 2\ Cu^{+} + Pd^{2+}$$

$$2\ Cu^{+} + 1/2\ O_2 + 2H^{+} \rightarrow 2\ Cu^{2+} + H_2O$$

At present the Wacker reaction should be regarded as a relatively slow process, with only a few hundred turnovers per hour at elevated temperatures and pressures. For internal alkenes the rate is one or two orders of magnitude lower and the reaction affords mixtures of products due to isomerisation. In the absence of isomerisation, the product of the Wacker oxidation of a 1-alkene is a

methyl ketone, a useful method in organic synthesis. Propene will give acetone, which we can explain both by electronic and steric arguments, as the internal carbon atom is the most electrophilic. There are a few rare examples of palladium catalysts that give aldehydes (<70%) from terminal alkenes [7], which probably involve cycloaddition reactions.

Process description

Here we will describe the one-stage process in which oxygen is used as the oxidant and all reactions take place in one vessel.

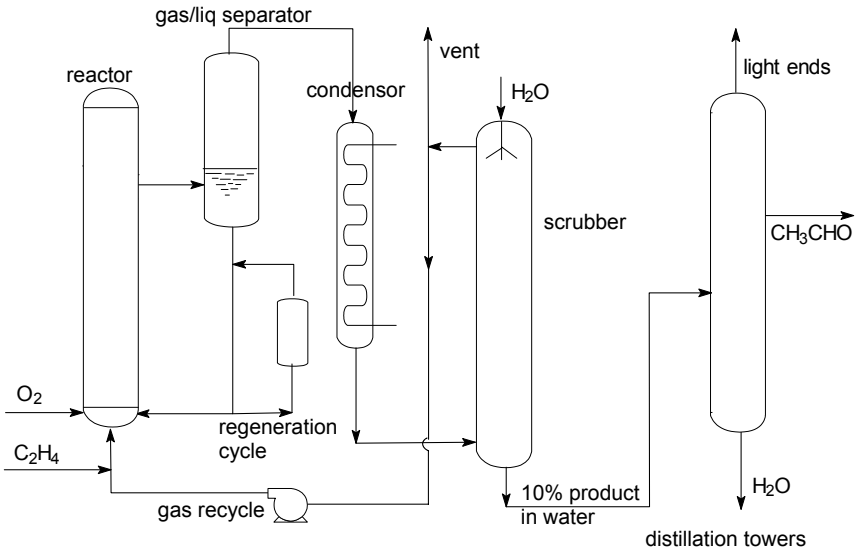

Figure 15.3. Simplified flow-scheme of the Wacker process

Figure 15.3 shows the flow diagram of the one-stage Wacker process (Hoechst). Oxygen and ethene are fed into the reactor (130 °C, 4 bar) containing an aqueous solution of palladium and copper chlorides. Catalyst concentrations have not been published. The reactor is a gas lift reactor and at the top the liquid/gas is removed. In a separate vessel, liquid and gas are separated and heat is removed by further evaporation. The gas contains acetaldehyde, unreacted ethene and oxygen, and side products such as carbon dioxide, hydrocarbons and water. Only the side-reactions give water and water has to be kept in balance in the reactor. The gases are cooled in the condenser and scrubbed in the next column with water. The unreacted gas is returned to the reactor and a vent balances the production of carbon dioxide and inert impurities in the feed such as ethane, methane and nitrogen. The water solution leaving the scrubber contains 10% of acetaldehyde. In a distillation unit, the last traces of light ends are removed and water and acetaldehyde (b.p. 20 °C, 1 bar)

are fractionated. Acetaldehyde is completely miscible with water and forms no azeotrope.

In the two-stage process, reoxidation of palladium is carried out in a second reactor with air. Both processes utilise the intermediacy of copper in the reoxidation reaction. In the first stage, a stoichiometric oxidation of ethene by palladium(II) (and perhaps some Cu(II)) takes place. The two-stage process can be compared with heterogeneous oxidation reactions operating via the Mars-van Krevelen mechanism [8] such as the oxidation of benzene to maleic anhydride (Monsanto, Dupont); a solid catalyst in the oxidised state is used to oxidise benzene in one reactor and in a separate reactor (fluidised bed) the solid is reoxidised with air (or oxygen). As in the two-stage Wacker process, this circumvents the danger of explosions when the hydrocarbon and oxygen are mixed in one reactor.

When air is used as the oxidant, the gas cannot be recycled since inert nitrogen would accumulate in the system. The one-stage process requires recycling of the gas, because it contains unconverted ethene and thus oxygen is used.

A major disadvantage of the Wacker chemistry using chloride catalysts is the production of chlorinated byproducts such as chloroethanal. These have to be removed since they are toxic and cannot be allowed in the wastewater. In the small recycle loop the catalyst solution is heated to 160 °C which leads to decomposition of chlorinated aldehydes under the influence of the metal chlorides. The traces going over the top in the gas/liquid separator have to be removed from the wastewater by different means. The toxicity inhibits biodegradation. Chlorine free catalysts have been studied but have not (yet) been commercialised.

15.3 Wacker type reactions

A development of the last two decades is the use of Wacker activation for intramolecular attack of nucleophiles to alkenes in the synthesis of organic molecules [9]. In most examples, the nucleophilic attack is intramolecular, as the rates of intermolecular reactions are very low. The reaction has been applied in a large variety of organic syntheses and is usually referred to as Wacker (type) activation of alkene (or alkynes). If oxygen is the nucleophile, it is called oxypalladation [10]. Figure 15.4 shows an example. During these reactions the palladium catalyst is often also a good isomerisation catalyst, which leads to the formation of several isomers.

The mechanism of the reaction in Figure 15.4 involves coordination of palladium to the alkene and nucleophilic attack of oxygen at the internal carbon atom to form the five-membered ring. Palladium is bonded to the exocyclic carbon atom. β-hydride elimination gives the exocyclic methylene,

and thus a re-insertion and another β-hydride elimination must take place to form the product observed. A rapid, intramolecular sequence of insertions and eliminations is not uncommon in Wacker type chemistry.

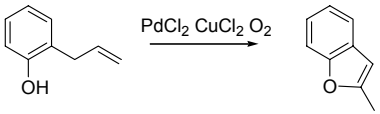

Figure 15.4. Oxypalladation of 2-allylphenol

The palladium zero has to be reoxidised after the first turnover has occurred. The turnover number is often not very high, even though copper is used to catalyse the reoxidation. The exact nature of the palladium/copper intermediates is not known; it is presumed that they form larger aggregates with mixed valences. In the absence of copper, the re-oxidation of palladium is slow. In certain cases it was found (or only postulated) that large palladium clusters are formed containing Pd(0) in the inner part and Pd(II) at the surface. The reaction shown in Figure 15.5 is an example for which nicely the occurrence of "giant" palladium clusters as the catalysts has been proven (nano-particles in today's jargon) [11]. The most abundant cluster in this system is Pd_{561}, carrying acetate and sulfoxide ligands at the surface.

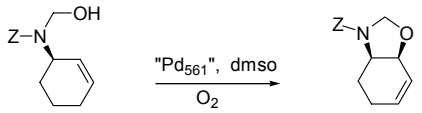

Figure 15.5. Giant palladium cluster in Wacker reactions

Asymmetric Wacker type cyclisations have also been explored with the use of 3,3'-diisopropyl 2,2'-bis(oxazolyl)-1,1'-binaphthyls as the chiral ligand [12]. The reaction and ligand are shown in Figure 15.6. The catalyst loading is 10% and an ee of 85% is obtained at 88% yield. Such a high loading is not unusual in this type of applications. When the amount of ligand was doubled, the ee increased to 97%. This was explained by the relative instability of the complexes formed due to the wide bite angle of the ligand. On the other hand, the embracing effect of the ligand is needed to ensure that there is sufficient steric bulk near the coordinating alkene substrate. Interestingly a tetrasubstituted alkene is used for which one would not expect a facile coordination to palladium. Secondly, three of the substituents at the alkene are alike (methyl groups) and thus the enantiodiscrimination remains remarkable even for an intramolecular reaction.

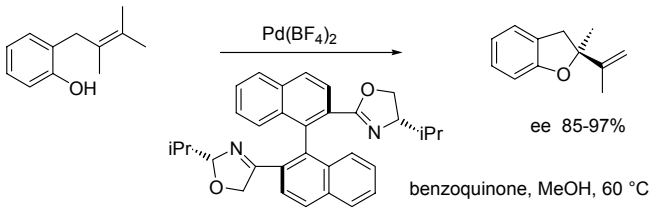

Figure 15.6. Enantioselective Wacker-type ring-closure of an allylphenol

Nitrogen nucleophiles. The oxygen nucleophiles discussed so far are weak ligands towards palladium^{2+}, and thus ligand complexation does not interfere with alkene co-ordination. Amines, however, form strong bonds with electrophilic metals, and this reduces the activity of palladium as a catalyst in Wacker reactions. Figure 15.7 shows an interesting example how this problem can be solved [13]. Cyclopentyl amine coordinates to palladium and no further reaction takes place. After acylation of nitrogen, the nitrogen donor will no longer coordinate to palladium and the nucleophilic attack now occurs, but the metallacycle formed does not react further and palladium is retained in the complex as shown. When the amine is tosylated, however, complete conversion to the unsaturated "Wacker" product is obtained.

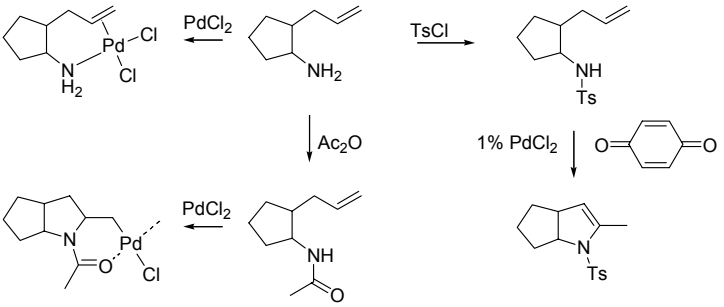

Figure 15.7. Palladium catalysed addition of nitrogen nucleophiles to alkenes

Again we see that an alkene isomerisation reaction has taken place. Another important, useful reagent applied in this field is also pictured in Figure 15.7, *viz*. the use of benzoquinone as the re-oxidant for palladium. Quinone takes the role of dioxygen as oxidising agent. It is very efficient and both quinone and hydroquinone are inert towards many substrates. Furthermore, no water is formed, as is the case when dioxygen is used.

Interception of the palladium-carbon bond by inserting another molecule such as an alkene or a carbon monoxide molecule is a very useful tool. In

Figure 15.8 a simple example is presented of a subsequent insertion of CO and methanolysis of the palladium acyl intermediate [14]. This is not a very common reaction, because both the ligand requirements and the redox conditions for Wacker and carbonylation chemistry are not compatible. For insertion reactions one would use *cis* coordinating diphosphines or diimines, which makes the palladium centre more electron-rich and thus the nucleophilic attack in the Wacker part of the scheme will be slowed down. In addition, the oxidants present may lead to catalytic oxidation of carbon monoxide.

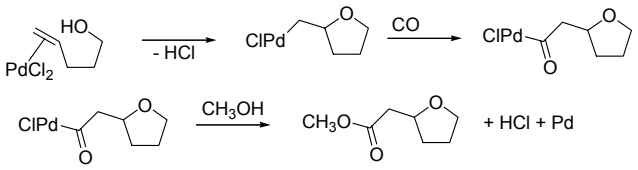

Figure 15.8. Cascade reactions involving a Wacker reaction and methoxycarbonylation

Many nitrogen nucleophiles have been used in this reaction yielding a wide variety of products [15].

15.4 Terephthalic acid

Introduction. The production of terephthalic acid (1,4-benzenedicarboxylic acid) has several interesting features. First, it is one of the examples of a homogeneous, radical-catalysed oxidation with the use of dioxygen and cobalt salt initiators. Secondly, it is an example of a catalyst/product separation involving a filtration of the product from the liquid that contains the catalyst. Crystallisation on such a huge scale is not very attractive, but the low solubility of phthalic acid in many solvents and the high boiling point do not allow any other solution. Theoretically, a solvent-solvent extraction would be an option, but we are not aware of a viable combination of solvents.

Terephthalic acid is used for the production of polyesters with aliphatic diols as the comonomer. The polymer is a high-melting, crystalline material forming very strong fibres. In production volume it is the largest synthetic fibre and the production of terephthalic acid is the largest scale operated process based on a homogeneous catalyst. More recently, the packaging applications (PET, the recyclable copolymer with ethylene glycol) have also gained importance. Terephthalic acid is produced from p-xylene by catalytic oxidation with oxygen. The overall reaction for making terephthalic acid reads as shown in Figure 15.9. The reaction is carried out in acetic acid and the catalyst used is cobalt (or manganese) acetate and bromide. Phthalic anhydride is made from naphthalene or o-xylene by air oxidation over a heterogeneous catalyst. The

main application of phthalic anhydride is in the form of dialkyl esters used as plasticisers (softeners) in PVC. The alcohols used are for instance 2-ethylhexanol obtained from butanal, a hydroformylation product.

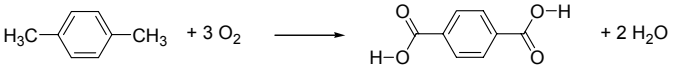

Figure 15.9. Oxidation of paraxylene to terephthalic acid

The reaction produces two moles of water per mole of terephthalic acid. The oxidation reaction is a radical process. The key step of the reaction scheme involves the cobalt(III) bromide catalysed H-abstraction to give a benzylic radical, hydrogen bromide and a divalent cobalt species (Figure 15.10). This is the initiation process of the radical chain reaction. Without cobalt or manganese and bromide the reaction would be very slow. The benzylic radical reacts with dioxygen to give a peroxo radical. The peroxo radical can continue the cycle in various ways. Like all other oxo radicals formed later in the cycle it can abstract hydrogen from another substrate molecule or it can react with a divalent cobalt complex and oxidise cobalt(II) again to cobalt(III). This is the second important reaction in this scheme because it regenerates the initiator. As a result of radical coupling reactions the radicals will disappear and thus trivalent cobalt is needed to start new radical chain reactions.

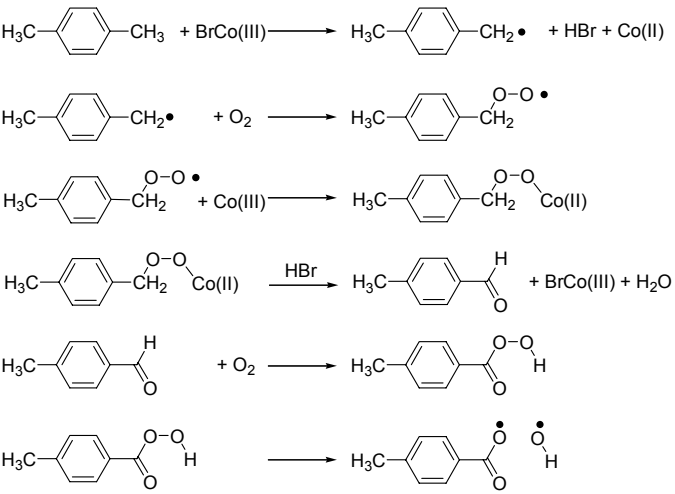

Figure 15.10. Abridged reaction scheme for catalytic, radical oxidation of p-xylene

When one methyl group has been oxidised, 4-toluic acid is formed. This intermediate is soluble in the solvent used, acetic acid. In the next step it is oxidised to terephthalic acid, which is almost insoluble in acetic acid. The intermediate product is 4-formylbenzoic acid. This cocrystallises with the final product. Since it is a mono-acid it will cause a termination of the polymerising chain.

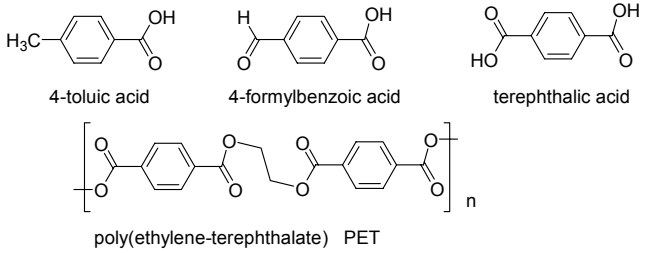

Figure 15.11. Important structures involved in PET manufacture

High molecular weights are needed to obtain strong materials. Thus, the presence of mono-acids is detrimental to the quality of terephthalic acid and they have to be carefully removed. One approach involves a second oxidation carried out at higher temperatures and the other method involves reduction of the formylbenzoic acid to toluic acid. The latter is more soluble and stays behind in the liquid. The reduction is done with a palladium catalyst on carbon support. This method gives the highest quality terephthalic acid.

The polymerisation with ethylene glycol can be carried out directly from the acid if this is very pure. Older processes are based on a transesterification process using dimethyl terephthalate. The intermediacy of the latter gives another opportunity for further purification. The esterification/ polymerisation is conducted at high temperatures (200–280 °C) using metal carboxylates as homogeneous catalysts. In the laboratory high molecular weights are obtained by removing the last traces of water under vacuum.

Process description

Most of the terephthalic acid is produced with a catalyst system developed by Scientific Design. It was purchased by Amoco and Mitsui and is referred to as the Amoco Oxidation. The solvent is acetic acid. Compressed air is used as the source for oxygen. The catalyst dissolved in acetic acid and the two reactants are continuously fed into the reactor. The temperature is around 200 °C and the pressure is approximately 25 bar. The reaction is very exothermic (1280 $kJ.mol^{-1}$, calculation from data in Stull et al [16]; often a much higher, erroneous value is cited). This heat of reaction is removed by evaporation/condensation of acetic acid and can be used in the solvent distillation/purification part of the plant. A scrubber washes the vent gases

(inert gas traces and by-products such as carbon dioxide resulting from over-oxidation). See Figure 15.12 for a simplified flow-scheme.

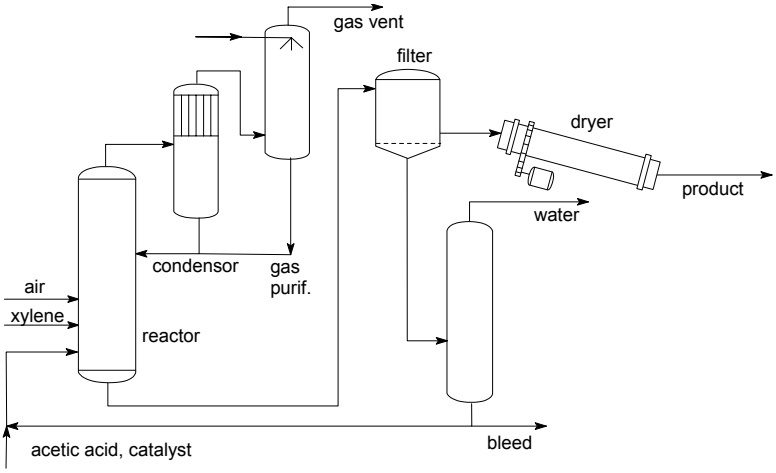

Figure 15.12. Simple flow-scheme for terephthalic acid production

The oxidation proceeds in two steps, p-toluic acid is the intermediate. This mono-acid has a high solubility in this medium and undergoes the second oxidation. The conversion is high, approaching 100% and the yield based on p-xylene is ~95%. The solubility of terephthalic acid in most solvents is extremely low, even at this high temperature. The solubility in acetic acid at room temperature is 0.1 g/l and at 200 °C it is still only 15 g/l. Thus, most of the product crystallises while it is being formed and as mentioned above the intermediate formylbenzoic acid cocrystallises. The mixture of liquid and solid is led to a filter in which the crude product containing 0.5% of mono-acid is collected. The liquid, containing traces of xylene, p-toluic acid, water, the catalyst, and some product is sent to a distillation unit to remove water and to recover acetic acid and the catalyst. The catalyst is relatively cheap, but the heavy metals cannot be simply discarded and a recycle of these robust catalysts would seem to be in place.

As outlined above a purity of "only" 99.5% is not sufficient for a polymer feedstock and the mono-acid intermediate has to be removed either by oxidation under more forcing conditions (Mitsubishi) or reduction (Amoco). In the Amoco process (not shown) the crude di-acid is dissolved in water (275 °C) (15 % weight) and hydrogenated over a palladium on carbon catalyst. The intermediate 4-formylbenzoic acid is hydrogenated to 4-toluic acid which has a much higher solubility and does not cocrystallise with terephthalic acid. The solution is carefully cooled while the product crystallises and the by-product remains in the water. The final content of 4-formylbenzoic acid is as low as 15

ppm. The proportion of toluic acid may be an order of magnitude higher. Aldehydes usually cause colouring of polymers and that is an additional reason to remove them carefully.

Present developments. One might think that an established reaction such as aerobic oxidation (or autoxidation) is not the subject of further research and improvement, but this is definitely not the case and both new homogeneous and heterogeneous catalysts are in development. In the introduction we already mentioned the drawbacks of oxidation of cyclohexene to adipic acid and several researchers address this challenge. Also a highly developed reaction such as the oxidation of paraxylene is subject to further improvements.

We mention one example of a recent catalyst modification, with the risk of omitting several important other ones. Cobalt or manganese initiated autoxidation requires the presence of bromide ions for the initial abstraction of a hydrogen radical. Halides in such a medium of acids and oxygen, and high temperatures, are highly corrosive and replacement by another initiator would be of interest. Ishii and co-workers reported on potential organic replacement molecules [17]. One example is N-hydroxyphthalimide (NHPI), which presumably reacts with a cobalt oxygen complex to give the radical phthalimide N-oxyl (PINO) which starts the autoxidation cycle(s) in the normal fashion. It works for the aerobic oxidation of benzylic compounds, alkylbenzenes, cyclohexene, polycyclic alkanes, and alcohols (Figure 15.13). Another active molecule is N,N'N''-trihydroxycyanuric acid (THICA), which also produces a related N-oxyl radical.

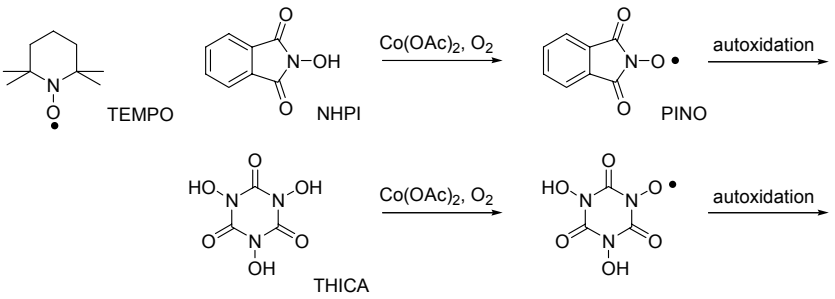

Figure 15.13. Carbon-centred radical producing catalysts

Synthesis of aldehydes from alcohols is an important transformation in several applications. In small scale oxidations still chromic acid is being used as a stoichiometric oxidant of alcohols, which leads to a large amount of toxic waste and it is also expensive. Catalytic routes have been reported using palladium catalyst [18], or TEMPO (see also Figure 15.13) as a radical catalyst for the oxidation of alcohols [19], or combinations of TEMPO and copper [20]; related work is mentioned in the references of these articles. The mechanism of

the palladium-catalysed reaction has been studied. One of the catalysts used is shown in Figure 15.14; in general dipyridine type ligands can be used with palladium acetate, in water at high pH, and a 30 bar pressure of air. Turnover frequencies are 50 $m.m^{-1}.h^{-1}$ or less at 100 °C, which may not seem extremely high yet, but compared to stoichiometric means producing large amounts of toxic waste this catalytic route is superior. The highest rate and 100% selectivity were obtained for 3,3-dimethylbutan-2-ol. For hexan-1-ol the selectivity amounted to 90%, but with TEMPO added it increased to 97%, see below.

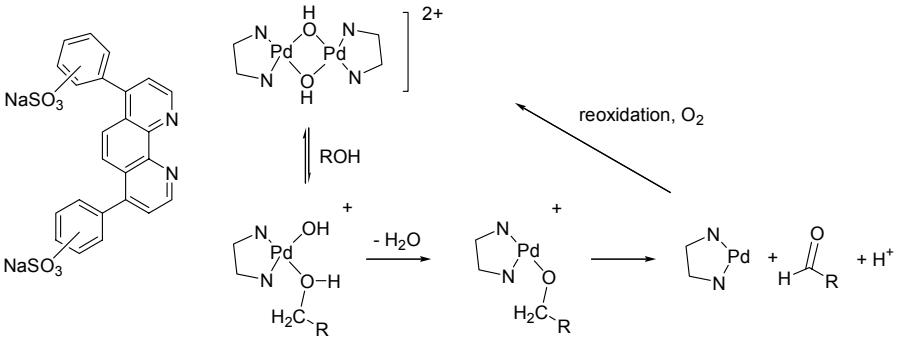

Figure 15.14. Catalytic oxidation of alcohols [18]

The reaction rate is half-order in palladium and dimeric hydroxides of the type shown are very common for palladium. The reaction is first order in alcohol and a kinetic isotope effect was found for CH_2 versus CD_2 containing alcohols at 100 °C (1.4–2.1) showing that probably the β-hydride elimination is rate-determining. Thus, fast pre-equilibria are involved with the dimer as the resting state. When terminal alkenes are present, Wacker oxidation of the alkene is the fastest reaction. Aldehydes are prone to autoxidation and it was found that radical scavengers such as TEMPO suppressed the side reactions and led to an increase of the selectivity [18].

15.5 PPO

Poly(phenylene oxide) PPO, or poly(phenylene ether) PPE, is an engineering polymer developed by General Electric. It concerns the oxidative coupling of phenols discovered in 1956 by Allan S. Hay [21]. Oxidative coupling leads to the formation of carbon-oxygen bonds between carbon atoms 2, 4, and 6 and the phenolic oxygen atom. To avoid coupling with carbon atoms 2 and 6, alkyl substituents at these two positions were introduced. In addition to the polymer a 4,4' dimer is formed, named diphenoquinone (DPQ). The

commercial product is made from 2,6-dimethylphenol DMP or 2,6-xylenol). Copper catalysts with nitrogen ligands and dioxygen as the oxidant are used (Figure 15.15). With methyl and ethyl groups at the 2 and 6 positions of phenol polymer is formed, but larger groups such as two isopropyl groups, or one t-butyl and one methyl group give 4,4' coupling to diphenoquinone, because of steric hindrance at the oxygen atom. When pyridine is used as the ligand for copper a large excess of pyridine is required, but for a bidentate such as tetramethylethylene-1,2-diamine (TMEDA) a one to one ratio with copper is optimal. The TMEDA catalyst is much more active than the pyridine-based one. Water, formed as the by-product, diminishes catalyst activity. N,N'-tBu_2-ethylene diamine gives a hydrolytically stable and active catalyst [22].

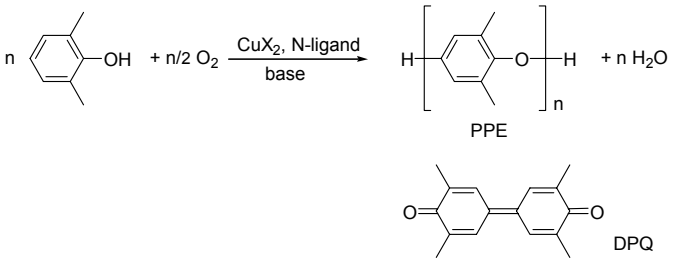

Figure 15.15. Copper catalysed oxidative coupling of phenols

The mechanism is not known in all details in spite of a large amount of research devoted to it. Phenols form readily the phenoxy radical by abstraction of hydrogen, but the free phenoxy radical is not involved in the reaction leading to polymer. Typical hydrogen abstracting reagents such as Fenton's reagent and benzoyl peroxide lead to large amounts of DPQ, the 4,4' coupled dimer. For this reason most authors agree that the reaction giving polymer requires a two-electron oxidation with the formation of phenoxonium cations.

The polymerisation reaction is a step growth polymerisation similar to a condensation polymerisation of amides or esters. The reaction starts with monomers, which dimerise, trimerise, etc. continuously maintaining a Flory-Schulz distribution.

Monovalent copper salts were initially found to be better catalyst precursors than divalent copper salts. The latter needed the addition of base. In the presence of dioxygen the copper(I) salts are oxidised to copper(II) hydroxides forming hydroxide bridged dimers. The hydroxides can be replaced by phenolates, thus producing the key-intermediate [23] (Figure 15.16). From this equilibrium we understand that water concentration should be kept low in order to have a maximum amount of phenoxides coordinated to the copper dimers.

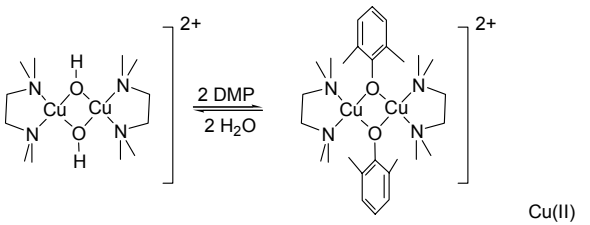

Figure 15.16. Key intermediates for oxidative 2,6-Me_2-phenol polymerisation

When two electrons are transferred from a phenoxide anion to the copper dimer, we form the phenoxonium cation and two copper(I) ions are formed. Most likely, the phenoxonium cations are not free in solution, but they are still coordinated to copper. The valence state cannot be rapidly deducted from the picture and thus we have indicated that below the respective complexes. A nucleophilic attack by another phenol (or phenoxide anion) takes place at carbon-4 of the phenoxonium ion (Figure 15.17).

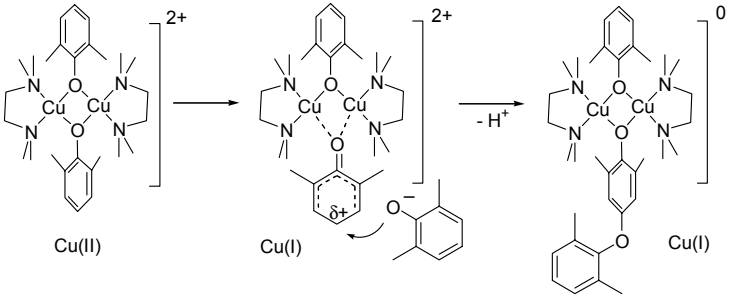

Figure 15.17. C-O bond formation in oxidative coupling of DMP

Phenolates and phenols form very strong hydrogen bonds and thus the actual complexes will be more complicated than the ones shown in Figure 15.17 and more phenolate anions or solvent molecules can coordinate to the Cu(II) dimer. Reoxidation of the copper(I) dimer takes place with dioxygen, which may involve oxygen complexes also relevant to biological systems, such as μ– η^2:η^2 peroxo complexes [24]. An interesting finding that supports the mechanism shown in Figure 15.17 is the initial, selective formation of a quinone ketal intermediate when dimethylphenol dimers are oxidatively coupled, rather than the expected linear tetramer [25]. The reaction shows (Figure 15.18) that as expected the phenoxoium ion of the dimer is much more readily formed than that of the monomer because of the stabilisation by the phenoxy substituent at carbon-4. The "branched" tetramer, quinone ketal, converts to the linear tetramer via a rearrangement reaction.

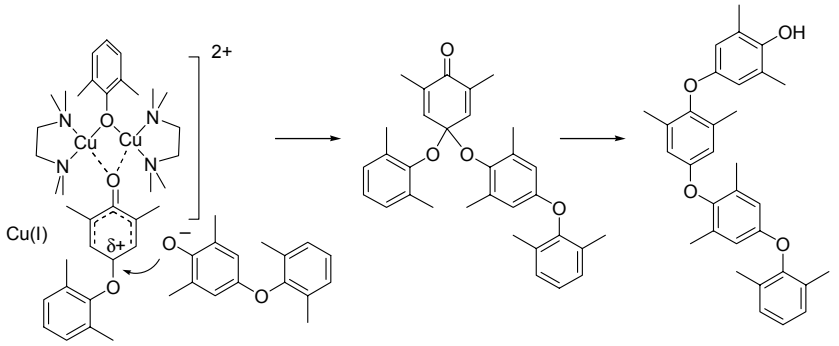

Figure 15.18. Oxidative coupling of dimethylphenol dimers to tetramers

Commercial application. 2,6-Dimethylphenol, the starting material, can be made from cyclohexanone and formaldehyde at high temperatures over a calcium phosphate catalyst or from phenol and methanol with the use of magnesium oxide as the catalyst also at 350 °C. The polymerisation reaction can be carried out in toluene at temperatures up to 65 °C, in the presence of copper source and amine ligands under a stream of oxygen. The copper salts are removed by a liquid-liquid extraction with water and amine ligands. Copper is precipitated from the water solution as the sulphide salt. The toluene solution is concentrated and the remaining syrup is used in blenders or the product is precipitated by adding a solvent. The molecular weight is in the order of 40,000.

PPO (now PPE) has been commercially available from General Electric since 1960. PPO has a very high T_g (208 °C) and therefore it must be processed at a high temperature. The product has high impact strength at high and low temperatures, it has a high hydrolytic stability and flame resistance, and a high heat distortion temperature. Its most important properties are the low electric conductivity and the high miscibility with many other polymers. Blending with polystyrene leads to a whole range of resins sold as Noryl® by GE. We find the product in numerous applications as the "plastic" parts of electric devices (tv sets, computers), and also in medical applications for which repeated steam sterilisation is required.

References

1 Thiemens, M. H.; Trogler, W. C. *Science,* **1991,** *251,* 932. Corrigenda, *Angew. Chem. Int. Ed.* **2003,** *42,* 2443.

2 Sato, K.; Aoki, M.; Noyori, R. *Science,* **1998**, *281,* 1646. Deng, Y.; Ma, Z.; Wang, K.; Chen, J. *Green Chem.* **1999,** 275.

3 Draths, K. M.; Frost, J. W. *J. Am. Chem. Soc*. **1994**, *116*, 399.

4 Bäckvall, J. E.; Akermark, B.; Ljunggren, S. O. *J. Am. Chem. Soc.* **1979***, 101,* 2411. Nelson, D. J.; Li, R.; Brammer, C. *J. Am. Chem. Soc.* **2001***, 123*, 1564.
5 Hamed, O.; Henry, P. M.; Thompson, C. *J. Org. Chem.* **1999***, 64*, 7745.
6 Smidt, J. *Angew. Chem. Int. Ed.* **1962***, 1*, 80.
7 Kiers, N. H.; Feringa, B. L.; van Leeuwen, P. W. N. M. *Tetrahedron Lett.* **1992***, 33*, 2403.
8 Khenkin, A. M.; Weiner, L.; Wang, Y.; Neumann, R. *J. Am. Chem. Soc.* **2001***, 123*, 8531. Doornkamp, C.; Ponec, V. *J. Mol. Catal. A Chem.* **2000***, 162*, 19.
9 Hegedus, L. S. *Tetrahedron,* **1984***, 40*, 2415.
10 Hosokawa, T.; Murahashi, S.-I. *Acc. Chem. Res.* **1990**, *23*, 49.
11 van Benthem, R.; Hiemstra, H.; van Leeuwen, P. W. N. M.; Geus, J. W.; Speckamp, W. N. *Angew. Chem. Int. Ed.* **1995***, 34***,** 457.
12 Uozumi, Y.; Kyota, H.; Kato, K.; Ogasawara, M.; Hayashi, T. *J. Org. Chem.* **1999***, 64,* 1620.
13 Hegedus, L. S.; McKearin J. M. *J. Am. Chem. Soc.* **104***, 1982*, 2444.
14 Semmelhack, M. F.; Kim, C. R.; Dobler, W.; Meier, M.; *Tetrahedron Lett.* **1989***, 30*, 4925.
15 Hegedus, L. S.; Allen, G. F.; Olsen, D. J. *J. Am. Chem. Soc.* **1980***, 102*, 3583.
16 Stull, D. R.; Westrum Jr, E. F.; Sinke, G. C. *The Chemical Thermodynamics of Organic Compounds,* Wiley, New York, **1969**.
17 Ishii, Y.; Nakayama, K.; Takeno, M.; Sakaguchi, S.; Iwahama, T.; Nishiyama, Y. *J. Org. Chem.* **1995**, *60,* 3934. Iwahama, T.; Syojyo, K.; Sakaguchi, S. Ishii, Y. *Org. Process Res. Dev.* **1998***, 2*, 255. Hirai, N.; Sawatari, N.; Nakamura, N.; Sakaguchi, S.; Ishii, Y. *J. Org. Chem.* **2003,** *68,* 6587.
18 Ten Brink, G.-J.; Arends, I. W. C. E.; Sheldon, R. A. *Adv. Synth. Catal.* **2002**, *344,* 355.
19 Dijksman, A.; Arends, I. W. C. E.; Sheldon, R. A. *Synlett.* **2001**, 102.
20 Gamez, P.; Arends, I. W. C. E.; Reedijk, J.; Sheldon, R. A. *Chem. Commun.* **2003**, 2414.
21 Hay, A. S.; Blanchard, H. S.; Endres, G. F.; Eustance, J. W. *J. Am. Chem. Soc.* **1959**, *81,* 6335. Hay, A. S. *J. Polym. Sci. Part A. Polym. Chem.* **1998***, 36,* 505.
22 Mobeley, D. P. *J. Pol. Sci. Part A: Polym. Chem.* **1984**, *22,* 3202.
23 Challa, G.; Chen, W.; Reedijk, J. *Makromol. Chem. Makromol. Symp.* **1992**, *59,* 59.
24 Kitajima, N.; Morooka, Y. *Chem. Rev.* **1994***, 94*, 737;
25 Mijs, W. J.; van Lohuizen, O. E.; Bussink, J.; Vollbracht, L. L. *Tetrahedron,* **1967**, *23,* 2253.

Chapter 16

ALKENE METATHESIS

Resisting functional groups ...

16.1 Introduction

Metathesis of alkenes has been known for a long time. The initial catalysts were based on tungsten, molybdenum, and rhenium. Both homogeneous and heterogeneous catalysts find application. A complete review can be found in the book by Ivin and Mol [1]. Well known homogeneous catalysts can be formed from $MoCl_5$ or WCl_6 and an alkylating reagent. These are actually Ziegler-type procedures for preparing a catalyst for polymerisation, but it was noted that the reaction did not yield alkene insertion products with loss of the double bonds, but instead the double bonds were retained. The name "olefin metathesis" was coined by Calderon [2]. Alkylation of the metal chloride follows a different pathway in this instance. After dialkylation with reagents such as Et_2AlCl or R_4Sn, α-elimination occurs and a metal alkylidene is formed, $Cl_4W{=}CR_2$, see Chapter 2, Elementary steps. Often oxygen-containing promoters including O_2, EtOH, or PhOH are added. Turnover frequencies as high as 300,000 mol (product).mol^{-1}(cat).h^{-1} can be achieved, even at room temperature. The metal halides react with these species to give more active and stable alkoxide and oxo metal complexes.

Figure 16.1. Metathesis of lower alkenes

Heterogeneous catalysts were first reported by Eleuterio [3] and the reaction concerned metathesis of light olefins over MoO_3 on alumina at high temperature, 160 °C. Heterogeneous applications involve the conversion of

propene into ethene and 2-butene, or the reverse reaction depending on demand and availability of the feedstocks. Butenes can also be made from ethene via dimerisation and in this way the flexibility in the feedstock coming from the naphtha cracker is increased, but it does add an extra step to the whole. The ethene-propene-butene process was known as the Phillips Triolefin process and it was on stream for a number of years during the sixties for the conversion of propene. The overall reaction is shown in Figure 16.1. Since 2001 there is another plant from BASF-FINA in Texas using this reaction to increase the mount of propene coming from the cracker. Now it is named the OCT (Olefin Conversion Technology) process. Mitsui Chemicals will install the OCT technology to meet increasing propene demand in Asia.

Another heterogeneous metathesis process forms part of the Shell Higher Olefins Process. The oligomerisation reaction of ethene gives a Schulz-Flory mixture of oligomers that all have to be converted to C_{11} and C_{12} alkenes (Chapter 9). The 1-alkenes for which there is a market are being sold directly, but the remaining part, which may be more than 50% by weight of the product of the oligomerisation reaction, is sent to the ”isomerisation-metathesis” section. All by-products leave the plant as internal C_{11} and C_{12} alkenes after ”many” recycles, because the fraction of $C_{11–12}$ is relatively small in this very broad mixture. The catalyst used is a molybdenum oxide catalyst on silica; its commercial source is the so-called CoMo catalyst also used for the hydrodesulfurisation of petroleum fractions (HDS)!

Early applications of homogeneous catalysts in industry were polymerisation reactions, in particular the ring-opening metathesis polymerisation (ROMP) of cyclopentene and cyclooctene. Hüls (Germany) brought *trans*-poly(1-octylene) on the market in 1982 as Vestenamer 8012. Tungsten catalysts are used containing a number of chloride anions and substituted phenoxides. Activation often took place with DEAC, diethylaluminium chloride. Mainly *trans* (80%) is produced as drawn in Figure 16.2. It is used in blends with other polymers.

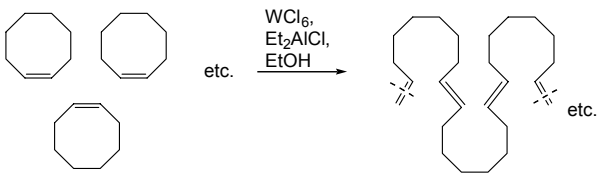

Figure 16.2. ROMP of cyclooctene

The Ziegler-like character of the initial catalyst systems prohibited the use of alkenes containing functional groups, even very simple ones as carboxylic esters, amides or ethers, as they will coordinate to the electrophilic metal, or

worse, react with the alkylating agents. The search for functional-group resistant catalysts has always been a key issue in metathesis research. A first break-through, showing that it was not intrinsically impossible to accomplish this, even with early-transition metals, was the metathesis of methyl oleic esters with the use of tungsten halide catalysts activated with tetramethyltin by Van Dam and co-workers [4]. The latter does react with tungsten hexachloride to form the initial carbene-tungsten species, but it is not sufficiently active as a metal alkyl species to react with methyl esters. Turnover numbers were only in the order of 100–500, but many of today's catalysts for applications in organic syntheses do not reach higher turnover numbers.

16.2 The mechanism

For didactic reasons we will not show mechanistic proposals that have been abandoned, because the "carbene" mechanism now is well established. It is referred to as the Chauvin-Hérisson mechanism, as they were the first to propose the intermediacy of metal-alkylidene species [5]. Their proposal was based on the observation (simplified for our purposes) that initially in the ring-opening polymerisation of cyclopentene in the presence of 2-pentene a mixture of compounds was obtained rather than the single products if a pair-wise reaction of cyclopentene (or higher homologues) and 2-pentene would occur. Figure 16.3 shows the results.

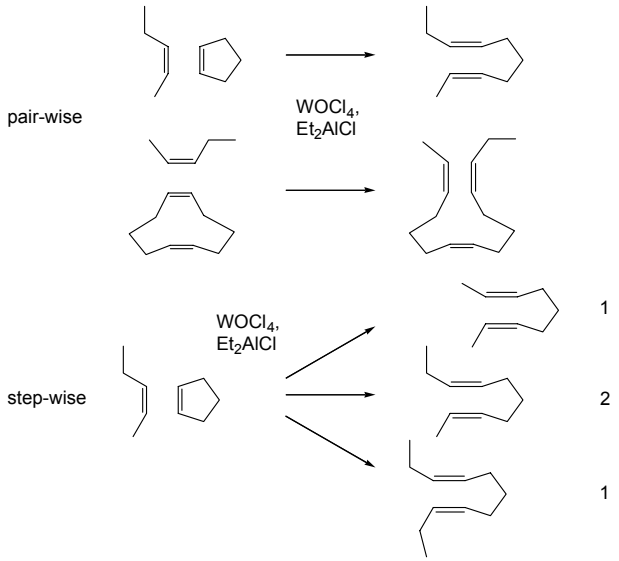

Figure 16.3. Result of pair-wise reactions (top) and step-wise reactions

If cyclopentene would react pair-wise with 2-pentene, only one product would form, namely 2,7-decadiene, and a similar result for cyclodimers etc. of cyclopentene. If somehow, the alkylidene species would be transferred one by one, we would obtain a mixture of 2,7-nonadiene, 2,7-decadiene, and 2,7-undecadiene in a 1:2:1 ratio. The latter turned out to be the case, which led the authors to propose the participation of metal-carbene (metal alkylidene) intermediates [6]. Via these intermediates the alkylidene parts of the alkenes are transferred one by one to an alkene. The mechanism is depicted in Figure 16.4. In the first step the reaction of two alkylidene precursors (ethylidene – bottom- and propylidene –top) with cyclopentene is shown. In the second step the orientation of the next 2-pentene determines whether nonadiene, decadiene or undecadiene is formed. It is clear that this leads to a statistical mixture, all rates being exactly equal, which need not be the case. Sometimes the results are indeed not the statistical mixture as some combinations of metal carbene complex and reacting alkene may be preferred, but it is still believed that a metal-carbene mechanism is involved. Deuterium labelling of alkenes by Grubbs instead of differently substituted alkenes led to the same result as the experiments with the use of 2-pentene [7].

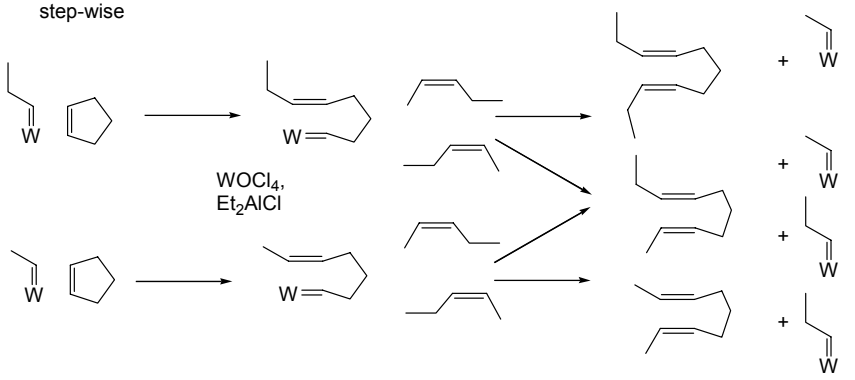

Figure 16.4. Metal alkylidene mechanism for cyclopentene/2-pentene metathesis

Another observation was that the ring-opening polymerisation of cyclic alkenes led to a polymer growth reaction rather than a condensation polymerisation reaction. In a condensation polymerisation we would see a steady growth of the oligomers to mixtures of C_5, C_{10}, C_{15}, C_{20}, etc while continuously a Schulz-Flory distribution is maintained. Instead, a chain growth mechanism is observed [8], i.e. the growing chain remains attached to the catalyst and we observe the growing chains in addition to the excess of monomer, see Figure 16.5.

Initially the polymer molecular weight distribution obeys a Poisson distribution, typical of a chain growth reaction without chain transfer. Since the reactions are reversible, at a later stage, also the equilibration between the polymers becomes important and a broad distribution of molecular weights is obtained. As can be seen from Figure 16.5 the presence of linear alkenes causes chain termination (chain transfer) and thus low molecular weights are produced if the cycloalkenes are not sufficiently pure.

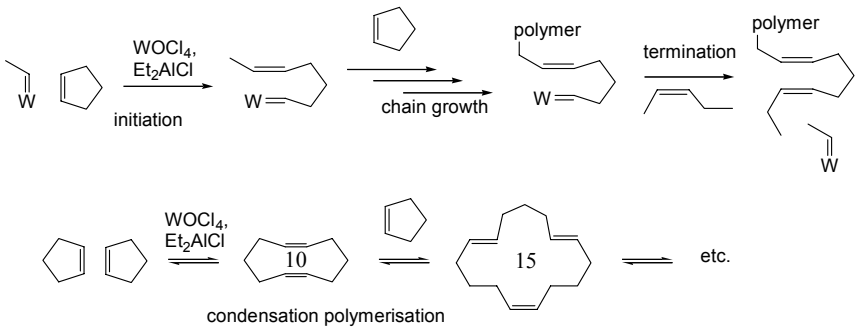

Figure 16.5. Condensation polymerisation versus chain growth

Early reports about involvement of metal alkylidene complexes in a chain growth polymerisation reaction and how metal alkylidenes may form via elimination reactions include suggestions by Dolgoplosk and co-workers [9]. In a subsequent paper they initiated the ring-opening metathesis reaction of cyclopentene or cyclooctadiene by the addition of (diazomethyl)benzene to tungsten hexachloride. In the absence of cycloalkene stilbene was formed, showing that tungsten is able to accommodate the carbene moiety [10].

The chemistry of alkylidene and alkylidyne complexes of early transition metals was developed by Schrock and co-workers and these complexes turned out to be of crucial importance to alkene and alkyne metathesis. Initially their research focused on tantalum complexes of the type $CpTaCl_2R_2$, which after α-elimination (Figure 16.6) led to alkylidene complexes $Cp(R)Cl_2Ta{=}CHR'$ [11].

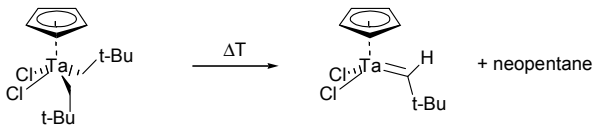

Figure 16.6. Formation of well-defined alkylidene complexes

In subsequent publications reactions were reported relevant to alkene metathesis, such as 2+2 additions with alkenes giving metallacyclobutanes

(Figure 16.7), but as catalysts tantalum alkylidenes were extremely slow. This marks the beginning of the synthesis of well-characterised metal carbene complexes as active catalysts, for metals of practical importance in metathesis such as molybdenum and tungsten. The carbene complexes used until then, e.g. $(OC)_5W{=}CPh_2$ [12] or the in situ prepared Ziegler-type catalysts for molybdenum [6] are not active before they have undergone considerable changes.

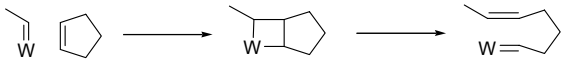

Figure 16.7. Metallacyclobutane mechanism

A prerequisite for the α-elimination is the absence of β-hydrogen atoms in the alkyl groups and this was successfully achieved by using the neopentyl substituents at the metal centre. The nature of the double bond between the metal and carbon was established by its bond length and the occurrence of stereoisomers [13]. Typical feature of the "Schrock" carbenes is that they contain an electrophilic, high-valent metal atom and an electron rich carbene carbon atom. The reverse is true for the older, Fischer carbene compounds, such as the one mentioned, $(OC)_5W{=}CPh_2$.

Involvement of α-elimination reactions for in situ prepared catalysts from WCl_6 and Me_4Sn was demonstrated by the use of ^{13}C in tetramethyltin. The norbornene polymers formed contained the $^{13}CH_2$ alkene moiety as the end-group. Also unstable $Cl_4W{=}CH_2$ and $Cl_4W{=}^{13}CH_2$ species were observed by ^1H NMR spectroscopy [14].

The expected intermediate for the metathesis reaction of a metal alkylidene complex and an alkene is a metallacyclobutane complex. Grubbs studied titanium complexes and he found that biscyclopentadienyl-titanium complexes are active as metathesis catalysts, the stable resting state of the catalyst is a titanacyclobutane, rather than a titanium alkylidene complex [15]. A variety of metathesis reactions are catalysed by the complex shown in Figure 16.8, although the activity is moderate. Kinetic and labelling studies were used to demonstrate that this reaction proceeds through the carbene intermediate.

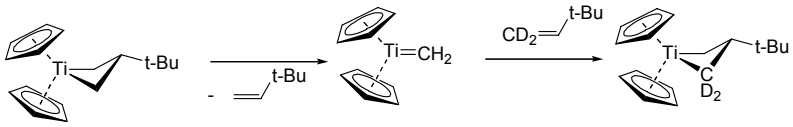

Figure 16.8. Grubbs's titanacyclobutane catalyst for metathesis

The most common method for the generation of the metal alkylidene species seems to be α-elimination from an intermediate dialkyl-metal species. This procedure gives the most active catalysts. Above we mentioned the addition of other carbene precursors, which leads to active catalysts. Other methods to generate the metal alkylidene species involve alkylidene transfer from phosphoranes [16] or ring-opening of cyclopropenes [17]. In Chapter 16.4 we will describe a few compounds that are active by themselves as metathesis catalysts.

16.3 Reaction Overview

Numerous catalysts and metathesis reactions have been reported and it is not possible to do justice to all authors, not even to those who have contributed to the development of the mechanistic proofs summarised above. In Figure 16.9 we have collected a schematic overview of the type of reactions that are usually distinguished in metathesis catalysis.

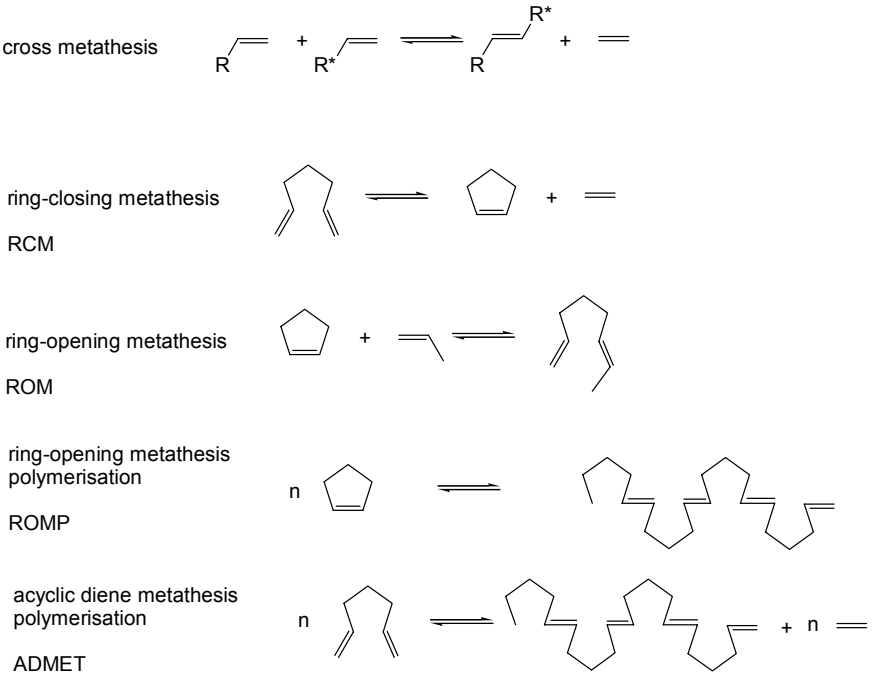

Figure 16.9. Types of metathesis reactions

16.4 Well-characterised tungsten and molybdenum catalysts

Since the late seventies efforts were directed toward the development of *well-defined catalysts* that would be active without addition of additives or further modification. A wide variety of tungsten and molybdenum alkylidene complexes have been prepared. Many of them show some activity, but only few are good catalysts. The synthesis is often not straightforward and a range of synthetic procedures varying solvents, alkylating reagents, anions, and alkylidene moieties have to be tried before a desired compound will be obtained.

Probably the first isolated tungsten alkylidene complex active in metathesis and completely characterised is the one shown in Figure 16.10 reported by Wengrovius and Schrock; the analysis included an X-ray structure determination by Churchill and co-workers [18]. The alkylidene was transferred from a tantalum complex to yield the hexacoordinate tungsten complex containing two PEt_3 ligands. One of these can be removed by the addition of half an equivalent of palladium chloride. The total turnover number of these catalysts with Lewis acids added was ~50 in 24 hours.

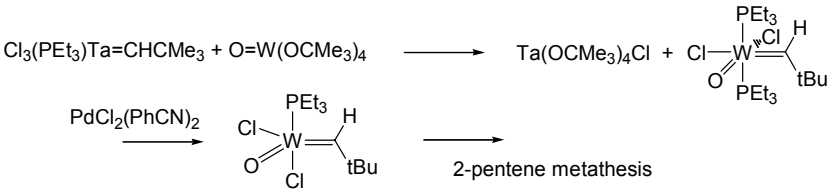

Figure 16.10. Synthesis of the first isolated metathesis catalyst

An example of a much faster catalyst, equally well characterised is depicted in Figure 16.11. This catalyst gives thousands of turnovers of cis-2-pentene in a few minutes at 25 °C. The electron withdrawing fluoroalkoxides make the metal centre nucleophilic and the steric bulk prevents dimer formation or other degradation reactions.

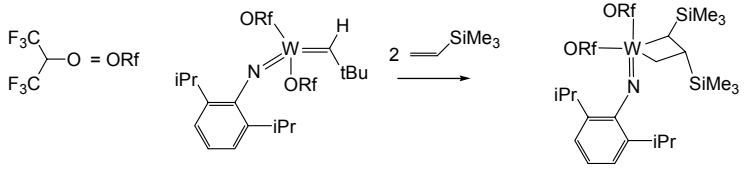

Figure 16.11. Highly active tungsten alkylidene complex and tungstenacyclobutane complex

With two molecules of vinyltrimethylsilane it gives the tungstenacyclobutane containing two Me_3Si groups. Apparently, the silyl groups stabilise the metallacyclobutane species relative to the alkylidene species.

The molybdenum analogue of this tungsten catalyst is known as Schrock's catalyst [19]. It is less active than its tungsten counterpart, but it is much more resistant to polar groups in the substrate.

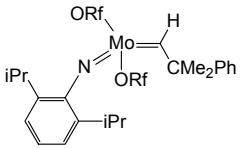

Figure 16.12. Schrock's catalyst for polar substrates

Instead of neopentylidene $Me_3C(H)=$ it contains $PhMe_2C(H)=$, a cheaper analogue, for which the starting halide precursor is cheaper than neopentyl chloride. By replacing the two alkoxides by a chiral bulky bisphenol also asymmetric metathesis has been achieved [20]. This is called the Schrock-Hoveyda catalyst, see Figure 16.13, coordinating tetrahydrofuran omitted. It can be used for example for asymmetric RCM, see below. Since the metathesis reaction is reversible, if possible one must remove one of the alkene products, for instance when this is ethene one can bubble nitrogen through the solution. Otherwise, eventually the racemic mixture will form. Another interesting solution is shown in Figure 16.13 in which a five-membered ring rearranges to the more stable six-membered ring. The ee of the product can range from 14 to 91% depending on the substituents at the aryl rings of the bisphenol and the aryl amide. The crucial part of the reaction is the asymmetric ring opening metathesis (AROM) of the five-membered ring, because at this point the ee has been determined.

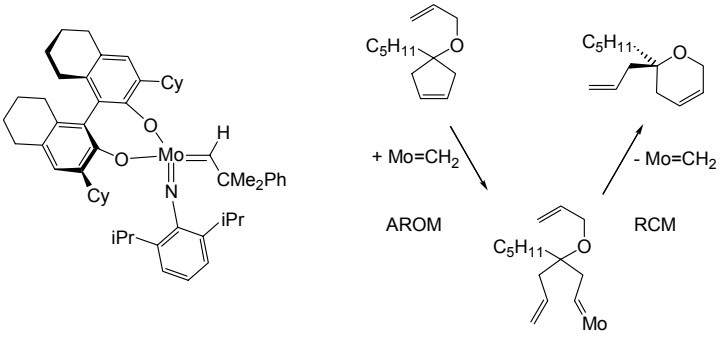

Figure 16.13. Schrock-Hoveyda catalyst for asymmetric metathesis

Likewise asymmetric ring closing metathesis has been achieved (ARCM) on acyclic trienes [21]. An example is shown in Figure 16.14. One can easily imagine that these types of reactions will be extremely useful in asymmetric organic synthesis; the remaining double bond can be hydrogenated to obtain alkyl group substituents that are very similar in nature. Such an asymmetric carbon centre is difficult to make by other means.

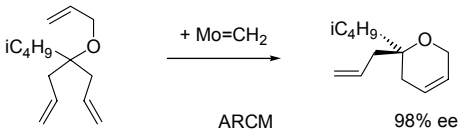

Figure 16.14. Asymmetric Ring Closing Metathesis

Alternatively one might continue the synthesis with further substitution reactions at the remaining allyl group. Ethers containing chiral tertiary carbon atoms adjacent to the oxygen atom are scarcely accessible and metathesis is a very convenient tool.

16.5 Ruthenium catalysts

The activity of ruthenium for ring-opening polymerisation has been known for a long time. As early as 1965 Natta reported that cyclobutene and 3-Me-cyclobutene can be ring-opening polymerised by ruthenium chloride in protic media [22]. Reports on ROMP of norbornene and ruthenium in protic media appeared in the same year [23]. In 1972 the metathesis nature of this ruthenium system and other catalyst systems based on titanium, vanadium, rhodium, nickel, iridium, etc. was recognised [24]. Porri continued research along these lines and in 1974 he reported the ROMP of norbornene with ruthenium and iridium salts in protic media [25]. Reaction times reported were rather long. Ruthenium showed activity for ROMP of cyclopentene as well, but only after the addition of dihydrogen. These were the first reports on catalysts made from elements of the right-hand side of the periodic table. This was very remarkable, because until then metathesis catalysts were incompatible with polar and certainly protic solvents. The work remained relatively unnoticed, although an industrial process was based on it in 1976 (CdF-Chimie, Norsorex; now Atofina). Like in the Porri system, $RuCl_3$ is used in an alcohol as the solvent (t-BuOH) and in situ formation of the presumed ruthenium alkylidene took place. Norsorex is the *trans* (90%) polymer of ROMP of norbornene with a molecular weight of 2 M.

In 1988 Novak and Grubbs reexamined the ruthenium catalysed ROMP in protic media with 7-oxanorbornene as the substrate [26]. As catalysts they used

$RuCl_3$ in water or the more active $Ru(H_2O)_6(tos)_2$. They found that considerable incubation occurred and that after the incubation period a small portion of ruthenium was active, which showed a very high activity. Molecular weights of 0.5 M were obtained and other R-groups were studied as well. Re-use of the catalyst solutions led to much shorter or no initiation times. Figure 16.15 shows the reaction.

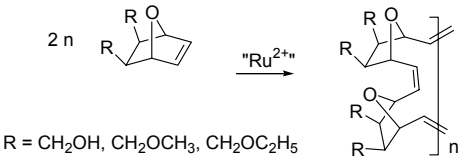

Figure 16.15. ROMP of oxanorbornene derivatives in water with a ruthenium catalyst

It was evident that the ruthenium catalyst was highly resistant to polar functionalities and that potentially it could compete successfully with the rhenium and tungsten based catalysts using alkyl tin compounds as the initiating agent to generate the alkylidene species, if only its activity could be generated in a controllable fashion. The preparation of tungsten and molybdenum alkylidene complexes active as metathesis catalysts without further activation stimulated research into this direction for the ruthenium catalysts. Addition of ethyl diazoacetate as a carbene precursor (as Dolgoplosk did for tungsten [10]) to ruthenium hydrated salts gave active catalysts [27]. The first successful synthesis of a ruthenium alkylidene was obtained with the use of diphenylcyclopropene as the carbene precursor [28], Figure 16.16.

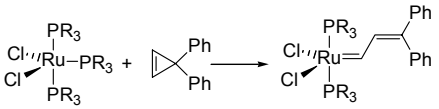

Figure 16.16. The first isolated ruthenium carbene catalyst

The latter method was utilized in the synthesis of ruthenium vinylalkylidene complexes of the type $RuCl_2(=CHCH=CPh_2)(PR_3)_2$ (R = Ph [29] and R=Cy [30]. The phenyl carbene species was isolated when diazomethylbenzene was used [31], Figure 16.17.

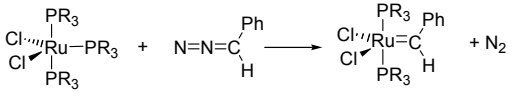

Figure 16.17. Ruthenium phenylcarbene catalyst

While ruthenium dichlorides always showed an undesirable initiation time, these novel catalysts start the reaction without delay. For compounds not containing functional groups their turnover frequencies can be several thousands per hour, but for polar molecules the total turnover may be as low as fifty, obtained in several hours.

Initially the presence of the two phosphine molecules in the complex was considered to be of crucial importance. Grubbs has shown that in fact the complex containing only *one* phosphine ligand is more active [32]. Higher activities were obtained when CuCl was added to the reaction mixture; CuCl removes free phosphine from the solution thus shifting the equilibrium to the side of the mono-substituted ruthenium complex. Ligands with lower χ-values (e.g. cyclohexylphosphine) give higher rates. Anions follow the reverse order: Cl > Br > I. This detailed study was conducted on the RCM reaction shown in Figure 16.18, often chosen as the model test reaction after Grubbs had introduced his catalysts. In general the ruthenium catalysts are still not as fast as the tungsten or molybdenum based ones, but their flexibility and scope is enormous.

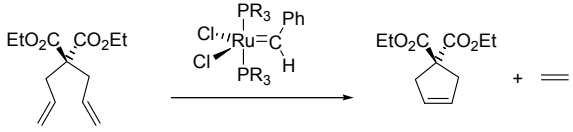

Figure 16.18. RCM model reaction with Grubbs catalyst

An important development has been the introduction of carbene ligands replacing one of the phosphine ligands. The structure of the complex is the same, carbene and phosphine occupying *trans* positions. The catalyst is known as the second generation Grubbs catalyst, which in many applications is more active than the first generation Grubbs catalyst. As we have learnt in Chapter 1 diamino-carbene ligands are very strong σ-donors and very poor π-acceptor ligands; since PCy_3 ligands perform better than PPh_3 ligands one might expect that carbene ligands are even better. Asymmetric variations of carbene ligands have also been reported. Figure 16.19 illustrates the three most common Grubbs ligands.

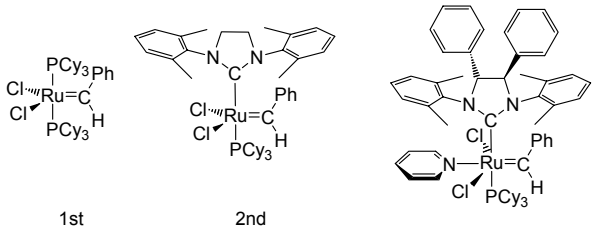

Figure 16.19. The first and second generation Grubbs catalysts and an asymmetric catalyst

Many applications of these new catalysts to organic chemistry have appeared recently and excellent reviews have appeared [33], but with the present rate of publications we cannot keep up with the most recent developments! Large rings can be prepared this way, and subsequently the alkene linker can be hydrogenated or functionalised. Also, multiple links between molecules containing several alkene substituents can be accomplished [34], etc. In view of the relative ease with which allyl groups can be introduced in organic molecules one might expect that the method will find very wide application in organic synthesis. Within a very short period the Grubbs catalyst has become an indispensable tool in organic synthesis.

16.6 Stereochemistry

The final stereochemistry of a metathesis reaction is controlled by the thermodynamics, as the reaction will continue as long as the catalyst is active and eventually equilibrium will be reached. For 1,2-substituted alkenes this means that there is a preference for the *trans* isomer; the thermodynamic equilibrium at room temperature for *cis* and *trans* 2-butene leads to a ratio 1:3. For an RCM reaction in which small rings are made, clearly the result will be a *cis* product, but for cross metathesis, RCM for large rings, ROMP and ADMET both *cis* and *trans* double bonds can be made. The stereochemistry of the initially formed product is determined by the permanent ligands on the metal catalyst and the interactions between the substituents at the three carbon atoms in the metallacyclic intermediate. *Cis* reactants tend to produce more *cis* products and *trans* reactants tend to give relatively more *trans* products; this is especially pronounced when one bulky substituent is present as in *cis* and *trans* 4-methyl-2-pentene [35]. Since the transition states will resemble the metallacyclobutane intermediates we can use the interactions in the latter to explain these results.

The metallacyclobutane ring is not flat, but puckered, with carbon-2 above the plane formed by the metal and the other two carbon atoms. This leads to equatorial and axial positions for the substituents. In the ring 1,2 and 1,3

interactions play a role and all substituents will prefer equatorial sites. Only the productive pathways have been depicted in Figure 16.20. From the figure we can see that if two small methyl groups are at positions 1 and 2, the 1,3 interaction dominates, and the *trans* or *cis* structure of the reactant is mostly retained in the 2-butene products. When the two isopropyl groups are in 1 and 2 positions, they cannot assume *cis* positions, and only *trans* "bulky" alkene is formed (*trans*-2,5-dimethyl-3-hexene). The data in the Figure refer to the catalyst WCl_6, Et_2O, $SnBu_4$ [35].

For ROMP of cyclopentene dominant 1,2 interactions will lead to *trans* polymer, but dominant 1,3 interactions will give an initial *cis* polymer. The latter seems to be the case in more crowded catalysts.

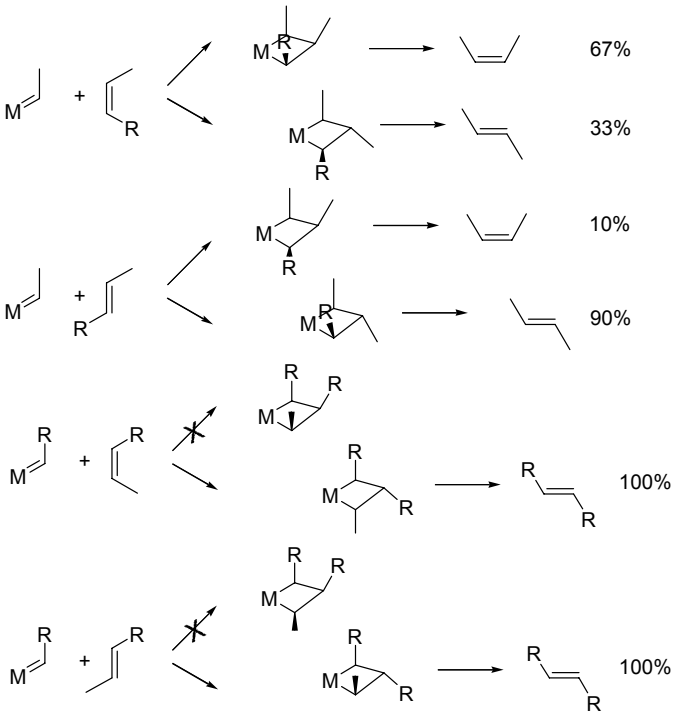

Figure 16.20. Metathesis of 4-methyl-2-pentene (R=i-Pr)

16.7 Catalyst decomposition

Early transition metal based catalysts react with a variety of polar substrates and impurities, except the molybdenum ones substituted electronically and sterically (Figure 16.12) in such a way that they become less "oxophilic". In

general early transition metal alkylidenes will for instance react with aldehydes to form a metal oxo species and an alkene. This type of heteroatom metathesis reaction is very common (Figure 16.21).

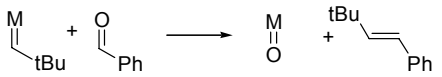

M, see Figure 16.12

Figure 16.21. Reaction of aldehydes and ETM alkylidene complex

The Schrock catalyst shown in Figure 16.12 does react cleanly with benzaldehyde according to the equation shown in Figure 16.21, a Wittig- type reaction [19]. The compound did not react with ethyl acetate or N,N-dimethylformamide for several weeks at room temperature.

Simple alkenes can give turnover numbers in the order of several 100,000 with tungsten or molybdenum based catalysts, including the in situ prepared catalysts (e.g. WCl_6, PhOH, $SnBu_4$), provided that the alkene is thoroughly purified. A convenient purification method is percolation of the alkene over neutral alumina to remove peroxides.

In the synthetic protocols for organic chemistry the Grubbs catalysts are usually applied in quantities of 1-5 mol% and one may wonder why so much catalyst is needed. Reasons for this may include that the catalyst is not totally stable towards the functional groups, or perhaps the ingress of air and water leads to decomposition of the catalyst. Therefore it is of interest to have a look at unmodified alkenes with the use of ruthenium catalysts. Several authors have found that the intrinsic activity of the Grubbs catalyst or in situ prepared ruthenium catalysts can be very high, and turnover numbers approaching one million have been reported for 1-octene. Removal of peroxides from the alkene feed is again important [36].

Metathesis of 1-octene leads cleanly to ethene and 7-tetradecene, but as the reaction proceeds also 2-octene is formed and metathesis products derived from the isomerisation reaction. It was found that after prolonged reaction times decomposition of the ruthenium alkylidene catalyst occurs. At least eight different products were formed and several of them have been identified [37]. Figure 16.22 shows the identified compounds derived from Grubbs 1st generation catalyst (the 2nd generation gives basically the same result [38]).

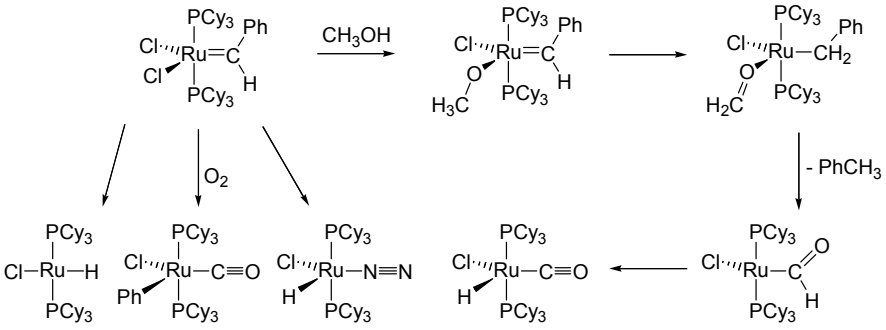

Figure 16.22. Decomposition products of Ru=CHPh and methanol, water and O_2

The mechanisms proposed contain pathways for generating a carbonyl species either from an alcohol added or it may form from the carbene ligand with either water or dioxygen. In the presence of dioxygen $Cy_3P{=}O$ was also found as the product. Even in very carefully cleaned glassware still decomposition to some of these products occurred and thus decomposition seems hard to avoid in the laboratory. The hydrides and phenyl compounds formed this way were shown to be good isomerisation catalysts (100,000 turnovers!) for 1-octene to 2-octene and they can also be used as hydrogenation catalyst. The selectivity to 2-octene was 95% if the reaction is stopped in time as 1-octene is much more reactive than 2-octene, as the chemical equilibrium tells us. It was reported that the alkylidene catalyst could be on purpose transformed into these hydride species in order to carry out a tandem metathesis/ hydrogenation reaction [39].

From these studies it is evident that the intermediates obtained during an organic synthesis will likely contain impurities at the percentage level that may make the use of similar catalyst levels necessary, unless still better catalysts that are more resistant to alcohols and water will be developed.

16.8 Alkynes

Metathesis of alkynes has also been known since the sixties. In this instance it is more curious that the reaction indeed follows a metathesis mechanism via a metallacyclobutadiene mechanism, starting from a metal alkylidyne and an alkyne, and not a breaking of the σ-bond and exchange of groups. Metathesis of $BuC{\equiv}{}^{14}CH$ gave indeed $BuC{\equiv}CBu$ and $H{}^{14}C{\equiv}{}^{14}CH$ [40]. The history of alkyne metathesis is interesting because it is an example how mechanistic ideas can lead to far better catalysts.

Initially a catalyst was obtained by in situ mixing, using a method that was relatively satisfactory for alkenes. Heating molybdenum carbonyl with resorcinol or chlorophenol at high temperatures (110-160 °C) gave a few

turnovers per hour for aryl substituted alkynes [41]. A considerable improvement was obtained by using $O_2Mo(acac)_2$ with phenols and $AlEt_3$ as the alkylating agent, a much more likely way to arrive at molybdenum alkylidyne species. Turnover frequencies as high as 17,000 per hour were now achieved at 110 °C [42]. Many tungsten alkylidyne (also named tungsten carbyne) complexes were tried, but many showed no reactivity. Besides the synthesis was not straightforward in many cases and the efficient procedures had to be developed (Schrock and co-workers). Wengrovius and Schrock [43] found that t-BuC≡W(O-t-Bu)$_3$ was an extremely efficient catalyst for the metathesis of 3-heptyne with a turnover frequency of hundreds of thousands per hour! Depending on the size of the alkoxide groups used the reaction has as a resting state the metallacyclobutadiene complex or the alkylidyne state, as is concluded from the kinetics. The former reaction is zero order in alkyne (dissociative"), the latter is first order in alkyne concentration ("associative") [44], see Figure 16.23.

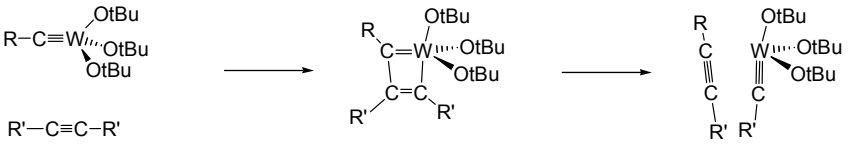

Figure 16.23. Alkyne metathesis

Initially alkynes were polymerised by trial and error with the use of Ziegler type recipes and the mechanism for these reactions may well be an insertion type mechanism. Undefined metathesis catalysts of ETM complexes were known to give poly-acetylene in their reaction with alkynes (acetylene) [45] and metallacycles were proposed as intermediates. Since the introduction of well-defined catalysts far better results have been obtained. The mechanism for this reaction is shown in Figure 16.24 [46]. The conductive polymers obtained are soluble materials that can be treated and deposited as solutions on a surface.

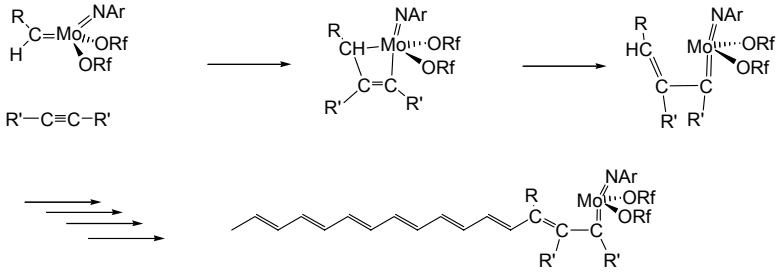

Figure 16.24. Reaction of metal alkylidenes and alkynes

Metathesis of enynes is another intriguing application in the laboratory. It would seem from the outcome, that it is a completely intramolecular reaction, but if the mechanism involves a metal alkylidene this is not true and the alkylidene group moves on from one substrate molecule to the next, see Figure 16.25. The methylene group moves to the next ring-closed diene. This is a useful tool in organic synthesis [47].

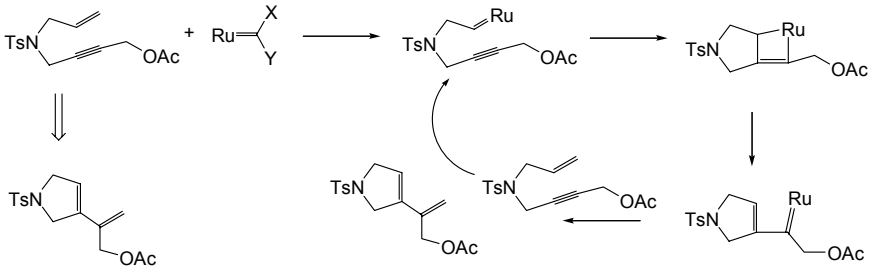

Figure 16.25. Reaction of tungsten alkylidene with enynes

16.9 Industrial applications

Above we have mentioned several heterogeneous applications such as the OCT process and SHOP. Neohexene (3,3-dimethyl-1-butene), an important intermediate in the synthesis of fine chemicals, is produced from the dimer of isobutene, which consists of a mixture of 2,4,4-trimethyl-2-pentene and 2,4,4-trimethyl-1-pentene. Cross-metathesis of the former with ethene yields the desired product. The catalyst is a mixture of WO_3/SiO_2 for metathesis and MgO for isomerisation at 370 °C and 30 bar. The isobutene is recycled to the isobutene dimerisation unit [48].

We also mentioned Vestenamer 8012, a predominantly *trans* polymer of cyclooctene made with a WCl_6 based catalyst (Degussa-Hüls), used in blends and poly-norbornene made by a catalyst generated from $RuCl_3$ in t-BuOH in the presence of air (Norsorex by Atofina, a polymer with a very high molecular weight).

As a last example we mention polydicyclopentadiene (DCPD). Dicyclopentadiene is the Diels-Alder adduct of cyclopentadiene, an abundant product from the cracker in the refinery. It contains a strained norbornene ring and a less strained cyclopentene ring. ROMP leads to opening of the norbornene ring, but some reaction of the cyclopentene ring also takes place, which leads to cross-linking (Figure 16.26).

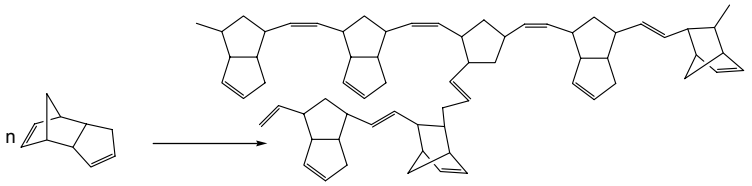

Figure 16.26. ROMP of DCPD

The polymer is a yellowish material with very high impact strength. It is made via a so-called reaction injection moulding procedure (RIM). Two stable solutions, each containing a catalyst component, e.g. $WCl_x(OAr)_{6-x}$ and $SnBu_4$ are brought together in a warm mould. An exothermic reaction occurs and the temperature rises up to 190 °C and within two minutes the fabricated parts are obtained. Reaction should go to high conversion as the smell of DCPD is unpleasant. They are marketed as Metton (initially Hercules and Shell) and Telene (Goodrich) and the parts made are for instance panels for trucks, snowmobile hoods, and fenders for tractors.

For a recent update of industrial applications see [49].

References

1 Ivin, K. J.; Mol, J. C. *Olefin Metatheis and Metathesis Polymerization,* Academic Press, **1997**, San Diego USA, London UK. Special issue on metathesis: *Adv. Chem. Cat.* **2002,** *344,* issue 6/7.

2 Calderon, N. *Chem. Eng. News,* **1967**, *45,* 51. Calderon, N.; Chen, H. Y.; Scott, K. W. *Tetrahedron Lett.* **1967**, 3327.

3 Eleuterio, H. S. *US Patent* 3,074,918; *Chem. Abstr.* **1961**, *55,* 16005. Eleuterio, H. S. *J. Mol. Catal.* **1991**, *65,* 55.

4 Van Dam, P. B.; Mittelmeijer, M. C.; Boelhouwer, C. *J. Chem. Soc. Chem. Commun.* **1972**, 1221. Verkuylen, E.; Boelhouwer, C. *ibid.* **1974**, 793. Verkuylen, E.; Kapteijn, F.; Mol, J. C.; Boelhouwer, C. *ibid.* **1977**, 198.

5 Hérisson, J.-L.; Chauvin, Y. *Makromol. Chem.* **1971**, *141,* 161.

6 Katz, T. J.; McGinnis, J. *J. Am. Chem. Soc.* **1975***, 97*, 1592.

7 Grubbs, R. H.; Burk, P. L.; Carr, D. D. *J. Am. Chem. Soc.* **1975***, 97*, 3265.

8 Many industrial polymer chemists will have observed this phenomonon in the early days: e.g. van der Ven, S.; van Leeuwen, P.W. N. M. **1969**, Shell Research, unpublished.

9 Dolgoplosk, B. A.; Makovetskii, K. L.; Tinyakova, E. I. *Dokl. Akad. Nauk SSSR* **1972***, 202*, 871 (Engl. transl. p. 95-97).

10 Dolgoplosk, B. A.; Golenko, T. G.; Makovetskii, K. L.; Oreshkin, I. A.; Tinyakova, E. I. *Dokl. Akad. Nauk SSSR* **1974***, 216*, 807.

11 Schrock, R. R. *J. Am. Chem. Soc.* **1974***, 96*, 6796.

12 Casey, C. P.; Burkhardt, T. J. *J. Am. Chem. Soc.* **1974***, 96*, 7808.

13 Schrock, R. R. *Acc Chem. Res.* **1975***, 12*, 98.

14 Ivin, K. J.; Milligan, B. D. *Makromol. Chem., Rapid Commun.* **1987***, 8*, 269.

15 Howard, T. R.; Lee, J. B.; Grubbs, R. H. *J. Am. Chem. Soc.* **1980**, *102*, 6876. Lee, J. B.; Ott, K. C.; Grubbs, R. H. *J. Am. Chem. Soc.* **1982**, *104*, 7491. Straus, D. A.; Grubbs, R. H. *J. Mol. Catal.* **1985**, *28,* 9.
16 Sharp, P. R.; Schrock, R. R. *J. Organomet. Chem.* **1979**, *171,* 43. Johnson, L. K.; Frey, M.; Ulibarri, T. A.; Virgil, S. C.; Grubbs, R. H.; Ziller, J. W. *J. Am. Chem. Soc.* **1993**, *115*, 8167.
17 Binger, P.; Müller, P.; Benn, R.; Mynott, R. *Angew. Chem., Int. Ed. Engl.* **1989**, *28*, 610. Johnson, L. K.; Grubbs, R. H.; Ziller, J. W. *J. Am. Chem. Soc.* **1993**, *115*, 8130.
18 Wengrovius, J. H.; Schrock, R. R.; Churchill, M. R.; Missert, J. R.; Youngs, W. J. *J. Am. Chem. Soc.* **1980**, *102*, 4515.
19 Schrock, R. R.; Murdzek, J. S.; Bazan, G. C.; Robbins, J.; DiMare, M.; O'Regan, M. *J. Am. Chem. Soc.* **1990**, *112,* 3875.
20 Zhu, S. S.; Cefalo, D. R.; La, D. A.; Jamieson, J. Y.; Davis, W. M.; Hoveyda, A. H.; Schrock, R. R. *J. Am. Chem. Soc.* **1999**, *121*, 8251.
21 Cefalo, D. R.; Kiely, A. F.; Wuchrer, M.; Jamieson, J. Y.; Schrock, R. R.; Hoveyda, A. H. *J. Am. Chem. Soc.* **2001**, *123*, 3139.
22 Natta, G.; Dall'Asta, G.; Porri, L. *Makromol. Chem.* **1965**, *81*, 253.
23 Michelotti, F. W.; Keaveney, W. P. *J. Pol. Sci.* **1965**, *A3,* 895. Rinehart, R. E.; Smith, H. P. *Poly. Lett.* **1965**, *3,* 1049.
24 Porri, L.; Rossi, R.; Diversi, P.; Lucherini, A. *Polymer Preprints (Am. Chem. Soc. Div. of Polymer Chem.)* **1972**, *13*, 897.
25 Porri, L.; Rossi, R.; Diversi, P.; Lucherini, A. *Makromol. Chem.* **1974**, *175*, 3097.
26 Novak, B. M.; Grubbs, R. H. *J. Am. Chem. Soc.* **1988**, *110*, 960 and 7542.
27 France, M. B.; Paciello, R. A.; Grubbs, R. H. *Macromolecules* **1993**, *26,* 4739.
28 Johnson, L. K.; Grubbs, R. H.; Ziller, J. W. *J. Am. Chem. Soc.* **1993**, *115*, 8130. For this method, see also: Binger, P.; Müller, P.; Benn, R.; Mynott, R. *Angew. Chem., Int. Ed. Engl.* **1989**, *28*, 610.
29 Nguyen, S. T.; Johnson, L. K.; Grubbs, R. H.; Ziller, J. W. *J. Am. Chem. Soc.* **1992**, *114*, 3974.
30 Nguyen, S. T.; Grubbs, R. H.; Ziller, J. W. *J. Am. Chem. Soc.* **1993**, *115*, 9858.
31 Schwab, P.; Grubbs, R. H.; Ziller, J. W. *J. Am. Chem. Soc.* **1996**, *118*, 100.
32 Dias, E. L.; Nguyen S. T.; Grubbs R. H. *J. Am. Chem. Soc.* **1997**, *119*, 3887.
33 Fürstner, A. *Angew. Chem. Int. Ed.* **2000**, *39*, 3012. Trnka, T. M.; Grubbs, R. H. *Acc. Chem. Res.* **2001**, *34,* 18.
34 Clark, T. D.; Ghadiri, M. R. *J. Am. Chem. Soc.* **1995**, *117*, 12364.
35 Ofstead, E. A.; Lawrence, J. P.; Senyek, M. L. Calderon, N. *J. Mol. Catal.* **1980**, *8,* 227.
36 Dinger, M. B.; Mol, J. C. *Adv. Synth. Catal.* **2002**, *344,* 671. Nubel, P. O.; Hunt, C. L. *J. Mol. Catal. A: Chem.* **1999**, *145,* 323.
37 Dinger, M. B.; Mol, J. C. *Organometallics,* **2003**, *22,* 1089. Fürstner, A.; Ackermann, L.; Gabor, B.; Goddard, R.; Lehmann, C. W.; Mynott, R.; Stelzer, F.; Thiel, O. R. *Chem. Eur. J.* **2001,** *7,* 3236.
38 Dinger, M. B.; Mol, J. C. *Eur. J. Inorg. Chem.* **2003**, 2827.
39 Drouin, S. D.; Zamanian, F.; Fogg, D. E. *Organometallics,* **2001**, *20,* 5495.
40 Mortreux, A.; Blanchard, M. *Bull. Soc. Chim. France* **1972**, 1641.
41 Mortreux, A.; Blanchard, M. *J. Chem. Soc. Chem. Commun.* **1974**, 786.
42 Bencheick, A.; Petit, M.; Mortreux, A.; Petit, F. *J. Mol. Catal.* **1982**, 15, 93.
43 Wengrovius, J. H.; Sancho, J.; Schrock, R. R. *J. Am. Chem. Sco.* **1981**, *103***,** 3932**.**
44 Freudenberger, J. H.; Schrock, R. R.; Churchill, M. R.; Rheingold, A. L.; Ziller, J. W. *Organometallics,* **1984**, *3,* 1563.
45 Masuda, T.; Sasaki, N.; Higashimura, T. *Macromolecules,* **1975**, *8,* 717.

46 Schrock, R. R. Luo, S.; Lee Jr. J. C.; Zanetti, N. C. Davis, W. M. *J. Am. Chem. Soc.* **1996**, *118*, 3883.
47 Kinoshita, A.; Mori, M. *Synlett.* **1994**, 1020.
48 Banks, R. L.; Banasiak, D. S.; Hudson, P. S.; Norell, J. R. *J. Mol. Catal.* **1982**, *15*, 21.
49 Mol, J. C. *J. Mol. Catal.* **2004**, in press.

Chapter 17

ENANTIOSELECTIVE CYCLOPROPANATION

In just one step to valuable products ...

17.1 Introduction

Cyclopropane molecules can be synthesised by the addition of carbenes to alkenes. The carbene can be generated via the transition metal catalysed decomposition of diazo compounds, which has been known for about a century. The catalysed reaction occurs at considerably lower temperatures and in particular metallic copper and copper complexes were initially reported as being effective catalysts. Widely used diazo compounds are those containing a carbonyl group such as diazo acetates N_2=C(H)COOEt, which are stable up to 100 ºC. The diazocarbonyls react with the copper complex, to give a copper-carbenoid complex, which then transfers the carbene fragment to another substrate, e.g. an alkene for forming a cyclopropane. In addition to cylopropanation other typical carbene reactions take place such as insertion into X-H bonds. Figure 17.1 gives a simple representation of carbene insertion and cyclopropanation. Many transition metal compounds are active catalysts for these reactions, but we will only give examples of the more developed systems.

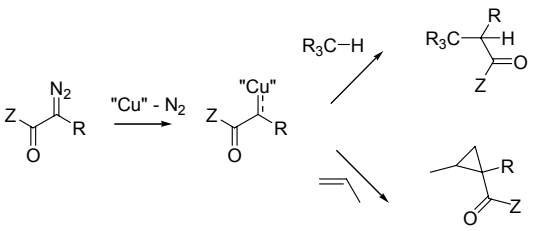

Figure 17.1. Reactions of diazocarbonyls with the aid of copper catalysts

17.2 Copper catalysts

The initial question was whether the active catalyst is copper metal, copper(I), or copper(II), because all metal precursors gave results. Without the proper control of the valence state and the ligand environment the selectivities for the copper catalysed cyclopropanations (or carbene insertion reactions) have remained low or inconsistent for a long period of time. It was only in the sixties that a more systematic study of these issues was started. Several divalent copper salts were successfully used, but Kochi and Salomon [1] showed with the use of Cu(I)OTf that most likely copper(I) was the actual species needed for this reaction.

Apart from cycloaddition to ethene, cyclopropanation immediately brings along the question of control of the formation of *cis* and *trans* products, the diastereoselectivity, and enantioselectivity, depending on the structure of the carbene and the alkene. In the last three decades a great deal of work has been devoted to the development of enantiospecific and diastereoselective catalysts. Derivatives of salicylaldehyde and chiral aminoalcohols were amongst the first effective ligands for copper catalysts [2]. They were used as dimeric copper(II) salts and elaborate changes to the substituents were made. Increasing the size of the aromatic substituent increases the enantioselectivity. A successful example is shown in Figure 17.2. Further derivatisation of the product of isobutene and ethyl diazoacetate gives cilastatin, a widely used *in situ* stabiliser of the antibiotic Imipenum, made commercially via the cyclopropanation route by Merck.

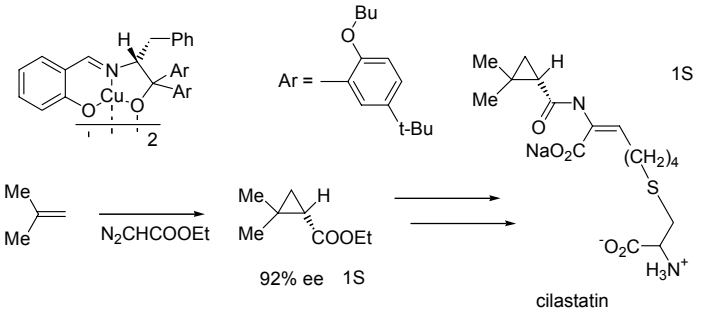

Figure 17.2. Aratani's salicylaldimine catalyst

Cyclopropanation of 2,5-dimethyl-2,4-hexadiene provides chrysanthemic acid, a natural product of the group of pyrethroic acids, used as an insecticide, see Figure 17.3 [3]. The appropriate esters of the 1R stereomers are the active compounds, which are obtained industrially by resolution of the racemates.

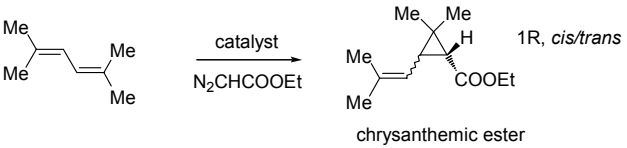

Figure 17.3. Synthesis of chrysanthemic acid

The next "generation" of catalysts started with the introduction of chiral semicorrin ligands by Pfaltz [4], which led to stable copper(II) complexes. They were effective catalyst precursors to cyclopropanation that were reduced in situ to their copper(I) analogues by the diazo compounds or before the catalytic reaction by phenylhydrazine to the copper(I) complex containing one semicorrin ligand. Later publications disclosed 5-azacorrins [5] and C_2-symmetric bis-oxazolines [6,7,8] as highly efficient asymmetric ligands, Figure 17.4.

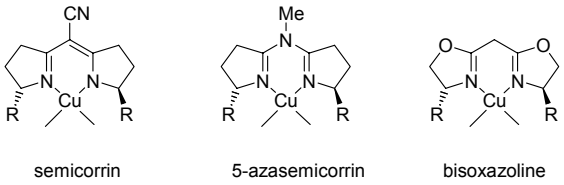

Figure 17.4. Semicorrin, 5-azasemicorrin and bisoxazoline ligands

Direct, controlled preparation of copper(I) complexes was achieved by Evans [7] from bisoxazolines and copper(I)triflate, which avoids the use of other methods for reduction or accidental reduction by the substrate, which may not always be efficient. When isobutene is the substrate one obtains only two enantiomers and no other products; for styrene we obtain a *cis* and a *trans* product each occurring as a pair of enantiomers. We will illustrate this with styrene and the results of Pfaltz's semicorrin-copper.

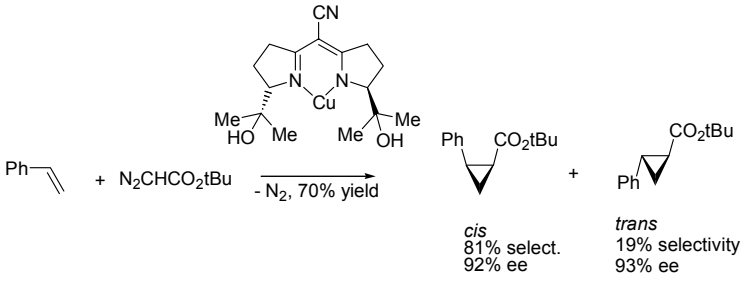

Figure 17.5. Products obtained with styrene

A variety of ester groups were reported, but for the present purposes one example suffices. For large ester groups (Figure 17.5) e.e.'s are high, surprisingly, both for the *cis* and for the *trans* isomers, but always a considerable amount of the second isomer is obtained. Even today the synthesis of a single product, be it *trans* or *cis*, is a major issue. The ester group has an influence as one can also see from the use of chiral groups in this position; *l*-menthyl diazoacetate with the ligand above gave lower e.e.'s than *d*-menthyl diazoacetate.

During these studies [4] it was again proven that copper(I) containing one semicorrin was the species needed and thus preparing the catalyst from Cu(I)OTf saves one molecule of ligand and avoids other problems.

Bisoxazolines can be readily made from chiral aminoalcohols of which a large number are commercially available. Changes in substitution in the ligand and the ester group are used to arrive at the best result. In Figure 17.6 we have collected three examples that show the influence of these parameters [6]. The reaction concerns the synthesis of chrysanthemic esters, already presented in Figure 17.3 (to avoid the current confusion about carbon numbering we assign carbon-1 only).

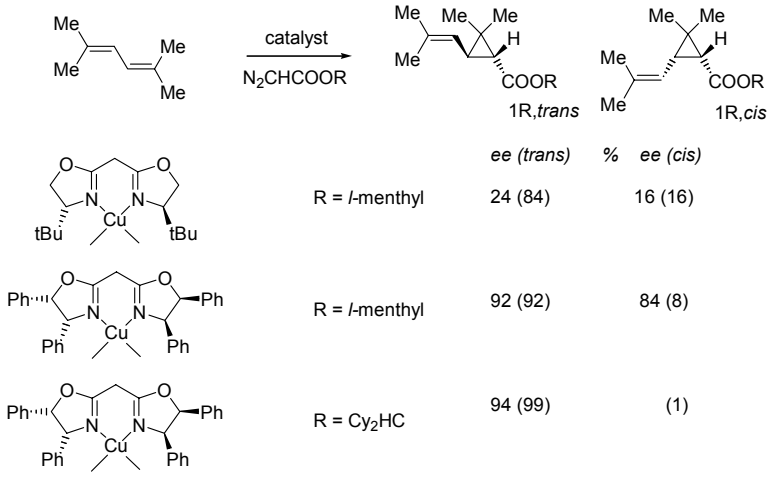

Figure 17.6. Substitution effects in bisoxazolines and ester on cyclopropanation [6]

The data from Masamune's papers underscore the impressive range the results can cover when the substituents are varied. The last reaction utilises a very bulky ester group to make practically one diastereomer in 94% e.e.! The catalyst is $CuClO_4$ or CuOTf. For styrene cyclopropanation Evans [7] found a similar relationship between the steric bulk of the ester group of the diazo-compound and the selectivity for *trans* products.

There are no mechanistic details known from intermediates of copper, like we have seen in the studies on metathesis, where both metal alkylidene complexes and metallacyclobutanes that are active catalysts have been isolated and characterised. The copper catalyst must fulfil two roles, first it must decompose the diazo compound in the carbene and dinitrogen and secondly it must transfer the carbene fragment to an alkene. Copper carbene species, if involved, must be rather unstable, but yet in view of the enantioselective effect of the ligands on copper, clearly the carbene fragment must be coordinated to copper. It is generally believed that the copper carbene complex is rather a copper carbenoid complex, as the highly reactive species has reactivities very similar to free carbenes. It has not the character of a metal-alkylidene complex that we have encountered on the left-hand-side of the periodic table in metathesis (Chapter 16). Carbene-copper species have been observed in situ (in a neutral copper species containing an iminophosphanamide as the anion), but they are still very rare [9].

Ruthenium complexes that are precursors for both cyclopropanation and metathesis perhaps show the relationship between the two reactions for this metal, but as yet it seems that different species are involved in the two reactions [10].

Most authors agree on the valence state of copper and thus we are dealing with a d^{10} electron configuration at Cu(I). The preferred geometry for such a complex would be tetrahedral: the C_2 symmetric bidentate, a carbene ligand and a vacancy. Alternatively one could reduce this to a trigonal geometry. When the carbene ligand (C(H)COOR') lies in the plane perpendicular to that of the ligand, there is no preferred mode of coordination i.e. at this stage there is no enantiodiscrimination. Most likely, the alkene does not coordinate to the metal when the reaction starts, but the electron deficient carbene attacks the π-orbital at the most nucleophilic carbon, initially. Most likely the two large groups in the reactants, COOR' and Ph, will assume up and down positions. Thus preferably a *trans* product will be formed.

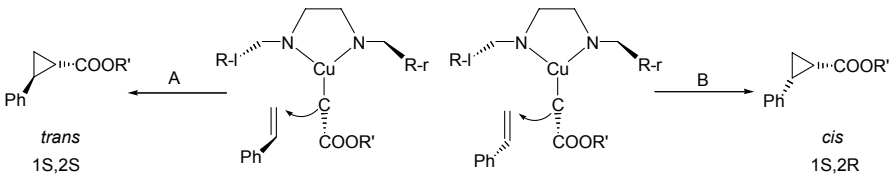

Figure 17.7. Enantiodiscrimination in a trigonal copper complex

In Figure 17.7 we show how enantiodiscrimination might take place as proposed by Pfaltz [11]. The copper complex in the centre is viewed along the trigonal axis. The alkene will approach always from the left-hand side, to avoid

the steric interaction between the ligand substituent R-r and COOR'. The styrene molecules in the respective pathways approach the carbene centre in the orientation as shown in the figure. Both for the up and down orientations of the phenyl group this leads to formation of a 1S centre. *Trans* disposition of phenyl and ester will be preferred, which can be achieved via route A to give mainly the product diastereomer 1S,2S. In this transition state an alternation up and down of all large groups is obtained.

17.3 Rhodium catalysts

17.3.1 Introduction

The catalytic activity of rhodium diacetate compounds in the decomposition of diazo compounds was discovered by Teyssié in 1973 [12] for a reaction of ethyl diazoacetate with water, alcohols, and weak acids to give the carbene inserted alcohol, ether, or ester product. This was soon followed by cyclopropanation. Rhodium(II) acetates form stable dimeric complexes containing four bridging carboxylates and a rhodium-rhodium bond (Figure 17.8).

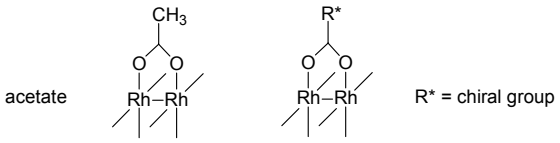

Figure 17.8. Rhodium(II) carboxylate dimer, only one bridging carboxylate drawn

Substitution of the acetate anions by chiral carboxylates was started simultaneously by a number of groups [13]. For cyclopropanation the first generation of catalysts was not very effective. As the interaction with the substrates takes place at the axial position of the dimer, the R* group is relatively remote. Replacing one of the carboxylate oxygens by a nitrogen atom, which can carry a substituent, brings the chiral steering group much closer to the reactive centre. These dirhodium(II) carboxamidates were developed by Doyle and coworkers [14] and to date they are the most selective catalysts known both for enantioselective insertion in C-H bonds and for stereoselective and enantioselective cyclopropanation.

Before turning to specific results we will have a look at the properties of rhodium(II) acetates/carboxamidates as catalysts for reactions with diazo-compounds as the substrates via carbenoid intermediates. Rhodium(II) has a d^7 electron configuration, forming the "lantern" type dimers with bridging carboxylates. The single electrons in the respective d_{z^2} orbitals form an electron

pair in the dimer (Rh-Rh distance 2.45 Å), which results in a diamagnetic compound. Two axial positions are unoccupied and are available as Lewis acid sites, with the anti-bonding combination of the two d_{z2} orbitals as the receptor orbital. The antibonding combination of the d_{xz} and d_{yz} combination can participate in back-donation to axial ligands, including carbene ligands.

The first kinetic study was reported by Noels and Teyssié [15] for the cyclopropanation reaction of ethyl diazoacetate and styrene. As activation parameters they found $\Delta H^{\ddagger}$ 63 kJ mol^{-1} and $\Delta S^{\ddagger}$ –13 J mol^{-1} K^{-1}. The reaction is first order in catalyst; this and later studies [16] support the presence of intact dimers throughout the catalytic cycle (there is one report suggesting dissociation of the rhodium dimer [17]). The classic model of Yates [18] can be applied to the transformation of diazo compounds by rhodium(II) complexes [16], *i.e.* the negatively polarised carbon atom of the diazo compound interacts with the Lewis acidic rhodium centre followed by loss of dinitrogen to give the carbenoid intermediate. The kinetics by Pirrung [16] show a substrate saturation effect and a rate-determining loss of dinitrogen (Michaelis–Menten kinetics), see Figure 17.9. The carbene intermediate is extremely reactive and the subsequent reactions, be they cyclopropanations or C-H insertions, are fast and therefore the rates of many reactions are the same, and depend only on the diazocompound used.

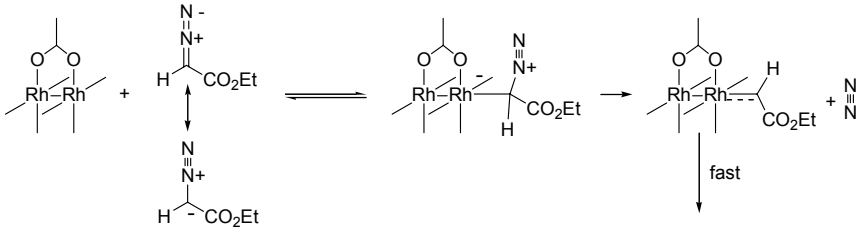

Figure 17.9. Formation of rhodium(II) carbene intermediate

The rhodium dimer has two Lewis acidic sites and thus the catalyst could coordinate to two substrate molecules under saturation kinetics, which would make the Michaelis–Menten plots complicated. This does not happen and the second site becomes less acidic once the other site is occupied by the substrate. What does happen, though, is that other Lewis bases compete with the substrate, as might be expected. The ligand dissociation reaction may be part of the rate equation of the process. Coordination of one Lewis base reduces already the activity of the catalyst. The solvent of choice is often anhydrous dichloromethane. The polar group may also be part of one of the substrates and in this instance one cannot avoid inhibition.

The carbenoid fragment reacts as an electron-deficient carbon centre. Substituents both at rhodium and at the carbene centre can make it more electron-deficient. If the carbenoid is given the choice between a cyclopropanation and C-H insertion reaction, the preference for C-H insertion increases with the electron deficiency [19], Figure 17.10.

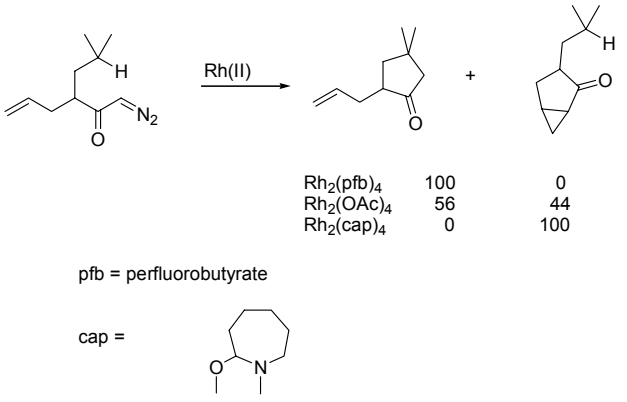

Figure 17.10. Influence of electron density of catalyst on chemoselectivity

The electron density in the carbene acceptor also plays a role as is illustrated by the next example. The competing reactions are again cyclopropanation and insertion into a C-H bond. Cyclopropanation occurs at an aromatic ring forming a norcaradiene where it is followed by a ring-opening reaction, overall named a Buchner reaction. An electron-rich aromatic ring undergoes cyclopropanation, but the nitro-substituted aromatic ring is less reactive and insertion in the benzylic C-H bond takes place (Figure 17.11).

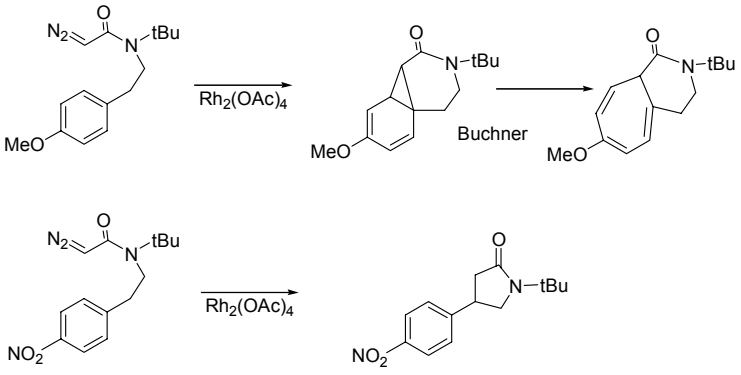

Figure 17.11. Electronic influence of carbene acceptor

17.3.2 Examples of rhodium catalysts

Chiral carboxylates such as α-phenylcarboxylic acids, lactic acid, and mandelic acid were used by Brunner [13], but, as mentioned above, these ligands did not afford very enantioselective catalysts. Aminoacids provided the possibility of introducing bulky substituents at the nitrogen atom, but these ligands based on proline and phenylanaline also gave modest results (Figure 17.12).

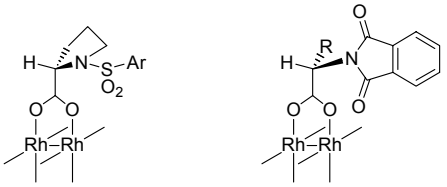

Figure 17.12. Proline and phenylalanine based carboxylate ligands [13]

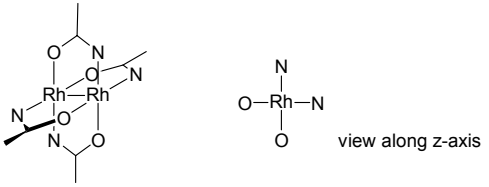

Figure 17.13. Rhodium(II) carboxamidite dimer

Carboxamidites are the most generally applicable ligands for all enantioselective reactions [14]. Interestingly, the two nitrogen atoms and the two oxygen atoms of the N,O bidentates occupy *cis* positions in the rhodium dimer complex, as drawn in Figure 17.14. All crystal structures for *selective* catalysts obtained so far show the *cis-2,2* arrangement of the carboxamidite groups [20]. Some typical examples are depicted in Figure 17.14. The catalysts are usually prepared and stored as their bis-acetonitrile complexes. Clearly, a whole range is available by changing the substituents in the ring and at the ester or amide positions.

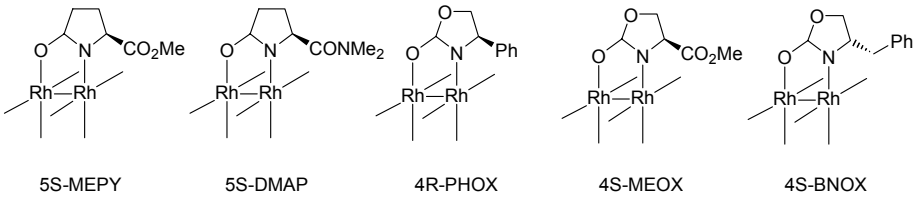

Figure 17.14. Examples of carboxamidite complexes

The axial alignment of $Rh_2(5R\text{-}MEPY)_4$ leads to probable structures for the carbene intermediate as shown in Figure 17.15. Approach of styrene will occur with the phenyl group pointing away from the rhodium complex, and also in a *trans* (*anti*) fashion with respect to the ester group of the carbene moiety. The 2-phenylcyclopropane-1-carboxylic ester resulting from this is indeed the 1R,2R (1R-*trans*) diastereomer.

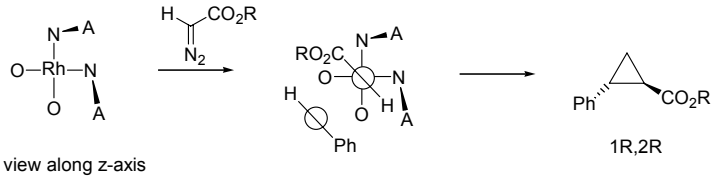

Figure 17.15. Mechanism of enantioselection with 5R-MEPY-rhodium

Intramolecular additions to alkenes and insertions into C-H bonds, in which the ester R group contains the "acceptor" site for carbene reagent, follow the same scheme as that depicted in Figure 17.15. Thus, for the substrate shown in Figure 17.16 the use of 5S-MEPY having an ester as the "steering" group afforded 98% e.e., whereas the benzyl analogue 4S-BNOX gave only 56% e.e. [21]. Ester or amides are often the most effective steering group, whereas the oxazolidinone analogues are usually more reactive.

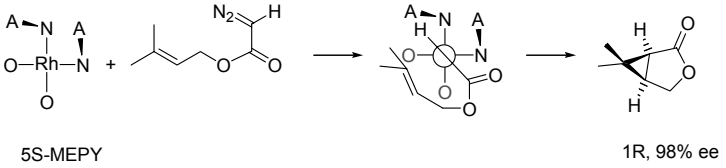

Figure 17.16. Intramolecular enantio-control

Because of the condensed ring structure, the *cis/trans* issue does not exist and only the *cis* products are formed.

References

1 Salomon, R. G.; Kochi, J. K. *J. Am. Chem. Soc.* **1973***, 95,*3300.
2 Aratani, T.; Yoneyoshi, Y.; Nagase, T. *Tetrahedron Lett.* **1975**, 1707; **1977**, 2599; **1982**, 685.
3 Matsuo, N.; Miyamoto, J. ACS Symposium Series **1997**, 658 (Phytochemicals for Pest Control), 183. *Chem. Abstr.* **1997***, 126*, 234688, AN:219961.
4 Fritschi, H.; Leutenegger, U.; Pfaltz, A. *Angew. Chem. Int. Ed. Engl.* **1986***, 25,* 1005.
5 Leutenegger, U.; Umbricht, G.; Farni, C.; von Matt, P.; Pfaltz, A. *Tetrahedron,* **1992**, *31*, 6005.
6 Lowenthal, R. E.; Abiko, A.; Masamune, S. *Tetrahedron Lett.* **1990,** *31,* 6005. Lowenthal, R. E.; Masamune, S. *Tetrahedron Lett.* **1991**, *32,* 7373.
7 Evans, D. A.; Woerpel, K. A.; Hinman, M. M.; Faul, M. M. *J. Am. Chem. Soc.* **1991***, 113,* 726.
8 Müller, D.; Umbricht, G.; Weber, B.; Pfaltz, A. *Helv. Chim. Acta* **1991,** *74*, 232.
9 Straub, B. F.; Hofmann, P. *Angew. Chem. Int. Ed.* **2001***, 40,* 1288.
10 Noels, A. F.; Demonceau, A. *J. Phys. Org. Chem.* **1998***, 11,* 602.
11 Fritschi, H.; Leutenegger, U.; Pfaltz, A. *Helv.Chim. Acta* **1988***, 71,* 1553.
12 Paulissen, R.; Reimlinger, H.; Hayez, E.; Hubert, A. J.; Teyssié, Ph. *Tetrahedron Lett.* **1973**, *14,* 2233.
13 Brunner, H.; Kluschanzoff, H.; Wutz, K. *Bull. Soc. Chim. Belg.* **1989**, *98,* 63. Kennedy, M.; McKervey, M. A.; Maguire, A. R.; Roos, G. H. P. *J. Chem. Soc. Chem. Commun.* **1990,** 361. Hashimoto, S.; Watanabe, N.; Ikegami, S. *Tetrahedron Lett.* **1990**, *31,* 5173.
14 Doyle, M. P. *Recl. Trav. Chim. Pays-Bas,* **1991**, *110,* 305. Doyle, M. P.; Forbes, D. C. *Chem. Rev.* **1998**, *98,* 911.
15 Anciaux, A. J.; Hubert, A. J.; Noels, A. F.; Petinot, N.; Teyssié, Ph. *J. Org. Chem.* **1980,** *45,* 695.
16 Pirrung, M. C.; Liu, H.; Morehead Jr., A. T. *J. Am. Chem. Soc.* **2002**, *124,* 1014.
17 Alonso, M. E.; García, M. del C. *Tetrahedron* **1989***, 45,* 69.
18 Yates, P. *J. Am. Chem. Soc.* **1952**, *74,* 5376.
19 Padwa, A.; Austin, D. J.; Hornbuckle, S. F.; Semones, M. A.; Doyle, M. P.; Protopopova M. N. *J. Am. Chem. Soc.* **1992**, *114,* 1874.
20 Timmons, D. J.; Doyle, M. D. *J. Organomet. Chem.* **2001***, 617-8,* 98.
21 Doyle, M. P.; Winchester, W. R.; Hoorn, J. A. A.; Lynch, V.; Simonsen, S. H.; Ghosh, R. *J. Am. Chem. Soc.* **1993***, 115,* 9968.

Chapter 18

HYDROSILYLATION

So common and yet unknown

18.1 Introduction

Silicon can be introduced in organic compounds in several ways, typical of making organometallics, such as reaction of the metal with organic halides, "cross-coupling" of silicon halides and reactive organometallics of magnesium or lithium, cross-coupling of anionic silicon compounds with organic halides, addition of silicon hydrides to unsaturated organic compounds, etc. Silyl ethers are made from alcohols and silicon halides; bulky silyl groups are often used as protecting groups in organic syntheses.

Many silicon compounds play an important role in organic synthesis, but the final products rarely contain silicon. Industrially the reaction of silicon (made from SiO_2 and C) with organic halides is important for making a number of starting materials [1]. The catalytic reaction (General Electric, ~1940, Müller-Rochow reaction) produces a mixture that is separated by distillation. For instance dimethyldichlorosilane is made in this fashion, which via hydrolysis is converted into silicone rubbers. The HCl by-product is reacted with methanol to give methyl chloride, which can be used again in the oxidative addition to silicon. When $RSiCl_3$ is added during the silicon rubber synthesis cross-linking is obtained. Silicone rubbers have been on the market since 1940 (Dow Corning Corporation). The production today amounts to ~0.5 M tons per year.

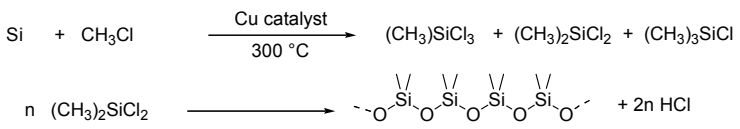

Figure 18.1. Silicone formation

Application of silicone putty or cements containing these silicone rubbers in the household or construction produces the smell of acetic acid during the hardening (curing) of the cement. This is because the end-groups contain acetate groups, which upon exposure to moisture hydrolyse and form new Si-O-Si bonds while acetic acid evaporates. There is a trend towards using alkoxides to avoid the smell and corrosion side effects, but the reaction may be slower. For surface modification alkoxides are the most common precursors. One also finds silicone sealants, Room Temperature Vulcanisation silicone rubbers, which are used in moulds and lead to hard materials after curing in moist air.

The reaction that concerns us here is the hydrosilylation reaction [2], which is also used in the hardening of silicone polymers, but it is important in itself for making silyl derivatives used in a very broad range of applications. They are applied extensively for the modification of surfaces, such as fabrics, cloths, glass, stone (e.g. conservation of archaeological treasures). Glass fibres used for the strengthening of plastics (glass-reinforced plastic) are treated with an organic silylating agent to make the surface compatible with the organic polymers (the lower surface tension enhances "wetting" by the polymer). Fillers in rubbers may also be pre-treated by organylsilyl trialkoxides to obtain better binding between rubber and filler. Other applications include paper release coatings, cosmetics, pressure sensitive adhesives, lubricants, etc. [3].

Controlled hydrolysis of $RSiX_3$ compounds gives so-called silsesquioxanes or POSS compounds (Polyhedral Oligomeric SilSesquioxane), which can be used as models for silica surfaces or supports for catalysts [4] (Figure 18.2, schematic structure on the right).

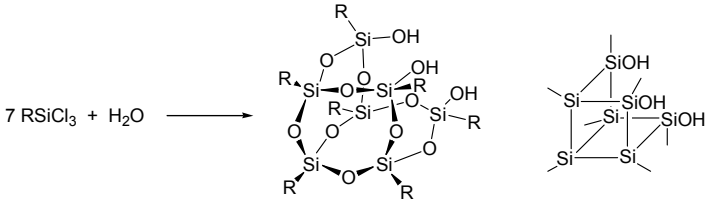

Figure 18.2. Example of a silsesquioxane or POSS compound

Hydrosilylation of allyl chloride with $HSiCl_3$ leads to $Cl(CH_2)_3SiCl_3$ that can be used for many surface modifications after substitution of the chlorides by suitable functional groups [5]. For instance it can be used to anchor soluble hydroformylation catalysts to a silica surface (Figure 18.3). Many examples have been reported and we present only one example of a selective Xantphos type ligand [6].

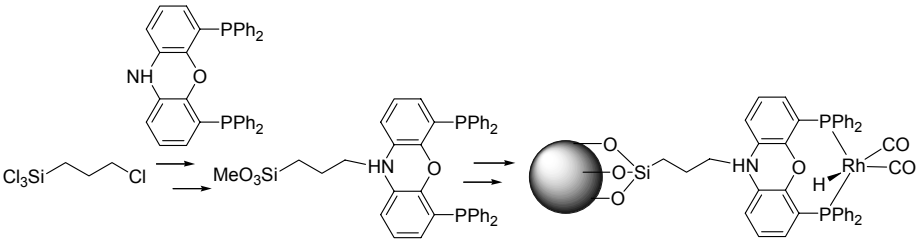

Figure 18.3. Immobilisation of a homogeneous hydroformylation catalyst to silica

Silicones can be prepared in such a way that they contain only one percent or less of vinyl groups and silicon hydrides, which undergo a catalytic hydrosilylation reaction to give the desired cross-linking (Figure 18.3). Vinyl silanes are made by Si-H addition to acetylene, and thus two hydrosilylations are involved.

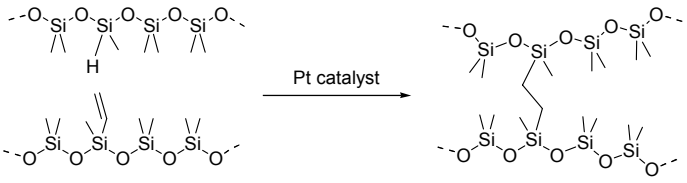

Figure 18.4. Cross-linking of silicone rubber via hydrosilylation

Hydrosilylation can be applied to alkenes, alkynes, and aldehydes or ketones. A wide range of metal compounds can be used as a catalyst. The most common and active ones for alkenes and alkynes are undoubtedly based on platinum. Hydrosilylation of C-O double bonds gives silyl ethers, which are subsequently hydrolysed to their alcohols. The reaction is of interest in its enantioselective version in organic synthesis for making chiral alcohols, as the achiral hydrogenation of aldehydes or ketones does not justify the use of expensive silanes as a reagent.

18.2 Platinum catalysts

The catalytic hydrosilylation by soluble platinum compounds was discovered by Speier in the late 1950's. The catalyst he used was H_2PtCl_6. Other well-known catalysts are those developed by Lukevics [7] and Karstedt [8]. The crystal structure of the latter complex was solved by Lappert [9]. The catalysts are depicted in Figure 18.5.

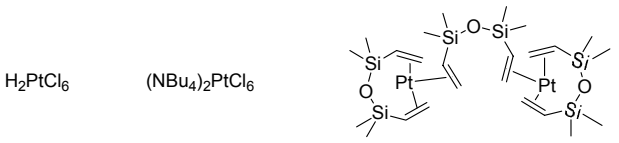

Figure 18.5. Platinum catalysts for hydrosilylation

The mechanism of the reaction was first described by Harrod and Chalk [10]. It involves the general mechanism of H–X additions to unsaturated organic compounds, starting with an oxidative addition of HX to a zerovalent platinum complex. The process is the same as that of addition of HCN to double bonds (Chapter 11).

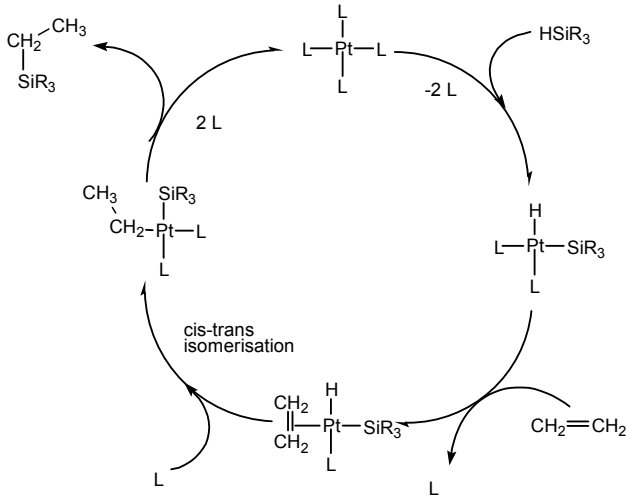

Figure 18.6. Chalk-Harrod mechanism for hydrosilylation

Interestingly, in addition to the "normal" hydrosilylation reaction, involving the insertion of alkene into a metal-hydride, insertion of alkene in the metal-silyl bond takes place as shown in Figure 18.6. Its occurrence can be deduced from the side-products obtained. After insertion of the alkene into the metal-silicon bond, β-hydride elimination happens and a vinyl-silyl compound is obtained as the product. The by-product hydrogen is used for the hydrogenation of the substrate to give alkane. Characteristic of this side-reaction is the 1:1 generation of vinylsilane and alkane. Figure 18.7 shows the complete mechanism for this product distribution.

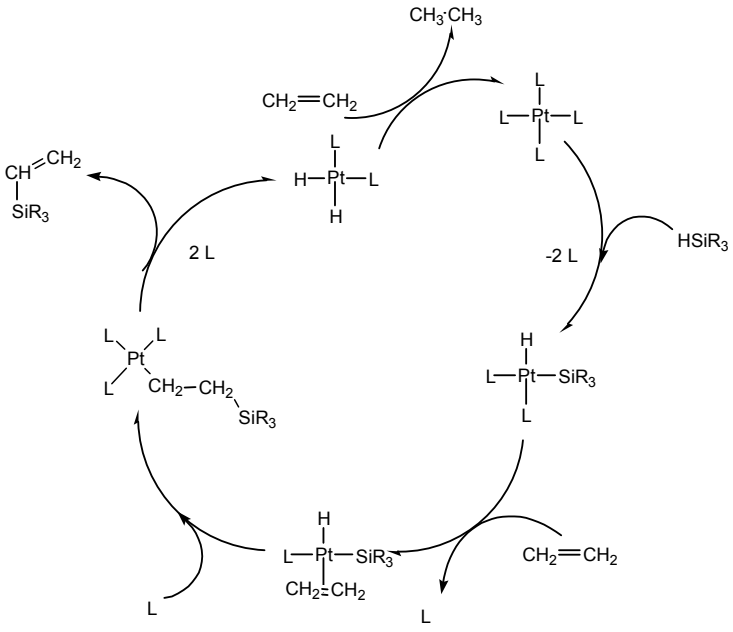

Figure 18.7. Formation of side products in hydrosilylation

Hydrosilylation of alkenes is highly exothermic; the heat of reaction is comparable to that of the hydrogenation of alkenes (~120 kJ.mol^{-1}). As a result, a very vigorous reaction may follow in the laboratory when a catalyst is added to an alkene and $HSi(CH_3)Cl_2$ (the exotherm will be between 100 and 200 °C for a product with MW of 240 without solvent!). Thus it is necessary to control the reaction by using solvent or by reducing the amount of catalyst.

Industrially, with the use of Speier type catalysts for the addition of $HSiCl_3$, turnover numbers as high as one million are achieved. In the laboratory these numbers are often not equalled (in particular for $HSiCl_3$) and it is not unusual to add an extra amount of catalyst precursor when the catalytic reaction does not start or stops prematurely. In industrial procedures, oxygen-containing components are added to the catalyst such as alcohols, dioxygen, and many other compounds, which will lead to partial formation of silicon-oxygen bonds. When making precursors for silicone polymers or surface modifiers the introduction of oxygenates is not problematic, but for the synthesis of highly pure silane dendrimers (Figure 18.8), for instance, the coupling of silicon via Si-O-Si bonds spoils the beauty of it. For many years we worked on this reaction and eventually Van der Made [11] succeeded in making up to the 6th generation of silane dendrimers. They are made via a repetitive sequence of hydrosilylations with $HSiCl_3$ and Grignard coupling of allylmagnesium bromide.

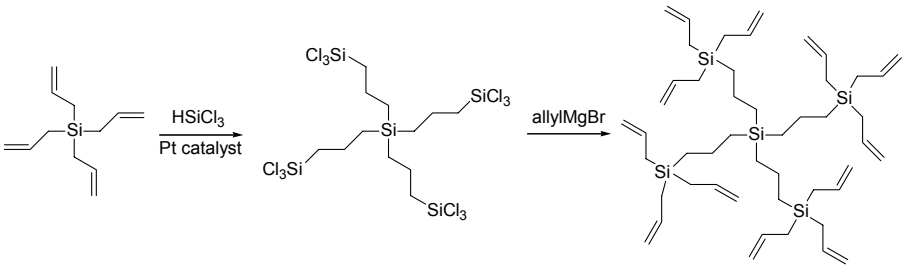

Figure 18.8. Silane dendrimers via hydrosilylation and Grignard coupling

Repeating the sequence shown in Figure 18.8 another five or six times (when congestion at the periphery occurs) is not an easy task without the introduction of Si-O-Si links and very few silane dendrimers of such a high generation have been prepared. The reaction is much more facile when $HSi(CH_3)Cl_2$ is used. Equipped with phosphine complexes either in the core or at the periphery the dendrimeric systems are used as catalysts [12]. Controlling the "state" of platinum seems to be a key problem.

The platinum catalysts show an induction period and during this period and during catalysis one observes changes in the colour of the solution, from yellow, to orange, and red, then darkening to blue, and eventually also black metal particles form. The colour of the solution was ascribed to the occurrence of platinum clusters and for a long time the work by Lewis, Lewis, and Uriarte (General Electric) had lent support to an active role of platinum clusters and colloids in the catalytic reaction. In their first paper in 1986 [13] they showed that addition of silanes to the precursor (Speier's catalyst, or $[1,5\text{-cod}]PtCl_2$) gave colloid particles as identified by light scattering and transmission electron microscopy. The smaller particles gave the most active catalysts. Silanes reduced the platinum precursor salts to Pt(0), which then forms clusters and colloids, and eventually platinum metal particles that are inactive. Thus, controlling the valence state and aggregation state of platinum is essential to obtain good performance.

While several *molecular* complexes (Rh, Ru, Ir, Pd) had been discovered as catalysts for the hydrosilylation reaction, for platinum catalysts, support was being gathered for the involvement of large clusters or small *colloids*. In a second paper Lewis [14] outlined the influence of oxygen on such catalysts. Dioxygen has a positive effect on such reactions and it was shown to stabilise the metal clusters as a ligand, without participating or reacting with any of the components. Alcohols and water react with silanes under the influence of platinum catalysts to form dihydrogen and silicon-oxygen bonds, a reaction related perhaps to the well controlled reaction reported by Crabtree [15], to which we referred in Chapter 2, as an activation of silanes for nucleophilic

attack by alcohols. Thus, in addition to the cross-linking described in Figure 18.4 also a coupling of Si-H bonds can be accomplished by water or alcohols, leading to Si-O-Si bonds. Most likely, platinum(II) is involved in this reaction, rather than platinum(0), the precursor for hydrosilylation (Figure 18.9).

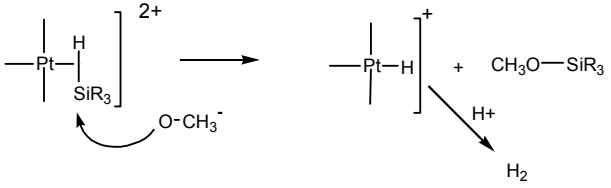

Figure 18.9. Activation of Si-H bonds by platinum

The simultaneous presence of clusters and catalytic activity is no proof for the participation of clusters in the catalytic cycle; one might argue that the catalysis requires zerovalent "naked" platinum and that this may easily be accompanied by cluster and metal particle formation. Most authors note that the most active catalysts are accompanied by a yellow colour. It should also be remembered that the reagent (ranging from $HSiEt_3$ to $HSiCl_3$), solvent (no solvent, thf, or dichloromethane), and source of platinum (Speier's catalyst or Karstedt's) have a large influence on incubation times and the stability of the state platinum. Electron-withdrawing alkenes, such as maleates, stabilise platinum(0) and complexes of this type are not active at room temperature in hydrosilylation. This property is used to deactivate platinum present in an oligomer mixture of silicones to allow processing in e.g. moulds as a liquid at room temperature, while the "curing" can be initiated by raising the temperature of the system.

The most recent findings support a mononuclear platinum complex as the resting state and active state of the platinum hydrosilylation catalyst when the zerovalent Karstedt complex is used as the precursor [16]. In situ EXAFS (extended X-ray absorption fine structure), SAXS (small-angle X-ray scattering), and UV spectroscopy were used to show that monomeric platinum complexes having silicon and carbon in the first coordination sphere were present. An excess of alkene gives mainly Pt-C bonds, and an excess of silanes leads to multinuclear Pt-Si compounds as well. EXAFS typically gives information about the valence state of the metal and the first coordination sphere around the metal, and other metals surrounding it. Speier's catalyst in the presence of 2-propanol and a hydrosilylating mixture gives the same intermediate as the Karstedt catalyst after incubation, during which the chlorides are removed from the first coordination sphere.

In conclusion, in the instance of the platinum-catalysed hydrosilylation reaction the molecular insight is behind the industrial practice; for an industrial

application a window of conditions is needed to allow the operation, and surely this is known, but the detail on the molecular level is not yet known. As a result conditions found in literature vary considerably. We can conclude that neither too strongly oxidative conditions nor too strongly reducing conditions will lead to highly active catalysts.

18.3 Asymmetric palladium catalysts

Catalytic asymmetric hydrosilylation of alkenes is an important goal in organic syntheses. As mentioned in the introduction, silicon compounds by itself are not in demand in pharmaceutical applications. It could be a useful tool for asymmetric synthesis of optically active alcohols, because carbon-silicon bonds can be readily oxidised to carbon-oxygen bonds with retention of the sterogenic centre. Here we will focus on only one example, namely the palladium-catalysed reaction with the use of the so-called MOP ligands developed by Tamio Hayashi [17]. MOP ligands are like BINAP derived from the atropisomeric 1,1'-dinaphthyl moiety, but they contain only one phosphine group, and at the other position a group X is placed from which the name is derived, "X-MOP" (Figure 18.10).

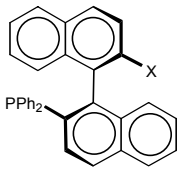

X = OMe, OBz, OiPr, Et, Ar, CN, COOMe, COOH, OH

X-MOP

Figure 18.10. MOP ligands

While hydrosilylation of 1-alkenes and $HSiCl_3$ with platinum catalysts provides linear products (1-trichlorosilylalkanes), palladium chloride modified with phosphines gives products carrying the trichlorosilyl group at the secondary carbon. This is highly remarkable because all other metal complexes studied so far lead to 1-substituted products. This regioselectivity leads to the possibility to carry out asymmetric hydrosilylation.

The asymmetric hydrosilylation of 1-octene with $HSiCl_3$ in the presence of 0.1 mole % of a palladium catalyst generated from π-allylpalladium chloride dimer and (*S*)-MeO-MOP gave 2-octyltrichlorosilane [18]. The resulting 2-octanol is the *R* enantiomer in 93% e.e. (Figure 18.11). So far, the relatively bulky, chiral monodentate MOP ligand seems to be the only ligand giving this peculiar selectivity. Complexes of bidentate diphosphines do not catalyse the hydrosilylation. It was thought that only monodentate phosphines can give square planar complexes of the correct composition for the catalysis, *viz.*

$PdH(SiCl_3)(MOP)(CH_2{=}CHR)$, obtained by oxidative addition of $HSiCl_3$ to palladium(0). MOP ligands with other substituents also gave good selectivities: X = $PhCH_2O$–, *i*-PrO–, Et–. This list shows that the X group has little influence on the course of the reaction and is not coordinating during part of the catalytic cycle. In the X-ray structure of *trans*-$(MeO\text{-}MOP)_2PdCl_2$ it can be seen that the MeO group is rather well removed from the metal centre [19]. Most likely, insertion of alkene into palladium-hydride occurs giving 2-alkylpalladium under the steric constraints of the ligand, followed by reductive elimination. Reductive elimination from a monophosphine ligated palladium species resembles the reductive elimination in palladium-catalysed cross-coupling reactions (Chapter 13).

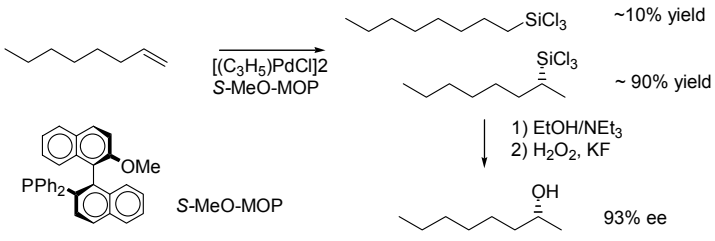

Figure 18.11. Asymmetric hydrosilylation of 1-octene

Another interesting example involves the dihydrosilylation of alkynes [20], which is carried out at room temperature in two steps, the first one with platinum chloride (0.01%) and the second one with palladium-MOP catalysts (0.3%). The reaction can be done with solely the palladium catalyst, but in that case the yield for the first step is low. The work-up leads to the formation of a chiral diol in high optical yield when the MOP derivative shown is used (Figure 18.12).

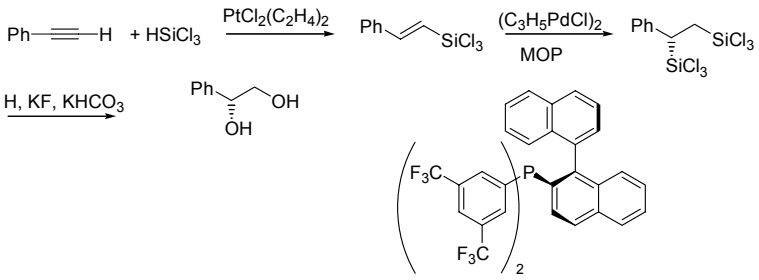

Figure 18.12. Double hydrosilylation of alkynes to form 1,2-diols

18.4 Rhodium catalysts for asymmetric ketone reduction

Asymmetric hydrosilylation of ketones was developed almost simultaneously with the better known asymmetric hydrogenation of cinnamic acid derivatives as described in Chapter 4. Many metal complexes catalyse the addition of silanes ($PhMe_2SiH$, Et_2SiH_2, etc.) to ketones and aldehydes (for copper hydrides as catalysts, and references to other metals see Lipshutz [21]). Here we will restrict ourselves to rhodium catalysts, in particular the enantioselective ones. In the early 1970's this chemistry was developed by Iwoa Ojima and co-workers [22], Kagan and co-workers [23], and Tamio Hayashi, Keiji Yamamoto, and Makoto Kumada [24]. In those days asymmetric hydrogenation of ketones or asymmetric hydrogen transfer to ketones had not yet been developed and thus hydrosilylation provided an excellent tool for making chiral alcohols. Figure 18.13 shows a simple scheme.

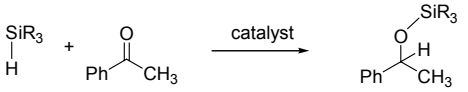

Figure 18.13. Hydrosilylation of ketones

In view of the oxophilicity of silicon compared to carbon, the addition takes place in such a way that a carbon-hydrogen bond and an oxygen-silicon bond is formed, giving RR'HC-OSiX_3. This silyl ether can be hydrolysed to give an alcohol. Ojima, in his first report, used two equivalents of a phosphorus-stereogenic monodentate *S*-benzylmethylphenyl-phosphine with an optical purity of only 62% to add diphenylmethylsilane to phenyl methyl ketone and alkene complexes of rhodium(I) chloride as the catalyst precursor. 1-Phenylethanol was obtained in 43% e.e.. This value might be disturbed by non-linear effects (!) (Chapter 4.5), as more than one ligand coordinates to rhodium. An oxidative addition of the silane to rhodium(I) was proposed since such addition complexes were already known. Coordination of ketone to rhodium(III) might be involved and they proposed an insertion of the ketone into the rhodium-silyl bond, analogous to alkene hydrogenation. If this were the case, one might expect, as in other hydrosilylation reactions (Figure 18.7), that β-hydride elimination at this point should give rise to vinyl silyl ethers as by-products.

Asymmetric hydrosilylation of ketones has developed enormously since these early reports and probably there are few catalytic reactions for which the variety in ligand structure is so immense as for this reaction. Numerous reports have been published and in general oxazoline-based ligand systems seem to give the highest enantioselectivities. In the following we will mention a few

examples, without saying that these represent the "best" catalysts. In addition some mechanistic findings will be presented.

For many years nitrogen-based ligands were the ligands of choice for the asymmetric hydrosilylation of ketones and especially pyridineoxazolines were highly effective [25]. In Figure 18.14 a few typical examples have been collected.

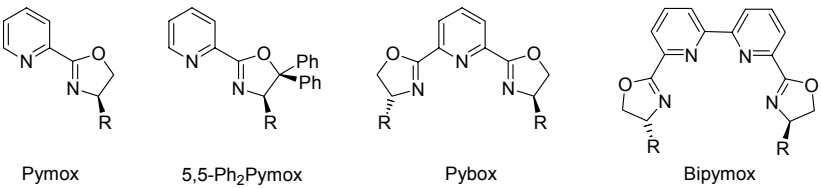

Figure 18.14. Typical examples of pyridineoxazoline ligands

A wide variety of these ligands can be envisaged, including pyridine derivatives containing chiral appendices. The rhodium precursor is usually $[(1,5\text{-cod})RhCl]_2$ or better a cyclooctene complex. A trivalent rhodium chloride can also be used, which is most likely reduced in situ by the silane component, very often Ph_2SiH_2. An early successful ligand is a thio analogue of Pymox (pyridinethioazolidine) reported by Brunner in 1983, with e.e.'s spanning a wide range, with values up to 97% [26]. Many derivatives have been reported. It was shown [27] that 5,5-diphenyl substituted Pymox gives much higher e.e.'s than Pymox, showing that the large phenyl groups increase the effectiveness of the R group at the chiral carbon atom.

Another interesting observation in Brunner's work was the co-production of silyl enol ethers. Often they remain unnoticed, because after aqueous workup they regenerate the starting ketone. They are important though as a clue to a mechanistic pathway as can be seen from Figure 18.15 (randomly chosen geometry, although we did keep σ-bonds in *cis* positions).

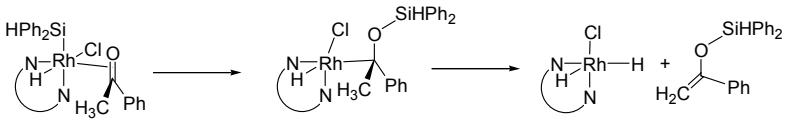

Figure 18.15. Formation of silyl enol ether

We start the scheme after the oxidative addition of diphenylsilane and coordination of acetophenone has taken place, after the classic mechanism by Ojima [28]. The formation of enol ethers proves, that at least for this part of the products formed (up to 22%, Brunner [27], 40% [29]), the reaction proceeds

via migration of the silyl group to the oxygen atom of the ketone. In Chapter 2 we wrote that a migratory insertion involves in general the migration of a σ-bonded nucleophile to an electron deficient centre (often π-bonded), but here clearly the reverse takes place; a silyl group connected to trivalent rhodium surely is an electrophile. The bonding of acetophenone to rhodium(III) may not resemble the bonding of an alkene either, but instead can be best described as an oxygen bonded ligand. We do conclude that subsequently the carbon atom forms a "normal" C-Rh bond, because in the following step β-hydride elimination occurs.

A concerted mechanism has also been discussed [29,30], involving either a 2+2+1 or 3+2 mechanism. To avoid trimolecular reactions this requires an interaction between Rh(I) and silanes prior to the reaction with a ketone. Interaction of silanes not leading to oxidative addition usually requires high-valent metals as we have seen in Chapter 2. The model is shown in Figure 18.16; it proved useful for the explanation of the enantiomers formed in different instances. The formation of a rhodium-carbon bond is included and thus formation of silyl enol ethers remains a viable side-path.

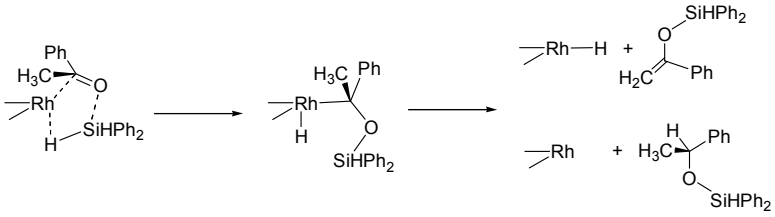

Figure 18.16. Concerted mechanism for ketone hydrosilylation

A number of P–N ligands has been reported as efficient ligands for the asymmetric hydrosilylation of ketones. We mention the phosphinooxazolines developed by Helmchen, Pfaltz, and Davis, we have seen before and mixed ligands containing planar-chiral heterocycles such as ferrocene [31] (Figure 18.17). For several ketone and silane combinations e.e.'s in the high nineties were obtained.

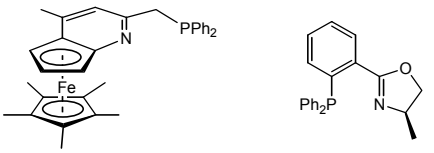

Figure 18.17. Ferrocene-based chiral-planar P–N ligand, and phosphinooxazolines [32]

Diphosphines initially gave poor results compared to nitrogen based ligands; the reason for this is not entirely clear. The coordination number of the crucial intermediate may be six for a rhodium(III), but this is not necessarily different from a hydrogenation reaction where oxidative addition of dihydrogen takes place prior to the insertion of the alkene. All N–N and P–N ligands known form *cis* complexes, but an early example of a P–P ligand was the TRAP ligand series developed by Ito [33], which led to the suggestion that perhaps *trans* diphosphines were needed, as TRAP often coordinates in a *trans* fashion, at least in its resting states. While the initial experiments with the common *cis* diphosphines were perhaps not very successful, in recent years several diphosphine based catalysts have been discovered. Their bite angles range from very narrow to relatively wide, for respectively bridges of methylene, MiniPHOS [34], ferrocene [35], and binaphthyl, BINAP [36]. The four diphosphines are shown in Figure 18.18.

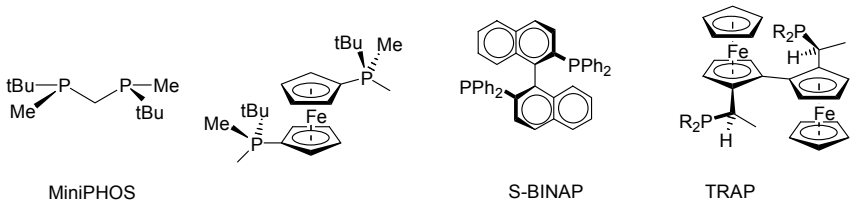

Figure 18.18. Diphosphines used in asymmetric ketone hydrosilylation

The wide variety of metals and ligands makes the mechanism somewhat mysterious and after so many years of study still many questions remain. The basic scheme, mentioned above [28], involves oxidative addition of R_3SiH to Rh(I), coordination of the ketone to rhodium, migration of the silyl group to oxygen and formation of a rhodium-carbon bond, and finally reductive elimination liberating a silyl ether. The reaction is first order in rhodium and silane concentrations (ionic rhodium complexes of *cis* diphosphines, DIOP [37] and BINAP [36]), but an inhibiting effect of ketone occurs at higher ketone concentrations. In addition, the studies using RhCl(BINAP) have shown that secondary silanes react much faster than tertiary silanes, the reason for which might be steric. Electron withdrawing substituents at triarylsilanes led to faster reactions as well, in accord with an oxidative addition as the rate-determining step.

With the use of NMR spectroscopy Giering and coworkers studied the reaction of acetophenone and $HSiBu_3$ in more detail. The catalyst was $[(1,5\text{-cod})RhCl]_2$ and R-BINAP [36]. They noted that the silyl enol ether by-product was formed mainly at the beginning of the reaction and thus this must form via an independent pathway. The common intermediate for silyl ether product and

enol ether by-product, which we have shown in Figure 18.16, may be an oversimplification, as the complexes involved will not be completely the same. Formation of alcohol was also observed, which makes up for the hydrogen stemming from the 5-20% of silyl enol ether being produced. Thus it would seem that more catalytic species are involved in the complicated reaction scheme. As yet, much less is known for this reaction than for the asymmetric hydrogenation with similar complexes.

References

1 Lewis, L. N.; Ligon, W. V.; Carnahan, J. C. *Silicon Chem.* **2002***, 1,* 23.
2 Marciniec, B. *Silicon Chem.* **2002***, 1,* 155.
3 Lewis, L. N.; Stein, J.; Gao, Y.; Colborn, R. E.; Hutchins, G. *Platinum Met. Rev.* **1997**, *41,* 66.
4 Feher, F. J.; Schwab, J. J.; Phillips, S. H.; Eklund, A.; Martinez, E. *Organometallics* **1995**, *14*, 4452. Feher, F. J.; Budzichowski, T. A.; Blanski, R. L.; Weller, K. J.; Ziller, J. W. *Organometallics* **1991***, 10*, 2526. Abbenhuis, H. C. L. *Chem. Eur. J.* **2000***, 6*, 25.
5 Deschler, U.; Kleinschmit, P.; Panster, P. *Angew. Chem. Int. Ed. Engl.* **1986**, *25*, *236.*
6 Sandee, A. J.; van der Veen, L. A.; Kamer, P. C. J.; Lutz, M.; Spek, A. L.; van Leeuwen, P. W. N. M. *Angew. Chem. Int. Ed. Engl.* **1999***, 38*, 3231.
7 Iovel, I. G.; Goldberg, Y. Sh.; Shymanska, M. V.; Lukevics, E.; *Organometallics* **1987***, 6,* 1410.
8 Karstedt, B. D. U.S. Patent, 3,775,452, (to General Electric Co.) 1973. *Chem. Abstr.* **1969**, *71*, 91641.
9 Hitchcock, P. B.; Lappert, M. F.; Warhurst, N. J. W. *Angew. Chem. Int. Ed. Engl.* **1991***, 30,* 438.
10 Harrod, J. F.; Chalk, A. J. in *Organic Synthesis Via Metal Carbonyls;* Wender, I.; Pino, P. Eds. Wiley, New York, **1977**, p 673.
11 Van der Made, A. W.; van Leeuwen, P. W. N. M. *Chem. Commun.* **1992**, 1400. Van der Made, A. W.; van Leeuwen, P. W. N. M.; de Wilde, J. C.; Brandes, R. A. C. *Adv. Mater. (Weinheim, Fed. Repub. Ger.),* **1993***, 5*, 466. Zhou, L. L.; Roovers, J. *Macromolecules* **1993***, 26*, 963. Seyferth, D.; Son, D. Y.; Rheingold, A. L.; Ostrander, R. L. *Organometallics* **1994***, 13*, 2682.
12 Oosterom, G. E.; Reek, J. N. H.; Kamer, P. C. J.; Van Leeuwen, P. W. N. M. *Angew. Chem., Int. Ed.* **2001***, 40*, 1828. *C.R. Chimie,* **2003**, *6*, 1061.
13 Lewis, L. N.; Lewis, N. *J. Am. Chem. Soc.* **1986***, 108,* 7228.
14 Lewis, L. N. *J. Am. Chem. Soc.* **1990***, 112,* 5998.
15 Luo, X.-L.; Crabtree, R. H. *J. Am. Chem. Soc.* **1989***, 111*, 2527.
16 Stein, J.; Lewis, L. N.; Gao, Y.; Scott, R. A. *J. Am. Chem. Soc.* **1999***, 121,* 3693.
17 Hayashi, T. *Acc. Chem. Res.* **2000***, 33,* 354.
18 Uozomi, Y.; Hayashi, T. *J. Am. Chem. Soc.* **1991***, 113,* 9887.
19 Uozomi, Y.; Kitayama, K.; Hayashi, T.; Yanagi, K.; Fukuyo, E. *Bull. Chem. Soc. Jpn.* **1995***, 68,* 713.
20 Shimada. T.; Mukaide, K.; Shinohara, A.; Han, J. W.; Hayashi, T. *J. Am. Chem. Soc.* **2002**, *124***,** 1584**.**
21 Lipshitz, B. H.; Noson, K.; Chrisman, W.; Lower, A. *J. Am. Chem. Soc.* **2003***, 125,* 8779.
22 Ojima, I.; Kogure, T.; Nagai, Y. *Chem. Lett.* **1973**, 541. *Tetrahedron Lett.* **1972**, 5035.
23 Dumont, W.; Poulin, J.-C.; Dang, T.-P.; Kagan, D. B. *J. Am. Chem. Soc.* **1973***, 95,* 8295.

24 Hayashi, T.; Yamamoto, K.; Kumada, M. *Tetrahedron Lett.* **1974**, 4405. *J. Organomet. Chem.* **1972***, 46,* C65.
25 Brunner, H.; Obermann, U. *Chem. Ber.* **1989**, *122,* 499. Nishiyama, H.; Sakaguchi, H.; Nakamura, T.; Horihata, M.; Kondo, M.; Itoh, K. *Organometallics,* **1989***, 8,* 846. Balavoine, G.; Clinet, J. C.; Lellouche, I. *Tetrahedron Lett.* **1989**, *30*, 5141. Brunner, H.; Nishiyama, H.; Itoh, K. in "Catalytic Asymmetric Synthesis" Ed. Ojima, I. VCH Publishers, New York, **1993**, p. 303.
26 Brunner, H.; Becker, R.; Riepl, G. *Organometallics,* **1984**, *3*, 1354. Brunner, H.; Riepl, G.; Weitzer, H. *Angew. Chem. Int. Engl. Ed.* **1983**, *22*, 331.
27 Brunner, H.; Henrichs, C. *Tetrahedron Asymm.* **1995***, 6,* 653.
28 Ojima, I.; Kogure, T.; Kumagai, M.; Horiuchi, S.; Sato, Y. *J. Organomet. Chem.* **1976***, 122,* 83.
29 Nishiyama, H.; Yamaguchi, S.; Park, S.-B.; Itoh, K. *Tetrahedron Asymm.* **1993***, 4,* 143.
30 Akita, M.; Mitani, O.; Morooka, Y. *J. Chem. Soc. Chem. Commun.* **1989**, 527.
31 Tao, B.; Fu, G. C. *Angew. Chem. Int. Ed.* **2002**, *41,* 3892.
32 Sudo, A.; Yoshida, H.; Saigo, K. *Tetrahedron Asymm.* **1997***, 8,* 3205.
33 Sawamura, M.; Kuwano, R.; Ito, Y. *Angew. Chem. Int. Ed.* **1994***, 33,* 111. Kuwano, R.; Sawamura, M.; Shirai, J.; Takahashi, M.; Ito, Y. *Bull. Chem. Soc. Jpn.* **2000**, *73*, 485.
34 Yamanoi, Y. Imamoto, T. *J. Org. Chem.* **1999**, *64,* 2988.
35 Tsuruta, H.; Imamoto, T. *Tetrahedron Asym.* **1999,** *10***,** 877.
36 Reyes, C.; Prock, A.; Giering, W. P. *Organometallics,* **2002**, *21*, 546.
37 Kolb, I.; Hetflejs, J. *Collect. Czech. Chem. Commun.* **1980***, 45,* 2808.

Chapter 19

C–H FUNCTIONALISATION

Future trends ....

19.1 Introduction

Direct conversion of alkanes or arenes to oxygenates, nitrogenates, and other compounds is an important reaction that has been the target of research for a long while. Carbon-hydrogen bonds are very stable towards many reagents, except reactive oxygen compounds. Functionalisation therefore requires "activation of C–H bonds" and usually we refer to metal mediated activation when this expression is used [1]. Attack by oxygen-centred species is relatively common and we have come across this mechanism a number of times. For instance the partial burning of butane to give acetic acid was mentioned in Chapter 6. Production of terephthalic acid from paraxylene with oxygen also uses a cobalt catalyst (Chapter 15.4), but the function of the metal is only to generate a reactive oxygen centred radical that starts the radical chain oxidation reaction. In these reactions there is no direct interaction between the metal and the C–H bond.

An intermediate case involves the interaction of a ligand coordinated to a metal with the C–H bond of an alkane or arene substrate. For example the oxidation of organic substrates with the use of metal porphyrin oxo complexes belongs to this class. Reactions of this type have been extensively studied as mimicks of the natural enzyme Cytochrome P450, which plays a central role in living cells. The porphyrin moiety in P450 contains a reactive Fe(V)=O species that can attack C–H bonds to give alcohols and can also attack alkene double bonds to produce epoxides. A very wide variety of porphyrins of iron and manganese (and related complexes, see Chapter 14 for a few examples) have been studied. Oxygen centred activation of C–H bonds is not the topic of this chapter.

Another example of a fragment X attached to a metal centre that attacks a C–H bond is the carbenoid fragment attached to copper or rhodium as

discussed in Chapter 17. A diazo compound loses N_2 first, the carbenoid left forms a weak bond to the metal, and inserts into a C–H bond the same way as a free carbene would do.

Activation of a C–H bond as an organometallic chemist would define it involves coordination of a C–H bond to a metal complex, which activates, or weakens the C–H bond. For functionalisation, such activation must be followed by C–X bond formation. Alternatively, the activation will proceed as an oxidative addition to the metal, after which a C–X bond should be formed to obtain functionalisation. The key issue of this general scheme is that the interaction of a metal ion and a C–H bond is very weak and that this must occur in the presence of a reagent X. The reagent X is expected to react with an activated carbon atom, a carbon atom coordinated to a metal, or a metal complex, but it should react with the complex only after the "activation" has taken place. Such molecules "X" tend to be much better ligands toward metal complexes than hydrocarbons and this outlines the problem; most reagents X will react with the reactive metal complex and, for example, oxidise it. After many years of research in this area there are many complexes now that activate C–H bonds and form interesting organometallic complexes; subsequent functionalisation with the use of electron-rich complexes, however, is relatively rare. Subsequent functionalisation may also pose a thermodynamic problem as we will see.

In heterogeneous metal catalysis alkanes, alkenes, and aromatics adsorbed on the metal surface rapidly exchange hydrogen and deuterium. The multiple adsorption of reactants and intermediates lowers the barriers for such exchange processes. Hydrogenation of unsaturated aliphatics and isomerisation can be accomplished under mild conditions. Catalytic dehydrogenation of alkanes to alkenes requires temperatures >200 °C, but this is because of the thermodynamics of this reaction.

We are not aware of any industrial application that uses metal activation of C–H bonds to obtain functionalised molecules. We have included this topic, because it is potentially of great importance by providing a short-cut for the conversion of hydrocarbons to its functionalised derivatives. Two extreme cases will be discussed, reactions with electron-rich metal complexes and reactions with electrophilic metal complexes. As always in organometallic chemistry there are cases in between that utilise both bonding interactions.

For each case we will also present catalytic analogues, namely (1) the activation of methane to form methanol with platinum, the reaction of certain aromatics with palladium to give alkene-substituted aromatics, and (2) the alkylation of aromatics with ruthenium catalysts, and the borylation of alkanes and arenes with a variety of metal complexes.

19.2 Electron-rich metals

Intramolecular oxidative addition of C–H bonds to an electron-rich metal is a very common reaction in organometallic chemistry. Maybe it was discovered via H–D exchange of the ligand with deuterium present as $^2H_2$. It has been encountered many times for triphenylphosphine, in which case it was called orthometallation, because the ortho-hydrogen moves to the metal and a metal-carbon bond to the ortho-carbon is formed. If now this hydrogen is exchanged with deuterium present in the solution and the reaction reverses, we find the incorporation of deuterium in the ligand (Figure 19.1).

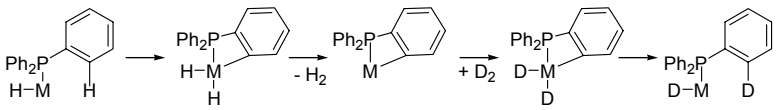

Figure 19.1. Schematic representation of orthometallation and H-D exchange

Incorporation of deuterium was also found for alkyl groups attached to ligands and the general name for the formation of the intermediates now is cyclometallation. One might wonder if such cyclometallation reactions always involve oxidative additions, and many intermediate cases with electrophilic metal complexes can be imagined. For example, a very common sequence of reactions includes a formal reductive elimination of HX after the formation of the metal-carbon bond, and this we can write equally well as an electrophilic mechanism (see Figure 19.2 for a general reaction). Numerous intramolecular, stoichiometric C–H reactions have been reported, and often the metal organic compound obtained can undergo insertion reactions.

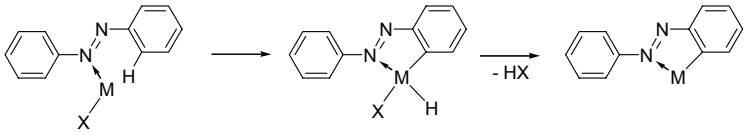

Figure 19.2. Cyclometallation with elimination of HX

These findings have stimulated enormously the search for intermolecular activation of C–H bonds, in particular those of unsubstituted arenes and alkanes. In 1982 Bergman [2] and Graham [3] reported on the reaction of well-defined complexes with alkanes and arenes in a controlled manner. It was realised that the oxidative addition of alkanes to electron-rich metal complexes could be thermodynamically forbidden as the loss of a ligand and rupture of the C–H bond might be as much as 480 kJ.mol^{-1}, and the gain in M–H and M-C

bond energies might be less or at best very close in magnitude. Therefore, it is advantageous if the initial creation of the vacant site can be carried out photochemically. A photochemically generated unsaturated iridium species undergoes oxidative addition of cyclohexane and other substrates (Figure 19.3).

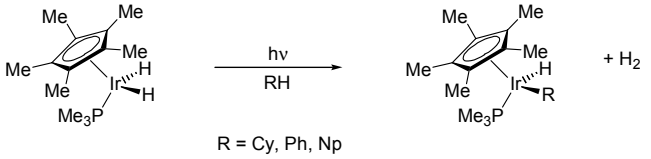

Figure 19.3. Oxidative addition of cyclohexane [2]

Interestingly, the triphenylphosphine analogue underwent mainly the "normal" cyclometallation reaction (Figure 19.4).

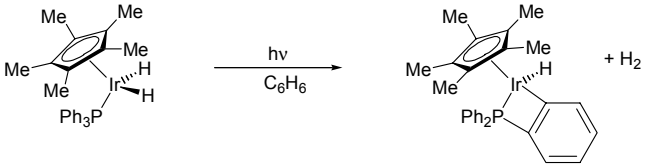

Figure 19.4. Cyclometallation for PPh_3

Many related complexes of iridium and rhodium undergo the oxidative addition reaction of alkanes and arenes [1]. Alkane C–H bond oxidative addition and the reverse reaction is supposed to proceed via the intermediacy of σ-alkane metal complexes [4], which might involve several bonding modes, as shown in Figure 19.5 (for an arene the favoured bonding mode is η^2 via the π-electrons).

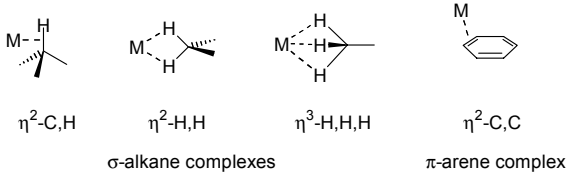

Figure 19.5. Alkane bonding modes

The first reports on σ-alkane metal complexes date back to the 1970s, the work of Perutz and Turner on photochemically generated unsaturated metal carbonyls of Group 6 [4], which is well before the C–H oxidative addition studies of alkanes. The enthalpy gain of formation of σ-alkane metal complexes

is estimated to be 20–40 kJ.mol^{-1}. The occurrence of such intermediates in alkane activation reactions was probed by isotopic substitution in mixed H/D hydrocarbons and by comparing rate measurements at per-protio and per-deuterio hydrocarbyl hydride complexes [5]. In mixed H/D hydrocarbyl hydride complexes equilibration occurs intramolecularly between hydride and deuterium prior to loss of alkane from the complex, see below.

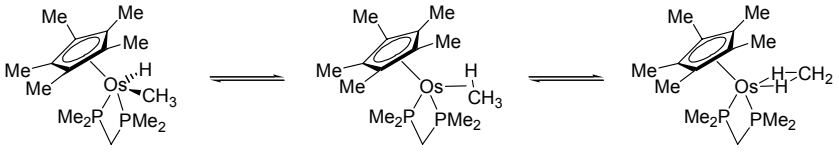

Figure 19.6. Intramolecular hydride methyl-hydrogen exchange

Exchange of hydrogen between C–H and M–H can be very fast as in the osmium compound shown in Figure 19.6 in which H/H exchange can be observed by NMR spectroscopy (intermediates shown are speculative). At –100 °C the exchange rate is as high as 170 s^{-1} [6].

Kinetic isotope effect studies have contributed greatly to our understanding of the details of C–H activation by these types of metal complexes. The simplest energy scheme for kinetic isotope effects is presented schematically in Figure 19.7.

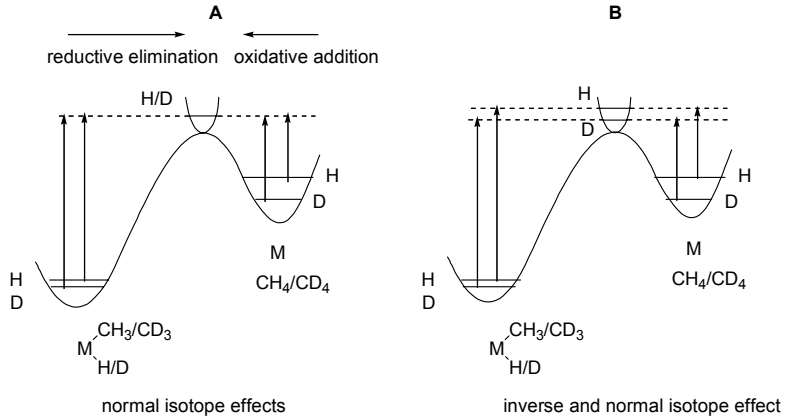

Figure 19.7. Isotope effects in alkane-metal reactions

The general phenomenon of a primary kinetic isotope effect is caused by the higher zero-point vibration energy of a C–H bond compared to a C–D bond. If in the transition state where this bond is being broken the intermediate is linear (C–H–X), the energies of the deuterio and protio species are equal and

thus the barrier for the protio species is lower. Therefore, the rate for the protio species is higher than that of the deuterio species; this is the general rule for organic reactions. Normal isotope effects have been measured for the formation of alkanes from hydrido alkyl platinum complexes [7]. This situation is sketched in Figure 19.7-**A** and it represents the overall process for perdeuterio and perprotio complexes. The normal isotope effect holds for the reactions in both directions, the reductive elimination and the oxidative addition of the alkane. The isotope effect is higher for the oxidative addition.

For a late transition state, however, the vibrational energies of the transition state will not be equal for the two isotopes, but will be closer to the vibrational energies of the alkane product. Likewise, this may be the case for non-linear transition states. This has been depicted in Figure 19.7-**B**. It is seen that in the metal deuteride/hydride the energy difference between the two species is smaller than in a carbon-hydrogen/deuterium bond (exaggerated in the figure), because the stretching frequencies for M–H are lower than those of C–H. As a result the reductive elimination barrier is lower for the deuterated species. Secondary isotope effects for the H/D atoms not participating in bond breaking/making are not considered, as they are supposed to be much smaller. For many complexes the elimination of CD_4 from $MD(CD_3)$ is indeed faster than the elimination of CH_4 from the perprotio analogue.

There is ample evidence that the reductive elimination of alkanes (and the reverse) is a not single-step process, but involves a σ-alkane complex as the intermediate. Thus, looking at the kinetics, reductive elimination and oxidative addition do not correspond to the elementary steps. These terms were introduced at a point in time when σ-alkane complexes were unknown, and therefore new terms have been introduced by Jones to describe the mechanism and the kinetics of the reaction [5]. The reaction of the σ-alkane complex to the hydride-alkyl metal complex is called reductive cleavage and its reverse is called oxidative coupling. The second part of the scheme involves the association of alkane and metal and the dissociation of the σ-alkane complex to unsaturated metal and free alkane. The intermediacy of σ-alkane complexes can be seen for instance from the intramolecular exchange of isotopes in D–M–CH_3 to the more stable H–M–CH_2D prior to loss of CH_3D.

The kinetics of the overall loss of alkane must be treated as a two-step-process with the elementary steps rc (reductive coupling), oc (oxidative cleavage) and d (dissociation). If the elimination is irreversible the kinetic equation reads $k_{cr}k_d/(k_{cr}+k_{oc}+k_d)$ and depending on the relative magnitudes the equation can be simplified [8]. In Figure 19.8 the situation has been depicted for transition states having different zero-point energies for protio and deuterio systems, and a rate-determining dissociation reaction. For clarity the arrows for the dissociation have been omitted. The isotope effect of this step is usually considered to be close to unity. The oxidative cleavage according to this sketch

shows a normal isotope effect, and the reductive coupling shows an inverse isotope effect. The inverse isotope effect in elimination reactions was taken as an indication that σ-alkane complexes are intermediates. An accurate treatment should include the effects on the elementary steps involved. The inverse isotope effect has values $k_H/k_D = 0.3–0.7$. It has been observed for complexes of Ir, Rh, W, Re, and Pt [9]. For a complete treatment and a discussion of many pitfalls we refer to Jones and references therein [5,9].

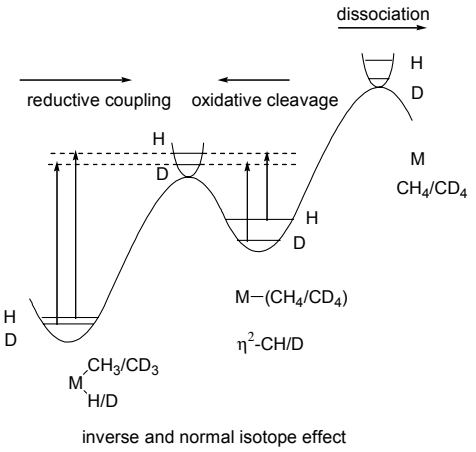

Figure 19.8. Inverse isotope effects in C–H activation [5]

In H/D mixed hydrocarbyl metal complexes, the differences in zero-point energies also lead to equilibrium isotope effects, as it does in H/D complexes with agostic hydrogen-metal interactions (Chapter 10.5). Like in agostic interactions the most favourable situation is to have deuterium at a carbon atom and the protium interacting with the metal, as this gives the lowest total zero-point vibration energy. Prior to loss of alkane equilibration takes place. We will not discuss here the interesting details of such mixed complexes.

In summary, once the reactive vacant site has been created activation of alkanes is a facile process, much more facile than might have been thought during the 1970s, when only intramolecular ligand-cyclometallation reactions were known. The C–H activation shown in Figure 19.3 occurs in the related carbonyl complex at very low temperature; IR spectroscopic evidence, including deuterium labelling, showed that photolysis of $(\eta5\text{-}CpMe_5)Ir(CO)_2$ in CH_4 matrices at 12 K lead quickly to $[(\eta5\text{-}CpMe_5)Ir(CO)H(Me)]$ species [10]. As we said in the introduction the overall thermodynamics of the process pose the problem: the loss of a ligand costs energy and the metal-carbon bond made is too weak. Since aryl metal-carbon bonds are stronger than alkyl metal bonds, aryl carbon-metal bonds are formed preferentially and more easily. In the

reaction with alkanes there is a preference for activation of the terminal hydrogens, probably for steric reasons, which makes the reaction even more interesting for catalysis.

Several catalytic processes are known, see below, but it is clear that the compatibility of the above chemistry with functionalisation is limited. Many reagents used to introduce functional groups will react with the reactive intermediates described above, and the alkanes will have no opportunity to react with the catalyst. Below a few catalytic reactions will be described of relatively electron-rich metal complexes.

19.3 Hydrogen transfer reactions of alkanes

Hydrocarbons that might be compatible with electron-rich organometallic complexes capable of C–H activation are alkenes. A potential reaction therefore is dehydrogenation of alkanes to alkenes. Thermodynamics require high temperatures and low hydrogen pressures otherwise the process is energetically uphill. The stoichiometric reaction was discovered for cycloalkanes and iridium complexes $L_2IrH_2^+$ with the use of hydrogen acceptors such as t-butylethene [11] (Figure 19.9). Stoichiometric reactions were also reported for rhenium complexes; $(PPh_3)_2ReH_7$ was shown to dehydrogenate cyclopentane to give cyclopentadienyl-rhenium complexes [12]. These (and other) intermolecular C–H activation reactions with electron-rich metal complexes preceded the stoichiometric reactions that started to appear in 1982.

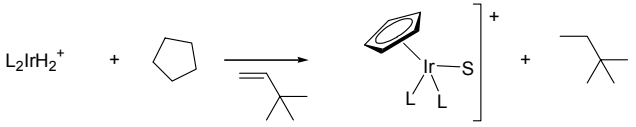

Figure 19.9. Hydrogen transfer from alkanes to alkenes

Highly stable complexes for the catalytic hydrogen transfer reaction are the so-called pincer complexes of iridium as reported by Jensen [13]. They are even sufficiently stable to allow dehydrogenation of alkanes to alkenes and dihydrogen in refluxing cyclooctane (b.p. 151 °C) or cyclodecane (b.p. 201 °C). During reflux the hydrogen escapes from the solvent and can be removed from the system (Figure 19.10). Turnover frequencies of several hundreds per hour were measured [14]. As mentioned above, C–H activation occurs preferentially at the terminal carbon atom of n-alkanes; thus, the primary product of such a reaction are predominantly 1-alkenes, a desirable product (Chapter 9). Indeed, the initial product is 1-alkene, but at longer reaction times

isomerisation takes place. Also higher concentrations of alkene prohibit the reaction as alkenes coordinate more strongly to the metal catalyst than alkanes.

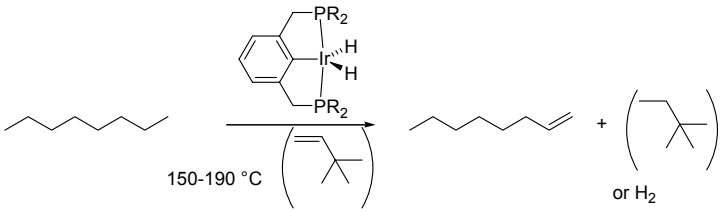

Figure 19.10. Dehydrogenation of alkanes with pincer complexes

19.4 Borylation of alkanes

Activation of alkane C–H bonds is much easier than one might have thought before 1980. Substitution of the carbon atom after its addition to a low-valent metal complex, however, remains a difficult task *and* an important target. The key issue is to find a reagent that can transfer a functional group or atom in such a way that the reactive metal complex is retained. Alkenes and alkynes are candidates as we have seen above, but the products of such reactions are alkenes (via dehydrogenation of alkanes or alkane addition to alkynes) or alkanes (alkane addition to alkenes). It was found that boron compounds are suitable candidates, in terms of reactivity and thermodynamics [15]. The first examples required photochemical activation, but now there are several examples of thermal reactions. Interestingly, many metals catalyse this reaction: Mo, W, Fe, Ru, Rh, and Ir. A typical example is shown in Figure 19.11.

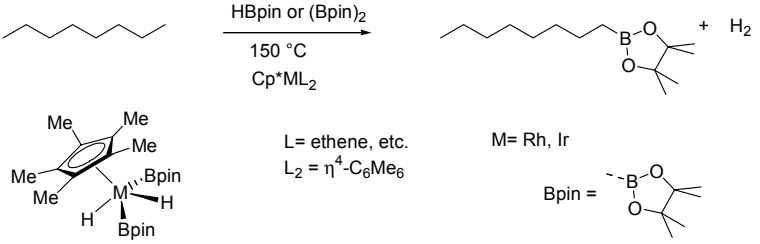

Figure 19.11. Borylation of alkanes

Instead of the borohydrido pinacol ester one can also use the boron dimer. Several metals, intermediates as the one shown in Figure 19.10 have been isolated. They may contain 1-3 Bpin units and 3-1 hydrides. For the mechanism

one can imagine a series of oxidative addition and reductive elimination reactions. For iron and tungsten systems also σ-bond metathesis type mechanisms were proposed [16].

The boron group can be displaced by oxygen via oxidation with hydroperoxide. For making simple alcohols this is not an industrial option. For making aryl boronic esters, starting materials for the Suzuki reaction (Chapter 13) for the use in agrochemicals and pharmaceuticals [17], it seems a promising route, as it avoids the use of Grignard reagents, and it reduces the number of steps, especially if one could continue with the Suzuki coupling reaction in the same reactor without purification.

19.5 The Murai reaction

An efficient catalytic addition of aromatic carbon-hydrogen bonds to alkenes was developed by Murai and co-workers [18]. The aromatic compound usually contains a functionality such as a ketone or imine and the "activation" takes place ortho to this group. Thus the Murai reaction is more akin to the older C–H activation in ligands coordinated to the activating metal than to the alkane/arene activation described in the previous sections. The conversion is catalytic, though, and the number of compounds subjected to this reaction is very high. Ruthenium is the metal of choice and a range of precursors has given good results. Turnover numbers are often below 100 and temperatures are often high, 150 °C. The "base" example is presented in Figure 19.12 together with a simplified mechanism.

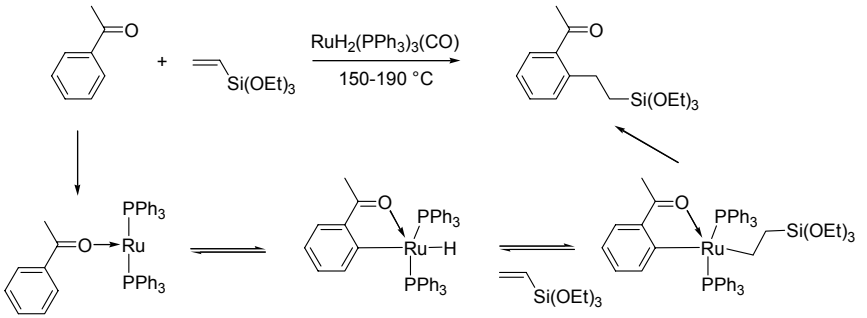

Figure 19.12. Addition of aromatics to alkenes (Murai reaction)

According to isotope studies the rate-determining step of this sequence is the reductive elimination, and all other reactions (C–H activation, insertion of alkene) are reversible. The first indication of this behaviour was the H/D exchange of the ortho proton of acetophenone. Secondly, and perhaps useful for many other systems, was the kinetic isotope effect observed for ^{13}C natural

abundance in the starting material. If all reactions are reversible and the reductive elimination is rate-determining there will be a small, but distinct ^{13}C isotope effect, because the intermediates containing ^{13}C at the crucial positions will react more slowly than the molecules containing ^{12}C at the Ru-C bonds. The isotope effect is small because the masses differ only slightly, but especially at high conversions one can measure this effect in the unreacted substrate, which is enriched in ^{13}C at the positions involved in the reductive elimination. As the natural abundance does not change at the other positions, the enrichment can be relatively easily measured by ^{13}C spectroscopy [19].

19.6 Catalytic σ-bond metathesis

Another effective way of staying clear of the thermodynamic barriers of C–H activation/substitution is the use of the σ-bond metathesis reaction as the crucial elementary step. This mechanism avoids intermediacy of reactive metal species that undergo oxidative additions of alkanes, but instead the alkyl intermediate does a σ-bond metathesis reaction with a new substrate molecule. Figure 19.13 illustrates the basic sequence [20].

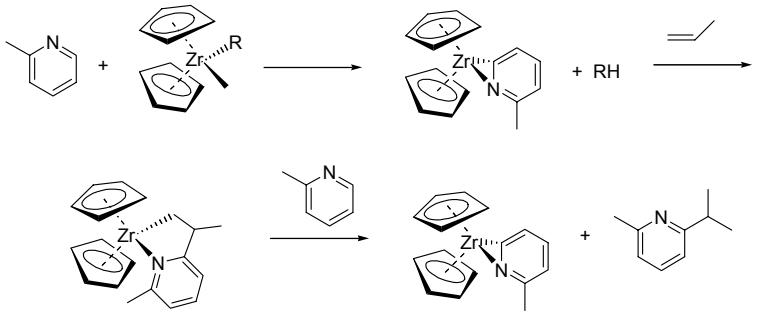

Figure 19.13. Catalytic σ-bond metathesis

Effectively, this is another example of the addition of a functional aromatic compound to an alkene, as the Murai reaction, but the mechanism is different. Alkyl substituted pyridine derivatives are interesting molecules for pharmaceutical applications. The σ-bond metathesis reaction is typical of early transition metal complexes as we have learnt in Chapter 2.

19.7 Electrophilic catalysts

The earliest catalytic application of C–H bond activation and functionalisation is that of methane using platinum chlorides as the catalyst and oxidising reagent. The exchange of hydrogen atoms in arenes with D_2O was

discovered in 1967 by Garnett and Hodges [21] and the exchange with alkanes two years later by Shilov and co-workers [22]. The effective functionalisation of methane involves platinum(II) [23] as the activating metal complex and platinum(IV) as the oxidising species to generate methyl chloride and methanol [24]. The methane activating species is platinum(II), which is compatible with the oxidising agent, Pt(IV). The process is different from the one we have seen above; an electrophilic metal ion forms a bond with the σ-C–H-bond of methane, and a base abstracts the proton, under formation of a metal-carbon bond [25]. The process is the analogue of the heterolytic cleavage of dihydrogen and the cleavage of a silicon-hydride bond by a methoxide forming a silicon-oxygen bond (Chapter 2). The mechanism is shown in Figure 19.14.

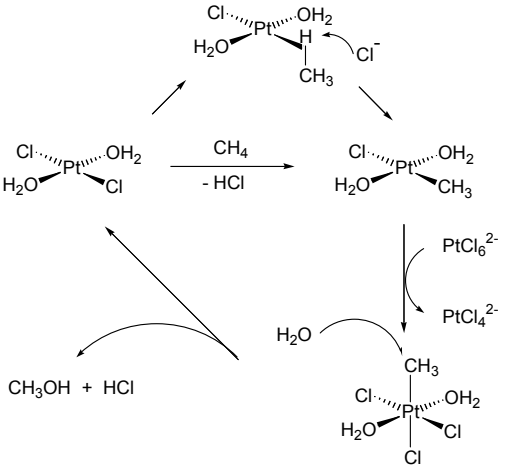

Figure 19.14. Mechanism of methanol formation in the "Shilov" system

Pentane gives 1-pentyl chloride as the main product, which is highly interesting as all other oxidative functionalisations will give a secondary alkyl derivative as the product, because for radical attack the secondary hydrogens are more reactive than the primary ones.

It has been shown that Pt(IV) functions as an oxidant and that no methyl transfer is involved from Pt(II) to Pt(IV). This is promising, in that other oxidising agents might be used instead of Pt(IV). Ligand modified platinum complexes can activate methane under very mild conditions in pentafluoropyridine or trifluoroethanol as a weakly coordinating solvent. Bidentate nitrogen ligands were preferred [26]. The divalent dimethylplatinum complexes can be oxidised to Pt(IV) by dioxygen [27], which indicates there is still room for progress towards a useful system.

An important breakthrough on the route toward avoidance of expensive tetravalent platinum as the oxidising agent was reported by Periana and co-

workers [28] who succeeded in using sulfuric acid in combination with Pt(II). The product of this reaction is the monomethyl ester of sulfuric acid. Re-oxidation of SO_2 and recovery of methanol is not an easy task either, but as yet it is one of the best catalytic functionalisation reactions of methane using C–H activation.

Other metals capable of electrophilic substitution of C–H bonds are salts of palladium and, environmentally unattractive, mercury. Methane conversion to methanol esters have been reported for both of them [29]. Electrophilic attack at arenes followed by C–H activation is more facile, for all three metals. The method for making mercury-aryl involves reaction of mercury diacetate and arenes at high temperatures and long reaction times to give aryl-mercury(II) acetate as the product; it was described as an electrophilic aromatic substitution rather than a C–H activation [30].

Palladium salts will attack C–H bonds in functionalised aromatics such as acetoaniline to form palladium-carbon bonds that subsequently undergo insertion of alkenes [31]. β-Hydride elimination gave styryl derivatives and palladium hydride, which requires re-oxidation of palladium by benzoquinone. The reaction can be regarded as a combined Murai reaction (C–H activation, if electrophilic) and a Heck reaction (arylalkene formation), notably without the production of salts as the cross-coupling reactions do. An example is shown in Figure 19.15.

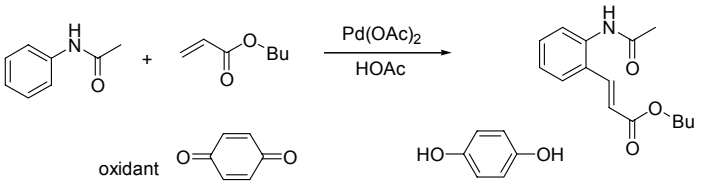

Figure 19.15. Electrophilic C–H activation by palladium(II)

Perhaps, many of the intramolecular C–H activations that are known for metal ligand complexes are actually best described as electrophilic substitutions rather than oxidative additions. A very large number of palladium(II) complexes are known to react intramolecularly to the metallated species.

C–H activation remains an important topic for catalysis even after thirty years of intensive research. The potential shortcuts it offers for many present routes to a wide variety of chemicals that are produced will continue to inspire industrial and academic research [32]. An interesting example involves the enantiospecific, coordination-directed C–H bond functionalisation in the synthesis of a natural product, rhazinilam, an anti-tumor agent. The resulting vinyl moiety obtained in the dehydrogenation was subsequently carbonylated to form a cyclic amide [33].

References

1 Shilov, A. E.; Shul'pin, G. B. *Activation and Catalytic Reactions of Saturated Hydrocarbons in the Presence of Metal Complexes.* **2000**. Catalysis by Metal Complexes, Volume 21. James, B. R.; van Leeuwen, P. W. N. M. Eds. Kluwer Academic Publishers, Dordrecht.

2 Janowicz, A. H.: Bergman, R. G. *J. Am. Chem. Soc.* **1982***, 104,* 352.

3 Hoyano, J. K.; Graham, W. A. G. *J. Am. Chem. Soc.* **1982***, 104,* 3732.

4 Hall, C. Perutz, R. *Chem. Rev.* **1996**, *96,* 3125. Perutz, R. N.; Turner, J. J. *J. Am. Chem. Soc.* **1975***, 97*, 4791.

5 Jones, W. D. *Acc. Chem. Res.* **2003**, *36,* 140.

6 Gross, C. L.; Girolami, G. S. *J. Am. Chem. Soc.* **1998**, *120*, 6605.

7 Abis, L.; Sen, A.; Halpern, J. *J. Am. Chem. Soc.* **1978**, *100*, 2915. Hackett, M.; Ibers, J. A.; Whitesides, G. M. *J. Am. Chem. Soc.* **1988**, *110*, 1436.

8 Churchill, D. G.; Janak, K. E.; Wittenberg, J. S.; Parkin, G. *J. Am. Chem. Soc.* **2003**, *125*, 1403.

9 Periana, R. A.; Bergman, R. G. *J. Am. Chem. Soc.* **1986**, *108*, 7332. Bullock, R. M.; Headford, C. E. L.; Hennessy, K. M.; Kegley, S. E.; Norton, J. R. *J. Am. Chem. Soc.* **1989**, *111*, 3897. Gould, G. L.; Heinekey, D. M. *J. Am. Chem. Soc.* **1989**, *111*, 5502. Stahl, S. S.; Labinger, J. A.; Bercaw, J. E. *J. Am. Chem. Soc.* **1996**, *118*, 5961. Wang, C.; Ziller, J. W.; Flood, T. C. *J. Am. Chem. Soc.* **1995**, *117*, 1647. Chernega, A.; Cook, J.; Green, M. L. H.; Labella, L.; Simpson, S. J.; Souter, J.; Stephens, A. H. H. *J. Chem. Soc. Dalton Trans.* **1997**, 3225. Wick, D. D.; Reynolds, K. A.; Jones, W. D. *J. Am. Chem. Soc.* **1999**, *121*, 3974.

10 Rest, A. J.; Whitwell, I.; Graham, W. A. G.; Hoyano, J. K.; McMaster, A. D. J. *Chem. Soc. Chem. Commun.* **1984**, 624.

11 Crabtree, R. H.; Mihelcic, J. M.; Quirk, J. M. *J. Am. Chem. Soc.* **1979**, *101*, 7738.

12 Baudry, D.; Ephritikhine, M.; Felkin, H.; Zakrewski, J. *J. Chem. Soc. Chem. Commun.* **1980**, 1235.

13 Gupta, M.; Hagen, C.; Flesher, R. J.; Kaska, W. C.; Jensen, C. M. *Chem. Commun.* **1996**, 2083. Jensen, C. M. *Chem. Commun.* **1999**, 2443.

14 Liu, F. C.; Goldman, A. S. *Chem. Commun.* **1999**, 655.

15 Waltz, K. M.; Hartwig, J. F. *Science* **1997**, *277,* 211. Waltz, K. M.; He, X.; Muhoro, C.; Hartwig, J. F. *J. Am. Chem. Soc.* **1995**, *117*, 11357. Iverson, C. N.; Smith III, M. R. *J. Am. Chem. Soc.* **1999**, *121*, 7696. Shimida, S.; Batsanov, A. S.; Howard, J. A. K.; Marder, T. B. *Angew. Chem. Int. Ed.* **2001**, *40*, 2168. Takagi, J.; Sato, K.; Hartwig, J. F.; Ishiyama, T.; Miyaura, N. *Tetrahedron Lett.* **2002**, *43,* 5649.

16 Webster, C. E.; Fan, Y.; Hall, M. B.; Kunz, D.; Hartwig, J. F. *J. Am. Chem. Soc.* **2003**, *125*, 858.

17 Mertins, K.; Zapf, A. Beller, M. *J. Mol. Catal. A: Chem.* **2004**, *207*, 21.

18 Murai, S.; Kakiuchi, F.; Sekine, S.; Tanaka, Y.; Kamatani, A.; Sonoda, M.; Chatani, N. *Nature,* **1993**, *366,* 529. Kakiuchi, F.; Murai, S. *Acc. Chem. Res.* **2002**, *35,* 826.

19 Kakiuchi, F.; Ohtaki, H.; Sonoda, M.; Chatani, N. Murai, S. *Chem. Lett.* **2001**, 918.

20 Jordan, R. F.; Taylor, D. F. *J. Am. Chem. Soc.* **1989**, *111*, 778.

21 Garnett, J. L.; Hodges, R. J. *J. Am. Chem. Soc.* **1967**, *89,* 4546.

22 Gold'shleger, N. F.; Tyabin, M. B.; Shilov, A. E.; Shteinman, A. A. *Zh. Fiz. Khim.* **1969**, *43*, 274 (in Russian); *Chem. Abstr.* **1969**, *71,* 505782.

23 Tyabin, M. B.; Shilov, A. E.; Shteinman, A. A. *Dokl. Akad. Nauk. SSSR* **1971***, 198*, 380.

24 Shilov, A. E.; Shul'pin, G. B. *Russ. Chem. Rev.* **1987**, *56,* 442.

25 Luinstra, G. A.; Wang, L.; Stahl, S. S.; Labinger, J. A.; Bercaw, J. E. *J. Organometal. Chem.* **1995**, *504,* 75. *Organometallics,* **1994**, *13*, 755.

26 Holtcamp, M. W.; Labinger, J. A.; Bercaw, J. E. *J. Am. Chem. Soc.* **1997**, *119*, 848.
27 Rostovtsev, V. V.; Labinger, J. A.; Bercaw, J. E.; Lasseter, T. L.; Goldberg, K. I. *Organometallics* **1998**, *17*, 4530.
28 Periana, R. A.; Taube, D. J.; Gamble, S.; Taube, H.; Satoh, T.; Fujii, H. *Science,* **1998**, *280,* 560.
29 Periana, R. A.; Mironov, O.; Taubde, D.; Bhalla, G.; Jones, C. J. *Science,* **2003**, *301,* 814, and references therein.
30 Lau, W.; Kochi, J. K. *J. Am. Chem. Soc.* **1986**, *108*, 6720. Olah, G. A.; Yu, S. H.; Parker, D. G. *J. Org. Chem.* **1976**, *41*, 1983.
31 Boele, M. D. K.; van Strijdonck, G. P. F.; de Vries, A. H. M.; Kamer, P. C. J.; de Vries, J. G.; van Leeuwen, P. W. N. M. *J. Am. Chem. Soc.* **2002**, *124*, 1586.
32 Labinger, J. J.; Bercaw, J. E. *Nature,* **2002**, *417,* 507.
33 Johnson, J. A.; Li, N.; Sames, D. *J. Am. Chem. Soc.* **2002**, *124*, 6900.

Subject index